LIGAND ISOTOPE VIBRATIONAL STUDIES OF METAL(II) COMPLEXES WITH PARTICULAR REFERENCE TO HETEROCYCLIC *N*-OXIDES

A thesis submitted to the

UNIVERSITY OF CAPE TOWN

in fulfilment of the requirements for the degree of

DOCTOR OF PHILOSOPHY

by

GARETH MOSTYN WATKINS

B.Sc.(Hons.)(University of Cape Town)

Department of Inorganic Chemistry
University of Cape Town
Rondebosch 7700
South Africa

(December 1987)

' Great are the works of the LORD;

they are pondered by all who

delight in them.

Glorious and majestic are his deeds,

and his righteousness endures

forever. '

(*Psalm 111* $^{2+3}$)

ACKNOWLEDGEMENTS

My sincere thanks to Professor D.A. Thornton for introducing this field of work to me and for his supervision, to Professor B.J. van der Veken and Dr. P.F.M. Verhoeven (University of Antwerp) for the Raman spectral data, to Miss B. Williamson for the mass spectral data, to Mr. W.R.T. Hemstedt for the microanalyses and to my colleagues of the Department of Inorganic Chemistry.

Financial assistance from the South African Council for Scientific and Industrial Research is gratefully acknowledged.

Finally, I would like to thank my mother for the typing of this thesis and Mr. P.S. Hall for proof-reading.

SUMMARY

A critical examination of the characteristic N-O vibrational frequencies of aromatic *N*-oxides questions the widely held assignment of αN-O ($840cm^{-1}$) and γN-O ($470cm^{-1}$). The present investigation supports the assignments of αN-O ($470cm^{-1}$) and γN-O ($280cm^{-1}$), with the assignment of the band at $840cm^{-1}$ as being νring coupled with νN-O.

The infrared and Raman spectra ($4000-50cm^{-1}$) of pyrazine *N,N'*-dioxide, pyrazine *N*-oxide, their fully deuterated analogues and 1,10 phenanthroline have been fully assigned. The infrared spectra ($4000-50cm^{-1}$) of 2,2' bipyridine *N,N'*-dioxide, quinoline *N*-oxide, their fully deuterated analogues and 1,10-phenanthroline -d_8 have been fully assigned. Vibrational coupling within these ligands is discussed by comparison with similar molecules and by employing their ν^D/ν^H ratios.

The infrared spectra ($4000-50cm^{-1}$) of 62 complexes of the type $ML_n(ClO_4)_2$ (M = Mn-Zn; n = 4-6, L = pzO, quinO, $bipyO_2$, bipy, phen and their fully deuterated analogues) are fully assigned. Strong coupling between νM-O and internal ligand vibrations is suggested for the Jahn-Teller distorted $[Cu(bipyO_2)_3](ClO_4)_2$ complex, the $[Mn(quinO)_6](ClO_4)_2$ complex and the $[Cu(quin\text{-}d_7O)_4](ClO_4)_2$ complex. Previous reports on the preparation of M(II) $(ClO_4)_2$ complexes with pyrazine *N,N'*-dioxide are questioned in light of the present study.

Detailed infrared assignments ($4000-50cm^{-1}$) are made of 41 π-acid complexes of the type *cis*-$[Pt(bipyO_2\cdot H)AX_2]X$ and *trans*-$[Pt(L)AX_2]$ (A = C_2H_4, CO; X = Cl, Br; L = pdz, pzO, quin, quinO, bipy, phen) and their fully deuterated (L) and C_2D_4 analogues. The uncertainty in the assignments of νPt-O (aromat-

ic *N*-oxides) is raised, and strong coupling between νPt-N(aza-nitrogen) and νPt-Br is demonstrated. The employment of ν_{12} (CH_2 scissors ∿ 1460cm^{-1}) of π-ethene as a diagnostic tool to distinguish between four and five coordination is suggested, while the summed percentage decrease of $\nu_2+\nu_3$ ($\nu C{=}C/\delta CH_2$) may be used to distinguish between N- and O- coordination. The use of chemical shifts (^{1}H nmr spectroscopy) is confirmed as a suitable means to distinguish between four and five coordination and is also shown to be suitable to distinguish between N- and O- coordination in four coordinate Pt(II) π-ethene complexes. In contrast to previous reports J_{Pt-H} cannot be employed to determine the coordinate number.

ABBREVIATIONS

naphth = naphthalene
phenanth = phenanthrene
py = pyridine
pz = pyrazine
pdz = pyridazine
γ-pic = γ-picoline
bipy = 2,2'-bipyridine
quin = quinoline
phen = 1,10-phenanthroline
pyO = pyridine *N*-oxide
pzO = pyrazine *N*-oxide
pzO_2 = pyrazine *N*,*N'*-dioxide
$bipyO_2$ = 2,2'-bipyridine *N*,*N'*-dioxide
quinO = quinoline *N*-oxide
phenO = 1,10-phenanthroline *N*-oxide

ν = stretch
α = inplane bend (of heterocyclic ligand)
γ = out-of-plane bend (of heterocyclic ligand)
δ = inplane bend (of ligand or metal complex)
π = out-of-plane bend (of metal complex)
τ = twist
ω = wag
ρ = rock

The terms hypsochromatic and bathochromatic are employed instead of hypsochromic and bathochromic since *-chromatic* is the *adj.* relating to colour whereas *-chromic* is the *adj.* relating to chromium (Collins English Dictionary, 1986).

TABLE OF CONTENTS Page No.

CHAPTER 1

GENERAL CONSIDERATIONS

The assignment of metal-ligand vibrations in metal complexes is important since their frequencies, species and number give direct information about the nature of the metal-ligand bond and about the structure of the compound. These bands generally occur below $600cm^{-1}$ in the vibrational spectrum, due to the high mass of metal and to the relatively weak nature of the metal-ligand bond. Their frequency is such as to permit vibrational coupling with both low-lying internal vibrations of the ligand and possibly with the lattice modes, thereby complicating their assignments.

In vibrational spectroscopy, those vibrations which result in a change in dipole moment of the molecule are infrared active, while those giving rise to a change in the polarisability of the molecule are Raman active. For simple molecules it is easy to distinguish whether the polarisability or the dipole moment is changed, by simple inspection. For instance a homopolar diatomic molecule, such as H_2, is Raman active but infrared inactive, whereas a heteropolar molecule, such as HCl is both Raman and infrared active.

For polyatomic molecules it becomes difficult to apply simple inspection. If the polyatomic molecule has a center of symmetry, the vibrations that are symmetric with respect to the center of symmetry (the *gerade* or *g* vibrations) are Raman active but infrared inactive, while those vibrations that are antisymmetric with respect to the center of symmetry (the *ungerade* or *u* vibrations) are infrared active but Raman inactive. However, this rule of mutual exclusion is subject to change by the presence of other symmetry elements. For example in the square planar MY_4 type of molecule, the symmetric A_{2g} vibrations are not Raman active and the antisymmetric A_{1u}, B_{1u} and B_{2u} vibrations are not infrared active, as a result of the other symmetry elements associated with D_{4h} symmetry. The concept of symmetry clearly plays

an important role in the understanding of vibrational spectroscopy.

1. APPLICATION OF GROUP THEORY TO MOLECULAR VIBRATIONS

1.1 Group Theory

The quantitative discussion of symmetry is called Group Theory. Molecules may be classified within a group according to their symmetry elements, the name of the point group to which a particular molecule belongs being determined by the symmetry elements that characterise it. These point groups, with their specific symmetry elements, constitute the character tables and may be found in the majority of texts dealing with vibrational spectroscopy [1-4]. Their use is best seen by example.

Consider a molecule composed of N atoms. All the movements of the atoms within the molecule - translational, rotational and vibrational displacements may be resolved into components along the x-, y- and z- axes. This gives a total of 3N possible movements within the molecule, of which six (for non-linear molecules) are translational and rotational and 3N-6 are internal molecular vibrations. The symmetries of the vibrational modes are characterised by labelling each atom within the molecule with 3 Cartesian coordinates describing the unit displacement vectors. These vectors represent all 3N degrees of freedom, and on performing the symmetry operations, the new vector positions can be related to the old by [3N x 3N] matrices whose character χ forms a reducible representation, Γ_{total}

Consider more specifically the molecule *trans*-[PtX_2(CO)L] (Figure 1.1), which we will be examining in Chapter 5.

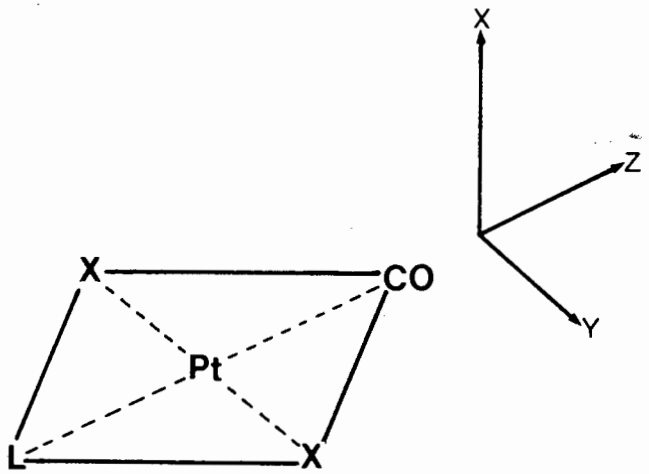

Fig. 1.1 Square planar structure of *trans*-$[PtX_2(CO)L]$

By regarding the ligands as point masses, the point group of the molecule is C_{2v} for which Γ_{total} is:

C_{2v}	E	C_2	σ(xz)	σ'(xy)
Γ_{total}	15	-3	3	5

To determine the symmetry species of all the possible molecular motions, the following formula is applied:

$$N_i = \frac{1}{n} \sum \chi_R \chi_I N$$

where N_i = the number of times each irreducible representation appears in the reducible representation,

n = the order of the group,

χ_R = character of the reducible representation,

χ_I = character of the irreducible representation,

N = the number of symmetry operations in each class.

Thus the 15 possible molecular motions for *trans*-[$PtX_2(CO)L$] are:

$$\Gamma_{3N} = 5A_1 + A_2 + 4B_1 + 5B_2$$

The molecular translations and rotations are obtained from the character tables, which list the transformation properties of x, y, z, x^2, y^2, z^2, xy, xz and yz associated with the point group. The translational properties are listed as T_x, T_y and T_z and the rotational properties as R_x, R_y and R_z. The representations responsible for vibrations are then obtained by removing the translational and rotational representation. For *trans*-[$PtX_2(CO)L$] this yields:

Symmetries for all molecular vibrations	$5A_1$	+	A_2	+	$4B_1$	+	$5B_2$
Symmetries for translations	A_1			+	B_1	+	B_2
Symmetries for rotations			A_2	+	B_1	+	B_2
Symmetries for vibrations (Γ_{vib})	$4A_1$			+	$2B_1$	+	$3B_2$

To determine the number of stretches and bends which constitute Γ_{vib} internal displacement vectors are chosen as a new basis for point group representation. To determine the reducible representation for the stretches, vectors are drawn along the bends. Any vector which is affected by a symmetry operation contributes zero to the character of the matrix, while any unaffected vector contributes +1. For *trans*-[$PtX_2(CO)L$] this yields:

C_{2v}	E	C_2	σ(xz)	σ'(xy)
$\Gamma_{stretch}$	4	2	2	2

which reduces to

$$\Gamma_{stretch} = 3A_1 + B_2$$

The bends can then be obtained by subtracting $\Gamma_{stretch}$ from Γ_{vib},

$$\Gamma_{bend} = A_1 + 2B_1 + 2B_2$$

It now becomes easier to determine which fundamentals are infrared active, Raman active, or both.

It is the interaction of the dipole of the molecule with the oscillating vector of the radiation which produces a change in dipole moment. Therefore, a vibration will be infrared active if it belongs to the same representation as any of the internal displacement vectors. This can be read directly from the character table, any irreducible representation having the transformation properties of x, y or z being infrared active. Similarly, a vibration will be Raman active if it belongs to the same representation as any one of the components of the polarisability tensor of the molecule. Any irreducible representation having the transformation properties of x^2, y^2, z^2, xy, xz or yz is therefore Raman active.

Thus for *trans*-[PtX_2(CO)L] all the stretches and bends (shown in Figure 1.2) are both infrared and Raman allowed.

Another aspect that can be determined from symmetry elements is the likelihood of coupling between vibrations.

Firstly, interactions (*i.e.* coupling) between two or more vibrations of

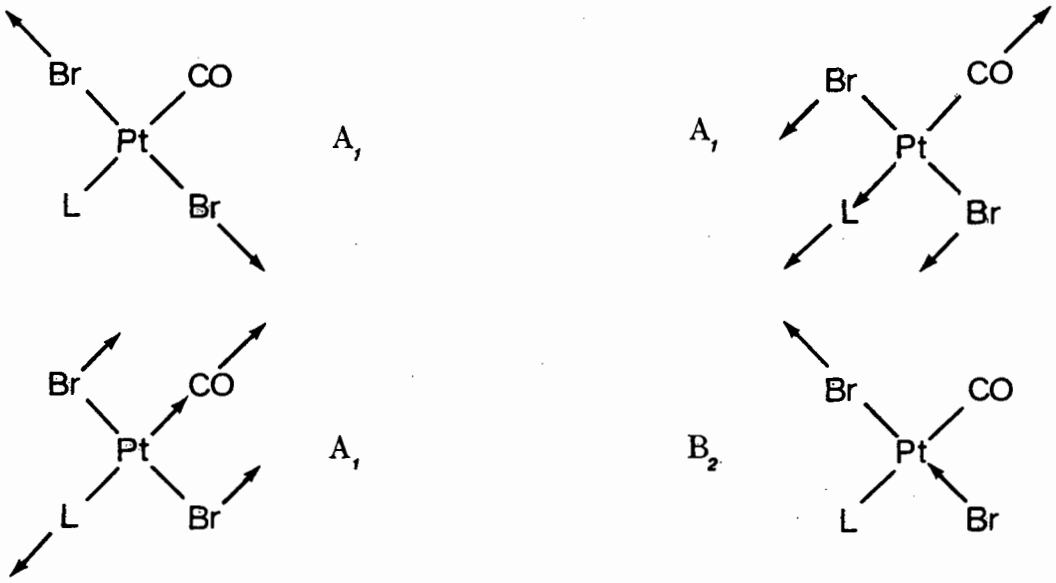

Stretches

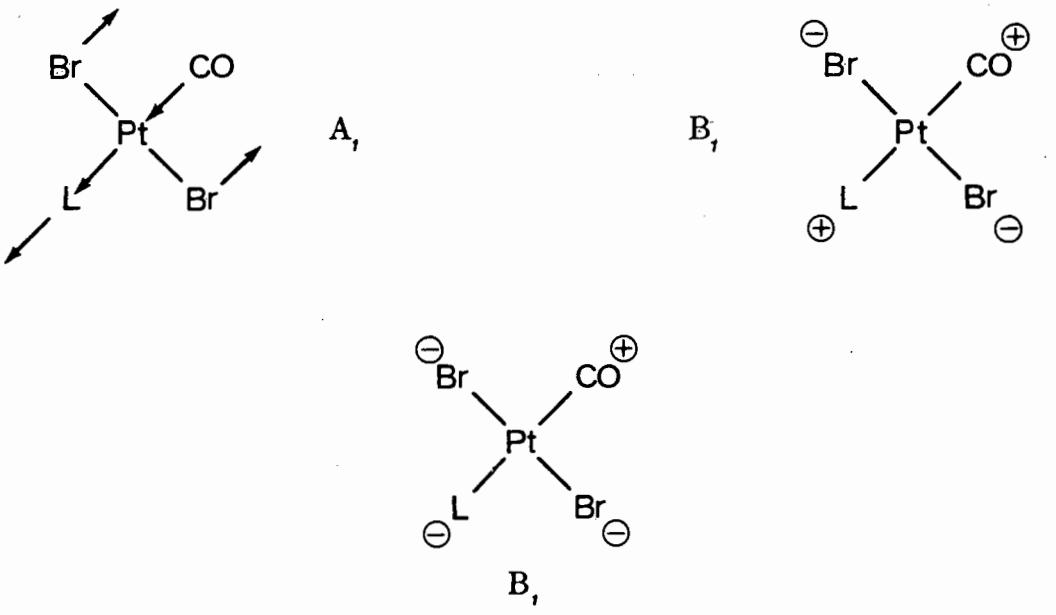

Bends

Fig. 1.2 Stretches and bends of *trans*-[$PtBr_2(CO)(L)$]

different representation (*e.g.* between the A_1 stretch and the B_2 stretch in *trans*-[$PtX_2(CO)L$]) is symmetry forbidden since these are orthogonal representations. Secondly, although symmetry does not allow for the separation of two or more vibrations of the same irreducible representations, there is usually a large frequency difference between stretching and bending modes as a result of the different energies of their force constants. Coupling may only be expected between vibrations of the same irreducible representation if there is not a significant energy difference between them. Therefore interaction between a symmetric A_1 stretch and the symmetric A_1 bend in *trans*-[$PtX_2(CO)L$] is not expected, although it is symmetry allowed.

The discussion so far applies only when one considers the molecule to be an isolated unit [1-3]. Strictly, this only occurs in the gaseous phase where the vibrations of the molecule are restricted by its own intrinsic point symmetry. In the solid state the molecule is subject to symmetry restrictions arising out of its crystalline environment. Any rigorous vibrational analysis would need to consider the entire array of molecules, a task that, for all practical purposes, is impossible. Two approximations, site group and factor group analysis, can however be used. For both approximations, a full x-ray crystal structure with atomic coordinates is necessary.

1.2 Site Group Analysis

The site group approximation [5] assumes that the interactions between one molecule and its neighbouring molecules may be ignored. That is, the only relevant property of the surroundings is its symmetry as seen by the molecule occupying a site within it.

Determination of site symmetry is subject to two conditions, (i) the site

group must be a subgroup of both the space group of the crystal and the point group of the isolated molecule, and (ii) the number of equivalent sites must be equal to the number of molecules in the unit cell. If the space group, the point group and the number of molecules per unit cell are known, the site group may be determined from Halford's Tables [5] listing possible site symmetries.

In general, the site symmetry is lower than the molecular symmetry. On grounds of a change in selection rules, vibrations forbidden by molecular symmetry may appear as weak bands if allowed by site symmetry. Low site symmetry may also result in the splitting of molecular symmetry degeneracies. However, the degree to which the vibrational spectrum of a molecule in a site of low symmetry will deviate *observably* from the behaviour of the free molecule depends on just how strongly the molecule interacts with its surroundings.

1.3 Factor Group Analysis

Factor group analysis [6], being the more rigorous approximation, considers the interaction of one molecule in the unit cell with another. That is, the entire set of molecules in the unit cell is regarded as the vibrating unit and so is subject to symmetry restrictions of the space group. Factor group analysis accounts for lattice modes and solid state splitting of non-degenerate vibrations of the free molecule (or correlation field splitting).

Correlation field splitting depends on dipole-dipole interactions, which vary inversely with the cube of the dipole-dipole separation [1]. Therefore factor group analysis is applicable mainly to neutral molecules with highly dipole-active oscillators. For polyatomic ions, which are separated from

each other by intervening counterions, the correlation field splitting is negligible [1,3,6] and these are suitably described by site group analysis.

The above discussion serves as an illustration of the application of group theory to assisting vibrational assignments. The vibrational spectrum of a metal complex may be understood by considering the molecular symmetry, with possible activation of the molecular symmetry forbidden vibrations through the lowering of symmetry by site symmetry or space group symmetry.

The assignment task may, however, be simplified for, while the vibrations of the molecule can be classified on the basis of overall molecular symmetry, more information on the position and intensity of the bands is obtained by the application of the local symmetry perturbed by the molecular environment. The bands forbidden by local symmetry will only give rise to weak bands if they are allowed by overall molecular symmetry. Those bands which arise from a common origin in the localised symmetry may not be separately resolved [7,8]. This principle was in effect adopted in the discussion of *trans*-$[PtX_2(CO)L]$ above, where the ligands CO and L were considered point masses. In this manner, the local symmetry of the ligands and local symmetry of the metal-ligand nucleus may be considered separately to build up an understanding of the overall molecular symmetry.

This is more suitably illustrated by the example of the complexes $[M(II)(pyO)_6]$ $(ClO_4)_2$ which have space group $R\bar{3}$, with the cation having S_6 point group symmetry [9,10]. This allows for the calculation of the metal-oxygen vibrations based on local symmetry S_6 [11-13]. The metal-oxygen stretches have even been considered in terms of the lower symmetry O_h [11]. The ligand vibrations may be assigned using C_{2v} localised symmetry [14]. The vibrational assignments for $[M(II)(pyO)_6]$ $(ClO_4)_2$ have thus been proposed on

the basis of the metal nucleus [11-13] and on the ligands [15-17].

In order to identify the metal-ligand vibrations several techniques may be applied.

2. TECHNIQUES APPLIED TO THE ASSIGNMENT PROBLEM

2.1 Comparison between the Spectra of the Free Ligand and the Complex ('empirical' method)

Based on the above considerations, comparison between the spectra of the free ligand and the complex yields the metal-ligand vibrations.

Adoption of this simplistic method is limited by possible activation of some ligand vibrations, forbidden by the molecular structure of the free ligands, but allowed by the molecular symmetry of the complex. These may occur in the same region as the metal-ligand vibrations [1] and may result in incorrect assignments. As discussed above, the bands activated by lowering of symmetry are expected to be weak, unless they result from the removal of degeneracy.

A further difficulty may rise where the localised ligand symmetry is different to the free ligand molecular symmetry, as seen for $[M(II)(bipy)_3](ClO_4)_2$. The free ligand has molecular symmetry C_{2h}, being *trans*-coplanar in the solid [18]. The complex has overall molecular symmetry D_3 [19,20], in which the 2,2'-bipyridine ligands are cisoid, non-planar, with the two pyridyl rings twisted 6-12° with respect to each other. This lower C_2, localised symmetry for the dipyridyl moiety results in the activation of some ligand vibrations, forbidden by C_{2h} symmetry.

Clearly an understanding of the behaviour of the ligand modes of vibration is advantageous to establish which of the new bands in the spectrum are likely to be activated ligand bands.

2.2 Comparison between Spectra of Isostructural Complexes

On the basis of symmetry considerations isostructural complexes should give rise to similar vibrational spectra, the actual position of the bands being determined by any difference in the nature of the bonding. There are a number of variations that might be applied.

2.2.1 For isostructural complexes of identical ligands with differing metals or differing oxidation states, the metal-ligand vibrations follow the order of Crystal Field Stabilization Energies of the metal ions [21,22].

2.2.2 For isostructural complexes of a particular metal with a range of similar ligands, the metal-ligand bands should be found within a small frequency range since the nature of the bonding should be similar. If there is some measure of the chemical similarity of such a set of ligands, the resultant correlation with the degree of variation expected by the metal-ligand bands may aid their assignment. Use of the Hammett substituent parameter, σ, as an index of the electronic effects of the substituent, R, can be so employed [23-25].

2.2.3 For isostructural complexes containing coordinated halogens, the large change in the masses of the halogen ligand yields dramatic shifts of the metal-halogen vibrations. This allows for their easy identification [26,27].

2.3 Isotopic Labelling

Replacement of an atom by one of its isotopes results in a change in frequency in those vibrations that involve the particular species. The expected isotopic shifts can be calculated, to a reasonable approximation, by assuming the labelled atom to be a part of a *simple harmonic diatomic* molecule [28]. The vibrational frequency of such a system is represented by the equation:

$$\nu = \frac{1}{2\pi c}\left[\frac{f}{\mu}\right]^{\frac{1}{2}}$$

while that for the isotopically labelled system is given by:

$$\nu = \frac{1}{2\pi c}\left[\frac{f}{\mu^{i}}\right]^{\frac{1}{2}}$$

where ν = the vibrational frequency,

f = the harmonic force constant,

π = the reduced mass of the molecule,

c = the velocity of light,

and superscript i refers to the labelled system.

Assuming the force constants are unaltered by isotopic substitution, the expected isotopic shifts may be calculated from:

$$\frac{\nu^{i}}{\nu} = \left[\frac{\mu}{\mu^{i}}\right]^{\frac{1}{2}}$$

where ν^{i} is always taken to be the *heavier* isotopomer [28].

This ratio, although based on harmonic diatomic molecules, is a very good approximation for real, anharmonic molecules, if their anharmonicity is not appreciable and it changes only moderately with isotopic labelling [28]. For polyatomic molecules, the R-X stretching fundamentals may behave as independent oscillators, isolated from the rest of the polyatomic vibration, so allowing application of the ratio. This is true where X has a low atomic weight (less than 25 a.m.u.) or where the R-X bond is strong [28,29]. For the R-X bending fundamentals, the ratio only holds if the kinetic energy of these vibrations is localised predominantly to one fundamental. This requirement is less common for polyatomic molecules [28,29].

The ν^i/ν ratio is therefore useful in determining the expected frequency shifts on isotopic labelling, subject to the conditions above, namely, the number and nature of the atoms in the molecule that have been labelled, the extent to which the labelled atom participates in a particular vibration and the extent of couplings or of hydrogen bonding. Ideally, if the isotopically substituted atom is the metal or the ligand donor atom, then the metal-ligand vibration may be assigned unambiguously.

2.3.1 For metal isotopic labelling, several metal isotopes are commercially available [30]. Since the magnitude of the isotopic shift is dependent on the mass difference between the isotopes, isotopic pairs with the greatest mass difference are preferred. The metal isotope pairs $^{57}Fe/^{54}Fe$, $^{62}Ni/^{58}Ni$, $^{68}Zn/^{64}Zn$ and $^{53}Cr/^{50}Cr$ have been successfully employed to aid vibrational assignments [30-33]. It has been found, however, that metal isotopic labelling is not effective for the assignment of the metal-ligand bending vibrations. The reasons for this have been attributed to the small difference between the masses of the metal isotopes as well as to the weakness of the metal-ligand bond [30]. However, since these factors should affect the

metal-ligand stretching in the same manner, the failure of the simple harmonic diatomic molecule approximation for bending fundamentals (discussed above) would possibly be a better explanation. Other limiting factors towards the use of this technique are that pure and stable metal isotopes are available only for certain elements, observed shifts are too small for heavy elements such as Os, Pt and Pb, and some metal isotopes are too expensive for even milligram scale synthesis [30].

2.3.2 In ligand isotopic labelling, specific labelling of the ligand atom allows assignment of the metal-ligand vibrations, including the bending modes. The most frequently applied ligand donor isotopes are ^{18}O and ^{15}N [28]. However, since the metal-ligand vibration may also be described by considering the ligand as a point mass vibrating against the rest of the molecule [17,34,35], other isotopes which effect a larger mass difference than $^{15}N/^{14}N$ and $^{18}O/^{16}O$ - thereby increasing the metal-ligand shifts - may be employed. Deuteration gives the largest mass difference and is often used to label the atom α to the ligand donor atom as well as atoms further removed [36,37].

Labelling of the ligands is advantageous in identifying any low frequency internal ligand vibrations, since these usually reflect larger shifts than the metal-ligand vibrations. Further, by multiple isotopic labelling [38-40] a complete understanding of the vibrational purity of the fundamentals, (*i.e.* the degree of coupling) of both the metal-ligand and the internal ligand vibrations can be ascertained. Other advantages of labelling the ligand are the availability of many isotopic pairs yielding large mass difference ratios, and the ready availability and relatively reasonable price of a variety of common labelled ligands.

The disadvantage of ligand isotopic labelling lies principally in the possibility of incorrectly assigning a ligand vibration that is only slightly sensitive to the isotope, to a metal-ligand vibration. Other potential problems are inability to label the preferred atom due to synthetic difficulties and the change in symmetry which may occur on partial isotopic labelling. This could activate some previously forbidden modes making assignments complicated (although this may also be used to aid the assignment problem [29]).

2.4 The ν^D/ν^H Ratio

Since deuteration results in the largest isotopic shifts and is generally the most accessible type of labelling, most labelling studies have employed this isotope [28]. Based on the simple harmonic diatomic equation discussed above, work by THORNTON and his co-workers [41,42] have established ν^D/ν^H ratios for aromatic and heterocyclic ligand systems. They found that ν^D/ν^H for the ring (skeletal) modes of vibration falls within the range 0,85 to 1,00, while for C-H modes, the range 0,68 to 0,85 is observed.

The ranges of the ν^D/ν^H ratios gives an indication of the degree of coupling between the vibrations. The skeletal ratio will be lowered from unity by a slight participation of a C-H vibration through coupling. This introduces a degree of deuterium-sensitive potential energy into the otherwise insensitive skeletal vibration [43]. Similarly, the C-H ratio is raised from its theoretical value of 0,73 by the participation of the potential energy of the insensitive skeletal vibration in the C-H vibration. Values less than 0,73 may indicate a change in the nature of coupling as a result of the labelling. This could arise from the greater displacement experienced by carbon atoms attached to deuterium, than that for carbons attached to

hydrogen [43,44].

The main criticism with the use of the ν^D/ν^H ratio is that, being based on a simple harmonic diatomic model, it is over simplistic. Yet it proves extremely helpful in identifying vibrational modes in which the absolute molecular structure is not necessarily known, preventing the application of more rigorous methods.

2.5 The Teller-Redlich Product Rule

Based on the equation to describe a simple harmonic non-linear polyatomic molecule, TELLER and REDLICH independently developed a rule for any pair of isotopic molecules. This states that since the force fields of isotopic molecules are practically identical, the product of the harmonic frequency ratios for normal vibrations belonging to any one symmetry species depends only upon the masses of their constituent atoms and their geometrical structure [28]. Hence:

$$\frac{\nu_1^i}{\nu_1} \cdot \frac{\nu_2^i}{\nu_2} \cdots \frac{\nu_f^i}{\nu_f} = \sqrt{\left[\frac{m_1}{m_1^i}\right]^{\alpha} \left[\frac{m_2}{m_2^i}\right]^{\beta} \cdots \left[\frac{M^i}{M}\right]^{t} \left[\frac{I_x^i}{I_x}\right]^{\delta x} \left[\frac{I_y^i}{I_y}\right]^{\delta y} \left[\frac{I_z^i}{I_z}\right]^{\delta z}}$$

where $\nu_1^i, \nu_2^i .. \nu_f^i$ = the harmonic frequencies of all the f normal vibrations of a given species,

$m_1, m_2 ..$ = the atomic masses of each of the various existing sets of identical nuclei (*i.e.* reproduced by the allowed symmetry operations),

$\alpha, \beta ..$ = the number of normal vibrations (including non-genuine ones) contributed by each of these sets

of species in question (found in character tables),

M = molecular weight,

t = the number of translations which belong to the species considered,

I_x, I_y, I_z = the molecular moments of inertia about the x-, y- and z-axes, passing through the center of mass,

and superscript i refers to the labelled system and where δx, δy and $\delta z = 1$ only when a rotation about the x-, y-, or z-axis belongs to this species. Otherwise they equal zero. In this calculation a degenerate vibration is counted once only.

This is a more precise definition than is the ν^D/ν^H ratio, and as such can be used to predict more precisely to which frequency a mode of vibration is expected to move on isotopic labelling. Alternatively, it may be used as a measure of correctness of the overall vibrational assignment by comparing the observed ratio for each symmetry species with the theoretical one.

The disadvantage of the Product Rule is that the molecular dimensions need to be known to determine the moments of inertia.

2.6 Normal Coordinate Analysis

The final test of a vibrational assignment would be to attempt to model the molecule by normal coordinate analysis, which may lead to the reassignment of a number of the fundamental vibrations. As seen above the vibrational frequencies are determined by molecular geometry, atomic masses and the nature of the force field providing the restoring forces during the vibra-

tion (the force constant). This force field is characteristic of the electron density within the molecule and calculation of it can give an understanding of the bonding within the molecule.

Normal coordinate treatment by WILSON's *GF* matrix method [45,46] derives a solution of the vibrational problem in terms of the matrix equation:

$$|GF - E\lambda| = 0$$

where F = the potential energy matrix involving normal coordinates and potential force constants,

G = the kinetic energy matrix, calculated from the geometry and atomic masses of the molecule,

E = the unit matrix,

λ = the frequency parameter $(4\pi^2 c^2 \omega^2)$.

Solutions to the equation are expressed in terms of Potential Energy Distribution and may also be used to give Cartesian displacement diagrams. However when the matrix is expanded there are many more terms involving the force constant than there are vibrational frequencies. So to arrive at a possible solution, the model must be set up to ignore some of the interactions between atoms on the grounds that they are expected to be less important than the terms included [1,2,30,46,47]. The two most commonly used methods in transition metal vibration analysis are various modifications of the Valence Force Field (VFF) and the Urey-Bradley Force Field (UBFF).

2.6.1 The basic VFF assumption is that there is no interaction between the bending and stretching motions in the molecule (*i.e.* the off-diagonal elements in the *GF* matrix are zero) [29,45-47]. As this assumption has been

shown to be incorrect for generalised calculations, the application of the VFF requires some of the off-diagonal elements to be non-zero, the number of such terms being determined by the experimental frequencies available. Unfortunately, the choice of which terms are non-zero is generally not justified on theoretical grounds [46].

2.6.2 The UBFF combines the assumption that the off diagonal elements are zero with the postulate that there are also important interactions between the non-bonded atoms [29,45-47]. The simple model thus contains interaction terms in the form of repulsive constants. However, adjusting force constants to fit the observed frequencies is made difficult by ignorance of the interactions between non-neighbouring stretching vibrations. These require non-Urey-Bradley force constants to be introduced, such as the Kekulé constant, ρ, in aromatic systems [48,49], and the torsional out-of-plane bending and internal torsional interactions of SHIMANOUCHI [50,51]. The number of such extra terms is determined by the number of experimental frequencies.

Each approach to the vibrational analysis problem is held by their proponents to be superior to the other in various ways, yet they do lead to comparable results with very little difference between the Cartesian displacements produced by the two methods [52]. This indicates that the normal coordinates of either model is a good first order approximation of the true forms of vibration. However, the bending and interaction force constants differ greatly, requiring caution in their interpretation and in their transference to similar systems [52].

While a good fit between the calculated and experimental data might be considered the conclusive proof of a vibrational assignment, the difficulty in evaluating the force constants used in the modelling of a molecule may be

demonstrated by two normal coordinate analyses of acetylacetonate conducted by NAKAMOTO and his co-workers. In their earlier work NAKAMOTO and MARTELL [53] used a simple UBFF calculation, while in their later work NAKAMOTO and BENKE [54] used a modified UBFF calculation. As seen from Table 1.1 below,

1960 Calculation [53]		1967 Calculation [54]	
Assignment	Frequency	Frequency	Assignment
C ⋯ C assym. stretch (B_2)	1580cm^{-1}	1563cm^{-1}	C ⋯ O sym. stretch (A_1)
C ⋯ O sym. stretch (A_1)	1554cm^{-1}	1538cm^{-1}	C ⋯ O assym. stretch (B_2)
C ⋯ O assym. stretch (B_2)	1534cm^{-1}	1429cm^{-1}	C – CH_3 deg. def.
C – CH_3 deg. def.	1415cm^{-1}	1380cm^{-1}	C ⋯ O assym. stretch (B_2)
C ⋯ C sym. stretch (A_1)	1274cm^{-1}	1288cm^{-1}	C ⋯ C sym. stretch (A_1)

Differences between the calculations

1) The band assignments for the C ⋯ O and C ⋯ C stretches above 1500cm^{-1} are interchanged.

2) The band assignments for the C – CH_3 degenerate deformation and the lower C ⋯ O stretch are interchanged.

Table 1.1 Normal coordinate analyses of acetylacetonate

both models originally gave a satisfactory comparison with the experimental data, yet their conclusions are contradictory. The 1960 normal coordinate calculation was disproved by ^{18}O-labelling of a metal acetylacetonate [56] which showed that the higher frequency component of the doublet absorption in the carbonyl region was far more sensitive to ^{18}O-labelling than the lower frequency component. This suggests that the former is predominently νC ⋯ O and the latter is predominently νC ⋯ C. Indeed, it was this finding which led to the revision of the normal coordinate anaylsis in 1967, and which again displays the importance of isotopic labelling of the ligand.

Clearly, since the solution to any calculation is dependent upon the method by which the force field is constructed, the ultimate criterion is 'what is

a good fit?' It does appear in general that, the higher the complexity of the molecule being spectroscopically examined, the more important do experimental rather than theoretical techniques become [56].

In conclusion, it should be emphasised that of the several techniques available that aid the correct assignment of the metal-ligand vibrations, no one technique is the golden key which alone unlocks the puzzle. Each method has its strengths and its weaknesses. The assignment problem can only be truly solved by weighing up the information produced by *all* the techniques. The more information that is available, the more correct the final assignment should be. This is the principle employed in this present work. For although (as the title indicates) the work is predominently directed to ligand isotopic studies, the conclusions reached in the vibrational assignments are equally dependent on information derived by other techniques.

REFERENCES

1. K. NAKAMOTO,
Infrared and Raman spectra of Inorganic and Coordination Compounds, 3rd Ed., (1978) Wiley-Interscience, New York.

2. P. GANS,
Vibrating Molecules: Introduction to the Interpretation of Infrared and Raman Spectroscopy, (1975) Chapman and Hall, London.

3. F.A. COTTON,
Chemical Application of Group Theory, 2nd Ed., (1971) Wiley-Interscience, New York.

4. N.B. COLTHUP, L.H. DALY and S.E. WIBERLEY,
Introduction to Infrared and Raman Spectroscopy, (1964) Academic Press, New York.

5. R.S. HALFORD,
J. Chem. Phys., *14* (1946) 8.

6. D.M. ADAMS,
Coord. Chem. Rev., *10* (1973) 183.

7. R.D. GILLARD, H.G. SILVER and J.L. WOOD,
Spectrochim. Acta, *20* (1964) 63.

8. O. POIZAT and C. SOURISSEAU,
J. Phys. Chem., *88* (1984) 3007.

9. T.J. BERGENDAHL and J.S. WOOD,
Inorg. Chem., *14* (1975) 338.

10. D. TAYLOR,
Aust. J. Chem., *31* (1978) 713.

11. A.D. VAN INGEN SCHENAU, W.L. GROENEVELD and J. REEDIJK,
Spectrochim. Acta, *30A* (1974) 213.

12. A.D. VAN INGEN SCHENAU, C. ROMERS, D. KNETSCH and W.L. GROENEVELD,
Spectrochim. Acta, *33A* (1977) 859.

13. A.M. GREENAWAY, C.J. O'CONNOR, E. SINN and J.R. FERRARO,
Spectrochim. Acta, *37A* (1981) 575.

14. A. GAMBI and S. GHERSETTI,
Spectrosc. Letters, *8* (1977) 627.

15. Y. KAKIUTI, S. KIDA and J.V. QUAGLIANO,
Spectrochim. Acta, *19* (1963) 201.

16. S. KIDA, J.V. QUAGLIANO, J.A. WALMSLEY and S.Y. TYREE,
Spectrochim. Acta, *19* (1963) 189.

17. A.T. HUTTON and D.A. THORNTON,
J. Mol. Struct., *39* (1977) 33.

18. L.L. MERRITT and E.D. SCHROEDER,
Acta Crystallogr., 9 (1956) 801.

19. O.P. ANDERSON,
J. Chem. Soc. Dalton, (1972) 2597.

20. A. WADA, N. SAKABE and J. TANAKA,
Acta Crystallogr., B 32 (1976) 1121.

21. J.M. HAIGH, R.D. HANCOCK, L.G. HULETT and D.A. THORNTON,
J. Mol. Struct., 4 (1969) 369.

22. D.A. THORNTON,
Coord. Chem. Rev., 55 (1984) 113.

23. J.M. HAIGH, N.P. SLABBERT and D.A. THORNTON,
J. Mol. Struct., 7 (1971) 199.

24. T.P.E. AUF DER HEYDE, G.A. FOULDS, D.A. THORNTON and G.M. WATKINS,
Spectrosc. Letters, 14 (1981) 455.

25. R. WHYMAN, W.E. HATFIELD and J.S. PASCHAL,
Inorg. Chim. Acta, 1 (1967) 113.

26. G.A. FOULDS and D.A. THORNTON,
Spectrochim. Acta, 37A (1981) 917.

27. T.P.E. AUF DER HEYDE, G.A. FOULDS, D.A. THORNTON and G.M. WATKINS,
J. Mol. Struct., 77 (1981) 19.

28. S. PINCHAS and I. LAULICHT,
Infrared Spectra of Labelled Compounds, (1971) Academic Press, London.

29. G. VARSÁNYI and S. SZÖKE,
Vibrational Spectra of Benzene Derivatives, (1969) Academic Press, New York.

30. K. NAKAMOTO,
Angew. Chem. (Int. ed.), 11 (1972) 666.

31. Y. SAITO, J. TAKEMOTO, B. HUTCHINSON and K. NAKAMOTO,
Inorg. Chem., 11 (1972) 2003.

32. B. HUTCHINSON, J. TAKEMOTO and K. NAKAMOTO,
J. Amer. Chem. Soc., 92 (1970) 3335.

33. M.L. NIVEN and D.A. THORNTON,
Spectrosc. Letters, 13 (1980) 419.

34. A. MULLER, K.H. SCHMIDT and G. VANDRISH,
Spectrochim. Acta, 30A (1974) 651.

35. P.F.M. VERHOEVEN,
PhD Thesis, (1984) University of Cape Town.

36. A.T. HUTTON and D.A. THORNTON,
Spectrochim. Acta, 34A (1978) 645.

37. T.P.E. AUF DER HEYDE, C.S. GREEN, D.E. NEEDHAM, D.A. THORNTON and G.M. WATKINS,
J. Mol. Struct., 70 (1981) 121.

38. G.A. FOULDS, G.C. PERCY and D.A. THORNTON,
Spectrochim. Acta, 34A (1978) 1231.

39. M.L. NIVEN and D.A. THORNTON,
Inorg. Chim. Acta, 32 (1979) 205.

40. J.B. HODGSON, G.C. PERCY and D.A. THORNTON,
Transition Met. Chem., 4 (1979) 218.

41. G.A. FOULDS, J.B. HODGSON, A.T. HUTTON, M.L. NIVEN, G.C. PERCY, P.E. RUTHERFORD and D.A. THORNTON,
Spectrosc. Letters, 12 (1979) 25.

42. J.B. HODGSON, G.C. PERCY and D.A. THORNTON,
J. Mol. Struct., 66 (1980) 75.

43. J.R. SCHERER,
Spectrochim. Acta, 24A (1968) 747.

44. Y. KAKIUTI, H. SAITO and T. YOKOYAMA,
J. Mol. Spectrosc., 32 (1969) 247.

45. E.B. WILSON, J.C. DECIUS and P.C. CROSS,
Molecular Vibrations, (1955) McGraw Hill, New York.

46. I.M. MILLS,
"Calculation of Force Constrants" in *Infrared Spectra and Molecular Structure,* (1963) M. Davies (Ed.), Elsevier, Amsterdam.

47. I.M. MILLS,
"Harmonic Force Field Calculations" in *Critical Evaluation of Chemical and Physical Structural Information,* (1974) D.R. Lide and M.A. Paul (Eds.), National Academy of Science, Washington.

48. J.R. SCHERER and J. OVEREND,
Spectrochim. Acta, 17 (1961) 719.

49. G. ZERBI, B. CRAWFORD and J. OVEREND,
J. Chem. Phys., 38 (1963) 127.

50. T. SHIMANOUCHI,
Pure Appl. Chem., 7 (1963) 131.

51. M. MIKAMI, I. NAKAGAWA and T. SHIMANOUCHI,
Spectrochim. Acta, 23A (1967) 1037.

52. J.R. SCHERER,
Spectrochim. Acta, 20 (1964) 345.

53. K. NAKAMOTO and A.E. MARTELL,
J. Chem. Phys., 32 (1960) 588.

54. G.T. BEHNKE and K. NAKAMOTO,
Inorg. Chem., 3 (1967) 433.

55. G. ZERBI and S. SANDRONI,
Spectrochim. Acta, 26A (1970) 1951

56. S. PINCHAS, B.L. SILVER and I. LAULICHT,
J. Chem. Phys., 46 (1967) 1506.

57. S. CALIFANO,
Pure Appl. Chem., 18 (1969) 353.

CHAPTER 2

EXPERIMENTAL

1 PHYSICAL METHODS

1.1 Infrared Spectra

The infrared spectra were recorded on a Perkin Elmer model 983 spectrophotometer using both Nujol mulls (2000 to 200cm^{-1}) and hexachlorobutadiene mulls (4000 to 2000cm^{-1} and 1500 to 1200cm^{-1}), between caesium iodide or KRS 5 [Tl (Br,I)] plates. The far-infrared spectra were recorded as Nujol mulls (500 to 50cm^{-1}) between polyethylene plates on a Digilab FTS 16B/D interferometer.

The mull technique was adopted in preference to the pellet die technique because of the probability that these aromatic *N*-oxides and their complexes will yield undesirable reactions with the matrix [1], or may undergo molecular rearrangements brought about by the effect of pressure [2].

The model 983 spectrophotometer is a double-beam, ratio-recording instrument with pre-sample chopping, and has integral data handling as well as digital display facilities. The optics are a purgable F 4.2 monochromator with four gratings and nine fitters. The quoted wave number accuracy is ± 2cm^{-1} over the range 4000 to 2000cm^{-1} and ± 1cm^{-1} over the range 2000 to 180^{-1}, with a reproducibility of better than 0,1cm^{-1}. A resolution of 0,5cm^{-1} is obtainable using the highest scan mode [3].

The FTS 16B/D is an automatic ratio recording, far-infrared vacuum interferometer with a resolution of 0,5cm^{-1} throughout the spectral range 500 to 10cm^{-1}. The instrument consists of a model 296A Michelson interferometer, four interchangeable Mylar beam splitters, a high pressure mercury arc source, stored ratio optics and a remotely controlled sample carriage, a triglycine

sulphate detector, an analog-to-digital converter, a data system with 8K of core memory, a 1,2 million word moving disc head, a digitally controlled plotter and related hard- and software [4].

1.2 Raman spectra

The Raman spectra of the solid compounds were determined by employing a spinning cell to reduce burning of the sample. These spectra were recorded on a Coderg PHO instrument using a Spectra Physics Model 164 Ar^+-laser for excitation and the 488.0 nm line with interference fitters to remove plasma lines. Laser powers were kept at about 100mW over the range 1800 to 20cm^{-1} and at about 200mW (with one exception) over the range 3100 to 2800cm^{-1} (or 2400 to 2000cm^{-1} for the deuterated samples). For pyrazine-d_4 *N,N'*-dioxide the laser power was kept at 50mW over the range 2400 to 2000cm^{-1} to reduce burning. The spectra were recorded over separate regions to overcome the increasing background resulting from fluorescence.*

1.3 ^{1}H-Nuclear magnetic resonance spectra

The ^{1}H-nmr spectra were recorded at 90MHz on a Bruker WH-90D/S Fourier transform spectrometer. Deuterated water and chloroform were used as solvents and locks, depending upon solubility, while tetramethylsilane (TMS) was used as the reference. Spectra were recorded at operating temperature (ambient = 298K) unless otherwise stated.

---

* Fluorescence is frequently observed in Raman spectroscopy of organic materials, particularly where an aromatic ring is substituted (or fused to another ring) and is due to impurities which may 'burn up' after prolonged exposure to the laser beam [5]. While some workers find less fluorescence employing an Ar^+ laser, others find more [6].

1.4 Mass Spectra

Mass spectra were obtained on a VG Micromass 16F mass spectrometer operating in the electron impact mode, with an electron beam energy of 70eV and ion accelerating voltage of 4kV, and with an ion source temperature in the range 180 to 210°C.

1.5 Microanalyses

Microanalyses were performed by Mr. W.R.T. Hemsted, Department of Organic Chemistry, University of Cape Town, on a Heraeus universal combustion analyser model CHN-MICRO.

2 PREPARATION OF THE LIGANDS

		Experimental			Calculated		
	Colour	%C	%H	%N	%C	%H	%N
pzO_2	white	42,85	3,65	25,00	42,86	3,60	24,99
pz-d_4O_2	white	41,50	3,50	24,10	41,37	3,47	24,12
pzO	white	50,10	4,20	29,05	50,00	4,20	29,15
pz-d_4O	white	48,20	4,10	27,80	47,99	4,03	27,98
$bipyO_2$	white	63,70	4,40	14,85	63,82	4,28	14,89
bipy-d_8O_2	white	61,05	4,15	14,30	61,20	4,11	14,27
quinO·$2H_2O$	tan	59,75	6,00	7,90	59,66	6,07	7,73
quin-d_7O·$2H_2O$	tan	57,65	5,80	7,50	57,42	5,89	7,44

Table 2.1 Microanalyses of the ligands

All deuterated starting materials were purchased from Merk, Sharp and Dohme (Canada) Ltd.

2.1 Pyrazine *N,N'*-dioxide (pzO_2)

Pyrazine *N,N'*-dioxide was prepared by the method of KOELSCH and GUMPRECHT [7].

To 2,0g pyrazine (25 mmole) was added 15ml glacial acetic acid (250 mmole) and 3,40ml 50% H_2O_2 (50 mmole). The solution was heated to 95°C for four hours. A further 3,40ml 50% H_2O_2 was added (total ratio 4:1 H_2O_2:pyrazine) and heating continued for an additional 20 hours. After cooling, the volume was reduced to one third, upon which the pyrazine *N,N'*-dioxide was removed by filtration. A second crop was obtained by neutralising the fitrate with Na_2CO_3 and extracting with chloroform. The pyrazine *N,N'*-dioxide was purified by sublimation *in vacuo* (110-115°C/0,5mmHg), after removing any mono *N*-oxide impurity collected at lower temperatures. Yield: 2,17g (78%).

This compound was characterised by ^1H nmr; singlet at 8.46ppm(D_2O), and by melting point:sublimes 240°C, melts (with partial decomposition) 300-302°C. Purity was established by microanalysis (Table 2.1) and by mass spectrometry (Appendix 1).

There is some dispute in the literature as to the melting point of pyrazine-*N,N'*-dioxide. KOELSCH and GUMPRECHT [7] originally reported a melting point of 285-295°C. On the other hand, KLEIN and BERKOWITZ [8] reported a decomposition temperature of 300°C, while POPP and GARLOUGH [9] report a much lower decomposition temperature of 250°C. SZÖKE *et al.* [10] recognised that the compound sublimes, but equate the sublimation point with the melting point figures originally quoted by KOELSCH and GUMPRECHT.

2.2 Pyrazine-d_4 *N,N'*-dioxide (pz-d_4O_2)

To 0,5g pyrazine-d_4 (6 mmole, 99% isotopic purity) was added 3,50ml glacial acetic acid (59 mmole) and 0,80ml 50% H_2O_2 (11,8 mmole). The solution was heated to 95° for 3 hours. A further 0,82ml 50% H_2O_2 (12 mmole) was added and heating continued for another 20 hours. After cooling, the solution was poured into 20ml absolute ethanol, to form a white precipitate. This was removed by filtration and washed well with absolute ethanol and dried under reduced pressure over silica gel. A second crop was obtained from the filtrate by reducing to one third of its original volume, neutralising with Na_2CO_3 and extracting with chloroform. The pyrazine-d_4 *N,N'*-dioxide was purified by sublimation (115-120°/0,5mmHg), after removing any mono *N*-oxide impurity collected at lower temperatures. Yield: 0,47g (69%).

The compound was characterised by melting point: sublimes 245°C, decomposes >350°C. Purity was established by microanalysis (Table 2.1) and by mass spectrometry (Appendix 1).

2.3 Pyrazine *N*-oxide (pzO)

Pyrazine *N*-oxide was prepared by the method of KOELSCH and GUMPRECHT [7].

To 2,0g pyrazine (25 mmole) was added 7,5ml glacial acetic acid (125 mmole) and 1,70ml 50% H_2O_2 (25 mmole). The solution was heated to 70°C for 3 hours. A further 1,70ml 50% H_2O_2 (total ratio 2:1 H_2O_2:pyrazine) was added and heating continued for an additional 5 hours. The solution was cooled and the volume reduced to one third. After neutralising with Na_2CO_3, the pyrazine *N*-oxide was extracted into chloroform. After evaporation, the crude product was purified by sublimation *in vacuo* (50-60°C/0,5mmHg).. Yield: 1,70g (71%).

The compound was characterised by ^1H nmr (D_2O); doublet 8.44ppm (2H), doub-

let 8.11ppm (2H), $J_{2,3}$ = 4Hz [11], and by melting point: sublimes 85°C, melts 112-113°C. Purity was established by microanalysis (Table 2.1) and by mass spectrometry (Appendix 1).

Again, there is some question in the literature as to the correct melting point of this compound. KOELSCH and GUMPRECHT [7] report it to be 113-115°C, while KLEIN and BERKOWOTZ [8] reported 104°C.

2.4 Pyrazine-d_4 *N*-oxide (pz-d_4O)

To 1,0g pyrazine-d_4 (12 mmole, 99% isotopic purity) was added 3,5ml glacial acetic acid (58 mmole) and 0,80ml 50% H_2O_2 (11,9 mmole). The solution was heated to 70°C for 3 hours. A further 0,82ml 50% H_2O_2 (12 mmole) was added and heating continued for another 5 hours. After cooling, the volume was reduced to one third and the solution neutralised with Na_2CO_3 and extracted with chloroform. The pyrazine-d_4 *N*-oxide was purified by sublimation *in vacuo* (60-70°C/0,5mmHg). Yield: 0,81g (68%).

The compound was characterised by melting point: sublimes 83°C, melts 110-112°C. Purity was established by microanalysis (Table 2.1) and by mass spectrometry (Appendix 1).

2.5 2,2'-Bipyridine *N,N'*-dioxide (bipyO_2)

2,2'-bipyridine *N,N'*-dioxide was prepared by the method of SIMPSON *et al.* [12].

To 1,0g 2,2'-bipyridine (6,4 mmole) was added 7,5ml glacial acetic acid (125 mmole) and 0,80ml 50% H_2O_2 (11,8 mmole). The solution was heated to 70°C for

3 hours. A further 0,52ml 50% H_2O_2 (total ratio 3:1 H_2O_2:2,2'-bipyridine) was added and heating continued for another 18 hours. The solution was allowed to cool and was poured onto 150ml acetone. The fine white needles were filtered off, recrystallised from a hot aqueous solution and dried *in vacuo* over silica gel. Yield: 0,96g (80%).

The compound was characterised by ^1H nmr (D_2O); multiplet 8.35 ppm (2H), multiplet 7.67 ppm (2H), multiplet 7.31 ppm (4H) [13], and by melting point: 297-300°C (decomposition) Literature Melting Point: 297°C (decomposition) [12]. Purity was established by microanalysis (Table 2.1) and by mass spectrometry (Appendix 1).

2.6 2,2'-Bipyridine-d_8 *N,N'*-dioxide (bipy-d_8O_2)

To 0,7g 2,2'-bipyridine-d_8 (4,25 mmole, 98% isotopic purity) was added 5,25ml glacial acetic acid (87,5 mmole) and 0,55ml 50% H_2O_2 (8 mmole). The solution was heated to 70°C for 3 hours. A further 0,35ml 50% H_2O_2 (5 mmole) was added and heating continued for 18 hours. The solution was allowed to cool and was poured into 150ml acetone. The white needles were filtered off, recrystallised from a hot aqueous solution and dried *in vacuo* over silica gel. Yield: 0,62g (74%).

The compound was characterised by melting point: 303°C (decomposition). Purity was established by microanalysis (Table 2.1) and by mass spectrometry (Appendix 1).

2.7 Quinoline *N*-oxide dihydrate (quinO·$2H_2O$)

Quinoline *N*-oxide was prepared by the method of OCHIAI [14].

To 2ml quinoline (16,9 mmole) was added 5ml glacial acetic acid (84,6 mmole) and 1,15ml 50% H_2O_2 (16,8 mmole). The solution was heated to 70°C for 3 hours and an additional 1,15ml 50% H_2O_2 (total ratio 3:1 H_2O_2:quinoline) was added and heating continued for a further 3 hours. The solution was concentrated, neutralised with Na_2CO_3 and extracted with chloroform. The extract was taken down to dryness and the quinoline *N*-oxide broken up under ether and filtered. The compound was purified by preparative layer chromatography (10:1 $CHCl_3$:MeOH on silica gel F_{254}). Yield: 1,98g (77%).

The compound was characterised by ^1H nmr((CDCl$_3$); doublet of doublets 8.79 ppm (1H), doublet 8.50 ppm (1H), multiplet ~ 7.75 ppm (3H), doublet of doublets 7.60 ppm (1H), doublet of doublets 7.31 ppm (1H). $J_{2,3}$=6Hz, $J_{2,4}$=1Hz, $J_{3,4}$= 8,5Hz, $J_{5,6}$=8,5Hz, $J_{5,7}$=2Hz, $J_{6,8}$=1,5Hz, $J_{7,8}$=9Hz [15], by mass spectrometry (Appendix 1) and by melting point: 49,5-63°C (melts with deliquescence). Purity was established by microanalyses (Table 2.1).

There is some question in the literature concerning the true melting point of this compound. OCHIAI reports 60-62°C [14], while POUCHERT reports two different melting points: 52-55°C [16] and 60-64°C [17]. This is possibly due to the hygroscopic nature of the compound.

2.8 Quinoline-d_7 *N*-oxide dihydrate (quin-d_7O·2H$_2$O)

To 1,5ml quinoline-d_7 (9 mmole, 97% isotope purity) was added 2,75ml glacial acetic acid (45,8 mmole) and 0,6ml 50% (H_2O_2 8,9 mmole). The solution was heated to 70°C for 3 hours and a further 0,55ml 50% H_2O_2 (8 mmole) was added and heating continued for an additional 3 hours. The solution was concentrated, neutralised with Na_2CO_3 and extracted with chloroform. The extract was reduced to dryness and the product crushed under ether and filtered. The

product was purified by preparative layer chromatography (10:1 $CHCl_3$:MeOH on silica gel F_{254}). Yield: 1,17g (69%).

The compound was characterised by mass spectrometry (Appendix 1) and by melting point: 62-63°C (with deliquescence). Purity was established by microalysis (Table 2.1).

2.9 Attempted preparation of 1,10-phenanthroline *N*-oxide (phenO) and its fully deuterated analogue (phen-d_8O)

1,10-phenanthroline *N*-oxide was prepared after the method by COREY *et al.* [18].

A solution of 1,0g 1,10-phenanthroline monohydrate (5,0 mmole) in 6ml glacial acetic acid (100 mmole) and 0,40ml 50% H_2O_2 (5,9 mmole) was heated to 75°C for 3 hours. Another 0,40ml 50% H_2O_2 (total ratio 2.35:1 H_2O_2:1,10-phenanthroline) was added and heating continued for a further 3 hours. The solution was neutralised with Na_2CO_3 and was reduced to dryness. The solid mass was crushed and extracted by refluxing in 100ml dried chloroform in a Soxhlet extractor. The impure brown product (obtained by taking the chloroform solution down to dryness) was found to be extremely hygroscopic.

Repeated attempts to produce the bright yellow needles of the pure product by recrystallising in toluene [19], in chlorobenzene [18,20,21] and in 96% ethanol [22] were unsuccessful due to the extremely hygroscopic nature of the crystals. (They rapidly turned from bright yellow needles, through a tan, to a light brown and to a darker brown precipitate before they could be filtered off). Microanalysis revealed varying degrees of hydration. Low melting points (melting with deliquescence) indicate impure products (Lit-

erature Melting Points vary depending upon the method of recrystallisation, 179-180°[19,20], 181-183°[21] and 188-190°[22]).

Attempts to purify the product by preparative layer chromatography (75:15:10 *n*-hexane : *i*-butylamine (or *i*-propylamine) : Chloroform on silica gel F_{254} gave the best separation) were unsuccessful according to the mass spectral data discussed below.

Attempts to prepare 1,10-phenanthroline-d_8 *N*-oxide by the same method using 1,10-phenanthroline-d_8 monohydrate (98% isotopic purity, Merck, Sharp and Dohme (Canada) Ltd.) experienced the same difficulties.

Mass spectroscopy was used to establish the purity of the products, not only because of its greater sensitivity, but also because the presence of water in the hygroscopic products excludes the use of microanalysis, while the complexity of the ^{1}H nmr spectrum of the product and of phen does not make it a suitable diagnostic tool. The multiplicity at *ca.* 7.55 ppm, the doublet at 7.75 ppm and the three sets of doublets at 8.20 ppm, 8.72 ppm and 9.29 ppm in the nmr of phenO are sufficiently similar to that of phen (doublet of doublets 7.55 ppm (2H), singlet 7.67 ppm (2H) and two sets of doublet of doublets (2H each) at 8.16 ppm and 9.12 ppm) to make identification of starting material impurity difficult. (Both spectra were run in $CDCl_3$). Furthermore, the deuteration labelling study employed excludes the use of ^{1}H nmr as a diagnostic tool.

In mass spectrometry the principal fragmentation pattern in fused aromatic *N*-oxides is a loss of CO and HCN [23]. The most likely fragmentation for phenO (and its fully deuterated analogue) is given in Figure 2.1. The presence of an (M-16) ion in phenO (Figure 2.2) might be attributed to thermal fragmenta-

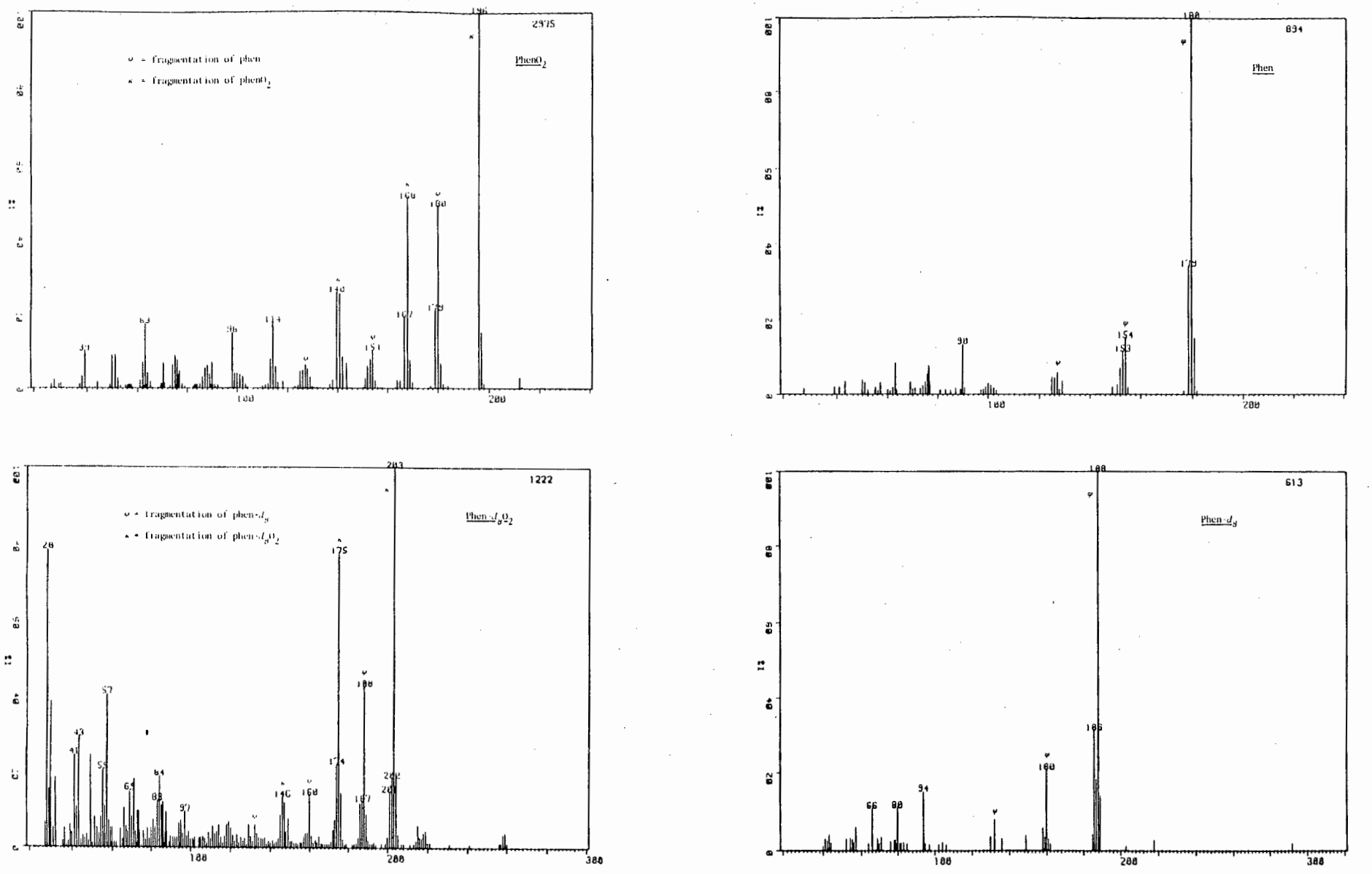

Figure 2.2 Mass spectra of PhenO and its deuterated analogue

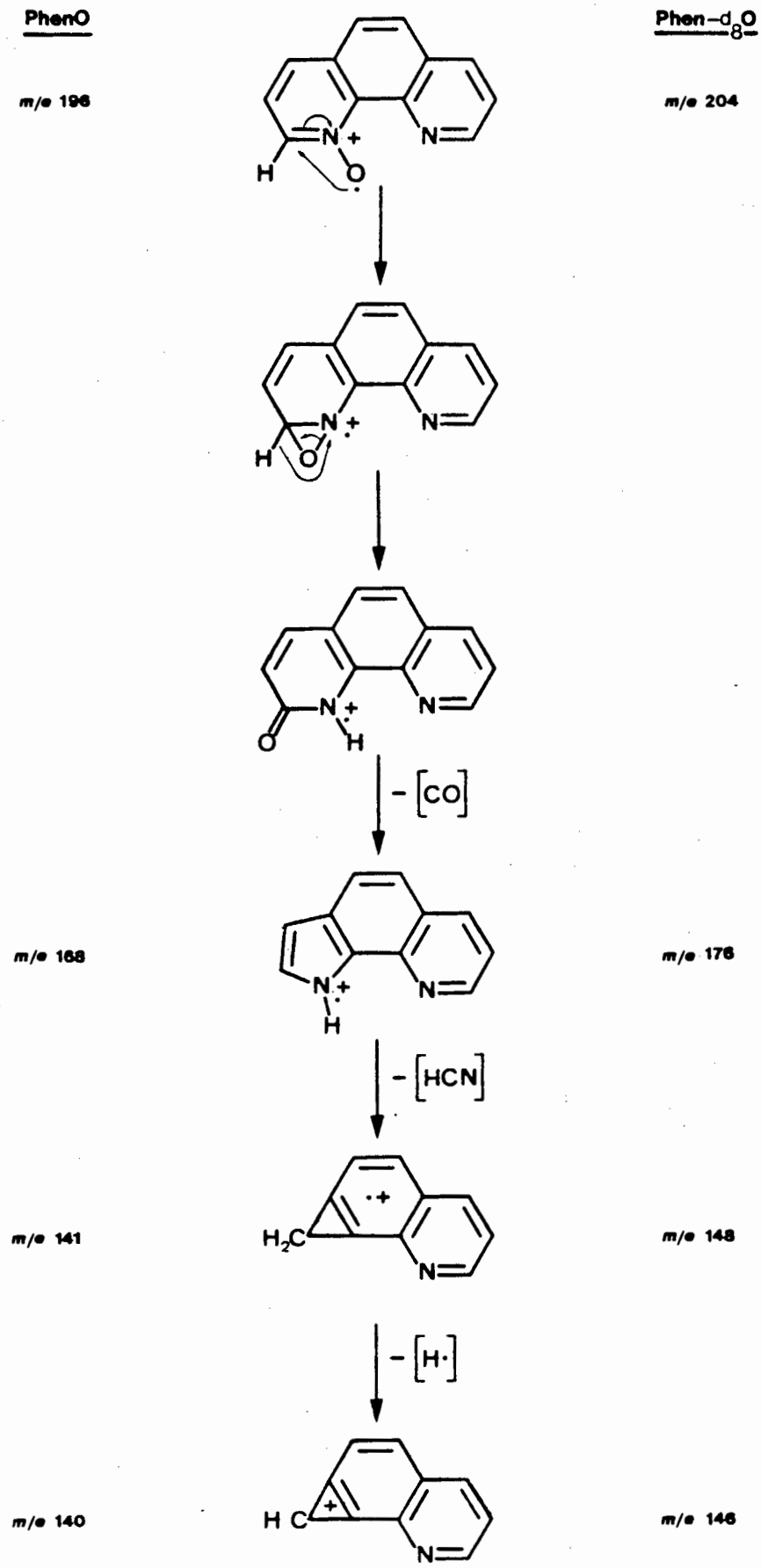

Figure 2.1 Probable fragmentation pattern of PhenO and its -d_8 analogue

tion (as is experienced by quinO [24]); alternatively it may indicate the presence of starting material. Doping the phenO sample with phen and running the mass spectra showed that both compounds volatalise simultaneously, and so the purity of the phenO cannot be determined by examining the mass chromatogram of the ion at m/e 180 (the molecular ion of phen).

In the mass spectrum of the deuterated phenanthroline *N*-oxide the presence of ion at m/e 203 (phen-d_7O) in a relative five-fold excess to that at m/e 204 (phen-d_8O), to that at m/e 202 (phen-d_6O) and to that at m/e 201 (phen-d_6O) indicates that H/D exchange has occurred either in the preparation of the *N*-oxide, or within the ionisation chamber of the mass spectrometer.* The occurrence of the latter was ruled out by swamping the mass spectrometer with D_2O (99,8% isotopic purity, Aldrich Chemical Co.) before re-running the mass spectrum of the deuterated phenanthroline *N*-oxide. The m/e 203 ion remained the predominant peak in the spectrum. (A similar run with phenO in a D_2O swamped instrument also revealed no D/H exchange within the instrument).

The presence of the (M-15) ion (at m/e 188) in the mass spectrum of the deuterated product is clear evidence of the presence of starting material within the product. The ratios of the m/e 188 to the m/e 187 and m/e 186 ion in phen-d_8 is similar to that observed in the deuterated *N*-oxide; consequently thermal fragmentation with loss of [O] from the m/e 203 ion to produce a m/e 187 ion is not a significant mechanism in the deuterated *N*-oxide fragmentation. It is therefore most likely that the corresponding m/e 180 ion in the undeuterated analogue is also a result of the presence of starting material.

---

* Formation of the *N*-oxide makes the protons, particularly in positions 2 and 4, more labile than in the parent diimine.

Since the fully-deuterated *N*-oxide was not prepared by this method, and in view of the inability to produce pure ligands, this section of the work was terminated.

3 PREPARATIONS OF THE M(II) PERCHLORATE COMPLEXES

All Fe(II) complexes were prepared under nitrogen, using nitrogen-purged solvents.

3.1 Preparation of $[M(bipy)_3](ClO_4)_2$ (M = Mn, Fe, Co, Ni, Cu, Zn)

A 5ml hot aqueous solution of 0,1g (0,27 mmole) metal perchlorate (as the hydrated salt) was added to a hot solution of 0,17g (1,10 mmole: 4:1 mole ratio) 2,2'-bipyridine in 10ml EtOH with stirring. The solution was allowed to cool and the precipitate filtered and washed with absolute EtOH. The complex was recrystallised from a minimal amount of hot acetone and dried over silica gel, under reduced pressure. Yields of 86 to 98% were obtained. Microanalytical data are given in Table 2.2.

3.2 Preparation of $[M(bipy\text{-}d_8)_3](ClO_4)_2$ (M = Mn, Fe, Co, Ni, Cu, Zn)

The deuterated complexes were prepared as described in 3.1, using one-half quantities of reactants. 2,2'-bipyridine-d_8 of 98% isotopic purity was purchased from Merck, Sharp and Dohme (Canada) Ltd. Yields of 80 to 94% were obtained. Microanalytical data are given in Table 2.2.

3.3 Preparation of $[M(phen)_3](ClO_4)_2$ (M = Mn, Fe, Co, Ni, Cu, Zn)

A solution of 0,1g (0,27 mmole) metal perchlorate (as the hydrated salt) in

Table 2.2 Microanalyses of $M(II)(ClO_4)_2$ complexes

	Colour	Experimental %C	%H	%N	Calculated %C	%H	%N
$[Mn(bipy)_3](ClO_4)_2$	lemon yellow	49,60	3,45	11,70	49,88	3,35	11,63
$[Fe(bipy)_3](ClO_4)_2 \cdot 1\frac{1}{2}H_2O$	crimson	48,10	3,45	10,95	48,02	3,63	11,20
$[Co(bipy)_3](ClO_4)_2$	sand-yellow	49,65	3,35	11,65	49,60	3,33	11,57
$[Ni(bipy)_3](ClO_4)_2$	pink	49,70	3,40	11,55	49,62	3,33	11,57
$[Cu(bipy)_3](ClO_4)_2$	royal blue	49,10	3,30	11,50	49,29	3,31	11,50
$[Zn(bipy)_3](ClO_4)_2$	white	49,10	3,30	11,45	49,17	3,30	11,47
$[Mn(bipy\text{-}d_8)_3](ClO_4)_2$	lemon yellow	48,10	3,30	11,20	48,26	3,24	11,26
$[Fe(bipy\text{-}d_8)_3](ClO_4)_2 \cdot \frac{1}{2}H_2O$	crimson	47,65	3,45	11,00	47,63	3,33	11,11
$[Co(bipy\text{-}d_8)_3](ClO_4)_2$	sand-yellow	47,90	3,25	11,25	48,01	3,22	11,20
$[Ni(bipy\text{-}d_8)_3](ClO_4)_2$	pink	47,55	3,25	11,20	48,02	3,22	11,20
$[Cu(bipy\text{-}d_8)_3](ClO_4)_2$	royal blue	47,60	3,25	11,20	47,71	3,20	11,13
$[Zn(bipy\text{-}d_8)_3](ClO_4)_2$	white	47,45	3,30	11,10	47,60	3,20	11,10
$[Mn(phen)_3](ClO_4)_2 \cdot H_2O$	mustard	53,25	3,35	10,40	53,21	3,22	10,34
$[Fe(phen)_3](ClO_4)_2 \cdot 3\frac{1}{2}H_2O$	post box red	50,15	3,55	9,70	50,37	3,64	9,79
$[Co(phen)_3](ClO_4)_2 \cdot H_2O$	dark yellow	53,00	3,20	10,30	52,96	3,21	10,29
$[Ni(phen)_3](ClO_4)_2 \cdot H_2O$	flesh pink	53,20	3,20	10,30	52,97	3,21	10,30
$[Cu(phen)_3](ClO_4)_2 \cdot \frac{1}{2}H_2O$	duck egg blue	53,25	3,10	10,30	53,24	3,10	10,35
$[Zn(phen)_3](ClO_4)_2 \cdot H_2O$	white	52,70	3,20	10,25	52,54	3,18	10,21
$[Mn(phen\text{-}d_8)_3](ClO_4)_2 \cdot H_2O$	mustard	52,00	3,20	10,00	51,68	3,13	10,04
$[Fe(phen\text{-}d_8)_3](ClO_4)_2 \cdot 3H_2O$	post box red	49,85	3,45	9,50	49,50	3,46	9,62
$[Co(phen\text{-}d_8)_3](ClO_4)_2 \cdot H_2O$	dark yellow	51,60	3,20	10,00	51,43	3,12	10,00
$[Ni(phen\text{-}d_8)_3](ClO_4)_2 \cdot H_2O$	flesh pink	51,60	3,15	9,95	51,45	3,12	10,00
$[Cu(phen\text{-}d_8)_3](ClO_4)_2 \cdot H_2O$	duck egg blue	51,40	3,10	9,85	51,15	3,10	9,94
$[Zn(phen\text{-}d_8)_3](ClO_4)_2 \cdot H_2O$	white	51,30	3,00	10,00	51,04	3,09	9,92
* $[Mn(bipyO_2)_3](ClO_4)_2 \cdot 1\frac{1}{2}H_2O$	burnt orange	42,40	3,20	9,90	42,62	3,22	9,94
$[Co(bipyO_2)_3](ClO_4)_2 \cdot 1\frac{1}{2}H_2O$	brick red	43,35	3,10	9,85	42,42	3,20	9,89
$[Ni(bipyO_2)_3](ClO_4)_2 \cdot 1\frac{1}{2}H_2O$	lime green	42,30	3,15	9,95	42,43	3,20	9,90
$[Cu(bipyO_2)_3](ClO_4)_2 \cdot 1\frac{1}{2}H_2O$	light green	42,50	3,10	9,90	42,19	3,19	9,84
$[Zn(bipyO_2)_3](ClO_4)_2 \cdot 1\frac{1}{2}H_2O$	white	42,15	3,20	9,80	42,10	3,18	9,82
* $[Mn(bipy\text{-}d_8O_2)_3](ClO_4)_2 \cdot 1\frac{1}{2}H_2O$	burnt orange	41,60	3,10	9,60	41,43	3,13	9,66
$[Co(bipy\text{-}d_8O_2)_3](ClO_4)_2 \cdot 1\frac{1}{2}H_2O$	brick red	41,30	3,15	9,65	41,25	3,12	9,62
$[Ni(bipy\text{-}d_8O_2)_3](ClO_4)_2 \cdot 1\frac{1}{2}H_2O$	lime green	41,40	3,10	9,65	41,26	3,12	9,65
$[Cu(bipy\text{-}d_8O_2)_3](ClO_4)_2 \cdot 1\frac{1}{2}H_2O$	light green	41,10	3,00	9,65	41,03	3,10	9,57
$[Zn(bipy\text{-}d_8O_2)_3](ClO_4)_2 \cdot 1\frac{1}{2}H_2O$	white	41,10	3,10	9,65	40,93	3,09	9,55

Table 2.2 (continued)

	Colour	Experimental %C	%H	%N	Calculated %C	%H	%N
* $[Mn(quinO)_6](ClO_4)_2 \cdot \frac{1}{2}H_2O$	deep red	57,10	3,75	7,45	57,20	3,82	7,41
$[Co(quinO)_6](ClO_4)_2$	ochre	57,45	3,75	7,50	57,46	3,75	7,44
$[Ni(quinO)_6](ClO_4)_2 \cdot H_2O$	orange	56,60	3,80	7,30	56,57	3,85	7,33
$[Cu(quinO)_4](ClO_4)_2$	chocolate	51,00	3,35	6,60	51,29	3,35	6,64
$[Zn(quinO)_5](ClO_4)_2$	ivory	54,70	3,65	7,00	54,59	3,56	7,07
* $[Mn(quin\text{-}d_7O)_6](ClO_4)_2 \cdot \frac{1}{2}H_2O$	deep red	54,95	3,70	7,10	55,14	3,68	7,14
$[Co(quin\text{-}d_7O)_6](ClO_4)_2 \cdot H_2O$	ochre	54,45	3,60	7,00	54,45	3,73	7,07
$[Ni(quin\text{-}d_7O)_6](ClO_4)_2 \cdot 2H_2O$	orange	53,70	4,05	7,00	53,74	3,84	6,96
$[Cu(quin\text{-}d_7O)_4](ClO_4)_2$	chocolate	49,40	3,25	6,45	49,62	3,24	6,43
$[Zn(quin\text{-}d_7O)_5](ClO_4)_2 \cdot \frac{1}{2}H_2O$	ivory	52,10	3,25	6,75	52,25	3,51	6,77
$Mn(pzO)_6(ClO_4)_2 \cdot \frac{1}{2}H_2O$	yellow	34,10	2,80	19,95	34,34	3,00	20,02
$Mn(pzO)_5(ClO_4)_2 \cdot 1\frac{1}{2}H_2O$	yellow	31,45	2,85	18,40	31,55	3,04	18,40
$Fe(pzO)_5(ClO_4)_2$	red	32,50	2,75	19,00	32,67	2,74	19,05
$Fe(pzO)_5(ClO_4)_2 \cdot 2H_2O$	yellow	31,05	3,60	18,10	31,15	3,14	18,16
$Co(pzO)_5(ClO_4)_2 \cdot 1\frac{1}{2}H_2O$	tangerine	31,60	2,85	18,10	31,40	3,03	18,30
$Co(pzO)_4(ClO_4)_2 \cdot H_2O$	light pink	29,35	2,95	17,05	29,11	2,75	16,97
$Ni(pzO)_4(ClO_4)_2 \cdot H_2O$	light green	29,05	2,75	16,95	29,11	2,75	16,98
$Cu(pzO)_4(ClO_4)_2$	grey-green	29,60	2,55	17,10	29,71	2,49	17,32
$Zn(pzO)_5(ClO_4)_2 \cdot H_2O$	white	31,50	2,80	18,20	31,49	2,91	18,36
$Mn(pz\text{-}d_4O)_6(ClO_4)_2 \cdot 2\frac{1}{2}H_2O$	yellow	31,80	2,75	18,35	32,04	3,02	18,68
$Mn(pz\text{-}d_4O)_5(ClO_4)_2 \cdot 3H_2O$	yellow	29,60	3,35	17,25	29,71	3,24	17,32
+ $Fe(pz\text{-}d_4O)_5(ClO_4)_2 \cdot \frac{1}{2}H_2O$	red	31,20	3,10	18,10	31,43	2,77	18,32
$Fe(pz\text{-}d_4O)_5(ClO_4)_2 \cdot 2H_2O$	yellow	30,20	3,50	17,55	30,35	3,06	17,70
$Co(pz\text{-}d_4O)_5(ClO_4)_2 \cdot 1\frac{1}{2}H_2O$	tangerine	30,50	2,90	17,65	30,58	2,95	17,85
$Co(pz\text{-}d_4O)_4(ClO_4)_2 \cdot 1\frac{1}{2}H_2O$	light pink	28,10	2,65	16,20	28,04	2,79	16,35
$Ni(pz\text{-}d_4O)_4(ClO_4)_2 \cdot H_2O$	light green	28,40	2,60	16,40	28,42	2,68	16,57
$Cu(pz\text{-}d_4O)_4(ClO_4)_2 \cdot \frac{1}{2}H_2O$	grey-green	28,65	2,50	16,50	28,60	2,55	16,68
$Zn(pz\text{-}d_4O)_5(ClO_4)_2 \cdot H_2O$	white	30,55	2,85	17,75	30,68	2,83	17,89

* light sensitive

\+ extremely hygroscopic

3ml 96% EtOH was added to a solution of 0,16g (0,82 mmole; 3:1 mole ratio) 1,10-phenanthroline monohydrate in 7ml 96% EtOH with stirring. The resultant precipitant was filtered and washed with small amounts of water and ethanol. The complex was recrystallised from a minimal amount of hot acetone and dried over silica gel under reduced pressure. Yields of 64 to 98% were obtained. Microanalytical data are given in Table 2.2.

3.4 Preparation of $[M(phen\text{-}d_8)_3](ClO_4)_2$ (M = Mn, Fe, Co, Ni, Cu, Zn)

The deuterated complexes were prepared as in 3.3, using one-half quantities of reactants. 1,10-phenanthroline-d_8 of 98% isotopic purity was purchased from Merck, Sharp and Dohme (Canada) Ltd. Yields of 73 to 98% were obtained. Microanalytical data are given in Table 2.2.

3.5 Preparation of $[M(bipyO_2)_3]\cdot 1\frac{1}{2}H_2O$ (M = Mn, Co, Ni, Cu, Zn)

A 2ml hot aqueous solution of 0,1g (0,27 mmole) metal perchlorate (as the hydrated salt) was added to a hot solution of 0,15g (0,81 mmole; 3:1 mole ratio) 2,2'-bipyridine *N,N'*-dioxide in 5ml H_2O with stirring. On cooling, the precipitate was filtered and washed with 2ml cold H_2O. The complex was recrystallised from a minimum amount of hot water and dried over silica gel under reduced pressure. Yields of between 65 and 92% were obtained. Microanalytical data are given in Table 2.2.

3.6 Preparation of $[M(bipy\text{-}d_8O_2)_3](ClO_4)_2\cdot 1\frac{1}{2}H_2O$ (M = Mn, Co, Ni, Cu, Zn)

The deuterated complexes were prepared as described in 3.5, using one-half quantities of reactants. Yields of between 70 and 87% were obtained. Microanalytical data are given in Table 2.2.

3.7 Preparation of $[M(quinO)_n](ClO_4)_2$ (n = 6 for Mn, Co, Ni; n = 5 for Zn and n = 4 for Cu)

A solution of 0,1g (0,27 mmole) metal perchlorate (as the hydrated salt) in 5ml dried EtOH/dimethoxypropane (1:1 ratio) was allowed to stand for 20 minutes before being added with stirring to a similarly prepared solution of 0,35g (1,91 mmole; 7:1 mole ratio) quinoline *N*-oxide·dihydrate in 10ml dried EtOH/dimethoxypropane. The precipitate was collected by filtration, washed with cold dried EtOH and with dried ether, and was dried over silica gel under reduced pressure. Yields of between 60 and 87% were obtained. Microanalytical data are given in Table 2.2.

3.8 Preparation of $[M(quino\text{-}d_7O)_n](ClO_4)_2$ (n = 6 for Mn, Co, Ni; n = 5 for Zn and n = 4 for Cu)

The deuterated complexes were prepared as described in 3.7, using one-half quantities of reactants. Yields of between 69 and 91% were obtained. Microanalytical data are given in Table 2.2.

3.9 Preparation of $M(pzO)_n(ClO_4)_2 \cdot x\,H_2O$

3.9.1 For complexes where n = 5 for Mn, Fe, Zn; n = 4 for Co, Ni, Cu

A solution of 0,1g (0,27 mmole) perchlorate (as the hydrated salt) in 5 ml dried EtOH/dimethoxypropane (1:1 ratio) was allowed to stand for 20 minutes before being added with stirring to a similarly prepared solution of 0,18g (0,92 mmole; 7:1 ratio) pyrazine *N*-oxide in 10ml dried EtOH/dimethoxypropane. The precipitate was immediately collected by filtration under nitrogen and dried over P_4O_{10} under reduced pressure. These complexes readily absorb at-

mospheric water on standing. For the Fe(II) complex this is reversible, the yellow complex $Fe(pzO)_5H_2O(ClO_4)_2$ reverting back to the red complex $Fe(pzO)_5(ClO_4)_2$ by the addition of dimethoxypropane, or by drying under reduced pressure over P_4O_{10}. Yields of between 60 and 86% were obtained. Microanalytical data are given in Table 2.2.

3.9.2 For complexes where n = 6 for Mn, n = 5 for Co

These complexes were prepared as described in 3.9.1, but were not filtered immediately, being left to stand overnight before being filtered under nitrogen and dried over P_4O_{10} under reduced pressure. Yields of between 60 and 86% were obtained. Microanalytical data are given in Table 2.2.

3.10 Preparation of $M(pz\text{-}d_4O)_n(ClO_4)_2 \cdot xH_2O$

The deuterated complexes were prepared as described in 3.9, using one-half quantities of reactants. Yields of between 81 and 88% were obtained. Microanalytical data are given in Table 2.2.

3.11 Attempted preparation of M(II) perchlorate complexes with pyrazine *N,N'*-dioxide

In attempting the preparation of the M(II) perchlorate complexes following the method of POPP and GARLOUGH [9], the ligand was found to be insoluble in the solvent recommended (dried EtOH).

The ligand is soluble in 96% EtOH. However, use of this solvent lead to irreproducible results for the resulting complexes, with varying stoichiometry of between 2 and 5 molecules of pzO_2 and between 1 and 5 molecules of water

or ethanol per metal ion (for each of the metals Co, Ni, Cu or Zn). This is probably a result of competition between the oxygen donors of pzO_2, H_2O and EtOH for bonding within the inner coordination sphere.

The ligand is slightly soluble in chloroform and the following attempts to prepare the complexes from this solvent were made.

A solution of 0,1g (0,27 mmole) metal perchlorate (as the hydrated salt for the metals Co, Ni, Cu and Zn) was prepared in 5ml dried EtOH/dimethoxypropane (1:1 ratio) and allowed to stand for 20 minutes before being added to a suspension of 0,214g (1,91 mmole; 7:1 mole ratio) pyrazine *N,N'*-dioxide in 50ml dried $CHCl_3$/dimethoxypropane (10:1 ratio). The suspension was refluxed for 24 hours. On cooling, both the complex and excess of ligand were observed to co-precipitate. The precipitate was collected by filtration and dried over P_4O_{10} under reduced pressure.

In the attempts to find a suitable solvent for the recrystallisation of the metal complexes, both the ligand and the complexes were found to be insoluble in the majority of organic solvents (with the exception of slight solubility of pzO_2 in $CHCl_3$ and in 96% EtOH). The pink-red colour of the Co complex, the orange colour of the Ni complex and the brown hue of the copper complex undergo a change in colour (presumably undergoing dissociation) in dimethylformamide, in dimethylsulphoxide, in acetonitrile and in water.

Attempts to remove the excess of pzO_2 by extraction from the crude product (by refluxing with dried chloroform in a Soxhlet extractor under dry nitrogen for 48 hours) resulted in decomposition of the complexes via ligand displacement.

Finally, attempts to prepare the complexes by the slow addition of a 6:1 mole ratio (ligand:metal) of pzO_2 (by means of extracting the pzO_2 into dried chloroform in a Soxhlet extractor under dry nitrogen) into a solution of metal perchlorate (as the hydrated salt) in a $CHCl_3$/dimethoxypropane solution (10:1 ratio) result in co-precipitation of the complex and free ligand on cooling.

The impure complexes prepared above were found to be air-sensitive, slowly absorbing atmospheric water which displaces the pzO_2, the complexes thereby losing their colour.

4 PREPARATION OF ZEISE'S SALT DERIVATIVES AND THEIR CARBONYL ANALOGUES

4.1 Preparation of $K[Pt(C_2H_4)X_3]\cdot H_2O$ (X = Cl, Br) and $K[Pt(C_2D_4)Cl_3]\cdot H_2O$

These complexes were prepared in a similar manner to the synthesis described by CHATT and SEARLE [25].

A solution of $K_2[PtX_4]$ (9,28 mmole; 3,85g for X = Cl or 5,50g for X = Br) in 30ml water and 2ml conc. HX (sp.gr. 1,18 for HCl or 1,50 for HBr) in a 250ml round bottomed flask, under a positive pressure of ethene, was shaken until the solution changed from dark red to golden yellow (*ca.* three to five days). The solution was taken down to dryness, extracted with acetone, and the insoluble KX and unreacted $K_2[PtX_4]$ were removed by filtration. As aqueous solutions of $K[Pt(C_2H_4)X_3]$ were required, the acetone solution was evaporated to dryness and the Zeise's salt dissolved in water. Prior to use, the aqueous solution was filtered to remove traces of finely-divided platinum black which had precipitated out. Yields of between 65 and 89% were obtained.

The deuterated Zeise's salt $K[Pt(C_2D_4)Cl_3]\cdot H_2O$ was similarly prepared, employing ethene-d_4 of 99% isotopic purity supplied by Merck, Sharp and Dohme (Canada) Ltd.

4.2 Preparation of *trans*-$[Pt(quin)(C_2H_4)X_2]$ (X = Cl, Br) and their C_2D_4 and quin-d_7 analogues

These complexes were prepared by the dropwise addition of an ethanolic solution of quinoline (0,26 mmole in 5ml) to an aqueous solution of $K[Pt(C_2H_4)X_3]\cdot H_2O$ (0,26 mmole in 20ml) with stirring. After 20 minutes the product was filtered, washed well with water and dried over silica gel under reduced pressure.

The deuterated complexes were similarly prepared from quinoline-d_7 (97% isotopic purity from Merck, Sharp and Dohme (Canada) Ltd.) and from $K[Pt(C_2D_4)Cl_3]\cdot H_2O$.

Yields of between 74 and 91% were obtained. Microanalytical data are given in Table 2.3.

4.3 Preparation of *trans*-$[Pt(quinO)(C_2H_4)X_2]$ (X = Cl, Br) and their C_2D_4 quin-d_7O analogues

These complexes were prepared by the dropwise addition of an aqueous solution of quinoline *N*-oxide (0,26 mmole in 10ml) to an aqueous solution of $K[Pt(C_2H_4)X_3]\cdot H_2O$ (0,26 mmole in 20ml) with stirring. After 20 minutes, the product was filtered, washed well with water and dried over silica gel, under reduced pressure.

The deuterated complexes were similarly prepared from quinoline-d_7 *N*-oxide

Table 2.3 Microanalyses of complexes of Zeise's salt and their CO derivatives

	Experimental			Calculated		
	%C	%H	%N	%C	%H	%N
trans-[Pt(quin)(C_2H_4)Cl_2]	31,30	2,60	3,30	31,22	2,62	3,31
trans-[Pt(quin)(C_2H_4)Br_2]	25,75	2,20	2,70	25,80	2,17	2,74
trans-[Pt(quin)(C_2D_4)Cl_2]	30,80	2,60	3,30	30,92	2,60	3,28
trans-[Pt(quin-d_7)(C_2H_4)Cl_2]	30,80	2,60	3,25	30,71	2,58	3,26
trans-[Pt(quin)(CO)Cl_2]	28,25	1,65	3,30	28,38	1,67	3,31
trans-[Pt(quin)(CO)Br_2]	23,50	1,45	2,75	23,46	1,38	2,74
trans-[Pt(quin-d_7)(CO)Cl_2]	27,35	1,75	3,20	27,35	1,84	3,19
trans-[Pt(quinO)(C_2H_4)Cl_2]	30,30	2,60	3,15	30,08	2,52	3,19
trans-[Pt(quinO)(C_2H_4)Br_2]	25,15	2,20	2,65	25,02	2,10	2,65
trans-[Pt(quinO)(C_2D_4)Cl_2]	29,95	2,55	3,15	29,81	2,50	3,16
trans-[Pt(quin-d_7O)(C_2H_4)Cl_2]	29,85	2,50	3,15	29,61	2,48	3,14
trans-[Pt(quinO)(CO)Cl_2]	27,45	1,70	3,10	27,34	1,61	3,19
trans-[Pt(quinO)(CO)Br_2]	22,95	1,40	2,65	22,75	1,34	2,65
trans-[Pt(quin-d_7O)(CO)Cl_2]	27,20	1,65	3,20	26,92	1,58	3,14
trans-[Pt(pzO)(C_2H_4)Cl_2]	18,60	2,10	7,10	18,46	2,07	7,18
trans-[Pt(pzO)(C_2H_4)Br_2]	15,10	1,70	5,90	15,10	1,69	5,87
trans-[Pt(pzO)(C_2D_4)Cl_2]	18,70	2,10	7,10	18,28	2,05	7,11
trans-[Pt(pz-d_4O)(C_2H_4)Cl_2]	18,40	2,05	7,10	18,28	2,05	7,11
trans-[Pt(pzO)(CO)Cl_2]	15,45	1,05	7,15	15,39	1,03	7,18
trans-[Pt(pzO)(CO)Br_2]	12,45	0,85	5,75	12,54	0,84	5,85
trans-[Pt(pz-d_4O)(CO)Cl]	15,20	1,05	7,00	15,24	1,02	7,11
trans-[Pt(pdz)(C_2H_4)Cl_2]	19,25	2,15	7,40	19,25	2,16	7,49
trans-[Pt(pdz)(C_2H_4)Br_2]	15,55	1,75	6,00	15,62	1,75	6,07
trans-[Pt(pdz)(C_2D_4)Cl_2]	19,15	2,10	7,40	19,06	2,13	7,41
trans-[Pt(pdz-d_4)(C_2H_4)Cl_2]	18,95	2,15	7,35	19,06	2,13	7,41
trans-[Pt(pdz)(CO)Cl_2]	15,95	1,15	7,40	16,05	1,08	7,49
trans-[Pt(pdz)(CO)Br_2]	13,00	0,95	6,05	12,97	0,87	6,05
trans-[Pt(pdz-d_4)(CO)Cl_2]	16,05	1,10	7,35	15,88	1,07	7,41

Table 2.3 (continued)

	Experimental			Calculated		
	%C	%H	%N	%C	%H	%N
cis-[Pt(bipyO$_2$H)(C$_2$H$_4$)Cl$_2$]Cl	27,70	2,50	5,40	27,79	2,52	5,39
cis-[Pt(bipyO$_2$H)(C$_2$H$_4$)Br$_2$]Br	22,00	2,00	4,25	22,16	2,01	4,31
cis-[Pt(bipyO$_2$H)(C$_2$D$_4$)Cl$_2$]Cl	27,60	2,50	5,35	27,57	2,51	5,36
cis-[Pt(bipy-d_8O$_2$H)(C$_2$H$_4$)Cl$_2$]Cl	27,30	2,50	5,25	27,36	2,49	5,32
cis-[Pt(bipyO$_2$H)(CO)Cl$_2$]Cl	25,65	1,90	5,35	25,47	1,75	5,40
cis-[Pt(bipyO$_2$H)(CO)Br$_2$]Br	20,30	1,45	4,30	20,26	1,39	4,30
cis-[Pt(bipy-d_8O$_2$H)Cl$_2$]Cl	24,80	1,80	5,25	25,08	1,72	5,32
trans-[Pt(bipy)(C$_2$H$_4$)Cl$_2$]	31,80	2,50	6,25	32,01	2,69	6,22
trans-[Pt(bipy)(C$_2$H$_4$)Cl$_2$]	31,90	2,70	6,20	31,73	2,66	6,17
trans-[Pt(bipy-d_8)(C$_2$H$_4$)Cl$_2$]	31,55	2,60	6,15	31,45	2,64	6,11
trans-[Pt(phen)(C$_2$H$_4$)Cl$_2$]	35,35	2,60	5,95	35,46	2,55	5,91
trans-[Pt(phen)(C$_2$D$_4$)Cl$_2$]	35,00	2,65	5,75	35,16	2,52	5,86
trans-[Pt(phen-d_8)(C$_2$H$_4$)Cl$_2$]	34,40	2,40	5,90	34,86	2,51	5,81

and from $K[Pt(C_2D_4)Cl_3]\cdot H_2O$.

Yields of between 73 and 79% were obtained. Microanalytical data are given in Table 2.3.

4.4 Preparation of *trans*-$[Pt(pzO)(C_2H_4)X_2]$ (X = Cl, Br) and their C_2D_4 and pz-d_4O analogues

These complexes were prepared by the dropwise addition of an aqueous solution of pyrazine *N*-oxide (0,26 mmole in 5ml) to an aqueous solution of $K[Pt(C_2H_4)X_3]\cdot H_2O$ (0,26 mmole in 30ml) with stirring. After 20 minutes the product was filtered, washed well with water and dried over silica gel, under reduced pressure.

The deuterated complexes were similarly prepared from pyrazine-d_4 *N*-oxide and from $K[Pt(C_2D_4)Cl_3]\cdot H_2O$.

Yields of between 74 and 84% were obtained. Microanalytical data are given in Table 2.3.

4.5 Preparation of *trans*-$[Pt(pdz)(C_2H_4)X_2]$ (X = Cl, Br) and their C_2D_4 and pdz-d_4 analogues

These complexes were prepared by the addition of an aqueous solution of pyridazine (0,26 mmole in 10ml) to an aqueous solution of $K[Pt(C_2H_4)X_3]\ H_2O\cdot$(0,26 mmole in 20ml H_2O) with stirring. The precipitate was *immediately* filtered (if allowed to stir for ten minutes before filtering, the complex loses C_2H_4), and was washed with cold ($\sim$ 0°C) water and dried over silica gel, under reduced pressure.

The deuterated complexes were similarly prepared from pyradizine-d_4 (97% isotopic purity, from Aldrich Chemical Co.), and from $K[Pt(C_2D_4)Cl_3]\cdot H_2O$.

Yields of between 68 and 94% were obtained. Microanalytical data are given in Table 2.3.

4.6 Attempted preparation of *trans*-$[PtL(C_2H_4)X_2]$ (L = pzO_2, $bipyO_2$; X = Cl, Br)

Attempts to prepare these complexes were made by the addition of an aqueous solution of ligand, L (0,26 mmole in 5ml) to an aqueous solution of $K[Pt(C_2H_4)X_3]\cdot H_2O$ (0,26 mmole in 20ml) with stirring for up to 18 hours. No precipitate was formed, instead the Zeise's salt decomposed to platinum black.

This preparation was repeated in D_2O and was monitored by ^1H nmr. The absence of a change in chemical shift of the ligand protons (at 8.42 ppm) with pzO_2, and the absence of a change in chemical shift of the ethene protons (at 4.57 ppm) with pzO_2 and $bipyO_2$ shows that no complexation occurs with Zeise's salt for these two ligands in an aqueous medium.

4.7 Preparation of *cis*-$[Pt(bipyO_2H)(C_2H_4)X_2]X$ (X = Cl, Br) and their C_2D_4 and bipy-d_8O_2 analogues

The complexes were prepared as described in 4.6, with the exception that 2ml 5M HX was added to the solution of $K[Pt(C_2H_4)X_3]\cdot H_2O$. This results in the immediate precipitation of the cationic species upon addition of the $bipyO_2$. The precipitate was washed with cold water and dried over silica gel under reduced pressure. These complexes are insoluble in water and ethanol, and only very slightly soluble in acetone and chloroform.

The deuterated complexes were similarly prepared from 2,2'-bipyridine-d_8O_2 and from $K[Pt(C_2D_4)Cl_3]\cdot H_2O$.

Yields of between 63 and 98% were obtained. Microanalytical data are given in Table 2.3.

4.8 Attempted preparation of $[Pt(pzO_2H)(C_2H_4)X_2]X$ (X = Cl, Br)

The preparation of these complexes was attempted as described in 4.7, with the exception of employing pyrazine *N,N'*-dioxide in place of $bipyO_2$. No product was obtained, although the presence of the HX prevented decomposition to platinum black. The solution was taken down to dryness and extracted into absolute EtOH. After filtration, the yellow ethanolic solution was taken down to dryness. Microanalysis showed the yellow solid to be $K[Pt(C_2H_4)X_3]\cdot H_2O$.

4.9 Attempted preparation of $[Pt_2(C_2H_4)_2X_4L]$ (L = pzO, pzO_2 and $bipyO_2$; X = Cl, Br)

Attempts to prepare these bridged dinuclear complexes were made by the addition of an aqueous solution of the ligand, L (0,26 mmole in 10ml) to an aqueous solution of $K[Pt(C_2H_4)X_3]\cdot H_2O$ (0,26 mmole in 20ml) with stirring. For L = pzO the mononuclear complex $[Pt(pzO)(C_2H_4)X_2]$ only is formed, while the reactions with pzO_2 and $bipyO_2$ undergo slow decomposition to platinum black.

4.10 Preparation of $[Pt(bipy)(C_2H_4)Cl_2]$ and its C_2D_4 and bipy-d_8 analogues

These complexes were prepared by the addition of a cold ($\sim$ 0°C) aqueous solution of 2,2'-bipyridine (0,26 mmole in 10ml) to a cold ($\sim$ 0°C) aqueous sol-

ution of $K[Pt(C_2H_4)Cl_3]\cdot H_2O$ (0,26 mmole in 20ml) with stirring. The precipitate was immediately filtered and washed well with cold water (∿ 0°C), and dried and stored over silica gel, under reduced pressure at -5°C. These complexes rapidly lose ethene in solution at room temperature.

The deuterated complexes were prepared from 2,2'-bipyridine-d_8 (98% isotopic purity from Merck, Sharp and Dohme (Canada) Ltd.) and $K[Pt(C_2D_4)Cl_3]\cdot H_2O$. Yields of between 86 and 96% were obtained. Microanalytical data are given in Table 2.3.

The bromo analogues could not be prepared, repeated attempts yielding a mixture of $[Pt(bipy)(C_2H_4)Br_2]$ and $[Pt(bipy)Br_2]$.

4.11 Preparation of $[Pt(phen)(C_2H_4)Cl_2]$ and its C_2D_4 and phen-d_8 analogues

These complexes were prepared by the addition of a cold (∿ 0°C) ethanolic solution of 1,10-phenanthroline (0,26 mmole in 3ml) to a cold (∿ 0°C) aqueous solution of $K[Pt(C_2H_4)Cl_3]\cdot H_2O$ (0,26 mmole in 10ml) with stirring. The precipitate was immediately collected by filtration and washed well with cold (∿ 0°C) water, and dried and stored over silica gel, under reduced pressure, at -5°C. These complexes rapidly lose ethene in solution at room temperature.

The deuterated analogues were prepared from 1,10-phenanthroline-d_8 monohydrate (98% isotopic purity from Merck, Sharp and Dohme (Canada) Ltd.) and $K[Pt(C_2H_4)Cl_3]\cdot H_2O$. Yields of between 83 and 89% were obtained. Microanalytical data are given in Table 2.3.

The bromo analogues could not be prepared, repeated attempts yielding a mixture of $[Pt(phen)(C_2H_4)Br_2]$ and $[Pt(phen)Br_2)$.

4.12 Preparation of the CO analogues of the Zeise's salt derivatives

The complexes *trans*-[Pt(CO)X_2] (L = quin, quinO, pzO, pdz and their fully deuterated analogues; X = Cl, Br) and *cis*-[Pt(LH)(CO)X_2]X (L = bipyO_2 and bipy-d_8O_2; X = Cl, Br) were prepared by bubbling CO through a solution of the ethene analogue in dry chloroform (or a suspension in the case of the cation with bipyO_2), until the colour changed from bright yellow to pale yellow or ivory. Precipitation of the complex was induced by the addition of dry *n*-hexane. The precipitate was filtered, washed well with dry hexane and dried over silica gel, under reduced pressure. Yields were practically quantitative. Microanalyses are given in Table 2.3. The CO analogues decompose in the presence of water.

The CO analogues of the Zeise's salt derivatives with bipy and with phen could not be prepared because of rapid loss of ethene in solution from the latter.

1. J. PADMOS and A. VAN VEEN,
Spectrochim. Acta, 38A (1982) 97.

2. A.N. SPECA, L.L. PYTLEWSKI and N.M. KARAYANNIS,
Inorg. Nucl. Chem. Lett., 9 (1973) 365.

3. *Model 983 Infrared Spectrophotometer Operator's Manual,* (1981) Perkin-Elmer, England.

4. *Spectrometer Technical Manual M091-0033,* (1975) Digilab Inc., U.S.A. (Mass.).

5. T.R. GILSON and P.J. HENDRA,
Laser Raman Spectroscopy, (1970) Wiley-Interscience, London.

6. G.J. THOMAS,,
'Raman Spectroscopy' in *Physical Methods in Heterocyclic Chemistry, Vol. 3* (1971) A.R. Katritzky (Ed.), Academic Press, London.

7. C.F. KOELSCH and W.H. GUMPRECHT,
J. Org. Chem., 23 (1958) 1603.

8. B. KLEIN and J. BERKOWITZ,
J. Amer. Chem. Soc., 81 (1959) 5160.

9. C.J. POPP and G.D. GARLOUGH,
J. Inorg. Nucl. Chem., 43 (1981) 501.

10. S. SZÖKE, GY. VARSÁNYI and E. BAITZ,
Acta Chim., 54 (1967) 145.

11. A.G. MORITZ and D.B. PAUL,
Aust. J. Chem., 22 (1969) 1305.

12. P.G. SIMPSON, A. VINCIGUERRA and J.V. QUAGLIANO,
Inorg. Chem., 2 (1963) 282.

13. D. WENKERT and R.B. WOODWARD,
J. Org. Chem., 48 (1983) 283.

14. E. OCHIAI,
J. Org. Chem., 18 (1953) 534.

15. P. HAMM and W.V. PHILIPSBORN,
Helv. Chim. Acta, 54 (1971) 2363.

16. C.J. POUCHERT (Ed.),
The Aldrich Library of Infrared Spectra (3rd Ed.), (1981) 1423, Aldrich Chemical Co., Wisconsin.

17. C.J. POUCHERT (Ed.),
The Aldrich Library of NMR, Vol 2 (2nd Ed.), (1983) 778, Aldrich Chemical Co., Wisconsin.

18. E.J. COREY, A.L. BORROR and T. FOGLIA,
J. Org. Chem., 30 (1965) 288.

19. G.M. MERKER and F.H. CASE,
J. Amer. Chem. Soc., 80 (1958) 2745.

20. Z. DEGA-SZAFRAN,
Rocz. Chem., 46 (1972) 827.

21. E.J. HALBERT, C.M. HARRIS, E. SINN and C.J. SUTTON,
Aust. J. Chem., 26 (1973) 951.

22. L.C. NATHAN, J.E. ARMSTRONG and R.O. RAGSDALE,
Inorg. Chim. Acta, 35 (1979) 293.

23. O. BUCHARDT, A.M. DUFFIELD and R.H. SHAPIRO,
Tetrahedron, 24 (1968) 3139.

24. A.M. DUFFIELD and O. BUCHARDT,
Acta Chem. Scand., 26 (1972) 2423.

25. J. CHATT and M.L. SEARLE,
Inorg. Synth., 5 (1957) 210.

CHAPTER 3

THE LIGANDS

It was noted in Chapter 1 that an understanding of the ligand vibrations is advantageous in predicting the possible changes within the vibrational spectra on complexation. One of the most widely studied vibrational systems is that of benzene. The benzene modes were first described by WILSON [1], and are depicted in Fig. 3.1. VARSÁNYI and SZÖKE [2] have presented a comprehensive review of the vibrational spectra of benzene derivatives in which they account for the vibrational coupling experienced by the benzene derivatives in terms of the nature and position of the substituents.

The ligands being examined in the present investigation were chosen because of the absence in the literature of ligand isotopic studies of the metal complexes of these azines and their *N*-oxides. It is anticipated that, with the understanding of the coupling experienced by benzene derivatives, the vibrational assignment of both the free ligands and their complexes will be simplified because of the similarity of these ligands to benzene derivatives.

The validity of extending the nature of the coupling experienced by benzene to azines and their *N*-oxides, and the possibility of using a unified vibrational description (namely WILSON's notation) needs to be examined.

1. THE ADOPTION OF A UNIFIED VIBRATIONAL NOTATION

VARSÁNYI and SZÖKE [2] state that since the benzene nucleus dominates in the determination of the force field of the vibrating molecule, then for substituted benzenes the normal modes of a derivative can be *compared* to the appropriate normal modes of vibration of benzene. This remains a formal treatment, however, because the normal vibrations of a benzene derivative cannot be *directly related* to any normal mode of benzene by a continuous function since the substituent introduces qualitative changes into the properties of

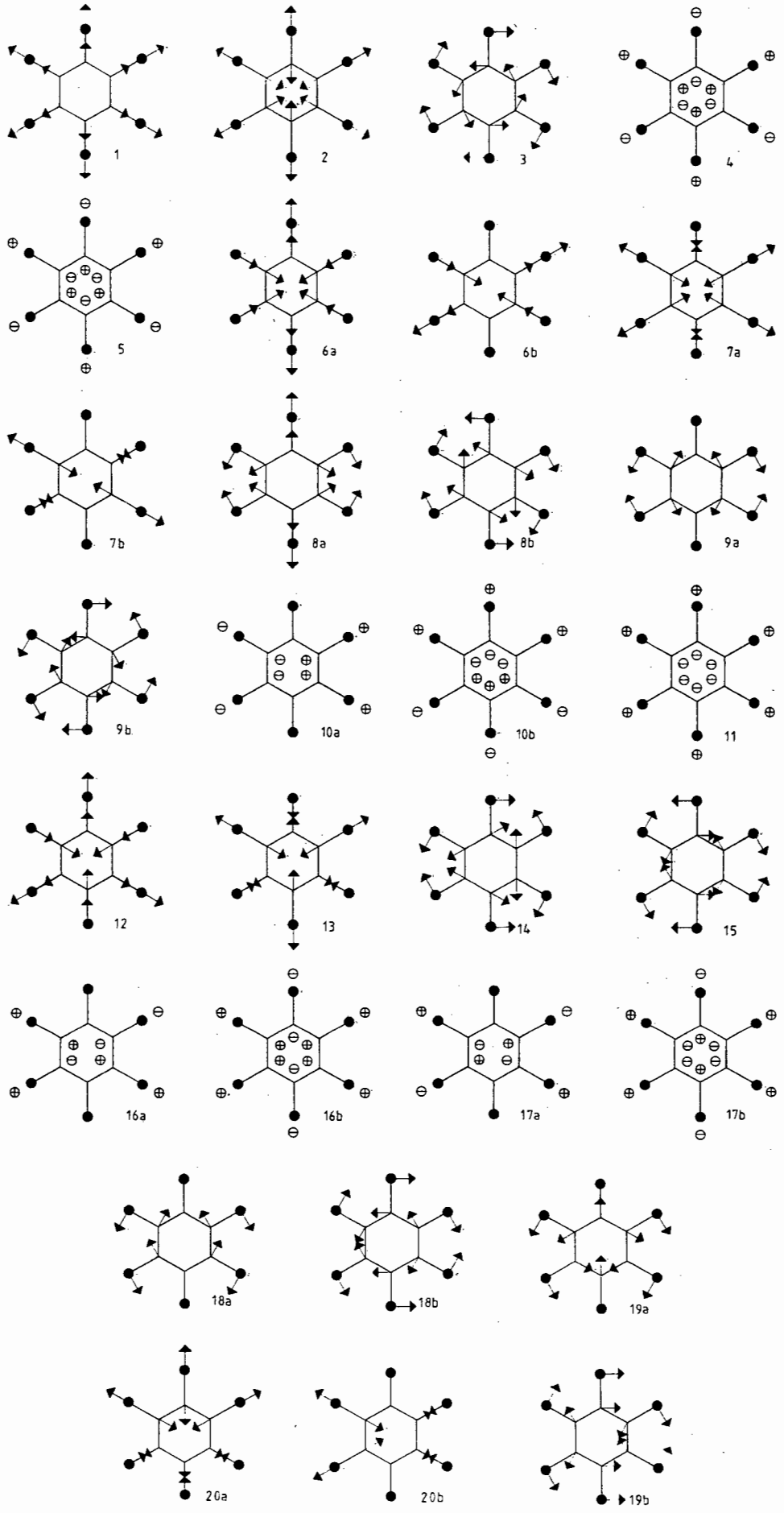

Figure 3.1 WILSON's Vibrational modes of benzene

the mechanical system represented by the molecule [2,3].

The extension of this comparison to azine *N*-oxides is based upon the similarity of the interatomic distances and reduced masses, and of the isoelectronic nature of a fluorobenzene and an azine *N*-oxide. Their force fields are transferable to a more satisfactory extent than is usual in related molecules [4,5]; the C-F and N-O bonds having nearly equal stretching force constants in the two force fields and - to a lesser degree - there is some agreement with the substituent bending and ring stretching force constants. Monocyclic azine *N*-oxide systems have therefore been described in terms of the WILSON notation and compared with substituted benzenes [4-8].

Application of the WILSON notation to a description of the normal modes of pyridine has long been employed by others [9-12].* This practice assumes that the force constants are not greatly affected on replacing the methine group by the isoelectronic nitrogen atom, neither is the mass effect regarded as significant.

Three C-H modes are 'lost' on passing from benzene to pyridine - one stretch, one planar bend and one out-of-plane bend. KLINE and TURKEVICH [9] presented the first extensive vibrational analysis of pyridine by comparison with benzene. The modes they chose to omit were WILSON's modes 7a, 9b and 17b [9], a choice which they acknowledged as being highly arbitrary. The omission of these modes has subsequently been adopted by other workers [10-14].

Normal coordinate treatments of various pyridines have been conducted by

---

* An alternate notation of the vibrational modes of benzene - that of WHIFFEN - has also been applied to substituted pyridine systems [12].

LONG and his co-workers [15-17] in which they transferred the valence force constants from benzene, allowing for the change in symmetry between the two molecules. They questioned the use of the WILSON notation since they found that many of the actual modes of pyridine are linear combinations of two or more symmetry coordinates of the same class [17]. Two slightly different schemes of frequency notation were then proposed; LONG, MURFIN and THOMAS [15] and LONG, THOMAS and GEORGE [16,17]. The latter scheme has been adopted by some authors [18-20], while others have retained the original WILSON notation [10-14,21,22].

HARSÁNYI and KILÁR [22] recently carried out a normal coordinate treatment in which a separate force field for pyridine was calculated. They too, employed the WILSON notation. This work showed that the nitrogen influences the force field (as compared with that of benzene) more than had been anticipated earlier, and that the greater complexity of the force field for pyridine discredits those simplifications made by LONG and others.

Since the transferability of the force constants from benzene to pyridine is not as justifiable as that found for the azine *N*-oxides, the use of the WILSON notation for pyridine and other azines might rightly be questioned. That the modes of pyridine are linear combinations of 2 of more symmetry coordinates is evident from their shifts to *both* higher and lower frequencies [9,13]. However, in light of the work of HARSÁNYI and KILÁR, the alternative scheme of LONG, THOMAS and GEORGE also needs to be re-examined.

While both schemes are therefore not fully satisfactory, in view of the utilisation of the WILSON notation by most authors, and for the sake of a unified discussion of the ligands under investigation, the normal vibrations referred to for both the monocyclic azines and their *N*-oxides are those of

benzene, as defined by WILSON [1].

In adopting WILSON's notation for the azines, a change is required to the choice of modes which were arbitrarily omitted by KLEIN and TURKEVICH [9]. VARSÁNYI [2,23-25] has identified two alternatives for describing the C-X vibrations of a substituent benzene. These are: 13, 9 and 17b for a *light* substituent, and 7b, 9b and 10b for a *heavy* substituent (*light* and *heavy* are defined below in Section 1.1).

Since the N-O group of azine *N*-oxides is considered *light* according to VARSÁNYI's classification, it is preferable to use mode 13 for the 'lost' C-H stretch rather than KLINE and TURKEVICH's 7b. The 'lost' C-H modes for the monocyclic azines defined in this work are thus: 13, 9b and 17b.

Due to the increasing complexity of the vibrational spectra of larger, fused polycyclic hydrocarbons, there is not a complete understanding of the vibrational coupling on substitution as in the case for benzene. Nevertheless, the WILSON notation has been used in some partial assignments of fused heterocycles [26-28]. These consider the overall spectrum of the molecule to be a composition of the spectra of two (or more) substituted benzene rings, where the vibration of one ring is regarded as being independent of the other(s) [28,29]. However, as shown by napthalene [30,31], the presence of the fused ring introduces an increased coupling within the molecule, compared with that of benzene. This makes such a direct relationship debatable.

Furthermore, in their normal coordinate work on the out-of-plane vibrations of aza-aromatic molecules, CHAPPELL and ROSS [32] comment on the difficulty of comparing these with those of napthalene because of the need to allow for

the loss of a degree of freedom (for the 'lost' γC-H) for each aza-substitution. For while the skeletal (ring) modes correlate well (in an intuitive way) the γC-H modes have slightly different forms of vibration [32]. This is in effect the same objection that LONG and his co-workers [15-17] raised to the employment of the WILSON notation to pyridine.

Thus in the same manner that the monocyclic azines and their *N*-oxides are compared with benzene in this work, and with the same reservations, the vibrations of the fused heterocycles are compared with their fused polycyclic hydrocarbon parent, and the respective notational system is adopted accordingly.

1.1 Factors affecting the Coupling experienced in Substituted Benzenes

An examination of the normal modes of benzene (Fig. 3.1) shows that in considering the individual atomic displacements, the modes of vibration (with the exception of the pair 19*) lie in three directions: RADIAL, TANGENTIAL and OUT-OF-PLANE. Within this classification, the modes of vibration may be further divided into C-H modes and ring, or skeletal, modes.

It is the coupling of these ring modes and C-H modes (or C-X modes for substituted benzenes) which makes even a qualitative assignment of the substituents complicated. As discussed in Chapter 1, the factors that determine which modes couple together are governed by both symmetry conditions and the similarity of the energies of the force constants. That is, the degree of coupling experienced in substituted benzenes is regulated by the *nature* of

---

* The displacements of the pair 19 do not fall into one category alone, but are nevertheless regarded as a C-C stretch and considered as tangential [2].

and *position* of the substituents, as well as the type of vibration being considered; radial, tangential or out-of-plane.

VARSÁNYI [2,23-25] found that the important influence in the nature of the substituent is the strength of the C-C bond. Based on the principle that the lighter atoms of the periodic table have *2p* electrons and so form stronger bonds than those atoms having *3p* orbitals, one can consider the substituent (X) as *light* (less than 25 a.m.u.) or *heavy*. There are a few exceptions to this where the bonding of the atom attached to the ring is so weak that it is considered *heavy*; for example $-CF_3$ [2,23].

For the radial vibrations the first atom of a polyatomic substituent is the one which has the decisive role in the classification of the substituent [2, 23]. This holds true since the kinetic energy of the internal vibrations of the substituent are localised predominantly to one fundamental, with the simple harmonic approximation being applicable [33]. As noted in Chapter 1, the simple harmonic diatomic approximation is not as strictly valid for bends as it is for stretches because the kinetic energy of the out-of-plane bends is not localised predominantly to one fundamental. Therefore, for the out-of-plane modes, the total mass of the whole substituting group is considered in the classification of *light* or *heavy*, so expressing the greater degree of coupling experienced by these modes [2,23].

The identification of the C-X modes in terms of WILSON's notation is important since, for symmetry reasons, the positions of the substituents regulate which modes couple together. There are twelve unique symmetry variations in which a six-membered ring might be substituted as shown in Table 3.1; each of which affects the classification of the C-X modes and hence the expected coupling. With the nature of the substituent also being important in defin-

Table 3.1 Classification of C-X modes of substituted benzenes

RADIAL

	mono	di			tri			tetra			penta
		para	meta	ortho	sym	asym	vic	para	meta	ortho	
20a							/		/		
2											/
13	/	/	/	/	/	/	/	/	/	/	/
7a		/		/	/	/		/	/	/	/
7b			/		/	/	/	/	/	/	/
20b								/		/	/

LIGHT SUBSTITUENTS

	mono	di			tri			tetra			penta
		para	meta	ortho	sym	asym	vic	para	meta	ortho	
20a											
2					/		/		/	/	/
13		/				/		/	/	/	/
7a	/	/	/	/	/	/	/	/	/	/	/
7b			/	/	/	/	/	/	/	/	/
20b								/			/

HEAVY SUBSTITUENTS

TANGENTIAL

	mono	di			tri			tetra			penta
		para	meta	ortho	sym	asym	vic	para	meta	ortho	
3								/	/	/	/
9a			/	/	/	/		/	/	/	/
9b	/	/			/	/			/	/	/
5		/	/		/		/	/	/	/	/
18a				/		/	/	/			/
18b							/				

Table 3.1 (continued)

OUT-OF-PLANE

	mono	di			tri			tetra			penta
		para	meta	ortho	sym	asym	vic	para	meta	ortho	
11											
10a											
10b											
17a											
17b											
5											

LIGHT SUBSTITUENTS

	mono	di			tri			tetra			penta
		para	meta	ortho	sym	asym	vic	para	meta	ortho	
5											
17a											
17b											
10a											
10b											
11											

HEAVY SUBSTITUENTS

(after VARSÁNYI & SZÖKE [2].)

ing the C-X mode, the number of variations further increases as substitution may also consist of a mixture of *light* and *heavy* substituents. A comprehensive discussion of all the variations of coupling experienced by substituted benzenes is beyond the scope of this work, having already been presented in the review by VARSÁNYI and SZÖKE [2]. Instead, the particular coupling expected for the relevant type of substitution will be considered while discussing each ligand in turn.

1.2 An Assessment of the Assignment of the N-O Vibrations in Pyridine *N*-oxide.

In view of the assignment of azine *N*-oxides being traditionally based upon those of pyridine *N*-oxide, it is necessary to examine the infrared assignment of the N-O vibrations of the latter.

In 1955 ITO and HATA compared the infrared and Raman spectra of pyridine *N*-oxide with those of pyridine [43]. They noted three new bands in the former at 280cm^{-1}, 470cm^{-1} and at 840cm^{-1}. These they assigned to the out-of-plane N-O bend (γN-O, WILSON mode 17b), the in-plane N-O bend (αN-O, mode 9b) and

Observed	Assignments		
cm^{-1}	ITO & HATA [34]	SHINDO [35,36]	NCA [65-68]
1250	αC-H	νN-O	νN-O (coupled)
840	νN-O	αN-O	νring (coupled)
470	αN-O	γN-O	αN-O (pure)
280	γN-O	-	γN-O (coupled)

Table 3.2 Previous assignments of the N-O vibrations of pyridine *N*-oxide

the N-O stretch (νN-O, mode 13) respectively. They assigned the strong band at 1250cm^{-1} to a C-H in-plane with some N-O character - i.e. WILSON mode 18b (Table 3.2).

SHINDO later conducted extensive investigations on pyridine *N*-oxide, examining the effect of hydrogen bonding and of substitution of the pyridine ring on the N-O modes [35,36]. He showed that the band at 1250cm^{-1} is present even in penta-substituted pyridine *N*-oxide, thereby discrediting ITO and HATA's assignment of this as being a C-H mode. SHINDO described this as being typical, rather, of a partially double bonded N-O stretch, and suggested that the band at 840cm^{-1} (ITO and HATA's N-O stretch) be better described as the in-plane, αN-O [35,36]. Unfortunately SHINDO did not extend his studies below 700cm^{-1} but, by default, the band at 470cm^{-1} has become recognised as the γN-O, while the band at 280cm^{-1} has been relegated to a non-fundamental or non-ligand vibration [37,38].

The wide acceptance of SHINDO's assignment was based upon the reduction of the frequency of the N-O stretch by hydrogen bond formation and upon the correlation of the N-O stretching frequencies with the HAMMETT substituent constant, σ [35,36]. While he did point out the probability of coupling of the N-O stretch, SHINDO did not consider it to be of significance in light of this correlation [35,36]. (By comparison, in substituted quinoline *N*-oxides, the greater coupling by the N-O stretch does not allow a correlation to be observed [39,40]). It should be noted that SHINDO found no correlation for the band at *ca.* 840cm^{-1}, his αN-O [35,36].

Acceptance of SHINDO's assignment has resulted in these N-O group frequencies being employed in vibrational assignments of pyrazine *N*-oxide and pyrazine *N,N'*-dioxide [41,42], in 2,2'-bipyridine *N*-oxide and 2,2'-bipyridine

N,N'-dioxide [43,44], in quinoline *N*-oxide [40], in quinoxaline-1-oxide [45] and quinoxaline-1,4-dioxide [46], in biquinolyl *N,N'*-dioxide [47], in 1,10-phenathroline *N*-oxide [48] and 1,10-phenathroline *N,N'*-dioxide [49,50], in phenazine-5-oxide [51] and phenazine-5,10-dioxide [52] and in various substituted analogues of these.

Moreover, recognition that the N-O stretch is sensitive to substituent effects has led to a wide usage of pyridine *N*-oxide as a ligand in transition metal chemistry [53-63]. However, HERLOCKER *et al.* [57] considered SHINDO's correlations as unsuccessful due to the substituent constant used. They preferred to use the HAMMETT substituent constants σ^+ (for strongly electron releasing substituents) and σ^- (for strongly electron with drawing substituents) [57], while NELSON *et al.* introduced σ_{pyO} constants, derived from the acid dissociation constants of protonated pyridine *N*-oxides [61]. These give better correlations with νN-O, but are unsuccessful for the *ca.* 840cm^{-1} band (SHINDO's αN-O).

It is also important to note that the band at *ca.* 840cm^{-1} in the metal complexes does not differ much from the free substituted pyridine *N*-oxides, showing small negative or positive shifts [53-60,62,63]. This has been explained as being due to the equally competitive effect of two opposing factors; the weakening of the N-O bond on complexation which would result in a shift to lower frequencies, and kinematic coupling of the N-O group with the bonded metal ion, which would increase the frequencies [54,63]. This does not, however, explain the non-correlation found in the free ligands, and indicates the possible misassignment of the 840cm^{-1} band to αN-O.

Further evidence for the misassignment of this band is the sensitive nature of the band at 280cm^{-1} to molecular interaction [64], as this suggests that

ITO and HATA's assignment of this band to γN-O is correct. This allows the 470cm^{-1} band to be assigned to αN-O and the 840cm^{-1} band to be explained as a coupled vibration. Four separate normal coordinate treatments of pyridine-*N*-oxide have been conducted [65-68], and all support such a revised assignment. They show that the band at 280cm^{-1} is best described at γN-O (mode 17b) coupled with a ring torsion (mode 16b) [66,68]. The band at 470cm^{-1} is best described as a pure αN-O (mode 9b), while the band at 1250cm^{-1} is best described as a highly coupled νN-O (mode 13), coupling predominantly with the ring-breathing mode (mode 1) at 840cm^{-1} [64-68] and lightly coupled with the ring vibrations at 1610cm^{-1} and 550cm^{-1} (modes 8a and 6a respectively) [66,68].

The identification of the band at 480cm^{-1} as the ring-breathing mode might initially be surprising, since it is found at 991cm^{-1} in pyridine and at 992cm^{-1} in benzene [13]. However, this lower frequency is in accord with mono-light substituted benzenes, in which the C-X stretching vibration (mode 13 - expected at about 1000cm^{-1}) couples with the ring-breathing vibration (mode 1 - also expected at about 1000cm^{-1})to produce two highly-coupled bands, one above 1100cm^{-1} (identified as νC-X) and one below 900cm^{-1} (identified as the ring-breathing mode) [2,23]. Such coupling is produced because modes 1 and 13 have the same symmetry (both A_1) and similar energy in their force constants. A similar type of coupling is also experienced in mono-light substituted pyridines [13,69].

The identification of αN-O at 470cm^{-1} and γN-O at 280cm^{-1} is important since the latter is often misassigned in metal complexes as a purely metal-ligand vibration, such as an O-M-O bend [38,70].

This revised assignment for the N-O vibrations has been adopted by several

authors for pyridine *N*-oxide [71-75], as well as for a few other azine *N*-oxides [4,7,8]. It has, however, not received mention in the most recent reviews on metal complexes of aromatic amine *N*-oxides [76,77] and most post-1980 literature still applies SHINDO's assignments to complexes of aromatic *N*-oxides [78-89]. This reveals the necessity of the present work in examining the vibrational assignments of such ligands.

2. VIBRATIONAL ASSIGNMENT OF SOME AZINE *N*-OXIDES

2.1 Pyrazine *N,N'*-dioxide (pzO_2)

The assignment of the fundamentals of pyrazine *N,N'*-dioxide (pzO_2) and its fully deuterated analogue ($pz\text{-}d_4O_2$) are based firstly upon considering pzO_2 as a *para*-di-light substituted benzene, secondly upon the vibrational assignment of pyO, thirdly upon the partial normal coordinate treatment, and the infrared and Raman spectra, of pzO_2, fourthly upon the ν^D/ν^H ratio, and fifthly by comparison with the reported spectra of pyrazine (pz) and its $-d_4$ analogue.

The latter comparison is made difficult by the existence of two phase transitions of pz: Form I <28°C; Form II 28-35°C and Form III 35-52°C [94,95]. This has led to some complications in the vibrational assignment since the crystal structure of Form I only is known, while the vibrational spectra have been collected at various temperatures and hence reflect different polymorphs. The assignments of pz and $pz\text{-}d_4$ in Tables 3.3 and 3.4 are generally those of SBRANA *et al.* [91], with the following exceptions:

Firstly, the assignment of modes 20b and 13 by SBRANA *et al.* [91] have been reversed. This is in accordance with ZAREMBOWITCH and BOKOBZA-SEBAGH [92]

WILSON Mode [1] (a)	pzO_2 (This work)	pzO_2 SZÖKE *et al.* [7]	pzO_2 Normal Coordinate Calc. [4]	p-$C_6H_4F_2$ [99-102]	p-xylene [96,97]	pyO [67,68]	pz [90-93]	pz-d_4O_2 (This work)	p-$C_6D_4F_2$ [101-103]	pz-d_4 [91,93]
20a	3075	3065	3073	3073	(3045)	3070	3015	2271	2277	2259
20b	3107	3115	3102	(3086)	(3056)	3102	3066	2308	2310	2278
19a	1487	1491	1525	1511	1522	1466	1483	1406	1435	1532
19b	1456	1450	1462	1437	1403	1482	1419	1355	1328	1264
18a	1047	1035	1029	1012	1022	1043	1139	900	859	1027
18b	1125	1130	1127	1085	1125	1070	1068	866	802	839
17a	(953)	(970)	-	(943)	(974)	977	(960)	(744)	(752)	-
17b	186	(200)	-	157	153	226	-	177	156	-
16a	(393)	(400)	-	(405)	(403)	415	(350)	(358)	(357)	-
16b	536	542	-	508	484	512	417	460	422	401
15	417	412	396	352	295	1149	-	412	348	-
14	1292	1306	1283	1306	1286	1364	1148	1252	1286	1105
13	1264	1265	1222	1225	1226	1252	-	1186	1130	-
12	874	880	825	737	730	1017	1026	791	685	882
11	805	810	-	836	801	769	785	737	732	597
10a	852	(830)	-	800	846	829	941	662	614	721
10b	958	952	-	928	936	909	975	830	793	840
9a	1191	1181	1151	1142	1182	1170	1248	882	867	1002
9b	519	(460)	442	(460)	389	468	-	492	(430)	-
8a	1637	1644	1658	1617	1619	1604	1581	1594	1595	1537
8b	1631	1620	1610	1617	1581	1556	1521	1589	(1585)	1502
7a	1286	1300	1270	1257	1205	3000	-	1290	1250	-
7b	3038	3020	3034	3084	(3042)	3070	3030	2301	2304	2273
6a	484	394	476	451	460	544	598	483	453	581
6b	684	(630)	628	635	646	636	697	660	(619)	680
5	374	294	-	375	313	977	-	351	366	-
4	699	694	-	692	699	675	754	627	600	647
3	1334	1310	1287	1285	1314	1329	1358	1038	1008	1027
2	3048	3060	3077	3084	(3059)	3012	3046	2313	2313	2286
1	879	888	851	858	830	837	1014	830	780	899

estimated frequencies in parenthesis

(a) for pz 20a ≡ 13, 18b ≡ 15, 10b ≡ 5 (see Text)

Table 3.3 The fundamentals of pyrazine *N*,*N'*-dioxide (pzO_2) and its -d_4 analogue (pz-d_4O_2) compared with similar molecules

WILSON Mode[a] [1]	pz [90-93]	pz-d_4 [91,93]	ν^D/ν^H	p-$C_6H_4F_2$ [99-102]	p-$C_6D_4F_2$ [91,93]	ν^D/ν^H	pzO_2 (This work)	pz-d_4O_2 (This work)	ν^D/ν^H	Assignment
20a	3015	2259	0,749	3037	2277	0,741	3075	2271	0,738	ν C-H/D
20b	3066	2278	0,743	(3086)	2310	0,748	3107	2308	0,743	ν C-H/D
19a	1483	1352	0,912	1511	1435	0,950	1487	1406	0,945	ν ring
19b	1419	1264	0,891	1437	1328	0,924	1456	1355	0,931	ν ring
18a	1139	1027	0,902	1012	859	0,849	1047	900	0,860	α C-H/D
18b	1068	839	0,786	1085	802	0,739	1125	866	0,770	α C-H/D
17a	(960)	-	-	(943)	(752)	0,797	(953)	(744)	0,780	γ C-H/D
17b	-	-	-	157	156	0,994	186	177	0,952	γ N-O + γ ring
16a	(350)	-	-	(405)	(357)	0,881	(393)	(358)	0,911	γ ring
16b	417	401	0,962	508	422	0,831	536	460	0,858	γ ring + γ N-O
15	-	-	-	352	348	0,989	417	412	0,988	α N-O
14	1148	1105	0,962	1306	1286	0,985	1292	1252	0,969	ν ring
13	-	-	-	1225	1130	0,922	1264	1186	0,938	ν N-O + ν ring
12	1026	882	0,860	737	685	0,929	874	791	0,905	ν ring + ν N-O
11	785	597	0,760	836	732	0,876	805	737	0,916	γ C-H/D
10a	941	721	0,766	800	614	0,768	852	662	0,777	γ C-H/D
10b	975	840	0,862	928	793	0,855	958	830	0,866	γ C-H/D
9a	1248	1002	0,803	1142	867	0,759	1191	882	0,740	α C-H/D
9b	-	-	-	(460)	(430)	0,936	519	492	0,948	α N-O
8a	1581	1537	0,972	1617	1595	0,986	1637	1594	0,974	α ring
8b	1521	1502	0,988	1617	(1585)	0,981	1631	1589	0,974	α ring
7a	-	-	-	1257	1250	0,994	1286	1290	1,003	ν N-O + ν ring
7b	3030	2273	0,750	3084	2304	0,747	3038	2301	0,757	ν C-H/D
6a	598	581	0,972	451	453	1,004	484	483	0,998	α ring
6b	697	680	0,976	635	614	0,967	684	660	0,965	α ring
5	-	-	-	375	366	0,976	374	351	0,938	γ N-O
4	754	647	0,858	692	600	0,867	699	627	0,897	γ ring
3	1358	1027	0,756	1285	1008	0,784	1334	1038	0,778	α C-H/D
2	3046	2286	0,750	3084	2313	0,750	3048	2313	0,759	ν C-H/D
1	1014	899	0,886	858	780	0,909	879	830	0,944	ν ring + ν N-O

estimated frequencies in parenthesis

(a) for pz 20a ≡ 13, 18b ≡ 15, 10b ≡ 5 (see Text)

Table 3.4 The ν^D/ν^H ratio for pyrazine *N*,*N'*-dioxide (pzO_2) and its -d_4 analogue (pz-d_4O_2) compared with similar molecules

to explain, among other things, a band at 3713cm^{-1} (which is otherwise unaccountable) as being the combination band (13+6b).

Secondly, the spectra of the metal complexes [92] have shown that the assignment by CALIFANO *et al.* [90] of the band at 1346cm^{-1} to mode 14 is incorrect, being instead a combination band. More preferable is the suggestion by SBRANA *et al.* [9] of the possibility of the band at 1148cm^{-1} being this fundamental. This brings into question the latter's assignment of the shoulder at 422cm^{-1} to mode 16a(A_u), since this was so assigned (despite having the wrong dichroism) by considering the 1148cm^{-1} band to be a combination of (16a+4) [91]. ZAREMBOWITCH and BOKOBZA-SEBAGH's assignment of 16a at 350cm^{-1}, on the basis of combination bands, is therefore employed.

Finally, the assignment of the three out-of-plane C-H modes - 5,10a and 17a - is not conclusive, and their assignment is open to debate [92,93]. However, ZAREMBOWITCH and BOKOBZA-SEBAGH [92] concur with the assignment of SBRANA *et al.* [91] of mode 5 at 975cm^{-1} and mode 10a at 914cm^{-1} (at 25°C). The latter's assignment of mode 17a(A_u) at 997cm^{-1} is based upon a very weak band in the infrared (only seen at 78K) and on the identification of a shoulder at 1128cm^{-1} as the combination (17a+3). Since the latter may also be described as the result of a Fermi resonance between the fundamental 18a and the combination (4+16a) [92], and because the assignment of mode 17a at 960cm^{-1} enables several combination bands to be explained, this latter assignment by ZAREMBOWITCH and BOKOBZA-SEBAGH [92] is preferred here.*

It should also be noted that the six benzene modes 'lost' in the assignment of pz are normally given as 20a and 7a (νC-H), 18b and 9b (αC-H) and 10b and

---

* The adoption of these changes are supported by the very recent vibrational studies of pyrazine and its -d_4 analogue by ARENAS *et al.* [93].

17b (γC-H). However, according to VARSÁNYI and SZÖKE [2], for a *para*-di-light benzene these modes are considered to be 13 and 7a, 15 and 9b, and 5 and 17b, respectively. This apparent contradiction is explained by considering the displacements of the hydrogens 2,3,4 and 5 only, for which displacements of 13 and 20a, of 15 and 18b and of 5 and 10b respectively, are identical (Fig. 3.1) [2,23-25]. Such ambiguity reveals the difficulty in transferring the WILSON notation to azine systems. The description of VARSÁNYI and SZÖKE is employed here for pz, in preference to the original nomenclature.

In considering the assignments for pyO, mode 3 (αC-H) has been assigned at 1329cm^{-1} by GAMBI and GHERSETTI [68] and at 1300cm^{-1} by SZÖKE *et al.* [67]. The former is preferred and is presented in Table 3.3. The Kekulé vibration, mode 14, is assigned at 1364cm^{-1} by GAMBI and GHERSETTI [68], and at 1207cm^{-1} by SZÖKE *et al.* [67]. The former is apparently too high and the latter too low compared with the other assignments.

In comparing pzO_2 with *para*-di-light substituted benzenes, it is noted that it is possible to have coupling occur between the internal vibrations of the substituent and the ring vibrations; for example, as occurs between mode 19b (αC-H) and a methyl C-H bend in toluene [96]. The assignments of *p*-xylene (Table 3.3) have been employed since the Potential Energy Distributions (PED's) of these have also been published [96,97] and the extent of such coupling can be examined. No significant coupling (greater than a 10% contribution to the overall PE of the vibration) between the ring vibrations and the internal methyl vibrations is observed. The assignments for *p*-$C_6H_4F_2$ are also included in view of the isoelectronic nature of the C-F and N-O groups.

Lastly, there have been few vibrational assignments undertaken for *para*-di-light substituted benzenes in which the ring protons have been fully deuterated, as reflected by the paucity of data in Table 3.4.

The molecule pz is planar and belongs to the point group D_{2h} [98]. As the N-O bonds are expected to be planar, the *N,N'*-dioxide (pzO_2) is also expected to have the same point group. The molecular axes adopted for pzO_2 are the same as for pz [90]. The Y-axis is taken perpendicular to the molecular plane and the X- and Z-axes in the plane, the Z-axis passing through the nitrogens and oxygens.

For D_{2h} symmetry, thirteen infrared active fundamentals ($5B_{1u}$, $3B_{2u}$ and $5B_{3u}$ species) and fifteen Raman active fundamentals ($6A_g$, $1B_{1g}$, $5B_{2g}$ and $3B_{3g}$ species) are expected. The two expected A_u vibrations are both Raman and infrared forbidden.

An investigation of the infrared and Raman spectra (Tables 3.5 and 3.6) reveals spectra rich in overtone, combination and difference bands, besides the expected fundamentals. These have been assigned following the procedure of BRODERSEN and LANGSETH [104]. Where more than one combination assignment is possible, all alternatives are given; polarisation studies will be necessary for the conclusive assignment of these.

Finally, the correctness of the assignments for pzO_2 and its fully deuterated analogue are assessed in light of the Product Rule. All species, except B_{1g}, B_{2g} and B_{3g}, are free of a rotation about the X, Y or Z axes and so are independent of the moments of inertia of the molecule. In the absence of crystallographic data for pzO_2, two slightly different models have been presented to determine the moments of inertia and hence the Product Rule for

3.5 Infrared and Raman spectra of pyrazine *N*,*N'*-dioxide (pzO_2)

Raman (cm^{-1})	Infrared (cm^{-1})	Assignment
Not recorded	3164 vw	Unassigned.
	3107 m	20b(B_{3u}) fundamental.
	3075 m	20a(B_{1u}) fundamental.
3048 vs		2(A_g) fundamental.
3038 sh	3035 ms	7b(B_{2g}) fundamental.
2969 wm		8a+3(B_{2g}); $19a^2$(A_g).
	2966 m	Unassigned.
	2935 m	14+8a(B_{3u}).
2933 wm		20b-17b(B_{1g}).
	2891 w	13+8b(B_{3u}).
	2820 w	19a+3(B_{3u}).
	2791 w	19b+3(B_{1u}).
	2719 vw	Unassigned.
	2676 w	19a+9a(B_{1u}); 18a+8b(B_{3u}).
	2664 w	Unassigned.
	2646 vw	19b+9a(B_{3u}); 7b-16a(B_{2u}).
	2564 w	20a-9b(B_{3u}).
	2544 wbr	13+7a(B_{1u}).
	2467 vvw	18b+3(B_{1u}).
	2420 vvw	Unassigned.
Not recorded	2283 vw	18a+3(B_{3u}).
	2335 vw	19b+1(B_{3u}); 18a+7a(B_{1u}).
	2276 vw	Unassigned.
	2170 vvw	14+1(B_{3u}); 16b+8a(B_{2u}); 2-12(B_{1u}); 7b-12(B_{1u}).
	2135 vvw	13+1(B_{1u}).
	2085 w	7b-17b(B_{2u}); 11+7a(B_{2u}).
	1991 w	7b-18a(B_{1u}); 11+9a(B_{1u}).
	1923 w	18a+1(B_{1u}); 2-18b(B_{3u}).
	1864 vw	19a+5(B_{2u}).
	1810 wbr	14+9b(B_{1u}); 17a+10a(B_{1u}).
	1764 w	11+10b(B_{1u}).
	1727 w	16a+3(B_{2u}); 16b+9a(B_{2u}).
1682 m		15+13(B_{2g}); 12+11(B_{3g}); 16a+14(B_{3g}).
1637 vs		8a(A_g) fundamental; 19a+17b(B_{1g}).
1631 sh		8b(B_{2g}) fundamental.
	1595 vw	2-9b(B_{3u}).
1589 wm		20a-19a(A_g); 18a+16b(B_{3g}).

Table 3.5 (continued)

Raman (cm^{-1})	Infrared (cm^{-1})	Assignment
1486 m		$7a+16b(B_{2g})$.
	1490 m 1484 m	$19a(B_{1u})$ fundamental; $16b+10b(B_{1u})$.
	1456 vs	$19b(B_{3u})$ fundamental; $8a-17b(B_{2u})$.
1397 w		$4^2(A_g)$; $9b+1(B_{2g})$; $7b-8a(B_{2g})$.
	1380 vw	$17b+9a(B_{2u})$.
1339 w		$3(B_{2g})$ fundamental; $16b+11(A_g)$; $10a+6a(B_{1g})$.
1295 sh		$12+15(B_{2g})$; $19a-17b(B_{3g})$.
	1292 m	$14(B_{3u})$ fundamental; $15+1(B_{3u})$; $11+6a(B_{2u})$.
1286 s		$7a(A_g)$ fundamental.
1276 ms		$19b-17b(B_{1g})$.
	1265 vssh 1263 vs	$13(B_{1u})$ fundamental; $15+10a(B_{2u})$.
	1235 m	$16b+4(B_{1u})$; $16a+8b(B_{2u})$.
1200 m		$16a+11(B_{2g})$.
1191 s		$9a(A_g)$ fundamental.
	1182 w	$11+5(B_{1u})$.
	1125 vw	$18b(B_{3u})$ fundamental.
1079 w		$13-17b(B_{3g})$; $5+4(A_g)$.
	1079 w	Unassigned.
	1047 s	$18a(B_{1u})$ fundamental.
	1003 vvw	$19a-9b(B_{3u})$; $9a-17b(B_{2u})$.
	965 vw	$19a-6a(B_{1u})$.
958 vw		$10b(B_{3g})$ fundamental; $3-5(B_{2g})$; $16b+15(B_{1g})$.
	899 w	$15+6a(B_{3u})$.
879 vs		$1(A_g)$ fundamental; $14-15(A_g)$.
	874 ms	$12(B_{1u})$ fundamental.
852 m		$10a(B_{1g})$ fundamental; $3-6a(B_{2g})$; $13-15(B_{2g})$.
	805 vs	$11(B_{2u})$ fundamental; $14-6a(B_{3u})$.
	735 wsh	Unassigned.
	720 w	Unassigned.
699 m		$4(B_{3g})$ fundamental.
684 vs		$6b(B_{2g})$ fundamental; $19a+11(B_{3g})$; $12-17b(B_{3g})$.
	684 vw	$17a-8a(B_{2u})$.
	536 m	$16b(B_{2u})$ fundamental.
519 vw		$9b(B_{2g})$ fundamental; $18a-16b(B_{3g})$.
484 vw		$6a(A_g)$ fundamental; $3-10a(B_{3g})$; $12-16a(B_{1g})$; $14-11(B_{1g})$.

Table 3.5 (continued)

Raman (cm^{-1})	Infrared (cm^{-1})	Assignment
	478 vw	7a-11(B_{2u}); $R_x(B_{1g})$-15(B_{2u}).
	431 m	1-5(B_{1u}); 5+$T_y(B_{1u})(B_{2u})$; 10a-15(B_{2u}).
	417 s	15(B_{3u}) fundamental; 14-1(B_{3u}).
374 m		5(B_{3g}) fundamental; $17b^2(A_g)$; 3-10b(B_{1g}).
	237 vw	18a-7a(B_{1u}).
	186 m	17b(B_{2u}) fundamental; 5-17b(B_{1u}).
	119 vw	$T_y(B_{1u})$+$R_x(B_{2g})(B_{3u})$.
118 m		$R_z(B_{3g})$ libration; 15-16b(B_{1g}).
	103 vw	17a-10a(B_{1u}); 17b-$R_z(A_g)(B_{2u})$; 11-4(B_{1u}).
	95 w	8b-19a(B_{3u}).
84 vs		$R_z(A_g)$ libration; 18a-10b(B_{2g}); 18b-18a(B_{2g}).
	74 vw	$T_x(B_{2u})$ translation; 1-11(B_{2u}); 13-9a(B_{1u}).
65 m		$R_x(B_{2g})$ libration; 12-11(B_{3g}).
	55 w	$T_y(B_{1u})$ translation; 20b-2(B_{3u}).

s = strong

m = medium

w = weak

v = very

sh = shoulder

br = broad

3.6 Infrared and Raman spectra of pyrazine-d_4 N,N'-dioxide (pz-d_4O_2)

Raman (cm^{-1})	Infrared (cm^{-1})	Assignment
Not recorded	3092 vw	7b+12(B_{3u}).
	3057 vw	11+2(B_{2u}).
	3017 vw	Unassigned.
	2944 vw	19b+8b(B_{1u}); 19b+8a(B_{3u}).
	2777 vw	13+8b(B_{3u}); 13+8a(B_{1u}); 16b+2(B_{2u}).
	2641 w	7a+19b(B_{3u}).
	2605 w	Unassigned.
	2467 w	18b+8a(B_{3u}).
	2393 vw	19b+3(B_{1u}).
	2365 vw	Unassigned.
2313 m		2(A_g) fundamental.
	2308 s	20b(B_{3u}) fundamental.
2301 s		7b(B_{2g}) fundamental.
	2289 m	19a+9a(B_{1u}); 3+14(B_{1u}).
2287 m		Unassigned.
2270 s	2271 s	20a(B_{1u}) fundamental; 19a+18b(B_{2g}).
	2215 w	Unassigned.
	2178 w	19b+1(B_{1u}).
2174 w		7a+9a(A_g).
Not recorded	2062 vw	19a+6b(B_{3u}); 13+9a(B_{1u}); 12+7a(B_{1u}).
	2025 w	7a+11(B_{2u}).
	1948 w	16a+8b(B_{2u}).
	1873 vw	Unassigned.
	1805 w	Unassigned.
	1780 wbr	20a-9b(B_{3u}); 18a+9a(B_{1u}); 3+17a(B_{2u}).
	1729 w	18a+1(B_{1u}); 14+6a(B_{3u}).
	1690 w	18b+1(B_{3u}).
	1669 w	13+9b(B_{3u}); 12+9a(B_{1u}).
	1627 w	12+1(B_{1u}).
1604 w		18b+11(A_g).
1594 m		8a(A_g) fundamental; 13+15(B_{2g}).
1589 sh		8b(B_{2g}) fundamental; 19a+17b(B_{3g}).
1578 w		12^2(A_g).
1562 vvw		20b-17a(B_{3g}).
	1562 w	11+1(B_{2u}); 18a+9a(B_{1u}).
1549 w		10a+9a(B_{1g}).
	1545 w	13+5(B_{2u}).

Table 3.6 (continued)

Raman (cm^{-1})	Infrared (cm^{-1})	Assignment
1486 w		$2\text{-}1(A_g)$; $10a\text{+}1(B_{1g})$: $20a\text{-}12(A_g)$.
	1480 vw	$20b\text{-}1(B_{3u})$.
1470 wsh		$7b\text{-}1(B_{2g})$; $11^2(A_g)$.
1463 w		$4\text{-}1(B_{3g})$.
	1435 w	$7b\text{-}18b(B_{1u})$; $20a\text{-}1(B_{1u})$.
	1429 w	$20b\text{-}9a(B_{3u})$.
1416 vw		$7b\text{-}9a(B_{2g})$.
	1406 m	$19a(B_{1u})$ fundamental; $7a\text{-}18a(B_{3u})$.
	1394 wm	$18a\text{+}9b(B_{3u})$; $16a\text{+}3(B_{2u})$.
	1355 vs	$19b(B_{3u})$ fundamental; $18b\text{+}9b(B_{1u})$; $18b\text{+}6a(B_{3u})$.
1359 vw		$18a\text{+}16b(B_{1g})$; $13\text{+}17b(B_{3g})$.
1314 vvw		$1\text{+}6a(A_g)$; $6b^2(A_g)$.
1290 m		$7a(A_g)$ fundamental; $10a\text{+}4(B_{2g})$; $4\text{+}6b(B_{1g})$.
	1288 mw	$9a\text{+}15(B_{3u})$; $9b\text{+}12(B_{3u})$.
1277 wm		$2\text{-}3(B_{2g})$; $15\text{+}18b(A_g)$.
	1252 w	$14(B_{3u})$ fundamental; $18a\text{+}5(B_{2u})$.
	1239 vw	$15\text{+}1(B_{2u})$; $9b\text{+}17a(B_{2u})$; $20a\text{-}3(B_{3u})$.
1205 vw		$16b\text{+}17a(B_{2g})$; $15\text{+}12(B_{2g})$.
	1191 w	Unassigned.
	1186 ms	$13(B_{1u})$ fundamental; $8a\text{-}15(B_{3u})$.
1150 w		$15\text{+}11(B_{1g})$; $6a\text{+}12(B_{1g})$; $9a\text{+}6b(A_g)$; $10a\text{+}9b(B_{3g})$.
	1148 w	$12\text{+}5(B_{2u})$.
	1117 w	$7b\text{-}13(B_{3u})$; $7a\text{-}17b(B_{2u})$; $16b\text{+}10a(B_{3u})$.
	1090 vw	$11\text{+}5(B_{1g})$; $16b\text{+}4(B_{1u})$; $5\text{+}17a(B_{3u})$.
	1040 vvw	Unassigned.
1038 vw		$3(B_{3g})$ fundamental; $2\text{-}7(A_g)$; $18b\text{+}17b(B_{1g})$.
	1001 vvw	$17b\text{+}1(B_{2u})$.
	984 w	$4\text{+}16a(B_{3u})$; $20a\text{-}7a(B_{1u})$.
	970 w	Unassigned.
967 w		$8a\text{-}4(B_{3g})$; $6a^2(A_g)$; $12\text{+}17b(B_{3g})$; $8b\text{-}4(B_{1g})$.
929 w		$8b\text{-}10a(B_{3g})$; $19a\text{-}16b(B_{3g})$; $8a\text{-}6b(B_{2g})$.
901 wsh		$20b\text{-}19a(B_{2g})$.
	900 s	$18a(B_{1u})$ fundamental; $15\text{+}9b(B_{1u})$; $15\text{+}6a(B_{3u})$.
894 wsh		$14\text{-}16a(B_{3g})$; $19b\text{-}16b(B_{2g})$.
882 s		$9a(A_g)$ fundamental.
	882 wsh	$7\text{-}15(B_{3u})$.
867 mw		$16b\text{+}15(B_{2g})$.

Table 3.6 (continued)

Raman (cm^{-1})	Infrared (cm^{-1})	Assignment
	866 w	18b(B_{3u}) fundamental; 19b-9b(B_{1u}).
830 ms		10b(B_{3g}) fundamental and 1(A_g) fundamental; 9b+5(B_{1g}).
	826 m	7a-16b(B_{2u}).
	791 w	12(B_{1u}) fundamental.
	774 w	19a-4(B_{2u}).
	737 s	11(B_{2u}) fundamental.
662 msh		10a(B_{1g}) fundamental; 7a-4(B_{3g}).
660 vs		6b(B_{2g}) fundamental.
	659 w	17b+6a(B_{2u}); 1-17b(B_{2u}).
657 sh		Unassigned.
627 w		4(B_{3g}) fundamental.
570 w		17b-17a(B_{2g}); 19b-12(B_{2g}).
	524 vw	19b-1(B_{1u}); 13-6b(B_{3u}); 17b+5(B_{1u}).
492 w		9b(B_{2g}) fundamental; 19b-18b(A_g).
483 wm		6a(A_g) fundamental; 1-5(B_{3g}).
	480 w	7a-12(B_{1u}).
	469 mw	9a-15(B_{3u}); 19b-9a(B_{3u}).
	460 w	16b(B_{2u}) fundamental.
412 w		7a-9a(A_g).
	412 ms	15(B_{3u}) fundamental; 18a-9b(B_{3u}); 8a-13(B_{1u}).
	380 vw	18b-6a(B_{3u}); 11-5(B_{1u}).
380 vw		12-15(B_{2g}); 11-16a(B_{2g}); 3-6b(A_g); 3-10a(B_{3g}); 14-18b(A_g).
351 w		5(B_{3g}) fundamental; 14-18a(B_{2g}); $17b^2$(A_g); 1-6a(A_g).
	339 vvw	8a-14(B_{3u}).
277 w		11-16b(A_g); 4-5(A_g); 16b-17b(A_g).
	232 vvw	8b-19b(B_{1u}).
	177 m	17b(B_{2u}) fundamental; 5-17b(B_{2u}).
	117 vw	19a-7a(B_{1u}); 4-17a(B_{3u}).
	95 w	9a-12(B_{1u}).
	74 vw	T_x(B_{2u}) translation; 11-10a(B_{3u}).
	53 w	T_y(B_{1u}) translation.

s = strong

m = medium

w = weak

v = very

sh = shoulder

br = broad

the other three species. (The motivation for these models, and the calculations of the moments of inertia are given in Appendix 2).

2.1.1 The infrared active fundamentals

The present assignment of the infrared allowed fundamentals of pzO_2 agrees well with that of SZÖKE *et al.* [7], with the exception of the N-O out-of-plane bend, mode 17b. Several other assignments need to be discussed, as well as some for pz-d_4O_2.

With the assignments of 20a(B_{1u}) and 20b(B_{3u}) for pzO_2 agreeing well with the calculated values (Table 3.3), the medium strong band at 3035cm^{-1} in the infrared (pzO_2) has tentatively been assigned to the infrared forbidden B_{2g} fundamental 7b as it cannot be accounted for as a combination band. Neither can it be considered as a Fermi resonance of 20a or even 20b since, according to BRODERSEN and LANGSETH [104], the Fermi doublet will be reproduced by the combination and difference bands of the fundamental in question. No such doublets are observed by the combination bands, neither do any combinations of B_{1u} or B_{2u} symmetry (necessary for possible Fermi resonance to occur with 20a or 20b respectively) occur in this region of the spectrum. All other major bands in the infrared spectra of both pzO_2 and pz-d_4O_2 have otherwise been assigned (Tables 3.5 and 3.6).

B_{1u} Species

The assignments of 20a, 18a, 12 and 13 for both pzO_2 and pz-d_4O_2 are unambiguous. While the ν^D/ν^H ratio of 0,938 for νN-O (mode 13) is lower than that found for pyO (ν^D/ν^H = 0,968) [105] the assignment of mode 15 to the medium strong band at 1186cm^{-1} is in agreement with the behaviour of this mode in p-$C_6H_4F_2$ (discussed below) and by the absence of a suitable band at

1225cm^{-1} (pz-d_4O_2).

The medium split band at 1490cm^{-1} and 1484cm^{-1} (pzO_2) is assigned to the first ring mode, 19a. While it is possible for Fermi resonance to exist with the B_{1u} combination 16b+10b (1494cm^{-1}), this is considered not to occur since a splitting of 6cm^{-1} in the combination bands of 19a is not observed. The splitting of the band at 1490cm^{-1} is possibly the result of a solid state effect. In the spectrum of pz-d_4O_2, 19a has been assigned to the medium band at 1406cm^{-1} rather than to the medium weak band at 1394cm^{-1}, since the latter may also be described as the B_{3u} combination 18a+9b (1392cm^{-1}). Again Fermi resonance is excluded on the basis of non-splitting of the combination bands. The unique assignments of the bands at 901cm^{-1} and 774cm^{-1} as 20b-19a(B_{2g}) and 19a+4(B_{2u}) supports this assignment of 19a (pz-d_4O_2).

The Product Rule for the B_{1u} species (Table 3.7) indicates the assignments to be reasonable. As the Rule is based upon the simple harmonic approximation, the experimental R value is likely to be higher* than the calculated R value, as the result of anharmonicity.

B_{2u} Species

The infrared allowed N-O out-of-plane bend, mode 17b, is assigned to the medium intensity bands at 186cm^{-1} (pzO_2) and 186cm^{-1} (pz-d_4O_2). This is significantly lower than that assigned by SZÖKE *et al.* [7] who calculated its frequency to be 200cm^{-1} (pzO_2) on the basis of four combination bands, since their infrared studies were only conducted to 400cm^{-1}. This new assignment

---

* Some authors define the Product Rule as the inverse of the definition given in Chapter I. This figure will therefore always be given in parenthesis. Accordingly, for this value the experimental R is expected to be *lower* than the calculated R.

Table 3.7 Product Rule of pyrazine N,N'-dioxide and its -d_4 analogue

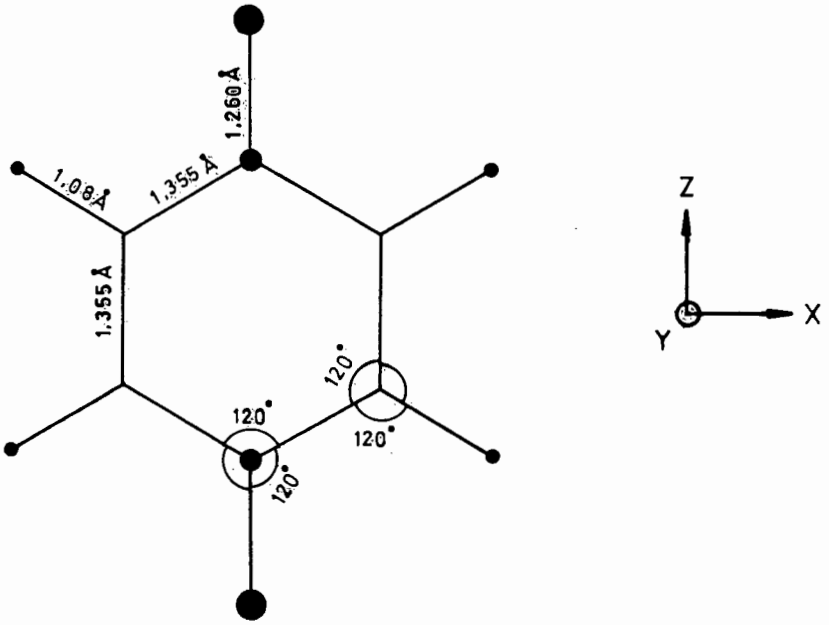

MODEL I

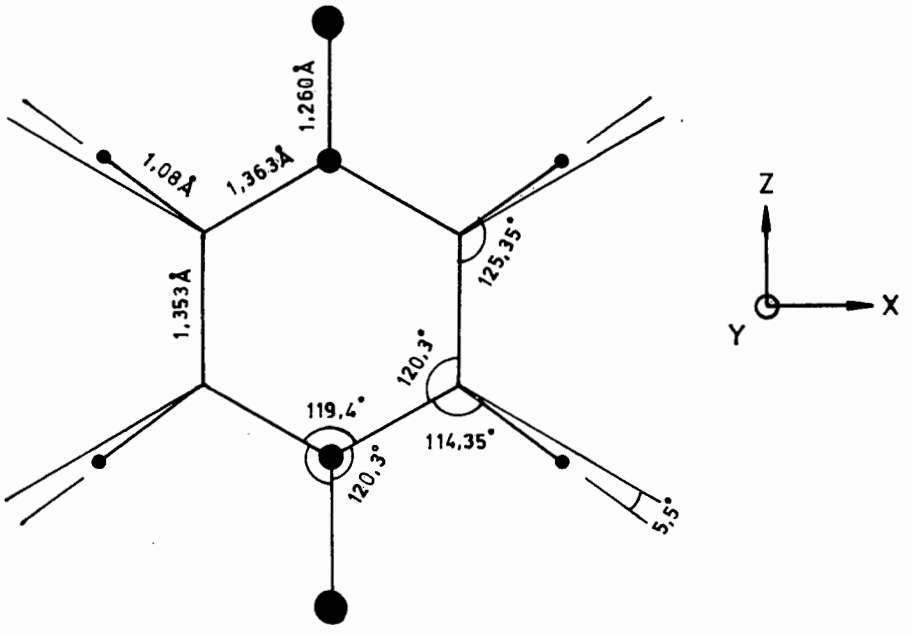

MODEL II

Table 3.7 (continued)

Species	R_{exp}		R_{calc} (a)			
			Model I		Model II	
B_{1g}	0,777	(1,287)	0,793	(1,261)	0,790	(1,266)
B_{2g}	0,525	(1,905)	0,525	(1,905)	0,525	(1,905)
B_{3g}	0,729	(1,371)	0,727	(1,375)	0,728	(1,374)
B_{1u}	0,510	(1,959)	0,509	(1,964)	0,509	(1,964)
B_{2u}	0,748	(1,337)	0,720	(1,389)	0,720	(1,389)
B_{3u}	0,509	(1,963)	0,509	(1,964)	0,509	(1,964)
A_g	0,517	(1,933)	0,500	(2,000)	0,500	(2,000)
A_u	0,711	(1,406)	0,707	(1,414)	0,707	(1,414)

(a) see Appendix 2

agrees well with that of *para*-di-light substituted benzenes.

In the infrared spectrum of pz-d_4O_2 either the medium weak band at 469cm^{-1} or the weak band at 460cm^{-1} may be assigned to the B_{2u} out-of-plane ring torsion, mode 16b. Fermi resonance is ruled out by the absence of any possible B_{2u} combinations in this region, as well as by the absence of any Fermi splitting of the combination bands of 16b. The band at 460cm^{-1} is assigned to 16b since this accounts for two unique assignments of the bands at 867cm^{-1} and 826cm^{-1} as the combinations 16b+15(B_{2g}) and 7a-16b(B_{2u}) respectively. The band at 469cm^{-1} is ascribed to the difference band 9a-15(B_{3u}) or 19b-9a(B_{3u}).

With the umbrella vibrations, mode 11, presenting no assignment difficulties, the Product Rule indicates a good assignment fit for the B_{2u} species (Table 3.7).

B_{3u} Species

The assignments of the B_{3u} fundamentals are unambiguous with the exception of that for 18b (pz-d_4O_2). Two alternatives exist, the weak band at 860cm^{-1} (with a ν^D/ν^H ratio of 0,770) or the weak shoulder at 882cm^{-1} (with a ν^D/ν^H ratio of 0,784). Comparing 18b with the equivalent vibration of *p*-$C_6H_4F_2$ is of no avail since its ν^D/ν^H ratio of 0,739 indicates that a slight difference in coupling is experienced by the two molecules. Furthermore, both assignments do not give rise to any unique combinations, and as both bands may be explained as combinations, the ambiguity of this assignment can only be clarified by their infrared gas phase contours or by a normal coordinate treatment of pz-d_4O_2. On the basis of the slightly better Product Rule (Table 3.7) the band at 866cm^{-1} is tentatively assigned to 18b.

The infrared active lattice modes

In the far infrared region, the very weak bands at 74cm^{-1} (pzO_2) and 74cm^{-1} (pz-d_4O_2) are assigned to the B_{1u} translational lattice mode (ν^D/ν^H = 1,000). The weak bands at 54cm^{-1} (pzO_2) and 53cm^{-1} (pz-d_4O_2) are assigned to the translation (ν^D/ν^H = 0,964). These agree well with those found for pz at 71cm^{-1} and 50cm^{-1} (at 270K) respectively [106]. Their ν^D/ν^H ratios also agree well with the square root of the ratio of the labelled and unlabelled molecular masses [107]; R = 0,965 (1,036). The B_{3u} translation is most likely spectroscopically silent [106].

2.1.2 The Raman active fundamentals

The assignment of the Raman allowed fundamentals of pzO_2 agree well with those of SZÖKE *et al.* [7] with the exception of the out-of-plane bend 5, and also with the in-plane N-O bend 9b, and the ring mode 6a. Several other assignments as well as some of the pz-d_4O_2 need to be discussed.

In the Raman spectrum of pz-d_4O_2 the strong band at 2270cm^{-1} has been ascribed to the Raman forbidden fundamental 20a(B_{1u}), while the medium band at 2287cm^{-1} is unassigned. All other major bands in the Raman spectra of both pzO_2 and pz-d_4O_2 have been assigned.

A_g Species

The assignment of 9a, 8a and 1 are unambiguous. The N-O stretch, mode 7a, is clearly assigned to the strong band at 1286cm^{-1} (pzO_2). In pz-d_4O_2 it is assigned to the medium band at 1290cm^{-1} (in spite of yielding a ν^D/ν^H ratio of greater than 1,000), since a Fermi resonance with the medium intensity band at 1270cm^{-1} is excluded on the basis of the absence of combinations with A_g symmetry over this range, and by the non-existence of Fermi split-

ting in the combinations involving 7a. This assignment is supported by the unique combination and difference bands (pz-d_4O_2) at 2174cm^{-1}, 984cm^{-1} and 826cm^{-1}, being 7+9a(A_g), 20a-7a(B_{1u}) and 7a-16b(B_{2u}) respectively. The significance of the ν^D/ν^H ratio of 1,003 is discussed below.

The planar ring vibration 6a is assigned to the very weak band at 483cm^{-1} (pzO_2). This is substantially higher in frequency than the assignment of SZÖKE *et al.* [7] who assigned it to a band at 394cm^{-1}, which is unobserved in our spectrum. This revised assignment is in agreement with the normal coordinate calculation, as well as with that for *p*-xylene and *p*-$C_6H_4F_2$ (Table 3.3).

The tentative assignment of mode 2, νC-H, to the medium band at 2313cm^{-1} (pz-d_4O_2) is based upon that for *p*-$C_6H_4F_2$ (also at 2313cm^{-1}). The possibility of the strong band at 2301cm^{-1} and the band at 2313cm^{-1} being in Fermi resonance is excluded on the basis that no A_g combinations occur in this region, although two sets of Fermi split difference bands might possibly exist; 1486cm^{-1} and 1470cm^{-1} being 2-1(A_g) and 1578cm^{-1} and 1562cm^{-1} being 2-11(B_{2u}). None of these four bands has a unique assignment. Polarisation studies would clearly be beneficial for an absolute assignment.

The A_g vibrations are the only Raman active vibrations which are independent of the moments of inertia, hence the Product Rule is absolutely determined. The experimental R value indicates a good assignment of the A_g vibrations.

B_{1g} Species

The single member of this species, 10a, has tentatively been assigned to the medium intensity band at 852cm^{-1} (pzO_2) and to the medium shoulder at 662cm^{-1} (pz-d_4O_2). The former is slightly higher than that calculated by SZÖKE *et*

al. [7] (from combination bands). The intensity and frequency of the band is similar to that found in *p*-xylene [97], but it is significantly higher in frequency than that of p-$C_6H_4F_2$ (Table 3.3). These assignments give an R experimental *lower* than that calculated by the Product Rule. This does not necessarily prove an incorrect assignment however, since the ratio of the moments of inertia ($I_{pz\text{-}d_4O_2}/I_{pzO_2}$) about the X-axis is that which is most sensitive to changes in the model of the molecule (Table 3.7). Polarisation studies are necessary to confirm these assignments, B_{1g} vibrations being Raman depolarised.

B_{2g} Species

The assignment of the planar ring vibration 8b is unambiguous. The assignment of 7b, νC-H, to the strong band at 2301cm^{-1} ($pz\text{-}d_4O_2$) is based upon that of p-$C_6H_4F_2$ (at 2295cm^{-1}). The possibility of Fermi resonance with the band at 2313cm^{-1} has been mentioned above.

The N-O in-plane bend, mode 9b, has been assigned to the weak bands at 519cm^{-1} (pzO_2) and 492cm^{-1} ($pz\text{-}d_4O_2$). The alternative assignment of 484cm^{-1} (pzO_2) and 483cm^{-1} ($pz\text{-}d_4O_2$) - assigned here to 6a(A_g) - is not preferred in light of the good agreement with the Product Rule for the A_g species. Polarisation studies would be necessary to confirm these assignments, 9b(B_{2g}) being Raman depolarised and 6a(A_g) being Raman polarised.

The planar ring vibration, 6b, is expected to give a strong Raman absorbance [97], and has therefore been assigned to the bands at 684cm^{-1}(pzO_2) and 660cm^{-1} ($pz\text{-}d_4O_2$). These are the only likely assignments, although both are higher than expected (Table 3.3).

The assignment of the planar C-H bend, mode 3, to the weak bands at 1334cm^{-1}

(pzO_2) and 1038cm^{-1} ($pz\text{-}d_4O_2$) is in accord with that of pyO, although slightly higher than that of SZÖKE *et al.* [7].

The ratio of the moment of inertia about the Y axis is the least sensitive to change in modelling of the molecule. The experimental R value therefore indicates a satisfactory assignment fit of the B_{2g} fundamentals.

B_{3g} Species

The assignment of the out-of-plane ring torsion, mode 4, and C-H bend, mode 10b, are unambiguous. The accidental degeneracy of 10b(B_{3g}) and 1(A_g) in the deuterated spectrum is noted. This is not unexpected since these are found to be close together in p-$C_6D_4F_2$ (Table 3.3) originally being thought to be accidentally degenerate themselves [101,103]. SZÖKE *et al.* [7] assigned the out-of-plane N-O bend, mode 5, to a weak band at 294cm^{-1} (pzO_2) which is not observed in our spectra, and which is at a much lower frequency than expected (Table 3.3). This vibration is rather assigned to the medium band at 374cm^{-1} (pzO_2) and the weak band at 351cm^{-1} ($pz\text{-}d_4O_2$). The revised assignments are in good agreement with those of p-di-fluorobenzene (Table 3.3).

The experimental R value indicates a reasonable assignment of the B_{3g} fundamentals, in light of the two models employed.

The Raman active lattice modes

The medium intensity band at 118cm^{-1}, the strong band at 84cm^{-1} and the medium intensity band at 65cm^{-1} in the Raman spectrum of pzO_2, have tentatively been ascribed to the rotational modes $R_z(B_{3g})$, $R_z(A_g)$ and $R_x(B_{2g})$, respectively, based upon those of pz [108]. Polarisation studies, in particular single crystal studies, would be needed to confirm these assignments.

2.1.3 The infrared and Raman forbidden vibrations

The out-of-plane ring torsion, 16a, and C-H bend, 17a, are expected to be spectroscopically silent. Their positions can however be determined from their combination and difference bands.

16a is calculated to be at 393cm^{-1} ± 2cm^{-1} (pzO_2) based upon six possible combinations of which that at 1200cm^{-1} is uniquely assigned to 16a+11(B_{2g}). In the deuterated spectrum the ring torsion is calculated to be at 358cm^{-1} ± 1cm^{-1}, also based upon six possible combination bands. The weak band at 1948cm^{-1} (pz-d_4O_2) is uniquely assigned to the combination 16a+8b(B_{2u}). These values agree well with the values calculated for the other systems (Table 3.3).

The out-of-plane C-H bend (pzO_2) is calculated to be at 953cm^{-1} ± 6cm^{-1} on the basis of six possible combinations. Two of these, at 1486cm^{-1} and 684cm^{-1}, are unique assignments: 17a+16b(B_{2g}) and 17a-8b(B_{2u}) respectively. 17a is calculated to be at 744cm^{-1} ± 3cm^{-1} in the deuterated spectrum. Of the seven possible combinations used, the very weak Raman band at 1562cm^{-1} is uniquely assigned to 20b-17a(B_{3g}). These values agree well with those for *p*-di-fluorobenzene, although 17a(pzO_2) is significantly lower than that estimated by SZÖKE *et al.* [7].

The Product Rule indicates a very good fit for the calculated frequencies of the A_u species.

2.1.4 Coupling within the molecule

Examination of the Potential Energy Distribution (PED) for *p*-xylene, and com-

parison of the ν^D/ν^H ratio of pzO_2 with that of pz, yields an understanding of the coupling experienced within the molecule.

Typical of 1,4 di-light substituted benzenes [2], in *p*-xylene the infrared allowed C-H stretch, mode 13(B_{1u}) is strongly coupled with the 'Star of David' ring-breathing vibration, mode 12(B_{1u}) [96,97]. The Raman active C-CH_3 stretch, 7a(A_g) couples strongly to the principal ring-breathing vibration, mode 1(A_g) and couples lightly with the lowest planar ring mode, 6a(A_g) [96,97]. A similar coupling is therefore expected for pzO_2.

The most striking feature of the data for pzO_2 (Table 3.4) is the difference between the ν^D/ν^H ratios of the two N-O vibrations. This clearly is the result of the difference in the frequencies observed in the *deuterated* spectrum - 1290cm^{-1} for 7a(A_g) and 1186cm^{-1} for 13(B_{1u}) - and suggests that a comparative change in the nature of the coupling is experienced by the two stretches upon deuteration. While, unfortunately, there are no published PED figures for *p*-xylene-d_4, the nature of this deuteration-induced coupling change may be deduced by examining the PED for toluene and toluene-d_8 [96, 97].

The lowering of symmetry in comparing toluene with *p*-xylene allows the single C-CH_3 stretch, mode 13(A_1), to couple strongly with the principal ring-breathing mode, 1(A_1) and lightly with the planar ring mode 6a(A_1), [96, 97]. On deuteration of the ring, the PED reveals a slight decoupling of 13 and 1 [96,97], resulting in mode 13 being a slightly more pure C-CH_3 vibration than that found for the undeuterated molecule. This reduction in coupling means that the coupling-induced bathochromatic* (of the C-CH_3 mode) and

---

* Bathchromatic (red) shift = a decrease in energy *i.e.* ν(cm^{-1}) increases,

hypsochromatic (of the ring mode) shifts would be smaller than those for the undeuterated molecule. The ν^D/ν^H ratio for the C-CH_3 stretch would therefore decrease from unity, while that for the ring-breathing mode would rise slightly from the expected value.

We could expect a similar decoupling between the N-O stretches (13 and 7a) and the ring vibrations (12 and 1) on deuterating pzO_2. This is indeed observed for the infrared active vibrations (13 and 12), but not for 7a and 1. The higher ν^D/ν^H ratio of mode 1 for pzO_2, compared with that for pz (Table 3.4) indicates that there *is* some decoupling of this vibration on deuteration (*i.e.* the deuterated ring vibration is not being displaced as far down in frequency). However, the higher ν^D/ν^H ratio of 7a would indicate an *increase* in coupling (the deuterated N-O stretch is being displaced further up in frequency). Since this coupling does not occur with the ring-breathing mode, there must be another vibration which is deuteration-induced to couple with the N-O stretch, 7a(A_g).

It is tentatively suggested here that this coupling possibly occurs with the planar C-H bend, mode 9a. The reasons for this choice are threefold. Firstly, it is symmetry allowed (both having A_g symmetry). Secondly, there should not be a significant energy difference to prevent coupling as mode 9a(pz-d_4O_2) is found at a frequency very similar to that of mode 1(pzO_2). Thirdly, the ν^D/ν^H ratio of 9a(pzO_2) is much lower than that for pz (Table 3.4), which would be the case if this vibration is showing a hypsochromatic shift resulting from coupling with 7a. Clearly this suggestion can only be confirmed by a normal coordinate analysis of both pzO_2 and pz-d_4O_2. However, in p-$C_6D_4F_2$, mode 9a becomes Frank-Condon active in the electronic spectrum, which

---

hypsochromatic (blue) shift = an increase in energy *i.e.* (cm^{-1}) decreases.

ZIMMERMAN and DUNN [102] attribute to "mixing with the 'ring-breathing' co-ordinate". This provides further support for the suggestion of the coupling of modes 9a and 7a, since the C-F stretch, mode 7a(A_g) involves the 'Star of David' vibration of its carbon atoms (Fig. 3.1) and is therefore a candidate for the coupling mode which causes this effect.

Again from the PED of *p*-xylene, the out-of-plane C-CH_3 bending vibrations, 5(B_{3g}) and 17b(B_{2u}) are coupled with the ring torsions 4(B_{3g}) and 16b(B_{2u}) respectively [96,97]. The latter reflects extreme coupling to the extent that it may be arguable to really define 17b as the C-CH_3 vibration. That the ring torsion is similarly coupled to the out-of-plane bend in pzO_2 is indicated by the former's lower ν^D/ν^H ratio for pzO_2 compared with those of pz.

The umbrella mode, 11, also indicates a change in coupling for pzO_2, compared with pz, as seen by its much higher ν^D/ν^H ratio (for a αC-H mode) than for pz. Since no coupling is observed in *p*-xylene [96,97], it is possible that this coupling with 17b is also deuteration-induced. Such deuteration-induced coupling of 11 and 17b is seen in toluene-d_8 [96]. Again this can only be verified by a normal coordinate analysis of the molecule.

Finally, as observed for αN-O in pyO [64-68], the PED of *p*-xylene indicates that the in-plane C-CH_3 bends, modes 15 and 9b, are very pure vibrations [96, 97]. The corresponding vibrations in pzO_2 are similarly expected to be pure. The slight difference in the ν^D/ν^H ratios for 9b and 15 is not taken as indicative of deuteration-induced coupling of 9b(B_{2g}), since there is no significant difference between the ν^D/ν^H ratios for pz and pzO_2 of 6b(B_{2g}), 3(B_{2g}) or 8b(B_{2g}). These are the only vibrations symmetrically allowed to couple with 9b. No change in coupling is expected for 15 on the basis of the PED

for toluene-d_8 [96].

Having presented a complete assignment of the ligands' vibrational spectra, assignment of the metal-ligand vibrations can now be made with more confidence. This is especially true since identifying which bands are N-O vibrations should possibly be able to explain why some of the ligand modes show metal sensitivity on complexation.

2.2 Pyrazine N-oxide (pzO)

The assignment of the fundamentals of pyrazine N-oxide (pzO) and its fully deuterated analogue (pz-d_4O) are based firstly upon considering pzO in terms of being a γ-mono-light substituted pyridine, secondly in terms of being a *para*-di-light substituted benzene, thirdly upon comparison with the previous assignment of the infrared and Raman spectra of pzO, fourthly by a comparison with pz and pzO_2 and their fully deuterated analogues and finally, upon the ν^D/ν^H ratio.

Due to the absence of published spectral data for γ-fluoropyridine the comparison of pzO with γ-picoline (*p*-methyl pyridine) [11-14,17] as a mono-light substituted pyridine is presented instead. Normal coordinate calculations by DRAEGER [13] have shown that with the exception of the planar ring mode 6a and the out-of-plane C-CH_3 bend, mode 5, there is no significant coupling (*i.e.* greater than a 10% contribution to the overall PE of the vibration) of the internal vibrations of the methyl substituent with those of the ring. The assignment of the Kekulé mode, 14, at 1228cm^{-1} in γ-picoline is based on DRAEGER [13].

In employing the WILSON notation for substituted pyridines there is consider-

able confusion in the literature as to the naming of the out-of-plane vibrations. There should be five B_2 out-of-plane vibrations for a γ-substituted pyridine; two ring modes, two C-H modes and one C-X mode.

In their classical work on substituted pyridines, GREEN *et al.* [11] attributed the lowest infrared band (substituent sensitive) to the WILSON ring mode 16b. In so doing they needed to ascribe one of the C-H modes of WILSON to a ring mode. They therefore regarded the umbrella mode, 11, as a ring vibration. They then attributed the very intense infrared band at 799cm^{-1} to the γC-H mode, 10b. CUNLIFFE-JONES [21] questioned this last assignment since the position and intensity of this band is typical of the umbrella vibration, and so reversed the assignments of 11 and 10b.

cm^{-1}	GREEN *et al.* [11]	CUNLIFFE-JONES [21]	ABDEL-SHAFY *et al.* [12]	Present
872	5 γC-H	5 γC-H	5 γC-H	10b γC-H[(a)]
799	10b γC-H	11 γC-H	10b γC-H	11 γC-H
728	4 γring	4 γring	4 γring	4 γring
490	11 γring	10b γring	11 γring/X sensitive	16b γring/γC-X
211	16b X sensitive	16b X sensitive	16b X sensitive	5 γC-X

(a) As for *p*-di-light substituted benzenes, considering the displacements of the hydrogens at 2,3,5 and 6, mode 10b is equivalent to 5. Therefore for a light substituent 10b is regarded as the C-H mode, while for a heavy substituent 5 is regarded as the C-H mode.

Table 3.8 Description of the B_1 fundamentals of a γ-substituted pyridine

In employing both the WILSON and the WHIFFEN notations to substituted pyridines, ABDEL-SHAFY *et al.*[12] questions the *nature* of the vibration at 490cm^{-1} since, according to the WHIFFEN notation, it should be considered as substituent sensitive.* They therefore regarded this as a mixed γring and

* Normal Coordinate Analyses by BEREZIN and ELKIN [109] and DRAEGER [13] on substituted pyridines confirm that the two bands at 490cm^{-1} and at 211cm^{-1} are both substituent sensitive. The former authors apply the nomenclature of GREEN *et al.*, while the latter does not employ any descriptive notation.

γC-X vibration but retain the notation of GREEN *et al.* [11]. In so doing they also identify the 799cm^{-1} band as 10b, despite the fact that this band is described by the WHIFFEN mode *f*, which corresponds to the WILSON umbrella mode 11 [2,25].

It is suggested here that the source of this confusion over the nomenclature of the two bands at 490cm^{-1} and at 799cm^{-1} lies not in the assignment of these two vibrations, but rather in the description of the substituent sensitive band at 211cm^{-1} as being the ring mode 16b.

Since the 'lost' vibrations of pyridine are equated to the C-X vibrations 13, 9 and 17b of benzene, the C-X modes of a γ-light substituted pyridine should be equated to 7a, 15 and 5 on the basis of *p*-di-light substituted benzenes. Accordingly, the band at 211cm^{-1} is better described as mode 5, γC-X, which strongly couples with the ring torsion, mode 16b, at 490cm^{-1} (as indicated by the NCA [12,109]). The assignment of the rest of the bands follows in accordance with that for a *p*-di-substituted benzene [2]. This revised description is also consistent with the later assignments of *p*-di-substituted benzenes proposed by GREEN [99], in which mode 16b is regarded as a *ring* vibration at 450cm^{-1} and *not* as the lowest infrared band, the γC-X vibration.

This conflict in the nomenclature of the B_2 fundamentals has a direct implication in the assignment of pzO made here since HASE [8] employed the nomenclature of GREEN *et al.* [11] to this system. To facilitate comparisons with the present work, four changes have been made to the nomenclature of HASE for the B_2 fundamentals. These are: mode 5 here replaces HASE's original mode 16b; mode 16b replaces HASE's mode 11; mode 11 replaces HASE's mode 10b, and mode 10b replaces HASE's mode 5. It is emphasised that these changes do not reflect a change in the *nature* of the bands described by HASE [8],

but rather shows an attempt to make the naming of these vibrations more consistent with the WILSON modes for benzene. Similarly, the same changes to the nomenclature of pz which were made while discussing pzO_2 above, have been retained (Tables 3.9 and 3.10).

The molecule of pyrazine *N*-oxide is expected to be planar with C_{2v} symmetry. The molecular axes adopted for pzO are the same as those for pz [90]. The Y-axis is taken perpendicular to the molecular plane and the X- and Z- axes in the plane, the Z-axis passing through the nitrogens and the oxygen.

For C_{2v} symmetry, 24 fundamentals are both infrared and Raman active ($10A_1$, $9B_1$ and $5B_2$ species), and three fundamentals are Raman active only (A_2). There are no spectroscopically silent fundamentals. An investigation of the infrared and Raman spectra for pzO and pz-d_4O_2 (Tables 3.11 and 3.12) reveals spectra rich in overtone, combination and difference bands, beside the expected fundamentals. As for pzO_2, where more than one combination assignment is possible, all alternatives are given. Polarisation and infrared gas phase contour studies would be necessary for any conclusive assignments of these to be made.

Finally, unlike pzO_2, the correctness of the assignments made for pzO and its fully deuterated analogue cannot be fully assessed in light of the Product Rule. This is the result of the absence of a centre of inversion in the molecule, through which the three axes of rotation would pass. Instead, the centre of gravity of the molecule is displaced along the Z-axis towards the oxygen, the extent of which will be dependent upon the molecular dimensions. Therefore the moments of inertia are significantly dependent upon the molecular dimensions and so, with the absence of crystallographic data of pzO, no model for the molecule is proposed (unlikely above for pzO_2, where the

WILSON Mode [1]	pzO (This work)	pzO HASE [8]	γ-pic [11-14]	pz [90-93]	pzO_2 (This work)	pz-d_4O (This work)	γ-pic-d_7 [14,17]	pz-d_4 [91,93]	pz-d_4O_2 (This work)
20a	3085	3083	3050	3015	3075	2275	2277	2259	2271
20b	3120	3075	3070	3066	3107	2297	(2302)	2278	2308
19a	1468	1469	1501	1483	1487	1373	1393	1352	1406
19b	1433	1433	1420	1419	1456	1331	1335	1264	1355
18a	1075	1080	1066	1139	1047	831	848	1027	900
18b	1090	1089	1112	1068	1125	809	825	839	866
17a	994	982	969	(960)	(953)	804	799	-	(744)
17b	-	-	-	-	186	-	-	-	177
16a	396	398	385	(350)	(393)	345	-	-	(358)
16b	540	626	482	417	536	455	427	401	460
15	475	477	344	-	417	468	296	-	412
14	1212	1348	1228	1148	1292	1159	1253	1105	1252
13	-	-	-	-	1262	-	-	-	1186
12	857	856	800	1026	874	791	735	882	791
11	836	838	800	785	805	725	683	597	737
10a	(871)	878	(890)	941	852	666	650	721	662
10b	863	865	(865)	975	958	854	(860)	840	830
9a	1169	1169	1157	1248	1191	934	887	1002	882
9b	-	-	-	-	519	-	-	-	492
8a	1594	1595	1603	1581	1637	1548	1575	1537	1594
8b	1554	1548	1575	1521	1631	1488	1538	1502	1589
7a	1307	1307	1228	-	1286	1251	1187	-	1290
7b	3042	3044	3038	3030	3038	2266	2245	2273	2301
6a	545	541	512	598	484	535	506	581	483
6b	681	681	668	697	684	659	650	680	660
5	226	226	203	-	374	222	198	-	351
4	714	716	727	754	699	614	613	647	627
3	1295	1295	1279	1358	1334	987	931	1027	1038
2	3071	3071	3070	3046	3048	2297	2277	2286	2313
1	1006	1009	996	1014	879	959	973	899	830

estimated frequencies in parenthesis

(a) for pz 20a ≡ 13, 18b ≡ 15, 10b ≡ 5 (see Text)

for pzO 7a ≡ 13, 5 ≡ 16b, 16b ≡ 11, 11 ≡ 10b, 10b ≡ 5 (see Text)

Table 3.9 The fundamentals of pyrazine *N*-oxide (pzO) and its -d_4 analogue (pz-d_4O) compared with similar molecules

WILSON Mode (a)	pz	pz-d_4	ν^D/ν^H	Y-pic	Y-pic-d_7	ν^D/ν^H	pzO	pz-d_4O	ν^D/ν^H	Assignment
[1]	[90-93]	[91,93]		[11-14]	[14,17]		(This work)	(This work)		
20a	3015	2259	0,749	3050	2277	0,746	3085	2275	0,737	ν C-H/D
20b	3066	2278	0,743	3070	(2302)	0,750	3120	2297	0,736	ν C-H/D
19a	1483	1352	0,912	1501	1393	0,928	1468	1373	0,935	ν C-H/D
19b	1419	1264	0,891	1420	1335	0,940	1433	1331	0,929	ν ring
18a	1139	1027	0,902	1066	848	0,795	1075	831	0,773	α C-H/D
18b	1068	839	0,786	1112	825	0,742	1090	809	0,742	α C-H/D
17a	(960)	-	-	969	799	0,824	994	804	0,809	Y C-H/D
17b	-	-	-	-	-	-	-	-	-	
16a	(350)	-	-	385	-	-	396	345	0,781	Y ring
16b	417	401	0,962	482	427	0,886	540	455	0,842	Y ring + Y N-O
15	-	-	-	344	296	0,860	475	468	0,985	α N-O
14	1148	1105	0,962	1228	1253	1,020	1212	1159	0,956	ν ring
13	-	-	-	-	-	-	-	-	-	
12	1026	882	0,860	800	735	0,919	857	791	0,923	ν ring + ν N-O
11	785	597	0,760	800	683	0,854	836	725	0,867	Y C-H/D
10a	941	721	0,766	(890)	650	0,730	(871)	666	0,765	Y C-H-D
10b	975	840	0,862	(865)	(860)	0,994	863	854	0,990	Y C-H/D
9a	1248	1002	0,803	1157	887	0,767	1169	934	0,799	α C-H/D
9b	-	-	-	-	-	-	-	-	-	
8a	1581	1537	0,972	1603	1575	0,983	1594	1548	0,971	α ring
8b	1521	1502	0,988	1575	1538	0,976	1554	1488	0,958	α ring
7a	-	-	-	1228	1187	0,967	1307	1251	0,957	ν N-O + ν ring
7b	3030	2273	0,750	3038	2245	0,739	3042	2266	0,745	ν C-H/D
6a	598	581	0,972	512	506	0,988	545	535	0,982	α ring
6b	697	680	0,976	668	650	0,973	681	659	0,968	α ring
5	-	-	-	203	198	0,975	226	222	0,982	Y N-O + Y ring
4	754	647	0,858	727	613	0,843	714	614	0,860	Y ring
3	1358	1027	0,756	1279	931	0,728	1295	987	0,762	α C-H/D
2	3046	2286	0,750	3070	2277	0,742	3071	2297	0,748	ν C-H/D
1	1014	899	0,886	996	973	0,977	1006	959	0,953	ν ring

estimated frequencies in parenthesis

(a) for pz 20a ≡ 13, 18b ≡ 15, 10b ≡ 5 (see Text)

for pzO 7a ≡ 13, 5 ≡ 16b, 16b ≡ 11, 11 ≡ 10b, 10b ≡ 5 (see Text)

Table 3.10 The ν^D/ν^H ratio of pyrazine *N*-oxide (pzO) and its -d_4 analogue (pz-d_4O) compared with similar molecules

3.11 Infrared and Raman spectra of pyrazine *N*-oxide (pzO)

Raman (cm^{-1})	Infrared (cm^{-1})	Assignment
	3161 vw	Unassigned.
3122 w	3120 m	$20b(B_1)$ fundamental.
	3085 s	$20a(A_1)$ fundamental.
3071 s		$2(A_1)$ fundamental.
3064 sh	3062 sh	$19a+8a(A_1)$.
3056 sh		Unassigned.
3042 m	3042 wsh	$7b(B_1)$ fundamental.
	3026 m	$19b+8a(B_1)$; $19a+8b(B_1)$.
	3004 m	Unassigned.
	2930 w	$19a^2(A_1)$.
	2890 w	$8a+3(B_1)$.
	2855 w	$8b+3(A_1)$; $8b+7a(B_1)$; $20a-5(B_2)$.
	2812 vw	Unassigned.
	2799 vw	$14+8a(B_1)$.
	2766 vw	$14+8b(A_1)$; $12+8a(A_1)$; $19+3(B_1)$.
	2672 vw	$18a-8a(A_1)$.
	2637 vw	$19a+9a(A_1)$.
	2589 m	$3^2(A_1)$.
	2516 vw	$2-16b(B_2)$; $14+7a(B_1)$.
	2460 vw	$10b+8a(B_2)$.
	2425 vw	$10a+8b(B_2)$; $14^2(A_1)$; $19b-17a(B_1)$; $11+8a(B_2)$.
Not recorded	2344 m	$9a^2(A_1)$.
	2332 m	$19a+2(A_1)$.
	2256 w	$18b+9a(B_1)$.
	2150 m	$18a^2(A_1)$; $19a+6b(B_1)$; $3+12(B_1)$.
	2080 vw	$20a-1(A_1)$; $18a+1(A_1)$; $14+10a(B_2)$; $18b+17a(B_2)$.
	2028 vw	$10b+9a(B_2)$; $15+8b(A_1)$; $20b-18b(A_1)$; $12+9a(A_1)$.
	1961 vw	$18b+10a(B_2)$; $7b-18a(B_1)$.
	1930 w	$18a+12(A_1)$.
	1910 wsh	$18a+11(B_2)$; $20b-14(A_1)$; $20a-9a(A_1)$.
	1868 vw	$20a-9a(A_1)$; $12+1(A_1)$; $7b-14(A_1)$; $17a+10a(A_1)$.
	1850 w	$7a+6a(A_1)$; $16b+7a(B_2)$.
	1800 vwbr	Unassigned.
	1768 vw	$15+3(B_1)$; $18b+6b(A_1)$; $2-7a(A_1)$.
	1705 w	$11+10a(B_1)$; $17a+4(B_2)$; $16b+9b(B_2)$; $10b+11(A_1)$.
	1682 wsh	$17a+6b(B_2)$; $20b-19b(A_1)$.
1650 w	1650 m	$20a-19b(B_1)$; $15+9a(A_1)$.

Table 3.11 (continued)

Raman (cm^{-1})	Infrared (cm^{-1})	Assignment
	1625 sh	18a-6a(A_1).
1593 vs	1595 s	8a(A_1) fundamental.
1587 sh		10a+4(B_1).
	1554 mw	8b(B_1) fundamental; 10a+6b(B_2); 6a+1(A_1).
1510 w	1509 w	2-8b(B_1).
1506 w	1498 mw	20a-8a(A_1).
1472 sh		18a+16a(A_2).
1469 s	1468 s	19a(A_1) fundamental; 17a+15(B_2).
1437 m		14+5(A_2).
1433 m	1432 s	19b(B_1) fundamental.
	1400 sh	12+6a(A_1); 10b+5(A_1).
1349 m	1344 mw	10a+15(B_2).
1339 mw	1338 m	15+10b(A_2).
1316 w		18b+5(A_2).
1304 s	1310 s	7a(A_1) fundamental.
1295 s	1270 sh	3(B_1) fundamental.
1226 m		16b+6b(A_2).
1211 s	1212 s	14(B_1) fundamental.
1171 vs	1168 mw	9a(A_1) fundamental.
1085 vwbr	1090 vw	18b(B_1) fundamental; $6a^2$(A_1).
	1075 m	18a(A_1) fundamental; 16a+6b(B_2).
1009 s	1003 s	1(A_1) fundamental; 8b-6a(B_1).
994 vw		17a(A_2) fundamental.
	978 sh	Unassigned.
	952 w	15^2(A_1); 19b-15(A_1).
862 s	865 s	10b(B_2) fundamental.
	857 s	12(A_1) fundamental.
	848 s	18a-5(B_2).
838 vw	835 vs	11(B_2) fundamental.
794 w		$16a^2$(A_1).
	772 w	6a+5(B_2); 1-5(B_2); 7a-16b(B_2); 16b+5(B_1).
740 w	735 vw	14-15(A_1); 8a-12(A_1).
720 vw	719 vw	19b-4(A_2); 8b-11(A_2); 8a-10a(A_2).
715 vw	713 w	4(B_2) fundamental.
689 vw		18b-16a(B_2).
686 vw		8b-10b(A_2).
682 m	679 w	6b(B_1) fundamental.

Table 3.11 (continued)

Raman (cm^{-1})	Infrared (cm^{-1})	Assignment
544 w	546 sh	6a(A_1) fundamental; 8b-1(B_1).
540 w	540 s	16b(B_2) fundamental.
474 w	475 s	15(B_1) fundamental.
396 vw	395 vw	16a(A_2) fundamental; 18a-6b(B_1).
	321 vw	6a-5(B_2); 1-6b(B_1).
227 vw	226 s	5(B_2) fundamental.
223 vw		18b-10a(A_2).
90 w		R_z(A_2) libration; 9a-19a(A_1); 18b-17a(B_2); 8b-19b(B_1).
81 w	82 w	R_x(B_1) libration; 20b-7b(A_1).
	65 w	T_z(A_1) translation.
52 vw	Not recorded	20b-2(B_1).
38 w		8a-8b(B_1); 20b-20a(B_1).
32 w		19a-19b(B_1); 2-7b(B_1); 10b-11(A_1).
23 w		12-11(B_2).

s = strong

m = medium

w = weak

v = very

sh = shoulder

br = broad

3.12 Infrared and Raman spectra of pyrazine-d_4 *N*-oxide (pz-d_4O)

Raman (cm^{-1})	Infrared (cm^{-1})	Assignment
	3125 vw	20b+18a(B_1); 18a+2(A_1); 20a+10b(B_2).
	3067 vw	20a+12(A_1); 17a+7b(B_2).
	2970 vw	$8b^2$(A_1).
	2923 vw	19a+8a(A_1); 7b+6b(A_1).
	2731 w	20a+16b(B_2); 15+7b(A_1).
	2691 vw	Unassigned.
Not recorded	2637 w	20b+16a(B_2)
	2605 m	7b+16a(B_2).
	2520 w	5+2(B_2).
	2483 w	19b+14(A_1).
	2400 vw	10b+8a(B_2).
	2370 vw	18a+8a(A_1).
	2342 w	Unassigned.
2331 w	2331 m	19a+1(A_1).
2297 m	2297 s	2(A_1) fundamental and 20b(B_1) fundamental; 18b+8b(A_1).
	2275 s	20a(A_1) fundamental; 11+8a(B_2); 12+8b(B_1).
2266 m		7b(B_1) fundamental.
2256 w		Unassigned.
	2224 m	19a+10b(B_2).
	2156 w	19a+12(A_1); 19b+18a(B_1); 8a+4(B_2).
	2031 vw	19a+6b(B_1); 8b+6a(B_1).
	1830 vw	20b-15(A_1); 2-15(B_1); 19a+16b(B_2); 10a+14(B_2).
	1815 vw	18b+3(A_1); 20a-16b(B_2).
Not recorded	1775 w	14+12(B_1); 14+8a(B_2).
	1695 vw	14+6a(B_1).
	1680 vw	2-4(B_2); 19b-16a(B_2); 11+1(B_2); 18a+10b(B_2).
	1645 w	12+10b(B_2); 6b+3(A_1); 18a+18b(B_1).
1617 vw	1614 w	17a+18b(B_1); 20a-6b(B_1); $18b^2$(A_1); 18a+12(A_1).
	1580 vw	12^2(A_1); 11+10b(A_1).
1548 s	1548 s	8a(A_1) fundamental; 9a+4(B_2); 20a-11(B_2).
	1515 w	12+11(B_2); 10a+10b(B_1); 6a+3(B_1).
1489 w	1488 m	8b(B_1) fundamental; 20b-18b(A_1); 2-18b(B_1); 18a+6b(B_1).
1450 vvw		10a+12(A_2).
	1438 vw	7b+18a(B_1); 2-10b(B_2); 20a-18a(A_1).
	1410 w	16b+1(B_2); 12+4(B_2).
1380 w		14+5(A_2); 11+6b(A_2).
1371 ms	1374 s	19a(A_1) fundamental.

Table 3.12 (continued)

Raman (cm^{-1})	Infrared (cm^{-1})	Assignment
1365 ms		6a+18a(A_1); 20b-9a(B_1).
1332 m	1330 s	19b(B_1) fundamental; $10a^2$(A_1); 7a-9a(A_1); 6a+3(B_2).
	1290 wsh	20a-3(B_1); 18a+16b(B_2).
	1267 w	15+17a(B_2).
1252 w	1250 s	7a(A_1) fundamental.
1245 w		16b+12(B_2).
	1168 w	18a+16b(B_2).
1160 s	1157 w	14(B_1) fundamental; 20a-14(B_1); 5-19a(B_2); 18b+16a(B_2).
	1135 w	15+10a(B_2); 20b-14(A_1); 2-14(B_1).
1068 vwbr	1070 vwbr	16a+11(B_1); 16b+4(A_1); $6a^2$(A_1); 10b+5(A_1).
1039 vwbr	1035 vw	8b-16b(A_2).
1031 vwbr	1028 vw	7a-5(B_2); 17a+5(B_1); 18b+5(A_2).
	1004 vvw	16a+6b(B_2); 6a+5(B_2).
999 w	998 w	16b+6a(B_2).
988 s	982 s	3(B_1) fundamental; 19a-16a(B_2).
959 ms	960 m	1(A_1) fundamental; 16a+4(B_1).
952 ms	950 msh	8b-6a(B_1).
941 m		14-5(A_2).
934 s		9a(A_1) fundamental; 8a-4(B_2); 7b-19b(A_1); 15^2(A_1).
863 w		19b-15(A_1).
855 w	852 wm	10b(B_2) fundamental.
838 w		5+4(A_1); 19a-6a(A_1).
830 w	832 wm	18a(A_1) fundamental.
	823 w	8a-11(B_2); 8b-10a(B_2).
809 w	808 wm	18b(B_1) fundamental; 16a+15(B_2).
804 w		17a(A_2) fundamental.
794 vs 791 s	792 s 788 s	12(A_1) fundamental; 19b-6a(B_1); 7a-16b(B_2).
748 w	750 wm	20b-8a(B_1); 2-8a(B_1).
726 w	724 s	11(B_2) fundamental; 20a-8a(A_1).
667 w	665 vw	10a(A_2) fundamental; 19b-10a(B_2).
659 vs	656 w	6b(B_1) fundamental; 18a+8b(B_1).
614 vw	613 vw	4(B_2) fundamental; 8a-9a(A_1).
607 vw	605 w	18a-5(B_2).
534 msh	537 w	6a(A_1) fundamental.
531 m		8b-1(B_1); 19b-17a(B_2).
468 vw	469 m	15(B_1) fundamental; 9a-15(B_1); 18b-16a(B_2).

Table 3.12 (continued)

Raman (cm^{-1})	Infrared (cm^{-1})	Assignment
454 m	456 s	16b(B_2) fundamental; 17a-16a(A_1).
345 w		16a(A_2) fundamental; 1-4(B_2); 19b-3(A_1).
342 wsh	342 w	18b-15(A_1).
222 w	222 s	5(B_2) fundamental; 14-9a(B_1).
218 wsh		19a-14(B_1).
	79 w	R_x(B_1) libration; 9a-10b(B_2); 6a-16b(B_2).
	64 w	T_z(A_1) translation; 10b-12(B_2); 6a-15(B_1).

s = strong

m = medium

w = weak

v = very

sh = shoulder

br = broad

moments of inertia are not significantly dependent on the molecular dimensions). The Product Rule is therefore only calculated for the A_1 fundamentals, since these are uniquely independent of the moment of inertia, being free from a rotation about the X-, Y- or Z-axes.

2.2.1 The infrared and Raman active fundamentals

Taking into account the different nomenclature employed, the assignment of the fundamentals of pzO in the present work agrees well with that of HASE [8] with the exception of the C-H stretch, mode 20b, the assignment of the Kekulé vibration, mode 14, and the out-of-plane ring torsion (coupled with γN-O), mode 16b. Several of the deuterated bands also need to be discussed.

A_1 Species

The planar ring bend 6a(A_1) for pzO has been ascribed to the strong infrared band at 541cm^{-1} by HASE [8], while the ring torsion 16b(B_2) is ascribed to a very weak infrared band at 626cm^{-1}. The latter is not observed in our spectrum, and as this ring torsion is expected to be of greater infrared intensity than mode 6a [11,12], assigning the strong infrared band at 540cm^{-1} to the ring torsion 16b(B_2) is preferred. The planar A_1 ring vibration has been assigned to the weak Raman band at 544cm^{-1} and the shoulder at 544cm^{-1} in the infrared spectrum. The assignment of the rest of the A_1 fundamentals of pzO agree well with HASE (Table 3.9).

The A_1 fundamentals of pz-d_4O agree with those of γ-picoline-d_7, with the exception of modes 7a,12 and 9a. The N-O stretching vibration, 7a, is assigned to the strong infrared band at 1250cm^{-1} (the weak Raman counterpart at 1252cm^{-1}) since this band shifts down some 40cm^{-1} on complexation involving metal-oxygen coordination.

The two double strong bands at 794cm^{-1} and 791cm^{-1} (Raman spectrum) and at 792cm^{-1} and 788cm^{-1} (infrared spectrum) are assigned to the 'Star of David' ring-breathing vibration, 12. This vibration, being coupled to the N-O stretch, 7a, is found at the same frequency in pzO_2 (Table 3.9). The splitting is not considered a result of Fermi resonance in view of the small degree of splitting (only 3 to 4cm^{-1}), the absence of any possible combinations or overtones with A_1 symmetry in this region, and the absence of a similar splitting being shown in the combinations involving mode 12. The splitting (which is removed on complexation) is therefore ascribed to some solid state effect.

From the spectra of γ-picoline-d_7, the in-plane bend, mode 9a, is expected to be found at approximately 890cm^{-1} (Table 3.9). It has been assigned here to the strong Raman band at 934cm^{-1} (with no infrared counterpart) as there is no strong Raman band in the region *ca.* 890cm^{-1}.

Finally, there is some ambiguity in the assignment of the principal ring-breathing mode, 1. In γ-picoline-d_7 mode 1 is found at 973cm^{-1} (Table 3.9). There are two suitable bands in pz-d_4O which may be ascribed to mode 1; the strong infrared band at 982cm^{-1} (strong Raman counterpart at 988cm^{-1}) and the medium strength band at 960cm^{-1} (medium strong Raman counterpart at 959cm^{-1}). The other band is that of the planar C-H bend, mode 3(B_1). With either polarisation or infrared gas contour studies necessary for confirmation, the present assignment of the infrared band at 960cm^{-1} (Raman counterpart at 959cm^{-1}) to the A_1 ring-breathing mode is based tentatively on its better Product Rule (Table 3.13). However, while the experimental and calculated Product Rule for the A_1 species give very good agreement, this should not be taken as a conclusive test of their assignments since the Product Rule for the other species has not been determined here.

(C_{2v})

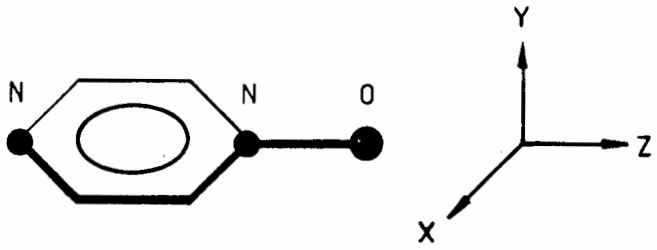

$$R_{calc} = \left[\left(\frac{100,117}{96,087}\right)^{1} \left(\frac{I_x'}{I_x}\right)^{0} \left(\frac{I_y'}{I_y}\right)^{0} \left(\frac{I_z'}{I_z}\right)^{0} \left(\frac{1,008}{2,015}\right)^{4}\right]^{\frac{1}{2}} = 0,225 \ (3,915)$$

A_1 Vibrations

	$-d_0$	$-d_8$
20a	3085	2275
2	3071	2297
8a	1594	1548
19a	1468	1373
7a	1307	1251
9a	1169	934
18a	1075	831
1	1006	959[a]
12	857	791
6a	545	535

$R_{exp} = 0,256 \ (3,909)$

[(a) alternate assignment for mode 1 at 987cm^{-1} (pz-d_4O)

$R_{exp} = 0,263 \ (3,798)$]

Note: Product Rule is calculated for the A_1 species since the other species are dependant upon an axis of rotation, hence upon the moment of inertia (I) about that axis.

Table 3.13 Product Rule of A_1 vibrations for pyrazine *N*-oxide (pzO) and its -d_4 analogue (pz-d_4O)

B_1 Species

Two B_1 assignments for pzO differ from those of HASE (Table 3.9). The strong infrared band recorded at 3075cm^{-1} by HASE [18] was not observed in our spectrum; mode 20b, a C-H stretch, has therefore been assigned to the medium intensity infrared band at 3120cm^{-1} (weak Raman counterpart at 3122cm^{-1}). Unlike that made by HASE, the assignment of 20b to a band of *higher* frequency than 20a is consistent with those of pz, γ-picoline and pzO_2 (Table 3.9).

The assignment of the Kekulé vibration, mode 14, to the strong bands at 1212cm^{-1} (infrared spectrum) and 1211cm^{-1} (Raman spectrum) is consistent with that for γ-picoline according to DRAEGER [13]. In his normal coordinate work he showed that the band at 1365cm^{-1} earlier assigned to mode 14 for γ-picoline is best described as an internal methyl vibration, and that the band at 1228cm^{-1} is the Kekulé vibration. Its much lower value (compared with that of benzene) is the result of coupling with the in-plane C-H bend, mode $3(B_1)$. As the lower of the two resultant shifted bands has the greater C-N and C-C stretching character, it is the one regarded as the Kekulé ring vibration [13].

The assignment of the B_1 fundamentals for pz-d_4O agree well with those found for γ-picoline-d_7 (Table 3.9).

B_2 Series

With the exception of the ring torsion 16b (already discussed) the assignment of the B_2 vibrations for pzO agree well with HASE (taking into account the different notation). 16b is found at 455cm^{-1} in pz-d_4O, which is higher than that found in γ-picoline-d_7, but is typical of pz-d_4O_2 (Table 3.10). This is a reflection of the N-O contribution to this vibration as a result of coupling with γN-O, mode $5(B_2)$. A similar behaviour is found for the umbrel-

1a mode, 11, in pz-d_4O. The other C-H out-of-plane bend, mode 10b, and the trigonal ring torsion, mode 4, are more typical of γ-picoline-d_7.

2.2.2 The Raman allowed infrared forbidden vibrations

Three A_2 vibrations, modes 10a, 16a and 17a, are expected to be Raman allowed only. Their assignments for pzO agree well with HASE, although 17a (γC-H) was not observed in our spectrum. Its frequency of 871cm^{-1} ± 2cm^{-1} (was calculated on the basis of nine combination bands of which three are unique. These are at 1587cm^{-1} (Raman), at 1349cm^{-1} (Raman) and 1344cm^{-1} (infrared) and at 223cm^{-1} (Raman), which are attributed to 10a+4(B_1), 15+10a(B_2) and 18b-10a(A_2) respectively.

These vibrations for pz-d_4O agree well with those found for γ-picoline-d_7 and pz-d_4O_2 (Table 3.9). The γC-D mode, 10a, is assigned to the weak Raman band at 667cm^{-1} with the very weak infrared counterpart forbidden for A_2 symmetry being explained as a difference band involving itself, namely 19a-10a(B_1). These two bands cannot be explained otherwise. The other two vibrations are infrared silent as expected.

2.2.3 The lattice modes

The weak infrared bands at 65cm^{-1} (pzO) and 64cm^{-1} (pz-d_4O) with a ν^D/ν^H ratio of 0,985 are tentatively ascribed to the A_1 translation on the basis of the spectrum of pz [106]. The ν^D/ν^H ratio agrees well with the square root of the ratio of the labelled and unlabelled molecular masses [107], R = 0,980 (1,021). In light of the lower ν^D/ν^H ratio 0,963, the weak infrared bands at 82cm^{-1} (Raman counterpart 81cm^{-1}) for pzO and 79cm^{-1} for pz-d_4O are ascribed to a librational rather than a translational mode. Similarly, the

weak Raman band at 90cm^{-1} (pzO) is tentatively ascribed to possibly the R_z (A_2) libration based upon the absence of the infrared counterpart and upon the spectrum for pz [106]. Unambiguous assignments in the lattice mode region would require further studies, preferably of single crystal form, at low temperatures.

Finally, the medium intensity infrared band at 280cm^{-1} interpreted by HASE as a possible combination of the lattice vibrations [8] is not observed in our spectrum of pzO.

2.2.4 Coupling within the molecule

By examining the Potential Energy Distribution for γ-picoline [13] and by comparing the ν^D/ν^H ratio of pzO with that of pz (Table 3.10) an understanding of the coupling experienced by the molecule may be presented.

In γ-picoline [13] the C-CH_3 stretch, mode 7a(A_1), is strongly coupled to the 'Star of David' ring-breathing mode, 12(A_1), rather than with the principal ring-breathing mode, 1(A_1), found in mono-substituted benzenes [2]. This is clear from the CCN, the NCN and the C-H in-plane bend (describing mode 12) found in the coupled vibration at 800cm^{-1}, rather than the uncoupled vibration at 996cm^{-1} [13]. Similarly; 7a(A_1) is expected to couple with mode 12(A_1) in pzO, rather than with mode 1(A_1) as occurs for pyO [67].

The possibility of a change in the nature of coupling on deuteration has been discussed for pzO_2. In the absence of published PED figures for γ-picoline-d_7, such behaviour for pzO may be deduced by examining changes in the ν^D/ν^H ratio proceeding from pz to pzO.

Firstly, the higher ν^D/ν^H ratio of mode 12 for pzO than that found for pz (Table 3.10) indicates that a reduction in the coupling between modes 12(A_1) and 7a(A_1) on deuteration (as is observed in toluene and pzO_2) does indeed occur.

Secondly, it was suggested that in pz-d_4O_2, νN-O, 7a(A_g) couples with mode 9a(A_g) as reflected by the high ν^D/ν^H ratio of the former and the low ν^D/ν^H ratio of the latter, compared with pz.

As the frequency of νN-O in pz-d_4O lies between those found for modes 7a and 13 in pz-d_4O_2, and as the ν^D/ν^H ratio for 7a in pzO is larger than that of mode 13 in pzO_2, a similar coupling in pz-d_4O is possible. Such coupling would be lighter than that which occurs for pzO_2 in view of the relatively lower frequency and ν^D/ν^H ratio of mode 7a for pzO (Table 3.10). The C-D bend, 9a(A_1) is found at 934cm^{-1} in pz-d_4O, significantly different to that of mode 12 in pzO. Therefore it is unlikely that coupling occurs between 7a(A_1) and 9a(A_1) in pz-d_4O. However, another A_1 vibration, mode 18a, is found at a suitable frequency at 831cm^{-1} (pz-d_4O). The much lower ν^D/ν^H ratio of 0,773 found for this vibration compared with that of 0,902 for pz is typically that expected for a hypsochromatic shift of this mode in the deuterated spectrum. This tentative suggestion of coupling between νN-O, 7a(A_1) and the C-D in-plane bend, 18a(A_1) can only be confirmed by a normal coordinate analysis of pz-d_4O.

Again from the PED of γ-picoline, the out-of-plane C-CH_3 vibration, mode 5 (B_1) is strongly coupled to the ring torsion, 16b(B_1). The extension of this to pzO is confirmed by the higher frequency (reflecting the N-O character) and the lower ν^D/ν^H ratio of 16b in pzO compared with those of pz (Table 3.10). The similar behaviour of the umbrella mode, 11(A_1) in pz-d_4O with

that found in pzO_2 and pz-d_4O_2 may indicate a deuteration-induced coupling with the γN-O vibration. This suggestion is supported by an observed deuteration-induced coupling found for the umbrella mode in toluene-d_7 [96]. The smaller change in the ν^D/ν^H ratio between pz and pzO, compared with that for pzO_2, would suggest that such coupling is not as extensive in pzO as is that of pzO_2.

In contrast the very high ν^D/ν^H ratio for the γC-H vibration mode 10b and its high frequency compared with that of mode 10a (as is also found for γ-picoline-d_7 [17]) indicates the occurrence of a considerable deuteration-induced coupling with the γN-O vibration.

The planar N-O bending vibration, mode 15b(B_2) is expected to be a pure vi-vibration as found in pyO and pzO_2 and as is observed for αC-CH_3 in γ-picoline, shown by its PED [13].

Finally, in extending the PED of γ-picoline, the Kekulé vibration, 14(B_2) couples with the planar C-H bend, 3(B_2). The lower frequency vibration is expected to show more C-C and C-N stretching character [13] and so is assigned to the ring mode. This accounts for the reversal in the assignment of modes 14 and 3 compared with that for a mono-substituted benzene [2] and with pyO [67,68]. Such coupling would be removed on deuteration, which explains the breaking of the isotopic rule that 'mass difference cannot bring about a crossing over of frequencies within the same species' [33].

The full vibrational assignment of pyrazine *N*-oxide made above should assist the vibrational assignments of its metal complexes, as well as helping to differentiate between complexes which are oxygen coordinated, nitrogen coordinated or bridged.

2.3 2,2'-Bipyridine *N,N'*-dioxide (bipyO_2)

The assignment of the fundamentals of 2,2'-bipyridine *N,N'*-dioxide (bipyO_2) and its fully deuterated analogue (bipy-d_8O_2) are made by firstly considering the two rings as mainly being independent of each other, so allowing a consideration of each ring in terms of being an *ortho*-di-light substituted benzene. Secondly, the molecule is considered as a whole with regard to the inter-ring effects. These are discussed with reference to the vibrational spectra of biphenyl and its -d_{10} analogue. Thirdly, the assignments are made in the light of previous partial infrared assignments for bipyO_2, by comparison of the Raman and infrared spectra of 2,2'-bipyridine (bipy) and its fully deuterated analogue (bipy-d_8) and, finally, with regard to the ν^D/ν^H ratio.

In considering the two rings behaving independently of each other, the modes of vibration of the molecule may be described in terms of (i) the WILSON modes and (ii) non-benzenoid modes. Both bipyO_2 and biphenyl have 54 benzene-type vibrations in which the two rings vibrate either in-phase or out-of-phase. Six non-benzene vibrations have been described by KATON and LIPPINCOTT [110] to replace the 'lost' benzene modes as a result of the ring-ring bond (Fig. 3.2). These are identified in this work by the first six uncial letters of the Greek alphabet. The interaction of these with the WILSON modes needs to be examined.

2.3.1 Vibrational coupling experienced by biphenyl-d_0 and -d_{10}

Tables 3.14 and 3.15 give the literature assignments of biphenyl and biphenyl-d_{10}. The work of KATON and LIPPINCOTT [110] was an attempt to assign the infrared and Raman spectra by a comparison with benzene. The papers of

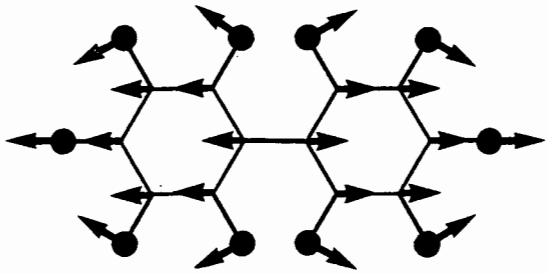

inter-ring stretch

(A ν inter-ring)

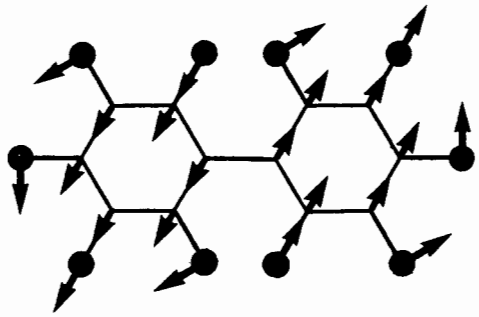

planar shear

(B i.p. shear)

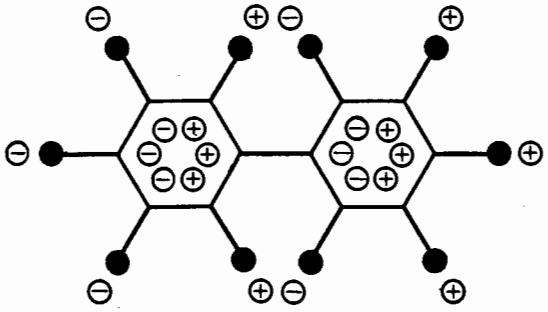

out-of-plane shear

(Γ o.p. shear)

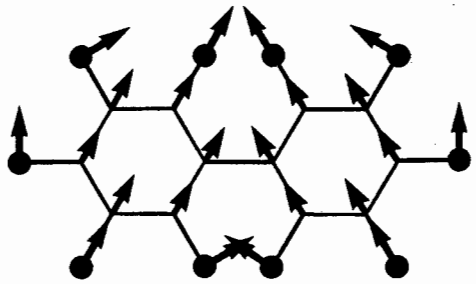

planar scissors

(Δ i.p. scissors)

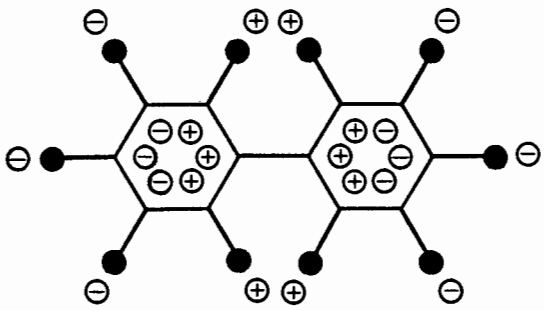

out-of-plane scissors

(E o.p. scissors)

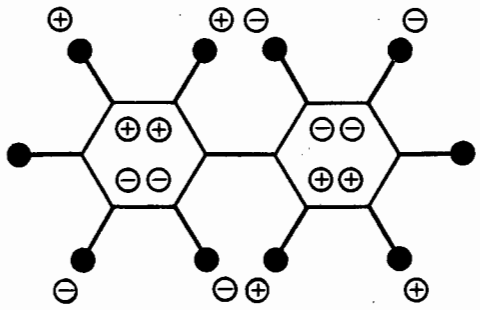

internal rotation

(Z i. rotation)

Figure 3.2 Non-benzenoid vibrational modes of biphenyl

Table 3.14 Assignments of biphenyl found in the literature

WILSON Mode [1]	benzene [13]	toluene [13]		OUT-OF-PHASE[a] biphenyl: KATON & LIPPINCOTT [110] (1959)	PEREGUDOV [111] (1960)	ZERBI & SANDRONI [114,115] (1968)	BARRETT & STEELE [112] (1972)	EATON & STEELE [113] (1973)	BREE *et al.* [116,117] (1971 & 75)
20a	3053	3056	B_{1u}	3086	3069	(3072/3082)[b]	(3073)	(3073)	3108
19a	1482	1500		1497	1492	1482	1480	1480	1481
18a	1037	1030		1046	1050	1040	1041	1041	1043
13	3048	1212		-	-	-	-	-	-
12	1010	1004		1012	1016	1008	1006	1006	1008
9a	1178	1178		1162	1190	1176	1181	1181	1183(?)
8a	1599	1611		1583	1600	1597	1597	1597	1599
7a	3048	3039		3038	3010	(3070/3075)[b]	(3069)	(3069)	3033
6a	606	521		738	(608)	609	610	610	608
2	3062	3067		3067	3047	(3069/3072)[b]	(3072)	(3072)	3059
1	993	786		993	996	965	985	985	990
20b	3053	3056	B_{2u}	3086	3096	(3070/3079)[b]	(3070)	(3070)	3085
19b	1482	1436		1440	1440	1432	1428	1428	1431
18b	1037	1083		1077	1080	1074	1072	1075	1093
15	1146	1155		1162	1170	1156	1155	1153	1156
14	1309	1278		1397	1280	1272	1268	1268	1272
9b	1178	341		1182	-	-	-	-	-
8b	1599	1585		1608	1580	1570	1568	1568	1569
7b	3048	3039		3067	3047	(3068/3070)[b]	(3069)	(3069)	3043
6b	606	623		606	(614)	628	626	626	627
3	1350	1330		-	1326	1383	1344	1344	1345
J	-	-		(140)	(105)	116	118	118	n/o
17a	967	964	A_u	969	n/o	n/o	964	963	969
16a	398	405		399	n/o	400	403	409	410
10a	846	843		841	n/o	838	838	833	841
E	-	-		n/o	n/o	70	n/o	n/o	n/o
17b	967	205	B_{3u}	-	-	-	-	-	-
16b	398	462		487	(430)	484	458	458	455
11	673	730		543	724	736	729	729	732
10b	846	894		778	904	903	903	903	904
5	990	980		904	974	n/o	968	968	1171(?)
4	707	695		695	688	698	695	695	698
Z	-	-		n/o	(95)	174	73	73	(73)[c]

Table 3.14 (continued)

WILSON Mode [1]	benzene [13]	toluene [13]		IN-PHASE[a] biphenyl: KATON & LIPPINCOTT [110] (1959)	PEREGUDOV [111] (1960)	ZERBI & SANDRONI [114,115] (1968)	BARRETT & STEELE [112] (1972)	EATON & STEELE [113] (1973)	BREE *et al.* [117] (1975)
20a′	3053	3056	A_g	3083	(3069)	(3072/3082)[b]	(3073)	(3072)	3070
19a′	1482	1500		1497	1504	1507	1513	1513	1512
18a′	1037	1030		1025	1032	1030	1036	1036	1038
13′	3048	1212		-	-	-	-	-	-
12′	1010	1004		1019	1003	1003	1006	1002	1001
9a′	1178	1178		1151	1185	1190	1205	1208	1209 or 1188
8a′	1599	1611		1583	1611	1612	1610	1610	1610[d]
7a′	3048	3039		3031	3047	(3068/3072)[b]	(3069)	(3069)	3021(?)
6a′	606	521		773	315	315	330	331	330
2′	3062	3067		3052	3060	(3070/3075)[b]	(3072)	(3074)	3051
1′	993	786		996	740	742	739	739	740
A	-	-		1275	1280	1285	1276	1276	1277
20b′	3053	3056	B_{3g}	3083	(3075)	(3069/3079)[b]	(3070)	(3070)	n/o
19b′	1482	1436		1448	1452	1452	1462	1462	1467
18b′	1037	1083		1035	1092	1090	1097	1097	n/o
15′	1146	1155		1145	1155	1158	1158	1165	1166
14′	1309	1278		1357	(1300)	1316	1262	1263	n/o
9b′	1178	341		1185	-	-	-	-	-
8b′	1599	1585		1603	1592	1595	1592	1592	n/o
7b′	3048	3039		3052	3047	(3068/3070)[b]	(3069)	(3069)	3056(?)
6b′	606	623		606	612	613	610	610	610
3′	1350	1330		-	1326	1376	1333	1333	1335(?)
B	-	-		302	407	407	(342)	395	n/o
17a′	967	964	B_{1g}	970	965	965	969	963	n/o
16a′	398	405		397	407	400	406	409	n/o
10a′	846	843		843	838	838	846	846	n/o
17b′	967	205	B_{2g}	-	-	-	-	-	-
16b′	398	462		470	540	441	546	546	547(?)
11′	673	730		531	780	708	782	775	785
10b′	846	894		775	897	903	908	909	n/o
5′	990	980		995	980	n/o	978	978	n/o
4′	707	695		696	(699)	545	(695)	694	633(?)
Γ	-	-		n/o	267	260	251	251	251

(a) refers to the vibrations of the two rings,

(b) calculated values simplified VFF/modified UBFF respectively,

(c) estimated, after EATON & STEELE [113],

(d) in Fermi resonance,

calculated values in parentheses,

n/o not observed.

Table 3.15 Assignments of biphenyl-d_{10} found in the literature

WILSON Mode [1]	benzene-d_6 [13]	toluene-d_8 [13]		OUT-OF-PHASE[a] biphenyl-d_{10} KATON & LIPPINCOTT [110] (1957)	PEREGUDOV [111] (1960)	ZERBI & SANDRONI [114,115] (1968)	EATON & STEELE [113] (1973)	BREE *et al.* [116,117] (1971 & 75)
20a	2276	2265	B_{1u}	2307	2274	(2288/2280)[b]	(2286)	2291
19a	1333	1378		1353	1360	1346	1343	1343
18a	814	842		843	816	816	813	813
13	2275	1144		-	-	-	-	-
12	970	961		986	988	983	991	1008(?)[c]
9a	869	871		913	868	846	854	864
8a	1558	1569		1555	1586	1568	1566	1567
7a	2266	2255		2255	2267	(2284/2267)[b]	(2279)	2273
6a	579	507		626	560	590	588	586
2	2293	2271		2287	2284	(2288/2280)[b]	(2284)	2253
1	945	741		952	956	952	950	982(?)
20b	2276	2265	B_{2u}	2307	2284	(2286/2270)[b]	(2281)	2284
19b	1333	1322		1330	1326	1328	1317	1319
18b	814	816		818	836	790	818	n/o
15	824	838		863	868	830	844	855
14	1282	1284		1269	1279	1266	1260	1266
9b	869	335		922	-	-	-	-
8b	1558	1556		1578	1570	1531	1522	1523
7b	2266	2255		2276	2250	(2279/2261)[b]	(2278)	2276
6b	579	597		592	(560)	565	594	594
3	1059	1035		-	1028	1010	1024	1119
λ	-	-		(137)	(97)	110	112	110
17a	787	(787)	A_u	783	n/o	n/o	780	790
16a	345	355		300	n/o	n/o	357	359
10a	660	660		660	n/o	n/o	648	n/o
ε	-	-		n/o	n/o	n/o	n/o	n/o
17b	787	208	B_{3u}	-	-	-	-	-
16b	345	413		435	(340)	466	410	409
11	496	551		462	(560)	540	538	538
10b	660	735		660	741	774	742	744
5	829	816		705	802	n/o	813	845
4	599	621		553	660	627	620	619
τ	-	-		n/o	(89)	160	73	73[d]

Table 3.15 (continued)

WILSON Mode [1]	benzene-d_6 [13]	toluene-d_8 [13]		IN-PHASE[a] biphenyl-d_{10} KATON & LIPPINCOTT [110] (1959)	PEREGUDOV [111] (1960)	ZERBI & SANDRONI [114,115] (1968)	EATON & STEELE [113] (1973)	BREE *et al.* [117] (1971)
20a'	2276	2265	A_g	2290	2297	(2287/2290)[b]	(2280)	2300
19a'	1333	1378		1335	1412	1412	1411	1415
18a'	814	842		838	840	835	846	853[e]
13'	2275	1144		-	-	-	-	-
12'	970	961		967	960	960	965	968
9a'	869	871		865	870	869	880	883
8a'	1558	1569		1551	1574	1571	1563	1562
7a'	2266	2255		2275	2272	(2280/2264)[b]	(2280)	2278
6a'	579	507		692	300	300	312	319
2'	2293	2271		2285	2286	(2284/2267)[b]	(2285)	2258
1'	945	741		840	692	688	690	693
A	-	-		1179	1188	1188	1188	1188
20b'	2276	2265	B_{3g}	2290	2297	(2285/2279)[b]	(2283)	n/o
19b'	1333	1322		1452	1345	1345	1347	1350
18b'	814	816		784	835	(813)	831	n/o
15'	824	838		865	870	840	850	853[e]
14'	1282	1284		1275	(1298)	1272	1280	1280
9b'	869	335		913	-	-	-	-
8b'	1558	1556		1571	1566	1566	1583	n/o
7b'	2266	2255		2285	2272	(2271/2261)[b]	(2279)	2278[e]
6b'	579	597		585	589	589	583	587
3'	1059	1035		-	1070	1070	1038	n/o
B	-	-		297	355	355	361	n/o
17a'	787	(787)	B_{1g}	790	780	n/o	780	n/o
16a'	345	355		346	355	n/o	354	n/o
10a'	660	660		652	654	n/o	655	n/o
17b'	787	208	B_{2g}	-	-	-	-	-
16b'	345	413		393	(453)	n/o	465	n/o
11'	496	551		500	530	n/o	544	543
10b'	660	735		646	780	n/o	759	821(?)
5'	829	816		775	835	n/o	816	836
4'	599	621		539	654	n/o	651	661
Γ	-	-		n/o	248	n/o	225	232

(a) refers to the vibrations of the two rings,

(b) calculated values simplified VFF/modified UBFF,

(c) in Fermi resonance,

(d) estimated, after EATON & STEELE [113],

(e) accidental degeneracy,

calculated values in parentheses,

n/o not observed.

PEREGUDOV [111] and of STEELE and his co-workers [112,113] yield assignments based upon normal coordinate calculations, while the findings of ZERBI and SANDRONI [114,115] result from normal coordinate calculations (planar vibrations only) plus extensive gas, solution and solid infrared and Raman studies. The papers of BREE and his co-workers [116,117] comprise single crystal infrared and Raman polarisation studies.

Two points are noted from the data. Firstly, agreement of the calculation and observed frequencies for the C-H stretching modes is relatively poor, reflecting possible anharmonicity and/or Fermi resonance. Secondly, there are a number of assignments which are in dispute, particularly the out-of-plane B_{2g} and B_{3u} vibrations. The earlier assignment of KATON and LIPPINCOTT has generally been superseded by that of ZERBI and SANDRONI, in light of their calculations. However, ZERBI and SANDRONI [118] point out the difficulty in making assignments of large polyatomic molecules based upon normal coordinate calculations since the introduction of another interaction constant into the force field may change the assignment slightly. In a molecule of high symmetry as is biphenyl, depolarisation studies, vapour band analyses and polarisation studies play a greater importance in the final analysis. Considering the nature of their work, the assignments by BREE *et al.* [116, 117] with the possible exception of $5(B_{3u})$ and $4'(B_{2g})$ (in view of those for toluene) are considered best where there is disagreement with the earlier workers. The assignments by BREE *et al.* [116,117] are also considered best for biphenyl -d_{10} with possibly the exception of $10b'(B_{2g})$ and $3(B_{2u})$, as shown in Table 3.15.

From the assignments of biphenyl it is important to note that the behaviour of the individual ring vibrations tends to follow that of toluene rather than that of benzene. The major exception to this observation lies with the B_{1u}

vibrations, which behave similarly to benzene. This behaviour is a reflection of the nature of the coupling experienced within the molecule (coupling which was not initially considered by KATON and LIPPINCOTT [110] as demonstrated by the subsequent assignment changes made by the later workers).

For the in-plane, in-phase A_g vibrations, the coupling seen is somewhat similar to that of a light substituted benzene. Coupling of the ring-breathing mode 1′ with the inter-ring stretch mode A typically results in the inter-ring stretch being found above 1100cm^{-1} and in mode 1′ being found below 900cm^{-1}. More significant though, is the coupling of the inter-ring stretch, mode A, with the planar ring mode, 6a′. Although a little coupling between mode 6a and the substituent stretching mode is found in pyO [72,74] and in toluene [104,105], the extent of coupling here is greater, to produce a much lower frequency band at 330cm^{-1} (315cm^{-1} biphenyl-d_{10}). The inter-ring stretch contributes about 30% to the potential energy of this vibration [114, 115] compared with only about 10% in toluene [104,105].* This vibration has been shown to be sensitive to a change in phase, decreasing in frequency from solid to liquid to gas [112], a reflection of the change in the force constant of the inter-ring bond. This type of coupling represents a significant difference from the two previous systems investigated, and as a similar behaviour is also observed in bipy and bipy-d_8, such coupling is to be expected in bipyO$_2$.

Although energetically allowed, the coupling described above does not occur in the analogous in-plane, out-of-phase B_{1u} vibrations since this is symmetry

---

* It may be added that the *change in the coupling* experienced by the inter-ring stretch of biphenyl compared with the C-CH$_3$ stretch of toluene invalidates the argument [110] that the higher frequency of the inter-ring stretch indicates a stronger than usual C-C bend.

forbidden (the inter-ring stretch being of A_g symmetry). This then accounts for the similarity of the B_{1u} vibrations to their benzene counterparts.

The other vibrations of the individual rings behave similarly to those of toluene apart from the C-H modes, 19b'(B_{3g}) and 11'(B_{2g}), and the ring mode, 16b'(B_{2g}). These three fundamentals are substantially higher in frequency than those found in toluene. From the normal coordinate analysis of biphenyl [115], the PED reveals a slight coupling of 19b'(B_{3g}) with the in-plane ring-shear, mode $B(B_{3g})$, which accounts for its variation to that of toluene. In the absence of published PED figures for the out-of-phase vibrations, a similar coupling with the out-of-plane shear mode $\Gamma(B_{2g})$ is tentatively postulated to explain the behaviour of modes 11'(B_{2g}) and 16b'(B_{2g}). The latter is supported by the extensive coupling of Γ and 16b' in bipy. The behaviour of the ring mode (16b') may also be the result of sensitivity to the dihedral angle between the rings.

According to BARRETT and STEELE [112], while no A vibrations are expected to be sensitive to the dihedral angle, some B vibrations below 1000cm^{-1} may be perturbed. In particular the coupling of the ring mode 16b(B_{2u}) with the in-plane shear, $B(B_{3g})$ increases as the dihedral angle is increased and the symmetry of the molecule is reduced. This occurs to a lesser extent for 16b'(B_{2g}) and 6b(B_{2u}), which couple with the in-plane scissors, mode $\Delta(B_{2u})$ and the out-of-plane shear, mode $\Gamma(B_{2g})$, respectively [112]. Such coupling is important for metal-ligand assignments since, in similar ligand systems, the non-benzenoid vibrations may be expected to reflect some degree of metal sensitivity as the result of kinematic coupling. This metal sensitivity might also then be seen in the coupled vibrations. Alternatively, the benzenoid vibrations might reveal significant frequency shifts as a result of complexation-induced decoupling from the non-benzenoid vibrations.

2.3.2 Vibrational coupling experienced by 2,2'-bipyridine-d_0 and -d_8

Tables 3.16 and 3.17 present the literature assignments for 2,2'-bipyridine (bipy) and 2,2'-bipyridine-d_8 (bipy-d_8). The work of PEARCE *et al.* [119] is an empirical assignment of the infrared spectrum of bipy based upon similar molecules. That of STRUKL and WALTER [120] reports the infrared assignments employing a fully deuterated labelling study, and a normal coordinate analysis. The work of SHIRO and KUWATA [121] presents a normal coordinate analysis of both the infrared active and the Raman active fundamentals (although only the infrared spectrum was recorded). The other two works represent three papers from the same research group. That of CASTELLI *et al.* [122] reports the polarised infrared and Raman spectra of single crystals, while the later two papers represent an extension of this work, plus a normal coordinate treatment of bipy (both internal and crystal vibrations) and of bipy-d_8 (internal modes only) [123,124].

It is noted that in comparing α-picoline (and hence bipy) with py, a change in the labelling of the 'missing' C-H modes is necessary. According to VARSANYI [2], the C-X modes for an *o*-dilight substituted benzene are 13 and 7a for the stretches, 9a and 18a for the planar bends and 17b and 17a for the out-of-plane bends. Thus mode 9a (α-picoline) replaces mode 9b (py) as the description of the 'lost' C-H planar bend. This is confirmed by the PED for α-picoline which shows that the C-H in-plane bend at 1055cm^{-1} contains some CN stretching character [13], this being typical of mode 9b rather than 9a. In the same way the assignment of the ring modes 8a and 8b have been reversed, the *higher* frequency band at 1594cm^{-1} showing CN stretching character is considered to be 8b in α-picoline (and correspondingly in bipy). PEARCE *et al.* [119] employed the WILSON notation for bipy, however their assignment did not reflect these two changes. For the sake of clarity, their assign-

Table 3.16 Assignments of 2,2'-bipyridine (bipy) found in the literature

WILSON[b] Mode [1]	pyridine [13]	α-picoline [13]		OUT-OF-PHASE[a] 2,2'bipy PEARCE *et al.*[c] [119] (1970)	STRUKL & WALTER [120] (1971)	SHIRO & KUWATA [121] (1972)	CASTELLUCI *et al.* [122] (1979)	NETO *et al.* [123,124] (1983)
20a	3034	3027	B_2	n/o	3054	3059	3054	3060
20b	3079	3064		n/o	3078	3085	3075	3083
19a	1483	1468		1458	1448	1435	1456	1456
19b	1437	1436		1417	1410	1405	1417	1420
18a	1069	355		-	-	-	-	-
18b	1069	1052		1066	1083	1050	1063	1067
15	1146	1148		1090	1138	1152	1139	1143
14	1293	1299		1310	1248	1307	1252	1271
13	-	-		-	-	-	-	-
12	1030	1036		1042	1063	1024	1039	1042
9a	1217	-		-	-	-	-	-
9b	-	1095		1140	1090	1070	1086	1088
8a	1581	1564		1560	1553	1566	1555	1565
8b	1574	1594		1580	1579	1599	1579	1585
7a	3057	(1176)		-	-	-	-	-
7b	3034	3046		n/o	3061	3059	3061	3068
6a	603	548		623	618	604	655	621
6b	665	624		(660)	651	638	892	654
3	1227	1246		1250	1210	1240	1210	1255
2	3079	3082		n/a	3086	3130	3085	3090
1	991	803		995	991	980	994	996
A				-	-	-	-	-
B				-	-	-	-	-
J				n/o	169	(154)	161	165
17a	980	194	A_2	-	-	-	-	-
17b	-	-		-	-	-	-	-
16a	380	401		410	398	388	403	403
16b	406	470		n/a	n/a	419	415	415
11	703	781		660	738	729	739	743
10a	884	883		760	753	833	758	808
10b	884	928		960	890	881	808	895
5	941	972		896	1039	964	974	975
4	747	729		744	710	742	620	765
Γ				-	-	-	-	-
E				n/o	94	133	111	117
Z				n/o	42	96	73	95

Table 3.16 (continued)

WILSON[b] Mode [1]	pyridine [13]	α-picoline [13]		IN-PHASE[a] 2,2'bipy SHIRO & KUWATA [121] (1972)	2,2'bipy CASTELLUCI *et al.* [122] (1979)	2,2'bipy NETO *et al.* [123,124] (1983)
20a'	3034	3027	A_g	3073	3011	3023
20b'	3079	3064		3078	3053	3058
19a'	1483	1468		1497	1482	1480
19b'	1437	1436		1449	1446	1442
18a'	1069	355		-	-	-
18b'	1069	1053		1039	1094	1048
15'	1146	1148		1160	1234	1145
14'	1293	1299		1198	1300	1236
13'	-	-		-	-	-
12'	1030	1036		993	995	993
9a'	1217	-		-	-	-
9b'	-	1095		1086	1047	1090
8a'	1581	1564		1581	1574	1570
8b'	1574	1594		1613	1591	1587
7a'	3057	(1176)		-	-	-
7b'	3034	3046		3076	3030	3048
6a'	603	548		295	332	330
6b'	665	624		603	615	614
3'	1227	1246		1321	1311	1308
2'	3079	3083		3082	3075	3074
1'	991	808		747	765	763
A				1292	1044	1299
B				396	412	413
Δ				-	-	-
17a'	980	194	B_g	-	-	-
17b'	-	-		-	-	-
16a'	380	401		361	353	355
16b'	406	470		245[d]	234[d]	236[d]
11'	703	781		775	741	742
10a'	884	883		847	816	815
10b'	884	928		890	738	906
5'	941	972		958	975	971
4'	747	729		743	906	736
Γ				458[d]	440[d]	440[d]
E				-	-	-
Z				-	-	-

(a) refers to the vibrations of the two rings,

(b) for py 13 ≡ 7a,

(c) 18b ≡ 18a; 17a ≡ 10b; 9a ≡ 9b; 8a ≡ 8b (see text),

(d) 16b(B_g) coupled to internal rotation (B_g) (see text),

calculated values in parentheses,

n/o not observed,

n/a not assigned.

WILSON Mode [1] (b)	py-d_5 [13]		OUT-OF-PHASE (a) 2,2'bipy-d_8 STRUKL & WALTER [110] (1971)	OUT-OF-PHASE (a) 2,2'bipy-d_8 NETO *et al.* [123,124] (1983)	IN-PHASE (a) 2,2'bipy-d_8 NETO *et al.* (c) [123,124] (1983)
20a	2252	B_u	2255	2259	A_g 2280
20b	2248		2280	2278	2285
19a	1339		1345	1333	1385
19b	1298		1300	1288	1341
18a	963		-	-	-
18b	835		801	783	791
15	867		850	822	820
14	1228		1245	1248	1183
13	-		-	-	-
12	888		1033	1025	983
9a	1009		-	-	-
9b	-		841	830	830
8a	1551		1529	1525	1530
8b	1537		1559	1550	1586
7a	2252		-	-	-
7b	2248		2270	2270	2282
6a	581		630	603	315
6b	624		664	631	728
3	963		965	963	963
2	2270		2295	2292	2288
1	824		990	983	593
A			-	-	1262
B			-	-	385
Δ			n/o	(149)	-
17a	(817)	A_u	-	-	B_g -
17b	-		-	-	-
16a	328		351	(369)	339
16b	368		n/o	(388)	210 (d)
11	536		602	578	558
10a	690		580	630	624
10b	768		734	668	672
5	824		827	792	775
4	582		690	727	685
Γ			-	-	414 (d)
E			n/o	(99)	-
Z			n/o	(66)	

see footnote of Table 3.16

Table 3.17 Assignments of 2,2'-bipyridine-d_8 (bipy-d_8) found in the literature

ments have been altered in Table 3.16 to follow those of α-picoline. To conform with the classification of VARSANYI, two other minor changes have also been made, namely, the 'lost' planar bend, 8a, and out-of-plane bend, 10b, of PEARCE *et al.* have been replaced by 18a and 17a, respectively.

Unfortunately there are no reports of either a PED or of the assignment of α-picoline-d_7 in the literature. In keeping with the reasoning above, the reversals of the ring modes 8a and 8b have been extended to the assignment of bipy-d_8. This however, will require confirmation through future PED calculations.

From Table 3.16 it is seen that, with a few exceptions, there is good agreement in the assignments for bipy. The greatest disagreement involves, surprisingly, the polarisation studies of CASTELLUCI *et al.* [122], from which several symmetry species [e.g. 6a(B_u), 6b(B_u) and 4(A_u), 10b(A_u)] and several mode descriptions [e.g. 14'(A_g), 15'(A_g), inter-ring stretch, 10b'(B_g), 5'(B_g) and 4'(B)] were later revised by NETO *et al.* [123,124]. Eight assignments still remain in question; the two Kekulé modes 14'(A_g) and 14(B_u); the two in-plane C-H bends 3'(A_g) and 3(B_u), the two out-of-plane bends 10b(A_u) and 5(A_u) and (more importantly) the out-of-plane scissors, mode E(A_u) and the internal rotation, mode Z(A_u).

The situation for bipy-d_8 is less satisfactory, with little experimental data available (Table 3.17), and for which there are several disagreements between STRUKL and WALTER [120] and NETO *et al.* [123,124] over the planar vibrations and for which there is *no* agreement for the out-of-phase vibrations. Furthermore, with the absence of published Raman spectra for bipy-d_8 and in the absence of the PED, the abnormal ν^D/ν^H ratios particularly of modes 1'(A_g) and 4'(A_g), may indicate the possibility of the calculated in-phase frequencies

being incorrect. This area clearly requires further investigation.

Nevertheless, the data do yield much information. As occurs in biphenyl, in bipy the inter-ring stretch, mode $A(A_g)$ is found to couple with the in-phase ring-breathing mode, $1'(A_g)$, and is strongly coupled with the in-phase ring mode $6a'(A_g)$. There are however two points of interest in which the coupling experienced within bipy differs from that of biphenyl.

The first involves the different behaviour of the Kekulé ring mode 14 and the planar C-H bend, mode 3, observed for the in-phase and out-of-phase vibrations. In the infrared active out-of-phase vibrations of bipy these two modes couple significantly. (In pyridine the higher frequency band, reflecting more ring character, is identified as the Kekulé mode [13]). This coupling in bipy is lost on deuteration and so follows, typically, the behaviour of pyridine [13]. However, there is apparently not such a significant degree of coupling in the Raman active in-phase vibrations, and therefore the C-H bend is found at a higher frequency than the Kekulé vibration (this being more typical of a substituted benzene [2,13]).

The second point of interest involves what appears to be extensive coupling of the out-of-plane shear, $\Gamma(B_g)$ and the ring torsion $16b'(B_g)$ which is such that there is a reversal of the assignment. The higher frequency band at $440cm^{-1}$ is considered to be the shear, while the lower band at $236cm^{-1}$ is considered to be the ring torsion [123,124]. This is clearly different from both α-picoline [13] and biphenyl [114-117]. The coupling is apparently maintained on deuteration of bipy [123,124].

The coupling above experienced by bipy needs to be considered in attempting the vibrational assignments of its metal complexes. However, in extending

the understanding of the behaviour of bipy to that of bipyO_2, the coupling involving the Kekulé vibration is unlikely to occur (rather, the behaviour of a substituted benzene is expected for both the in-phase and the out-of-phase vibrations). The second type of coupling unique to bipy, that involving the out-of-plane shear Γ, and the ring torsion 16b', may be of significance in bipyO_2, but in view of its being maintained on deuteration, the PED of bipyO_2 will be required to prove this since the ν^D/ν^H ratio will not show any 'abnormal' behaviour such as reflecting a deuteration-induced coupling.

Finally, in the absence of crystal structure data for bipyO_2, before the assignment of the infrared spectrum of bipyO_2 is attempted the final consideration to be pursued is that of predicting the most probable conformation of the molecule. Theoretically there are four conformational possibilities - *trans* coplanar with C_{2h} symmetry, *cis* coplanar with C_{2v} symmetry and the twisted non-planar conformations with C_2 symmetry, in which the molecule may be *syn* (cisoid) or *anti* (transoid) with respect to the N-O groups.

While an initial reflection might suggest that the least sterically hindered conformation would be that of the *anti* non-planar molecule, the 2,2'-dihalo biphenyls are found to have a *syn* non-planar conformation rather than the *anti* [125]. As would be expected, the dihedral angle increases with increasing size of the halogen. What is surprising however, is that the intramolecular halogen-halogen distance (with the exception of F) is *shorter* than that predicted by Pauling's Van der Waal's radii, a discrepancy which *increases* with the increase in the atomic number of the halogen (Table 3.18), thereby indicating the presence of some intramolecular attraction.

This intramolecular attractive force between the non-bonded halogen atoms has been suggested by DYNES *et al.* [126] to be similar to the stabilizing

	ø°	X-X(Å)	V.d. Waal's radii (Å)	Δ(X-X) (Å)	Pauling's Electroneg. Scale
2,2'-di-F-biphenyl	60°	2,85	2,70	-0,15	4,0
2,2'-di-Cl-biphenyl	74°	3,46	3,60	+0,14	3,0
2,2'-di-Br-biphenyl	75°	3,62	3,90	+0,28	2,8
2,2'-di-I-biphenyl	79°	3,82	4,30	+0,48	2,5
'2,2'-di-O-biphenyl'	-	-	2,80	(-0,03)	3,5

Table 3.18 Effect of electronegativity on the intramolecular distance (X-X) of 2,2'di-halo-biphenyl

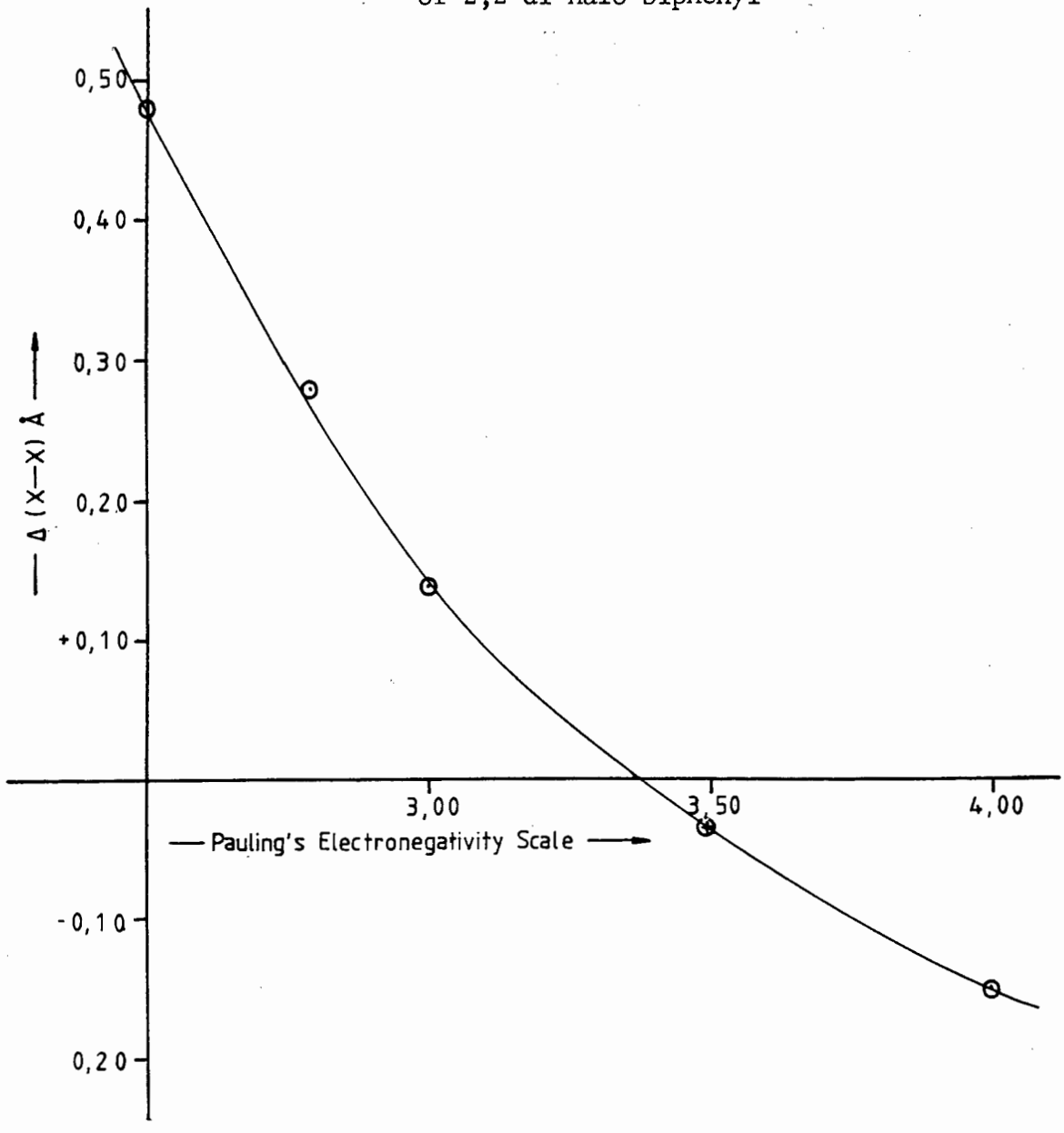

Figure 3.3 Plot of electronegativity *vs* the intramolecular distance (X-X) of 2,2'di-halo-biphenyls

effects experienced by the *cis* isomers of 1,2-dihalo-ethylenes. Their stability is considered to be a result of through-space interaction of the lone pair orbitals of the halogen [127,128]. This force may also be considered similar to the interatomic 'chlorine atom effect' of SCHMIDT and GREEN [129, 130], by which highly overlapped parallel molecules in the crystal structure of aromatic molecules are produced by halogen substitution of the phenyl ring.

The reason for the different behaviour of the fluorine substituent is considered here to be the competitive result of the electrostatic repulsion between the two highly electronegative fluorine atoms dominating the interaction of the lone pair orbitals of the halogens. While oxygen is isoelectronic with fluorine, it is less electronegative, falling midway between F and Cl on the Pauling electronegativity scale (Table 3.18). Therefore, from a plot of Pauling's electronegativity scale against the difference between the observed halogen-halogen distance for 2,2'-disubstituted biphenyl and the Van der Waal's radii (Fig. 3.3), it is observed that the expected O-O distance in a hypothetical *o*-di-O-substituted biphenyl would be equal approximately to the sum of the Van der Waal's radii. If such a distance is taken for the oxygens in bipyO_2, then for the molecule to exist in the *cis*-coplanar conformation would require a distortion in the CNO angle of some 30° (Fig. 3.4). The alternative conformation of the molecule would be for the two rings to be twisted with respect to each other, through a dihedral angle of 61° (Fig. 3.4).

Whether or not the molecule is likely to exist in the planar conformation in the solid state depends on whether the stabilisation by intra- and interatomic forces will overcome the energy barrier which would exist for the planar conformation. Such stabilisation in less sterically hindered molecules is demonstrated by biphenyl and 2,2'-bipyrimidine which have calculated

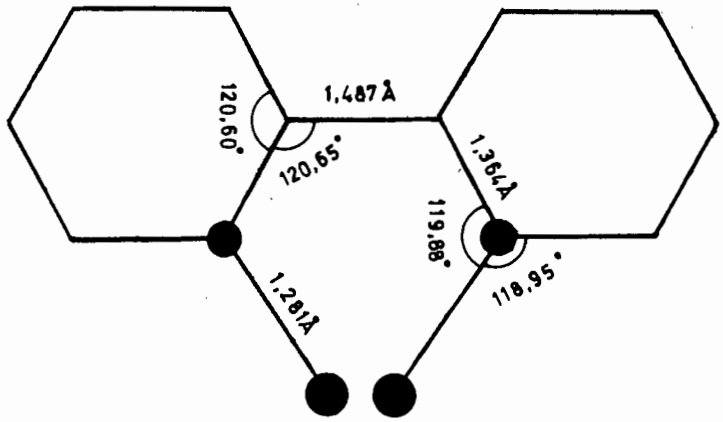

sideview through the plane of one ring

view down the inter-ring bond

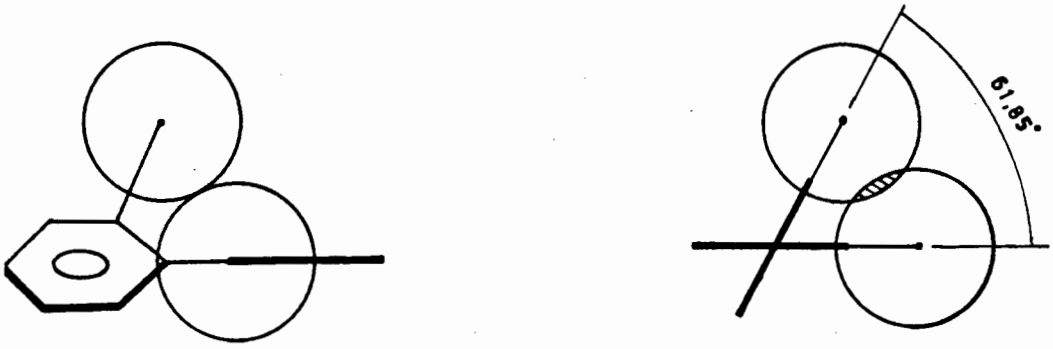

syn nonplanar model

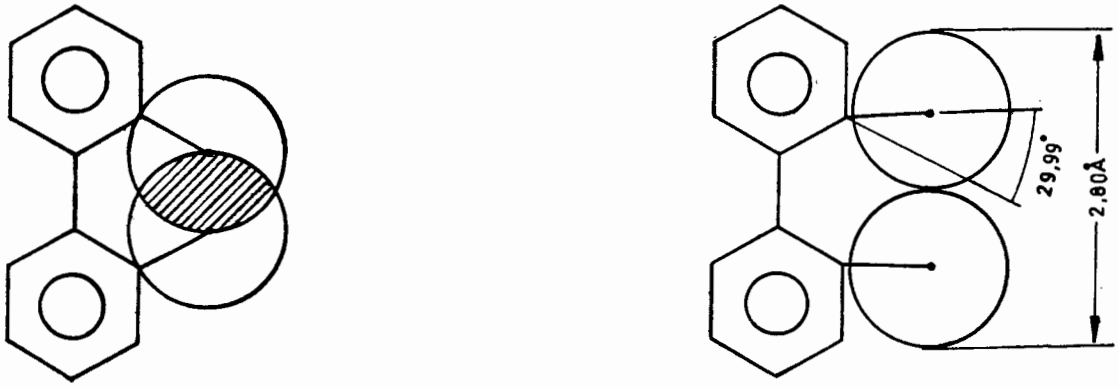

cis coplanar model

Figure 3.4 Possible conformations of 2,2'-bipyridine *N*,*N*'-dioxide (bipyO_2)

(See Appendix 2 for calculations)

gaseous phase torsion angles of 42° and of 49°, respectively, but which are both planar in the solid state [131].

While, from the discussion given above, the electrostatic repulsion between the electronegative oxygen atoms should exactly counterbalance the intramolecular interaction of the lone pair orbitals of the oxygens, the possibility of the intermolecular 'chlorine atom-type interaction' needs to be examined since this could provide the necessary stabilisation to overcome the intramolecular O-O repulsion.

The crystal structure of pyO [132] shows that it is the intermolecular interaction between the oxygen and two adjacent *carbons* which determines the crystal packing. Similarly, for phenazine 5-oxide [133], the overlaying of the ring systems is determined by carbon-carbon interactions rather than oxygen-oxygen interaction, since oxygens are found in opposite positions. Clearly the 'chlorine atom-type interaction' is minimal in aromatic *N*-oxides, undoubtedly the result of the participation of the lone pairs of the oxygen in the N-O bond.

With the stabilisation of bipyO_2 therefore likely to be predominantly due to the interatomic interaction of the rings, it is unlikely that such a sterically hindered molecule will exist in the *cis*-coplanar conformation in the solid state.

2.3.3 The vibrational assignment and coupling experienced by 2,2′-bipyridine *N*,*N*′-dioxide -d_0 and -d_8

For the *syn* non-planar configuration with C_2 symmetry all 60 fundamentals are expected to be both infrared and Raman active. The *A* species describe those

fundamentals in which the vibrations of the two rings are in-phase, while the *B* species describe those in which they are out-of-phase.

For the *cis*-coplanar configuration with C_{2v} symmetry the A_1 (in-plane, in-phase vibrations), the B_1 (out-of-plane, in-phase vibrations) and B_2 (out-of-plane, out-of-phase vibrations) are expected to be both infrared and Raman active, while the 10 A_2 fundamentals (in-plane, out-of-phase vibrations) are expected to be infrared silent and Raman active.

The systematic infrared silence of the in-plane, out-of-phase vibrations therefore presents a potential spectroscopic 'proof' of the solid state conformation of bipyO$_2$. The effectiveness of this, however, is reduced due to the difficulty in assigning such a vibrationally rich spectrum which arises from bipyO$_2$ being a large polyatomic molecule with low symmetry. The more numerous the spectral bands, the greater is the probability of accidental degeneracies, of Fermi resonance, and of compensating errors occurring in isotope labelling studies (such as the one conducted here). Nonetheless, by a comparison of bipyO$_2$ and bipy-d_8O$_2$ with similar molecules, the infrared activity of the in-phase, out-of-plane vibrations (Table 3.19) supports the conclusions drawn above, *viz.* the *syn*-non-planar conformation of the molecule in the solid state. The assignments made here of the infrared spectra of bipyO$_2$ and its -d_8 isotopomer (Tables 3.20 and 3.21) therefore accords C_2 symmetry to the molecule.

Another result of the low symmetry of the molecule and the substantial number of vibrations present is the large number of possible overtone, combination and difference bands. The assignment of these presented here are those calculated to fall within ± 6cm^{-1} of the observed frequency. The large number of possibilities of describing these bands does not, generally, make them use-

Table 3.19 The ν^D/ν^H ratio of 2,2'-bipyridine *N,N'*-dioxide (bipyO_2) and its -d_8 analogue (bipy-d_8O_2) compared with similar molecules

OUT OF PHASE[a]

WILSON	biphenyl			2,2'-bipy			*o*-di-F benzene			2,2'-bipyO_2		
Mode	-d_0	-d_{10}	ν^D/ν^H	-d_0	-d_8	ν^D/ν^H	-d_0	-d_4	ν^D/ν^H	-d_0	-d_8	ν^D/ν^H
20a	3108	2291	0,737	3060	2259	0,738	3081	2307	0,749	3105	2289	0,737
20b	3085	2284	0,740	3083	2278	0,739	3081	2296	0,745	3086	2280	0,739
19a	1481	1343	0,907	1456	1333	0,916	1469	1368	0,931	1479	1341	0,907
19b	1431	1319	0,922	1420	1288	0,907	1514	1448	0,956	1428	1332	0,933
18a	1042	813	0,780	-	-	-	440	420	0,954	466	432	0,927
18b	1093	818	0,748	1067	783	0,734	1025	818	0,798	1022	771	0,754
17a	969	790	0,815	-	-	-	560	498	0,889	214	204	0,953
17b	-	-	-	-	-	-	296	281	0,949	-	-	-
16a	410	359	0,876	403	(369)	0,916	200	189	0,945	(402)	(364)	(0,905)
16b	455	409	0,899	415	(388)	0,935	454	397	0,874	516	468	0,907
15	1156	855	0,740	1143	822	0,719	1155	858	0,743	1148	853	0,743
14	1272	1266	0,995	1271	1248	0,982	1298	1227	0,945	1299	1222	0,941
13	-	-	-	-	-	-	1206	1175	0,974	-	-	-
12	1008	991	0,983	1042	1025	0,984	857	788	0,919	856	795	0,923
11	732	538	0,735	743	578	0,778	748	592	0,791	768	597	0,777
10a	841	648	0,770	808	630	0,780	929	757	0,815	(848)	656	(0,770)
10b	904	744	0,823	895	668	0,746	850	706	0,830	892	721	0,808
9a	1183	864	0,730	-	-	-	287	288	1,003	-	-	-
9b	-	-	-	1088	830	0,763	1103	874	0,792	1097	876	0,798
8a	1599	1567	0,980	1565	1525	0,974	1618	1602	0,990	1602	1569	0,979
8b	1569	1523	0,971	1586	1550	0,977	1606	1583	0,986	1553	1526	0,983
7a	3033	2273	0,749	-	-	-	1270	1185	0,933	1265	1214	0,960
7b	3043	2276	0,748	3068	2270	0,740	3080	2272	0,738	3014	2246	0,745
6a	608	586	0,964	621	603	0,971	568	550	0,968	581	556	0,957
6b	627	594	0,947	654	631	0,965	548	530	0,967	541	519	0,959
5	968	845	0,873	975	792	0,812	908	806	0,833	960	830	0,865
4	698	619	0,887	765	727	0,950	705	605	0,858	724	609	0,841
3	1345	1024	0,761	1255	963	0,767	1282	1014	0,791	(1331)	1025	(0,770)
2	3059	2253	0,736	3090	2292	0,742	3065	2296	0,749	3048	2246	0,737
1	990	982	0,992	997	983	0,987	764	708	0,927	983	998	1,015
Δ	118	110	0,932	165	(149)	(0,903)				123	116	0,943
Ε	73-95	72-160	-	117	(99)	(0,845)				115	109	0,948
Z	70	n/o	-	95	(66)	(0,695)				104	100	0,961

Table 3.19 (continued)

IN PHASE[a]

WILSON	biphenyl			2,2'-bipy			*o*-di-F benzene			2,2'-bipyO$_2$		
Mode	$-d_0$	$-d_{10}$	ν^D/ν^H	$-d_0$	$-d_8$	ν^D/ν^H	$-d_0$	$-d_4$	ν^D/ν^H	$-d_0$	$-d_8$	ν^D/ν^H
20a'	3070	2300	0,749	3023	2280	0,754	3081	2307	0,749	3069	2280	0,743
20b'	(3069)	(2283)	(0,744)	3058	2285	0,747	3081	2296	0,745	3069	2271	0,740
19a'	1512	1415	0,936	1480	1385	0,936	1469	1368	0,931	1505	1431	0,951
19b'	1467	1350	0,920	1442	1341	0,930	1514	1448	0,956	1433	1368	0,955
18a'	1036	853	0,823	-	-	-	440	420	0,954	478	442	0,925
18b'	1097	831	0,758	1048	791	0,755	1025	818	0,798	1032	830	0,804
17a'	965	780	0,808	-	-	-	560	498	0,889	220	211	0,959
17b'	-	-	-	-	-	-	296	281	0,949	-	-	-
16a'	407	354	0,870	355	339	0,955	200	189	0,945	(402)	(364)	(0,905)
16b'	546	465	0,852	236	210	0,890	454	397	0,874	516	481	0,932
15'	1165	853	0,732	1145	820	0,716	1155	858	0,743	1148	853	0,743
14'	1263	1280	1,013	1236	1183	0,957	1298	1227	0,945	1307	1292	0,989
13'	-	-	-	-	-	-	1206	1175	0,974	-	-	-
12'	1002	968	0,966	993	983	0,990	857	788	0,919	839	778	0,927
11'	785	543	0,692	742	558	0,752	748	592	0,791	768	556	0,724
10a'	846	655	0,774	815	624	0,766	929	757	0,815	(850)	656	(0,772)
10b'	908	759	0,836	906	672	0,742	850	706	0,830	(933)	739	(0,792)
9a'	1188	883	0,743	-	-	-	287	288	1,003	-	-	-
9b'	-	-	-	1090	830	0,761	1107	874	0,790	1119	876	0,783
8a'	1610	1562	0,970	1570	1530	0,974	1618	1602	0,990	1621	1594	0,983
8b'	1592	1566	0,984	1587	1586	0,999	1606	1583	0,986	1602	1569	0,979
7a'	3021	2278	0,754	-	-	-	1270	1185	0,933	1255	1214	0,967
7b'	3056	2278	0,745	3048	2282	0,749	3080	2272	0,738	3002	2224	0,741
6a'	330	319	0,967	330	315	0,954	568	550	0,968	320	301	0,941
6b'	610	587	0,962	614	728	1,186	548	530	0,967	526	504	0,958
5'	978	836	0,855	971	775	0,798	968	806	0,833	976	806	0,826
4'	694	661	0,952	736	685	0,931	705	605	0,858	724	616	0,851
3'	1335	1070	0,801	1308	963	0,736	1282	1014	0,791	(1352)	1080	(0,799)
2'	3051	2258	0,740	3074	2288	0,744	3064	2296	0,749	3036	2271	0,748
1'	740	693	0,936	763	593	0,777	764	708	0,927	(741)	683	(0,922)
A	1227	1188	0,968	1299	1262	0,972				(1232)	1174	(0,953)
B	395	361	0,914	412	385	0,934				350	350	1,000
Γ	251	232	0,924	440	414	0,941				276	267	0,967

(a) refers to the vibrations of the two rings

calculated values in parentheses

Table 3.20 The infrared spectrum of 2,2'-bipyridine *N,N'*-dioxide

Infrared cm^{-1}	Assignment
3124 w	7b'+Δ(*B*); 19a'+8a'(*A*); 7b+Z(*A*).
3105 m	20a(*B*) fundamental.
3086 m	20b(*B*) fundamental.
3069 msh	20a'(*A*) fundamental; 20b'(*A*) fundamental.
3048 ssh	2(*B*) fundamental.
3036 s	2'(*A*) fundamental.
3014 s	7b(*B*) fundamental.
3002 s	7b'(*A*) fundamental.
2973 m	8a+3(*A*); 8b'+3(*B*); 20b-*E*(*A*); 19b+8b(*A*).
2934 w	2-*E*(*A*); 2'-Z(*B*); 19a+19b'(*B*); 14'+8a'(*A*).
2908 w	14'+8a(*B*); 14'+8b'(*A*); 8b+3'(*B*); 7b+Z(*A*); 19a+19b'(*B*); 2'-*E*(*B*).
2776 w	19+14(*A*); 19b+3'(*B*); 2-Γ(*B*); 19a'+7a(*B*).
2752 w	15+8a(*A*); 15+8a'(*B*); 15+8b(*A*); 15+8b'(*B*); 20a'-6a'(*A*); 20b'-6a'(*A*); 20a-*B*(*B*).
2648 vw	9b+8b(*A*); 2-16a(*A*); 2-16a'(*B*); 14+3'(*B*); 19a'+15(*B*); 19a'+15'(*A*); 18b'+8a'(*A*); 18b+8a'(*B*); 7b'-*B*(*B*).
2635 vw	18b'+8a(*B*); 18b'+8b'(*A*); 2'-16a(*B*); 2'-16a'(*A*); 14+3(*A*); 8a'+1(*B*).
2490 w	19a'+1(*B*); 7b-6b'(*B*); 20a-6a(*A*); 20b-6a(*A*); 7a'+A(*A*); 7b -16b(*B*); 7b'-16b'(*A*); 2'-6b(*B*); 10b+8a(*A*); 10b+8b'(*B*).
2411 vw	19b+1(*A*); 19a+10b'(*B*); 15+7a(*A*); 15'+7a(*B*); 12+8b(*A*); 19b'+5'(*A*); 19b+5'(*B*).
2367 vw	19b'+10b'(*A*); 11+8a(*A*); 11+8b'(*B*); 11'+8a(*B*); 11'+8b'(*A*); 20a-1'(*B*); 19a+10b(*A*); 18a'+1'(*A*); 20b-4(*A*); 20b-4'(*B*).
2313 vw	2'-4(*B*); 2'-4'(*A*); 20b-11(*A*); 20b-11'(*B*); 19a+12'(*B*).
2273 w	19a'+11(*B*); 19a'+11'(*A*); 7b-1'(*B*); 19a+12'(*B*); 14+ 5'(*B*); 8b+4(*A*); 8b+4'(*B*); 2'-11(*B*); 2'-11'(*A*); 7b'-4(*B*); 7b'-4'(*A*); 15+9b'(*B*); 15'+9b'(*A*); 19b+12'(*B*); 14'+5(*B*).
2080 w	15+10a'(*B*); 15'+10a'(*B*); 18a'+8a(*B*); 18a'+8b'(*A*); 9b'+5(*B*); 8b+6b(*A*); 7b+10b'(*B*); 20a-18b(*A*); 14'+11(*B*); 14'+11'(*A*); 20a'-1(*B*); 20b'-1(*B*); 19a'+6(*B*).
1986 vw	20a-9b'(*B*); 15+12(*A*); 15'+12(*B*); 20b-9b(*A*); 19a+18a'(*B*); 10b+9b(*A*); 7a+4(*A*); 7a+4'(*B*); 18b+4(*A*); 18b'+4(*B*); 7b-18b(*A*).
1955 w	16a+8b(*A*); 16a'+8b(*B*); 19a+18a(*A*); 19b'+6b'(*A*); 18b+16b'(*B*); 20a-15(*A*); 20a-15'(*B*); 12+9b(*A*); 5'²(*A*); 12+9b'(*B*); 8a+*B*(*B*); 8b'+*B*(*A*); 19b-6b'(*B*); 5'+1(*B*); 2-9b(*A*); 20a'-9b'(*A*); 20b'-9b'(*A*); 19b+16b(*B*); 19b'+16b'(*A*).
1930 w	2'-9b(*B*); 18b'+10b(*B*); 12'+9b(*B*); 5'+5(*B*).
1837 w	20a-7a(*A*); 20a'-A(*A*); 20b'-A(*A*); 9b+1'(*B*); 7a'+6a(*B*); 19b'-16a(*B*); 19b'-16a'(*A*); 17a+8a(*A*); 12+1(*A*); 14+6b(*A*); 14'+6b'(*A*); 12+5(*A*); 9b'+4(*B*); 9b'+4'(*A*).
1772 vw	18a+14(*B*); 18b'+1'(*A*); 16b+7a(*A*); 16b'+7a(*B*); 7b'-A(*A*); 2'-7a(*B*); 20a-3(*A*); 20a'-14(*B*); 20b'-14(*B*); 18a'+14(*B*); 17a+8b(*A*); 20b-14'(*B*); 19b+*B*(*A*).

Table 3.20 (continued)

Infrared cm^{-1}	Assignment
1726 w	19a'+17a'(A); 8a+Δ(A); 8a'+Z(B); 8b'+Δ(B); 5+11(A); 5+11'(B); 1+1'(B); 15+6a(A); 15'+6a(B); 2'-14'(A); 18a+7a(A); 12+10b(A).
1656 w	20b-19b(A); 16a+7a(A); 16a'+7a(B); 14'+B(A); 8b+Z(A); 19b'+17a'(A); 11+10b(A); 11'+10b(B); 9b'+6b(B); 7b'-3(B).
1621 w	8a'(A) fundamental.
1602 w	8a(B) fundamental; 8b'(A) fundamental.
1553 wm	8b(B) fundamental.
1505 m	19a'(A) fundamental.
1479 s	19a(B) fundamental.
1475 ssh	17a'+7a'(A); 5-16b(A); 5-16b'(B); 17a+7a(A); 8a+Δ(A); 8b'+Δ(B); 9b'-B(A).
1457 w	7b-8b(A); 18a'+5'(A); 18a'+1(B).
1433 ssh	19b'(A) fundamental.
1428 s	19b(B) fundamental.
1307 w	14'(A) fundamental.
1299 m	14(B) fundamental.
1265 vs	7a(B) fundamental.
1255 vs	7a'(A) fundamental.
1207 wm	19b-17a'(B); 12+B(B); 19a-Γ(B); 14-E(A); 8b-B(B); 17a'+1(B); 18a'+4(B); 18a'+4'(A); 10b+6a'(B); 9b+E(B); 19b'-17a'(A).
1148 s	15(B) fundamental; 15'(A) fundamental.
1119 m	9b'(A) fundamental.
1097 m	9b(B) fundamental.
1062 vw	8a-6b(A); 8b'-6b(B); 5+Z(A); 18a'+6a(B); 17a'+12'(A); 6b+6b'(B).
1055 vw	17a+12(B); 16b+6b(A); 16b'+6b(B); $6b'^2(A)$; 18a'+6b(B); 7a-17a(A); 8a-6b(A); 8b'-6b(B);
1047 vw	18a+6a(A); 7a-17a'(B); 11+Γ(B); 11'+Γ(A); 4+6a'(B); 4'+6a'(A); $6b'^2(A)$; 7a'-17a(B).
1032 w	18b'(A) fundamental.
1022 s	18b(B) fundamental.
1018 msh	18a'+6b(B); 10b+Δ(A); 9b'-Z(B); 8a-6a(A); 8b'-6a(B); 19a-18a(A); 14-Γ(B).
983 wm	1(B) fundamental.
976 w	5'(A) fundamental.
960 s	5(B) fundamental.
892 m	10b(B) fundamental.
856 s	12(B) fundamental.
839 s	12'(A) fundamental.
768 vs	11(B) fundamental; 11'(A) fundamental.
724 s	4(B) fundamental; 4'(A) fundamental.

Table 3.20 (continued)

Infrared cm^{-1}	Assignment
632 wm	15-16b(*A*); 15-16b'(*B*); 15'-16b(*B*); 15'-16b'(*A*); 16b+*E*(*A*); 16b'+*E*(*B*); 9b-18a(*A*); 16b+*Z*(*A*); 16b'+*Z*(*B*); 10b-17a'(*B*); 8a-5'(*B*); 8b'-5'(*A*); 16b+Δ(*A*); 16b'+Δ(*B*); *B*+Γ(*A*).
581 s	6a(*B*) fundamental.
541 wm	6b(*B*) fundamental.
526 s	6b'(*A*) fundamental.
516 s	16b(*B*) fundamental; 16b'(*A*) fundamental.
478 w	18a'(*A*) fundamental.
466 m	18a(*B*) fundamental.
350 vw	*B*(*A*) fundamental.
320 s	6a'(*A*) fundamental.
276 w	Γ(*A*) fundamental.
247 vw	19a-*A*(*B*); 18a-17a'(*B*); 8b-14'(*B*); 4-18a'(*B*); 4'-18a'(*A*); *B*-*Z*(*B*); Δ^2(*A*); 8a-3'(*B*); 8b'-3'(*A*); 6b'-Γ(*B*); 19a'-7a'(*A*); 9b-2(*A*); 11-6b'(*B*); 11'-6b'(*A*); 5'-4(*B*); 5'-4'(*A*).
220 w	17a'(*A*) fundamental.
214 w	17a(*B*) fundamental.
150 w	14-15(*A*); 14-15'(*B*); 10b-1'(*B*); 19a-3(*A*); 19a'-3'(*A*); Γ-Δ(*B*); 18a-6a'(*B*); 7a-9b'(*B*); 1-12'(*B*).
123 m	Δ(*B*) fundamental.
115 m	*E*(*B*) fundamental.
104 m	*Z*(*B*) fundamental.
71 m	libration.
66 m	libration.

s = strong

m = medium

w = weak

v = very

sh = shoulder

br = broad

Table 3.21 The infrared spectrum of 2,2′-bipyridine-d_8 *N,N′*-dioxide

Infrared cm^{-1}	Assignment
3155 vw	20a′+9b(*B*); 20a′+9b′(*A*); 20b+9b(*A*); 20b+9b′(*B*).
3059 vw	20a+18b(*A*); 20a′+12′(*A*); 20b+12′(*B*); 18b′+7b′(*A*); 7b′+5(*B*).
2724 vw	19a′+14′(*A*); 20a′+18a′(*A*); 20b+18a′(*B*); 20a+18a(*A*); 16b′+2(*B*); 16b′+7b(*B*); 7b′+6b′(*A*).
2665 vw	$19b^2$(*A*); 18a′+7b(*B*); 19b′+14′(*A*).
2535 w	20b′+Γ(*A*); 2′+Γ(*A*).
2416 w	19b+3′(*B*); 19a+3′(*B*); 15+8a(*A*); 15+8a′(*B*); 15′+8a(*B*); 15′+8a′(*A*).
2378 vw	15+8b(*A*); 15′+8b(*B*); 20a′+Z(*B*); 20b+Z(*A*); 20b′+E(*B*); 2+E(*A*); 12+8a(*A*).
2347 vw	12′+8a(*B*); 12′+8b′(*A*); 7b+Z(*A*); 2+Z(*A*); 7a+A(*B*); 7a′+A(*A*).
2289 m	20a(*B*) fundamental.
2280 s	20a′(*A*) fundamental; 20b(*B*) fundamental.
2271 s	20b′(*A*) fundamental; 2′(*A*) fundamental.
2246 mw	7b(*B*) fundamental; 2(*B*) fundamental.
2224 mw	7b′(*A*) fundamental.
2120 vw	19a+12′(*B*); 18b′+14′(*A*); 14′+5(*B*); 11+8b(*A*); 7b-Z(*A*); 11′+8a(*B*); 11′+8b′(*A*); 8a+6a(*A*); 8b′+6a(*B*); 7b′-E(*B*); 19a+2′(*B*).
2090 vw	9b+7a(*A*); 9b+7a′(*B*); 9b′+7a(*B*); 9b′+7b′(*A*); 19b′+10b(*B*); 19a′+10a′(*A*); 8a+6b(*A*); 8b′+6b(*B*); 20a-17a(*A*).
1978 vw	20a-6a′(*B*); 20b′-6a′(*A*); 7b-Γ(*B*); 2-Γ(*B*); 5′+A(*A*); 19b′+4(*B*); 14′+2′(*A*); 19b′+4′(*A*).
1890 w	16a+8b(*A*); 16a′+8b(*B*); 14′+11(*B*); 19b+11′(*B*); 19b+6a(*A*); 19b′+6b(*B*); 3′+5′(*A*); 10b+A(*B*); 8a′+6a′(*A*); 7b-B(*B*); 2-B(*B*).
1812 vw	20a′-16b(*B*); 20b-16b(*A*); 19b+16b′(*B*); 14′+6b(*B*); 11+7a(*A*); 11+7a′(*B*); 7b-18a(*A*); 2-18a(*A*); 19a+16b(*A*).
1762 w	20a′-6b(*B*); 20b-6b(*A*); 3′+2′(*A*); 19b+18a(*A*); 16b+14′(*B*); 10b′+3(*B*); 20b′-6b′(*A*); 2′-6b′(*A*); 7b-16b(*A*).
1732 w	19a′+6a′(*A*); 19b′+16a(*B*); 19a′+-6a′(*A*); 20a-11′(*B*); 20a-6a(*A*); 10a+3(*A*); 7a+6b(*A*); 7a′+6a(*B*); 17a+8b(*A*); 11′+A(*A*); 6a+A(*B*); 15+9b(*A*); 15+9b′(*B*); 15′+9b(*B*); 15′+9b′(*A*); 14+6b′(*B*); 10b′+1(*B*); 7b-6b(*A*); 2-6b(*A*).
1685 vw	$9b^2$(*A*); $9b'^2$(*A*); 8a+Δ(*A*); 8b+Δ(*B*); 18b′+15(*B*); 18b′+15′(*A*); 15+5(*A*); 15′+5(*B*); 20a′-11(*B*); 20b-11(*A*); 19b+B(*B*); 16b+7a(*A*); 18b+7a′(*B*); 10a′+3(*B*); 4+3′(*B*); 2′+1(*B*); 20a-4(*A*); 16b+14(*A*); 19a+B(*B*); 7b-11′(*B*); 7b-6a(*A*); 2-11′(*B*); 2-6a(*A*).
1620 vw	20b′-10a(*B*); 11+3(*A*); 2-10a(*A*); 20a′-10a′(*A*); 20b-10a′(*B*); 18b+15(*A*); 18b+15′(*B*); 20b′-10a′(*A*); 18b′+12(*B*); 10b′+9b(*B*); 10b′+9b′(*A*); 12+5(*A*); 7b′-4(*A*); 2′-10a′(*A*); 4′+1(*B*).
1611 vw	$5'^2$(*A*); 19a+Γ(*B*); 12+5(*A*); 7b′-4′(*A*); 4′+1(*B*); 20b′-10a′(*A*); 10b+9b(*A*); 10b+9b′(*B*); 2′-10a′(*A*); 20a-2′(*B*); 18a+A(*B*).
1594 m	8a′(*A*) fundamental.
1569 ms	8a(*B*) fundamental; 8b′(*A*) fundamental.
1526 ms	8b(*B*) fundamental.

Table 3.21 (continued)

Infrared cm^{-1}	Assignment
1448 w	19b+Δ(A); 12+10a(A); 20a'-18b'(A); 20a'-5(B); 20b-18b'(B); 20b-5(A); 19a+E(A); 18b'+4'(A); 15+11(A); 15+11'(B); 7b'-12'(A); 5+4'(B); 7b-12(A); 2-12(A); 7b'-18b'(A); 18b-2'(B); $10b^2(A)$; 8a+Δ(A); 8b'+Δ(B).
1431 m	19a'(A) fundamental.
1390 wsh	8a'-17a(B); 16a+3(A); 16a'+3(B); 14'+2(B); 12+11(A); 10a+10b'(B); 18b+4'(B); 12'+4(B); 7b-15(A); 7b-15'(B); 2-15(A); 2-15'(B); 18b'+11'(A); 18b'+6a(B); 11'+5(B); 7b'-18b'(A); 7b'-5(B); 6a+5(A); 20b'-9b(B); 20b-9b'(A); 17a'+Δ(B); 9b+6b(A); 9b'+6b(B); 2-15(A); 2-15'(B).
1368 s	19b'(A) fundamental.
1341 ssh	19a(B) fundamental.
1332 vs	19b(B) fundamental.
1292 m	14'(A) fundamental.
1269 msh	10a+4(A); 19b'+Z(B); 8a-6a'(B); 8b'-6a'(A); 18a'+18b'(A); 18a'+5(B); 10a'+4'(A); 20b-1(A); 2'-1(B); 1+Γ(B); 20a-3(A); 16b+5(A); 20a-3(A); 18b+6b'(B).
1255 m	20a'-3(B); 20b-3(A); 11+10'(B); 19b'-Δ(B); 18b+16b'(B); 10b'+6b(B); 16b'+12(B); 8b-Γ(B); 11+10a(A).
1247 m	20b'-3(B); 12'-16b(B); 7b-1(A); 5'-18a'(A); 2'-3(B); 2-1(A); 10a-11(A); 8a'-B(A); 10b'-6b'(A); 19b'-Δ(B); 19a-2(A); 10a'-11(B).
1222 m	14(B) fundamental.
1214 vs	7a(B) fundamental; 7a'(A) fundamental.
1195 sh	18b+16a(B); 18b'+16a'(A); 16a+5(A); 16a'+5(B); $11^2(A)$; 3'+Δ(B); 14'-Z(B); 20a'-3'(A); 20b-3'(B); 20b'-3'(A); 7b'-3(B); 2'-3'(A); 10b+16b(A).
1174 s	A(A) fundamental.
1126 w	8a-16b(A); 18a+2'(B); 3-Z(A); 2'-18a'(A); 19b-17a(A); 12'-B(A); 10a'-16b(B); 4-6b(A); 19a-17a'(B); 19a'-6a'(A); 14-Z(A); 18b'-6a'(A); 18b-B(B); 10a-16b(A); 5-6a'(B); 15-Γ(B); 15'-Γ(A); 4'-6b'(A).
1080 mbr	3'(A) fundamental.
1025 ms	3(B) fundamental.
1013 w	8a-11'(B); 8a-6a(A); 8b'-11'(A); 8b'-6a(B); 14-17a'(B); 7a-17a(A); 7a'-17a(A); 7b'-7a(B); 7b'-7a'(A); 17a+5'(B); 17a'+5'(A); 19b'-B(A); $6b'^2(A)$; 8b-6b(A).
998 s	1(B) fundamental.
945 w	18a+6b'(B); 18b'+Δ(B); 5+Δ(A); 11+B(B); 10b'+17a(B); 7a'-Γ(A); 7a -Γ(B); 20a-19a(A); 20a'-19b(B); 20b-19b(A); 14'-B(B); 8a'-10a(B); $16b'^2(A)$; 19a'-16b'(A); 2'+Γ(A); 20b'-19b(B); 8a-4(A); 8b-4'(B); 6b+18a(A); 2'-19b(B).
934 vw	19b'-18a(B); 18a+6b'(B); 17a'+10b(B); 18b'+E(B); $16b^2(A)$; 7b'-14'(A); 18b'+Z(B); 8a'-10a(B); 5+Z(A); 20a'-19a(B); 20b-19a(A); 20b'-19b(B); 18b'+E(B); 8b-11(A); 5+E(A); 2'-19b(B).

Table 3.21 (continued)

Infrared cm^{-1}	Assignment
928 w	16a+14′(*B*); 16a′+14(*A*); 19a′-6b′(*A*); 8b-11(*A*); 20b′-19a(*B*); 19b′-18a′(*A*); 18b′+2(*B*); 5+2(*A*); 2′-19a(*B*); 10b+17a(*A*); 3-Z(*A*); 7b′-14′(*A*); 18a+16b(*A*); 10a′+Γ(*A*); 5′+Δ(*B*).
921 vw	20a-19b′(*B*); 16a+11′(*B*); 16a′+11′(*A*); 16a+6a(*A*); 16a′+6a(*B*); 14-6a(*A*); 10a-Γ(*B*); 5′-Δ(*B*); 10a′-Γ(*A*); 8b-4(*A*); 4-6a(*A*); 3-Z(*A*); 19b-18a′(*B*); 3-E(*A*); 19a-6b(*A*).
898 w	18a+16b(*A*); 11+6a(*A*); 1-Z(*A*); 19a-18a′(*B*); 19b-18a(*A*); 19b′-16b(*B*); 12+Z(*A*); 17a′+2′(*A*); 20b′-19b′(*A*); 2-19b′(*B*); 12+E(*A*); 7b-19b(*A*).
876 s	9b(*B*) fundamental; 9b′(*A*) fundamental.
853 wm	15(*B*) fundamental; 15′(*A*) fundamental.
830 m	5(*B*) fundamental; 18b′(*A*) fundamental.
806 m	5′(*A*) fundamental.
795 s	12(*B*) fundamental.
778 s	12′(*A*) fundamental.
771 s	18b(*B*) fundamental.
752 m	19b′-4′(*A*); 15-Z(*A*); 15′-Z(*B*); 10a+Z(*A*); 20a′-8b(*B*); 20b-8b(*A*); 14′-16b(*B*); 11+6a(*A*); 8b-18b(*A*); 19a-2′(*B*); 10a′+Z(*B*); 7a-16b(*A*); 7a′-16b(*B*); 3-Γ(*A*).
739 w	10b′(*A*) fundamental.
721 w	10b(*B*) fundamental.
696 vw	8b-18b′(*B*); 8b-5(*A*); 20a-8a′(*B*); 14′-11(*B*); 12-Z(*A*); 11+Z(*A*); 7a-6b(*A*); 7a′-6b(*B*); 5′-E(*B*); 1-6a′(*B*); 7b′-8b(*B*); 18a+Γ(*B*); 8a-9b(*A*); 8a-9b′(*B*); 8b′-9b(*B*); 8b′-9b′(*A*); A-16b′(*A*); 19a′-10b′(*A*); 16b+16b′(*B*); $B^2(A)$.
683 w	1′(*A*) fundamental.
656 w	10a′(*A*) fundamental.
653 m	10a(*B*) fundamental.
641 w	15-17a′(*B*); 15′-17a′(*A*); 14′-10a(*B*); 10b′-Z(*B*); 18a+17a′(*B*); 19a′-12(*B*); 18a′-17a′(*A*); 14′-10a′(*A*); 19b′-10b(*B*); 6b+Δ(*A*); 3′-18a(*B*).
630 w	10b′-E(*B*); 7b-8a′(*B*); 19b′-10b′(*A*); 16a+Γ(*B*); 16a′+Γ(*A*); 6b+E(*A*); 14-11(*A*); 18b′-17a(*B*); 5-17a(*A*); 19a′-5′(*A*); 6b+Δ(*A*); 18a+17a(*A*); 14′-10a′(*A*).
623 m	10b′-Δ(*B*); 19a′-5′(*A*); 14-11(*A*); 19a-10b(*A*); 18a′-17a(*B*); 6b′+Δ(*B*); 5-17a(*A*); 6b+Z(*A*); 6b+E(*A*); A-11′(*A*); A-6a(*B*); 19b′-10b′(*A*); 7a-11(*A*); 7a′-11(*B*); B+Γ(*A*).
616 s	4′(*A*) fundamental.
609 s	4(*B*) fundamental.
597 s	11(*B*) fundamental.
556 s	6a(*B*) fundamental; 11′(*A*) fundamental.
519 s	6b(*B*) fundamental.
504 s	6b′(*A*) fundamental.
481 ms	16b′(*A*) fundamental.
468 ms	16b(*B*) fundamental.

Table 3.21 (continued)

Infrared cm^{-1}		Assignment
453	vw	A-10b(B); 10a'-17a(B); 10b-Γ(B); 14-18b(A); 19b-9b(A); 19b-9b'(B); 11'-Z(B); 6a-Z(A); 5'-B(A); B-E(B); 10a-17a(A); 11'-E(B); 6a-E(A); B•Z(B).
442	w	18a'(A) fundamental.
432	s	18a(B) fundamental.
350	vw	B(A) fundamental.
301	s	6a'(A) fundamental.
267	vw	Γ(A) fundamental.
211	w	17a'(A) fundamental.
204	w	17a(B) fundamental.
116	s	Δ(B) fundamental.
109	s	E(B) fundamental.
100	s	Z(B) fundamental.
68	mw	libration.
63	mw	libration.

s = strong

m = medium

w = weak

v = very

sh = shoulder

br = broad

ful in calculating with absolute certainty those fundamentals not observed in the infrared spectrum.

The infrared intensities of the in-phase vibrations of bipyO_2 are generally weaker than their out-of-phase counterparts, and following the assignments of biphenyl and bipy, an examination of the present assignments of bipyO_2 and bipy-d_8O_2 (Table 3.19) reveals a general trend in the frequencies of the in-phase and out-of-phase vibrations. The out-of-phase C-H stretches are, without exception, found at slightly higher frequencies than their in-phase counterparts. For the vibrations below 1600cm^{-1}, the situation is reversed and, with the exception of five pairs in bipyO_2 and seven in bipy-d_8O_2, the in-phase vibrations are found at a higher frequency than their out-of-phase vibrations.

The exceptions are explained by their being highly coupled vibrations. Thus the general trend is broken for the ring modes 1 and 6a (both isotopomers) since the in-phase vibrations of these are highly coupled to the inter-ring stretch (as discussed above). Similarly, the variance by the two pairs, the principal ring-breathing modes 12(12′) and the N-O stretches, modes 7a(7a′) (both isotopomers), indicates that a slight difference within the coupling of these modes is experienced by the in-phase and out-of-phase vibrations. Furthermore, as the frequency at which modes 6b and 6b′ are found in bipyO_2 is more typical of *o*-difluorobenzene than that of biphenyl or bipy (Table 3.19), the discontinuity of the ring vibrational pair, mode 6b(6b′) for both isotopomers is not surprising in view of the halogen sensitivity of this mode in the *o*-difluorobenzene analogues [134].

The sixth and seventh vibrational pairs which deviate from the general trend are the νC-D vibrational pairs, modes 5(5′) and 11(11′) for the -d_8 isotopo-

mer. That they also differ from their -d_0 analogues is explained by a deuteration-induced coupling with the ring torsion mode 4(4') and with the γN-O vibration mode 17a(17a'), respectively, with the out-of-phase partners showing a slightly greater degree of coupling. This explanation is supported by the similar deuteration-induced coupling of modes 4 and 5 and of modes 11 and 17b(γC-F) in *o*-difluorobenzene-d_4, in which the PED of the γC-D modes 5 and 11 for the -d_4 isotopomer show a greater contribution from the γring and γN-O, respectively, compared to that for the -d_0 isotopomer [134].

Since the vibrational spectrum reflects the dual effects of the N-O and interring moieties upon the WILSON modes of vibration, a fuller discussion of these is necessary.

The N-O stretching vibrations 7a(*B*) and 7a'(*B*) (-d_0 isotopomer) have been assigned to the very strong bonds at 1265cm^{-1} and at 1255cm^{-1}, respectively. These assignments agree well with the two previous partial assignments of bipyO_2 reported by DEGA-SZAFRAN [43] and by KIREEV *et al.* [44]. They also agree well with those found for pyO, pzO and pzO_2 (Table 3.22). The observed

	bipyO_2	pyO	pzO	pzO_2	(mean)	bipy-d_8O_2	py-d_5O	pz-d_4O	pz-d_4O_2	(mean)
νN-O	1255 1256	1252	1307	1290 1264	(1277)	1214 1214	1225	1251	1290 1186	(1236)
αN-O	478 466	468	475	519 417	(478)	442 432	-	468	492 412	(453)
γN-O	220 214	226	226	374 186	(280)	211 204	-	222	351 177	(263)

Table 3.22 The N-O vibrations of four azine *N*-oxides and their fully deuterated analogues

and calculated frequencies for the similar molecule 4,4'-bipyridine *N,N'*-dioxide [136] further support these assignments.

In the -d_8 isotopomer these vibrations are accidentally degenerate to give a very strong band at 1214cm^{-1}. This degeneracy is partially lifted in the M(II)$(ClO_4)_2$ complexes (Chapter 4) to give a split band or a band with shoulders. The slight deuteration-induced decoupling of the N-O stretch from either the 'Star of David' or the principal ring-breathing modes, together with the different degree of deuteration-induced coupling of the former with other fundamentals in pyO, pzO and pzO_2 (discussed above), does not allow a firm comparison between the molecules of the N-O stretches of the fully labelled compounds. However, that the accidentally degenerate N-O stretches are found at a frequency close to that of the stretch of pz-d_4O_2 which does not show deuteration-induced coupling, as well as being found close to that of py-d_5O suggests that if any secondary, deuteration-induced, coupling does occur in bipy-d_8O_2, then it must be a light coupling. In *o*-difluorobenzene-d_4 the C-F stretches show a slight deuteration-induced coupling with the ring modes 19a and 19b [134], which was not observed in pz-d_4O, pz-d_4O_2 or their benzene analogues. Bearing in mind the crossover in the description of the higher frequency band in biphenyl and *o*-difluorobenzene (Table 3.19), the frequencies and ν^D/ν^H ratios of 19a(19a') and 19b(19b') for bipy-d_8O_2 do indicate a possible coupling of 7a'(*A*) with both 19a'(*A*) and 19b'(*A*), and of 7a(*B*) with that of 19a(*B*). The hypsochromatic shift of 19b and absence of shift of 19b' in the -d_8 isotopomer M(II)$(ClO_4)_2$ complexes, support such a coupling. Clearly a normal coordinate analysis of the molecule is required to present a clearer picture of the coupling.

Following SHINDO's assignment of the N-O vibrations of pyO [35,36], both DEGA-SZAFRAN [43] and KIREEV *et al.* [44] incorrectly identified the strong bands at *ca.* 860 and 840cm^{-1} as the planar N-O bends, αN-O. The present assignment of the strong bands at 856cm^{-1} (-d_0) and 795cm^{-1} (-d_8) to the 'Star of David' ring-breathing mode 12(*B*) which couples with the N-O stretch, and

that of the strong bands at 839cm^{-1} ($-d_0$) and 778cm^{-1} ($-d_8$) to its *A* in-phase counterpart has been made on the basis of the coupling experienced in substituted benzenes. Both the $-d_0$ and $-d_8$ frequencies are similar to those found for pyO, pzO and pzO_2. The $-d_0$ assignments are further supported by the normal coordinate calculations for 4,4'-bipyridine *N,N'*-dioxide which shows the calculated frequency of 830cm^{-1} to be the out-of-phase vibration of a ring mode coupled to the N-O stretch. It was suggested above that the reversal of the trend of finding the *A* vibrations at higher frequencies than their *B* counterparts is indicative that a different extent of coupling is experienced by the two modes. This suggestion is supported by the difference in the shifts of these bands on coordination. In the $M(II)(ClO_4)_2$ complexes, the *B* vibration shifts down in frequency by 7 to 9cm^{-1}, while the *A* vibration shifts down by 4 to 6cm^{-1}. Their $-d_8$ analogues shift by 4 to 7cm^{-1} and by 3cm^{-1}, respectively, the smaller shifts reflecting the slight deuteration-induced decoupling of modes 12(12') and 7a(7a').

In the present work, the two αN-O modes 18a and 18a' have been assigned to the weak bands at 478cm^{-1} ($-d_0$) and 442cm^{-1} ($-d_8$) and to the medium intensity bands at 466cm^{-1} ($-d_0$) and 432cm^{-1} ($-d_8$). The weaker, higher frequency $-d_0$ and $-d_8$ bands have tentatively been assigned to the *A* vibration, rather than the out-of-plane *B* vibration, on the basis of their intensity. A normal coordinate analysis will be required to verify this. The $-d_0$ frequencies agree well with those found for pyO and pzO (Table 3.22) as well as with that of 486cm^{-1} calculated for the in-phase αN-O of 4,4'-bipyridine *N,N'*-dioxide [136]. (The out-of-phase vibration of 4,4'-bipyridine *N,N'*-dioxide is found to couple strongly with the in-plane scissors, Δ, and so cannot be used as a comparison). Neither DEGA-SZAFRAN [43] nor KIREEV *et al.* [44] continued their investigations below 550cm^{-1}, so neither group was in a position to observe any bands of lower frequency which show N-O character.

The two γN-O modes 17a and 17a′ have been assigned to the weak bands at 220cm^{-1}($-d_0$) and 214cm^{-1} ($-d_8$) and to the weak bands at 214cm^{-1} ($-d_0$) and 204cm^{-1} ($-d_8$). Since the bands are of the same intensity, the higher frequency bands are assigned to the *A* vibration in accordance with the general trend. However, in view of the exceptions to this trend brought about by coupling, and in view of the highly coupled nature of the γN-O, this requires confirmation through normal coordinate studies. The assignments for the $-d_0$ isotopomer agree well with those of pyO and pzO (Table 3.22), while those of the $-d_8$ isotopomer agree well with pz-d_4O. This would indicate that a similar degree of coupling is found for the γN-O vibrations of bipyO_2 as exists in the highly coupled systems of pyO and pzO. In the latter two ligands the γN-O mode is strongly coupled with the ring torsion, 16b. With a similar coupling of the in-phase γC-F (mode 17b) and the ring torsion 16b observed in *o*-difluorobenzene (such that a true definition of the γC-F vibration is difficult) modes 17a(17a′) and 16b(16b′) are probably very strongly coupled in both isotopomers of bipyO_2. It is also noted that the deuteration-induced coupling of the umbrella mode 11 with γN-O (suggested to explain the deviation of the trend of in-phase modes > out-of-phase modes of mode 11-d_8) is also observed in pz-d_4O, pz-d_4O_2 and toluene-d_7.

The final information to be drawn from the N-O vibrations is achieved by a comparison of these vibrations with the other azine *N*-oxide systems investigated in this work. From Table 3.22 it can be seen that where two N-O moieties exist on separate rings (as for bipyO_2), the in-phase and out-of-phase vibrations of the N-O moieties have little effect upon each other. In contrast, where the two N-O moieties occur on the same ring, there is apparently some interaction between the in-phase and out-of-phase vibrations such that the two vibrations undergo a shift, one to a higher frequency and one to a lower frequency. The mean of these two shifted frequencies is similar

to the 'characteristic' N-O frequency, unless there is extensive coupling with other ring modes - such as has been observed for γN-O (both isotopomers) and νN-O (-d_4 isotopomer) of pzO_2.

Before the effects of the inter-ring bond is examined, the non-planarity of $bipyO_2$ implies that the designation of the in-plane shear *B*, the out-of-plane shear *Γ*, the in-plane scissors Δ and the out-of-plane scissors *E* require redefining. The first two are torsional shears while the latter are torsional scissors.

In $bipyO_2$ the inter-ring stretch, mode *A*, is masked by the two strong bands of the N-O stretches. Its frequency has been calculated to be 1232 ± 1cm^{-1} on the basis of five combination and difference bands; 7a+*A* (2490cm^{-1}), 20a'-*A* (1837cm^{-1}), 20b'-*A* (1837cm^{-1}), 7b'-*A* (1772cm^{-1}) and 19a-*A* (247cm^{-1}). This calculated frequency is very similar to that for biphenyl. With the large hypsochromatic shift of the N-O stretches in the $M(II)(ClO_4)_2$ complexes, the inter-ring stretch is observed as a band of medium to strong intensity at 1257cm^{-1}, reflecting an increase in frequency of 25cm^{-1} on complexation. This is of a similar magnitude to the 33cm^{-1} shift on complexation observed for the -d_8 analogue, which is assigned to the strong band at 1174cm^{-1}, in the free ligand.

The inter-ring stretch couples with the in-phase ring vibrations, modes 1' and 6a'. The principal ring-breathing mode 1'(*A*) is masked by the strong band of the accidentally degenerate ring torsions, modes 4(*B*) and 4'(*A*), and has a calculated frequency of 741 ± 2cm^{-1}. This has been based upon seven possible combination and difference bands: 20a-1' (2367cm^{-1}), 18a'+1' (2367cm^{-1}), 7b-1' (2273cm^{-1}), 9b+1' (1837cm^{-1}), 18b'+1' (1772cm^{-1}), 1+1' (1726cm^{-1}) and 10b-1' (150cm^{-1}). In the $M(II)(ClO_4)_2$ complexes this masking

is removed and mode 1′ is seen as a weak band at 750 to 752cm^{-1}, a bathochromatic shift of 8 to 10cm^{-1}. The -d_8 analogue of 1′, assigned to the weak band at 683cm^{-1} in the free ligand, yields a smaller shift of 4 to 50cm^{-1} on complexation.

The out-of-phase principal ring-breathing mode 1(B) does not couple with the inter-ring stretch mode A(A). However, it yields a high ν^D/ν^H ratio of 1,015 - the result of an abnormally high -d_8 frequency (Table 3.19). Since there is no alternative band of suitable intensity which may either be assigned to mode 1(B) or may indicate the existence of Fermi resonance (Table 3.21), this feature must be the result of deuteration-induced coupling with either a C-H, a N-O or an inter-ring vibration. The most likely candidate is mode 18b(B) which has a much lower ν^D/ν^H ratio than its in-phase counterpart, as well as showing a much lower -d_8 frequency compared with o-difluorobenzene-d_4 and biphenyl-d_{10} (Table 3.21). This coupling (which is unique to bipy-d_8O_2) would not be expected to occur with the former because of the coupling of mode 1(A_1) with the C-F stretch 7a(A_1), nor with the latter on grounds of symmetry. This suggested coupling, however, will require confirmation through normal coordinate analysis.

The coupled ring mode 6a′(A) is found at 320cm^{-1} (-d_0) and 301cm^{-1} (-d_8). Both frequencies are some 10 to 15cm^{-1} lower than those of biphenyl and bipy. Since the similarity of the -d_0 frequencies of the inter-ring stretch of biphenyl and bipyO_2 indicates a similar extent of coupling, and considering the sensitivity of mode 6a′ to the dihedral angle between the two rings [112], the lower frequency of 6a′ in bipyO_2 compared with biphenyl provides further evidence for the non-planarity of the molecule.

In comparing the other inter-ring vibrations with their biphenyl analogues,

it is noted that the three *ex*-out-of-plane vibrations, modes Γ, *E*, Z, increase in frequency dramatically on removal of planarity, with shifts of between $20cm^{-1}$ and $34cm^{-1}$ for both isotopomers. By contrast, the *ex*-in-plane scissors, mode Δ, shifts up in frequency by only $5cm^{-1}$ ($-d_0$) and $6cm^{-1}$ ($-d_8$), while the *ex*-in-plane shear, mode *B*, shifts *down* in frequency by $40cm^{-1}$ ($-d_0$) and $1cm^{-1}$ ($-d_8$). An explanation for this behaviour is not as simple as is that for the inter-ring stretch.

In discussing the vibrational behaviour of biphenyl it was noted that the out-of-plane shear $\Gamma(B_{2g})$ was coupled to 6b(B_{2g}) and that this coupling was sensitive to the dihedral angle (θ), such that as θ increases, the frequency of 6b decreases while that of Γ increases. These changes are relatively small for 6b (calculated maximum of $9cm^{-1}$ for $\theta = 90°$ [112]) but are more significant for Γ (calculated maximum $36cm^{-1}$ for $\theta = 90°$ [112]). With the frequencies of 6b and 6b′ reflecting N-O sensitivity in bipyO_2, and in view of the small frequency difference expected between 6b and 6b′ on coupling with Γ, no conclusion can be drawn as to whether such coupling is observed in bipyO_2. The large $-d_0$ and $-d_8$ frequency shifts of Γ cannot be regarded as evidence for the existence of this coupling since the torsional scissors mode *E* and the internal rotation mode Z show a similar shift, yet do not display any such dihedral sensitivity in biphenyl [112]. It is therefor probable that, with the presence of the strongly electronegative *syn* oxygens, the large bathochromatic shifts of Γ, *E* and Z in bipyO_2 reflect some steric interaction. Only a normal coordinate analysis of the molecule will be able to establish the exact nature of this behaviour.

The different behaviour of the torsional shear mode *B* and the torsional scissors mode Δ compared with the analogous planar vibrations in biphenyl indicates a coupling difference between the two. In biphenyl, the in-plane scis-

sors mode Δ (B_{2u}) couples with the ring torsion 16b'(B_{2g}), and is sensitive to θ, such that as θ increases both 16b' and Δ decrease in frequency [112]. This θ-sensitivity is small for mode Δ (calculated maximum of 5cm^{-1} for θ = 90°) and moderate for 16b' (calculated maximum of 13cm^{-1} for θ = 90° [112]). From the behaviour of both 16b' and Δ in bipyO_2, such coupling is not present.

The coupling of the in-plane shear, mode *B* (B_{3g}) with the ring torsion 16b (B_{3u}) in biphenyl is such that as θ increases the frequency of 16b increases while that of *B* decreases. The θ-sensitivity of these vibrations is considerable, 16b yielding a calculated maximum of 71cm^{-1} for θ = 90° and *B* yielding a calculated maximum of 67cm^{-1} for θ = 90° [112]. A second means by which 16b' may couple is with the torsional shear mode Γ, as occurs in biphenyl and more dramatically in bipy. The resultant increase in frequency of 16' with such coupling is almost as large as that observed for 16b and *B* (Table 3.19). Both types of coupling may account for the accidental degeneracy of 16b and 16b' in bipyO_2, and for the similarity of their frequencies in bipy-d_8O_2 (explaining their higher frequencies compared with biphenyl). A slightly larger shift of 16b because of a greater extent of the first type of coupling would result in its approach to 16b'. This would also account for the dramatic hypsochromatic shift in mode *B* in bipyO_2. However, with the alternative explanation of the high frequency of both 16b and 16b' being the result of their coupling with the νN-O vibrations, modes 17a and 17a', the evidence for coupling between 16b and *B*, and between 16b' and Γ is not conclusive. A normal coordinate analysis could be necessary to evaluate this potential threeway coupling of 17a, 16b and *B*, and of 17a', 16b' and Γ.

While the evidence for the coupling described above is not clear cut, what is certain is that the extensive coupling of 16b' and Γ to the point of causing a reversal in the vibrational description (as observed in bipy) is

unlikely to occur for bipyO_2. This is indicated by the torsional shear, mode Γ, of bipyO_2 being higher in frequency than that of biphenyl for which there is no such reversal. (Whereas the lower frequency band of the two coupled bands in bipy is at a *lower* frequency than the out-of-plane shear in biphenyl). Again, this will need verification from normal coordinate analysis.

Having discussed the assignments of the extraordinary bands of bipyO_2 and their possible coupling effects, a number of other assignments in the spectra need to be discussed briefly. Several vibrations show accidental degeneracy or are masked by stronger vibrations, which is to be expected in such a vibrationally rich spectrum.

Five degeneracies are observed in both bipyO_2 and bipy-d_8O_2 (Tables 3.20 and 3.21). The accidental degeneracy of the ring torsion 16b(B) and 16b'(A) to give the strong band at 516cm^{-1} in the -d_0 isotopomer has already been mentioned. Observation of the lifting of this degeneracy in the M(II)$(ClO_4)_2$ complexes is complicated by the close proximity of two other bands derived from 6b(B) and 6a(B) (found at 526cm^{-1} and 541cm^{-1}, respectively, in the free ligand). The weak band at 1602cm^{-1} in the -d_0 isotopomer has been assigned to the accidentally degenerate vibrations 8a(B) and 8b'(A) on the basis of their analogous vibrations in biphenyl and in *o*-difluorobenzene. It is not possible to see whether this degeneracy is lifted in the M(II)$(ClO_4)_2$ complexes due to masking by the O-H bend in the water of hydration.

The assignment of the umbrella modes 11(B) and 11'(A) and the trigonal ring torsions, modes 4(B) and 4'(A), in bipyO_2 is difficult since they have similar frequencies and because the frequencies and relative intensities of modes 4 and 11 vary in various substituted pyridines and their *N*-oxides [21,

137]. The very intense band at 768cm^{-1} and the strong band at 724cm^{-1} in the -d_0 isotopomer both show evidence of a lifting of degeneracy in the M(II)$(ClO_4)_2$ complexes. The very intense band yields a high frequency shoulder of medium intensity on coordination, while the other band gives a complete resolution compared with the free ligand. The band at 768cm^{-1} in the free ligand has been assigned to the accidentally degenerate modes 11(B) and 11'(A) on the basis of the γC-H mode having the greater frequency in biphenyl and *o*-difluorobenzene. These assignments will require confirmation through normal coordinate analysis since these two bands should reflect the same spectral properties employing polarisation studies.

The αC-H bends, modes 15(B) and 15'(A) are found to be accidentally degenerate in the infrared spectra of both isotopomers, being assigned to the strong band at 1148cm^{-1} (-d_0) and to the medium to weak intensity band at 853cm^{-1} (-d_8). This degeneracy is partially lifted in the M(II)$(ClO_4)_2$ complexes of the -d_0 isotopomer, with a complete lifting of the degeneracy in the complexes of the -d_8 isotopomer into higher and lower frequency components.

Of the other four bipy-d_8O_2 bands showing accidental degeneracy, that at 1214cm^{-1} (the N-O stretches 7a and 7a') has been discussed above. The very intense band at 556cm^{-1} in bipy-d_8O_2 is assigned to the degenerate modes 6a(B) and 11'(A). This band is split on complexation into a higher frequency band of medium intensity and its strong companion. The last two degenerate bands are in close proximity to that of the accidentally degenerate αC-D, modes 15(B) and 15'(A) at 853cm^{-1}. The strong band at 876cm^{-1} is assigned to the αC-D modes, 9b(B) and 9b'(A). The medium intensity band is that of γC-D mode 5(B) and αC-D 18b'(A). These degeneracies are lifted in their M(II)$(ClO_4)_2$ complexes, each producing two separate bands.

A number of the weaker infrared vibrations are masked by the nearby presence of stronger bands, or are too weak to have been observed. Their frequencies may be tentatively established on the basis of possible overtones, combination or difference bands, or (with less confidence) from the predicted ν^D/ν^H ratios. Six fundamentals in bipyO$_2$ have been established from possible combination bands, while two for bipy-d_8O$_2$ have been so established. Two fundamentals of bipyO$_2$ have been determined from their predicted ν^D/ν^H ratios. The frequencies of all of these may be better established in the future through single crystal polarisation studies, Raman studies or by a normal coordinate analysis.

Of the six -d_0 fundamentals established from their combination bands, modes 1′(*A*) and A(*A*) have been fully discussed above. The in-phase γC-H mode 10b′(*A*) has been calculated to be at 932 ± 1cm^{-1} on the basis of six possible combination or difference bands: 19a+10b′ (2411cm^{-1}), 19b′+10b′ (2367cm^{-1}), 7b-10b′ (2080cm^{-1}), 15+10b′ (2080cm^{-1}), 15′+10b′ (2080cm^{-1}) and 18b+10b′ (1955cm^{-1}). This assignment is slightly lower than that of pzO and pzO$_2$ but higher than that of pyO. Taking into account the crossover in the description of the higher band in biphenyl and *o*-difluorobenzene (Table 3.19) the calculated frequency of 10b′ in bipyO$_2$ agrees well with *o*-difluorobenzene. The presence in the M(II)(ClO$_4$)$_2$ complexes of a shoulder on the weak infrared forbidden νClO$_4^-$ band at 930cm^{-1} may add support to this assignment.

The assignment of the -d_0 fundamentals of the αC-H modes 3(*B*) and 3′(*A*) is made difficult by the possibility of their being significantly coupled with the two Kekulé vibrations 14(*B*) and 14′(*A*). Since the frequencies of the Kekulé vibrations follow those of *o*-difluorobenzene for both isotopomers, the αC-H modes might be expected to follow those of *o*-difluorobenzene also. However, the -d_8 frequencies of 3(*B*) and 3′(*A*) are typical rather of those

of pzO_2 and biphenyl. The $-d_0$ fundamental 3(*B*) has therefore been calculated to be 1331 ± 2cm^{-1} on the basis of six possible combinations: 8a+3 (2973cm^{-1}), 8b'+3 (2973cm^{-1}), 14+3 (2635cm^{-1}), 20a-3 (1772cm^{-1}), 7b'-3 (1656cm^{-1}) and 19a-3 (150cm^{-1}). That of 3'(*A*) has been calculated to be 1352 ± 3cm^{-1}, also on the basis of six possible combinations: 8b+3' (2908cm^{-1}), 18b+3' (2776cm^{-1}), 14+3' (2648cm^{-1}), 8a-3' (247cm^{-1}), 8b'-3' (247cm^{-1}) and 19a'-3' (150cm^{-1}). These values agree well with those in pzO_2 and biphenyl.

The last two $-d_0$ fundamentals and the only two $-d_8$ fundamentals assigned from their possible combinations are the normally very weak infrared ring torsions 16a(*B*) and 16a'(*A*). Following the typical values of these modes in pyO, pzO, pzO_2 and biphenyl (and their fully deuterated analogues) rather than the very low values observed for *o*-difluorobenzene and its $-d_4$ analogue, these have been calculated to be at 402 ± 2cm^{-1} (for the $-d_8$ isotopomer) on the basis of five combinations and at 364 ± 1cm^{-1} (for the $-d_8$ isotopomer) on the basis of nine combinations (Tables 3.20 and 3.21). Two points about these assignments are to be noted. Firstly, while the assignments agree well with their models (pyO, *etc.*) they are very tentative since, without the presence of an observed band in the spectra of either of the isotopomers, there is no corroboration for the validity of the models used. Secondly, since the possible combinations did not yield (in either isotopomer) two distinct frequencies to which the in-phase and out-of-phase vibrations could be assigned, these have been assigned as being accidentally degenerate. Hopefully, future Raman or normal coordinate studies will secure the assignments of these four fundamental vibrations with greater certainty.

The other very tentative assignments are those of the γC-H modes 10a(*B*) and 10a'(*A*) ($-d_0$ isotopomers) which have been established on the basis of their

expected ν^D/ν^H ratios (based upon those of biphenyl since the -d_8 fundamentals are more typical of biphenyl-d_{10} than of *o*-difluorobenzene-d_4). Their assignments could not be calculated from the combination bands because of the presence of two -d_0 modes (12 and 12′) in close proximity to the expected frequencies of 10a and 10a , which increases the standard of deviations of the calculations to impractical levels. The absence of splitting of the observed strong bands on complexation limits the identification of 10a or 10a′ as being accidentally degenerate with 12 or 12′. Future polarisation studies, Raman studies or normal coordinate studies may locate these vibrations with greater accuracy.

Finally, a comment about the C-H stretches modes 7b and 7b′ is in order. While the rest of the C-H stretches agree well with those of the other molecules, modes 7b and 7b′ do not (Table 3.19). Assigned on the basis of their infrared intensities, their very low frequencies compared with biphenyl, bipy or *o*-difluorobenzene indicate a possible mis-assignment. That these low values might be the result of Fermi resonance (unlikely for all four assignments) is discounted by the absence of other bands of enhanced intensity in this region and by the absence of Fermi resonance pairs being found in the combination and difference bands. In view of the likelihood of significant anharmonicity in these vibrations [112], a normal coordinate analysis may fail to supply answers to this behaviour.

In conclusion, the infrared spectra of bipyO_2 and its fully deuterated analogue supports the suggested non-planarity of the molecule. The full vibrational assignments of the ligand, and the examination of the coupling within the molecule should assist a comprehensive assignment of its metal(II) complexes.

3 VIBRATIONAL ASSIGNMENT OF POLYCYCLIC AZA-*N*-OXIDES

3.1 Quinoline *N*-oxide (quinO)

The assignments of the fundamentals of quinoline *N*-oxide (quinO) and its fully deuterated analogue (quin-d_7O) are based firstly upon considering quinO in terms of its similarity with a 1-monosubstituted naphthalene, secondly by a comparison with naphthalene and quinoline and with their fully deuterated analogues, thirdly upon the ν^D/ν^H ratio and, finally, upon partial assignments of quinO and quin-d_7O that have been reported.

As mentioned previously, the numerous spectral bands arising from large polyatomic molecules present a greater number of possible force fields that may be constructed for the molecule, and an increasing probability of compensating errors occurring in isotope labelling work and of incorrect interpretations of polarisation studies due to accidental degeneracies.

The various vibrational assignments made for naphthalene reflect these difficulties for, although the molecule has only 48 vibrational modes, HANSEN and GEE [138] state that by 1969 twice as many frequencies had been assigned as fundamentals. The assignments of naphthalene and naphthalene-d_8 presented in Tables 3.23 and 3.24 are those given by BENLEN *et al.* [139] and by SELLERS *et al.* [140], and represent the latest experimental data and the latest normal coordinate treatment of this molecule, respectively.

3.1.1 Vibrational coupling experienced by naphthalene-d_0 and -d_8

The modes of naphthalene shown in Figure 3.5, as defined by LIPPINCOTT and O'REILLY [141] and by LUTHER and DREWITZ [142], have previously been employ-

Table 3.23 The fundamentals of quinoline *N*-oxide (quinO) and its -d_7 analogue (quin-d_7O) compared with similar molecules

Mode[a]	naphth [139,140]	quin [149]	1-F-naphth[b] [144,155,156]	quinO (This work)	naphth-d_8 [139,140]	quin-d_7[b] [150-152]	quin-d_7O (This work)
1	3056	3056	3068	(3055)	2291	2275[d]	2290[d]
2	3030	3014	3030	(3030)	2276	2256[d]	2270[d]
3	1383	1371	1384	1398	1386	1281	1357
4	1576	1571	1576	1577	1552	1551	1536
5	1163	1140	1144	1146	838	860	835
6	765	760	709	743	697	696	721
7	1020	1031	1032[c]	1054	862	876[d]	879[d]
8	1464	1469	1464	1455	1298	1303	1301
9	512	521	567	557	493	504[d]	508
10	(981)	970	1003	997	(815)	806	830
11	(825)	840	821	(828)	(647)	641	(646)
12	(622)	628	625	610	(531)	568	526
13	(188)	193	181	211	(169)	174[f]	196
14	3051	3056	3052	(3050)	2276	2276[d]	2270[d]
15	3006	2979	2986	(3000)	2261	2256[d]	2261
16	1629	1619	1641	(1639)	1605	1584	1594
17	1458	1431	1442	1447	1353	1366	1377
18	1243	1192	1239	1266	831	932	823
19	1158	1095	1157	1179	1027	838[d]	1011
20	509	(505)	529	545	494	504[d]	497
21	936	953	917	928	884	915	924
22	955	-	155	185[d]	791	-	175
23	780	786	788	798	629	613	627
24	474	479	459	466	404	409	416
25	166	178	181	185[d]	153	166	170
26	951	939	952	970	766	780	755
27	717	741	728	722	545	589	590
28	385	392	416	422	348	351	374
29	3060	-	1232	1230	2232	-	1147
30	3027	3036	3022	(3025)	2278	2256[d]	2270[d]
31	1601	1593	1603	1616	1545	1542	1581
32	1387	1392	1397	1377	1257	1257	1242
33	1128	1118	1115	1138[e]	879	876[d]	879[d]
34	1268	1256	1263	1275	1045	1036	1055
35	359	377	354	365	328	345	340
36	(789)	785	758	778	738	712	742

Table 3.23 (continued)

Mode[a]	naphth [139,140]	quin [149]	1-F-naphth[b] [144,155,156]	quinO (This work)	naphth-d_8 [139,140]	quin-d_7[b] [150-152]	quin-d_7O (This work)
37	983	980	961	984	(857)	825	854
38	772	804	770	802	646	674	676
39	875	867	858	878[e]	761	749	773
40	470	472	473	480	413	417	441
41	3086	3086	3090	(3090)	2284	2275[d]	2290[d]
42	3029	3004	2998	(3030)	2258	2256[d]	2258
43	1361	1314	1350	1313	1312	1239	1315
44	1508	1500	1510	1514	1445	1438	1453
45	1163	-	270	321	840	-	307
46	1210	1216	1216	1210	1082	1092	1073
47	1010	1013	876	878	828	838[d]	787
48	618	611	636	628	590	584	564

(a) nomenclature after LIPPINCOTT and O'REILLY [141]

(b) final assignment (see Text)

(c) split band

(d) accidental degeneracy

(e) possible Fermi resonance

(f) from GHERSETTI *et al.* [151,152]

estimated values in parentheses

Table 3.24 The ν^D/ν^H ratio for quinoline *N*-oxide (quinO) and its $-d_7$ analogue (quin-d_7O) compared with similar molecules

Mode[a]	naphth [139,140]	naphth-d_8 [139,140]	ν^D/ν^H	quin [149]	quin-d_7[b] [150-152]	ν^D/ν^H	quinO (This work)	quin-d_7O (This work)	ν^D/ν^H	Assignment
1	3056	2291	0,750	3056	2275[d]	0,745	(3055)	2290[d]	(0,750)	ν C-H/D
2	3030	2276	0,751	3014	2256[d]	0,749	(3030)	2270[d]	(0,749)	ν C-H/D
3	1383	1386	1,002	1371	1281	0,934	1398	1357	0,970	ν ring
4	1576	1552	0,985	1571	1551	0,987	1577	1536	0,974	ν ring + ν N-O
5	1163	838	0,720	1140	860	0,754	1146	835	0,726	α C-H/D
6	765	697	0,911	760	696	0,916	743	721	0,970	ν ring + ν N-O
7	1020	862	0,845	1031	876[d]	0,850	1054	879[d]	0,834	α C-H/D
8	1464	1298	0,887	1469	1303	0,881	1455	1301	0,894	ν ring
9	512	493	0,963	521	504[d]	0,967	557	508	0,912	ν ring + ν N-O
10	(981)	(815)	(0,831)	970	806	0,831	997	830	0,832	γ C-H/D
11	(825)	(647)	(0,784)	840	641	0,763	(828)	(646)	(0,780)	γ C-H/D
12	(622)	(531)	(0,854)	628	568	0,904	610	526	0,838	γ ring
13	(188)	(169)	(0,899)	193	174[c]	0,899	211	196	0,929	γ ring
14	3051	2276	0,746	3056	2276[d]	0,745	(3050)	2270[d]	(0,744)	ν C-H/D
15	3006	2261	0,752	2979	2256[d]	0,757	(3000)	2261	(0,754)	ν C-H/D
16	1629	1605	0,985	1619	1584	0,978	(1639)	1594	(0,972)	ν ring + ν N-O
17	1458	1353	0,928	1431	1366	0,954	1447	1377	0,952	ν ring + ν N-O
18	1243	831	0,669	1192	932	0,782	1266	823	0,650	α C-H/D
19	1158	1027	0,887	1095	838[d]	0,765	1179	1011	0,858	α C-H/D
20	509	494	0,970	(505)	504[d]	0,988	545	497	0,912	ν ring + ν N-O
21	936	884	0,944	953	915	0,960	928	924	0,995	ν ring + ν N-O
22	955	791	0,828	-	-	-	185[d]	175	0,946	γ N-O
23	780	629	0,806	786	613	0,780	798	627	0,782	γ C-H/D
24	474	404	0,852	479	409	0,854	466	416	0,893	γ ring
25	166	153	0,921	178	166	0,933	185[d]	170	0,919	γ ring
26	951	766	0,805	939	780	0,830	970	755	0,778	γ C-H/D
27	717	545	0,760	741	589	0,795	722	590	0,817	γ C-H/D
28	385	348	0,904	392	351	0,895	422	374	0,886	γ ring
29	3060	2232	0,729	-	-	-	1230	1147	0,932	ν N-O + ν ring
30	3027	2278	0,752	3036	2256[d]	0,743	(3025)	2270[d]	(0,750)	ν C-H/D
31	1601	1545	0,965	1593	1542	0,968	1616	1581	0,978	ν ring
32	1387	1257	0,906	1392	1257	0,903	1377	1242	0,902	ν ring + ν N-O
33	1128	879	0,779	1118	876[d]	0,783	1138[e]	879[d]	0,772	α C-H/D
34	1268	1045	0,824	1256	1036	0,824	1275	1055	0,827	α C-H/D
35	359	328	0,914	377	345	0,915	365	340	0,937	ν ring
36	(789)	738	0,935	785	712	0,907	778	742	0,954	ν ring + ν N-O

Table 3.24 (continued)

Mode[a]	naphth [139,140]	naphth-d_8 [139,140]	ν^D/ν^H	quin [149]	quin-d_7[b] [150-152]	ν^D/ν^H	quinO (This work)	quin-d_7O (This work)	ν^D/ν^H	Assignment
37	983	(857)	(0,872)	980	825	0,842	984	854	0,868	γ C-H/D
38	772	646	0,837	804	674	0,838	802	676	0,847	γ C-H/D
39	875	761	0,870	867	749	0,864	878[e]	773	0,880	γ ring
40	470	413	0,879	472	417	0,883	480	441	0,919	γ ring
41	3086	2284	0,740	3086	2275[d]	0,737	(3090)	2290[d]	(0,741)	ν C-H/D
42	3029	2258	0,745	3004	2256[d]	0,751	(3030)	2258	(0,745)	ν C-H/D
43	1361	1312	0,964	1314	1239	0,943	1313	1313	1,000	ν ring + ν N-O
44	1508	1445	0,958	1500	1438	0,959	1514	1453	0,960	ν ring
45	1163	840	0,722	-	-	-	321	307	0,957	α N-O
46	1210	1082	0,894	1216	1092	0,898	1210	1073	0,887	α C-H/D
47	1010	828	0,820	1013	838[d]	0,827	878[e]	787	0,896	ν ring + ν N-O
48	618	590	0,957	611	584	0,956	628	564	0,898	ν ring + ν N-O

(a) nomenclature after LIPPINCOTT and O'REILLY [141]

(b) final assignment (see Text)

(c) from GHERSETTI *et al.* [151,152]

(d) accidental degeneracy

(e) possible Fermi resonance (see Text)

estimated values in parentheses

Figure 3.5 Vibrational modes of naphthalene

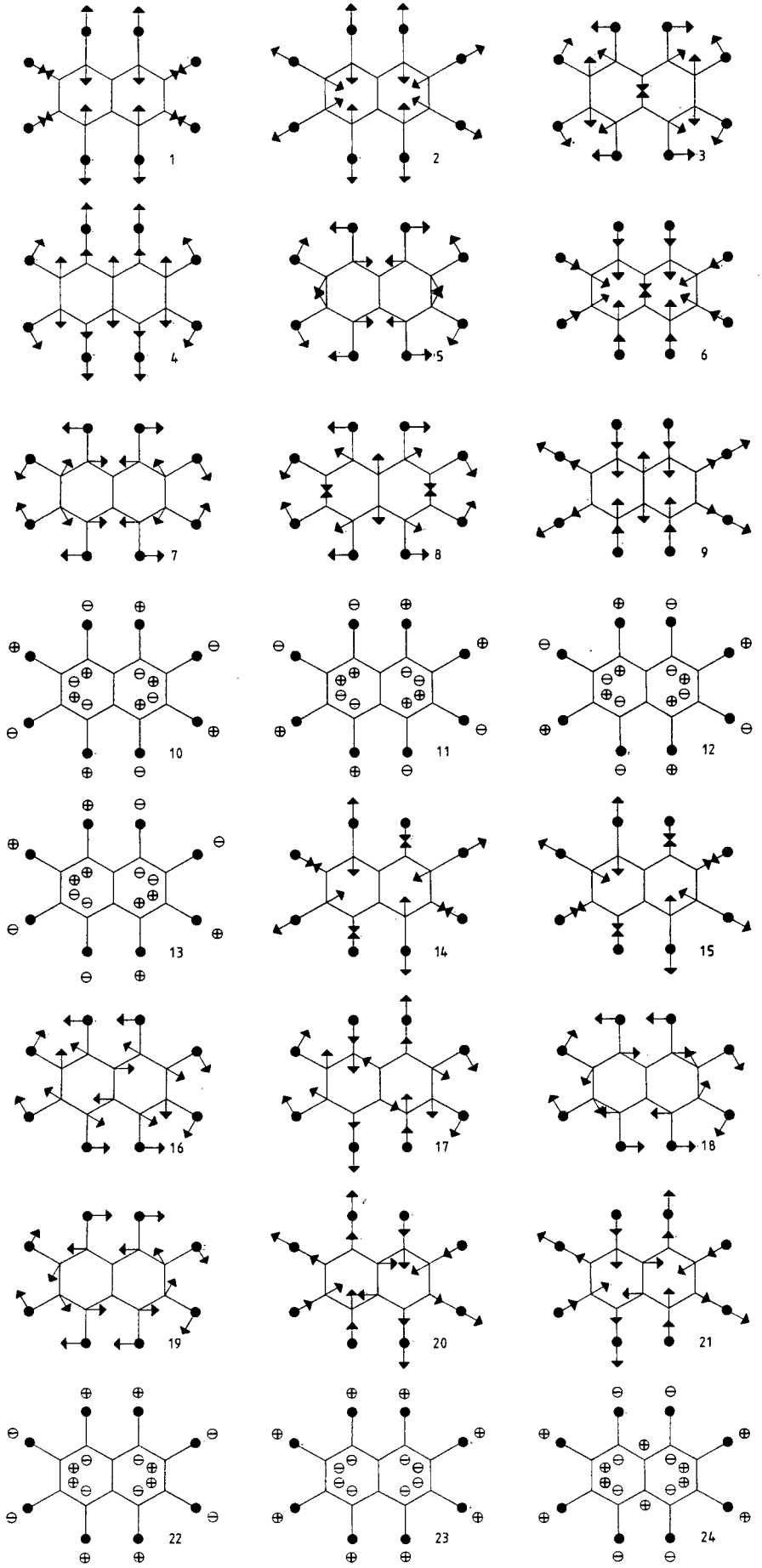

Figure 3.5 (continued)

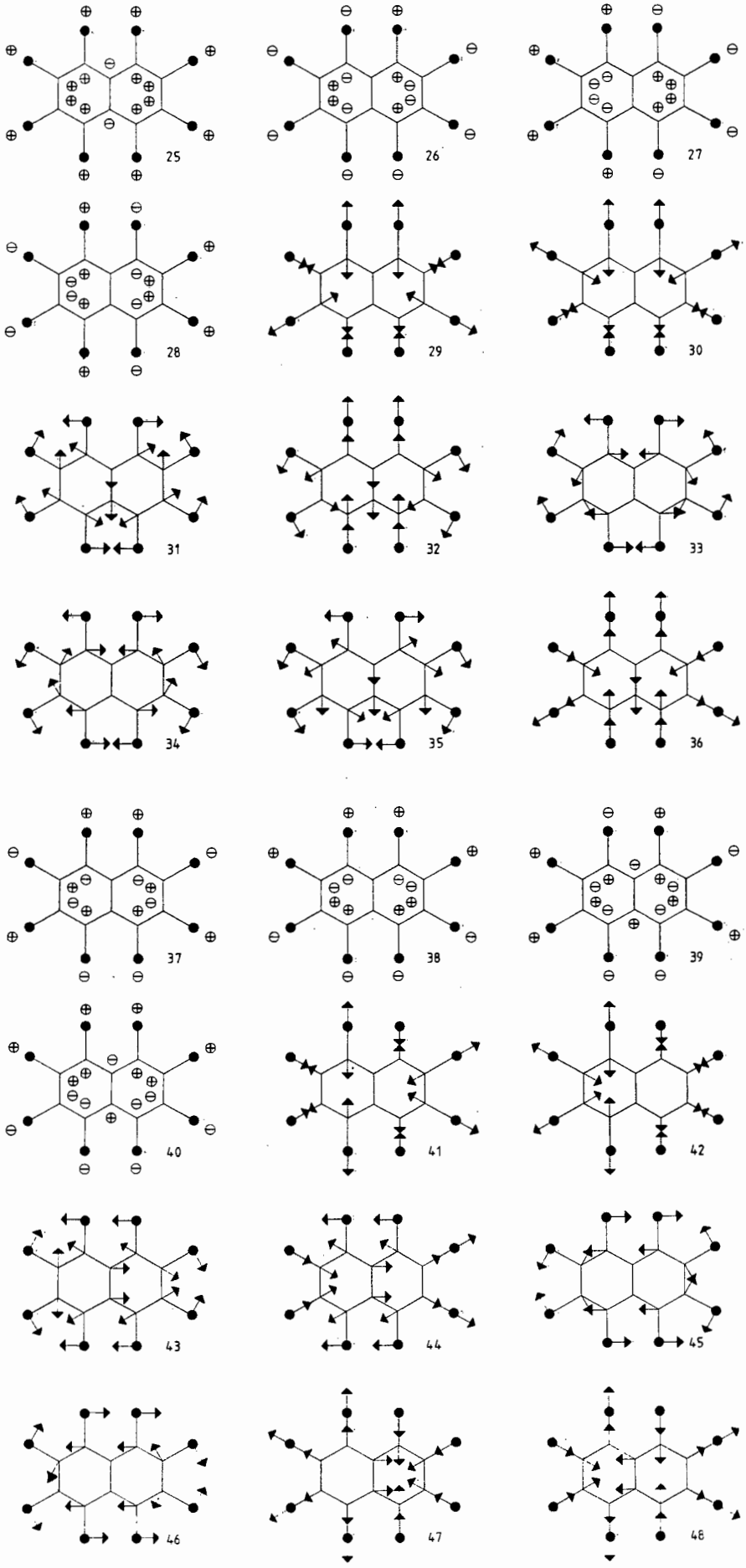

ed in the assignments of quinoline [143] and of 1-monosubstituted naphthalenes [144].

It is noted that, with the greater coupling of the planar vibrations as shown by Cartesian displacement diagrams [145,146], such a schematic set of vibrations is clearly idealised. It does however present a platform on which an understanding of both the vibrational behaviour and the potential coupling in similar molecules may be gained. Indeed, as a result of a number of normal coordinate analyses [145-147] the earliest assignments of LIPPINCOTT and O'REILLY [141] underwent some significant revision.

For example, the in-phase ring-breathing mode, $6(A_g)$, is not found at $1020cm^{-1}$ as originally thought, but occurs at $765cm^{-1}$. This is the result of its coupling with what LIPPINCOTT and O'REILLY called the gamma C stretching frequency, the inter-ring stretch mode $8(A_g)$, which is itself shifted to a higher frequency; found at $1464cm^{-1}$ [139,140] instead of $1394cm^{-1}$ [141]. (The band at $1020cm^{-1}$ is the lowest A_g in-plane C-H bending vibration, mode 7, rather than a ring mode, and is therefore of much higher frequency than its original assignment of $878cm^{-1}$ [141]). In contrast to this coupling, the out-of-phase ring-breathing vibration, mode $47(B_{2u})$, is found not to couple with the gamma C frequency due to symmetry restrictions. It is noted that both this coupling behaviour, and the frequency at which the in-phase ring-breathing mode is found are similar to that already seen for biphenyl, bipy and bipyO_2.

Other changes that have been introduced involve the assignment of all γC-H vibrations to bands below $1000cm^{-1}$, the revision of the B_{1g} ring torsion from *ca.* $390cm^{-1}$ to $470cm^{-1}$ and the reversal of the assignments of modes 13 and 40, both being ring modes. Similarly, the introduction of the Kekule

constants, ρ, into the normal coordinate calculations [146] also introduces a better understanding of the behaviour of the A_g and B_{2u} vibrations.

Apart from the coupling between the in-plane ring-breathing mode and the gamma C stretch mentioned above, an understanding of other coupling within the molecule may be elucidated. For example the planar vibrations between 1600cm^{-1} and 1000cm^{-1} are largely found to be coupled vibrations as reflected in their ν^D/ν^H ratios (Table 3.24) and from their PEDs [147,148].

Thus, the gamma C stretch, mode 8(A_g), and the lowest C-H planar bend, mode 7(A_g) are found to be coupled in naphthalene-d_0 but slightly decoupled in the -d_8 isotopomer, with the typically low ν^D/ν^H value of 0,887 for a ring-mode and high ν^D/ν^H value of 0,845 for a C-H mode clearly reflecting their mixed nature. In contrast, the in-phase Kekulé vibration, mode 3(A_g), and the C-H planar bend mode 5(A_g) are not significantly coupled in the -d_0, but *are* significantly coupled in the -d_8 isotopomer. This behaviour is reflected in the greater than unity ν^D/ν^H ratio for the ring mode and the low ν^D/ν^H ratio of 0,72 for the C-H mode. It also accounts for the non-adherence of the isotopic non-crossover rule, with a reversal on deuteration of the frequencies of modes 7 and 5 and of modes 8 and 3 (Table 3.23).

Coupling within the B_{3g} modes in naphthalene is more complicated. The PEDs [147,148] show that the three highly coupled -d_0 bands at 1458, 1247 and 1158cm^{-1} all consist of a C-H vibration, whereas the three -d_8 bands at 1353, 1027 and 831cm^{-1} reflect a coupled ring vibration, a coupled C-H vibration and an uncoupled C-H vibration respectively [147]. So while the very low ν^D/ν^H ratio of the C-H bend, mode 18, without the expected counterbalance of a high ratio for the ring mode may initially seem puzzling (Table 3.24), the B_{3g} vibrations can be understood as follows:

The very low ν^D/ν^H ratio of the C-H mode 18 is explained by an increase in the degree of coupling with mode 17 within the $-d_8$ isotopomer, as is indicated by the PED [147]. The high ν^D/ν^H ratio of 0,887 for the C-H mode 19 is typical of deuteration-induced decoupling between modes 19 and 17. This therefore explains the observed ratio of the ring mode, mode 17. The lowering of the ν^D/ν^H ratio of mode 17 on deuteration-induced coupling with mode 19 offsets the expected increase in the ratio with deuteration-induced coupling of mode 17 with mode 18. Thus, while the ν^D/ν^H ratio of mode 18 is smaller than its analogous A_g vibration (mode 5) this two way coupling of the B_{3g} modes prevents the counterbalance of the ν^D/ν^H ratio of mode 17 from being greater than that of the A_g Kekulé mode (mode 3).

In contrast to the B_{3g} vibrations, the coupling experienced by the B_{1u} planar modes is more straightforward. The PED for the $-d_0$ isotopomer [148] shows light coupling between the C-H bend, mode 34, and the ring mode 32. Their ν^D/ν^H ratios (Table 3.24) indicate a slight degree of deuteration decoupling. Coupling between modes 31 and 33 is insignificant.

The behaviour of the B_{2u} vibrations is complicated by the second Kekulé vibration. Firstly, unlike the A_g Kekulé vibration, the B_{2u} counterpart is strongly coupled in the $-d_0$ isotopomer. Two bands, at 1361cm^{-1} and at 1163cm^{-1}, both show a considerable Kekulé component, to the extent that it is questionable as to which to assign to the Kekulé vibration [146]. This coupling is maintained to some degree on deuteration (as is reflected by the ν^D/ν^H ratios) but a differentiation between the modes is now possible [146]. Secondly, in the $-d_0$ isotopomer there is slight coupling between the out-of-phase ring-breathing mode, $47(B_{2u})$ and the planar C-H bend, mode $46(B_{2u})$ [148]. In the $-d_8$ spectrum the band at 1082cm^{-1} shows considerable ring character, while that at 820cm^{-1} shows considerable C-D character [147].

That this is not a case of a crossover in the mode description due to extreme coupling (as observed above in pzO and in some substituted pyridines [13]) is indicated by the considerable Kekulé component of the 1082cm^{-1} band [147]. Clearly there is a complicated deuteration-induced coupling between the three modes, 43, 46 and 47. The PEDs given by NETO *et al.* [147] are not particularly helpful in determining the exact nature of this coupling.* Unfortunately the most recent normal coordinate analysis for naphthalene-d_8, that of SELLERS *et al.* [140], neither reports a full PED nor gives any Cartesian displacement diagrams, so a complete description of this coupling is not possible at present.

In comparison with the planar modes of naphthalene and its fully deuterated analogue, there have been no published PED figures for the non-planar vibrations. Nonetheless, the coupling experienced by the non-planar modes may be tentatively suggested, based upon their ν^D/ν^H ratios.

The A_u vibrations are spectroscopically silent. However, from their calculated frequencies and ν^D/ν^H ratios, it is suggested that the highest A_u ring torsion, mode 12, is coupled with the highest out-of-plane C-H bend, mode 10. This coupling is slightly lost on deuteration as seen by the ν^D/ν^H ratios of 0,854 and 0,831 respectively, which clearly reflects their mixed nature in the -d_0 isotopomer. The ν^D/ν^H ratios (Table 3.24) show that the lower ring torsion mode 11 and lower out-of-plane C-H bend, mode 13, either do not display a significant -d_0 coupling, or that this coupling is maintained in the -d_8 isotopomer.

---

* This is most probably a reflection of their employment of the least squares method in their calculation, being based upon the accepted assignment of naphthalene at that time.

A similar trend is observed for the B_{3u} vibrations. The highest ring torsion, mode 24 and the highest out-of-plane C-H bend, mode 23, show typical $-d_0$ coupling with deuteration-induced decoupling (Table 3.24). The lowest pair show smaller effects than their higher B_{3u} analogues, but more than their A_u (lower frequency) analogues.

For the B_{1g} vibrations the high ν^D/ν^H ratio for the out-of-plane C-H bend, mode 26, and the low ratio for the ring torsion, mode 28, indicates substantial $-d_0$ coupling between these vibrations, with $-d_8$ decoupling. In fact, the value of 0,805 for mode 26 is more typical of a ring vibration and it is likely that, because of extensive coupling, a clearcut assignment of these two vibrations in the $-d_0$ isotopomer may be debatable. PED figures would be desirable to examine this possibility.

Finally, the ν^D/ν^H ratios for the B_{2g} vibrations (Table 3.24) show typical $-d_0$ coupling with $-d_8$ decoupling between modes 38 and 39 and also between modes 37 and 40. The latter pair show almost identical ν^D/ν^H ratios and a future PED calculation is likely to show that a real identification of either as predominantly the ring mode is not fully justifiable.

Where these have been based upon the assignments of naphthalene and naphthalene-d_8, the plethora of differing naphthalene assignments found in the literature has resulted in much confusion in the vibrational assignments of like molecules. This is the case with the assignment problem in the spectra of quinoline-d_0 and $-d_7$ and of 1-fluoronaphthalene used here, necessitating a restructuring of the data in the present work to produce assignments which conform with the latest assignments of naphthalene.

3.1.2 The vibrational assignment of and coupling experienced by quinoline-d_0 and -d_7

The vibrational assignment of quinoline is taken from the re-examination of the infrared and Raman spectra with a normal coordinate analysis conducted by WAIT and NcNERNEY [149]. The data for quinoline-d_7 is taken from THORNTON *et al.* [150] which involves an examination of quinoline-d_0 and -d_7 in light of an earlier assignment of quinoline made by CHIORBOLI and BERTOLUZZA [143]. They, in turn, based their assignment on that of naphthalene made by LIPPINCOTT nad O'REILLY [141]. Since this latter work contains several errors, the data from THORNTON *et al.* [150] has been reworked with the aid of some partial quinoline-d_7 assignments [151,152] and by following the assignments of naphthalene-d_8 of BENLEN *et al.* [139] and SELLERS *et al.* [140] (Tables 3.23 and 3.24).

From the same Tables it is observed that the νC-H modes of naphthalene fall within two distinct ranges, four being found above 3050cm^{-1} and four being found below. The choice of mode 29 to be the 'lost' νC-H vibration in quinoline is based on the loss of one of the bands in the upper range [149].

The choice of assigning the 'lost' αC-H vibration to mode 45 is decided by the loss of a band in the 1160 to 1190cm^{-1} range for, (while in naphthalene, modes 5 and 45 are accidentally degenerate) in quinoline, the weak absorbance of the corresponding band at 1150cm^{-1} indicates absence of such degeneracy [149]. Support for this particular choice (as opposed to mode 5) will be shown below in the discussion of the coupling within the molecule.

The choice of mode 22 as the 'lost' γC-H vibration is made by the absence of a strong infrared, weak Raman band (being typically non-planar) in the 940

to 970cm^{-1} range [149].

We have already seen that the introduction of the aza-substituent into the ring resulted in a slightly different coupling being experienced by substituted pyridines, by pzO and by bipy, particularly that involving the Kekulé vibration. A similar situation also occurs for quinoline.

Firstly, from Table 3.23, the -d_0 frequencies of the first Kekulé vibration, mode 3, and the in-plane C-H bend, mode 5, are slightly lower than those found in naphthalene. This hypsochromatic shift reflects the CN character of these vibrations on aza-substitution [149]. Secondly, the choice of the band at 1281cm^{-1} in the -d_7 spectrum to be assigned to the in-phase Kekulé vibration, mode 3, is based upon its similar intensity to that of the -d_0 isotopomer, and on the absence of another strong band in the range 1250 to 1400cm^{-1} [150,151]. The correctness of this assignment is seen by the corresponding behaviour of mode 5, with which it couples. Thirdly, compared with naphthalene, the smaller and larger ν^D/ν^H ratios of modes 3 and 5, respectively, indicate that these vibrations are less coupled in the quinoline-d_7 isotopomer than occurs for naphthalene-d_8.

The second Kekulé vibration (the out-of-phase vibration, mode 43) might be expected to follow the same trend. Indeed, WAIT and McNERNEY interpreted the 47cm^{-1} lowering in the -d_0 frequency of mode 43 to be the result of the greater mass of the nitrogen atom and the difference in the force constant on aza substitution [149]. However, since the decrease in frequency for the in-phase Kekulé mode is smaller (being only 12cm^{-1}) this does not reveal the whole story. This behaviour is more fully comprehended by considering that the in-plane C-H bend, mode 45, to which the out-of-phase Kekulé mode couples, is the vibrational mode which is 'lost' on aza-substitution. The 47cm^{-1} de-

crease for the Kekulé mode is then seen to be the result of not merely the greater mass of the nitrogen, but of the complete removal of any possible coupling with mode 45. In contrast, for the in-phase Kekulé vibration, a potential for coupling still remains and the frequency shift is not as dramatic. Therefore the large decrease in the out-of-phase Kekulé mode, 43, supports the assignment of mode 45 as the 'lost' C-H planar bend in quinoline, or as the in-plane C-X bend or N-O bend in 1-monosubstituted naphthalene and quinoline *N*-oxide.

One other difference in the coupling experienced by the planar vibrations of quinoline compared with naphthalene is observed in the two-way coupling of the ring mode 17 and the two C-H planar bends, modes 18 and 19. This is demonstrated in the large changes in the frequencies of the two C-H modes and in their different ν^D/ν^H ratio (Table 3.24). It is suggested that the dominant C-H character exhibited by all three vibrations in naphthalene-d_0 has been differentiated more clearly into ring and C-H modes by a decoupling of these modes on introducing the aza-group. An investigation of the PED of both isotopomers would clearly be useful for examination of this possibility.

For the non-planar vibrations, the most significant effect of the aza-group involves the behaviour of the out-of-plane C-H bending vibrations. CHAPPELL and ROSS consider the hydrogen motions between the two rings as being weakly coupled and those of the α-H and β-H motions within the same ring as being strongly coupled, such that the mean range of the α-H and β-H are considered to be 755cm^{-1} and 945cm^{-1}, respectively [32]. However, from Table 3.25 it is clear that the designation of α-H and β-H does not describe the individual vibrations of the hydrogens at the α and β positions, with respect to the inter-ring C-C bond. Instead the lower β-H vibrations are those in which an *alpha* hydrogen and its *beta* neighbour vibrate *in-phase*, while the

higher α-H vibrations are those in which an *alpha* hydrogen and its *beta* neighbour vibrate *out-of-phase*. It is also seen that there is no clear distinction between the two rings, with respect to the effects of the introduced aza-group on the γC-H vibrations of quinoline.

mode	Type[a]	naphthalene [139,140]	quinoline [149]	Δ (cm^{-1})	out-of-plane displacement of H's
22	α-H	955	-	-	
38	β-H	772	804	+32	
27	β-H	717	741	+24	
11	β-H	825	840	+15	
23	β-H	780	786	+ 6	
37	α-H	983	980	- 3	
10	α-H	981	970	-11	
26	α-H	951	939	-12	

(a) after CHAPPEL & ROSS [32]

Table 3.25 The influence of the aza-group on the out-of-plane C-H bends in quinoline

The trends indicate that the introduction of the aza-group results in a mixing of *all* the γC-H vibrations. The data reflects the fact that the modes of vibration of quinoline are linear combinations of two or more of the symmetry coordinates of naphthalene. That is, since the displacement experienced by the neighbouring hydrogen to the aza-group in naphthalene will be less than is the case for its naphthalene analogue, the classification as to whether the C-H adjacent to the nitrogen is vibrating in-phase or out-of-phase grows less distinct. Thus the α-H vibrations will decrease in frequen-

cy, while the β-H vibrations will increase, as a result of their mixed force fields.

Clearly the practice of considering the two rings separately, equating bands found midway between the two ranges as indicating the presence of a ring containing *only* β hydrogens [32], or of identifying the band at 804cm^{-1} as being characteristic of *3 neighbouring* hydrogens [39,153,154] is not fully satisfactory.* Rather, these bands are merely evidence of the presence of the aza-group and of a difference in the coupling experienced within the molecule.

Unlike the out-of-plane C-H bends, the ring torsional modes appear in general to be little affected by the presence of the aza-substituent. The only significant difference in either their frequency or ν^D/ν^H ratio compared with naphthalene is observed for the ring mode 39(*A''*) which is found at a much lower frequency than that for naphthalene. As this is coupled to the C-H mode 38(*A''*), which shows the greatest aza-sensitivity of all the γC-H vibrations, and as the ν^D/ν^H ratios for both pairs are similar in quinoline to those in napthalene, (*i.e.* the same degree of coupling is maintained) the aza-sensitivity of this ring mode must be fully attributed to its coupling with the most aza-sensitive out-of-plane C-H vibration. Such a suggestion may only be firmly confirmed, however, by PED calculations.

An understanding of the behaviour of the naphthalene and quinoline modes of vibration as described above is useful in predicting the behaviour of both 1-monosubstituted naphthalenes and of quinoline *N*-oxide. For, in the same

---

* Further support for objecting to this practice is gained from the fact that the quinoline band at 741cm^{-1} is supposed to be characteristic of *4 neighbouring* hydrogen atoms [149], yet this band is the second most sensitive to aza-substitution.

manner that the WILSON nomenclature held for pzO_2 (which behaves like a *p*-substituted benzene) yet proved less rigorous for pzO, so should quinoline *N*-oxide behave more closely to a 1-monosubstituted naphthalene, which in turn should generally be more similar to naphthalene than to quinoline.

Unlike the more simple benzene system, there has been little systematic assignment of the vibrational spectra of substituted naphthalenes; a situation which appears to be complicated by the fact that the effects of substitution upon the *unsubstituted* ring are dependent upon the position and nature of the substituent [154,155].

3.1.3 The vibrational assignment of and coupling experienced by 1-fluoronaphthalene

Three comprehensive works on the vibrational assignments of 1-monosubstituted naphthalenes have been found in the literature [144,155,156]. These are reported in Table 3.26, giving all the vibrational assignments (apart from the C-H stretches) for 1-fluoronaphthalene. There is a significant difference of opinion between the authors, mostly the result of the use of the empirical method of making the assignments on the basis of naphthalene, enhanced by the uncertainty of the naphthalene data with which they were working. Several obviously incorrect assignments are noted in the Table; for example, where a band from a ring mode was incorrectly considered a C-H mode (and *vice versa*), as with modes 34(*A'*) and 32(*A'*) assigned by MICHAELSON and ZIEGLER, or where a γC-H mode was assigned to an abnormally high frequency, as with mode 37(*A''*) assigned by SINGH and SINGH.

Other obvious errors are the assignment of the band at 529cm^{-1} to the C-F stretch (made by MICHAELSON and ZIEGLER) and several assignments based upon

Table 3.26 Infrared assignments of 1-F-naphthalene found in the literature

Present Assignment	Observed (cm^{-1})	Previous Assignments [a] SINGH & SINGH [156]	MICHAELIAN & ZIEGLER [155]	CLAVERIE & GARRIGOU-LAGRANGE [144]
#16	1641 wm	16	n/o	n/o
31	1603 s	31	31	31
4	1576 s	4	4	4
44	1510 s	44	44	44
combination	1475 w			
8	1464 s	8	8	8
17	1442 m	17	17	17
combination	1426 w			
32	1397 s	32	34†	32
3	1384 s	3	3	3
combination	1365[b]			43
43	1350 w	43	43	
combination	1273 sh			
34	1263 s	34	32†	34
18	1239 vw	18		18
#29	1232 s	#29	46	#29 (?)
46	1216 sh	46	18	
combination	1166 sh			19
19	1157 m	5	19	
5	1144 sh	45	5 + 45	5
33[a]	1115[b]			33
combination[a]	1076[b]	19†		#21†
7	1035 s	7		
	1030 s	37†		7
10 (?)	1003 sh	10		46†
37	961 m	22	22 + 26	22
26	952 sh	21	21	26
#21	917 vw	24		39
combination	886[c]		47	
#47	876 s	47	# 6	#47
39	858 m		11 + 39	11
11	821 w	11		
combination	805 sh			
23	788 s	36	23 + 38	27
38	770[c]		27	
36	758 vs	23		23
combination	745[b,c]		36	36
27	728 w			

Table 3.26 (continued)

Present Assignment	Observed (cm^{-1})	Previous Assignments (a) SINGH & SINGH [156]	MICHAELIAN & ZIEGLER [155]	CLAVERIE & GARRIGOU-LAGRANGE [144]
#6	709 s	#6	#48	#6
#48	636 w	12		
12	625 w	48	12	12
#9	567 s	#9	#9	#48
#20	529 w	#20	#29+	20
combination	497 w		20	45
40	473 w	24	24	24
24	459 s	#33	#33	40
combination	425 sh			
28	416 m	40		
combination	383 sh	#13		
35	354 w	35	35	n/o
combination	302 w			
#45	270 m	#38	10 + #40+	
combination	241 vw	39+		
13 + 25	181 vw	28+		
#22	155 m	25	#13	

C-F Modes of Vibration

Mode	Present	SINGH & SINGH	MICHAELIAN & ZIEGLER	CLAVERIE & GARRIGOU-LAGRANGE
γC-F	22(155)	38(270)	10(270)	37 or 10(n/o)
αC-F	45(270)	33(459)	33(459)	45(482)
νC-F	29(1239)	29(1239)	29(529)	29(1239)

n/o not observed

\# substituted sensitive

\+ obvious incorrect assignment

(a) notation follows LIPPINCOTT and O'REILLY

(b) taken from CLAVERIE & GARRIGOU-LA GRANGE

(c) taken from MICHAELIAN & ZIEGLER

incorrect assignments for naphthalene, mode 46(A') (CLAVERIE and GARRIGOU-LEGRANGE) and modes 13(A'') and 28(A'') (SINGH and SINGH). Several unusually large shifts, either bathochromatic (mode 21(A') assigned by CLAVERIE and GARRIGOU-LEGRANGE) or hypsochromatic (modes 19(A') and 39(A'') assigned by SINGH and SINGH and mode 40(A'') assigned by MICHAELSON and ZIEGLER) are also questioned in light of the magnitude of the shifts or of the symmetry requirements necessary to allow coupling with the C-F vibrations.

One other source of difficulty is the different identification of the three 'lost' naphthalene modes of vibration which have been adopted by the authors, seen in the Table 3.27.

quinoline		1-F-naphthalene		
WAIT & McNERNEY [149]		SINGH & SINGH [156]	MICHAELIAN & ZIEGLER [155]	CLAVERIE & GARRIGOU-LEGRANGE [144]
22 (955)	γ C-F	39 (772)	10 (981)	37 (981) or 10 (983)
45 (1163)	α C-F	33 (1128)	33 (1128)	45 (1163)
29 (3060)	ν C-F	29 (3060)	-	-

(a) Figures in parentheses are for naphthalene (cm^{-1})

Table 3.27 Identity of the lost 'C-H modes' of quinoline

The choice of mode 29 (B_{1u} mode, naphthalene) as the νC-F fundamental is based upon the similarity of the intensity of the νC-H band which is lost and the high intensity of the C-F stretch [156]. In light of the discussion for quinoline above, the planar C-F bend (or 'lost' αC-H) is best described by mode 45 rather than mode 33. The presence of a CHAPPELL and ROSS β-H type band [32] at 770cm^{-1} in quinoline (which corresponds to mode 39 in naphthalene) does not support the description by SINGH and SINGH of this mode being the out-of-plane C-F bend (the 'lost' γC-H vibration). Similarly the quinoline bands at 980cm^{-1} and 970cm^{-1} are intuitively better described as modes 37 and 10 rather than either being mode 22. Therefore mode 22 best describes the 'lost' γC-H (the out-of-plane C-F bend).

Thus, in this work, the mode description for the C-F (1-F-naphthalene) or N-O (quinoline *N*-oxide) vibrations are after WAIT and McNERNEY [149]. Clearly a normal coordinate analysis of a 1-'light'-monosubstituted naphthalene, or of quinoline *N*-oxide itself, would help to establish the correctness (or otherwise) of this choice.

In spite of the differing assignments made by the three authors, six bands in the vibrational spectrum of 1-F-naphthalene are mutually recognised to be substituent sensitive; the bands at 1232cm^{-1}, 709cm^{-1}, 567cm^{-1}, 529cm^{-1}, 459cm^{-1} and 270cm^{-1} of which three describe the C-F vibrations and three are planar ring vibrations coupled to these. Several other bands which have been suggested to be substituent sensitive by one or other of the authors are influenced by the original naphthalene assignments they employed.

In view of this and in light of the latest vibrational assignment of naphthalene, the experimental data of SINGH and SINGH [156] have been re-examined and are presented in Table 3.26. Several changes are noted in comparison with the assignments given by SINGH and SINGH, with which there is a closer agreement than is the case for the other two works.

The first difference lies in the assignment of the medium intensity band at 1157cm^{-1} to mode 19(A'), a planar C-H bend. This follows better the assignment of naphthalene rather than assigning the band at 1076cm^{-1} to this mode [156] which follows more that of quinoline (Table 3.23). The assignment of the A' αC-H, mode 5 (which potentially couples to the first Kekulé mode) is then a little ambiguous. With increased coupling the vibration may be assigned to the shoulder at 1166cm^{-1}, or with the removal of coupling it may be assigned to the shoulder at 1144cm^{-1}. Since such coupling is expected to be decreased by a substituent, the latter assignment is preferred, and is in

fact supported by the vibrational assignment of quinoline *N*-oxide.

The above assignment of mode 19 does however present a difficulty in accounting for the strong band at 1076cm^{-1}. A possibility of Fermi resonance involving mode 33(*A'*) will be examined for quinoline *N*-oxide below, and this may account for the strong band at 1076cm^{-1} in 1-F-naphthalene. However, until more evidence is obtained, the assignment of mode 33 at 1115cm^{-1} made by CLAVERIE and GARRIGOU-LEGRANGE (in spite of being more similar to quinoline than to naphthalene and although not observed by SINGH and SINGH) is tentatively employed here.

The second difference lies in the reversal of the assignments of modes 23(*A''*), 38(*A''*) and 36(*A'*). These three fundamentals lie close together, and since the ring mode 36 is substituent sensitive, their assignments are difficult. The assignments made here are tentatively based upon that of naphthalene, taking into account the expected behaviour of the ring mode, 36. Clearly gas phase contour and polarisation studies are necessary for conclusive evidence of the correctness of these assignments. The two out-of-plane *A''* modes should give C-type bands and should be Raman depolarised.

The third difference is that the assignment of the two planar ring vibrations, modes 48(*A'*) and 12(*A'*), have been reversed. On grounds of symmetry (Fig. 3.5), the latter (unlike mode 48) is not likely to couple with the C-F stretch, and so is assigned to the weak band at 625cm^{-1}, which is typical of its position in both naphthalene and quinoline (Table 3.23). The band at 636cm^{-1} is considered to be the ring mode 48, its much higher frequency (18cm^{-1} higher than that of naphthalene) is attributed to its substituent sensitivity. A normal coordinate analysis of the molecule would be necessary to substantiate this view. A similar reversal of the substituent sensi-

tive ring mode 21(A') and the γC-H mode 26(A'') is made for the same reason.

The assignments of the ring torsion modes 24(A'') and 40(A'') also reflect an amendment of previous assignments. The two research groups, (SINGH and SINGH [156] and MICHAELIAN and ZIEGLER [155]) have both assigned the strong band at 459cm^{-1} to mode 33(A') (their choice, for describing the αC-F vibration) having both assigned the ring torsion mode 24(A'') to the weak band at 473cm^{-1} and further having assigned mode 40(A'') to a lower frequency (416cm^{-1} SINGH and SINGH; 270cm^{-1} MICHAELIAN and ZIEGLER). The assignment of the strong band at 459cm^{-1} to the αC-F vibration is examined below, and it will be suggested that this band is better ascribed to the ring torsion, mode 24, while the weak band at 473cm^{-1} is better assigned to mode 40. This latter assignment gives a better agreement with both naphthalene and quinoline (Table 3.23). Unlike the earlier assignments, the present assignments of modes 24 and 40 in 1-F-naphthalene also account for the observed intensities of both bands. The ring torsion, mode 24, having infrared allowed B_{3u} symmetry in naphthalene, is found to give a strong infrared absorption in quinoline [149]. Mode 40, on the other hand, has an infrared forbidden B_{2g} symmetry in naphthalene, and has a weak infrared absorption in quinoline [149].

Two present assignments for 1-F-naphthalene show unexpected differences compared with the analogous naphthalene assignments. The γC-H vibration, mode 27(A'') has been assigned to a higher frequency than its naphthalene counterpart. The similar assignment found for quinoline *N*-oxide (discussed below) would support this assignment as correct. By contrast, the assignment of the γC-H mode, 10(A'') to the shoulder at 1003cm^{-1}, which is considerably higher than its naphthalene counterpart, is only a very tentative assignment, following that of SINGH and SINGH [156]. Since this mode (being of

A_u symmetry) is spectroscopically silent in naphthalene, it is possible that a resultant very weak vibration in the region of 980cm^{-1} in the vibrational spectrum of 1-F-naphthalene may have been missed by SINGH and SINGH.

The greatest discrepancy with the previous assignments of 1-F-naphthalene, however, is to be found in the assignment of the in-plane and out-of-plane C-F bends. The previous assignments of these have been based upon their substituted benzene counterparts [155,156] for which the respective ranges are 400 to 210cm^{-1} and 250 to 140cm^{-1} [2]. However, studies of substituted quinolines [152] and substituted quinoline *N*-oxides [157] have shown that the substituent ranges for the fused ring systems are slightly lower, being 320 to 170cm^{-1} and 180 to 110cm^{-1}, respectively. This clearly shows that the band at 459cm^{-1} in 1-F-naphthalene is unlikely to be αC-F. Instead the band at 270cm^{-1} (which had been recognised as being substituent sensitive and therefor previously assigned to γC-F [155,156]) is here considered to be αC-F. The band at 155cm^{-1}, which was recognised by MICHAELIAN and ZIEGLER [155] to be substituent sensitive, is considered here to be γC-F. These new assignments agree well with the ranges expected for fused rings.

A comparison of the present assignments of 1-F-naphthalene with those of naphthalene shows that a number of other bands (besides the six mutually regarded so) possibly display substituent sensitivity. Their behaviour is understandable in terms of probable coupling with the C-F stretch. Table 3.28 shows these modes which, on grounds of symmetry (see also Fig. 3.5), are likely to couple with νC-F.

The ring modes found in the range 500 to 650cm^{-1} are seen to shift to higher frequencies on coupling with the C-F stretch. By contrast, those in the range 750 to 1050cm^{-1} are found at lower frequencies. Of these, the drama-

Mode	20	9	48	6	36	21	47	32	17	4
naphth	509	512	618	765	789	936	1010	1387	1458	1576
1-F-naphth	529	567	636	709	758	917	876	1397	1442	1576
difference	+20	+55	+18	-56	-31	-19	-134	+ 10	- 16	0

Table 3.28 Substituent sensitivity of planar ring modes in 1-F-naphthalene

tic shift of 134cm^{-1} in the out-of-phase ring-breathing mode 47(A') is reminiscent of the coupled behaviour of the ring-breathing mode of substituted benzenes. The ring modes above 1350cm^{-1} show no simple relationship. The shifts of modes 32 and 17 are probably a reflection of their coupling with planar C-H bends as described previously for naphthalene.

Two other observations about the effect of a substituent on the naphthalene vibrations are noted. With the introduction of the F-substituent the αC-H mode, 33(A') and the substituent sensitive ring mode 16(A') appear to couple, giving a hypsochromatic and bathochromatic shift of 13cm^{-1} and 13cm^{-1}, respectively. This is similar to the coupling experienced by WILSON modes 9a and 8a seen in pyO and pzO_2.

A further point of interest is the effect of the substituent on the out-of-phase Kekulé vibration, mode 43(A'). The fundamental to which this mode couples in naphthalene is mode 45(A') which has been shown to describe the planar C-F bend. However, with the large energy difference between the two in 1-F-naphthalene, it is unlikely that the coupling experienced in naphthalene is retained. Rather the sensitivity of this vibration must be the result of coupling in some manner with the C-F stretch. Further evidence for this is

developed below for quinoline *N*-oxide.

The absence of any coupling between the planar C-F bend, mode 45(*A'*), and those ring vibrations allowed on a symmetry basis, is evident by the similarity in frequency of the ring modes33(*A'*), 4(*A'*), 8(*A'*), 31(*A'*), 35(*A'*) and 44(*A'*) with the analogous naphthalene system. And, with only the ring torsion, mode 23(*A''*) showing a significant difference to its naphthalene analogue, the out-of-plane C-F bend, mode 22(*A''*), is also likely to be a pure vibration. The behaviour of mode 23 is explained by the *loss* of coupling on F-substitution, being coupled with the 'lost' C-H vibration (mode 22) in the naphthalene system. The absence of coupling of the out-of-plane vibrations and γC-X in fused ring systems is very much *unlike* substituted benzenes and reflects a significant difference between the two systems. Further evidence for the purity of these two substituted vibrations is developed below for quinoline *N*-oxide.

Clearly the arguments presented above depend upon the new assignments for 1-F-naphthalene made here. Future investigations involving labelling studies and normal coordinate treatments of 1-monosubstituted naphthalene may prove beneficial for a greater comprehension of these complex systems. However, since the present vibrational assignment yields a lucid understanding of the coupling within 1-F-naphthalene, it is anticipated that such work will not introduce any major changes.

The coupling behaviour described above also allows a better understanding of the behaviour of the quinoline *N*-oxide system. As for the 1-monohalogenated naphthalenes, quinoline *N*-oxide possesses C_s symmetry, for which all 35 planar *A'* vibrations and all 15 non-planar *A''* vibrations are expected to be both infrared and Raman active.

3.1.4 The vibrational assignment of and coupling experienced by quinoline *N*-oxide -d_0 and -d_7

The infrared spectra of quinoline *N*-oxide (quinO) and quinoline-d_7 *N*-oxide (quin-d_7O) are presented in Tables 3.29 and 3.30 respectively. With the low symmetry of the molecule and with the substantial number of vibrations present, the number of possible overtone, combination and difference bands is large. The assignments presented here are those combinations calculated to fall within ± 6cm^{-1} of the observed frequency. In the absence of polarisation and gas phase studies the conclusive assignment of these is not possible. Also, the number of possibilities of describing these bands does not, generally, make them useful in helping assign the fundamental vibrations of the molecule.

This is demonstrated by the fact that we are unable to determine the frequencies of the C-H stretches (which are masked by the O-H stretch of the water of hydration) from the combination bands. The values given in Tables 3.23 and 3.24 are estimated from the analogous naphthalene fundamentals and from their ν^D/ν^H ratios.

Three assignments have however been established on the basis of the combination bands. The assignment of the planar ring bend, mode 16(*A'*) in the -d_0 isotopomer is made difficult by its being masked by the O-H bend from the water of hydration. Its position has been calculated to be 1639 ± 1cm^{-1} on the basis of six possible combinations at 2850cm^{-1}(45+16), 2003cm^{-1}(35+16), 1159cm^{-1}(40+16), 1096cm^{-1}(20+16), 1012cm^{-1}(48+16) and 492cm^{-1}(16-5). This calculated upward shift in frequency of 10cm^{-1} compared with naphthalene (Table 3.23) is similar to observations for this vibration in 1-F-naphthalene.

Table 3.29 Infrared spectrum of quinoline *N*-oxide

Infrared (cm^{-1})	Assignment
3230 sbr	ν OH$_{(H_2O)}$.
2850 vw	46+16(*A'*); 43+3(*A'*); 18+7(*A'*); 33+4(*A'*).
2712 vw	8+3(*A'*); 31+29(*A'*); 8+3(*A'*).
2629 vw	29+3(*A'*); 43^2(*A'*); 17+9(*A'*); 7+4(*A'*).
2497 vw	44+37(*A''*); 29+18(*A'*); 39+31(*A''*); 47+31(*A'*); 17+7(*A''*); 43+19(*A'*).
2457 vw	47+4(*A'*); 39+4(*A''*); 43+5(*A'*); 29^2(*A'*); 34+19(*A'*); 10+8(*A''*); 7+3(*A'*).
2412 vw	18+5(*A'*); 34+33(*A'*); 31+23(*A''*); 29+19(*A'*); 26+17(*A''*).
2362 vw	37+31(*A''*); 31+6(*A'*); 19^2(*A'*); 43+7(*A'*); 33+29(*A'*); 46+5(*A'*).
2327 vw	21+3(*A'*); 47+16(*A'*); 39+16(*A'*); 19+5(*A'*); 34+7(*A'*); 39+8(*A''*); 47+8(*A'*).
2218 mbr	37+29(*A''*).
2116 vw	26+5(*A''*); 43+38(*A''*); 32+6(*A'*); 27+3(*A''*); 20+4(*A'*); 37+33(*A''*).
2095 vw	31+40(*A''*); 18+11(*A''*); 32+27(*A''*); 43+36(*A'*).
2003 wm	35+16(*A'*); 17+9(*A'*); 48+32(*A'*); 20+8(*A'*); 28+4(*A''*); 43+3(*A'*); 36+29(*A'*); 46+23(*A''*); 18+6(*A'*); 34+27(*A''*).
1990 vw	46+36(*A'*); 27+18(*A''*); 20+17(*A'*); 32+48(*A''*); 10^2(*A'*); 44+40(*A''*).
1972 w	29+16(*A'*); 11+5(*A'*); 37^2(*A'*); 23+19(*A''*); 26+10(*A'*).
1955 w	9+3(*A'*); 37+26(*A'*); 36+19(*A'*); 46+6(*A'*); 29+27(*A''*).
1935 vw	40+8(*A''*); 44+28(*A''*); 33+23(*A''*); 32+9(*A'*); 45+31(*A'*); 46+27(*A''*); 39+7(*A''*); 47+7(*A'*); 26^2(*A'*); 48+43(*A'*).
1917 vw	36+33(*A'*)[a]; 24+17(*A''*); 24+8(*A''*); 32+20(*A'*); 19+6(*A'*); 37+12(*A''*); 43+12(*A''*).
1876 w	36+33(*A'*)[a]; 18+12(*A''*); 39+10(*A'*); 47+10(*A''*); 28+8(*A''*); 40+3(*A''*); 44+35(*A''*); 33+6(*A'*); 43+9(*A'*).
1856 w	38+7(*A''*); 40+32(*A''*); 43+20(*A'*); 48+29(*A'*); 33+27(*A''*); 39+37(*A'*); 47+37(*A''*).
1844 w	32+24(*A''*); 29+12(*A''*); 39+26(*A'*); 48+46(*A'*); 47+26(*A''*).
1781 w	37+23(*A'*); 43+24(*A''*); 45+8(*A'*); 29+20(*A'*); 36+10(*A''*).
1743 wsh	35+32(*A'*); 40+18(*A''*); 10+6(*A''*); 33+12(*A'*); 36+26(*A''*).
1651 m	δ OH$_{(H_2O)}$.
1616 mw	31(*A'*) fundamental.
1585 w	22+3(*A''*); 25+3(*A''*); 45+18(*A'*); 32+13(*A''*); 26+12(*A'*); 36+23(*A''*).
1577 s	4(*A'*) fundamental.
1539 wsh	21+12(*A''*); 37+9(*A''*); 23+6(*A''*); 20+10(*A''*); 40+7(*A''*); 35+19(*A'*); 38+6(*A''*).
1514 s	44(*A'*) fundamental.
1495 wsh	43+22(*A''*); 43+25(*A''*); 45+19(*A'*); 36+27(*A''*).
1455 m	8(*A'*) fundamental.
1447 m	17(*A'*) fundamental.
1421 w	46+13(*A''*); 39+20(*A''*); 47+20(*A'*); (28+10(*A'*); 35+7(*A'*); 48+23(*A''*).
1398 s	3(*A'*) fundamental.

Table 3.29 (continued)

Infrared (cm^{-1})	Assignment
1377 m	32(*A'*) fundamental.
1349 w	37+35(*A''*); 33+3(*A'*); 28+21(*A''*); 48+27(*A''*); 38+20(*A''*); 12+6(*A'*); 23+9(*A''*); 39+24(*A'*); 47+24(*A''*).
1313 m	43(*A'*) fundamental.
1294 w	31-45(*A'*); 35+21(*A'*); 24+11(*A''*); 45+26(*A''*); 39+28(*A''*); 47+28(*A'*); 9+6(*A'*).
1275 wsh	34(*A'*) fundamental.
1266 s	18(*A'*) fundamental.
1230 s	29(*A'*) fundamental.
1210 ms	46(*A'*) fundamental.
1194 m	31-28(*A''*); 44-45(*A'*); 32-22(*A''*); 35+11(*A''*); 37+13(*A'*); 39+45(*A''*); 47+45(*A'*); 36+28(*A''*); 24+27(*A'*).
1179 s	19(*A'*) fundamental.
1159 w	40+16(*A'*); 4-28(*A''*); 26+22(*A'*); 26+25(*A'*); 35+23(*A''*); 20+12(*A''*); 28+6(*A''*).
1146 ms	5(*A'*) fundamental.
1138 ms	33(*A'*) fundamental[a].
1096 s	4-40(*A''*); 48+24(*A''*); 20+16(*A'*); 45+36(*A''*); 44-28(*A''*); 8-35(*A'*); 43-13(*A''*); 40+12(*A'*); 20+9(*A'*).
1054 m	7(*A'*) fundamental.
1040 wsh	13+11(*A'*); 45+27(*A''*); 40+9(*A''*); 29-22(*A''*); 29-25(*A''*); 44-40(*A''*).
1012 vw	32-35(*A'*); 38+13(*A'*); 24+20(*A''*); 48+16(*A'*); 23+13(*A'*); 22+11(*A'*); 25+11(*A'*); 31-12(*A''*).
997 vw	10(*A''*) fundamental.
984 w	37(*A''*) fundamental.
970 w	26(*A''*) fundamental.
928 w	21(*A'*) fundamental.
878 s	39(*A''*) fundamental; 47(*A'*) fundamental.
802 vs	38(*A''*) fundamental.
798 vs	23(*A''*) fundamental.
778 vs	36(*A'*) fundamental.
743 s	6(*A'*) fundamental.
722 s	27(*A''*) fundamental.
628 sbr	48(*A'*) fundamental.
610 sbr	12(*A''*) fundamental.
557 ms	9(*A'*) fundamental.
545 ms	20(*A'*) fundamental.
525 m	4-7(*A'*); 18-6(*A'*); 33-48(*A'*); 44-37(*A''*); 3-39(*A''*); 17-21(*A'*); 10-24(*A'*).
492 mw	16-5(*A'*); 26-40(*A'*); 46-27(*A''*); 18-36(*A'*); 29-6(*A'*).
480 w	40(*A''*) fundamental.

Table 3.29 (continued)

Infrared (cm^{-1})	Assignment
466 wm	24(A'') fundamental.
422 m	28(A'') fundamental.
365 vw	35(A') fundamental.
321 m	45(A') fundamental.
271 wm	11-9(A''); 18-10(A''); 17-19(A'); 5-39(A''); 39-12(A'); 47-12(A''); 40-13(A'); 10-27(A'); 6-24(A'').
211 m	13(A'') fundamental.
185 m	22(A'') fundamental; 25(A'') fundamental.
116 vw	44-3(A'); 6-48(A'); 40-35(A''); 10-39(A'); 18-5(A'); 27-12(A'); 32-18(A'); 45-13(A'').
82 w	dipole interaction.
68 wsh	librational mode.

s = strong

m = medium

w = weak

v = very

sh = shoulder

br = broad

Table 3.30 Infrared spectrum of quinoline-d_7 *N*-oxide

Infrared (cm^{-1})	Assignment
3300 sbr	ν OH$_{(H_2O)}$.
2773 vw	32+4(*A'*).
2604 w	19+16(*A'*); 8^2(*A'*); 44+29(*A'*); 32+3(*A'*); 46+4(*A'*).
2452 m	46+17(*A'*); 37+16(*A''*).
2378 w	44+21(*A'*); 46+8(*A'*); 29+8(*A'*).
2340 w	47+4(*A'*); 36+16(*A'*); 31+26(*A''*).
2311 m	19+8(*A'*); 39+4(*A''*); 44+37(*A''*); 46+3(*A'*); 16+6(*A'*).
2290 ms	1(*A'*) fundamental; 41(*A'*) fundamental.
2270 ms	2(*A'*) fundamental; 14(*A'*) fundamental; 30(*A'*) fundamental.
2261 msh	15(*A'*) fundamental.
2258 msh	42(*A'*) fundamental.
2225 msh	21+8(*A'*); 44+39(*A''*); 31+11(*A''*); 46+29(*A'*); 37+17(*A''*).
2163 w	47+3(*A'*); 23+4(*A''*); 43+37(*A''*); 48+16(*A''*); 29+19(*A'*).
2080 w	44+23(*A''*); 31+20(*A'*); 6+3(*A'*); 32+5(*A'*); 42-22(*A''*); 43+39(*A''*); 39+8(*A''*); 15-22(*A''*); 2-13(*A''*); 14-13(*A''*); 30-13(*A''*).
1936 w	21+19(*A'*); 35+16(*A'*); 34+7(*A'*); 43+23(*A''*); 48+17(*A'*); 2-35(*A'*).
1829 vw	2-40(*A''*); 14-40(*A''*); 30-40(*A''*); 46+26(*A''*); 39+34(*A''*); 12+8(*A''*); 44+28(*A''*); 32+27(*A''*); 19+18(*A'*); 38+29(*A''*).
1735 w	15-12(*A''*); 33+7(*A'*); 37+7(*A''*); 29+27(*A''*); 19+6(*A'*); 13+4(*A''*); 28+34(*A''*); 32+20(*A'*); 28+3(*A''*); 47+21(*A'*).
1651 s 1624 s	δ OH$_{(H_2O)}$.
1594 s	16(*A'*) fundamental.
1581 m	31(*A'*) fundamental.
1552 w	22+17(*A''*); 13+3(*A''*); 48+34(*A'*); 23+21(*A''*); 10+6(*A''*); 45+32(*A'*); 2-6(*A'*); 14-6(*A'*); 30-6(*A'*); 1-36(*A'*); 41-36(*A'*); 17+25(*A''*); 39^2(*A'*).
1536 s	4(*A'*) fundamental.
1453 m	44(*A'*) fundamental.
1429 wsh	34+28(*A''*); 42-10(*A''*); 24+19(*A''*); 26+38(*A'*); 15-5(*A'*); 21+9(*A'*); 27+5(*A''*); 47+23(*A''*).
1389 w	36+11(*A''*); 48+18(*A'*); 2-7(*A'*); 14-7(*A'*); 30-7(*A'*); 2-33(*A'*); 14-33(*A'*); 30-33(*A'*); 28+19(*A''*); 20+7(*A'*); 9+7(*A'*); 9+33(*A'*); 35+34(*A'*); 31-13(*A'*).
1377 ms	17(*A'*) fundamental.
1367 msh	11+6(*A''*); 1-19(*A'*); 41-19(*A'*); 4-25(*A'*); 40+21(*A''*); 36+23(*A''*); 39+27(*A'*); 45+34(*A'*); 37+9(*A''*); 12+5(*A''*).
1357 s	3(*A'*) fundamental.
1313 s	43(*A'*) fundamental.
1301 s	8(*A'*) fundamental.

Table 3.30 (continued)

Infrared (cm^{-1})	Assignment
1258 mw	2-19(A'); 14-19(A'); 30-19(A'); 44-13(A"); 38+27(A'); 23^2(A'); 16-35(A'); 28+7(A"); 26+9(A"); 28+33(A"); 27+26(A'); 40+18(A").
1242 s	32(A') fundamental.
1198 w	2-46(A'); 14-46(A'); 30-46(A'); 17-45(A'); 28+18(A"); 40+26(A'); 38+12(A'); 47+24(A"); 37+35(A"); 42-34(A'); 28+10(A').
1184 w	40+36(A"); 38+9(A"); 42-46(A'); 45+7(A'); 45+33(A'); 22+19(A"); 3-25(A"); 25+19(A"); 3-22(A"); 17-13(A"); 27^2(A'); 15-46(A'); 39+24(A"); 16-24(A").
1147 s	29(A') fundamental.
1073 s	46(A') fundamental.
1055 w	34(A') fundamental.
1026 m	13+10(A'); 45+6(A'); 37+25(A'); 2-32(A'); 14-32(A'); 30-32(A'); 20+12(A"); 16-48(A'); 40+27(A'); 13+5(A").
1011 s	19(A') fundamental.
954 w	31-23(A"); 44-20(A'); 26+13(A'); 42-8(A'); 2-43(A'); 14-43(A'); 30-43(A'); 29-13(A"); 47+25(A"); 40+9(A"); 15-8(A'); 39+22(A').
924 w	21(A') fundamental.
879 ms	7(A') fundamental; 33(A') fundamental.
854 m	37(A") fundamental.
835 m	5(A') fundamental.
830 msh	10(A") fundamental.
823 ms	18(A') fundamental.
807 s	16-47(A'); 44-11(A"); 29-35(A'); 42-44(A'); 15-44(A'); 8-20(A'); 20+45(A'); 23+25(A'); 17-48(A').
787 s	47(A') fundamental.
773 s	39(A") fundamental.
755 s	26(A") fundamental.
742 s	36(A') fundamental.
721 s	6(A') fundamental.
676 s	38(A") fundamental.
627 vs	23(A") fundamental.
615 ssh	3-36(A'); 32-23(A"); 34-40(A"); 40+22(A'); 24+13(A'); 45^2(A'); 21-45(A'); 47-25(A"); 4-21(A'); 44-5(A'); 18-13(A"); 40+25(A'); 12-29(A").
590 m	27(A") fundamental.
564 m	48(A') fundamental.
526 s	12(A") fundamental.
508 m	9(A') fundamental.
497 s	20(A') fundamental.

Table 3.30 (continued)

Infrared (cm^{-1})	Assignment
477 ms	32-47(A')[a]; 45+25(A''); 13^2(A'); 3-7(A'); 3-33(A'); 43-5(A'); 8-18(A'); 37-28(A'); 38-13(A'); 4-34(A'); 47-45(A'); 45+22(A''); 18-35(A'); 21-40(A''); 46-48(A'); 29-38(A'').
455 m	32-47(A')[a]; 10-28(A'); 23-25(A'); 17-21(A'); 23-22(A'); 43-37(A''); 5-28(A''); 36-28(A'').
441 mw	40(A'') fundamental.
416 m	24(A'') fundamental.
392 vw	13^2(A'); 29-26(A''); 48-25(A''); 27-13(A'); 5-40(A''); 48-22(A''); 10-40(A'); 43-21(A'); 29+4(A'); 32-37(A''); 46-38(A''); 44-34(A'); 21-12(A'').
374 m	28(A'') fundamental.
340 vw	35(A') fundamental.
307 ms	45(A') fundamental.
261 m	47-12(A''); 18-48(A'); 38-24(A'); 43-34(A'); 26-20(A''); 48-45(A'); 39-9(A'); 37-27(A'); 40-22(A''); 19-26(A'').
196 mw	13(A'') fundamental.
175 s	22(A'') fundamental.
170 msh	25(A'') fundamental.
123 w	20-28(A''); 48-40(A''); 33-26(A''); 7-26(A''); 23-9(A''); 26-23(A''); 31-44(A'); 43-29(A'); 8-29(A').
110 vw	12-24(A'); 45-13(A''); 24-45(A''); 10-6(A''); 29-46(A'); 26-11(A'); 47-38(A'); 37-36(A''); 38-48(A''); 33-39(A''); 7-39(A''); 5-6(A').
81 m	dipole interaction.
65 w	librational mode.

s = strong

m = medium

w = weak

v = very

sh = shoulder

br = broad

The other two assignments determined on the basis of combination bands are those for the out-of-plane C-H vibration, mode 11, of both the $-d_0$ and $-d_7$ isotopomers. This vibration, being a spectroscopically silent A_u vibration in naphthalene, is found to yield a weak infrared band in quinoline [149] and thus in quinoline *N*-oxide is possibly being masked by the very strong $-d_0$ absorption at 802cm^{-1}, and by the very strong $-d_7$ absorption at 627cm^{-1} (these two very strong bands being those of the out-of-plane umbrella vibration, mode 23).

The position of mode 11 for the $-d_0$ isotopomer is calculated to be at 828 ± 1cm^{-1} on the basis of seven possible combinations: 2095cm^{-1}(18+11), 1972cm^{-1}(11+5), 1294cm^{-1}(24+11), 1194cm^{-1}(35+11), 1040cm^{-1}(13+11), 1012cm^{-1}(22+11) and 271cm^{-1}(11-9). That of the $-d_7$ isotopomer is calculated to be at 646 ± 1cm^{-1} on the basis of five possible combinations: 2225cm^{-1}(31+11), 1389cm^{-1}(36+11), 1367cm^{-1}(11+6), 807cm^{-1}(44-11) and 110cm^{-1}(26-11).

While the veracity of these two assignments needs to be confirmed by gas phase contour and polarisation studies of the combinations upon which these are based, both assignments agree well with their naphthalene $-d_0$ and $-d_7$ analogues. The appearance of a weak infrared band at about 653cm^{-1} for the $-d_7$ isotopomer in both of the metal(II) complex series investigated in Chapters 4 and 5, provides strong evidence for at least the quinoline-d_7 *N*-oxide assignment.

The problem of accidental degeneracy which arises in a vibrational spectrum as rich as that of quinoline *N*-oxide, is displayed by the ring torsion, mode 39(A'') and the out-of-phase ring-breathing vibration, mode 47(A'), in the $-d_0$ isotopomer, and by five of the C-D stretches and by the two planar C-D bends, modes 7(A') and 33(A') in the $-d_7$ isotopomer.

In quinO, both mode 39(A'') and mode 47(A') have been assigned to the strong band at 878cm^{-1}. This accidental degeneracy is lifted in both series of metal(II) complexes (Chapters 4 and 5) to give a strong band at 876cm^{-1} (for the M(II) series; Mn-Zn) or at 880cm^{-1} (for the Pt(II) series) and a slightly weaker band at a lower frequency (about 868cm^{-1} for both series). The higher frequency band is that of the out-of-phase ring-breathing vibration, mode 47.

In quin-d_7O, modes 7(A') and 39(A') have both been assigned to the band of medium-strong intensity at 879cm^{-1}. This degeneracy is lifted in the Pt(II) complexes to give two weaker bands at 881cm^{-1} and 875cm^{-1}, respectively, but is not lifted in the M(II) series (Mn-Zn).

The assignment of the accidentally degenerate C-D stretches shown in Tables 3.23 and 3.30 are based upon their naphthalene analogues. Employing normal coordinate calculations to confirm these assignments may prove difficult because of the large anharmonicity of these vibrations [30,31,140].

A second complication with a rich vibrational spectrum, as previously mentioned, is the increasing probability of compensating errors occurring while employing isotopic labelling. Two regions in the spectra of the -d_0 and -d_7 isotopomers of quinoline *N*-oxide present such a potential danger.

In quinO there are six strong bands in the range 720 to 890cm^{-1}. These may be ascribed to the ring vibrations, modes 6(A'), 36(A') and 39(A''), and to the out-of-plane CH bends, modes 23(A''), 27(A'') and 38(A''). Their assignments in Tables 3.23, 3.24 and 3.29 have been made according to their expected behaviour (based upon their naphthalene, quinoline and 1-F-naphthalene analogues) and upon their ν^D/ν^H ratios.

In quin-d_7O there are nine vibrations within the range 625 to 825cm^{-1} which have medium to strong to very strong intensities. These bands may be ascribed to the four ring modes 6(A'), 36(A'), 39(A'') and 47(A') and to the four C-H bends, modes 18(A'), 23(A''), 26(A'') and 38(A''). Their assignment in Tables 3.23, 3.24 and 3.30 have been made in a similar manner to those above.

In view of the similar intensities of the bands and their close proximity to each other, polarisation and gas phase contour studies, followed by normal coordinate analyses of both isotopomers would be beneficial for final conclusions to be drawn.

The presence in quin-d_7O of the ninth strong band in the frequency range 625 to 825cm^{-1} introduces another difficulty experienced by large polyatomic systems, that being the increased probability of the occurrence of Fermi resonance.

While the strong band at 787cm^{-1} in quin-d_7O has presently been assigned as the γC-D vibration, a Fermi resonance may exist instead. If the two strong bands at 807cm^{-1} and 787cm^{-1} do represent a Fermi resonance system, then the splitting of some 20cm^{-1} should be seen in the combination bands in which mode 47 participates. There is one candidate for such a system; the bands at 477cm^{-1} and 455cm^{-1} ($\Delta\nu$ 22cm^{-1}) which may be the Fermi resonance split difference band 43-47(A').

Furthermore, in the metal(II) complexes, a strong band at about 790cm^{-1} is observed, with a weak band at a slightly higher frequency. Since this behaviour is typical of a loss of Fermi interaction through the removal of the degeneracy, it is possible that the two strong bands at 807cm^{-1} and 787cm^{-1} in quin-d_7O do indeed represent a Fermi resonance system. For more conclu-

sive evidence, gas phase and polarisation studies of the four bands at $807cm^{-1}$, $787cm^{-1}$, $477cm^{-1}$ and $455cm^{-1}$ need to be conducted, for which all four bands need to be Raman polarised, infrared *A+B* type bands to show that Fermi resonance does occur.

A similar possible Fermi resonance system also exists in the $-d_0$ isotopomer. Two bands may be assigned to the planar C-H bend, mode 33(*A'*); the medium strong band at $1138cm^{-1}$ or the strong band at $1096cm^{-1}$. While the former has been assigned here on the grounds of its greater similarity to the analogous naphthalene system, both bands may represent a Fermi resonance ($\Delta\nu$ $42cm^{-1}$). Such a suggestion is supported by a combination possibly reflecting this Fermi splitting; the bands at $1917cm^{-1}$ and $1876cm^{-1}$ ($\Delta\nu$ $41cm^{-1}$) may originate from the combination 36+33(*A'*).

Furthermore, as mentioned for 1-F-naphthalene, this C-H bend (mode 33) and the ring mode 16 are coupled. With the bathochromatic shift of about $10cm^{-1}$ calculated above for mode 16, as a result of introducing the N-O group, a hypsochromatic shift of similar magnitude is to be expected for mode 33. The centre of gravity of the two bands in question is $1117cm^{-1}$, yielding a frequency similar to that found in 1-F-naphthalene, and a shift of minus $11cm^{-1}$ compared with naphthalene, thus further supporting the suggestion of Fermi resonance. However, only in the complexes $[Pt(C_2H_4)(quinO)X_2]$ does the higher frequency band decrease in intensity. For the CO analogue [Pt(CO)-(quinO)X_2], both bands at $1158cm^{-1}$ and $1144cm^{-1}$ retain their intensity, while in the complexes $[M(II)(quinO)_n](ClO_4)_2$ (n=4,5 or 6) a strong band appears at ± $1140cm^{-1}$, while the lower band is masked by the ClO^-_4 mode. The latter two systems indicate either a retention of the Fermi resonance, or the absence of it in the free ligands. Again polarisation and gas phase studies are of importance to clearly establish the position. Until the ex-

istence of a Fermi resonance system is conclusively shown to exist, mode 33 is tentatively assigned to the medium-strong band at 1138cm^{-1}.

One other vibration needs some further comment. The -d_0 and -d_7 assignments of the out-of-plane C-H bend, mode 10, need to be considered. Both assignments are of high frequency compared with those of naphthalene, although they yield a ν^D/ν^H ratio that is comparable. Since the vibration is spectroscopically silent in naphthalene, the assignment of this mode to the weak band at 997cm^{-1} (-d_0) and the shoulder at 830cm^{-1} (-d_7) will need confirmation through normal coordinate calculations.

Finally, before the coupling within the molecule is discussed, the two bands of medium to weak intensity at 82cm^{-1} (-d_0) and 81cm^{-1} (-d_7) have been assigned to a dipole interaction in accordance with GHERSETTI *et al.* [152,157]. The weak shoulder at 68cm^{-1} (-d_0) and the weak band at 65cm^{-1} (-d_7) have been tentatively assigned to a librational mode.

The coupling experienced by quinoline *N*-oxide may be understood by the investigation of the hydrogen-bond sensitivity of the N-O vibrations and those

Vibration[a]	Mode[a]	quinO	Δ O---H shift	quin-d_7O	Δ O---H shift
νN-O(coupled)	29	1233	- 5	1184	-14
αN-O	45	318	+16	304	+12
γN-O	22	158	+22	148	+20
αC-H(coupled)	43	1307	- 6	1330	not reported

(a) present assignment (after GHERSETTI *et al.* [151,157]; frequency data in cm^{-1})

Table 3.31 Hydrogen bond sensitive bands in quinoline *N*-oxide

with which they couple. The data in Table 3.31 are that of GHERSETTI *et al.* [151,157], involving the infrared solution spectra of the anhydrous molecule.

The similarity of the shifts in both isotopomers that is experienced by modes 45(*A'*) and 22(*A''*) on hydrogen bond formation indicates the same degree of coupling, or lack of it, for both isotopomers. The magnitude of the shifts would indicate that *both* vibrations are pure (unlike the azine *N*-oxides) and this is supported by the absence of any other band showing hydrogen bond sensitivity below 500cm^{-1}.

By contrast the N-O stretch is clearly a coupled vibration. Two bands in substituted quinoline *N*-oxides have long been recognised as contenders for assignment to the N-O stretch, one in the range 1220 to 1260cm^{-1} and one in the range 1300 to 1340cm^{-1} [153]. However, their behaviour does not fit a simple relationship, with the higher frequency band being considered the predominant N-O stretch in some substituted quinoline *N*-oxides, and the lower frequency band in others [153]. Furthermore, the small shift (minus 5cm^{-1}) of the N-O stretch at 1233cm^{-1} (-d_0 isotopomer) on hydrogen bond formation compared with that experienced by the bending N-O vibrations indicates extensive coupling, while the corresponding shift of 14cm^{-1} in the -d_7 isotopomer indicates that a less extensive coupling occurs (Table 3.31). Unfornately, GHERSETTI *et al.* [152] do not report the shift for the -d_7 out-of-phase Kekulé vibration, mode 45. However, that this vibration is decoupled from the N-O stretch on deuteration, is evident from the increase of its ν^D/ν^H ratio compared with the situation in naphthalene (Table 3.24).

This deuteration-induced decoupling is also evident in the magnitude of the shift of νN-O on complexation. In the Pt(II) complexes (Chapter 5) the shift of νN-O in the -d_7 isotopomer is very small (of the order of 3 to

6cm^{-1}) while that for the -d_7 isotopomer is more significant (of the order of 15cm^{-1}). In this particular series the shift on complexation is enhanced by the *trans*-effect of the π-acceptor (either C_2H_4 or CO), since the shift for the $[M(II)(quinO)_n](ClO_4)_2$ (n=4,5 or 6) complexes is less significant (Chapter 4).

The deuteration-induced decoupling is also seen in the behaviour of the other ring modes to which the N-O stretch couples (which were not investigated by GHERSETTI *et al.* [152,157]). From Table 3.32, the coupling experien-

Mode	20	9	48	6	36	21	47	32	17	4
naphth	509	512	618	765	789	936	1010	1387	1458	1576
quinO	545	557	628	743	778	928	878	1377	1447	1577
difference	+36	+45	+10	-22	-11	- 8	-132	- 10	- 11	+ 1
change in ν^D/ν^H	↓	↓	↓	↑	↑	↑	↑	NIL	↑	↓

Table 3.32 Substituent sensitivity of planar ring modes in quinoline *N*-oxide

ced by these ring modes is seen to be very similar to that of 1-F-naphthalene (Table 3.28). For deuteration-induced decoupling of these ring modes from the N-O stretch, those ring vibrations which shift to higher frequencies in the -d_0 isotopomer compared with naphthalene (i.e. modes 20, 9 and 48 in the naphthalene range 500 to 650cm^{-1}) would be expected to yield ν^D/ν^H ratios lower than their naphthalene analogues. Those which are shifted to lower frequencies (modes 6, 36, 21 and 47 in the naphthalene range 750 to 1050cm^{-1}) would yield ν^D/ν^H ratios higher than their naphthalene counterparts. This behaviour is indeed observed to occur. As was observed for 1-F-naphthalene, the inconsistent behaviour of the three high frequency ring modes 32, 17 and

4 in quinoline *N*-oxide, again is probably a result of their being also coupled with planar C-H bends.

It would therefore appear that on full deuteration of quinoline *N*-oxide there is a general decoupling of the N-O stretch and all the ring modes with which it is coupled in the -d_0 isotopomer.*

Finally, a comparison with the assignments of the N-O vibrations made by GHERSETTI *et al.* [151,157] for the anhydrous molecule of quinoline *N*-oxide and its -d_7 isotopomer and those made here for quinoline *N*-oxide dihydrate and its -d_7 isotopomer, show some small differences. In the dihydrate, the N-O stretches are found at a lower frequency than in the anhydrous species, while the in-plane and the out-of-plane N-O bends are found at a higher frequency. Indeed, in the dihydrate -d_0 isotopomer the γN-O vibration, mode 22, is accidentally degenerate with the ring mode 25 (the wing-wagging vibration) whereas in the anhydrous species these two bands are completely resolved. Since this behaviour is typical of that found for the hydrogen-bonded molecule [151,157] it is clear that the hygroscopic nature of these aromatic *N*-oxide ligands is a result of their ability to form hydrogen bonds with the water of hydration at the oxygen site of the N-O group.

The full vibrational assignment of quinoline *N*-oxide and its fully deuterated analogue presented above, now makes possible a correspondingly complete assignment of their metal complexes.

---

* Consequently the lack of correlation between the N-O stretch and the electronic effect of the substituent in substituted quinoline *N*-oxides [39] may possibly be overcome by examining the fully deuterated analogues.

3.2 1,10-Phenanthroline *N*-oxide (phenO)

The vibrational assignment of 1,10-phenanthroline *N*-oxide (phenO) must be one of the least studied of the aromatic *N*-oxide ligand systems, with only one fairly comprehensive vibrational assignment found in the literature. This work by DEGA-SZAFRAN [48], which consists of a comparison of the infrared spectrum of phenO and its 1-oxide salts with those of 4,5-phenanthrene and 1,10-phenanthroline, regrettably does not extend below 700cm^{-1}.

Two strong bands at 1270cm^{-1} and 1250cm^{-1} were assigned to νN-O and two bands at 815cm^{-1} (strong) and 810cm^{-1} (very strong) were assigned to αN-O [48]. Based on the introduction to this chapter the latter assignments are questioned, being far too high in frequency compared with the true αN-O frequency of pyO. (Indeed, by comparison with quinO, the frequencies of αN-O and γN-O may well be expected to be *lower* than those of pyO). Since this region of the spectrum may contain both in-plane and out-of-plane ring modes (which are potentially coupled to νN-O) as well as out-of-phase C-H modes, the assignment of the bands at 815 and 810cm^{-1} is extremely complicated. The question of which of the two bands at 1270 and 1250cm^{-1} is predominently the νN-O also needs full clarification.

An attempt to present here an alternative assignment for phenO and its fully deuterated analogue (including the far-infrared spectra) was overruled by the difficulty (found in this work) to demonstrate the purity of the *N*-oxides. However, because of the absence in the literature of the vibrational assignment of the fully deuterated diimine parent (phen-d_8), an examination of the vibrational assignments of the hydrocarbon parent (namely 4,5-phenanthrene) and the diimine parent (1,10-phenanthroline) has been undertaken both to present the assignment of phen-d_8 as well as in the hope that such a study will

aid future investigations into the vibrational assignment of phenO and its deuterated analogue.

3.2.1 4,5-phenanthrene (phenanth) and 4,5-phenanthrene-d_{10} (phenanth-d_{10})

The difficulty in determining the vibrational assignments of large molecules has already been emphasised. 4,5-phenanthrene represents an even more complicated system than those previously considered and this is typified by the uncertainty of its assignment found in the literature. For while 4,5-phenanthrene has not undergone as extensive an investigation as has naphthalene, even so several different assignments have been made. The most comprehensive of these are presented in Table 3.33. The work of SCHETTINO *et al.* [158] represents a single crystal infrared polarisation, Raman and fluorescence study with a normal coordinate analysis of the planar vibrations. That of WITT and MECKE [159] involves infrared and Raman gas, solution and single crystal polarisation studies above 200cm^{-1}. BREE *et al.* [160] report single crystal infrared and Raman polarisation studies of both phenanthrene and its fully deuterated analogue above 40cm^{-1}. GODEC and COLOMBO [161] present the infrared and Raman spectra (single crystal and solution) of phenanthrene plus a normal coordinate analysis. ALTMANN and PERKAMPUS [162] report that a refinement of the planar normal coordinate analysis of phenanthrene, while the latest work, that of CYVIN *et al.* [163] presents both an in-plane and an out-of-plane normal coordinate analysis.

These works present two different assignment schemes. That of BREE *et al.* [160] is the first (consisting of slight modifications to the two earlier works) which is supported by the 1979 and 1980 normal coordinate calculations. The second is that of GODEC and COLOMBO [162] (in spite of their assertion of agreement with BREE *et al.*). That these do indeed represent different as-

Table 3.33 Assignments of 4,5-phenanthrene and 4,5-phenanthrene-d_{10} in the literature

Mode[b]		In-phase[a] phenanthrene-d_0						phenanthrene-d_{10}	
		SCHETTINO *et al.* [158] (1966)	WITT & MECKE [159] (1967)	BREE *et al.* [160] (1972)	GODEC & COLOMBO [161] (1976)	ALTMANN & PERKAMPUS [162] (1979)	CYVIN *et al.* [163] (1980)	SCHETTINO [164] (1967)	BREE *et al.* [160] (1972)
1	A_1	250	407	247	231	242	192	226	231
2		406	547	408	410	407	347	392	392
3		540	615	548	547	539	511	529	532
4		710	711	710	713	708	675	669	667
5		830	831	832	829	840	837	784	772
6		1038	865	1038	886	1035	877	(825)	813(?)
7		1100	1037	1094	968	1112	1003	843	(833)
8		1142	1093	1144	1037	1140	1045	864	860
9		1160	1142	1163(?)	1070	1171	1113	896	897
10		1200	1165	1203	1142	1204	1136	(980)	945
11		1244	1202	1247	1200	1233	1171	1122	1118
12		1303	1245	1304	1302	1288	1312	1203	1205
13		1365	1295	1352	1348	1352	1431	1304	1304
14		1417	1350	1431	1440	1439	1459	1326	1372
15		1441	1420	1443	1523	1455	1513	1396	1392
16		1524	1441	1526	1600	1541	1576	1475	1475
17		1567	1522	1606	1622	1579	1597	(1525)	1563
18		1608	1602	1626	1684	1628	1670	1565	1597
19		3020	3006	3002(?)	3015	3023	3030	2251	2253
20		3056	3038	3037	3035	3041	3031	2261	2263
21		3067	3046	3057	3055	3067	3032	2275	2277
22		3075	3063	3072	3081	3078	3036	2291	2290
23		(3088)	3086	3082(?)	3088	3089	3040	2310	2312(?)
46	B_1	951	950	1149(?)	1170		(980)	741	910
47		874	870	950	1153		950	690	777
48		819	818	871	946		871	649	691/746
49		735	793(?)	817	874		817	609	651
50		716	733	732	791		732	559	611
51		499	714	715	750		715	435	560
52		442	497	495	442		495	384	438
53		431	428	426	247		426	374	374
54		233	-	234	121		234	214	213
55		-	-	124	108		124	-	117

Table 3.33 (continued)

Mode[b]		Out-of-phase[a] phenanthrene-d_0 SCHETTINO *et al.* [158] (1966)	WITT & MECKE [159] (1967)	BREE *et al.* [160] (1972)	GODEC & COLOMBO [161] (1976)	ALTMANN & PERKAMPUS [162] (1979)	CYVIN *et al.* [163] (1980)	phenanthrene-d_{10} SCHETTINO [164] (1967)	BREE *et al.* [160] (1972)
24	B_2	(422)	240	441	429	453	404	411	414
25		(469)	398(?)	536	495	543	451	(430)	473(?)
26		618	442	619	616	610	626	594	597
27		(716)	618	712	734	724	707	676	677
28		(836)	980(?)	876	866	880	825	(737)	(737)
29		1002	1001	1001	950	993	896	(809)	830
30		1039	1147	1040	980	1041	1013	832	849
31		(1095)	1206(?)	1144	1000	1143	1062	845	863
32		1148	1223	1173(?)	1092	1176	1125	(958)	948(?)
33		1220	1280	1227	1163	1212	1181	975	971
34		1303	1303	1283	1244	1291	1285	1044	1022(?)
35		(1354)	1352	1340	1425	1353	1432	1270	1270
36		1430	1430	(1421)	1457	1405	1450	1352	1326
37		1458	1457	1458	1502	1449	1513	1382	1352
38		1500	1500	1502	1572	1495	1538	1431	1432
39		1548	1565	1572	1613	1586	1595	1525	1528
40		1670	1622	1616	1660	1624	1633	1597	1589
41		3024	3017	3019	3005	3023	3030	(2250)	2230(?)
42		(3034)	3021	3020	3024	3034	3032	(2255)	(2255)
43		(3042)	3056	3047	3047	3041	3035	2268	2265
44		(3064)	3071	3064	3070	3067	3038	2285	2273
45		3102	3100	3094	3100	3089	3040	2300	2286
56	A_2	928	944	1159(?)	-		(981)	-	(813)
57		880	-	969	972		969	-	831(?)
58		-	811	946	817		946	-	(757)
59		-	-	791(?)	760		880	672(?)	(732)
60		761	765	763	710		791(?)	621	621
61		594	-	(726)	396		761 or 763	-	(572)
62		513	-	(601)	283		594	475	(507)
63		-	-	(502)	142		513	-	(438)
64		352	-	395(?)	76		352 or 395	353	351
65		-	-	(258)	61		(266)	-	(239)
66		123	-	(138)	50(?)		(151)	-	165(?)

(a) refers to the vibrations of the two rings

(b) after SCHETTINO *et al.* [158]

signment schemes is demonstrated by the different interpretation of the polarisation studies made by the two groups (Table 3.34). From the Table it is seen that there is a disagreement as to the assignment of 31 of the 66 fundamentals of 4,5-phenanthrene.

Since both schemes have experimental as well as theoretical support, the employment of either scheme as the hydrocarbon 'parent' for subsequent determination of the fundamentals of phen and phenO, must be tentative until the ambiguity is resolved.* The assignment made by BREE *et al.* [160] is employin this work on two grounds. Firstly PERKAMPUS and his co-workers have previously used this scheme in their assignments of various phenanthrolines [165-167], secondly the scheme by BREE *et al.* includes the assignment of 4,5-phenanthrene-d_{10} whereas that of GODEC and COLOMBO does not. The vibrational notation adopted for this model (and therefore also for phen) is that of SCHETTINO *et al.* [158].

In employing the assignment of BREE *et al.* it is noted that while the assignment of the planar vibrations is fairly certain (demonstrated by the good agreement with the planar normal coordinate analysis by ALTMANN and PERKAMPUS [162]), the assignment of the out-of-plane vibration is less so, in particular the highest αC-H vibrations, modes 56(A_2) and 46(B_1). These two fundamentals have been assigned by BREE *et al.* to frequencies some 70 to 100cm^{-1} higher than their calculated frequencies, ascribing the differences to anharmonicity experienced by the two hydrogen atoms involved in the intramolecular crowding [160]. This suggestion is queried since, while it is true that the out-of-plane force field used neglected the repulsive interaction of the hy-

---

* This would be best achieved by extending the normal coordinate calculations of GODEC and COLOMBO to phenanth-d_{10} and so determine which of the two models is best.

cm^{-1}	BREE *et al.* [160]		GODEC & COLOMBO [161]	
234	B_1	fundamental	A_1	fundamental (?)
247	A_1	fundamental	B_1	fundamental
282		n/o	A_2	fundamental (?)
426	B_1	fundamental	B_2	fundamental (?)
441	B_2	fundamental	B_1	fundamental
495	B_1	fundamental	B_2	fundamental
536	B_2	fundamental	(?)	combination
710	A_1	fundamental	A_2	fundamental
713	B_1	fundamental	A_2	fundamental
732	B_1	fundamental	B_2	fundamental
755	A_1	combination	B_1	fundamental (?)
792	A_2	fundamental (?)	B_1	fundamental
817	B_1	fundamental	A_2	fundamental (?)
871	B_2	fundamental	B_2	fundamental
876	B_2	fundamental	B_1	fundamental
886	B_2	combination	A_1	fundamental (?)
946	A_2	fundamental	B_1	fundamental
950	B_1	fundamental	B_2	fundamental
969	A_2	fundamental	$A_2 + A_1$	fundamental
981	(?)	combination	B_2	fundamental
1040	B_2	fundamental		n/o
1069	A_1	combination	A_1	fundamental
1094	A_1	fundamental	B_2	fundamental
1144	$B_2 + A_1$	fundamental (?)	A_1	fundamental
1149	B_1	fundamental (?)		n/o
1159	A_2	fundamental (?)	B_1	fundamental
1163	A_1	fundamental (?)	B_2	fundamental
1173	B_2	fundamental (?)	B_1	fundamental
1229	B_2	fundamental	B_1	combination
1247	A_1	fundamental	B_2	fundamental
1283	B_2	fundamental	B_1	combination
1340	B_2	fundamental (?)	(?)	combination
1431	A_1	fundamental	B_2	fundamental
1660		n/o	B_2	fundamental
1684		n/o	A_1	fundamental
3003	A_1	fundamental (?)	B_2	fundamental
3015	B_2	fundamental	A_1	fundamental

(?) uncertain assignments (show mixed symmetry characteristics)

n/o not observed

Table 3.34 Different interpretation of the polarisation studies of 4,5-phenanthrene

drogen at positions 4 and 5, no such anharmonicity is observed for the in-plane vibrations, the calculation of which comprised the same simplification [158]. This point is, however, less relevant to the assignment of phen and phen-d_8 since any such interaction of these two hydrogens is removed and the two highest αC-H vibrations would therefore be closer to their calculated positions.

3.2.2 The monohydrates of 1,10-phenanthroline (phen) and 1,10-phenanthroline-d_8 (phen-d_8)

The infrared and Raman spectra of 1,10-phenanthroline hydrate (phen) are presented in Table 3.35, and the infrared spectrum of 1,10-phenanthroline-d_8 hydrate (phen-d_8) is presented in Table 3.36.

Since phen has C_{2v} point group symmetry the planar in-phase (A_1), planar out-of-phase (B_2), and out-of-plane out-of-phase (B_1) fundamentals are both infrared and Raman allowed. The out-of-plane in-phase (A_2) fundamentals are infrared forbidden but these may become very weakly activated in the solid state [165]. The A_2 fundamentals are also expected to yield Raman bands of weak intensity.

With the large number of fundamentals present, the number of possible overtone, combination and difference bands is substantial. The assignments presented here are those calculated to fall within ± 6cm^{-1} of the observed frequency, bearing in mind the spectroscopic characteristics of the A_2 bands. A more comprehensive assignment of the infrared active combination bands will require full polarisation studies.

The assignments of phen H_2O presented in this work agree well with those by

Table 3.35 Infrared and Raman spectra of phenanthroline monohydrate

Raman	Infrared	Assignment
Not recorded	3480 ssh 3380 sbr 3270 ssh	$\nu O\text{-}H_{(H_2O)}$.
	3115 wsh	$45(B_2)$ fundamental(?).
	3082 m	$23(A_1)$ fundamental.
3064 w	3068 ssh	$22(A_1)$ fundamental.
3058 sh	3059 s	$21(A_1)$ fundamental; $43(B_2)$ fundamental.
3032 vw	3032 m	$19(A_1)$ fundamental; $42(B_2)$ fundamental.
Not recorded	3008 mw	$41(B_2)$ fundamental.
	2991 mw	$40+36(A_1)$; $36+16(B_2)$.
	2985 wsh	$38^2(A_1)$; $39+37(A_1)$; $40+36(A_1)$.
	2862 vw	$45\text{-}65(B_1)$; $22\text{-}1(A_1)$; $15+14(A_1)$; $41\text{-}66(B_1)$; $37+15(B_2)$; $39+12(B_2)$.
	2607 vw	$22\text{-}53(B_1)$; $37+9(B_2)$; $19\text{-}24(B_2)$; $42\text{-}24(A_1)$; $35+12(B_2)$; $36+33(A_1)$; $41\text{-}2(B_2)$; $21\text{-}53(B_1)$.
	2588 w	$15+8(A_1)$; $46+18(B_1)$; $12^2(A_1)$; $38+7(B_2)$; $36+9(B_2)$; $29+17(B_2)$; $23\text{-}25(B_2)$; $31+15(B_2)$; $41\text{-}24(A_1)$.
	2346 vvw	$38+5(B_2)$; $58+36(B_1)$; $34+7(B_2)$; $23\text{-}51(B_1)$; $21\text{-}4(A_1)$; $43\text{-}4(B_2)$; $33+31(A_1)$; $49+16(B_1)$; $35+6(B_2)$; $28+15(B_2)$; $22\text{-}27(B_2)$; $27+18(B_2)$.
	2284 w	$8^2(A_1)$; $4\text{-}27(B_2)$; $45\text{-}59(B_1)$; $22\text{-}50(B_1)$; $39+27(A_1)$; $33+30(A_1)$; $49+15(B_1)$; $50+16(B_1)$; $43\text{-}50(A_1)$; $29+12(B_2)$; $21\text{-}50(B_1)$; $9+7(A_1)$; $31+8(B_2)$; $34+6(B_2)$.
	2128 vw	$36+27(A_1)$; $29+8(B_2)$; $52+18(B_1)$; $37+4(B_2)$; $26+16(B_2)$; $7+6(A_1)$; $50+13(B_1)$; $14+4(A_1)$; $41\text{-}29(A_1)$; $60+35(B_1)$.
	2112 w	$23\text{-}46(B_1)$; $41\text{-}28(A_1)$; $39+3(B_2)$; $28+10(B_2)$; $38+26(A_1)$; $36+4(B_2)$; $25+18(B_2)$; $52+17(B_1)$; $34+5(B_2)$; $30+6(B_2)$.
	2069 w	$48+9(B_1)$; $27+13(B_2)$; $26+15(B_2)$; $41\text{-}58(B_1)$; $10+5(A_1)$; $53+18(B_1)$; $50+12(B_1)$; $6^2(A_1)$; $46+7(B_2)$; $43\text{-}29(A_1)$; $30+29(A_1)$; $21\text{-}29(B_2)$; $42\text{-}58(B_1)$.
	2023 vw	$35+4(B_2)$; $45\text{-}7(B_2)$; $41\text{-}29(A_1)$; $21\text{-}6(A_1)$; $43\text{-}6(A_1)$; $29+6(B_2)$; $48+8(B_1)$; $24+17(B_2)$; $62+37(B_1)$; $49+9(B_1)$; $33+19(B_2)$; $22\text{-}6(A_1)$; $58+30(B_1)$; $27+12(B_2)$; $18+2(A_1)$; $36+26(A_1)$.
	1964 w	$39+2(B_2)$; $50+9(B_1)$; $43\text{-}7(B_2)$; $34+4(B_2)$; $21\text{-}7(A_1)$; $14+3(A_1)$; $59+31(B_1)$; $26+13(B_2)$; $53+16(B_1)$; $29^2(A_1)$; $22\text{-}7(A_1)$.
	1937 w	$42\text{-}7(B_2)$; $49+7(B_1)$; $35+26(A_1)$; $19\text{-}7(A_1)$; $46^2(A_1)$; $23\text{-}8(A_1)$; $58+29(B_1)$; $30+5(B_2)$; $28+6(B_2)$; $27+10(B_2)$.
	1908 w	$58+57(A_1)$; $59+30(B_1)$; $45\text{-}33(A_1)$; $27+9(B_2)$; $16+2(A_1)$; $64+38(B_1)$; $53+15(B_1)$; $25+14(B_2)$; $57^2(A_1)$; $41\text{-}7(B_2)$.
	1831 w	$36+24(A_1)$; $61+30(B_1)$; $64+37(B_1)$; $51+7(B_1)$; $33+26(A_1)$; $23\text{-}34(B_2)$; $58+28(B_1)$; $42\text{-}33(A_1)$; $19\text{-}33(B_2)$; $49+46(A_1)$.

Table 3.35 (continued)

Raman	Infrared	Assignment
Not recorded	1763 vw	43-12(B_2); 39+1(B_2); 21-12(A_1); 27+6(B_2); 26+8(B_2); 60+57(A_1); 48^2(A_1); 31+26(A_1); 23-35(B_2); 22-12(A_1); 10-3(A_1).
	1708 vw	61+5(A_1); 51+46(A_1); 5^2(A_1); 29+27(A_1); 66+39(B_1); 45-36(A_1); 16+1(A_1); 41-12(B_2); 59+48(B_2); 43-13(B_2); 30-26(A_1); 21-13(A_1).
	1642 m	δO-H$_{(H_2O)}$.
1617 vwbr	1615 m	18(A_1) fundamental.
1601 wbr	1597 vw	17(A_1) fundamental.
1587 mwbr	1585 ms	40(B_2) fundamental.
1562 wbr	1561 m	39(B_2) fundamental.
1541 vvw		59+4(A_2); 55+37(A_2); 53+30(A_2).
1507 sh		48+26(A_2); 64+7(A_2); 57+3(A_2); 50+27(A_2).
1502 m	1502 s	16(A_1) fundamental.
	1492 m	38(B_2) fundamental.
1446 s		15(A_1) fundamental.
1420 m	1422 s	37(B_2) fundamental.
1414 msh		14(A_1) fundamental.
1405 vs	1405 m	36(B_2) fundamental.
1397 msh		46+24(A_2); 65+8(A_2); 50+26(A_2).
1392 wsh		65+8(A_2); 46+24(A_2).
1345 ms	1345 ms	13(A_1) fundamental.
1314 vw	1312 vw	35(B_2) fundamental.
1295 vs	1295 w	12(A_1) fundamental.
1275 wm		50+25(A_2).
1270 wsh		66+14(A_2); 53+49(A_2); 64+5(A_2).
	1263 w	55+8(B_1); 4+3(A_1); 36-66(B_1); 60+53(B_2); 59+24(B_1); 5+2(A_1).
1253 w		34(B_2) fundamental.
1218 w	1217 wm	10(A_1) fundamental.
1204 w	1207 wsh	33(B_2) fundamental.
1187 w	1186 vw	9(A_1) fundamental.
	1170 vvw	33-66(B_1); 14-54(B_1); 37-65(B_1); 53+4(B_1); 17-24(B_2); 12-55(B_1); 40-64(B_1); 26+3(B_2).
1136 w	1137 m	31(B_2) fundamental.
1096 mw	1092 s	7(A_1) fundamental.
	1079 m	30(B_2) fundamental.
1036 s	1037 m	6(A_1) fundamental.
	1025 vvw	26+2(B_2); 66+48(B_2); 54+50(A_1); 8-55(B_1); 15-24(B_2); 62+24(B_1).
	1006 vvw	55+48(A_1); 53-3(B_1); 33-1(B_2); 16-25(B_2); 37-64(B_1); 36-2(B_2); 14-2(A_1); 34-65(B_1).

Table 3.35 (continued)

Raman	Infrared	Assignment
	997 w	$25^2(A_1)$; 37-24(A_1); 36-64(B_1); 38-25(A_1); 18-26(B_2); 16-52(B_1); 36-2(B_2); 65+51(B_2); 33-1(B_2); 16-25(B_2).
982 vw	988 m	29(B_2) fundamental.
971 vvwbr	969 w	46(B_1) fundamental.
958 vvwbr	956 w	57(A_2) fundamental.
	896 vvw	28(B_2) fundamental.
856 w	853 vs	5(A_1) fundamental.
	840 s	49(B_1) fundamental.
831 vw		59(A_2) fundamental(?); 30-54(A_2).
809 m	810 w	60(A_2) fundamental.
	779 m	50(B_1) fundamental.
	738 vs	51(B_1) fundamental.
	724 m	27(B_2) fundamental.
711 vs	708 wm	4(A_1) fundamental.
	695 mbr	$\rho N\cdots H_2O$.
622 vw	624 m	26(B_2) fundamental.
605 w		62(A_2) fundamental.
	596 wm	$\omega N\cdots H_2O$.
552 wm	550 vw	3(A_1) fundamental.
544 wsh		46-24(A_2); 12-61(A_2); 55+24(A_2); 40-6(A_2); 16-58(A_2).
509 w	509 w	52(B_1) fundamental.
	499 w	25(B_2) fundamental.
465 w		10-61(A_2); 12-59(A_2); 35-51(A_2); 27-54(A_2).
	457 w	53(B_1) fundamental.
426 vwbr	429 w	24(B_2) fundamental.
411 s	412 m	64(A_2) fundamental.
403 wm	406 vw	2(A_1) fundamental.
	281 vw	51-53(A_1); 24-66(B_1); 37-8(B_2); 31-5(B_2); 48-62(B_2); 4-24(B_2); 29-4(B_2); 37-31(A_1); 16-10(A_1); 14-31(B_2); 38-33(A_1); 35-6(B_2); 17-35(B_2); 38-10(B_2).
253 msh	254 vvw	65(A_2) fundamental.
246 ms	244 mw	54(B_1) fundamental.
Not recorded	203 vw	1(A_1) fundamental.
	167 vw	64-54(B_2); 37-34(A_1); 33-6(B_2); 18-15(A_1); 40-14(B_2); 35-8(B_2); 27-3(B_2); 8-46(B_1); 46-60(B_2); 48-4(B_1); 24-65(B_1); 14-34(B_2).

Table 3.35 (continued)

Raman	Infrared	Assignment
Not recorded	159 vwsh	34-7(B_2); 13-9(A_1); 65-66(A_1); 64-65(A_1); 12-31(B_2); 4-3(A_1); 2-54(B_1); 16-13(A_1); 14-34(B_2); 8-29(B_2); 46-49(A_1); 39-36(A_1); 29-59(B_1); 6-48(B_2); 40-37(A_1); 17-15(A_1); 12-8(A_1).
	122 wm	55(B_1) fundamental.
	110 wsh	libration(?); 36-12(B_2); 34-8(B_2); 12-9(A_1); 7-29(B_2); 45-41(A_1); 37-35(A_1); 33-7(B_2); 59-27(B_1); 35-33(A_1); 17-38(B_2); 9-30(B_2); 62-25(B_1); 18-16(A_1); 39-15(B_2); 8-6(A_1); 48-50(B_2); 46-5(B_1); 5-51(B_1).
	93 wsh	libration/translation.
	73 vwsh	libration.
	57 vwsh	libration.

s = strong

m = medium

w = weak

v = very

sh = shoulder

br = broad

Table 3.36 Infrared spectrum of phenanthroline-d_8 monohydrate

Infrared	Assignment
3490 sh 3392 sbr 3265 sh	$\nu O\text{-}H_{(H_2O)}$.
2955 vw	$66+45(B_1)$; $40+14(B_2)$; $39+15(B_2)$; $49+23(B_1)$; $21+4(A_1)$.
2877 vw	$50+20(B_1)$; $39+37(A_1)$; $16+15(A_1)$; $50+21(B_1)$.
2757 w	$52+23(B_1)$; $16+13(A_1)$; $25+21(B_2)$; $38+37(A_1)$.
2594 vw	$33+18(B_2)$; $37+35(A_1)$; $13^2(A_1)$.
2547 vw	$39+33(A_1)$; $35+13(B_2)$; $65+45(B_1)$; $40+10(B_2)$; $23+1(A_1)$.
2500 w	$43+1(B_2)$; $20+1(A_1)$; $21+1(A_1)$; $65+42(B_1)$; $34+16(B_2)$; $54+22(B_1)$; $37+12(B_2)$.
2413 vw	$35+12(B_2)$; $40+7(B_2)$; $34+14(B_2)$; $33+15(B_2)$; $55+22(B_1)$.
2371 w	$17+6(A_1)$; $55+19(B_1)$; $39+7(B_2)$; $37+34(A_1)$.
2364 w	$40+5(B_2)$; $37+34(A_1)$; $55+19(B_1)$; $17+6(A_1)$; $29+17(B_2)$.
2347 w	$16+9(A_1)$; $39+29(A_1)$; $36+34(A_1)$; $14+10(A_1)$.
2339 w	$37+33(A_1)$; $17+5(A_1)$; $57+39(B_1)$; $36+34(A_1)$.
2312 w	$23(A_1)$ fundamental.
2291 wm	$22(A_1)$ fundamental; $45(B_2)$ fundamental.
2274 m	$21(A_1)$ fundamental.
2269 msh	$20(A_1)$ fundamental; $43(B_2)$ fundamental.
2251 wm	$19(A_1)$ fundamental; $42(B_2)$ fundamental.
2240 wsh	$41(B_2)$ fundamental.
2230 w	$14+8(A_1)$; $35+10(B_2)$; $46+16(B_1)$; $31+14(B_2)$; $17+4(A_1)$; $15+6(A_1)$; $38+29(A_1)$; $49+18(B_1)$; $39+27(A_1)$.
2198 w	$49+17(B_1)$; $48+16(B_1)$; $28+16(B_2)$; $23-55(B_1)$; $50+18(B_1)$; $15+5(A_1)$; $36+9(B_2)$; $14+6(A_1)$.
2110 vw	$49+16(B_1)$; $35+31(A_1)$; $57+36(B_1)$; $43-66(B_1)$; $23-54(B_1)$; $48+14(B_1)$; $28+14(B_2)$; $40+26(A_1)$; $35+8(B_2)$; $27+15(B_2)$.
2055 wbr	$57+35(B_1)$; $14+4(A_1)$; $49+15(B_1)$; $46+13(B_1)$; $40+25(A_1)$.
1863 vwbr	$45-63(B_1)$; $24+16(B_2)$; $34+7(B_2)$; $33+31(A_1)$; $42-2(B_2)$; $19-2(A_1)$; $25+14(B_2)$; $33+8(B_2)$; $10+9(A_1)$.
1806 vw	$49+12(B_1)$; $40+1(B_2)$; $57+33(B_1)$; $24+15(B_2)$; $19-52(B_1)$; $10+7(A_1)$; $45-25(A_1)$; $22-25(B_2)$; $38+2(B_2)$.
1796 vw	$65+39(B_2)$; $15+2(A_1)$; $21-25(B_2)$; $33+5(B_2)$; $54+18(B_1)$; $36+25(A_1)$; $35+26(A_1)$.
1735 vw	$66+40(B_1)$; $35+25(A_1)$; $9+8(A_1)$; $43-26(A_1)$; $37+24(A_1)$; $20-26(B_2)$; $52+13(B_1)$: $31+9(B_2)$; $21-26(B_2)$; $46+10(B_2)$; $33+28(A_1)$.
1696 w	$26+12(B_2)$; $60+34(B_1)$; $36+2(B_2)$; $31+30(A_1)$; $22-51(B_1)$; $30+8(B_2)$; $24+13(B_2)$; $16+1(A_1)$; $33+27(A_1)$.
1683 w	$63+35(B_1)$; $30^2(A_1)$; $22-50(B_1)$; $33+4(B_2)$; $21-51(B_1)$; $8+7(A_1)$; $65+38(B_2)$; $13+2(A_1)$; $31+7(B_2)$.
1647 s	$\delta O\text{-}H_{(H_2O)}$
1607 w	$57+29(B_1)$; $14+1(A_1)$; $58+31(B_1)$; $43-60(B_1)$; $19-49(B_1)$; $52+12(B_1)$.
1590 m	$18(A_1)$ fundamental.
1577 mw	$40(B_1)$ fundamental.
1552 vs	$17(A_1)$ fundamental.

Table 3.36 (continued)

Infrared	Assignment
1542 vs	$39(B_2)$ fundamental.
1520 msh	$60+31(B_1)$; $43-58(B_1)$; $48+5(B_1)$; $28+5(B_2)$; $41-28(A_1)$; $30+4(B_2)$; $13+1(A_1)$.
1478 m	$49+7(B_1)$; $51+9(B_1)$; $45-6(B_2)$; $23-48(B_1)$; $23-28(B_2)$; $22-6(A_1)$; $43-5(B_2)$; $20-5(A_1)$; $29+4(B_2)$; $18-55(B_1)$; $35+1(B_2)$.
1464 vs	$16(A_1)$ fundamental.
1443 w	$42-29(A_1)$; $14-29(B_2)$; $57+41(B_1)$; $51+8(B_1)$; $21-7(A_1)$; $46+4(B_1)$; $45-30(A_1)$; $22-30(B_2)$.
1427 s	$38(B_2)$ fundamental.
1412 w	$15(A_1)$ fundamental.
1384 w	$39-66(B_1)$; $41-31(A_1)$; $43-9(B_2)$; $20-9(A_1)$; $51+5(B_1)$; $18-54(B_1)$; $49+48(A_1)$; $41-8(B_2)$; $27^2(A_1)$; $26+8(B_2)$; $12+1(A_1)$.
1378 w	$14(A_1)$ fundamental.
1360 w	$18-1(A_1)$; $10+2(A_1)$; $60+27(B_1)$; $54+12(B_1)$; $51+46(A_1)$; $41-9(B_2)$; $25+9(B_2)$.
1355 w	$51+46(A_1)$; $41-9(B_2)$; $26+6(B_2)$; $10+2(A_1)$; $4^2(A_1)$; $18-1(A_1)$; $17-54(B_1)$.
1334 vs	$37(B_2)$ fundamental.
1312 w	$36(B_2)$ fundamental.
1294 ms	$13(A_1)$ fundamental.
1276 w	$55+12(B_1)$; $52+7(B_1)$; $42-10(B_2)$; $14-10(A_1)$; $39-1(B_2)$; $50+4(B_1)$; $28+26(A_1)$; $24+9(B_2)$.
1270 w	$63+30(B_1)$; $28+26(A_1)$; $51+4(B_1)$; $25+5(B_2)$; $21-33(B_2)$; $9+2(A_1)$; $41-10(B_2)$; $55+12(B_1)$.
1255 s	$35(B_2)$ fundamental.
1236 wm	$63+29(B_1)$; $33+1(B_2)$; $16-1(A_1)$; $8+2(A_1)$; $43-34(A_1)$; $41-33(A_1)$; $20-34(B_2)$; $51+49(A_1)$; $52+5(B_1)$; $31+2(B_2)$; $24+7(B_2)$; $30+24(A_1)$; $27+26(A_1)$.
1206 vvw	$29+24(A_1)$; $18-2(A_1)$; $52+46(A_1)$; $41-34(B_1)$; $15-54(B_1)$; $10+1(A_1)$; $26+4(B_2)$; $51+50(A_1)$; $6+2(A_1)$.
1160 w	$12(A_1)$ fundamental.
1117 w	$52+4(B_1)$; $48+2(B_1)$; $28+2(B_2)$; $21-12(A_1)$; $9+1(A_1)$;
1097 vvw	$40-25(A_1)$; $35-66(B_1)$; $30-65(B_1)$; $16-35(B_1)$; $27+24(A_1)$; $53+48(A_1)$; $42-12(B_2)$; $19-12(A_1)$.
1084 vvw	$31+1(B_2)$; $36-1(B_2)$; $54+9(B_1)$; $37-65(B_2)$; $41-12(B_2)$; $27+2(B_2)$; $16-2(A_1)$; $55+10(B_1)$; $52+49(A_1)$.
1075 vw	$24+4(B_2)$; $26^2(A_1)$; $17-25(B_2)$; $30+1(B_2)$; $27+2(B_2)$; $16-2(A_1)$; $41-12(B_2)$; $8+1(A_1)$.
1034 m	$34(B_2)$ fundamental.
1006 mw	$33(B_2)$ fundamental.
994 vw	$46+1(B_1)$; $14-2(A_1)$; $50+2(B_1)$; $42-35(A_1)$; $14-35(B_2)$; $54+5(B_1)$; $45-13(B_2)$; $22-13(A_1)$; $18-51(B_1)$; $55+9(B_1)$.
974 ms	$10(A_1)$ fundamental.
955 vw	$58+54(B_2)$; $45-37(A_1)$; $43-36(A_1)$; $42-13(B_2)$; $22-37(B_2)$; $20-36(B_2)$; $14-13(A_1)$; $12-54(B_1)$; $17-51(B_1)$; $25^2(A_1)$; $37-2(B_2)$.
939 w	$42-36(A_1)$; $14-36(B_2)$; $21-37(B_2)$; $48+54(A_1)$; $23-14(A_1)$; $43-37(A_1)$; $37-24(A_1)$; $20-37(B_2)$; $26+24(A_1)$; $14-25(B_1)$; $17-50(B_1)$.

Table 3.36 (continued)

Infrared	Assignment
929 w	16-26(B_2); 55+6(B_1); 41-36(A_1); 36-2(B_2); 15-25(B_2); 12-1(A_1); 13-35(B_1); 37-24(A_1); 14-25(B_1); 43-37(A_1); 20-37(B_2).
923 w	27+1(B_2); 66+46(B_2); 26+2(B_2); 13-53(B_1); 41-36(A_1); 36-2(B_2); 35-1(B_2); 16-26(B_2); 42-37(A_1); 19-37(B_2).
908 vvw	63+25(B_1); 13-2(A_1); 41-37(A_1); 55+5(B_1); 4+1(A_1); 36-24(A_1); 17-49(B_1); 40-4(B_2); 23-15(A_1).
883 s	9(A_1) fundamental.
855 ms	31(B_2) fundamental.
852 ms	8(A_1) fundamental.
842 m	30(B_2) fundamental.
833 m	7(A_1) fundamental.
815 wmsh	6(A_1) fundamental.
808 s	29(B_2) fundamental.
788 s	5(A_1) fundamental.
764 m	46(B_1) fundamental.
734 s	28(B_2) fundamental; 48(B_1) fundamental.
702 sbr	$\phi N\cdots H_2O$.
694 vs	27(B_2) fundamental.
675 vs	4(A_1) fundamental.
646 vs	49(B_1) fundamental.
607 vs	50(B_1) fundamental.
593 s	51(B_1) fundamental.
536 mw	26(B_2) fundamental.
480 mw	25(B_2) fundamental.
444 w	52(B_1) fundamental.
428 vw	63(A_2) fundamental(?); 36-9(B_2); 18-12(A_1); 12-28(B_2); 6-2(A_1); 54+1(B_1); 29-2(B_2); 16-34(B_2); 35-7(B_2); 7-24(B_2).
399 ms	24(B_2) fundamental.
385 wsh	2(A_1) fundamental.
369 w	53(B_1) fundamental.
254 vw	64(A_2) fundamental(?); 28-25(A_1); 53-55(A_1); 33-58(B_1); 18-37(B_2); 15-12(A_1); 5-26(B_2); 25-1(B_2); 17-13(A_1); 35-33(A_1); 8-51(B_1).
229 m	1(A_1) fundamental.
203 vw	54(B_1) fundamental.
171 w	46-51(A_1); 38-35(A_1); 16-13(A_1); 6-49(B_1); 37-12(B_2); 17-14(A_1); 30-4(B_2); 53-54(A_1); 34-31(A_1); 33-30(A_1); 10-29(B_2); 40-15(B_2); 8-4(A_1).

Table 3.36 (continued)

Infrared	Assignment
150 w	66(A_2) fundamental(?); 40-38(A_1); 51-52(A_1); 33-31(A_1); 26-2(B_2); 9-28(B_2); 9-48(B_1); 36-12(B_2); 34-9(B_2); 30-27(A_1); 16-36(B_2); 33-8(B_2); 24-65(B_1); 12-33(B_2); 2-1(A_1).
116 m	55(B_1) fundamental.
107 msh	libration(?); 30-28(A_1); 26-63(B_1); 49-52(A_1); 29-27(A_1); 40-16(B_1); 5-4(A_1); 1-55(B_1).
91 wsh	libration/translation.
75 wsh	libration.
56 w	libration.

s = strong

m = medium

w = weak

v = very

sh = shoulder

br = broad

ALTMANN and PERKAMPUS [166,167] (Table 3.37) with the following exceptions.

The C-H stretch mode 45(B_2) has been tentatively assigned to the weak shoulder at 3115cm^{-1} (infrared spectrum), some 10cm^{-1} higher than that of ALTMANN and PERKAMPUS [166]. As no band is observed at 3092cm^{-1}, mode 43(B_2) has now been assigned at 3095cm^{-1} based upon the normal coordinate analysis, and thereby showing degeneracy with mode 21(A_1).

PERKAMPUS and his co-workers [165-167] found that the degree of polarisation and band dichroism for phenanthroline between 900 and 1350cm^{-1} does not allow for a proper determination of the symmetry species and that the normal coordinate analysis is more useful in determining the assignment.

On this basis, mode 29(B_2) is now assigned to the very weak Raman band at 892cm^{-1} and the medium intensity infrared band at 988cm^{-1} in preference to the tentative assignment of 1026cm^{-1} made by ALTMANN and PERKAMPUS [166]. This new assignment is in better agreement with the normal coordinate value of 997cm^{-1}. The band at 988cm^{-1} was considered by ALTMANN and PERKAMPUS as a possible alternative assignment of the infrared forbidden αC-H mode 57(A_2). The infrared intensity of this band makes such an assignment unlikely, while the weak infrared band at 1026cm^{-1} is now considered to be a combination band (Table 3.35).

Similarly, modes 10(A_1) and 33(B_2) are reversed in accordance with the normal coordinate analysis (Table 3.37). Mode 14(A_1) is assigned to the medium shoulder in the Raman spectrum at 1414cm^{-1} in preference to that of 1404cm^{-1} by ALTMANN and PERKAMPUS [166] (normal coordinate figure of 1420cm^{-1}), with mode 36(B_2) being assigned here to the very strong Raman and medium intensity infrared bands at 1405cm^{-1} (normal coordinate figure of 1411cm^{-1}) rather

Table 3.37 The fundamentals of 1,10-phenanthroline (phen) compared with that found in the literature

Mode		In-phase[a] 4,5-phenanthrene [160,162,163]	In-phase[a] 1,10-phenanthroline PERKAMPUS & ROTHER (1974) [165]	In-phase[a] 1,10-phenanthroline ALTMANN & PERKAMPUS (1979) [166,167]		Present work
1	A_1	247	408	249	(212)	203
2		408	550	408	(399)	403
3		548	618	550	(553)	552
4		710	708/743	704	(712)	710
5		831	856	852	(839)	854
6		1036	878/885	1033	(1042)	1037
7		1094	1033	1092	(1099)	1094
8		1144	1092	1140	(1142)	1142
9		1163	-	1180	(1172)	1186
10		1204	1140	1205	(1212)	1217
11		1247	1180	-	(-)	-
12		1304	1205	1292	(1282)	1295
13		1352	1292	1343	(1355)	1345
14		1431	1343	1404	(1420)	1414
15		1444	1404	1444	(1448)	1446
16		1526	1444	1505	(1524)	1502
17		1606	1505	1599	(1566)	1599
18		1626	1616	1616	(1595)	1616
19		3015	3026	3026	(3027)	3032
20		3037	3053	-	(-)	-
21		3057	3065	3053	(3054)	3058
22		3081	3076	3065	(3076)	3066
23		3088	-	3076	(3084)	3082
46	B_1	(980)	974	975	(964)	970
47		950	-	-	(-)	-
48		871	881	881	(892)	883
49		817	840	840	(813)	840
50		732	764	764	(773)	779
51		715	732	732	(743)	738
52		495	722	505	(510)	509
53		426	626	466	(432)	457
54		234	505	?	(234)	245
55		124	466	122	(106)	122

Table 3.37 (continued)

Mode		Out-of-phase[a] 4,5-phenanthrene [160,162,163]	PERKAMPUS & ROTHER (1974) [165]	1,10-phenanthroline ALTMANN & PERKAMPUS (1979) [166,167]	Present work
24	B_2	441	249	395 (435)	427
25		536	395	490 (496)	499
26		619	?	618/626 (606)	623
27		712	665	722 (734)	724
28		876	942	878 (890)	896
29		1001	-	1026? (997)	985
30		1040	1026?	1075 (1053)	1079
31		1144	1075	? (1136)	1137
32		1173	-	- (-)	-
33		1227	1214	1214 (1201)	1206
34		1283	1254	1254 (1222)	1253
35		1340	1262	1308? (1354)	1313
36		1425	1308	1382 (1411)	1405
37		1458	1417	1417 (1432)	1421
38		1502	1493	1493 (1499)	1492
39		1572	1558	1558 (1582)	1561
40		1616	1586	1586 (1615)	1586
41		3005	3000?	3000? (3027)	3008
42		3024	-	3038 (3035)	3032
43		3047	3038	3092? (3054)	3059
44		3064	3092	- (-)	-
45		3094	3105?	3105 (3084)	3115
56	A_2[b]	(981)	996	- (-)	-
57		966	985	996/985 (968)	957
58		946	964	964 (942)	(940)
59		880	925	925 (890)	831?
60		791	814	815 (800)	809
61		763	786	786 (751)	(752)
62		594	600	665? (627)	605
63		513	-	490 (504)	499
64		395	?	416 (402)	411
65		(266)	?	? (258)	253
66		(151)	122	? (142)	(144)

(a) refers to the rings

(b) infrared forbidden

calculated frequencies in parentheses

than at 1382cm^{-1} [166]. The band at 1382cm^{-1} recorded by ALTMANN and PERKAMPUS was not observed in this work.

On the basis that the B_1 fundamentals are expected to yield infrared bands of moderate to strong intensities, mode 50(B_1) is assigned to the infrared band of medium intensity at 779cm^{-1} rather than that of 764cm^{-1} made by ALTMANN and PERKAMPUS [167], a band which was not observed in this work. The new assignment is in good agreement with the figure calculated by normal coordinate analysis (Table 3.37). Similarly mode 54(B_1), which was not assigned by ALTMANN and PERKAMPUS [167], is here assigned to the Raman band of medium to strong intensity at 246cm^{-1} (medium to weak infrared band at 244cm^{-1}). This band was assigned to mode 1(A_1) by ALTMANN and PERKAMPUS, who did not observe the very weak band at 203cm^{-1} which is now assigned to the A_1 mode. This revised assignment is supported by the figures from the normal coordinate analysis (234cm^{-1} for mode 54; 212cm^{-1} for mode 1).

The B_2 vibration mode 24 is assigned to the broad weak Raman band at 426cm^{-1} (weak infrared band at 429cm^{-1}) in comparison with that of 395cm^{-1} by ALTMANN and PERKAMPUS [166], which was not observed in the present work.

The greatest difference between the present work and that of ALTMANN and PERKAMPUS lies in the assignment of the A_2 fundamentals. Two alternatives were given by the previous authors for assigning the highest αC-H vibration, mode 57 (Table 3.37). The assignment of the band at 985cm^{-1} has already been discussed. The second alternative, that of 996cm^{-1}, while being infrared active was not observed in the Raman spectrum, and is therefore considered to be a combination band in the present work (Table 3.35). In the present work this fundamental was assigned to the weak broad Raman band at 958cm^{-1} (weak infrared band at 956cm^{-1}) which possibly corresponds to the band as-

signed by ALTMANN and PERKAMPUS to mode 58(A_2), namely 964cm^{-1} [167]. This latter fundamental vibration was not observed in the present work and the calculated assignment of 940 ± 3cm^{-1} for mode 58 is based upon six combination bands: 58+36(2346cm^{-1}), 4+58(3069cm^{-1}), 58+30(2023cm^{-1}), 58+29 (1937cm^{-1}), 58+57(1908cm^{-1}) and 58+28(1831cm^{-1}).

The bands assigned by ALTMANN and PERKAMPUS to the A_2 modes 59, 61 and 62 were not observed in this work in either the Raman or the infrared spectra. Mode 59 is *very* tentatively assigned to the very weak Raman band at 831cm^{-1} in agreement with the assymetric phenanthrolines [167], but this assignment is discussed more fully below. In the absence of suitable bands in the Raman spectrum, mode 61 is calculated to be at 752 ± 1cm^{-1} on the basis of four combination and difference bands: 61+30(1831cm^{-1}), 61+57(1708cm^{-1}), 12-61(544cm^{-1}) and 10-61(465cm^{-1}). This fundamental is observed as a very weak band at about 765cm^{-1} in the infrared spectra of the M(II)$(ClO_4)_2$ complexes. Mode 62 is assigned to the weak Raman band at 605cm^{-1} in this work.

These new assignments of the A_2 fundamentals are, with the exception of mode 59, in better agreement with those values determined by the normal coordinate analysis than assignments given by ALTMANN and PERKAMPUS.

Several other assignments which do not show any major disagreement with ALTMANN and PERKAMPUS need to be considered more fully.

Mode 31(B_2) which was not observed by ALTMANN and PERKAMPUS, is seen in the Raman spectrum as a weak band at 1136cm^{-1} and in the infrared spectrum as a band of medium intensity at 1137cm^{-1}, and is therefore in excellent agreement with the normal coordinate analysis. Similarly, mode 65 (not observed by ALTMANN and PERKAMPUS) which is observed as a shoulder of medium intensity

at 253cm^{-1} in the Raman spectrum and as a very weak infrared band at 254cm^{-1} is also in good agreement with the normal coordinate analysis.

Mode 66(A_2) is unobserved by both ALTMANN and PERKAMPUS and in the present work. Its assignment here at 144 ± 2cm^{-1} is calculated from eight possible combinations: 41-66(2862cm^{-1}), 66+39(1708cm^{-1}), 14-66(1270cm^{-1}), 36-66 (1263cm^{-1}), 35-66(1170cm^{-1}), 66+44(1025cm^{-1}), 24-66(281cm^{-1}) and 65-66 (110cm^{-1}).

The accidental degeneracy of modes 25(A_1) and 63(A_2) observed by ALTMANN and PERKAMPUS [166,167] is supported by the lifting of this degeneracy in the M(II)$(ClO_4)_2$ complexes. The assignment in this work of the three fundamentals, modes 35(B_2), 41(B_2) and 49(B_1), are in agreement with those made by ALTMANN and PERKAMPUS although they differ with the calculated frequencies (Table 3.37).

Two medium intensity bands at 695cm^{-1} and 596cm^{-1} in the infrared spectrum show intensity sensitivity to dehydration of phen H_2O and are assigned to the rocking and wagging modes (respectively) of the hydrogen bonded water (bonded via the nitrogens of phen).

Finally, the three lowest bands observed in the infrared spectrum are assigned to lattice vibrations, their origin being tentatively based upon that of phenanthrene. The band at 110cm^{-1} may either be a lattice mode or a difference band. The complete identification of these bands by normal coordinate analysis may be difficult because of the likelihood of strong coupling between the lowest lying fundamentals and the lattice vibrations, as is observed for phenanthrene [161].

Two regions in the spectra of phenanthroline are of special interest. The first is that of the in-plane C-H bends. The use of a comparison of the PED of phenanthrene and phenanthroline must be tentative, firstly since the normal coordinate analysis of phenanth by SCHETTINO *et al.* [158] has been questioned by ALTMANN and PERKAMPUS [162], and secondly, in view of the absence of published PED by later workers. Nonetheless, several trends are noticeable. In phen all the B_2 vibrations between 1500 and 1000cm^{-1}, with the single exception of the ring mode 30, are lower in frequency than their phenanth analogues (Table 3.38). A comparison of the PED of the two molecules

B_2 Fundamentals			A_1 Fundamentals		
mode	phenanth	phen	mode	phenanth	phen
29	1001	985	6	1036	1037
30	1040	1079	7	1094	1094
31	1144	1137	8	1144	1142
32	1173	-	9	1163	1186
33	1227	1206	10	1204	1217
34	1283	1253	11	1247	-
35	1340	1313	12	1304	1295
36	1425	1405	13	1352	1345
37	1458	1421	14	1431	1414
38	1502	1493	15	1444	1446

Table 3.38 The influence of the aza-group on the planar C-H bends in phenanthroline

[158,162] shows that with the exception of mode 30 all the vibrations in phen show a slight contribution of the Kekulé vibration, thereby differing from phenanth. Indeed, the PED mode 31 (the Kekulé mode in phenanth) and mode 35 (αC-H in phenanth) shows such a degree of coupling that their description is reversed in phen. In contrast to the general increase of the

coupling experienced by phen, mode 30 (which showed an increase in frequency) reveals a loss of Kekulé contribution to this ring mode compared with its phenanth counterpart.

The A_1 fundamentals over this range differ from the B_2 modes in that they do not show such an extensive coupling. Three of the αC-H fundamentals of phen (modes 8,9 and 15) show either an increase in frequency or no change in frequency compared with the hydrocarbon parent. The fourth αC-H, mode 12 (in phenanth) shows a much stronger coupling with the Kekulé mode 7 (in phenanth) such that in the diimine a clear designation of either vibration to the ring mode is impractical.

The difference in coupling between phen and its hydrocarbon parent involving the Kekulé vibrations is not surprising in light of the behaviour observed for the azines as discussed above.

The second region of interest is that of the out-of-plane C-H bends. In discussing naphthalene and quinoline above, the αC-H were observed to fall into two frequency ranges. It was noted that these depended on whether the hydrogens in the alpha and beta positions (with respect to the fused C-C bond) were vibrating in-phase (β-H hydrogens) or out-of-phase (α-H hydrogens). Furthermore, the introduction of a nitrogen resulted in the general trend that the α-H hydrogens were lowered in frequency while the β-H hydrogens were increased in frequency.

Extending this to phenanthrene and phenanthroline, 5 α-H hydrogens are to be expected and also 5 β-H hydrogens. Following the assignment of ALTMANN and PERKAMPUS [167] the two lost αC-H modes in phen are $47(B_1)$ and $56(A_2)$, both α-H type vibrations. Based upon its frequency of $880cm^{-1}$ (phenanthrene) and

upon the number of β-H vibrations expected, mode 59(A_2) is expected to be a β-H type vibration. From Table 3.39 it is apparent that the present tenta-

B_1 Fundamentals				A_2 Fundamentals			
mode	phenanth	phen	Type[a]	mode	phenanth	phen	Type[a]
46	(980)	970	α-H	56	(981)	-	α-H
47	950	-	α-H	57	966	957	α-H
48	871	881	β-H	58	946	(940)	α-H
49	817	840	β-H	59	880	831(?)	β-H(?)
50	732	779	γ ring	60	791	809	β-H
51	715	738	β-H	61	763	(752)	γ ring

Calculated frequencies in parenthesis

(a) See text

Table 3.39 The influence of the aza-group on the out-of-plane C-H bends in phenanthroline

tive assignment of this fundamental to the very weak Raman band at 831cm^{-1} is most likely incorrect, since its behaviour on introducing the nitrogen into the ring is inconsistent with that expected for a β-H hydrogen. From the normal coordinate analysis [167] this mode is expected to be found at 890cm^{-1}. ALTMANN and PERKAMPUS [167] assigned this fundamental somewhat higher, at 925cm^{-1}. In the present work the Raman spectrum over this particular range (850 to 940cm^{-1}) was spectroscopically silent, so the present assignment has been suggested. Future single crystal polarisation studies will most likely clarify the true assignment of mode 59(A_2).

The assignment of the infrared spectrum of phenanthroline-d_8 hydrate is presented in Table 3.36. This assignment is strongly based upon that of phenanthrene-d_{10} (Table 3.40). The vibrational assignments of deuterated ligands are usually less certain than their hydrocarbon analogues. It is not sur-

Table 3.40 Assignment of 1,10-phenanthroline-d_8 compared with its hydrocarbon parent

Mode[a]		4,5-phenanthrene-d_{10} Calculated [160,164]	4,5-phenanthrene-d_{10} Experimental SCHETTINO [164]	4,5-phenanthrene-d_{10} Experimental BREE *et al.* [160]	1,10-phen-d_8 (This work)
1	A_1	(194)	226	231	229
2		(380)	392	392	385
3		(536)	529	532	?
4		(668)	669	667	675
5		(791)	784	772	788
6		(825)	-	813?	815
7		(833)	843	-	833
8		(842)	864	860	852
9		(845)	896	897	883
10		(980)	-	945	974
11		(1140)	1122	1118	-
12		(1178)	1203	1205	1160
13		(1294)	1304	1304	1294
14		(1354)	1326	1372	1378
15		(1398)	1396	1392	1412
16		(1470)	1475	1475	1464
17		(1525)	-	1563	1552
18		(1557)	1565	1597	1590
19		(2250)	2251	2252	2251
20		(2260)	2261	2263	-
21		(2280)	2275	2277	2274
22		(2288)	2291	2290	2291
23		(2296)	2310	2312?	2312
46	B_1	(809)	741	910	764
47		(760)	690	777	-
48		(706)	649	691 or 746	734
49		(646)	609	651	646
50		(621)	559	611	607
51		(542)	435	560	593
52		(442)	384	438	444
53		(352)	374	374	369
54		(203)	214	213	203
55		(96)	-	117	116

Mode[a]		4,5-phenanthrene-d_{10} Calculated [160,164]	4,5-phenanthrene-d_{10} Experimental SCHETTINO [164]	4,5-phenanthrene-d_{10} Experimental BREE *et al.* [160]	1,10-phen-d_8 (This work)
24	B_2	(411)	415	414	399
25		(430)	-	473?	480
26		(549)	594	597	536?
27		(686)	676	677	694
28		(737)	-	-	734
29		(809)	-	830	808
30		(833)	832	849	842
31		(858)	845	863	855
32		(958)	-	948?	-
33		(989)	975	971	1006
34		(1082)	1044	1022?	1034
35		(1246)	1270	1270	1255
36		(1331)	1352	1326	1312
37		(1382)	1382	1352	1334
38		(1444)	1431	1432	1427
39		(1515)	1525	1528	1542
40		(1610)	1597	1589	1577
41		(2250)	-	2230?	2240
42		(2255)	-	-	2251
43		(2264)	2268	2265	2269
44		(2282)	2285	2273	-
45		(2296)	2300	2286	2291
56	A_2[b]	(813)	-	-	-
57		(783)	-	831?	(799)
58		(757)	-	-	(752)
59		(732)	-	-	?
60		(654)	-	621	(664)
61		(572)	-	-	(568 or 554)
62		(507)	-	-	?
63		(438)	-	-	428
64		(335)	-	351	(331 or 350)
65		(239)	-	-	254
66		(126)	-	165?	150?

(a) after SCHETTINO *et al.* [158]

(b) infrared forbidden

calculated values in parentheses

prising, then, that there is a large disagreement between BREE *et al.* [160] and SCHETTINO [164] over the assignment of phenanth-d_{10}, the situation for the A_2 fundamentals being particularly poor, with little spectroscopic data available.

Generally the assignment by BREE *et al.* is the better of the two. This is evident in that the assignment of modes 14(A_1), 48(B_1), 49(B_1) and 52(B_1) made by BREE *et al.* are in better agreement with the normal coordinate analysis than those of SCHETTINO. The present assignment of phen-d_8 also supports the general assignment of BREE *et al.* over that of SCHETTINO, as well as suggesting that the second alternate assignment suggested by BREE *et al.* for mode 48(B_1) is the correct one (Table 3.40). Three assignments for phenanth-d_{10} made by BREE *et al.* which differ largely with the normal coordinate analysis, namely modes 18(A_1), 30(B_2) and 50(B_1), are nonetheless supported here by the assignments of their diimine analogues. So too are their suggested assignments of modes 25(B_2) and 55(B_1), which were not observed by SCHETTINO.

On the basis of their diimine analogues, the only assignments made by SCHETTINO for phenanth-d_{10} which are preferred to those of BREE *et al.* are of modes 5(A_1) and 46(B_1). The latter is complicated in that it is in a better agreement with the out-of-plane normal coordinate calculation of mode 47, the missing γC-D mode, rather than that calculated for mode 46 [160] (Table 3.40).

Since the infrared spectrum of phenanth-d_{10} is extremely rich in bands, several vibrations show possible degeneracy or are very close together and these merit further discussion.

The individual C-D stretches are not fully resolved and the following degen-

eracies have been suggested: modes 22(A_1) and 45(B_2), modes 20(A_1) and 43(B_2) and modes 19(A_1) and 42(B_2). Raman and polarisation studies would be necessary to validate these assignments. The accidental degeneracy of the planar ring, mode 28(B_2) and the γC-D, mode 48(B_1) is demonstrated by its being lifted in the M(II)$(ClO_4)_2$ complexes.

Based upon phenanth-d_{10} the three vibrations, the planar ring modes 3(A_1) and 26(B_2) and the γC-D mode 51(B_1), are expected to have frequencies close together and their identification is difficult. The assignment of the strong infrared band at 593cm^{-1} to mode 51 is based upon the expected intensity of a B_1 vibration. The band of moderate intensity at 536cm^{-1} is then tentatively identified as the B_2 vibration, mode 26 in preference to the A_1 vibration (although much lower in frequency than its phenanth-d_{10} analogue) since the A_1 ring vibration is much weaker in the infrared spectrum of phenanth-d_{10} than is that of the B_2 ring vibration [160]. The fundamental mode 3(A_1) has not been identified in the present work. As this region is too rich spectroscopically, an approximate assignment may not be established from possible combination and difference bands.

The assignment of the strong band at 808cm^{-1} to the ring mode 29(B_2) and that of the medium to weak shoulder at 815cm^{-1} to the ring mode 6(A_1), which is similarly based upon the expected intensities of the infrared bands, will require polarisation studies for confirmation. So too is the clear identification of the almost degenerate two medium to strong bands at 852cm and 855cm^{-1} - which are modes 8(A_1) and 31(B_2) - dependant on future polarisation studies.

A second difficulty resulting from a rich spectrum is the assignment of those A_1 modes which might yield bands of weak intensity and which are found

in regions of many combinations and difference bands. This is demonstrated by three modes in the present work.

Mode 12(A_1) may either be assigned to the medium weak band at 1236cm^{-1}, the very weak band at 1206cm^{-1} or the weak band at 1160cm^{-1}. The present assignment, that of 1160cm^{-1}, is made on the basis that the first two may be described by twelve and eight possible combinations respectively (Table 3.36), while the latter may be described by only three: 39-2(B_2), 53+5(B_1) and 25+4 (B_2). The latter is therefore more likely to be fundamental.

The assignment of mode 14(A_1) to the weak band at 1378cm^{-1} (alternatively poorly described by four possible combinations) is similarly made in preference to those of 1355cm^{-1} (well described by seven possible combinations) and 1360cm^{-1} (well described by six possible combinations). The assignment of mode 15(A_1) is even less certain with the weak band at 1412cm^{-1} yielding seventeen possible combinations - some of which are poor - while that at 1384cm^{-1} yields nine good possible combinations. The former is tentatively suggested here.

Clearly these A_1 assignments will need clarification through either Raman or polarisation studies.

The assignment of the infrared forbidden A_2 modes is more difficult. The very weak band at 428cm^{-1} may possible be explained as mode 63(A_2), an assignment which is supported by seven possible combinations and difference bands: 45-63(1863cm^{-1}), 63+35(1683cm^{-1}), 63+30(1270cm^{-1}), 63+29(1236cm^{-1}), 63+25(908cm^{-1}), 31-63(429cm^{-1}) and 26-63(107cm^{-1}). These yield a calculated frequency of 428 ± 1cm^{-1}.

The very weak band at 254cm^{-1} may possibly be assigned to mode 65(A_2). This is in agreement with that of 254 ± 3cm^{-1} from seven possible combinations: 65+45(2547cm^{-1}), 63+42(2500cm^{-1}), 65+39(1796cm^{-1}), 65+38(1683cm^{-1}), 30-65 (1097cm^{-1}), 37-65(1084cm^{-1}) and 24-65(150cm^{-1}). The last A_2 fundamental that might be observed in the infrared spectrum is that of mode 66 as the weak band at 150cm^{-1}. This assignment is less certain than the previous two assignments since the six combinations, namely 43-66(2110cm^{-1}), 66+40 (1735cm^{-1}), 39-66(1384cm^{-1}), 38-66(1270cm^{-1}), 35-66(1097cm^{-1}) and 66+46 (923cm^{-1}) suggest the assignment of 158 ± 1cm^{-1}.

The assignment of the other A_2 fundamentals which are not observed in the infrared spectrum may be estimated from possible combinations and difference bands. Mode 58 is calculated to be at 751 ± 2cm^{-1} on the basis of four combinations: 58+31(1607cm^{-1}), 43-58(1520cm^{-1}), 58+54(955cm^{-1}) and 33-58 (254cm^{-1}). This assignment is supported by the appearance of a weak infrared band at this frequency in the infrared spectra of some of the M(II)$(ClO_4)_2$ complexes (Chapter 4). Similarly the appearance of a weak band in the region of 670cm^{-1} in the M(II)$(ClO_4)_2$ complexes supports the calculated frequency for mode 60 as 664 ± 2cm^{-1} on the basis of five combinations: 60+45(2955cm^{-1}), 60+34(1697cm^{-1}), 43-60(1607cm^{-1}), 60+31(1520cm^{-1}) and 60+27 (1360cm^{-1}). Mode 57 is estimated to be at 799 ± 1cm^{-1} on the basis of six possible combinations: 57+39(2339cm^{-1}), 57+36(2110cm^{-1}), 57+35(2055cm^{-1}), 57+33(1806cm^{-1}), 57+29(1607cm^{-1}) and 57+41(1443cm^{-1}).

The assignment of modes 61 and 64 are more difficult since the possible combinations yield two alternate assignments for both modes (Table 3.41). A calculated frequency for modes 59 and 62 derived from the combination bands is not possible since their expected frequencies are sufficiently close to other fundamental vibrations as to render the calculations meaningless.

Assignment 1

Possible Combination	Mode 61
$2110cm^{-1}$ (61+39)	$568cm^{-1}$
$1683cm^{-1}$ (43-61)	$570cm^{-1}$
$1412cm^{-1}$ (61+30)	$568cm^{-1}$
$939cm^{-1}$ (61+33)	$570cm^{-1}$
Calculated frequency	(569 ± $1cm^{-1}$)

Assignment 2

Possible Combination	Mode 61
$1863cm^{-1}$ (61+36)	$551cm^{-1}$
$1806cm^{-1}$ (61+35)	$551cm^{-1}$
$1735cm^{-1}$ (45-61)	$556cm^{-1}$
$1696cm^{-1}$ (42-61)	$555cm^{-1}$
$1683cm^{-1}$ (41-61)	$557cm^{-1}$
$1360cm^{-1}$ (61+29)	$552cm^{-1}$
$1031cm^{-1}$ (61+25)	$551cm^{-1}$
$994cm^{-1}$ (61+52)	$550cm^{-1}$
$955cm^{-1}$ (61+24)	$556cm^{-1}$
$932cm^{-1}$ (61+53)	$554cm^{-1}$
$254cm^{-1}$ (29-61)	$554cm^{-1}$
Calculated frequency	(553 ± $2cm^{-1}$)

Assignment 1

Possible Combination	Mode 64
$2594cm^{-1}$ (64+41)	$354cm^{-1}$
$1683cm^{-1}$ (64+37)	$349cm^{-1}$
$1607cm^{-1}$ (64+35)	$352cm^{-1}$
$1384cm^{-1}$ (64+34)	$353cm^{-1}$
$1360cm^{-1}$ (64+33)	$353cm^{-1}$
$1355cm^{-1}$ (64+33)	$349cm^{-1}$
$1117cm^{-1}$ (64+46)	$353cm^{-1}$
$1084cm^{-1}$ (64+48)	$350cm^{-1}$
$1084cm^{-1}$ (64+28)	$350cm^{-1}$
$1075cm^{-1}$ (64+38)	$352cm^{-1}$
$994cm^{-1}$ (64+49)	$348cm^{-1}$
$955cm^{-1}$ (64+59)	$348cm^{-1}$
$939cm^{-1}$ (64+51)	$346cm^{-1}$
$908cm^{-1}$ (35-64)	$347cm^{-1}$
$254cm^{-1}$ (50-64)	$346cm^{-1}$
Calculated frequency	(350 ± $3cm^{-1}$)

Assignment 2

Possible Combination	Mode 64
$1360cm^{-1}$ (64+34)	$329cm^{-1}$
$1097cm^{-1}$ (64+46)	$333cm^{-1}$
$1097cm^{-1}$ (38-64)	$330cm^{-1}$
$939cm^{-1}$ (64+50)	$332cm^{-1}$
$923cm^{-1}$ (64+51)	$330cm^{-1}$
$923cm^{-1}$ (35-64)	$332cm^{-1}$
Calculated frequency	(331 ± $2cm^{-1}$)

Table 3.41 Alternate assignments for modes 61 and 64 of 1,10-phenanthroline-d_8

These assignments will require Raman studies, a study which failed in the present work due to excessive fluorescence by the molecule.

Finally, the remaining bands in the infrared need to be discussed. The strong broad band at $702cm^{-1}$ has been assigned to the rocking mode of the hydrogen bonded water. The wagging mode is not observed, being masked by the very strong band from the B_1 fundamental, mode 51.

As is the case of phen the lowest band observed in the infrared spectrum of phen-d_8 are assigned to lattice vibrations, with an uncertainty as to the band of medium intensity at $107cm^{-1}$ which may either be a libration or a difference band.

The above assignment of phen-d_8 completes the range of ligands under investigation and enables a full assignment of $[M(II)(phen)_3](ClO_4)_2$ to be made in the next chapter, and of $[Pt(phen)(C_2H_4)Cl_3]$ in Chapter 5.

REFERENCES

1. E.B. WILSON,
Phys. Rev., 45 (1934) 706.

2. G. VARSÁNYI and S. SZÖKE,
Vibrational Spectra of Benzene Derivatives, (1969) Academic Press, New York.

3. I.M. MILLS,
"Calculation of Force Constants" in *Infrared Spectra and Molecular Structure,* (1963) M. Davies (Ed.), Elsevier, Amsterdam.

4. S. SZÖKE, G. VARSÁNYI and E. BAITZ,
Acta Chim., 53 (1967) 347.

5. G. VARSÁNYI, E. BAITZ, F. BILLES, A. GROFCSIK, G. HORVÁTH, G. JALSOVSZKY, G. KERESZTURY, Á. KISS, S. SZÖKE, L. SZTRAKA and H. TÓTH,
Acta Phys., 35 (1974) 219.

6. G. VARSÁNYI, S. SZÖKE, G. KERESZTURY and A. GELLÉRI,
Acta Chim., 65 (1970) 73.

7. S. SZÖKE, G. VARSÁNYI and E. BAITZ,
Acta Chim., 54 (1967) 145.

8. Y. HASE,
An. Acad. brasil. Ciênce., 53 (1981) 109.

9. C.H. KLINE and J. TURKEVICH,
J. Chem. Phys., 12 (1944) 300.

10. L. CORRSIN, B.J. FAX and R.C. LORD,
J. Chem. Phys., 21 (1953) 1170.

11. J.H.S. GREEN, W. KYNASTON and H.M. PAISLEY,
Spectrochim. Acta, 19 (1963) 549.

12. H. ABDEL-SHAFY, H. PERLMUTTER and H. KIMMEL,
J. Mol. Struct., 42 (1977) 37.

13. J.A. DRAEGER,
Spectrochim. Acta, 39A (1983) 809.

14. V.I. BEREZIN and M.D. ELKIN,
Opt. Spektrosk., 34 (1973) 685.

15. D.A. LONG, F.S. MURFIN and E.L. THOMAS,
Trans. Faraday Soc., 59 (1963) 12.

16. D.A. LONG and E.L. THOMAS,
Trans. Faraday Soc., 59 (1963) 783.

17. D.A. LONG and W.O. GEORGE,
Spectrochim. Acta, 19 (1963) 1777.

18. J. LOISEL and V. LORENZELLI,
J. Mol. Struct., 1 (1967-68) 157.

19. S. AKYUZ, A.B. DEMPSTER, R.L. MOREHOUSE and S. SUZUKI,
J. Mol. Struct., 17 (1973) 105.

20. S. SUZUKI and W.J. ORVILLE-THOMAS,
J. Mol. Struct., 37 (1977) 321.

21. D.B. CUNLIFFE-JONES,
Spectrochim. Acta , 21 (1965) 747.

22. L. HARSÁNYI and F. KILÁR,
J. Mol. Struct., 65 (1980) 141.

23. G. VARSÁNYI,
Acta Chim., 50 (1966) 225.

24. G. VARSÁNYI,
Acta Chim., 50 (1966) 237.

25. G. VARSÁNYI,
Acta Chim., 57 (1968) 51.

26. H.M. FRIEDMAN,
Spectrochim. Acta, 22 (1966) 1465.

27. S.S. SINGH,
Z. Naturforsch., 24A (1969) 2015.

28. S.S. SINGH,
Z. Inorg. Allg. Chem., 384 (1971) 81.

29. C. KARR, P.A. ESTEP and A.J. PAPA,
J. Am. Chem. Soc., 81 (1959) 152.

30. L-O. PIETILÄ and F. STENMAN,
Comment. Phys.-Math., 46 (1976) 85.

31. L-O. PIETILÄ and F. STENMAN,
Comment. Phys.-Math., 48 (1978) 145.

32. P.J. CHAPPEL and I.G. ROSS,
J. Mol. Spectrosc., 66 (1977) 192.

33. S. PINCHAS and I. LAULICHT,
Infrared Spectra of Labelled Compounds, (1971) Academic Press, London.

34. M. ITO and N. HATA,
Bull. Chem. Soc. Japn., 28 (1955) 353.

35. H. SHINDO,
Bull. Chem. Pharm., 4 (1956) 460.

36. H. SHINDO,
Bull. Chem. Pharm., 5 (1957) 472.

37. A.R. KATRITZKY and A.P. AMBER,
"Infrared Spectra" in *Physical Methods in Heterocyclic Chemistry, Vol 2*, (1963) A.R. Katritzky (Ed.), Academic Press, London.

38. S.A. COTTON and J.F. GIBSON,
J. Chem. Sec. A., (1970), 2105.

39. H. SHINDO,
Bull. Chem. Soc. Japn., 8 (1960) 845.

40. J.J. MacDOUGALL, L.C. NATHAN and J.H. NELSON,
Inorg. Chim. Acta, 17 (1976) 243.

41. A.N. SPECA, N.M. KARAYANNIS and L.L. PYTLEWSKI,
J. Inorg. Nucl. Chem., 35 (1973) 3113.

42. C.J. POPP and G.D. GARLOUGH,
J. Inorg. Nucl. Chem., 43 (1981) 501.

43. Z. DEGA-SZAFRAN,
Rocz. Chemii, 44 (1970) 2371.

44. G.V. KIREEV, V.B. LEONT'EV, Y.U. KURBATOV, O.S. OTROSHCHENKO and A.S. SADYKOV,
Bull. Acad. Sci. USSR, 29 (1980) 740.

45. D.E. CHASAN, L.L. PYTLEWSKI, C. OWENS and N.M. KARAYANNIS,
J. Inorg. Nucl. Chem., 38 (1976) 1799.

46. D.E. CHASAN, L.L. PYTLEWSKI, C. OWENS and N.M. KARAYANNIS,
J. Inorg. Nucl. Chem., 40 (1978) 1019.

47. A. SEMINARA, A. MUSUMECI and R.P. BONOMO,
Inorg. Chim. Acta, 90 (1984) 9.

48. Z. DEGAN-SZAFRAN,
Rocz. Chemii, 46 (1972) 827.

49. C. CHASSAPIS and G. PNEUMATIKAKIS,
Inorg. Chim. Acta, 27 (1978) 67.

50. A.K. SRIVASTAVA, S. SHARMA and R.K. AGARWAL,
Inorg. Chim. Acta, 61 (1982) 235.

51. D.E. CHASAN, L.L. PYTLEWSKI, C. OWENS and N.M. KARAYANNIS,
J. Inorg. Nucl. Chem., 39 (1977) 1137.

52. D.E. CHASAN, L.L. PYTLEWSKI, C. OWENS and N.M. KARAYANNIS,
J. Inorg. Nucl. Chem., 41 (1979) 13.

53. S.I. SHUPALK and M. ORCHIN,
J. Am. Chem. Soc. 85 (1963) 902.

54. S. KIDA, J.V. QUAGLIANO, J.A. WALMSLEY and S.Y. TYREE,
Spectrochim. Acta, 19 (1963) 189.

55. Y. KAKIUTI, S. KIDA and J.V. QUAGLIANO,
Spectrochim. Acta, 19 (1963) 201.

56. H.H. JAFFE and H. LLOYD-JONES,
Advan. Heterocycl. Chem., 3 (1964) 209.

57. D.W. HERLOCKER, R.S. DAGO and V.I. MEEK,
Inorg. Chem., 5(11) (1966) 2009.

58. F.E. DICKSON, E.W. GOWLIN and F.F. BENTLEY,
Inorg. Chem., 6 (1967) 1099.

59. F.E. DICKSON, E.W. BAKER and F.F. BENTLEY,
J. Inorg. Nucl. Chem., 29 (1967) 559.

60. R.G. GARVEY and R.O. RAGSDALE,
J. Inorg. Nucl. Chem., 29 (1967) 745.

61. J.H. NELSON, R.G. GARVEY and R.O. RAGSDALE,
J. Heterocycl. Chem., 4 (1967) 591.

62. R.G. GARVEY and R.O. RAGSDALE,
J. Inorg. Nucl. Chem., 29 (1967) 1527.

63. J. REEDJIK,
Recueil, 88 (1969) 499.

64. S. GHERSETTI, S. GIORGIANNI, P.L. CAPUCCI and G. SPUNTA,
Spectrochim. Acta, 29A (1973) 1207.

65. V.I. BEREZIN,
Opt. Spektrosk., 18 (1965) 119.

66. G. COSTA and V. GALASSO,
Atti Accad. Naz. Lincei, Rend. Classe Sci. Fiz. Mat. Nat., 37 (1964) 289; *C.A. 61* 7843b (1964).

67. S. SZÖKE, A. GELLÉRI and E. BAITZ,
Acta Chim., 48 (1966) 343.

68. A. GAMBI and S. GHERSETTI,
Spectrosc. Letters, 10 (1977) 627.

69. G.N.R. TRIPATHI and S.R. TRIPATHI,
Spectrosc. Letters, 9 (1976) 789.

70. A.D. VAN INGEN SCHENAU, W.L. GROENVELD and J. REEDIJK,
Spectrochim. Acta, 30A (1974) 213.

71. H.D. BIST and J.S. PARIHAR,
Chem. Phys. Letters, 32 (1975) 244.

72. H.D. BIST, J.S. PARIHAR and J.C.D. BRAND,
J. Mol. Spectrosc., 59 (1976) 435.

73. A.D. VAN INGEN SCHENAU, C. ROMERS, D. KNETSCH and W.L. GROENVELD,
Spectrochim. Acta, 33A (1977) 859.

74. A.M. GREENWAY, C.J. O'CONNOR, E. SINN and J.R. FERRARO,
Spectrochim. Acta, 37A (1981) 575.

75. Z. MIELKE,
J. Phys. Chem., 68 (1984) 3288.

76. N.M. KARAYANNIS, L.L. PYTLEWSKI and C.M. MIKULSKI,
Coord. Chem. Rev., 11 (1973) 93.

77. N.M. KARAYANNIS, A.N. SPECA, D.E. CHASEN and L.L. PYTLEWSKI,
Coord. Chem. Rev., 20 (1976) 37.

78. A. SEMINARA and E. RIZZARELLI,
Inorg. Chim. Acta, 40 (1980) 249.

79. I.S. ASHUJA, R. SINGH and R. SRIRAMULLU,
J. Inorg. Nucl. Chem. (1980) 1034.

80. R.K. AGARWAL, C. JAIN, V. KAPUR, S. SHARMA and A.K. SRIVASTAVA,
Trans. Met. Chem., 5 (1980) 237.

81. L.B. ZINNER and G. VINCENTINI,
An. Acad. brasil. Ciênc., 52 (1980) 23.

82. C. OWENS, A.K. FILO, J.M. WOODS, L.L. PYTLEWSKI, A.N. SPECA and N.M. KARAYANNIS,
J. Inorg. Nucl. Chem., 43 (1981) 177.

83. A.K. SRIVASTAVA, R.K. AGARWAL, M. SRIVASTAVA and N. SRIVASTAVA,
J. Inorg. Nucl. Chem., 43 (1981) 2144.

84. I.S. AHUJA, R. SINGH and C.L. YADAVA,
J. Mol. Struct. 74 (1981) 143.

85. G. VICENTINI and M.A. da SILVA,
An. Acad. brasil. Ciênc., 52 (1980) 23.

86. C. CHASSAPIS and G. PNEUMATIKAKIS,
Inorg. Chim. Acta, 59 (1982) 49.

87. A.K. SRIVASTAVA, S. SHARMA and R.K. AGARWAL,
Inorg. Chim. Acta, 61 (1982) 235.

88. G. VICENTINI and M.S. da SILVA,
An. Acad. brasil. Ciênc., 54 (1982) 71.

89. W.A. BUENO, N.A. BLAZ and M.J.M. SANTOS,
An. Acad. brasil. Ciênc., 56 (1984) 63.

90. S. CALIFANO, G. ADEMBRI and G. SBRANA,
Spectrochim. Acta, 20 (1964) 385.

91. G. SBRANA, V. SCHETTINO and R. RIGHINI,
J. Chem. Phys., 59 (1973) 2441.

92. J. ZAREMBOWITCH and L. BOKOBZA-SEBAGH,
Spectrochim. Acta, 32A (1976) 605.

93. J.F. ARENAS, J.T. LOPEZ-NAVARRETE, J.C. OTERO and J.I. MARCOS,
J. Chem. Soc. Faraday Trans. 2, 81 (1985) 405.

94. V. SCHETTINO, G. SBRANA and R. RIGHINI,
Chem. Phys. Lett., 13 (1972) 284.

95. B. PASQUIER, D. BOUGEARD, N. LE CALVE and R. ROUMAIN,
Mol. Cryst. Liq. Crys. 32 (1976) 17; *C.A. 84* 186843q.

96. C. LA LAU and R.G. SNYDER,
Spectrochim. Acta, 27A (1971) 2073.

97. J.A. DRAEGER,
Spectrochim. Acta, 41A (1985) 607.

98. P.J. WHEATLEY,
Acta Cryst., 10 (1957) 182.

99. J.H.S. GREEN,
Spectrochim. Acta, 26A (1970) 1503.

100. V.J. EATON and D. STEELE,
J. Mol. Spectrosc., 48 (1973) 446.

10. R.A.R. PEARCE, D. STEELE and K. RADCLIFFE,
J. Mol. Struct., 15 (1973) 409.

102. R.L. ZIMMERMAN and T.M. DUNN,
J. Mol. Spectrosc., 110 (1985) 312.

103. P.N. GATES, K. RADCLIFFE and D. STEELE,
Spectrochim. Acta, 25A (1969) 507.

104. S. BRODERSEN and A. LANGSETH,
Mat. Fys. Skr. Dan. Vid. Selsk., 1 (1956) 1.

105. S. GHERSETTI, G. MACCAGNANI, A. MANGINI and F. MONTANARI,
J. Heteroc. Chem., 6 (1969) 859.

106. X. GERBAUX and A. HADNI,
J. Chem. Phys., 49 (1968) 955.

107. G. HERZBERG,
Molecular Spectra and Molecular Structure II: Infrared and Raman Spectra of Polyatomic Molecules, (1945) Van Nostrand, Princeton.

108. R.H. LARKIN and H.D. STIDHAM,
Spectrochim. Acta, 29A (1973) 781.

109. V.I. BEREZIN and M.D. ELKIN,
Opt. Spektrosk., 32 (1972) 1030.

110. J.E. KATON and E.R. LIPPINCOTT,
Spectrochim. Acta, 15 (1959) 627.

111. G.V. PEREGUDOV,
Opt. Spektrosk., 9 (1960) 155.

112. R.M. BARRETT and D. STEELE,
J. Mol. Struct., 11 (1972) 105.

113. V.J. EATON and D. STEELE,
J. Chem. Soc. Faraday Trans. 2, 69 (1973) 1601.

114. G. ZERBI and S. SANDRONI,
Spectrochim. Acta, 24A (1968) 483.

115. G. ZERBI and S. SANDRONI,
Spectrochim. Acta, 24A (1968) 511.

116. A. BREE, C.Y. PANG and L. RABENECK,
Spectrochim. Acta, 27A (1971) 1293.

117. A. BREE, M. EDELSON and R.A. KYDD,
Spectrochim. Acta, 31A (1975) 1569.

118. G. ZERBI and S. SANDRONI,
Spectrochim. Acta, 26A (1970) 1951.

119. C.K. PEARCE, D.W. GROSSE and W. HESSEL,
J. Chem. Eng. Data, 15 (1970) 567.

120. J.S. STRUKL and J.L. WALTER,
Spectrochim. Acta, 27A (1971) 209.

121. Y. SHIRO and H. KUWATA,
Mem. Fac. Eng. Hiroshima Univ., 4 (1972) 117.

122. E. CASTELLUCCI, L. ANGELONI, N. NETO and G. SBRANA,
Chem. Phys., 43 (1979) 365.

123. N. NETO, M. MUNIZ-MIRANDA, L. ANGELONI and E. CASTELLUCCI,
Spectrochim. Acta, 39A (1983) 97.

124. M. MUNIZ-MIRANDA, E. CASTELLUCCI, N. NETO and G. SBRANA,
Spectrochim. Acta, 39A (1983) 107.

125. O. BASTIANSEN and S. SAMDAL,
J. Mol. Struct., 128 (1985) 115.

126. J.J. DYNES, F.L. BAUDAIS and R.K. BOYD,
Can. J. Chem., 63 (1985) 1292.

127. N.D. EPIOTIS,
J. Am. Chem. Soc., 95 (1973) 3087.

128. N.D. EPIOTIS, R.L. YATES, J.R. LARSON, C.R. KIRMAIER and F. BERNARD,
J. Am. Chem. Soc., 99 (1977) 8379.

129. G.M.J. SCHMIDT,
Pure Appl. Chem., 27 (1971) 647.

130. Z. LUDMER, M.D. COHEN, A. ELGAVI, B.S. GREEN and G.M.J. SCHMIDT,
J. Am. Chem. Soc., 94 (1972) 6776.

131. L. FERNHOLT, C. RØMMING and S. SAMDAL,
Acta Chem. Scand., Ser A, 35 (1981) 707.

132. B.D. ÜLKÜ, B.P. HUDDLE and J.C. MORROW,
Acta Cryst., B27 (1971) 432.

133. R. CURTI, V. RIGANTI and S. LOCCHI,
Acta Cryst., 14 (1961) 133.

134. B. LUNELLI and M.G. GIORGINI,
J. Mol. Spectrosc., 64 (1977) 1.

135. B. LUNELLI and M.G. GIORGINI,
J. Mol. Spectrosc., 104 (1984) 203.

136. V.P. GUPTA,
Indian J. Pure Appl. Phys., 7 (1969) 423.

137. Y. KAKIUTI, H. SAITO and M. AKIYAMA,
J. Mol. Spectrosc., 35 (1970) 66.

138. D.M. HANSON and A.R. GEE,
J. Chem. Phys., 51 (1969) 5052.

139. F.M. BEHLEN, D.B. McDONALD, V. SETHURAMAN and S.A. RICE,
J. Chem. Phys., 75 (1981) 5685.

140. H. SELLERS, B. PULAY and J.E. BOGGS,
J. Am. Chem. Soc., 107 (1985) 6487.

141. E.R. LIPPINCOTT and E.J. O'REILLY,
J. Chem. Phys., 23 (1955) 230.

142. H. LUTHER and H.-J. DREWITZ,
Z. Electrochem., 66 (1962) 546.

143. P. CHIORBOLI and A. BERTOLUZZA,
A Ann. Chim. (Italy), 49 (1959) 245.

144. N. CLAVERIE and C. GARRIGOU-LAGRANGE,
J. Chim. Phys., 61 (1964) 889.

145. D.E. FREEMAN and I.G. ROSS,
Spectrochim. Acta, 16 (1960) 1393.

146. J.R. SCHERER,
J. Chem. Phys., 36 (1962) 3308.

147. N. NETO, M. SCROCCO and S. CALIFANO,
Spectrochim. Acta, 22 (1966) 1981.

148. A. GROFCSIK, M. KUBINYI and G. FOGARASI,
J. Mol. Struct., 89 (1982) 63.

149. S.C. WAIT and J.C. McNERNEY,
J. Mol. Spectrosc., 34 (1970) 56.

150. G.A. FOULDS, J.B. HODGSON, A.T. HUTTON, M.L. NIVEN, G.C. PERCY,
P.E. RUTHERFORD and D.A. THORNTON,
Spectrosc. Letters, 12 (1979) 25.

151. S. GHERSETTI, S. GIORGIANNI, M. MINARI and G. SPUNTA, *Spectrosc. Letters, 6* (1973) 167.

152. S. GHERSETTI, S. GIORGIANNI and G. SPUNTA, *Spectrosc. Letters, 6* (1973) 505.

153. H. SHINDO, *Bull. Chem. Pharm., 8* (1960) 845.

154. T.S. WANG and J.M. SANDERS, *Spectrochim. Acta, 12* (1959) 1118.

155. K.H. MICHAELIAN and S.M. ZIEGLER, *Appl. Spectrosc., 27* (1973) 13.

156. S.N. SINGH, H.S. BHATTI and R.D. SINGH, *Spectrochim. Acta, 34A* (1978) 985.

157. S. GHERSETTI, S. GIORGIANNI, M. MINARI and G. SPUNTA, *Spectrochim. Acta, 31A* (1975) 445.

158. V. SCHETTINO, N. NETO and S. CALIFANO, *J. Chem. Phys., 44* (1966) 2724.

159. K. WITT and R. MECKE, *Z. Naturforsch., A22* (1967) 1247.

160. A. BREE, F.G. SOLVEN and V.V.B. VILKOS, *J. Mol. Spectrosc., 44* (1972) 298.

161. J. GODEC and L. COLOMBO, *J. Chem. Phys., 65* (1976) 4693.

162. W. ALTMANN and H.H. PERKAMPUS, *J. Mol. Spectrosc., 78* (1979) 156.

163. S.J. CYVIN, G. NEERLAND, J. BRUNVOLL and B.N. CYVIN, *Spectrosc. Letters, 14* (1981) 37.

164. V. SCHETTINO, *J. Chem. Phys., 46* (1967) 302.

165. H.H. PERKAMPUS and W. ROTHER, *Spectrochim. Acta, 30A* (1974) 597.

166. W. ALTMANN and H.H. PERKAMPUS, *Spectrochim. Acta, 35A* (1979) 253.

167. W. ALTMANN, H. KLEINDIENST and H.H. PERKAMPUS, *Spectrochim. Acta, 35A* (1979) 259.

CHAPTER 4

METAL (II) PERCHLORATE COMPLEXES

In this Chapter the vibrational assignments of homo-ligand complexes of the first transition metal(II) ions (Mn-Zn) are investigated, employing ligand isotope labelling studies. Of the sixty-two complexes investigated here, forty are newly reported. These are the metal(II) complexes with pyrazine *N*-oxide (excluding that for Cu), $[Zn(quinO)_5](ClO_4)_2$ and all thirty-one fully deuterated complexes.

In Chapter 1 the assignment of metal complexes was discussed by means of a breakdown of molecular symmetry in terms of localised symmetry perturbed by the molecular environment. Thus, for octahedral homo-ligand complexes the ligand description (in terms of internal coordinates) will be unchanged, provided that the coupling between the central metal atom and the ligand is not too strong [1-3], while the number of modes for the ML_6 cation is 33 (as calculated from group theory) regardless of the nature of the ligand - so long as it is non-linear [1,2].

Of the 33 modes for the ML_6 cation, 15 modes of vibration describe (applying O_h symmetry) six stretches (νM-L) and nine bends (δLML) (Figure 4.1). This leaves 18 modes of vibration which arise from the ligand rotations and which are transmuted into rocking, wagging and twisting modes on complexation. Where the ligand is a heterocyclic molecule the rocking and the wagging modes of the six ligands yield six planar (with respect to the plane of the ligand) bends (δM-N) and six out-of-plane bends (δ'M-N) respectively. The final six modes are the M-N torsions, τ(MN). Where the ligand is an aromatic *N*-oxide the 18 ligand rotations yield six M-O torsions, τ(MO); six bends, δMON and six N-O torsions, τ(NO) respectively.*

---

* In their normal coordinate analyses of $[M(pyO)_6]^{2+}$ complexes VAN INGEN SCHENAU *et al.* [4,5] and GREENWAY *et al.* [6] incorrectly define the six

Figure 4.1 Breakdown of molecular symmetry of M(II) complexes with mono- or bidentate ligands

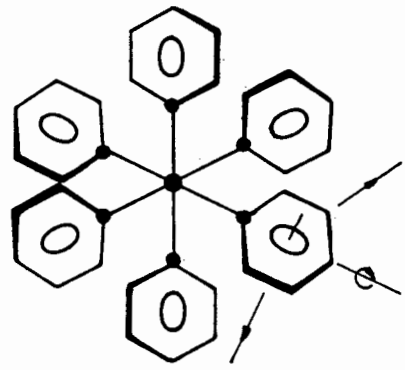

$[M(py)_6]^{2+}$ = 67 atoms (= N)

(3N-6) = 195 fundamentals

Fundamental breakdown

1 MN_6 component = 15

2 ligand (C_6H_5N) component = 6 x 27 = 162

3 inplane δM-N = 6

out-of-plane δM-N = 6

rotation about M-N = 6

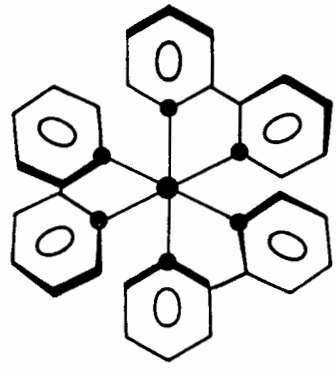

$[M(bipy)_3]^{2+}$ = 61 atoms (= N)

(3N-6) = 177 fundamentals

Fundamental breakdown

1 MN_6 component = 15

2 ligand $(C_{10}H_8N_2)$ component = 3 x 54 = 162

Figure 4.1 (continued)

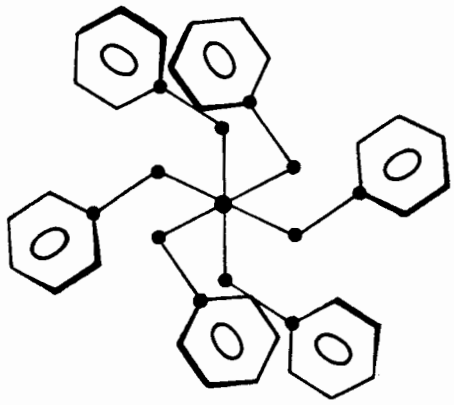

$[M(pyO)_6]^{2+}$ = 73 atoms (= N)

(3N-6) = 213 fundamentals

Fundamental breakdown

3 unit model (This Work)	2 unit model [4-6]
1 MO_6 component = 15	1 $M(ON)_6$ component = 33 (a)
2 ligand (C_6H_5NO) component = 6 x 30 = 180	2 ligand (C_6H_5NO) component = 6 x 30 = 180 (b)
3 rotation about M-O (τMO) = 6	
rotation about N-O (τNO) = 6	(a) includes 6 νN-O, 6 τMO and δMON
δMON = 6	(b) includes 6 νN-O

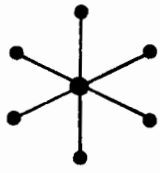

1

2

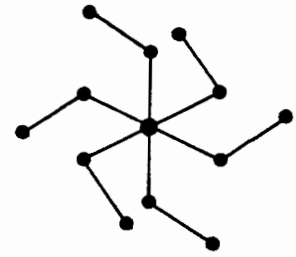

1

3

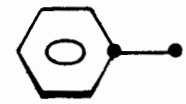

2

The ligand torsional modes are found below the metal-ligand stretching fundamentals [4-8] and are a major feature of the low-frequency spectra, although they are of little diagnostic value [7].

Where the ligand is bidentate the number of modes for the localised symmetry of the ML_3 cation is 15, regardless of the nature of ligand (Figure 4.1). These describe six stretches (νM-L) and nine bends (δLML).

Metal-nitrogen modes are among the most quoted vibrational assignments, especially where the neutral ligand is a heterocyclic molecule. Earlier studies of M(II) complexes generally did not scan below $200cm^{-1}$ thereby restricting themselves to the M-N stretches. Of the more recent studies which have been extended below $200cm^{-1}$, several were limited to the assignment of the metal-nitrogen stretching fundamentals [9-16]. Those vibrational studies in which more complete metal-ligand assignments were attempted [17-27], invariably entirely neglected the ligand rocking, wagging and twisting vibrations, and are therefore partially or wholly incorrect [4-8].

A similar situation exists for the far-infrared assignments of M(II) complexes with oxygen donors [28-32]. Clearly much investigation into the low-frequency spectra of M(II) complexes still remains to be done.

Since the far-infrared spectrum is influenced primarily, not by the nature of

---

νN-O as part of the 33 modes of the ML_6 cation, and introduce an additional six modes to account for the τ(NO). Rather, the six νN-O (being internal ligand modes) belong to the *localised symmetry of the ligand* and are simply reproduced in the NCA of the ML_6 cation as a result of the dissolution of the molecular symmetry into *two* localised symmetry components - these being the ligand and $M(ON)_6$ - by these authors, rather than into *three* (Figure 4.1).

the donor atom of the ligand, but rather by whether it is monodentate or bidentate, the M(II) $(ClO_4)_2$ complexes investigated will be considered in these categories rather than whether the ligand is coordinated via a nitrogen or donor atom.

1. M(II) $(ClO_4)_2$ COMPLEXES WITH BIDENTATE LIGANDS.

1.1 M(II) complexes with bipy and phen and their fully deuterated analogues

The deuteration study of the M(II) $(ClO_4)_2$ complexes with *tris*-bipy and *tris*-phen has been undertaken for several reasons.

Firstly, it was initially thought that a comparison between the spectra of the Cu(II) tris-complexes with these two ligands clearly demonstrated restriction of the JAHN-TELLER induced tetragonal distortion in a Cu(II) complex by the limited capacity of a ligand for expanding its bite (N-N distance). In noting the splitting of the 625,660cm^{-1} bipy doublet into a triplet INSKEEP [33] was the first to suggest spectroscopic evidence for tetragonal distortion in the $[Cu(bipy)_3]^{2+}$ cation. He also suggested that the absence of splitting in the infrared spectrum of the $[Cu(phen)_3]^{2+}$ cation indicated the absence of tetragonal distortion as a result of the more rigid ligand. PERCY and THORNTON [34-36] extended the infrared investigation of these complexes to 200cm^{-1}, and from the splitting of the M-N stretching frequencies in $[Cu(II)(bipy)_3](ClO_4)_2$ and its apparent absence in $[Cu(phen)_3](ClO_4)_2$, concurred with INSKEEP. Unfortunately these studies were at the extreme end of the range for the instrumentation used, and therefore subject to poor resolution. Two far-infrared metal isotope labelling studies (down to 150 and 100cm^{-1} respectively) of these complexes made by NAKAMOTO and his co-workers [23,24] later revealed both more vibrational bands and a greater splitting

by the Cu(II) complex in the metal-nitrogen stretching and bending region than had previously been reported. Finally publication of the crystal structures of both $[Cu(bipy)_3](ClO_4)_2$ and $[Cu(phen)_3](ClO_4)_2$ [37,38] conclusively shows that *both* tris-bidentate complexes are tetragonal as a result of a static JAHN-TELLER distortion.* Therefore a full assignment of the $[M(II)(phen)_3](ClO_4)_2$ complexes is necessary to investigate whether spectroscopic evidence for the tetragonal distortion of the Cu(II) was previously overlooked or, alternatively, to determine why it is absent.

Secondly, the far-infrared assignments (below $200cm^{-1}$) reported for these complexes did not take into account the metal-ligand bending modes. In the complexes of both ligands, several bands were generally described by NAKAMOTO and his co-workers as being activated ligand bands [23-25]. A full vibrational assignment should therefore be useful in distinguishing between internal ligand modes and the metal-nitrogen vibrations.

Thirdly, although several deuteration studies of M(II) complexes with bipy have been made [16,39,40] no systematic ligand isotope labelling study has been attempted for the metal(II) complexes of the first transition metal series. Neither has there yet been a ligand isotope study reported for any metal complex with phen.

---

*The restriction of the ligand bite in phen is evident in both the slightly shorter equatorial M-N bonds ($\Delta 0{,}04$ Å) of the two ligands involved in the longer axial M-N bonds (as compared with the third equatorial ligand) and by the planarity of the ligands. The bond lengthening of the axial bonds is thus accompanied by a twisting away of the ligand with a reduction of its bonding ability [38]. In $[Cu(bipy)_3](ClO_4)_2$ the 4 equatorial bonds are of equal length, with the tetragonal distortion accommodated by a twisting of the pyridine rings through a dihedral angle of some 31° [37].

Full infrared assignments of the M(II) complexes of bipy, phen and their fully deuterated analogues are given in Tables 4.1 to 4.4. The far-infrared assignments reflecting the deuteration shifts found in this work as well as reported metal-isotope shifts [23-26] are presented in Table 4.5 and 4.6.

The spectra reveal that the bands which arise from a common origin within the localised symmetry of the ligand (*e.g.* the A_1 and B_1 or the A_2 and B_2 twin components of the pyridyl ring vibrations in *cis*-bipy) are not completely resolved into the full number of components expected for the D_3 complex (*e.g.* the four components of the pyridyl ring vibrations, A_1, A_2 and $2E$). With the exception of the Cu(II) complexes only six bands show splitting in the tris(bipy) metal complexes, modes 14($-d_0$), 6b($-d_0$), 5'($-d_0$), 15'($-d_8$), 12($-d_8$),and 6a($-d_8$) while only four are split in the phen analogues; modes 50($-d_0$), 40($-d_0$), 33($-d_8$) and 15($-d_8$). This weak splitting of the localised ligand symmetry is typical of the tris(bipy) metal complexes [16].

In both series of metal(II) complexes, several ligand bands show metal sensitivity which follows the IRVING-WILLIAMS sequence [41].

This metal sensitivity may be explained by investigating the metal sensitive ligand vibrations in M(II) complexes with pyridine. The planar ring modes 12, 8a, 6a and 1 and the out-of-plane ring mode 16b have long been recognised as being strongly metal sensitive, while the planar ring modes 19a and 19b, the out-of-plane ring mode 4 and the C-H modes 15 and 5 are lightly metal sensitive [3,42-45]. The combination band at *ca.* 1640cm^{-1} (6a+1) is metal sensitive due to its components [45]. This metal sensitivity is a result of kinematic coupling with the M-N vibrations [3,45]. The nature and extent of this coupling may be comprehended by comparing it with the coupling experienced in pyO or in a mono-substituted benzene, since the same ring modes reflect

Table 4.1 Infrared assignment (4000-350cm^{-1}) of $[M(bipy)_3](ClO_4)_2$ complexes

Mn	Fe	Co	Ni	Cu	Zn	Assignment
-	3533 mbr	-	-	-	-	$\nu O\text{-}H_{(H_2O)}$
3196 vw	-	-	-	3135 w	3145 vw	comb
3110 m	3114 m	3110 m	3112 m	3112 m 3102 m	3113 m	2 (νC-H)
3079 ms	3086 ms	3077 ms	3081 ms	3089 ms	3082 ms	20b (νC-H)
3069 ms	3078 msh	3069 msh	3065 msh	3071 ms 3067 ms	3070 msh	2', 7b, 20a and 20b' (νC-H)
3050 mwsh	3037 vw	3046 mw	3046 mw	3040 msh	3046 m	7b' (νC-H)
3021 mw		3024 mw	3027 mw	3023 w	3024 m	20a (νC-H)
2988 vw	2979 w	-	2960 vw	2970 vw	2956 vw	
2781 w	2780 w	2778 w	2782 w	2783 vw	2782 vw	
2736 w	2738 vw	2738 w	2736 vw	2732 vw	2738 vw	
-	2685 vw	-	2648 vw	-	2670 vw	
2551 w	-	-	2558 vw	-	2555 vw	
2523 w	-	2525 vw	2527 vw	-	2524 vw	
2462 vw	2465 vw	2463 w	2462 vw	2465 vw	2465 vw	
2340 w	2340 vw	-	2335 vw	2334 w	2340 vw	
2265 w	2266 w	2264 w	2264 w	2265 w	2262 w	
2015 mw	2006 mw	2008 m	2009 mw	2014 wm	2010 w	
1990 wsh	1994 mw	1996 mw	1998 mw	-	-	comb
1951 vw	1950 vw	1955 vw	1955 vw	1951 vw	1958 w	
1921 w	-	1925 w	1923 w	1936 w	1928 w	
1892 vwsh	1908 w	1915 w	1913 w	1915 vw	1920 w	
1867 vw	-	1853 w	1850 w	1856 w	1868 w	
1780 wbr	-	1775 w	1773 w	1780 vw	1780 vwbr	
1720 wbr	-	1728 w	1731 w	1730 wbr	-	
-	-	1700 w	1702 w	1709 w	1715 wbr	
1673 vw	1682 vw	-	1680 vw	-	1675 w	
1634 vw	1627 wm	1634 vw	1650 vw	1665 wbr	1644 w	
1621 vw		1620 vw	1625 vw	-	-	
1602 vs	1607 vs	1607 vs	1607 vs	1607 vs 1597 s	1607 vs	8b' (νring)
1596 s	1600 s	1602 s	1602 vs	1602 vs 1591 s	1598 s	8b (νring)
1575 m	1574 wm	1574 m	1574 m	1575 m	1577 ms	8a' (νring)
1566 wm	1567 m	1564 wm	1564 m	1567 m	1567 m	8a (νring)

Table 4.1 (continued)

Mn	Fe	Co	Ni	Cu	Zn	Assignment
1491 ms	1495 m	1496 m	1494 ms	1497 ms 1492 ms	1492 m	19a' (ν ring)
1475 s	1465 s	1473 s	1471 s	1486 ms 1472 s	1474 s	19a (ν ring)
1440 vs	1443 vs	1439 vs	1441 vs	1441 vs	1440 vs	19b' (ν ring)
-	1425 ms	1418 m	1419 msh	-	-	19b (ν ring)
1366 w	1372 m	1372 m	1375 w	1368 w	1368 w	comb
1315 ms	1315 ms	1315 ms	1315 ms	1320 ms 1314 ms	1315 ms	A (ν inter-ring)
1281 vw	1281 vw	1285 w	1281 w	1281 vw	1284 w	3' (αC-H)
1262 vw	1272 w	1265 w	1265 w	1270 w	1266 w	14' (ν ring)
1246 s	1246 s	1246 s	1246 s	1247 s	1250 s	3 (αC-H)
1226 m 1219 m	1222 m	1220 m	1219 m	1218 m	1222 m	14 (ν ring)
1172 s	1168 s	1172 s	1171 s	1173 m 1167 m	1172 s	15' (αC-H)
1157 s	1160 s	1159 m	1158 m	1159 s	1158 s	15 (αC-H)
-	-	-	-	1105 vssh	-	9b' (αC-H)
1082 vsbr	1092 vsbr	1088 vsbr	1089 vsbr	1087 vsbr	1085 vsbr	$\nu_a(ClO_4)$ and 9b (γC-H)
-	1070 s	1070 s	1072 s	-	-	18b (αC-H)
1044 ssh	-	1045 s	1044 ssh	1047 s	1044 s	18b' (αC-H)
1018 ssh	1024 s	1021 s	1023 s	1027 ms	1021 s	12 (ν ring)
1014 s	1012 ms	1016 s	1017 ssh 1008 ssh	1020 ms 1006 msh	1014 s	1 (ν ring)
1001 s	1000 mw	998 w	1000 wsh	996 ms	1000 ms	12' (ν ring)
984 w 973 wm	-	-	-	985 ms 971 w	986 w	5 (γC-H)
960 w	956 w	964 wm 959 wsh	964 m	967 mw	966 w 962 w	5' (γC-H)
930 w	930 w	929 w	929 w	930 w	929 w	$\nu_s(ClO_4)$
903 w	-	896 w	895 w	905 w	899 wm	10b' (γC-H)
891 wsh	879 mw	892 mw	890 mw	891 w	894 wm	10b (γC-H)
-	826 w	-	816 wsh	813 w	819 wsh	10a' (γC-H)
812 w	-	813 w	813 w	809 w	815 w	10a (γC-H)
772 s	768 s	775 s	775 s	770 s	777 s	4 (γ ring)
760 s	765 s	768 s	768 s	765 s 762 s	767 sbr	1' (ν ring)

Table 4.1 (continued)

Mn	Fe	Co	Ni	Cu	Zn	Assignment
747 s	-	-	-	749 ms	-	11' (γC-H)
737 s	734 s	736 s	736 s	735 s	737 s	11 (γC-H)
723 wsh	727 wsh	723 wsh	725 wsh	722 wsh	720 wsh	4' (γring)
651 ms 646 m	656 m 650 m	653 ms	653 ms	658 m 652 m	653 ms	6b (νring)
-	-	634 m	635 m	634 wsh	632 ms	6a (νring)
623 s	623 s	623 s	623 s	623 s	623 s	$\delta(ClO_4)$ and 6b' (νring)
550 vw	550 vw	550 vw	-	550 vw	-	comb
-	497 w	481 w	483 w	496 w 481 w	494 vw	comb
467 w	475 wm	465 vw	468 w	465 vw	478 w	E (ring scissors)
-	456 w	455 vw	458 vw	458 w	459 w	Γ (ring shear)
424 w	438 wsh	433 m	439 m	441 m 423 m	428 ms	16b (γring)
412 ms	418 ms	413 ms	413 s	410 ms 393 msh	413 s	16a (γring)

s = strong

m = medium

w = weak

v = very

sh = shoulder

br = broad

comb = combination

Table 4.2 Infrared assignment (4000-350cm^{-1}) of $[M(bipy\text{-}d_8)_3](ClO_4)_2$ complexes

Mn	Fe	Co	Ni	Cu	Zn	Assignment
-	3524 wmbr	-	-	-	-	νO-H$_{(H_2O)}$
-	3189 wbr	-	-	-	-	
-	-	-	3143 vw	3140 vw	3136 vw	comb
3131 wbr	-	-	3130 vw	3130 vw	3128 vw	
2993 vw	-	2997 vw	2995 vw	-	2994 vw	
2923 w	2925 w	2925 w	2920 vw	2920 vw	2922 w	
2854 vw	2850 vw	2853 vw	2850 vw	2850 vw	2854 vw	
2780 w	2780 vw	2776 w	2778 w	2778 w	2778 w	
2656 w	2664 w	2656 w	2666 w	2665 w	2660 w	
2583 w	-	2581 vw	2576 vw	-	2584 vw	
2505 w	2506 w	2516 w	2519 w	-	2511 w	
2474 w	2470 vw	2472 vw	2480 vw	-	2480 vw	
2408 vw	2410 wbr	2410 w	2408 vw	2405 vw	2407 vw	
-	-	2334 wm	2335 w	2334 w	-	
2308 wm	2312 wm	2310 wm	2312 w	2305 wm	2308 wm	2 (νC-D)
2295 m	2298 m	2282 wmsh	2288 wm	2295 msh	2294 ms	2', 20b' and 7b' (νC-D)
2275 wsh	2280 msh		2282 wmsh	2291 m	2283 msh	20b and 20a' (νC-D)
2270 wsh	2263 wsh	2270 m	2273 m	2261 w	2274 msh	20a and 7b (νC-D)
2186 w	2188 w	-	-	2182 vw	2188 w	comb
2017 mw	2012 w	2029 w	2032 w	2022 mw	2022 mw	
2003 wsh	-	2006 wm	2008 wm	-	2005 msh	
-	-	1996 wm	1998 wm	1998 wmsh	1990 wsh	
1919 w	1920 w	1919 w	1918 w	1918 w	1920 w	
1804 w	-	1802 w	1804 w	1802 w	1804 w	
-	1798 w	1796 mw	-	1797 wm	1796 w	
1698 vw	1699 w	1700 vw	-	1694 vw	1700 wsh	
1682 w	-	-	1683 w	-	1683 w	
1645 w	1634 w	1640 vw	1643 vw	1650 w	1650 vw	
1601 w	1608 w	1594 w	1595 w	1598 w	1599 w	
1574 s	1576 s	1576 s	1578 s	1577 ms 1569 ms	1572 s	8b' (νring)
1560 s	1564 s	1566 s	1566 s	1562 ms	1563 ms	8b (νring)
1543 s	1542 s	1542 s	1546 s	1544 s	1544 s	8a' (νring)
1530 vs	1538 s 1532 s	1530 s	1532 s	1532 s	1350 s	8a (νring)
1466 w	1466 w	1466 w	-	1468 w	1463 w	comb

Table 4.2 (continued)

Mn	Fe	Co	Ni	Cu	Zn	Assignment
1420 ms	1428 ms	1425 ms	1428 ms	1433 ms 1418 ms	1420 ms	19a' (νring)
1389 vw	1389 w	-	1389 vw	1391 vw	1387 vw	comb
1361 vw	1370 w	1367 vw	1361 vw	1361 vw	1366 vw	comb
1344 vw	1342 msh	1342 w	1342 w	-	1345 w	19b' (νring)
1330 vs	1334 vs	1334 vs	1334 vs	1333 s 1326 s	1331 vs	19a (νring)
1308 m	1301 m	1306 mw	1308 mw	1303 mw	1307 mw	19b (νring)
1271 vw	-	1270 vw	1271 vw	1270 vw	1267 w	comb
1257 vw	1259 vw	1261 vw	1262 vw	1262 vw	1256 vw	14 (νring)
1237 s	1236 s	1240 s	1240 s	1240 s	1240 s	A (νinter-ring)
1200 w	1201 w	1201 vwbr	1202 vwbr	1206 w	1201 w	comb
1169 vw	-	1167 vw	1167 vw	1167 vw	1169 vw	14' (νring)
1095 vsbr	1088 vsbr	1108 ssh 1091 vsbr 1070 ssh	1109 ssh 1095 vsbr	1088 vsbr	1091 vsbr	$\nu_a(ClO_4)$
1031 m	-	-	-	1029 ms	1030 s	12 (νring)
1023 ms	1023 mssh	1020 m	1021 mw	1021 m	1022 s	
1005 wm	1003 s	1003 s	1004 s	1009 wm 1003 wm	1004 s	1 (νring)
989 s	993 s	993 m	994 ms	996 m 992 ms	992 s	12' (νring)
978 s	980 s	983 s	985 s	978 m	983 s	3 (αC-D)
964 wm	966 mw	964 mw	-	970 m	970 m	3' (αC-D)
931 w	929 wm	929 w	930 w	931 w	929 w	$\nu_s(ClO_4)$
877 vw	-	-	875 vw	879 vw	-	comb
866 s	867 s	868 s	868 ms	865 m	870 s	9b' (αC-D)
		860 s	862 ms	855 msh	861 s	9b (αC-D)
853 s		-	-	851 ms	-	
843 mw	-	840 ms	843 msh	840 ms	839 m	15' (αC-D)
-	829 ms	836 m	839 ms	-	-	15 (αC-D)
832 s	820 ms	832 ms	833 m	832 m	832 s	
810 w	-	804 vw	805 w	806 vw	807 w	5 (γC-D)
796 w	-	789 w	790 w	799 w	790 w	18b' (αC-D)
771 w	775 mw	772 w	774 w	777 w	770 vw	18b (αC-D)
-	-	760 vwsh	760 vwsh	-	762 vw	5' (γC-D)

Table 4.2 (continued)

Mn	Fe	Co	Ni	Cu	Zn	Assignment
731 ms	730 m	732 ms	733 ms	731 ms	732 ms	4 (γring)
726 ms	-	-	-	722 m	725 m	6b' (νring)
718 m	719 m	718 mw	718 m		718 ms	4' (γring)
667 vw	680 vw	676 vw	675 vw	687 vw 681 vw	678 vw	10b' (γC-D)
658 wm	657 w	654 wm	654 wm	667 w 658 w	655 w	10b (γC-D)
623 vs	622 s	629 s 623 vs	629 s 623 vs	622 vs	629 s 623 vs	6b (νring) and 10a (γC-D) $\delta(ClO_4)$
608 m	-	610 m	611 m	617 w 606 w	609 m	6a (νring)
583 s 570 s	585 s	590 ms 586 s	590 ms 586 s	597 ms 583 s	594 s 587 s	1' (νring) 11 (γC-D)
472 vw	472 vwsh	470 vw	478 vw	477 vw	475 vw	comb
462 vw	464 w	457 vw	458 vw	454 wm	459 vw	comb
444 vw	444 w	446 vw	448 w	-	443 vw	E (ring scissors)
432 vw	426 vw	431 vw	439 vw	437 vw	430 vvw	Γ (ring shear)
392 w	397 w	400 wm	405 m	403 wm 389 wm	396 m	16b (γring)

s = strong

m = medium

w = weak

v = very

sh = shoulder

br = broad

comb = combination

Table 4.3 Infrared assignment (4000-350cm^{-1}) of $[M(phen)_3](ClO_4)_2 \cdot H_2O$ complexes

Mn	Fe	Co	Ni	Cu	Zn	Assignment
3598 mbr	3604 mbr	3611 mbr	3608 mbr	3608 mbr	3612 mbr	νO-H(H_2O)
3525 mbr	3520 mbr	3521 mbr	3523 mbr	3522 mbr	3509 mbr	
3080 msh	3085 m	3084 msh	3088 msh	3086 msh	3082 msh	23 (νC-H)
3064 m	3063 m	3064 m	3066 m	3065 m	3064 m	43, 22 and 21 (νC-H)
3024 w	3024 w	3022 w	3024 w	3020 w	3022 w	42 and 19 (νC-H)
-	-	2995 w	3000 wsh	3000 wsh	3002 w	41 (νC-H)
2924 w	2923 w	2928 vw	2929 w	2931 w	2935 w	comb
-	2855 wbr	-	2860 wbr	-	-	
2778 w	2780 vw	2778 w	2778 w	2778 w	2772 w	
2612 vw	-	2610 w	2619 w	2617 w	2624 wbr	
2508 vw	-	2510 w	2510 w	2508 w	2512 w	
2462 vw	2460 vw	2463 w	2461 w	2465 w	2462 vw	
-	-	2414 vw	2419 vw	2411 w	2412 w	
2300 vw	2296 vw	2291 vw	2294 w	2294 w	2295 w	
2265 vw	2263 w	2263 w	2265 w	2263 w	2264 w	
2008 wbr	2003 wbr	2010 wbr	-	2011 wbr	2009 wbr	
1987 wbr	1985 wbr	1986 wbr	1990 wbr	1975 wbr	1975 wbr	
1942 wbr	1943 wbr	1945 w	1948 wbr	1945 wbr	1948 wbr	
1918 wbr	1917 w	1917 mbr	1919 wbr	1919 wbr	1908 wbr	
1810 wbr	1792 vw	1795 w	1819 wbr	1817 vw	1818 w	
1716 w	1711 w	1716 ww	1711 w	1715 w	-	
1708 w	-	1703 w	-	1702 w	1700 w	
1625 ms	1626 ms	1624 m	1625 m	1623 m	1625 m	18 (νring)
1605 w	1603 wm	1604 w	1604 wm	1604 w	1605 w	17 (νring)
1592 m	1586 m	1588 msh	1587 ms	1588 msh	1594 w	40 (νring)
				1583 ms	1585 msh	
1578 m	1579 m	1580 s	1581 ms	1578 ms	1580 ms	39 (νring)
1518 vs	1518 vs	1517 vs	1516 s	1518 s	1518 s	16 (νring)
1496 ms	1494 m	1494 m	1494 ms	1495 ms	1495 ms	38 (αC-H)
1451 vw	1455 vw	1460 vw	1461 vw	1456 vw	1454 vw	15 (αC-H)
1425 vs	1426 vs	1424 s	1424s	1426 vw	1425 vs	37 (νring) and 14 (νring)
-	1411 w	-	-	-	1400 m	36 (νring)
1375 vw	1372 vw	1376 vw	1378 vw	1376 vw	1377 vw	comb
1342 m	1342 m	1339 m	1339 ms	1339 ms	1339 m	13 (νring)
1314 vw	1320 wsh	1314 vw	1318 w	1318 w	1319 w	35 (νring)
1303 mw	1309 mw	1303 mw	1304 m	1305 m	1303 m	12 (νring)

Table 4.3 (continued)

Mn	Fe	Co	Ni	Cu	Zn	Assignment
1252 vw	1253 vw	1257 vw	1258 vw	1254 vw	1255 vw	34 (αC-H)
1224 m	1225 ms	1222 m	1223 ms	1223 m	1225 m	10 (ν ring)
1209 w	1210 w	1209 w	1210 w	1209 w	1210 w	33 (αC-H)
1191 vw	1202 vwsh	1179 vw	1199 vw	1200 vwsh	1195 w	9 (αC-H)
1146 s	1146 ms	1147 s	1147 s	1148 s	1148 s	8 (αC-H) and 31 (αC-H)
1076 sbr	1082 vsbr	1082 vsbr	1088 vsbr	1094 vsbr	1080 vsbr	$\nu_a(ClO_4)$, 30 and 7 (ν ring)
-	-	-	1037 msh	1035 ms	1033 msh	6 (ν ring)
-	1001 wsh	1004 mw	1006 mwsh	1007 w	1011 w	29 (ν ring)
992 w	-	994 mw	992 m	994 w	1001 w	46 (γC-H)
969 w	-	973 w	973 wsh	975 w	975 w	57 (γC-H)
	-	963 w	962 w	964 w	965 w	58 (γC-H)
929 w	930 w	931 w	931 w	932 w	934 w	$\nu_s(ClO_4)$
902 vw	905 vw	903 vw	904 vw	909 w 900 vw	904 vw	28 (ν ring)
866 m	869 m	868 m	869 m	871 wm 865 m	867 ms	48 (ν ring)
842 vs	845 vs	852 s 849 s 842 s	851 s 848 s 842 s	849 s 842 s	855 s 848 s	5 (ν ring) and 49 (γC-H)
-	829 msh	-	-	831 w	834 wsh	59 (γC-H)
806 vw	-	811 vw	-	811 vw	811 vw	60 (γC-H)
773 mw	782 mw	779 w	777 vw 772 vw	780 w 776 vwsh	782 w 776 wm	50 (γ ring)
763 vwsh	770 wsh	767 w	767 wm	767 wm	-	61 (γ ring)
728 ssh	732 s	727 ssh	-	731 ssh	-	51 (γC-H)
723 vs	724 vs	724 vs	723 vs	726 s 721 s	725 vs	27 (γC-H) 4 (ν ring)
642 m	642 m	644 m	646 m 643 m	647 m 639 m	645 m 641 m	26 (ν ring)
623 s	623 s	624 s	623 s	623 s	623 s	$\delta(ClO_4)$
556 vw	560 w	558 vw	559 vw	557 vw	558 w	3 (ν ring)
543 vw	548 vwsh	546 vw	547 vw	546 vw	547 vw	comb
527 vw	531 wm 526 wm	-	529 vvw	-	539 vw	comb
512 vw	511 vw	511 vw	511 vw	511 vw	512 w	52 (γ ring)
500 vw	500 vw	-	-	507 vwsh	500 vwsh	63 (γ ring)

Table 4.3 (continued)

Mn	Fe	Co	Ni	Cu	Zn	Assignment
477 vw	477 vw	482 vw	485 vw	489 vw 478 vw	482 vw	25 (νring)
457 vw	457 vw	458 vw	-	458 vvw	458 vvw	53 (γring)
438 vw	438 vwsh	441 vw	446 vw	-	437 vw	24 (νring)
421 m	426 m	425 wm	426 wm	422 wm	423 m	2 (νring)

s = strong

m = medium

w = weak

v = very

sh = shoulder

br = broad

comb = combination

Table 4.4 Infrared assignment (4000-350cm^{-1}) of $[M(phen\text{-}d_8)_3](ClO_4)_2 \cdot H_2O$ complexes

Mn	Fe	Co	Ni	Cu	Zn	Assignment
3615 wbr	3600 wbr	3615 wbr	3611 wbr	3603 wbr	3614 wbr	νO-H(H_2O)
3481 wbr	3524 wbr	3525 wbr	3521 wbr	3519 wbr	3479 wbr	
2966 wm	2968 w	2966 w	2960 vw	2958 vw	2963 w	comb
2925 w	2924 w	2923 w	2928 w	2922 w	2925 w	
2880 wbr	-	2858 vw	2860 vw	2854 w	2885 wbr	
2780 w	2780 w	2778 w	2781 w	2780 vw	2783 w	
-	-	-	2577 w	2575 vvw	2572 vvw	
-	2460 vvw	2462 vw	2463 w	2460 vvw	2463 vvw	
2309 w	2307 w	2304 w	2306 w	2305 w	2306 w	23 (νC-D)
2284 w	2290 w	2283 w	2280 w	2280 w	2290 w	22 and 45 (νC-D)
	2277 w					21 and 43 (νC-D)
2270 wsh	2270 wsh	2266 w	2264 w	2268 wsh	2275 w	comb
2022 w	2020 wbr	2019 wbr	2019 wbr	2016 wbr	2023 wbr	
-	1918 vw	1915 w	1920 w	1922 w	-	
1792 vw	1797 w	-	1804 w	1802 vw	-	
1716 w	1706 wbr	1735 wbr	1728 w	1718 vw	1716 w	
1685 vw	-	1686 vw	1680 vwbr	1682 vw	1685 vw	
1650 vw	-	1649 vw	1650 w	1649 w	1652 w	
1611 wbr	1616 wbr	1622 wbr	1622 wbr	1629 vw	1613 w	
1599 m	1604 w	1601 wm	1601 w	1600 w	1601 wm	18 (νring)
1586 m	1588 m	1586 m	1588 m	1590 m	1589 m	40 (νring)
1553 vw	1551 s	1551 s	1551 s	1553 s	1555 s	17 (νring) and 39 (νring)
1474 vs	1474 s	1473 vs	1474 vs	1474 vs	1476 vs	16 (νring)
-	-	1446 vw	1443 vw	-	1448 vw	comb
1431 s	1431 s	1431 s	1431 s	1431 s	1431 s	38 (αC-D)
1421 ms	-	-	-	1422 m	1425 mw	15 (αC-D)
1398 mw	-	-	-	-	1398 m	
1388 w	1386 w	1387 w	1388 w	1388 w	1389 w	14 (νring)
-	1365 w	1366 vw	1369 vw	1368 vw	1370 vw	comb
1342 vs	1341 vs	1344 vs	1345 vs	1344 vs	1346 vs	37 (νring)
1320 wsh	-	1326 msh	1329 wsh	-	1322 w	36 (νring)
1304 m	1308 m	1307 m	1307 m	1307 m	1307 m	13 (νring)
-	1269 wsh	-	-	1275 w	-	comb
1262 s	1262 ms	1263 ms	1264 ms	1263 s	1263 s	35 (νring)
1215 mw	1222 w	-	-	-	1219 w	comb
1168 w	1165 w	1168 w	1160 w	1168 w	1169 w	12 (νring)

Table 4.4 (continued)

Mn	Fe	Co	Ni	Cu	Zn	Assignment
-	-	1129 msh	1126 ssh	1128 ssh	1130 ssh	$\nu_a(ClO_4)$
1098 vsbr	1093 vs	1098 vsbr	1094 vsbr	1099 vsbr	1100 vsbr	
1037 s	1037 ssh	1036 s	1036 m	1037 s	1037 s	34 (αC-D)
1023 s	1020 s	1023 s	1023 s	1022 s	1024 s	33 (αC-D)
1013 m	-	-	-	-	1014 m	
976 s	974 ms	975 ms	975 ms	976 s	977 s	10 (νring)
947 vw	-	946 vw	945 vw	946 vw	947 vw	comb
934 w	928 w	932 w	931 w	932 w	935 w	$\nu_s(ClO_4)$
894 s	892 ms	892 s	893 s	898 ms	895 ms	9 (αC-D)
				892 ms		
870 m	869 w	870 w	871 vw	870 vw	871 m	31 (αC-D)
853 m	-	854 m	854 m	854 m	854 m	8 (αC-D)
840 w	-	833 w	834 w	836 w	838 w	30 (νring) and 7 (νring)
816 w	815 m	818 w	818 w	818 vw	817 w	6 (νring) and 29 (νring)
793 m	782 m	790 m	789 m	792 m	792 s	5 (νring)
				787 m		
772 vw	-	769 vw	767 vw	768 vw	772 vw	46 (γC-D)
761 vw	-	-	-	-	761 vw	58 (γC-D)
750 vw	-	-	-	-	750 vw	48 (γC-D)
735 m	730 m	733 m	733 mw	732 mw	736 wm	28 (νring)
722 m	722 msh	722 m	722 mw	721 w	722 w	48 (γring)
691 s	694 s	692 s	694 s	699 s	692 s	27 (νring)
				689 s		
675 vw	677 wsh	-	-	674 vw	673 vw	60 (γC-D)
667 vw	663 w	668 vw	667 vw	669 vw	667 vw	4 (νring)
				662 w		
640 s	636 s	639 s	639 s	638 s	637 s	49 (γC-D)
		634 m	632 s	630 s	631 ssh	50 (γring)
623 s	621 vs	623 s	623 s	623 s	624 s	$\delta(ClO_4)$
594 ms	590 ms	596 ms	595 s	592 s	595 s	51 (γC-D)
541 w	542 w	540 vw	540 vw	541 vw	543 w	26 (νring)
482 vw	494 w	482 vw	483 vw	483 vw	483 vw	25 (νring)
	478 w			471 vw		
453 w	459 w	458 w	461 w	460 w	457 w	52 (γring)
409 m	413 w	412 m	413 m	411 m	410 m	2 (νring)

see footnote of Table 4.3

	bipy		Mn		Fe			Co		Ni			Cu			Zn			Assignment	
	$-d_0$	$-d_8$	$-d_0$	$-d_8$	$-d_0$	$-d_8$	$^{54/57}\Delta$ Fe[a]	$-d_0$	$-d_8$	$-d_0$	$-d_8$	$^{58/62}\Delta$ Ni[a]	$-d_0$	$-d_8$	$^{63/66}\Delta$ Cu[a]	$-d_0$	$-d_8$	$^{64/68}\Delta$ Zn[a]	Previous[a]	This Work
6a	620	(603)	623 s	(623 vs)	623 s	(622 vs)		623 s	(623 vs)	623 s	(623 vs)		623 s	(623 vs)		623 s	(623 vs)			δClO_4
6b'	614	(728)		(608 m)		(masked)			(610 m)		(611 m)			(617 w) (606 w)			(609 m)			6a (νring)
			550 vw	(472 vw)	550 vw	(472 vwsh)		550 vw	(470 vw)	-	(478 vw)		550 vw	(477 vw)		-	(475 vw)			comb
			-	(462 vw)	497 w	(464 w)		481 w	(457 vw)	483 w	(458 vw)		498 w 481 w	(454 wm)		494 w	(459 vw)			comb
E	440	(414)	467 w	(444 vw)	475 w	(444 w)		465 w	(446 vw)	465 w	(448 w)		-	(-)		478 w	(443 vw)			E (ring scissors)
Γ	413	(385)	-	(432 vw)	456 w	(426 vw)		458 vw	(431 vw)	458 vw	(439 vw)		458 w	(437 vw)		459 w	(430 vvw)			Γ (ring shear)
16b	415	(388)	424 w	(392 w)	438 wsh	(397 w)		439 m	(400 wm)	439 m	(405 m)		441 m 423 m	(403 wm) (389 wm)		428 ms	(396 m)		ligand A	16b (Yring)
16a	403	(369)	412 m	(364 ms)	418 ms	(368 ms)	(+0,1)	413 ms	(365 ms)	413 ms	(366 s)		410 ms 393 mwsh	(376 msh) (367 ms)		413 s	(364 s)		ligand A	16a (Yring)
					382 wm		(+6,0)													
			365 wsh	-	372 w	(353 mw)	(+5,2)	365 wsh	(-)	361 w	(345 w)	(-0,6)	365 vw	(-)	(+0,2)	365 vw	(-)		ligand B	comb
6a'	330	(315)	355 w	(343 w)	-	(325 w)		356 w	(345 w)				357 vw 349 w	(352 wm)	(+0,1) (+0,2)	358 vw	(355 wsh)	(+0,5)	ligand B	6a' (νring)
										293 ms	(289 m)	(+7,1)	286 m	(279 m)	(+2,7)					
			280 vw	(275 vw)	285 m	(285 m)		280 wm	(275 wm)	281 m	(276 m)	(+5,4)	271 m	(264 wm)	(+1,3)	262 w	(245 w)	(+0,3)	ligand C	νM-N + comb
								264 m	(257 wm)	266 w	(264 w)	(+7,3)	266 msh		(+2,0)					
16b'	236	(210)	(masked)		247 wsh	(240 wbr)	(-0,6)	249 w	(-)	256 wsh	(236 w)		255 w	(237 w)	(+0,0)	248 wsh	(232 wmsh)	(+0,0)	ligand D	16b' (Yring)
			241 ms	(239 m)	241 w			231 w	(229 w)							235 ms	(223 ms)	(+2,5)	ligand D	νM-N
			206 wm	(204 wm)									217 w	(204 w)	(+0,0)				ligand E	δNMN
								206 vw	(-)	215 vw	(200 vw)	(+1,0)	209 wsh	(198 w)	(+0,0)					
			190 w	(179 vwsh)	192 w	(184 w)	(+0,0)			183 w	(174 vwsh)		199 wm	(189 w)	(+0,8)	188 m	(180 mw)	(+3,5)	ligand E	δNMN
B	165	(149)	169 w	(171 w)	165 vw	(-)		175 sh	(169 w)	177 vvw	(170 w)		175 wm	(164 w)	(+0,0)	170 w	(171 wsh)	(+0,1)	ligand F	B (ring shear)
								166 w	(160 vw)	162 w	(154 w)	(+0,5)	163 wm	(154 wm)	(+0,0)	161 vw	(154 vw)			
			150 wsh	(139 wm)	149 vw	(143 w)		150 w	(143 w)	147 w			151 vw	(-)		145 vw.	(139 w)			δNMN
			140 wsh	(133 wsh)									138 vw	(130 wsh)		125 vvw				
Δ	117	(99)	118 vvw	(-)	110 vw	(100 wsh)		-	(-)	116 wsh	(-)		116 w	(107 wsh)		109 vw	(-)			Δ (ring scissors)
Z	95	(66)	-	(-)	99 w	(84 w)		-	(89 wsh)	95 vwsh	(90 wsh)		98 wm	(90 wm)		95 wsh	(-)			Z (i. rotation)
			82 wsh	(83 wsh)	79 wsh	(75 w)		83 wsh	(80 wsh)	82 w	(80 wsh)		-	(83 wm)		80 wsh	(78 wsh)			δNMN or lattice
			67 w	(69 w)	66 w	(65 w)		68 w	(69 m)	67 w	(68 m)		65 w	(66 wm)		67 w	(69 m)		lattice	
			56 wsh	(56 wsh)	60 wsh	(-)		59 wsh	(57 wsh)	59 wsh	(59 wsh)		56 w	(-)		-	(-)		lattice	

(a) from NAKAMOTO and his co-workers [23-25]

N.B. $-d_8$ bands at 590cm^{-1} (medium strong) and 585cm^{-1} (strong) not included as they arise from $-d_0$ bands (modes 1' and 11) above 630cm^{-1} (see Tables 4.1 and 4.2)

Table 4.5 Far infrared assignment (625-50cm^{-1}) of $[M(bipy)_3](ClO_4)_2$ complexes and their fully deuterated analogues

phen			Mn		Fe			Co		Ni			Cu			Zn			Assignment	
	$-d_0$	$-d_8$	$-d_0$	$-d_8$	$-d_0$	$-d_8$	$^{54/57}\Delta$ Fe[a]	$-d_0$	$-d_8$	$-d_0$	$-d_8$	$^{58/62}\Delta$ Ni[a]	$-d_0$	$-d_8$	$^{63/65}\Delta$ Cu[a]	$-d_0$	$-d_8$	$^{64/68}\Delta$ Zn[a]	Previous[a]	This Work
26	623	(536)	623 s	(623 s)	623 s	(622 s)		624 s	(623 s)	623 s	(623 s)		**623** s	(623 s)		623 s	(624 s) (595 s)			$\delta(ClO_4)$
62	605	(507)	556 vw	(541 w)	560 w	(542 w)		558 vw	(540 vw)	559 vw	(540 vw)		**557** vw	(541 vw)		558 w	(543 w)			3 (νring)
3	552	(536)	543 vw	(-)	548 vwsh	(-)		546 vw	(-)	547 vw	(-)		**546** vw	(-)		547 vw	(-)			
			527 vvw	(-)	531 wm 526 wm	(-)		-	(-)	529 vvw	(-)		-	(-)		531 vw	(-)			comb
52	509	(444)	512 vw	(453 w)	511 vw	(469 vw)		511 vw	(458 w)	511 vw	(461 w)		**511** w	(460 w)		512 w	(457 w)			52 (νring)
25	499	(480)	500 vw		-	(495 vw)		-	(-)	-	(-)		**507** vwsh	(-)		500 vwsh	(-)			63 (νring)
63	499	(428)	477 vw	(482 vw)	484 vw	(482 w)		482 vw	(482 vw)	485 vw	(483 vw)		**489** vw **478** vw	(483 vw) (471 vw)		482 vw	(483 vw)			25 (νring)
53	457	(369)	457 vw	(369 vw)	464 vw	(364 vw)		458 vw	(370 vvw)	-	(372 vvw)		**458** vvw	(372 vvw)		458 vvw	(372 vvw)			53 (νring)
24	427	(399)	438 vwsh	(masked)	439 vw	(masked)		441 vw	(masked)	446 vw	(masked)		-	(masked)		437 vw	(masked)	(+0,0)	ligand A	24 (νring)
64	411	(350)	421 m	(409 m)	426 m	(437 m)		425 wm	(412 m)	426 m	(413 m)	(-0,1)	**422** wm	(411 m)		423 m	(410 m)	(+0,0)		2 (νring)
2	402	(385)	394 vvw	(369 wv)	-	(398 w)	(+4,4)	406 vw	(370 vvw)	395 vw	(372 vvw)		**392** vw	(372 vvw)		-	(372 vvw)			64 (νring)
			366 vvw	(-)	360 vvw	(363 w)	(+6,3)	-	(-)	366 vvw	(-)		**366** vvw	(-)		-	(-)			comb
			-	(-)	-	(339 w)		-	(-)	338 vvw	(-)		**334** vvw	(-)		-	(-)			
65	253	(254)	276 w	(260 wm)	293 m	(281 m)	(+0,0)	288 m	(275 m)	300 m	(288 m)	(+2,3)	**301** w	(306 vw) (286 w)	(+0,5)	285 wm	(271 mw)	(-0,5)	ligand B	65 (νring)
54	245	(203)	-	(-)	271 w	(237 wm)	(-0,6)						**286** wm	(273 w)	(+0,2)	255 vw	(241 w)			54 (νring)
										258 wm	(247 w)	(+3,9)	**267** w	(255 w)	(+1,5)				ligand C	νM-N
								237 m	(239 wm)	246 wm		(+2,8)	**246** wm	(236 vw)	(+2,0)					
1	203	(229)	236 w	(-)	244 w	(220 wm)	(+0,0)		(217 w)	236 wsh	(219 w)	(+0,9)		(217 w)		242 w	(217 w)	(+0,0)		1 (νring)
			219 m	(217 m)	212 mw	(198 wsh)	(+0,2)													νM-N + δNMN
			200 wm	(201 wsh)	192 wsh	(185 wsh)	(+0,1)				(-)	(-0,5)	-	(191 vw)	(+0,0)	192 m	(191 m)	(+4,0)		
					175 vw	(-)	(+0,0)	179 w	(170 vw)	189 w	(178 w)	(-0,5)	**180** wm	(172 mw)		176 w	(170 vw)	(+3,0)	ligand D	
66	[144]	(150)	159 wsh	(151 wsh)	155 vwsh	(144 w)		153 w	(143 vw)	160 w	(152 vw)	(+0,5)				159 w	(149 vw)	(+0,0)		66 (νring)
			147 w	(139 w)									**147** w	(141 mw)	(+0,0)	144 w	(143 wsh)		ligand E	δNMN
													-	(135 mw)						
55	122	(116)	-	(-)	-	(117 w)		127 vvwsh	(123 vw)	136 vw	(128 vw)		-	(129 wsh)		-	(-)			55 (νring)
			-	(-)	117 wbr	(103 w)		-	(108 vwsh)	109 vw	(105 vwsh)		**105** vw	(108 vwsh)		109 vw	(107 vw)			δNMN
			80 wsh	(90 wsh)	77 w	(78 w)		76 wm	(72 wsh)	76 w	(72 w)		**72** wsh	(77 mw)		78 wbr	(78 w)			
			70 w	(77 w)	66 w	(62 wsh)		63 w	(65 w)	65 w	(62 wsh)		**68** w	(69 mw)		65 wsh	(59 wsh)			lattice
			54 w	(55 wsh)	-			-	(55 wsh)	-	(-)		-	(-)		-	(-)			

(a) from NAKAMOTO and his co-workers [23-25]

N.B. $-d_8$ band at 595cm^{-1} (strong) is not included as it arises from $-d_0$ band (mode 51) above 630cm^{-1} (see Tables 4.3 and 4.4)

Table 4.6 Far infrared assignment (625-50cm^{-1}) of $[M(phen)_3](ClO_4)_2$ complexes and their fully deuterated analogues

either strong or weak N-O or C-X sensitivity.

In bipy and its -d_8 analogue, several ring modes show metal sensitivity - 19a, 19a', 19b(-d_0), 16b, 16b', 16a, 14(-d_0), 12(-d_0), 12', 8b, 8b', 6a(-d_8), 6b(-d_0), 1 and 1'. Five C-H bends, modes 18b, 15(-d_0), 15'(-d_0), 10b'(-d_8), and 9b(-d_8), and two C-H stretches at 3070cm^{-1} (degenerate vibration) and at 3080cm^{-1} (mode 20b) show metal sensitivity. Three of the non-benzenoid inter-ring vibrations, modes B(-d_0), Γ(-d_8) and E(-d_8) show metal sensitivity. The poor resolution of the far-infrared prevents an examination of the metal sensitivity of the lowest two inter-ring modes. The metal sensitivity of these modes may be understood in light of their N-O and inter-ring sensitivity of bipyO_2. The loss or acquisition of metal sensitivity on deuteration reflects a change in the kinematic coupling and is similar to the loss of metal sensitivity by mode 6a in py-d_5 [44].

Kinematic coupling between the ligand modes and the M-N vibrations in the phen complexes is not as extensive, showing fewer metal sensitive bands. Metal sensitive ring modes are modes 65, 54, 52(-d_8), 28(-d_0), 25, 24(-d_0), 12(-d_0), 5(-d_8), 4(-d_8) and 2(-d_8). One C-H stretch (mode 23), two planar C-H bends (modes 34 and 9) and one out-of-plane C-H bend (mode 48) show metal sensitivity in the phen-d_0 complexes.

With the JAHN-TELLER distortion experienced by the Cu(II) complexes, the localised symmetry of the ligand is altered to yield two different ligand environments, thereby presenting a potential for splitting of the ligand bands. From Tables 4.1 and 4.2 a number of such split bands are observed in the complexes with bipy-d_0 and bipy-d_8, including mode 6b(-d_0) which accounts for the splitting of the 625,660cm^{-1} bipy doublet noted by INSKEEP. Those bands which show this splitting are generally metal sensitive. It is also of in-

terest that the inter-ring stretch, mode $A(-d_0)$ shows splitting as a result of JAHN-TELLER distortion.

The $[Cu(phen)_3](ClO_4)_2$ complex shows only three split bands, namely modes 48 (δC-H), 28 (νring) and 25(νring) (Table 4.3). Since the infrared spectra of this complex is extremely rich it is not surprising that in the absence of a complete vibrational assignment this evidence for tetragonal distortion was overlooked. The phen-d_8 complex shows twice as many bands which are sensitive to tetragonal splitting; these being modes 64(γring), 27(νring), 9(αC-H), 5(νring) and 4(νring). Again, these are generally metal sensitive bands.

Finally, of the fifteen metal-ligand vibrations, three infrared active M-N stretches (A_2 and $2E$) and four M-N bends (A_2 and $3E$) are theoretically expected for D_3 symmetry, while the full six stretches ($3A$ and $3B$) and nine bends ($5A$ and $4B$) are expected for the tetragonal Cu(II) complexes. Site and correlation field splitting of the bands into several components is not expected in these complexes because of the large size of the ligands [46].

The assignment of the metal-ligand vibrations is made difficult because of the presence in both series of low lying ligand bands in this region, as well as the sensitivity of the metal-ligand bands to the Crystal Field Stabilisation Energy. The assignment of the M(II) tris-bipy and tris-phen complexes below 625cm^{-1} are given in Tables 4.5 and 4.6. These have been based upon the assignment of the ligand bands, upon their metal sensitivity and upon deuteration and metal isotope sensitivity.

The metal-nitrogen stretches are found in the region 400 to 180cm^{-1} for both series and, with the exception of Fe(II), follow the IRVING-WILLIAMS sequence (namely Mn<*Fe*<Co<Ni>Cu Zn). The M-N stretches for Fe(II) are some 90 to

150cm^{-1} higher than the other metals as a result of their greater CFSE, being low spin complexes [35].

Within the bipy complexes all three of the expected infrared active M-N stretches are observed. Their assignment is complicated by the presence in this region of two ligand bands at *ca.* 355cm^{-1}($-d_0$) and at *ca.* 250cm^{-1}($-d_0$) (being modes 6a' and 16b') and of a combination or difference band at 280cm^{-1}($-d_0$) (Table 4.5). Indeed mode 6a' was assigned as a metal-nitrogen stretch by PERCY and THORNTON [35] based upon its metal sensitivity.

Within the phen complexes, generally only two of three expected M-N stretches are observed (Table 4.6). This is no doubt due to accidental degeneracy with an incomplete resolution of the bands. The presence of twice as many combination bands (at 340cm^{-1} and 370cm^{-1}) and twice as many ligand bands at 390cm^{-1}($-d_0$), 285cm^{-1}($-d_0$), 260cm^{-1}($-d_0$) and 240cm^{-1}($-d_0$) (being modes 64, 65, 54 and 1 respectively) makes the νM-N assignments more difficult than is the case for the bipy complexes. Consequently, with the stretching frequencies lying below the frequency range examined, PERCY and THORNTON incorrectly assigned the ligand modes 1 and 65 as νM-N for the metals Mn and Zn [35]. A further such difficulty is observed in the Cu(II) complex for which the bands at 301cm^{-1} and 286cm^{-1} might also be considered as highly coupled νM-N (particularly the former in light of its metal isotope sensitivity) rather than as ligand modes 65 and 54.

The metal-nitrogen bends show less metal sensitivity than the stretches as shown by the Fe(II) frequencies being only some 30 to 70cm^{-1} higher than the other metals. These bends are found in two ranges. The highest bends are found between 240 and 140cm^{-1} in both metal series. In ML_6 heterocyclic complexes the two lowest δM-N vibrations occur at *ca.* 100cm^{-1} and at *ca.* 80cm^{-1}

[7], and since chelation causes the M-N bends to be found at slightly higher frequencies than for monodentate complexes [47], the lowest δM-N is assigned to the band at 150 to 125cm^{-1} in the bipy complexes and at 115 to 105cm^{-1} in the phen complexes. The band at 80 to 70cm^{-1} (both series) which is the highest lattice vibration may also mask the lowest δM-N for the Mn and Zn complexes. Of the 4 δM-N expected, two to four are observed depending upon the metal. (For Mn and Zn only two of the bends are clearly identified in both series). The assignments of these bends are complicated by the presence of three ligand modes (modes B, Δ and Z) for bipy and two ligand modes (modes 66 and 65) for phen (Tables 4.5 and 4.6).

It is necessary to comment on the behaviour of the Cu(II) complexes with bipy and phen. Six M-N stretches and nine bends are expected for C_2 symmetry; however, only three stretches and six bends are observed for the Cu(bipy)$_3$ cation and two stretches (with a possible third) and five bends are observed for the Cu(phen)$_3$ cation. It is therefore clear that the splitting of the M-N fundamentals expected for tetragonal distortion does not occur for the stretches, although it does for some of the bends. This may be accounted for by the stretching modes being accidentally degenerate and hence not fully resolved. Support for this suggestion is obtained from the infrared and Raman spectra of the Zn tris-phen complex in which the polarised Raman line at 286cm^{-1} has a strong infrared counterpart at 288cm^{-1}, which is evidence that the symmetric and antisymmetric Zn-N stretches are degenerate [48]. The infrared and Raman spectra of the Ru tris-bipy cation reveals the same situation [16].

In conclusion, the fully deuterated ligand study has enabled a full assignment of the low lying frequencies of the M(II) tris-bipy complexes and their phen analogues. It has allowed a more complete assignment of the 'ligand

vibrations' made by NAKAMOTO and his co-workers [23-25] (Tables 4.5 and 4.6).

Indeed, some of the 'ligand bands' identified by these authors have been found to consist of two ligand modes, *e.g.* Ligand A in bipy complexes is more correctly identified as modes 16a and 16b, while for the phen complexes Ligand A consists of modes 2 and 24, and Ligand C is more correctly modes 1 and 54. Of these 'ligand bands' previously considered as activated ligand vibrations, some have been clearly identified (*e.g.* Ligand D in the bipy complexes is mode 16b') while others are identified as consisting of two vibrations, *e.g.* Ligand B (in bipy complexes) is identified as being a combination band and mode 6a, with Ligand F consisting of mode *B* and a δM-N, while in the phen complexes Ligand D describes the ligand mode 66 and a δM-N. Some of the bands considered by NAKAMOTO and his co-workers to be activated ligand bands are clearly incorrectly assigned and instead are M-N bends, *e.g.* Ligand E in the bipy complexes and Ligand E in the phen complexes. The two lowest-lying ligand modes in the bipy complexes (modes Δ and Z) and the lowest mode in the phen complexes (mode 55) have been newly identified, being found at frequencies lower than previously investigated.

Finally, the present deuteration study in conjunction with previous metal-isotope studies [23-26] show that the M-N fundamentals are coupled vibrations, corroborating the kinematic coupling experienced by some of the ligand vibrations.

1.2 M(II) complexes with bipyO$_2$ and its fully deuterated analogue

The employment of bipyO$_2$ as a ligand has been fairly extensive [49], although no isotope spectroscopic study has yet been reported. Several studies of M(II) tris-bipyO$_2$ complexes for the metals Mn, Co, Ni, Cu and Zn are to be

found in the literature [50-54]. Of these only in the works of VINCIGUERRA *et al.* [51] and by AHUJA and SINGH [53] are νM-O assignments made. No assignment of the vibrations below the M-O stretches are to be found in the literature, hence the importance of the present study.

$BipyO_2$ coordinates through both oxygens in these complexes, to yield a stable seven membered chelate ring in which the two pyridal rings are twisted through a dihedral angle of some 67° [55]. The M-O-N angle in $[Ni(bipyO_2)_3](ClO_4)_2$ is calculated to be 117° [55]* which is typical of an aromatic *N*-oxide. While this angle is generally accepted as evidence for sp^2 hybridisation of the oxygen (*i.e.* the two lone pairs plus the N-O bond pair, with the third lone pair in a *p* orbital for π-interaction with the pyridine ring) and so indicating a significant contribution of the canonical form *II* in the complex, NG *et al.* [57] disagree.

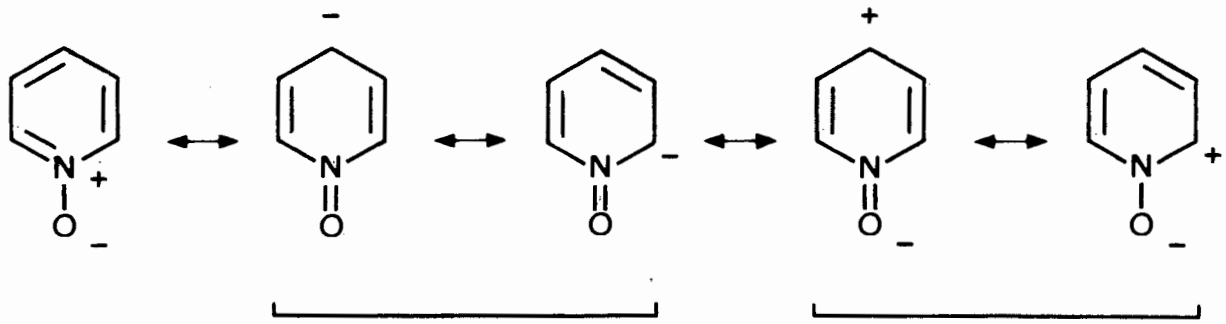

I *II* *III*

They note that if the π-interaction is important then the planes of the M-O-N and the pyridine ring should be coincident. Since this orientation is between 34° and 93° for a wide range of pyO complexes which have been crystallographically examined, NG *et al.* recently suggested that this is evidence of distorted sp^3 hybridisation, resulting from the fact that forcing the M-O-N

---

* In $[La(bipyO_2)_4](ClO_4)_3$ the M-O-N angle is crystographically determined to be 123° [56].

and pyridine rings into coincidence would maximise the steric interference of the aromatic ring with the other ligands on the metal atom [57].

Delocalisation of the second lone pair at the oxygen into the aromatic ring is retarded on the grounds of the poor geometry and energetics involved, considering the high *s* character of the oxygen orbital [57,58]. Furthermore, overlap of the second lone pair with the acceptor of the metal atom is said to be energetically poor since a positive charge on the nitrogen would reduce electron flow from the oxygen [57,58].

The *N*-oxides are therefore poorer π acceptors and weaker δ donors compared with the imine parents. As a result $bipyO_2$, while giving rise to a stronger ligand field than that of pyO (being bidentate), does not have sufficient field strength to cause the spin-pairing that is found for bipy and phen [49,52,54] (Table 4.7). Any metal sensitive vibration in the M(II) complexes with $bipyO_2$ are then expected to follow more exactly the IRVING-WILLIAMS series (Mn<Fe<Co<Ni<Cu>Zn). In particular the Fe(II) is expected to be high spin as is the complex $[Fe(pyO)_6](ClO_4)_2$.

	low spin			high spin	
ligand	quinO	pyO	$bipyO_2$	py	bipy
$10Dq\,(cm^{-1})$[(a)]	7900	8400	8600	11500	11500
Reference	[59]	[52]	[52]	[52]	[52]

(a) For Ni^{2+} cation

Table 4.7 Literature values of $10Dq$ for several imines and their *N*-oxides

$[Fe(bipyO_2)_3](ClO_4)_2$ has not been reported in the literature and repeated attempts to prepare this complex and its fully deuterated analogue were unsuccessful as the infrared spectrum clearly showed oxidation to Fe(III) (two νM-O at 412cm^{-1} and 380cm^{-1}; Literature 408cm^{-1} and 377cm^{-1} for the Fe(III) $(bipyO_2)_3$ cation [51]). A further difficulty experienced is the ability for the Fe(III) complex to be formed with more than three moles of $bipyO_2$ per mole of iron [52].

The full vibrational assignments of the M(II) complexes of $bipyO_2$ and their fully deuterated analogues are presented in Tables 4.8 and 4.9. The far-infrared assignments (below 625cm^{-1}) reflecting the deuteration shifts are presented in Table 4.10.

As is observed for the bipy and phen complexes the bands arising from a common origin within the localised ligand symmetry are not completely resolved. Excluding the Cu(II) complexes, only three bands (these being νN-O, modes 7a' and 7a, and γC-H mode 11) are split in the $bipyO_2$ complexes, while only one is split in the bipy-d_8O_2 complexes (the νring mode 19b).

Several fundamentals reflect metal sensitivity; modes 18a(-d_8), 18b(-d_0), 17a, 16b'(-d_8), 14(-d_8), 6a and 6b. The non-benzenoid inter-ring modes Γ, Δ, E and Z also show metal sensitivity in $bipyO_2$. The inter-ring stretch, mode A, does not reflect metal sensitivity, while the last inter-ring mode B is masked by the highest M-O stretch. Two combination bands at *ca.* 1940cm^{-1} (-d_8) and 1840cm^{-1}(-d_0) also reveal metal sensitivity, which is most probably a result of their components being one of the metal sensitive fundamentals mentioned.

The tetragonal JAHN-TELLER distortion experienced by the Cu(II) complex with

Table 4.8 Infrared assignment (4000-400cm^{-1}) of $[M(bipyO_2)_3](ClO_4)_2 \cdot 1\frac{1}{2}H_2O$ complexes

Mn	Co	Ni	Cu	Zn	Assignment
3596 mbr	3592 mbr	3591 mbr	3562 mbr	3596 mbr	$\nu O\text{-}H_{(H_2O)}$
3512 mbr	3506 mbr	3480 mbr	3460 mbr	3511 mbr	
3220 vw	3220 vvw	-	3220 vvw	3220 vvw	comb
3123 m	3123 m	3128 m	3128 m	3125 m	20a (νC-H)
3105 m	3107 m	3092 ms	-	3109 m	20b (νC-H)
3092 msh	3087 msh		3088 ms	3095 m	20a' and 20b' (νC-H)
3057 msh	3060 msh	3060 m	3059 m	3060 m	2 (νC-H)
3051 m	3045 m	-	-	3050 m	2' and 7b' (νC-H)
3034 mwsh	-	3038 msh	3038 msh	-	7b' (νC-H)
2986 vw	2990 w	2988 wsh	2990 w	2988 wsh	
2920 vw	2930 w	2930 w	2923 w	2928 w	
2860 vw	2856 w	2856 w	2860 w	2855 w	
2783 w	2788 w	2783 w	2783 w	2782 w	
2733 vw	2730 vw	2732 vw	2730 vw	2735 vw	
2651 w	2638 w	2642 vw	2640 vw	2652 w	
2455 wsh	2464 wsh	2456 wsh	2460 w	2455 w	
2425 w	2418 wbr	2416 w	2410 w	2424 w	comb
2333 vw	2320 vw	2329 vw	2329 vw	2333 vw	
2266 vw	2263 w	2264 w	2265 w	2267 w	
2046 wm	2036 wm	2039 wm	2033 wm	2042 wm	
2005 wbr	2005 w	2006 w	-	2008 wbr	
1957 w	1954 w	1956 w	1960 w	1960 wsh	
1918 vw	1918 vw	-	-	1918 w	
1842 w	1845 w	1842 w	1848 w	1841 w	
1628 mbr	1626 mbr	1630 mbr	1637 w	1631 mbr	$\nu O\text{-}H_{(H_2O)}$ and 8a' (νring)
			1626 mbr		
1605 w	1606 wsh	1605 wsh	1602 w	1604 wsh	8b' (νring) and 8a(νring)
1573 w	1572 w	1574 w	1574 w	1574 w	8b (νring)
1506 wm	1506 w	1505 w	1505 w	1505 w	19a' (αC-H)
1479 s	1474 s	1447 s	1480 ssh	1474 s	19a (αC-H)
			1474 s		
1441 s	1440 s	1442 s	1440 s	1442 s	19b' (αC-H)
1426 s	1424 s	1425 s	1425 s	1426 s	19b (αC-H)
1370 vw	1375 vw	1370 vw	1375 vw	1368 vw	3' (αC-H)
1313 vw	1317 w	1317 vw	1316 vw	1317 vw	14' (νring)
1293 w	1292 w	1292 w	1290 w	1293 w	A (νinter-ring)

Table 4.8 (continued)

Mn	Co	Ni	Cu	Zn	Assignment
1257 ms	1258 ms	1258 ms	1257 ms	1258 ms	14 (ν ring)
1232 vw 1226 vssh	1231 ssh 1221 vs	1223 vs	1231 vs	1229 s	7a' (νN-O/ν ring)
1216 vs	1211 vssh 1203 vs	1211 vs	1216 vs 1209 vs	1211 vs	7a (νN-O/ν ring)
1164 s	1165 s 1163 s	1163 s 1161 s	1158 s	1166 ssh 1163 s	15' (αC-H) 15 (αC-H)
-	1111 ssh	1111 ssh	1110 ssh	1110 ssh	9b' (αC-H)
1095 vsbr -	1090 vsbr 1061 ssh	1088 vsbr 1060 ssh	1085 vsbr 1057 ssh	1083 vsbr 1056 ssh	$\nu_a(ClO_4)$ and 9b (αC-H)
-	1050 msh	1048 msh	1049 msh	1048 msh	18b' (αC-H)
1032 m	1032 m	1035 m	1033 m	1033 m	18b (αC-H)
1004 w	1005 mw	1003 mw	1004 mw	1003 m	1 (ν ring)
965 wsh 961 m	962 w	962 w	964 w 952 w	959 w	5' (γC-H) 5 (γC-H)
930 w	930 w	932 w	931 w	932 w	$\nu_s(ClO_4)$
925 wsh	927 wsh	929 w	-	-	10b' (γC-H)
890 w	891 vw	889 vw	891 vw	885 vw	10b (γC-H)
849 s	847 s	848 s	848 s	848 s	12 (ν ring/νN-O)
835 s	834 s	835 s	834 s	834 s	12' (ν ring/νN-O)
787 msh	788 msh	787 msh		786 msh	11' (γC-H)
779 vs 773 vs	780 vs 776 vs 773 vs	780 vs 776 vs	775 vsbr	775 vs	11 (γC-H)
750 w	751 w	752 w	751 w	751 w	1' (ν ring)
733 m	733 m	733 m	732 w	733 w	4' (γ ring)
725 ms	726 s	723 ms	723 ms	722 ms	4 (γ ring)
639 w	638 w	638 w	637 w	639 w	comb
623 s	624 s	624 s	623 s	624 s	$\delta(ClO_4)$
584 s	582 s	584 s	582 s	581 s	6a (ν ring)
559 w	559 w	559 w	559 w	560 w	comb
540 s	542 m	542 m	546 mw	539 ms	6b (ν ring)
527 m	-	-	531 mwsh	-	6b' (ν ring)
517 s	518 s	518 s	518 s	518 s	16b and 16b' (γ ring/γN-O)
481 m	479 m	479 m	479 m	479 m	18a' (αN-O)
452 s	453 s	452 s	452 s	452 s	18a (αN-O)

see footnote of Table 4.9

Table 4.9 Infrared assignment (4000-400cm^{-1}) of $[M(bipy\text{-}d_8O_2)_3](ClO_4)_2 \cdot 1\frac{1}{2}H_2O$ complexes

Mn	Co	Ni	Cu	Zn	Assignment
3597 wbr	3593 wbr	3593 wbr	3496 wbr	3593 wbr	νO-H$_{(H_2O)}$
3512 wbr	3506 wbr	3506 wbr	3512 wbr	3509 wbr	
3135 vw	3150 vw	3160 vw	1352 vw	3150 vw	
-	2950 vw	-	2956 vw	2950 vw	
2917 vw	2923 w	2920 vw	2924 w	2920 w	comb
-	2852 w	-	2846 w	2850 w	
2778 vw	2779 w	2771 vw	2778 w	2776 vw	
2503 vw	2496 w	2497 w	2500 w	2504 w	
2323 wm	2323 wm	2325 wm	2324 w	2324 w	20a (νC-D)
2309 wsh	2308 w	2307 wm	2309 wm	2309 w	20b and 20a' (νC-D)
2290 wsh	2285 wsh	2287 wm	2290 w	2285 wsh	20b' and 2' (νC-D)
2283 w	2280 wm	2279 wm	2281 w	2281 w	2 and 7b (νC-D)
2185 w	2185 vw	2190 wv	-	-	
-	2110 vw	2113 vw	2115 vw	2119 w	
2045 w	2040 wsh	2045 wsh	2040 wsh	2048 w	comb
-	2020 w	2018 w	2022 w	2016 w	
-	1944 w	1948 w	1946 w	1943 w	
1920 w	-	1916 w	1920 w	1917 w	
1628 ms	1626 ms	1627 ms	1626 ms	1627 ms	δO-H$_{(H_2O)}$ and 8a' (νring)
1575 w	1574 w	1574 w	1574 w	1575 w	8a and 8b (νring)
1542 m	1543 m	1544 m	1543 m	1544 m	8b (νring)
1438 mw	1438 mw	1439 mw	1439 mw	1439 m	19a' (νring)
1391 wsh	1391 vwsh	1390 vwsh	1392 wsh	1393 wsh	comb
1370 ms	1369 s	1369 s	1370 s	1370 s	19b' (νring)
1350 s	1350 vs	1351 vs	1349 s	1351 s	19a (νring)
1330 ssh	1321 vs	1323 vs	1332 ssh	1332 ssh	19b (νring)
1324 s			1322 vs	1326 vs	
1310 w	-	-	-	1308 mwsh	14' (νring)
1224 mw	1226 mw	1227 wm	1226 wm	1226 wm	14 (νring)
1207 s	1207 ms	1208 ms	1207 ms	1208 ms	A (νinter-ring)
1179 vs	1174 ssh	1176 ssh	1187 msh	1173 vs	7a' (νN-O/νring)
			1172 vs		
1175 vs	1166 vs	1173 vs	1166 vs		7a (νN-O/νring)
1110 ssh	-	1109 ssh	1111 ssh	1113 ssh	
1098 vsbr	1095 vsbr	1094 vsbr	1094 vsbr	1094 vsbr	$\nu_a(ClO_4)$ and 3'(αC-D)
			1080 vssh	1084 vssh	
		1056 ssh	1050 mssh	1055 ssh	

Table 4.9 (continued)

Mn	Co	Ni	Cu	Zn	Assignment
1024 w	1025 mwsh	-	1025 wsh	-	3 (αC-D)
1010 ms	1010 ms	1010 ms	1010 ms	1009 ms	1 (νring)
929 w	930 w	930 w	930 w	930 w	$\nu_s(ClO_4)$
926 vwsh	926 w	926 w	926 wsh	926 wsh	
881 s	879 s	880 ssh	880 s	880 s	9b' (αC-D)
874 s	873 s	873 s	874 s	874 s	9b (αC-D)
864 w	864 w	864 w	864 w	864 w	15' (αC-D)
850 w	850 w	850 w	850 w	850 w	15 (αC-D)
835 m	835 ms	833 m	835 m	835 m	5 (γC-D)
824 w	824 w	825 w	824 w	825 w	18b' (αC-D)
791 s	788 s	789 s	788 s	789 s	18b (αC-D)
776 vs	776 s	776 s	776 vs	776 vs	12 (νring/νN-O)
765 s	766 m	766 m	766 ms	766 ms	12' (νring/νN-O)
738 m	740 w	738 w	739 w	740 w	10b' (γC-D)
723 m	723 w	723 w	722 w	723 w	10b (γC-D)
688 wm	688 wm	687 wm	688 wm	687 wm	1' (νring)
650 wm	651 wm	650 wm	651 wm	651 wm	10a (γC-D)
640 wsh	639 w	639 w	639 vw	637 w	10a' (γC-D)
625 vs	624 vs	622 vs	622 vs	622 vs	$\delta(ClO_4)$ and 4 (γring)
619 ssh	619 ssh	617 ssh	616 ssh	617 ssh	11 (γC-D)
611 s	611 s	609 s	611 s	611 s	4 (γring)
566 ms	566 ms	565 s	566 s	564 s	6a (νring)
556 vs	556 vs	557 vs	556 vs	556 vs	11' (γC-D)
509 s	505 ssh	506 ssh	504 s	507 s	6b (νring)
501 s	502 s	501 s		499 s	16b (γring) and 6b' (νring)
472 s	477 wm	476 wm	477 wm	475 wm	16b' (νring)
444 vw	443 vw	443 vw	443 w	442 vw	18a' (αN-O)
419 s	420 s	419 s	417 s	416 s	18a (αN-O)

s = strong

m = medium

w = weak

v = very

sh = shoulder

br = broad

comb = combination

	bipyO$_2$		Mn		Co		Ni		Cu		Zn		Assignment
	$-d_0$	$-d_8$	$-d_0$	$-d_8$	$-d_0$	$-d_8$	$-d_0$	$-d_8$	$-d_0$	$-d_8$	$-d_0$	$-d_8$	
			623 s	(625 vs)	624 s	(624 vs)	624 s	(622 vs)	623 s	(622 vs)	624 s	(622 vs)	$\delta(ClO_4)$
6a	581	(556)	584 s	(566 m)	583 s	(566 ms)	584 s	(565 s)	582 s	(566 s)	581 s	(564 s)	6a (νring)
			559 w	(-)	559 w	(-)	559 w	(-)	559 w	(-)	560 w	(-)	comb
6b	541	(519)	540 s	(509 s)	542 m	(505 ssh)	542 m	(506 ssh)	546 mw		539 ms	(507 s)	6b (νring)
6b'	526	(504)	527 m	(501 s)	518 s	(502 s)	518 s	(501 s)	531 mwsh	(504 s)	518 s	(499 s)	6b' (νring)
16b'	516	(481)	517 s						518 s	(477 wm)			16b (γring/γN-O)
16b	516	(468)		(472 s)		(477 wm)		(476 wm)				(475 wm)	16b' (γring/γN-O)
18a'	478	(442)	481 m	(444 vw)	479 m	(443 vw)	479 m	(443 vw)	480 s	(443 vw)	479 s	(442 vw)	18a' (αN-O)
18a	466	(432)	452 s	(419 s)	453 s	(420 s)	452 s	(419 s)	452 s	(417 s)	452 s	(416 s)	18a (αN-O)
B	350	(350)	357 s	(345 s)	367 s	(351 s)	377 s	(359 s)	395 s	(379 s)	362 s	(314 wm)	νM-O
6a	320	(301)	331 ms	(311 m)	349 mssh	(326 wsh)	353 msh	(335 wsh)	326 m	(305 m)	336 ms	(315 wm)	6a (νring)
			294 mw	(278 w)	298 mw	(297 w)	300 mw	(300 w)	299 vw	(277 vvw)	296 w	(227 vw)	νM-O
						(278 w)		(282 w)					
Γ	276	(267)	265 w	(258 w)	268 w	(257 vw)	280 vw	(248 w)	285 vvw	(-)	261 w	(255 w)	Γ (ring shear)
									255 w	(246 w)			
17a'	220	(211)	227 vw	(227 vw)	-	(-)	229 wsh	(-)	-	(-)	-	(-)	17a' (γN-O/γring)
17a	214	(204)	200 ms	(195 ms)	208 ms	(205 ms)	219 ms	(214 m)	212 mw	(207 wm)	189 s	(184 ms)	17a (γN-O/γring)
			159 vvw	(150 w)		(142 vw)	158 vvw	(-)	159 vw	(157 wm)	-	(-)	δMON
Δ	123	(116)	135 vvw	(-)	135 vwsh	(-)	-	(132 vwsh)	145 vvw	(130 vw)	133 vvw	(128 vwsh)	Δ (ring scissors)
E	115	(109)	116 w	(110 w)	123 w	(109 w)	128 vwsh	(-)	129 w	(-)	120 vw	(114 vw)	E (ring scissors)
Z	104	(100)	88 w	(80 w)	94 w	(90 w)	100 w	(91 w)	96 w	(92 w)	92 w	(91 w)	Z (in rotation) or δOMO
			72 w	(74 w)	73 w	(74 w)	71 w	(72 w)	73 w	(72 w)	72 w	(73 w)	δOMO
					61 vwsh				62 vwsh		62 vwsh		δOMO

N.B. $-d_8$ bands at 556cm^{-1} (very strong) and 611cm^{-1} (strong) not included as they arise from $-d_0$ bands (modes 11' and 1) above 630cm^{-1} (see Tables 4.8 and 4.9)

Table 4.10 Far infrared assignment (625-50cm^{-1}) of $[M(bipyO_2)_3](ClO_4)_2$ complexes and their fully deuterated analogues

its perturbed localised symmetry of the ligand is reflected in the splitting of the ligand bands 19a($-d_0$), 19b($-d_8$), 8a'($-d_0$), 7a, 7a'($-d_8$), 8a'($-d_0$) and Γ (Tables 4.8 and 4.9).

The assignment of the M-O fundamentals is made difficult by the presence of eight ligand modes below 400cm^{-1} (Table 4.10). VINCIGUERRA *et al.* assigned two bands to νM-O in the infrared spectra of the M(II) complexes, one found between 392 and 355cm^{-1} and the other between 354 and 430cm^{-1} [51]. They made this assignment on the (incorrect) basis that no ligand band is observed between the frequencies 434 and 340cm^{-1}. AHUJA and SINGH [53] only considered the higher frequency as being suitable to assign to νM-O since they observed a ligand band at *ca.* 360cm^{-1} which they consider to give rise to the band between 354 and 340cm^{-1}. (This ligand band has been identified in this work as mode 6a).

From the infrared spectra (Table 4.10) and in agreement with the two previous assignments, the strong band in the range 395 to 357cm^{-1} is assigned to a metal-oxygen stretch. This stretch masks the inter-ring torsion, mode *B*.

The ligand mode 6a is tentatively assigned to the band of medium to strong intensity (sometimes appearing as a shoulder on the higher νM-O band) between 353 and 326cm^{-1}. It clearly reflects metal sensitivity and must therefore be coupled to νM-O. Evidence for the assignment of this band to 6a is found in its frequency in the Cu(II) complex. The medium band at 326cm^{-1} is much lower than is found in either the Mn or Zn complex, and therefore in complete disagreement with the CFSE order expected from a M-O stretch. The low frequency of the band at 326cm^{-1} in the Cu(II) complex may be explained by there being a change in the coupling between νM-O and 6a compared with the other complexes. This may be possible in view of the much higher M-O stretch in Cu

(at 395cm^{-1}) in comparison with the other metals.

However, an alternate explanation is that both the strong band at 395cm^{-1} and the medium band at 326cm^{-1} are a result of 'splitting' of the highest νM-O due to JAHN-TELLER distortion of the Cu(II) complex. But this would require an explanation for the absence of the ligand band (mode 6a) expected at *ca.* 330 to 350cm^{-1}.

The present ligand isotope study indicates that the former explanation is the more suitable (the 326cm^{-1}($-d_0$)/305cm^{-1}($-d_8$) band frequencies in the Cu(II) complex is typical of the ligand mode rather than of a M-O stretch).* However, a more suitable method to resolve this assignment would require the use of a metal-isotope study, since if the band at 326cm^{-1} to 350cm^{-1} is a ligand band which is coupled to νM-O, it will show only slight metal isotope sensitivity (with no ^{63}Cu/^{65}Cu sensitivity), while if the band is a pure νM-O it will be significantly shifted on metal isotope labelling.

A metal sensitive band of weak to medium intensity found between 300 and 294cm^{-1} in the bipyO_2 complexes is assigned to νM-O. Its frequency is such as to exclude it from being assigned to a ligand mode. (The only ligand mode suitable is the shear, Γ, which is better assigned to the band between 285 and 265cm^{-1}). This band was not assigned by VINCIGUERRA *et al.* [51] and was masked by νM-NCS in the study conducted by AHUJA and SINGH [53].

---

* An examination of the Fe(III) complexes for both the $-d_0$ and $-d_8$ isotopes with their higher M-O stretches at 412cm^{-1}(394cm^{-1}) and 380cm^{-1}(371cm^{-1}) shows both ligand modes 6a at 320cm^{-1}(305cm^{-1}) and *B* at 355cm^{-1}(340cm^{-1}) and so adds further support for the assignment of the $-d_0$ band between 353 and 326cm^{-1} to mode 6a.

Of the three M-O stretches expected for D_3 symmetry two (three in some of the deuterated spectra) are observed.

The M-O bends are found below 200cm^{-1} in pyO [4-6,29]. This region also contains three of the non-benzenoid vibrations of bipyO$_2$, modes Δ, E and Z, thereby making the assignments difficult. As is observed for the bipy and phen complexes the metal-ligand bends are found in two regions. The highest is at about 158cm^{-1}, and is similar in frequency to δMON in M(II) complexes with pyO [4-6,29]. Therefore, while it is a δMO bend, it is likely to have a significant contribution of bending by the N-O bond and so is described in Table 4.10 as δMON. Two bands are observed in the second region which is found below 90cm^{-1}. The two δMO bands at *ca.* 70cm^{-1} and *ca.* 60cm^{-1} are found slightly higher than the δOMO bends in M(II) complexes with pyO [5] as expected from the chelate effect [47], and these two bands in bipyO$_2$ are therefore described as δOMO. The two δOMO's are metal insensitive as was observed for the same vibrations in pyO [5].

Of the four M-O bends expected, only three are observed. This may be ascribed to three causes. Firstly, the bends may be accidentally degenerate as is observed for δOMO in M(II)(pyO)$_6$ complexes [5]. Secondly, the fourth δMO might lie beyond the range investigated. Thirdly, a band found between 100 and 80cm^{-1} might also be identified as δMO, but is considered here to be best assigned to the internal rotation, Z based upon its metal sensitivity.

Finally, a comment needs to be made concerning the Cu(II) complex. The infrared spectrum (Table 4.10) shows no sign of splitting of the M-O fundamentals into the six νM-O and the nine δM-O bends expected for C_2 symmetry. The absence of such splitting in the stretches may possibly be ascribed to a different coupling within the Cu(II) complex, while the richness of the ligand

spectrum in the region in which the bends are expected would make the obsercation of splitting of the δMON and δOMO bands difficult. Clearly the best indication of JAHN-TELLER distortion in the bipyO_2 complex with Cu(II) lies in the splitting of some of the ligand bands as a result of the perturbation of the localised ligand symmetry.

2 M(II)$(ClO_4)_2$ COMPLEXES WITH MONODENTATE LIGANDS

Of the three series of complexes examined in this Section, those with the potentially bidentate pzO and pzO_2 offer the possibility of forming bridged complexes. This makes the assignments more complicated, so the M(II) complexes with quinO are discussed first.

2.1 M(II) complexes with quinO and its fully deuterated analogue

In view of the extensive work done on metal complexes with pyO, the similarity of quinO to pyO makes it a natural choice for metal complex studies. Previous studies of [M(II)$(quinO)_6$]$(ClO_4)_2$ complexes (M = Mn,Co,Ni,Zn) have been limited to partial assignments (conducted down to 250cm^{-1}) made by RAGSDALE and his co-workers [59-61]. These have relied upon the assignment of their pyO analogues, employing SHINDO's assignments for the N-O fundamentals (hence the necessity of the present study). No quinO complexes with Cu(II) or Fe(II) perchlorates are found in the literature, although the hexakis complex with Fe(III)$(ClO_4)_3$ is included in the study by NATHAN and RAGSDALE [61].

Quinoline *N*-oxide gives rise to a slightly weaker $10Dq$ than that of pyridine *N*-oxide (Table 4.7). The strength of the ligand field parameter $10Dq$ of a ligand is determined by the basicity of the ligand, by metal to ligand π

bonding, by ligand to metal π bonding and by steric effects. An increase in the first two increases $10Dq$, while an increase in the last two decreases it.

RAGSDALE and his co-workers [59-61] examined these factors in quinO and compared them with those of pyO. With the presence of electrons in the t_{2g} (π) orbitals in these metal complexes, ligand donation to these orbitals (ligand to metal π bonding) is unlikely. Furthermore, the basicity of quinO (pk_a 0,86), which is only slightly greater than that of pyO (pk_a 0,79) is not considered by NELSON *et al.* [59] to be a significant factor affecting $10Dq$.

The presence of the second aromatic ring in quinO introduces a steric restriction to complexation which results in a smaller $10Dq$. However, it is of the same order of magnitude as that for pyO, which has led to NATHAN and RAGSDALE suggesting that 4-substituted quinoline *N*-oxides are better π acceptors than the 4-substituted pyridine *N*-oxides [60,61] as this would counter the decrease in $10Dq$ resulting from the steric factor. The absence of a shift of the N-O stretch to lower frequencies on complexation is considered evidence of the greater metal to ligand π bonding experienced by quinO [59]. However, in view of the highly coupled nature of the N-O stretch in quinO, such evidence must be treated with caution. Nevertheless, a greater contribution of orbital angular momentum to the magnetic moments of the quinO complexes (as compared to the pyO analogues) indicates a lowering of the π* orbitals in quinO relative to pyO [59], making such π bonding energetically more favourable.

The only crystal structure found in the literature of a complex with quinO is that of the adduct: $(p\text{-tolyl})_3SnBr\cdot$quinO [62]. This reveals a Sn-O-N angle of some 119°, with a near orthogonality (87°) of the Sn-O-N plane with the mean plane of the quinoline rings. Clearly, as is the case for the complexes with pyO, the geometry of quinO on complexation is not suitable for

any major metal-ligand π bonding, and it is questionable whether it would be significant enough to cause a large increase in $10Dq$. It is therefore suggested that the similar magnitude of $10Dq$ for pyO and quinO is the result of a counter influence to the steric effect in quinO by the moderate cumulative effects of both a slightly larger basicity and a slightly greater metal to ligand π bonding compared with pyO.

Unlike the three previous series of metal complexes, in the present series with quinO the complexes are not isostructural. The Mn(II), Co(II) and Ni(II) complexes have a coordination number of six. As shown below, Cu(II) has a combination of four, while Zn(II) has a coordination number of five. The latter complex (and its fully deuterated analogue) differs from that found by NATHAN and RAGSDALE [61], who report the hexakis-quinoline *N*-oxide complex with Zn(II) perchlorate. Repeated attempts to produce the six-coordinate complex yielded only the five-coordinate species. Similarly, repeated attempts to prepare $[Fe(quinO)_6](ClO_4)_2$ and its fully deuterated analogue were unsuccessful, with the infrared spectra showing oxidation to Fe(III).

The six-coordinated complexes are likely to be octahedral with a localised symmetry of S_6 for the $M(ON)_6$ unit, similar to their pyO analogues [4-6,29].

With a coordination of five, the molecule may adopt either a trigonal bipyramidal (with $d_{z^2}sp^3$ hybridisation) or a square planar (with $d_{x^2-y^2}sp^3$ hybridisation) conformation (often existing as a highly distorted intermediate of these). On the basis of ligand repulsions alone (whether considered as purely electrostatic or as Pauli repulsions from the bonding pairs) trigonal bipyramidal symmetry is favoured, being slightly more stable than square planar [63]. However, the difference in stability between the two is so slight that the presence of crystal field effects and/or the presence of π

bonding can favour square planar geometry. Zn(II), being a d^{10} ion, has no Crystal Field Stabilisation Energy, while the geometry of the ligand restricts the presence of π bonding. Hence the most likely structure for $[Zn(quinO)_5](ClO_4)_2$ is trigonal bipyrimidal.

In four-coordinate complexes the tetrahedral conformation is generally considered to be favoured by steric requirements in terms of either simply electrostatic repulsions of charged ligands or Van der Waal's repulsions of large ones. Square planar complexes are sterically less favoured, being prohibitively crowded by large ligands, and it is generally accepted that a prerequisite for their stability is the presence of nonbulky, strong field ligands which are sufficiently good π binders (to make up the energy 'lost' through 4- rather than 6-coordination) [63]. However, according to KARAYANNIS *et al.* [64,65], the presence of the pyridine ring (particularly when 2,6-disubstituted) is effective in stabilising the square planar structure in four coordinate complexes with various pyridine *N*-oxides. Magnetic susceptibilities show four coordinate square planar structure for [M(II)(2,6-dimethy pyridine *N*-oxide)$_4$] perchlorates (M = Fr-Zn), rather than tetrahedral or octahedral bridged structures [64,65]. Indeed, $[Cu(pyO)_4](ClO_4)_2$ is crystallographically shown to be square planar [66]. The structure of the Cu(II) complex is therefore most likely to be square planar.

The full infrared assignments for $M(II)(ClO_4)_2$ complexes with quinO and its $-d_7$ analogue are given in Tables 4.11 and 4.12. The far-infrared spectra ($625cm^{-1}$ to $50cm^{-1}$) reflecting the deuteration shifts of these complexes are given in Table 4.13.

The absence of perchlorate coordination of either the Cu(II) and Zn(II) complex, to produce a coordination of six, is evident from the infrared spectra.

Table 4.11 Infrared assignment (4000-400cm^{-1}) of M(II)$(ClO_4)_2$ complexes with quinoline *N*-oxide

Mn	Co	Ni	Cu	Zn	Assignment
3553 vwbr	-	3526 wbr	-	-	νO-H$_{(H_2O)}$
3156 vw	3152 w	3155 w	3160 w	3158 w	comb
3100 mssh	3104 wm	3104 m	3110 s	3108 m	41 (νC-H)
3077 s	3073 m	3076 s	3085 m	3079 m	1, 14 and 42 (νC-H)
3021 m	3021 wm	3020 mw	3027 w	3025 wm	2 and 15 (νC-H)
			3020 wsh		30 (νC-H)
2969 wm	2966 w	2970 w	2964 w	-	
-	2928 w	2930 vw	2929 w	2928 w	
2848 w	2854 w	2853 w	2849 w	2844 w	
-	2781 w	2773 vwbr	2782 wbr	2792 wbr	
2716 w	2711 w	2713 w	2715 vvw	2709 w	
2629 w	2622 vw	2625 vw	2624 vw	2623 w	
2586 w	2582 vw	2580 vw	2586 vw	2582 w	
2530 vw	2525 vw	2500 vw	2500 vw	-	
2458 w	2456 w	2456 w	2460 w	2456 w	
2407 w	2404 wbr	2416 wbr	2414 wbr	2402 w	
2366 vw	2359 vw	2373 w	2355 vw	2350 vw	
2326 w	2319 vw	2324 w	2321 w	2324 w	comb
2284 w	2291 vw	2284 w	2292 vvw	-	
2262 vw	2264 w	-	2265 w	2263 w	
2191 w	2189 w	2193 w	2195 w	2194 w	
2112 w	2110 vw	2111 w	2107 vw	2111 w	
2015 w	1999 w	2003 w	2027 w	2010 w	
-	1951 w	1954 w	1955 w	1952 w	
1844 w	1846 w	1844 w	1866 w	1868 w	
1816 w	1816 w	1817 w	1831 w	1835 w	
1762 w	-	1762 vw	1772 w	1750 w	
-	1712 w	1713 w	1717 w	-	
1685 w	-	-	1673 w	1677 vw	
1642 vwsh	1644 w	1642 vw	1638 w	1632 wsh	16 (νring)
1620 wm	1620 wm	1621 wm	1618 wm	1619 m	31 (νring)
1601 w	1603 w	-	1601 w	1602 w	comb
1587 w	1587 msh	1586 m	1588 m	1588 msh	comb
1576 s	1577 s	1578 s	1582 s	1581 s	4 (νring/νN-O)
1537 w	1527 w	-	1528 w	-	comb
1514 ms	1515 s	1516 s	1516 s	1515 s	44 (νring)

Table 4.11 (continued)

Mn	Co	Ni	Cu	Zn	Assignment
1501 w	1502 wsh	-	-	1491 w	comb
1456 ms	1456 s	1455 s	1457 m	1456 ms	8 (ν ring)
1444 wsh	1445 msh	1445 msh	1447 m	1447 m	17 (ν ring/ν N-O)
1398 vs	1398 vs	1398 vs	1397 vs	1395 vs	3 (ν ring)
1377 s	1374 s	1375 s	1379 s	1375 s	32 (ν ring/ν N-O)
1335 wm	1335 wm	1336 w	-	1344 w	comb
1317 m 1309 m	1315 ms	1319 ms 1311 ms	1315 m 1308 m	1315 m	43 (ν ring/ν N-O)
1268 s 1262 ssh	1266 s	1269 s 1262 s	1280 wsh 1271 s	1265 s	34 (α C-H) 18 (α C-H)
1229 s	1228 s	1228 s	1229 s	1229 s	29 (ν N-O/ν ring)
1213 vs	1211 vs	1211 vs	1217 vs	1214 vs	46 (α C-H)
1184 s 1178 ssh	1184 s 1177 mssh	1187 s 1179 ssh	1176 s	1176 s	19 (α C-H)
1148 s	1149 s	1151 ms	1153 s	1149 s	5 (α C-H)
1141 s	1139 s	1140 s	1146 s	1141 s	33 (α C-H)
1080 vsbr	1087 vsbr	1085 vsbr	1090 vsbr	1083 vsbr	$\nu(ClO_4)$
1055 s	1057 ssh 1046 ssh	1054 s	1051 s	1057 s 1048 ssh	7 (α C-H)
1016 wm	1016 wm	1016 sm	1017 wm	1016 wm	10 (γ C-H)
989 w	991 w	991 w	995 wm	989 w	37 (γ C-H)
980 wm	979 wm	980 wm	977 w	974 w	26 (γ C-H)
968 wsh	968 w	969 w	965 w	961 w	comb
948 wsh	957 w	957 w	-	-	comb
938 w	937 w	938 w	937 wm	937 wsh	21 (ν ring/ν N-O)
929 w	930 wsh	929 w	930 w	930 w	$\nu(ClO_4)$
913 w	913 w	-	910 w	910 w	comb
-	908 w	908 w	-	903 w	comb
882 s	880 s	880 s	880 s	880 s	47 (ν ring/ν N-O)
861 m	868 ms	868 ms	870 m	868 m	39 (γ ring)
816 s	816 s	817 ms	-	815 s	11 (γ C-H)
805 s 799 vs	803 vs 798 vs	804 ssh 799 vs	806 vs 801 s	797 vs	38 (γ C-H) 23 (γ C-H)
778 s 767 vs	774 vs 762 s	774 m 764 s	770 s	772 s 767 s	36 (ν ring/ν N-O)
736 m	735 s	734 ms	737 m	735 mwsh	6 (ν ring/ν N-O)

Table 4.11 (continued)

Mn	Co	Ni	Cu	Zn	Assignment
725 s	724 s	724 s	727 s	723 s	27 (γC-H)
621 s	622 s	622 s	622 s	622 s	$\delta(ClO_4)$ and 48 (νring/νN-O)
583 s	581 ms	583 s	590 s	582 ms	12 (γring)
567 s 561 ms	567 s	569 s	571 s	566 s	9 (νring/νN-O)
552 s	550 s	550 s	550 ms	548 s	20 (νring/νN-O)
499 ms	497 s	498 s	507 ms	500 s	40 (γring)
483 m	488 ms 483 ms	490 ms 483 m	479 mw	482 w	24 (γring)
476 vw	475 vw	-	-	-	comb
468 vw	468 vw	468 vw	466 vw	-	comb
464 vw	463 vw	463 vw	-	464 w	comb
422 wm	422 wm	420 wm	450 m	420 w	28 (γring)

s = strong

m = medium

w = weak

v = very

sh = shoulder

br = broad

comb = combination

Table 4.12 Infrared assignment (4000-400cm^{-1}) of M(II)$(ClO_4)_2$ complexes with quinoline-d_7 *N*-oxide

Mn	Co	Ni	Cu	Zn	Assignment
3440 wbr	3530 w	3380 wbr	-	3416 mbr	νO-H$_{(H_2O)}$
3153 w	3155 vw	3152 w	3152 vw	3152 mbr	
-	2973 wm	2960 vw	2958 w	-	
2925 w	2935 w	2923 w	2929 w	2923 wsh	
2854 w	2861 w	2857 vw	2854 w	-	
2781 w	2792 vw	2780 w	-	2778 wsh	
-	2780 vw	-	2769 vw	-	comb
2680 vw	2680 vw	-	2684 vw	-	
-	2614 vwbr	2613 w	2622 vw	2623 w	
2463 w	2465 vwbr	2460 w	2455 w	2462 w	
2378 w	2377 w	2380 vw	2378 w	2378 w	
2338 wsh	2330 wsh	2342 w	2337 w	2336 wsh	
2312 mw	2314 m	2312 w	2317 wm	2316 m	1 (νC-D)
2296 mw	2296 wm	-	2300 wm	2296 wm	41 (νC-D)
2283 wm	2285 wsh	2287 w	-	-	30 (νC-D)
2268 wm	2278 wsh	2277 w	2272 w	2276 wm	2 and 14 (νC-D)
-	-	2218 w	2222 w	2216 vw	
-	2145 vw	-	2159 vw	2163 vw	
2101 vw	2094 w	2096 w	2098 w	2098 w	
2023 w	2019 w	2018 w	2036 w	2023 w	
-	-	2000 w	2004 w	2010 wsh	comb
1938 vw	1925 vw	1920 w	1935 w	1932 w	
1835 vw	-	1830 w	1830 w	-	
-	1818 vw	-	1815 vw	-	
1715 w	1712 w	-	1720 w	1708 wm	
1665 vw	-	-	1667 vw	1669 wmbr	δO-H$_{(H_2O)}$
1631 w	1640 w	1645 vw	1645 vw	1645 wbr	
-	1620 w	1621 w	1621 w	-	comb
1598 m	1599 m	1599 ms	1599 ms	1597 ms	16 (νring/νN-O)
-	1576 w	1571 w	1582 w	-	31 (νring)
1557 w	1556 w	1558 w	1562 w	1565 w	comb
1536 s	1537 s	1537 s	1541 s	1538 s	4 (νring/νN-O)
1490 w	1490 w	-	1515 vw	-	comb
1456 s	1458 s	1459 s	1461 s	1458 s	44 (νring)
1437 wsh	1446 wm	1445 wmsh	1451 wmsh	1442 wm	comb
1424 vw	1427 vw	1429 vw	1428 vw	1425 vw	comb

Table 4.12 (continued)

Mn	Co	Ni	Cu	Zn	Assignment
1397 vw	1392 vw	1396 vw	1391 vw	1390 vwsh	comb
1378 ms	1380 ns	1380 ms	1380 m	1379 m	17 (νring/νN-O)
1361 s	1359 s	1359 vs	1361 s	1359 s	3 (νring)
1314 s	1314 vs	1312 vs	1311 vs	1314 vs	43 (νring/νN-O)
1302 vs	1305 vs	1303 vs	1305 vs	1305 vs	8 (νring)
1242 s	1250 s	1248 s	1257 s 1251 s	1249 s	32 (νring/νN-O)
1213 w	1220 vw	1214 vw	1223 vw	-	comb
1204 w	1197 w	1204 w	1204 vwsh	1195 w	comb
1188 vw	1184 m	1189 vw	1194 w	1188 w	comb
1151 vs	1157 ssh 1147 vs	1160 ssh 1149 vs	1149 vs	1166 ssh 1148 vs	29 (νN-O/νring)
1080 vsbr	1092 vsbr	1087 vsbr	1109 vsbr	1089 vsbr	$\nu(ClO_4)$ and 46 (αC-D)
1028 s 1024 s	1027 ms	1028 s 1024 s	1026 s	1025 s	34 (αC-D)
1011 s	1012 s	1013 s	1012 vs	1012 s	19 (αC-D)
953 w	953 wm	953 w	955 vw	955 vw	comb
930 w 928 w	931 w	931 w	930 w	932 w	$\nu(ClO_4)$ and 21 (νring/νN-O)
877 s	877 s	878 ssh 876 s	879 s	878 s	7 (αC-D) and 33 (αC-D)
-	857 w	850 w	-	-	comb
842 wm	844 m	843 m	845 w	845 wm	37 (γC-D)
828 m	830 m	838 wm	831 m	830 msh	5 (αC-D)
825 msh	827 m	827 wm	827 wmsh	827 m	10 (αC-D)
-	814 wsh	812 w	813 w	811 w	18 (αC-D)
807 vw	806 w	806 w	-	-	comb
784 s	788 ssh 781 s	783 s	793 s 788 s	786 s	47 (νring/νN-O)
-	770 wsh	768 w	773 wm	770 w	39 (γring)
760 s	759 w	764 w	756 vw	753 w	26 (γC-D)
744 ms	743 ms	743 m	746 m	744 m	36 (νring/νN-O)
721 m	720 w	722 w	727 w 722 w	722 w	6 (νring/νN-O)
680 s	679 s	682 s	684 s	683 s	38 (γC-D)
666 w	668 vw	668 vw	672 vw	-	comb

Table 4.12 (continued)

Mn	Co	Ni	Cu	Zn	Assignment
650 wsh	651 w	651 wm	653 m	651 w	11 (γC-D)
639 ms	636 vs	629 vs	632 vs	633 vs	23 (γC-D)
623 vs	622 vs	622 vs	623 vs	624 vs	$\nu(ClO_4)$
594 m	600 m 596 msh	600 s	605 s	599 m	27 (γC-D)
564 ms	567 ms	563 s	572 s	567 s	48 (νring/νN-O)
-	544 m	544 m	547 m	548 w	comb
539 ms 529 msh	536 ms	532 s	532 s	536 m 529 m	12 (γring)
497 s	494 s	496 s	508 s	500 s	9 (νring/νN-O)
487 ms	485 ms	489 s 485 ssh	592 ms	487 s	20 (νring/νN-O)
460 mw	464 m	471 w 463 w 455 w	455 mw	462 wsh 456 wm	40 (γring)
416 w 411 wm	412 m	419 wm 412 wm	412 m	411 wm	24 (γring)

s = strong

m = medium

w = weak

v = very

sh = shoulder

br = broad

comb = combination

	quinO		Mn		Co		Ni		Cu		Zn		Assignment
	$-d_0$	$-d_7$	$-d_0$	$-d_7$	$-d_0$	$-d_7$	$-d_0$	$-d_7$	$-d_0$	$-d_7$	$-d_0$	$-d_7$	
48	628	(564)	621 s	(623 vs) (564 ms)	622 s	(622 vs) (567 ms)	622 s	(623 vs) (563 s)	622 s	(623 vs) (573 s)	622 s	(624 vs) (567 s)	$\delta(ClO_4)$ 48 (νring/νN-O)
			-	(-)	-	(544 m)	-	(545 w)	-	(547 m)	-	(548 wm)	comb
12	610	(526)	583 s	(536 ms) (529 msh)	581 ms	(536 ms)	583 s	(532 s)	590 s	(532 s)	582 ms	(563 ms) (529 ms)	12 (γring)
9	557	(508)	567 s 561 ms	(497 s)	567 s	(494 s)	569 s	(496 s)	571 s	(508 s)	566 s	(500 s)	9 (νring/νN-O)
20	545	(497)	552 s	(487 ms)	550 s	(485 ms)	550 s	(489 s) (485 ssh)	550 ms	(492 ms)	548 s	(487 s)	20 (νring/νN-O)
40	480	(441)	499 ms	(460 mw)	497 s	(464 m)	498 s	(471 w) (463 w) (455 w)	507 ms	(455 mw	500 s	(462 wsh) (456 wm)	40 (γring)
24	466	(416)	483 m	(416 w) (411 wm)	488 ms 483 msh	(412 m)	490 ms 483 m	(419 wm) (412 wm)	479 mw	(412 m)	482 w	(411 wm)	24 (γring)
			476 vw	(-)	475 vw	(-)	-	(-)	-	(-)	-	(-)	comb
			468 vw	(-)	468 vw	(-)	468 vw	(-)	466 vw	(-)	-	(-)	comb
			463 vw	(-)	463 vw	(-)	463 vw	(-)	-	(-)	464 w	(-)	comb
28	422	(374)	422 wm	(378 wm) (370 wm)	422 wm	(371 wsh)	420 wm	(373 w)	450 m	(362 s)	420 w	(379 w) (373 w)	28 (γring)
									397 ms				
					366 s	(352 s)	371 s	(350 s)			364 s	(349 s)	νM-O and 35 (νring)
35	365	(340)	349 s	(333 s)	354 s	(346 s)	358 s	(341 m)					
			388 s	(323 s)		(329 wsh)	350 mssh	(330 msh)			334 w	(-)	
45	321	(307)	297 m	(275 m)	320 mw	(302 m)	322 m	(305 m)	321 m	(308 ms)	320 m	(304 wm)	45 (αN-O)
			-	(-)	300 w	(277 vw)	301 vw	(279 w)	-	(-)	300 wsh	(283 wsh)	comb
			-	(-)	280 vw	(-)	280 vvw	(264 vvw)	-	(-)	285 vvw	(-)	comb
			227 m	(217 m)	238 w	(221 wsh)	243 wm	(229 wm)	262 wm	(248 wm)	239 w	(223 wm)	τMO/τNO
			-	(-)	-	(-)	-	(-)	-	(-)	230 w	(217 wm)	τMO/τNO
13	211	(196)	211 m	(199 m)	215 w	(210 m)	233 vwsh	(-)	217 vw	(-)	219 wm	(207 wm)	13 (γring)
			-	(-)	204 w	(-)	209 wm	(200 m)	-	(-)	-	(-)	τMO/τNO
25	185	(170)	188 m	(174 ms)	189 m	(177 msh)	196 m	(186 wm)	194 w	(181 wmsh)	189 m	(174 wm)	25 (γring)
22	185	(175)	172 wm	(165 ms)	178 wsh	(169 m)	180 wsh	(172 wsh)	181 wm	(173 m)	166 m	(159 m)	22 (γN-O)
			134 vw	(128 vw)	135 vw	(122 vw)	140 vw	(-)	141 vwsh	(135 wsh)	145 vw	(-)	δMON
			114 vw	(112 w)	-	(-)	-	(-)	127 w	(120 w)	129 w	(122 w)	δMON or τMO/τNO
			83 w	(81 w)	93 vwsh	(90 vwsh)	-	(105 vw)	99 w	(96 wm)	102 vw	(103 w)	τMO/τNO and δOMO
			75 w	(69 w)	74 w	(70 wm)	76 w	(75 w)	-	(-)	75 w	(72 w)	δOMO or τMO/τNO
			64 w	(55 wsh)	60 w	(59 wsh)	50 w	(50 w)	63 w	(60 w)	60 vwsh	(-)	δOMO

N.B. $-d_8$ band at 600 cm^{-1} (medium to strong) not included as it arises from $-d_0$ band (mode 27) above 630cm^{-1} (see Tables 4.11 and 4.12)

Table 4.13 Far infrared assignments (625-50cm^{-1}) of $M(II)(ClO_4)_2$ complexes with quinoline *N*-oxide and quinoline-d_7 *N*-oxide

The perchlorate ion with T_d symmetry is characterised by the very intense broad infrared band (with shoulders) at 1100 cm^{-1} (ν_3), the strong sharp band at 625cm^{-1} (ν_4) and the weak (infrared forbidden) band at 930cm^{-1} [67]. The broadness and shoulders present in ν_3 may be ascribed to it being a triply degenerate F_2 vibration, to ClO_4^- being disordered, as well as to the natural isotope ^{37}Cl (24% natural relative abundance).

The local symmetry of the perchlorate ion is reduced to C_{3v} in monodentate perchlorate and to C_{2v} or C_s in bidentate perchlorate. Monodentate perchlorate is characterised by two very strong bands between 1200 and 1000 cm^{-1}, a strong band at 930cm^{-1}, a strong band at 625cm^{-1} (sometimes split) and a weak to medium band at 480cm^{-1} [67]. Bidentate perchlorate is characterised by an additional strong band between 1270 and 1245cm^{-1} and by further splitting of the two bands at 625cm^{-1} and 480cm^{-1} [67].

As expected with the large size of the ligand quinO, resolution of the localised ligand symmetry into the molecular symmetry components is not complete. Even so, fourteen ligand fundamentals show band splitting, namely modes 47($-d_7$), 43($-d_0$), 40($-d_7$), 36($-d_0$), 34($-d_7$), 32($-d_7$), 28($-d_7$), 24, 20($-d_0$), 12($-d_7$), 9($-d_0$), 7($-d_0$) and 6($-d_7$). Of these only two are αC-H bends (modes 34 and 7) while the rest are ring modes; modes 40, 28, 24 and 12 being γ-ring modes, the others being νring modes coupled with νN-O. As band splitting is experienced by only two αC-H bends (out of the 14 αC-H modes expected with both isotopomers) this splitting may be a result of the energy of these two vibrations since the frequency of mode 34($-d_7$) (the free ligand being found at 1055cm^{-1}) is similar to that of mode 7($-d_0$) (the free ligand being found at 1054cm^{-1}).

Since only the trigonal bipyrimidal Zn(II) complex is expected to yield a

perturbation of the localised ligand symmetry (with a different axial and equatorial ligand environment), and as the split bands include those of the other metals, this splitting may simply indicate a better resolution of the localised ligand symmetry into the molecular symmetry components. However, the number of fundamentals showing splitting on complexation is (with the exception of the Cu(II) complexes experiencing JAHN-TELLER perturbation of the localised symmetry of the ligand) larger than that found for the three previous series of complexes. It is possible, therefore, that the splitting of the ligand bands in this series of complexes may rather be indicative of a slight distortion of the octahedral and the square planar structures, thereby giving rise to a greater perturbation of the localised ligand symmetry within these complexes. Future crystal structures of the ML_6 and ML_4 complexes with quinO would therefore be of some interest.

The assignment of the M-O fundamentals (Table 4.13), particularly the M-O stretches, is made difficult by the presence of five low-lying internal ligand fundamentals below 450cm^{-1}. The assignment of the ligand wagging vibrations (δMON, τNO and τMO) are based upon those of pyO [4-6]. The two bands in the regions *ca.* 300cm^{-1} and *ca.* 285cm^{-1} have been assigned as combination or difference bands since they lie above the expected region for the highest τMO/τNO region [4-6]. Considering the increased mass of the ligand, it is unlikely that these ligand wagging vibrations are to be found at higher frequencies than their pyO analogues.

Of the six νM-O, six δMON, six τNO, six τMO and nine δOMO vibrations associated with the $M(ON)_6$ unit, for S_6 symmetry four δOMO ($2A_u$ and $2E_u$) and two each of νM-O, δMON, τNO and τMO (each set with the representation of A_u and E_u) are infrared active.

For Mn(II), Co(II) and Ni(II) the expected two M-O stretches and five of the six expected ligand wagging modes (δMON, τNO and τMO) are observed. Of the four δOMO bands expected, two are undoubtedly to be found below $50cm^{-1}$ (the limit of this work) as is observed for their pyO analogues [4-6]. The band at *ca.* $60cm^{-1}(-d_0)$ is assigned to δOMO. The similar assignment of the band at *ca.* $75cm^{-1}(-d_0)$ is only tentative since the increased mass of the ligand may result in lower δOMO bends compared with pyO. An alternative assignment of this band is the sixth ligand wagging motion. Studies below $50cm^{-1}$, or alternatively a normal coordinate analysis, would be necessary to finalise this assignment.

The difficulty in assigning the M-O vibrations because of the presence of internal ligand vibrations is demonstrated by the coupling experienced between the αN-O (mode 45) and the lowest νM-O in the Mn(II) complex. Mode 45 for the Mn(II) complex is found some 20 to $25cm^{-1}$ lower in frequency than the other complexes and below the free ligand $(-d_0)$. It is suggested that this abnormal frequency is a result of coupling of mode 45 (expected at $320cm^{-1}$ for quin-d_0) with the lowest νM-O (*ca.* $325cm^{-1}$) to result in a higher coupled νM-O at $338cm^{-1}$ and a lower coupled αN-O at $297cm^{-1}$. This suggestion is supported by the fact that while the lowest νM-O of Zn(II) (being five-coordinate) is at a similar frequency to that of Mn(II), αN-O of Zn(II) is at the expected frequency of $320cm^{-1}(-d_0)$. Furthermore, νM-O for $[Mn(pyO)_6](ClO_4)_2$ is found at $312cm^{-1}$ [29] and therefore a frequency of *ca.* $325cm^{-1}$ is expected for the quinO analogue. Clearly, the lowest νM-O for the Mn(II) complex is not a pure vibration.

A further illustration of the difficulty in assigning the M-O vibrations because of the presence of ligand bands is seen in the masking of the ring mode (mode 35) by the strong M-O stretches and which is only observed as a

weak shoulder in the deuterated complexes with Co(II) and Ni(II).

Tetra-coordination theoretically gives rise to four each of νM-O, δMON, τNO and τMO and to five δOMO vibrations. For tetrahedral coordination with T_d symmetry (viewing the MO_4 unit) one νM-O(F_2) and one δOMO(F_2) are infrared active. Considering the $M(ON)_4$ unit with C_{2v} symmetry, four infrared active νM-O($2A_1$, B_1 and B_2) and four δOMO($2A_1$, B_1, B_2) are expected, while the twelve wagging modes of the ligands yield ten infrared active vibrations ($4A_1$, $3B_1$ and $3B_2$).

For square planar symmetry, the most likely conformation is that described by LEE *et al.* as the *swastika* [66]. That is, D_{4h} symmetry for the MO_4 unit yielding one infrared active νM-O (E_u) and two δOMO(A_{2u} and E_u), or C_{4h} symmetry for the $M(ON)_4$ unit, for which one infrared active νM-O(E_u) and two δOMO(A_u and E_u) are still expected and for which four infrared ligand wagging vibrations (A_u, B_u and $2E_u$) are expected.

From Table 4.13 the presence of one νM-O, two δOMO and three of the ligand wagging vibrations for the Cu(II) complex fully supports the square planar conformation rather than the tetrahedral. The higher frequency of νM-O and δOMO compared with their hexa-coordinate counterparts is expected due to a decrease in the coordination number [29]. However, compared with νM-O for $[Cu(pyO)_4](ClO_4)_2$ (at 322cm^{-1} [29]) the M-O stretch for Cu(II) complex with quinO is very low, while the frequency of 450cm^{-1} for the ring torsion (mode 28) is abnormally high. This indicates probable coupling between these two vibrations (which is possible since both are expected at *ca.* 420-430cm^{-1}). This coupling differs from that experienced by Mn(II). Future metal isotope labelling with the isotope pair $^{63}Cu/^{65}Cu$ is likely to prove the most suitable means of proving the existance of this coupling (both bends are predict-

ed to show isotope shifts).

Five νM-O, seven δOMO and fifteen ligand wagging modes (five each of δMON, τNO and τMO) are associated with the five-coordinate $M(ON)_5$ unit. The trigonal bipyramidal conformation has C_1 symmetry in which all the vibrations are expected to be infrared active. Considering the simpler model (the MO_5 unit) which has D_{3h} symmetry, two infrared active stretches (A_2'' and E') and three δOMO bends (A_2'' and $2E'$) are expected.

The alternative square based pyramidal structure has C_{4v} symmetry for the MO_5 unit, giving rise to three infrared active νM-O($2A_1$ and E) and three δOMO(A_1 and $2E$). This symmetry is similarly lowered to C_1 in considering the $M(ON)_5$ unit.

The presence of only two νM-O (at 364cm^{-1} and 334cm^{-1}) and three δOMO bands in the infrared spectrum of Zn(II)-d_0 complex tentatively supports predicted tetragonal bipyramidal conformation. The Raman spectrum would present more conclusive evidence, with its greater difference between the two conformations (three νM-O and three δOMO expected for trigonal bipyramidal, four νM-O and five δOMO expected for square-based pyramidal).

The high frequency of νM-O in the Zn(II) complex is accounted for by its lower coordination number [29]. The highest νM-O for Zn(II) is of the order of Co(II). That this is indicative of penta-coordination and that it does not fit the IRVING-WILLIAMS series is demonstrated by a very naïve calculation which may be derived for the expected increase in frequency of νM-O for the loss of one ligand. From the infrared data of M(II) complexes with pyO [29], the predicted M-O stretching frequency for five coordinate $Zn(PyO)_5$ [$\nu Zn_{(5)}$] may be very roughly calculated as:

$$\nu Zn_{(5)} = \left[\frac{\left(\frac{\nu Cu_{(4)}}{\nu Cu_{(6)}} - 1 \right)}{2} + 1 \right] \nu Zn_{(6)} = 369 cm^{-1}$$

This is similar for the δM-O frequency of $[Zn(quinO)_5](ClO_4)_2$ and therefore supports the latter's assignment. The three bands at $102 cm^{-1}(-d_0)$, $75 cm^{-1}$ $(-d_0)$ and $60 cm^{-1}(-d_0)$ are tentatively assigned to δOMO; their higher frequencies than those for Mn(II), Co(II) and Ni(II) are ascribed to the higher bond order.

In conclusion, the full infrared assignment of M(II) complexes with quinO and its fully deuterated analogues reveals the formation of hexa-, penta- and tetra-coordinate complexes having (possibly distorted) octahedral, trigonal bipyramidal and square planar conformations, respectively. The metal-oxygen stretches of the Mn(II) and Cu(II) complexes are in particular strongly coupled to internal ligand vibrations, this coupling being determined by the coordination numbers of the complex.

2.2 M(II) complexes with pzO_2 and its fully deuterated analogues

Only two accounts of metal complexes with unsubstituted pyrazine *N,N'*-dioxide are known in the literature. ZINNER and VICENTINI [68] report the preparation of $M(pzO_2)_4(ClO_4)_2$ (M = La,Pr,Eu,Er,Y). POPP and GARLOUGH [69] report, among several other azine *N*-oxides, three $M(II)(ClO_4)_2$ (M = Co,Ni,Cu) complexes with pzO_2.

In the former study no speculation concerning the coordination number or structure was attempted.

In the latter work the new complexes were fully characterised by elemental analysis, infrared spectra, molar electrolytic conductance measurements, magnetic susceptibility measurements and electronic spectra [69]. These complexes were identified as 'complexes with a low ligand/metal stoichiometry. The complexes may be polynuclear with bridging pzO_2 to insure the coordination number to six' [69]. Further, the low magnetic susceptibilities were interpreted as evidence of unidentate bridging pzO_2 (M-O-M bridges) [69].

There does, however, appear to be some contradiction within the paper by POPP and GARLOUGH. In contrast to their conclusions quoted above, according to their elemental analyses the complexes have the formulae $Co(pzO_2)_6(ClO_4)_2$; $Ni(pzO_2)_4(ClO_4)_2$ and $Cu(pzO_2)_6(ClO_4)_2$. These formulae were employed in determining the $10Dq$'s for the complexes, the electronic spectra being run as Nujol mulls and in acetonitrile solutions. In the discussion of the electronic spectra, the formulation of the Cu complex, which is given in the text as the hydrate - $Cu(pzO_2)_3(ClO_4)_2 \cdot H_2O$ - (note the *tris* complex) conflicts with the anhydrous *hexakis* complex in their Table 5 (the electronic spectra of the complexes). In contrast, the molecular formulae given for the molar conductivity, the magnetic data and the infrared spectra (their Tables 2 and 3) are $Co(pzO_2)_3(ClO_4)_2$, $Ni(pzO_2)_4(ClO_4)_2$ and $Cu(pzO_2)_3(ClO_4)_2$.

Furthermore, it was suggested from the colour change that the Cu complex dissociates in acetronitrile [69] (present studies show a similar colour change in acetonitrile for the Co and Ni complexes with pzO_2), yet the conductive measurements were recorded with acetonitrile as solvent.

There seems to be some confusion in the report concerning the stoichiometry and structure of these M(II) complexes with pzO_2. Present work attempting to repeat the preparation of these complexes proved unsuccessful (Chapter 2),

and in view of the non-reproducibility of the complexes a full vibrational analysis of the spectra has not been attempted.

2.3 M(II) complexes with pzO and its fully deuterated analogue

The ligand pyrazine *N*-oxide is unique in the present study of ligands complexed to metal (II) perchlorates in that it contains both a nitrogen and an oxygen donor atom, and hence possesses the ability of yielding terminal N-, terminal O-coordinated and N,O-bridged complexes. Various lanthanide (III) complexes with pzO reportedly reveal exclusive terminal M-O bonding [70-73], while Ag(I) complexes yield either bridging or terminal N-bonding by the ligand [74], M(II) complexes (M = Mn-Zn) are more complicated, showing all three types of bonding with pzO [75-76].

Identification of the nature of coordination has previously been based upon the infrared spectra, specifically considering three regions; that containing the C=N stretch (mode 8a) [70-73], that containing the N-O stretch [70-77], and that containing both the M-O and M-N stretches [75-77].

The ring mode 8a (described by VICENTINI and his co-workers as the νC=N [70-73]) is observed at 1594cm^{-1} in pzO. It has been suggested that the absence of a shift in this mode on complexation is indicative of oxygen coordination [70,71,73]. This is not, however, absolute since VICENTINI and ZINNER [70] recognise no shift of νC=N (giving the free ligand as 1585cm^{-1}) for the lanthanide perchlorate complexes, while the same authors also recognise no shift of νC=N (giving the free ligand as 1600cm^{-1}) for the lanthanide chlorides and hexaflurophosphates [71]. Furthermore, there exists a difference of between 11 and 16cm^{-1} in the assignment of νC=N for these complexes, as given in the two papers [70,71]. The use of mode 8a as an indicator of M-O or

M-N coordination is therefore open to question.

The N-O stretch for free pzO gives rise to a strong infrared band at 1307cm^{-1}. In the absence of M-O bonding this vibration is expected to shift to higher frequencies on complexation, while it is expected to shift to lower frequencies with M-O bonding. The position of the N-O stretch has been widely used to determine the nature of the coordination [70-77]. However, employing the N-O frequencies as an indicator of the nature coordination has the difficulty that the Kekulé vibration (mode 14) and the αC-H mode to which it couples (mode 3) (being found at 1212cm^{-1} and 1295cm^{-1}, respectively, for the free ligand) are expected to fall within the same region on complexation.

The use of the M-O and M-N stretching frequencies to evaluate the nature of the coordination by complexes with pzO has a threefold disadvantage. Firstly, the frequencies at which these vibrations are found are subject to CFSE effects; secondly, they are subject to the coordination number and, thirdly, they are dependant upon whether the ligand is bridged or terminally coordinated. The result of this is that no clear range to distinguish between the coordination by the two different donor atoms, although νM-O and νM-N are reported to lie between 360 to 290cm^{-1} and between 290 to 225cm^{-1}, respectively, for M(II) complexes [75-77]. According to KARAYANNIS *et al.* [49] νM-N for the bridged ligand is found at a higher frequency than its terminal counterpart, while νM-O (bridged) occurs at a *lower* frequency than the terminal νM-O. While this author agrees with the behaviour of the M-N stretches (based upon similar observations for pyrazine [10,13,19-21]) it is suggested that KARAYANNIS *et al.* [49] are possibly incorrect in their identification of the bridged νM-O being found at lower frequencies than terminal νM-O. Their proposition was based upon the behaviour of νM-O for the binuclear oxygen bridged complexes of various picoline *N*-oxides reported by WHYMAN and

HATFIELD [78]. However, it must be pointed out that these involve bridging by one donor atom (oxygen) between two metal atoms, whereas the bridging experienced by pzO involves bridging between two metal atoms by two different donor atoms within the same ligand. For the former the increase in bond order experienced by the single donor atom yields lower frequencies (compared with the terminal ligand). In the latter case, since the chelate effect results in higher metal-ligand frequencies for bidentate ligands [47], the bridged νM-O might also be expected at higher frequencies, especially in view of the behaviour of bridged pyrazine and of the higher frequencies of νM-N (bridged) reported for pzO.

The present series of metal (II) perchlorate complexes with pzO differ from that reported by SPECA *et al.* [76] in that (with the exception of the Cu complex) the present complexes all contain higher ligand to metal ratios than previously recorded. (This being the result of preparing the complexes with a greater than 6:1 ligand:metal salt ratio).

Full infrared spectra for these $M(II)(ClO_4)_2$ complexes with pzO and its $-d_4$ analogues are given in Tables 4.14 and 4.15. The far-infrared spectra (625 to 50cm^{-1}) reflecting the deuteration shifts of these complexes are given in Table 4.16.

As may be expected for a ligand with such a varied coordinating ability, the present complexes of pzO are not isostructural. This is illustrated by the large degree of splitting of the ligand bands, reflecting a greater perturbation of the localised ligand symmetry as a result of the differing ligand environments.

Before the most probable structures (as determined from their infrared spec-

Table 4.14 Infrared assignment (4000-400cm^{-1}) of M(II)$(ClO_4)_2$ complexes with pyrazine *N*-oxide

Mn n = 6	Mn n = 5	Fe (Red)	Fe (Yellow)	Co n = 5	Co n = 4	Ni n = 4	Cu n = 4	Zn n = 5	Assignment
3502 mbr	-	3528 vwbr	3533 msbr	3537 msbr	3538 wbr	-	-	-	νO-H(free H_2O)
3517 mbr	3429 mbr	-	-		-	-	3436 mbr	3410 wbr	
-	3378 ms	-	-	-	3305 wbr	3360 sm	-	-	νO-H(coord H_2O)
3162 mvbr	3188 mshbr	-	-	3100 mbr	3105 wbr	3176 sbr	-	3121 m	νO-H(free H_2O)
-	-	-	3024 msvbr		3012 mwbr	-	-	-	
-	-	-	-	-	-	-	2965 w	2976 w	
-	2925 w	2928 w	2837 m	-	-	-	2923 w	-	
-	2783 w	2780 w	-	2795 wsh	-	2795 wsh	2773 w	2777 w	
-	-	-	-	-	-	2727 w	2736 vw	-	
-	2657 vw	2656 vw	-	-	-	2640 wbr	-	2656 vw	
2633 w	2622 w	2631 vw	-	2636 vw	-		2633 wm	2632 w	
2590 w	2589 w	-	2611 w	2607 vw	2615 wbr	-	-	2613 vw	
	2576 vw	-	-	2577 w	-	-	-	2576 vw	
-	-	-	2540 vw	-	2542 vw	-	2556 w	-	comb
2526 w	2522 w	2523 vw	-	2526 vw	2512 vw	2522 w	-	2522 w	
2502 vw	2500 vvw	-	2508 vw	2498 vw	-	-	2500 w	-	
2460 vwsh	-	2462 w	2466 vw	2462 vw	2469 w	2462 vw	-	2473 vw	
2432 w	2429 w	-	-	-	-	-	-	-	
-	2418 w	2419 w	-	2417 wbr	2402 w	2402 w	2408 w	2418 vw	
-	2387 vw	2386 vw	2374 w	2391 w	2375 vvw	2370 w	2387 w	2374 w	
2346 wm	2340 msh	2343 wsh	2348 wsh	2350 wsh	2348 wsh	-	2346 m	2347 mw	
-	-	2325 msh	2328 wm	-	2330 ms		-	2328 ms	2 (νC-D)
2313 ms	2313 ms	2314 ms	2320 ms	2315 ms	2320 ms	2319 ms	2318 ms	2313 ms	20b (νC-D)
2273 wmsh	2270 wsh	2280 w	-	2280 msh	-	-	2276 m	2272 wm	20a (νC-D)
			-	2270 vw	-	-			7b (νC-D)
2176 w	2176 w	2174 wbr	2176 w	-	2174 wbr	2183 wbr	2189 w	2175 w	
2152 w	2151 w	2150 w	2150 vw	2152 w	-	2156 wsh	-	2150 w	
2020 wsh	2019 wbr	2018 wbr	2029 wbr	2022 wbr	2033 wbr	2026 wbr	2047 w	2036 wbr	comb
2005 w	2010 w	-	-	-	-	-	-	2000 w	
1832 w	-	-	1827 vw	1829 vw	-	1825 wbr	1826 vw	1829 w	
1794 vw	-	-	1793 vvw	1796 vw	-	-	-	1792 vw	
1668 vwbr	-	1645 vvwbr	1647 wbr	-	1649 mbr	1652 wbr	1652 vw	1646 wbr	δO-H(H_2O)
1633 w	1633 mbr	1628 vvw	1624 w	1630 w	-	1635 w	1633 vw		
1613 w	1611 w	1602 wbr	1602 w	1611 w	-	-	-	-	comb
1569 ssh	-	-	-	1567 ssh	1570 s	1568 vs	1573 vs	1571 vssh	
1560 s	-	-	1561 sbr	-	-	-	-	1562 s	8a (νring)
1557 s	1557 s	1557 s	-	1558 s	1557 s	-	-	-	
1546 s	1545 s	1545 s	1548 ssh	1546 s	1550 ssh	1550 ssh	-	1546 s	
-	1512 w	1513 wm	-	1510 w	-	-	-	-	
1507 w	1503 w	1505 w	-	1503 vw	1507 w	-	-	1507 wm	8b (νring)
1502 w	1500 wsh	1497 vw	1497 w	-	1498 w	-	-	1499 w	
1490 w	1488 w	1490 w	1490 w	1489 w	1490 w	1491 w	1492 wm	1492 w	
-	-	1467 vw	1467 w	-	1454 vw	-	1456 vw	1454 vw	comb
1413 m	1411 m	1408 m	1411 mw	1411 m	1412 wm	1412 wsh	1423 m	1419 m	comb
1407 m							1418 m		
1374 s	1371 s	1372 vsbr	1372 s	1371 vs	1380 s	1376 vs	1393 vs	1381 vs	19a (νring)
							1373 s		
-	-	1358 vs	-	-	-	1362 ssh	1356 vs	1359 s	
1338 s	-	-	1339 s	1348 s	1343 s	1347 s	-	1346 s	19b (νring)
1331 s	1331 s	1331 s	-	1332 s	-	-	-	1332 s	
1320 s	1321 s	1322 s	-	1322 ms	-	1321 m	-	1320 s	

Table 4.14 (continued)

Mn n = 6	Mn n = 5	Fe (Red)	Fe (Yellow)	Co n = 5	Co n = 4	Ni n = 4	Cu n = 4	Zn n = 5	Assignment
1281 sbr	-	1289 ms	1289 ms	-	-	1284 vsbr	-	-	
	1275 s		1271 s	-	1277 vsbr		1274 vw	-	
1266 sbr	1265 s	-		-	-	-	-	1262 ms	7a (νN-O)$_{coord}$
-	-	1257 sbr	-	1258 s	-	-	-	1252 ms	
-	-	1249 ssh	-	-	-	-	-	1243 ms	
1209 ssh	1212 ssh	1208 ssh	-	-	-	-	-	-	
-	1207 s	1205 s	1205 s	1204 s	1204 s	1207 s	1206 s	1204 s	14 (νring)
1201 s	1197 ssh	1195 ssh	-	-	-	-	1194 m	1199 s	
-			1179 m	1179 mw	1180 ms	1181 ms		1179 ms	9a (αC-H)
-	1162 ms	1165 ms	-	1169 m	1169 ms	1168 ms	-	1164 ms	
							1135 s	-	
							1112 s	1115 ssh	
1093 vsbr	1090 vsbr	1091 vsbr	1100 sbr	1084 vs	1102 vsbr	1103 vsbr	1096 s	1097 vs	$\nu(ClO_4)$
1079 vssh	1072 vssh	1070 vssh	1071 ssh	1072 vssh	1070 ssh	-	1073 s	1079 vssh	
							-	1069 vssh	
1025 s	1027 s	1029 s	1029 s	1032 s	1032 s	1032 s	1044 vs	1032 s	
			1022 s	1027 s	1026 s	-	1036 ssh	1025 s	
1007 m	1012 s	1012 s	1012 m	1013 s	-	1012 msh	-	1012 s	1 (νring)
	1002 s	1002 s	-	1004 s	-	-	1006 m	-	
980 vw	-	990 msh	981 msh	985 vw	984 vwsh	981 w	980 w	973 w	comb
-	962 wsh	965 wsh	967 w	-	969 w	-	969 vw	968 wsh	comb
965 w	940 vw	941 wsh	958 w	953 w	961 w	955 wsh	-	-	comb
934 w	931 w	932 w	930 w	933 w	933 w	930 w	935 s	931 w	$\nu(ClO_4)$
-	918 vw	-	918 vwbr	-	928 vwsh	920 vwsh	912 vw	-	comb
			866 s		871 s	877 s	877 s		10a (γC-H)
866 sbr	863 vsbr	860 sbr		864 sbr			874 s	870 s	10b (γC-H)
			861 s		852 s	860 s	855 m	859 s	12 (νring/νN-O)
			847 ms				850 m		
838 s	838 s	836 s	833 s	839 s	833 s	843 ssh	842 s	839 s	11 (γC-H)
	828 ms	828 ms					832 wsh	823 m	
-	769 w	-	-	-	764 w	769 w	-	-	ρM-OH_2
731 mbr	733 wsh	720 wm	735 wsh	735 wsh	738 wsh	732 wsh	735 wsh	738 w	comb
703 mbr	719 wm	715 wm	719 wm	720 w	722 wm	720 wm	721 w	719 m	4 (νring)
678 mbr	683 vw	683 w	684 w	668 w	690 w	686 w	682 w	686 w	6b (νring)
625 s	622 s	622 s	622 s	624 s	625 s	623 s	628 ms	622 s	$\delta(ClO_4)$
							624 s		
571 m	569 w	571 m	571 m	575 w	573 m	-	580 w	574 w	6a (γring)
				570 mw					
542 ms	549 wm	543 m	543 m	558 m	545 s	546 s	551 s	558 wsh	16b (γring)
537 msh	537 m			545 s			542 s	542 s	
-	-	-	-	509 m					
491 s	491 m	481 wsh	491 wmsh	495 wm					
-	-	-	485 ms	485 wm	484 s	484 s	488 s	484 s	15 (αN-O)
478 wm	474 m	473 s	479 mssh	475 s					
	458 wsh		450 wsh					464 w	
-	-	-	-	-	-	-	460 w	-	$\delta(ClO_4)$
397 vw	397 w	398 vw	400 vw	401 vw	409 vw	408 vw	416 vw	407 w	16a (γring)
387 vw	389 vw	386 vw	387 w	387 vw	396 vw	395 vw	401 w	399 vw	

Table 4.15 Infrared assignment (4000-400cm^{-1}) of M(II)$(ClO_4)_2$ complexes with pyrazine-d_4 *N*-oxide

Mn n = 6	Mn n = 5	Fe (Red)	Fe (Yellow)	Co n = 5	Co n = 4	Ni n = 4	Cu n = 4	Zn n = 5	Assignment
3947 w	3949 vw	3945 vw	3942 wbr	3951 w	3953 w	3950 w	-	3945 w	comb
3797 vw	3795 vw	3797 vw	-	3798 vw	3798 w	3086 vw	-	3798 vw	comb
3589 wvbr	3590 vwbr	-	3529 mvbr	3539 wvbr	-	-	-	3547 wvbr	νO-H$_{(free\ H_2O)}$
3517 wvbr	3517 wvbr	3534 vvw	-	-	-	-	-	-	
-	3380 wvbr	-	3300 mbr	-	3360 mbr	3357 wmbr	-	-	νO-H$_{(coord\ H_2O)}$
3123 mbr	3109 s	3110 ms	3117 ms	3111 s	3119 ms	3119 ms	3118 ssh	3113 ssh	20b (νC-H)
							3099 s	3106 s	20a (νC-H)
-	3042 msh	-	-	-	3055 ssh	3057 mssh	3059 ms	3058 msh	2 (νC-H)
3031	3032 m	3033 ms	3030 ms	3032 m	3034 ssh	3040 ms	3040 ms	-	7b (νC-H)
2954 w	2952 w	2975 wsh	2975 msh	2959 wmsh	-	2960 msh	2944 mw	2948 mwsh	
2923 m	2924 m	2925 wm	2925 ms	2929 wm	2929 wsh	2927 wsh	-	-	
2851 w	2853 w	2852 wmsh	2852 m	2856 wsh	-	2858 wsh	2851 vw	-	
-	2805 vw	2810 vw	2777 w	-	-	-	2800 vw	2790 w	
2690 w	2689 w	2687 vw	-	2682 vw	2687 vw	2690 vw	2695 vw	2685 vw	
2636 vw	-	-	-	2634 vw	2640 vw	-	-	2636 w	
2599 vvw	2597 vw	2599 w	2590 vw	2590 vw	-	-	-	2588 w	
2524 w	2527 wbr	2520 w	2520 vw	2529 w	2520 vw	2528 w	2530 vw	2514 w	
-	-	-	-	-	-	2485 vw	2485 vw	2487 w	
2466 w	2463 vvw	2460 w	2464 w	2462 w	2464 vw	2466 w	-	-	
-	-	2380 vw	-	2388 vvw	-	2377 w	2386 wm	2389 w	
2356 wm	-	2360 vw	2363 wm	2363 vw	2364 w	-	-	2368 vw	comb
2344 wm	2335 w	2336 w	2340 wsh	2332 w	2340 w	2342 w	2342 w	2339 vw	
2332 wm								2333 w	
2258 w	2263 vw	2265 vw	2263 vw	2263 vw	2267 w	2269 w	2281 w	2271 w	
2148 w	2149 w	2159 w	2153 wbr	2160 vw	2158 w	2172 wbr	2188 wm	2167 w	
2126 w	2122 vw	2120 w	-	2122 w	-	-	-	2113 vvw	
2068 w	2066 vw	2068 vw	2073 vw	2070 vw	2076 vw	2075 vw	2074 w	-	
2028 w	2020 wbr	2034 wbr	2034 w	2032 wbr	2028 wbr	2029 wbr	2038 w	2022 w	
1934 w	1949 wbr	1945 w	1942 w	1944 w	1941 w	1939 wbr	1940 w	1937 w	
-	1917 vw	-	1914 vw	1910 vw	1919 w	-	1911 w	1902 vw	
1887 vw	-	-	-	-	1892 wbr	1820 wbr	-	1800 vw	
1800 vw	-	-	-	1804 vw	1802 wbr	-	1796 vw	1773 vw	
-	1733 vwbr	1730 vwbr	-	-	1750 wbr	-	1770 vvw	-	
1655 mbr	-	-	1665 wbr	1662 vwbr	1665 w	1668 wbr	1677 m	1676 w	
	1643 w	1644 wm	1645 wm	1642 vw	1642 vw	1642 wbr	-	1646 w	δO-H$_{(H_2O)}$
1605 s	1605 ms	1608 msh	1608 s	1611 s	1610 s	1613 s	1614 sbr	1618 s	8a (νring)
								1603 ssh	
1588 s	1595 s	1594 s	1595 ssh	1595 s	-	-	1589 m	1588 s	8b (νring)
	1589 s	1587 s		1580 ssh					
1527 vw	1539 w	1539 w	-	1520 vw	-	-	-	-	comb
1496 mw	1492 vw	1489 w	1489 m	1489 wsh	-	-	1501 wmsh	1490 w	comb
1465 s	1466 s	1468 s	1468 s	1467 s	1471 s	1473 s	1471 s	1464 s	19a (νring)
1434 s	1459 s	1435 s	1434 s	1435 s	1435 s	1441 s	1444 s	1443 s	19b (νring)
	1434 s							1428 s	
-	-	-	-	-	-	-	1409 w	1402 vw	comb
1396 w	1390 w	1392 vw	1390 vw	-	-	-	1392 w	1387 vw	comb
1327 wsh	1340 w	1338 w	1330 w	1330 sbr	1329 vw	-	1340 s	1331 ms	7a (νN-O)$_{free}$
-	-	-	-	-	-	-	1324 vs	1223 s	
1308 m	1305 s	1306 s	1304 s	1308 sbr	1309 ssh	1315 ssh	1317 vs	1293 sbr	3 (αC-H)

Table 4.15 (continued)

Mn n = 6	Mn n = 5	Fe (Red)	Fe (Yellow)	Co n = 5	Co n = 4	Ni n = 4	Cu n = 4	Zn n = 5	Assignment
-	-	-	-	1317 mssh	-	-	1310 vw	-	comb
1283 vw	1292 vw	-	1288 vw	-	-	-	1280 w	1283 vw	comb
1265 vw	1274 vw	1271 w	1273 w	1267 vw	1272 vw	1272 wsh	-	1271 w	comb
1254 mw	1249 m	1253 s	-	1247 s	-	-	1255 vs	1256 s 1249 s	7a (νN-O)$_{free}$
1238 m	-	1243 s	1242 vssh	1237 s	-	-	-	1239 vs	7a (νN-O)$_{coord}$
1227 ms	1226 s	1227 vsbr	1232 vs	1232 vs	1225 sbr	1223 sbr	-	1218 s	
1214 s	1219 s	1208 s	1218 vssh	-	-	-	1213 w	1209 s	
1166 m	1166 s	1167 s	1166 m	1168 ms	1168 s	1167 m	1174 m	1168 m	14 (νring)
1080 vsbr	1094 vsbr	1088 vsbr	1088 vsbr	1095 vsbr	1080 vsbr	1100 sbr	1133 sbr 1100 sbr 1055 vs	1089 sbr	$\nu_a(ClO_4)$
1029 mw	1026 w	1025 msh	1023 ms	1025 w	1027 ms	1024 m	1026 vs	1026 m	
-	1009 s	-	-	-	-	-	1012 s	1010 s	1 (νring)
1003 s	-	1001 s	1004 s	1006 s	1006 s	1005 s	-	1003 s	
988 s	990 s	990 s	988 s	991 ms	989 mssh	989 msh	-	990 ms	3 (αC-D)
981 mssh	-	982 s	-	984 ms	-	-	-	-	
942 w	944 w	947 w	946 vw	948 vw	942 w	944 w	-	940 w	9a (αC-D)
930 w	931 w	931 w	930 w	933 w	930 w	931 w	935 s	932 w	$\nu(ClO_4)$
-	909 vw	-	-	896 vwbr	906 wm	-	912 vw	-	comb
875 vw	870 vwbr	870 vw	-	-	-	-	883 vw	881 vw	comb
848 ms	850 ms	852 m 841 m	849 m	851 m 842 wm	851 m	850 m	858 s	851 ms	10b (γC-D)
826 mw	829 wm	829 w	828 w	827 w	827 w	824 w	838 w	829 w 824 w	18a (αC-D)
815 m	816 m	817 wm	-	819 w	-	-	811 s	817 w	18b (αC-D)
787 vs	794 vs	791 vs	787 vs	792 vs	795 vs	792 vs	802 s 794 s	790 s	12 (νring/νN-O)
	-				761 wm	760 w	-	-	ρM-OH_2
729 s	731 m	725 ms	731 m	735 m	727 msh	734 m	738 s	734 m	11
719 ms	720 m	-	720 ms	723 ms	720 ms	727 wsh	722 m	724 ms	
710 m	710 m	710 ms	-	711 m	-	-	-	710 wsh	10a (γC-D)
-	670 w	-	665 vwsh	-	667 w	671 w	660 vw	-	6b (νring)
662 vw	664 vw	660 w	659 w	664 vw	663 w	664 w	652 vw	663 vw	
621 s	623 s	622 s	621 s	624 s	622 s	623 s	628 ssh 620 s	623 s	$\delta(ClO_4)$
610 wsh	607 w	605 wsh	-	-	-	-	-	614 wsh	4 (γring)
560 wsh 552 wm	551 wm	561 wm 522 w	558 w 530 w	564 wm -	571 wm 540 wsh	563 w 540 wsh	567 w -	563 w 548 wm	6a (νring)
-	-	496 s	-	500 wm	490 wmsh	495 wmsh	-	495 wm	15 (αN-O)
473 s	471 ssh	470 s	470 ssh	469 vs		469 s	477 s	475 ms	
462 vs	462 s	465 s	466 s		466 s		467 vs	464 vs	16b (γring)
455 ssh	445 s	453 s	-	454 ms		-	-	444m	
431 w	-	-	-	-	-	-	-	-	comb
-	389 vw	-	349 vw	365 vw	393 vw	-	363 vw	-	16a (γring)
342 vw	-	348 vwsh	334 vw	-	336 vw	350 vw	350 vw	353 vw	

pzO			Mn L_6		Mn L_5		Fe (red)		Fe (yellow)		Co L_5		Co L_4		Ni L_4		Cu L_4		Zn L_5		Assignment
$-d_0$	$-d_4$		$-d_0$	$-d_4$	$-d_0$	$-d_4$	$-d_0$	$-d_4$	$-d_0$	$-d_4$	$-d_0$	$-d_4$	$-d_0$	$-d_4$	$-d_0$	$-d_4$	$-d_0$	$-d_4$	$-d_0$	$-d_4$	
			625 s	(621 s)	622 s	(623 s)	622 s	(622 s)	622 s	(621 s)	624 s	(624 s)	625 s	(622 s)	623 s	(623 s)	628 ms 624 s	(628 ssh) (620 s)	622 s	(623 s)	$\delta(ClO_4)$
			571 m	(560 wsh) (552 wm)	569 w	(551 wm)	571 m	(561 wm) (522 w)	571 m	(558 w) (530 w)	575 w 570 wm	(564 wm)	573 m	(571 wm) (540 wsh)	-	(536 w) (540 wsh)	580 w	(567 w)	574 w	(563 w) (548 wm)	6a (νring)
6a	545	(535)																			
16b	540	(455)	542 ms 537 msh	(455 ssh)	549 wm 537 m	(445 s)	553 m 537 ms	(455 s)	534 m	(466 vs)	558 m 545 s	(454 ms)	545 s	(-)	546 s	(-)	551 s 542 s	(-)	558 wsh 542 s	(495 wm) (475 ms)	16b (γring)
								(496 s)			509 m	(500 wm)									
			491 s	(473 s)	491 m	(471 ssh)	481 msh	(470 s)	491 wmsh		495 wm			(491 wmsh)		(495 wmsh)		(477 s)			15 (αN-O)
							473 s	(465 s)	485 ms	(466 vs)	485 wm	(469 vs)	484 s	(466 s)	484 s	(469 s)	488 s	(467 vs)	484 s	(464 vs)	
15	475	(468)	478 wm	(462 vs)	474 m	(462 s)			479 mssh		475 ms								464 w	(444 m)	
			-	(431 w)	-	(-)	-	(-)	450 wsh	(-)	-	(-)	-	(-)	-	(-)	460 w	(masked)	-	(-)	$\delta(ClO_4)$
			-	(-)	458 wsh	(masked)	-	(-)	-	(-)	-	(-)	-	(-)	-	(-)	-	(-)	-	(-)	
16a	396	(345)	397 vw	(-)	397 w	(389 vw)	398 vw	(-)	400 vw	(349 vw)	401 vw	(365 vw)	409 vw	(393 vw)	408 vw	(-)	416 vw	(363 vvw)			16a (γring) and νM-OH_2
			387 vw	(342 vw)	390 vw	(-)	386 vw	(348 vwsh)	387 w	(334 vw)	387 vw	(-)	396 vw	(336 vw)	395 vw	(350 vw)	401 w	(350 vvw)			
							329 ms	(324 m)			338 ms	(336 m)									νM-O
			313 m	(308 ms)	313 m	(307 m)			290 msh	(289 msh)							314 vw	(-)	-	(296 wsh)	
			266 mw	(261 m)	265 m	(261 s)	269 ms	(263 ms)	267 s	(259 s)	271 s	(267 ms)	273 sbr	(268 mw)	285 msbr	(273 m)	297 s	(288 s)	283 m	(282 mw)	νM-N
				(241 m)		(244 m)													264 s	(255 m)	
			-	(-)	-	(-)	-	(-)	-	(-)	-	(-)	-	(-)	-	(-)	249 wm	(247 mw)	-	(-)	νM-$OClO_3$
																	240 wsh	(238 wsh)			
							239 m	(236 m)			241 m	(236 mw)	235 wm	(229 wbr)	235 wm	(230 wm)					νM-N(bridged)
5	226	(222)	228 wmsh	(226 wm)	230 m	(223 wsh)			227 m	(223 m)											15 (γN-O/γring)
			222 m	(204 m)	221 m	(215 ms)	221 m	(215 m)			219 w	(216 w)	218 vw	(218 wsh)	-	(-)	216 wm	(212 mw)	209 mw	(208 wm)	
							196 mbr	(193 ms)	195 ms	(194 ms)	200 m	(192 mw)	206 vw	(207 wsh)							τNO/τMO
			187 mw	(187 w)	185 mw	(187 mw)	187 mwsh	(175 wsh)			181 wm	(175 wsh)			182 w	(168 wsh)			190 wm	(184 vw)	
									170 wm	(175 wmsh)			173 vw	(161 w)	171 w	(163 w)	-	(168 s)	171 m	(166 w)	δMON + δMN
			162 vw	(-)	161 w	(158 w)			158 wm	(152 wm)			155 w	(146 vw)			151 ms	(-)			
			142 vw	(-)	143 w	(141 w)	136 vwsh	(135 w)	137 wm	(135 wm)			128 w	(137 vw)					135 w	(131 w)	τMO/τNO + δMN
			-	(110 vwsh)	123 vw	(109 w)	-	(113 wsh)	122 wsh	(123 wsh)	120 w	(118 vw)	-	(102 vw)	108 vw	(102 vw)	105 m	(106 m)			
			92 w	(87 w)	84 wbr	(89 w)	101 w	(98 w)			92 w	(93 w)	95 w	(90 vw)	-		92 m	(87 w)	87 w	(88 vw)	δMN + τMO/τNO
			-	(-)		(83 w)	81 w	(83 w)	85 w	(85 w)	80 wbr	(87 w)	83 w	(76 vw)	80 w	(80 w)	72 vw	(75 vwsh)	-	(75 vw)	
			61 w	(62 w)	62 w	(62 vw)	66 w	(57 w)	-	(66 vw)	-	(71 vwsh)	65 w	(-)	64 vw	(64 w)	55 vw	(55 vw)	60 wbr	(54 vw)	δOMO + δMN

Table 4.16 Far infrared assignment (625-50cm^{-1}) of M(II)$(ClO_4)_2$ complexes with pyrazine *N*-oxide and pyrazine-d_4 *N*-oxide

tra) of these complexes are discussed, it is necessary to comment further upon the regions used to determine the nature of coordination.

Firstly, in considering the employment of mode 8a as an indicator of the presence of metal-nitrogen coordination, the full infrared assignment of the M(II) complexes with pzO and their -d_4 analogues reveals a bathochromatic shift of this ring mode on coordination for *all* the complexes, independantly of whether the nitrogen or the oxygen is the donor atom (Tables 4.14 and 4.15). Although it is true that this vibration is split in the deuterated complexes and that a band is found at a frequency similar to the free ligand in some of these complexes, the absence of this behaviour for the -d_0 analogues must exclude the use of this mode as a means to prove metal-nitrogen coordination. The band(s) at *ca.* 1585cm^{-1} in the complexes with lanthanide perchlorates which were assigned as νC=N (mode 8a) by VICENTINI and ZINNER [70] are preferably to be assigned to mode 8b, and in so doing also reflect a bathochromatic shift. This accounts for the previously mentioned different assignment of νC=N made by these authors [70,71].

Secondly, the present deuteration study, with its full vibrational assignment, helps to clarify the assignments of mode 3 (αC-H) and the Kekulé vibration (mode 14) from those bands reflecting free and coordinated νN-O (mode 7a) in the -d_0 isotopomer. From Table 4.14, it is clear that on coordination the Kekulé mode is to be found at a sufficiently lower frequency (more than 40cm^{-1}) to prevent possible misassignment as coordinated N-O stretch. Furthermore, in the absence of any other ligand band being found in the region of the N-O stretch in the deuterated complexes, by identifying the nature of coordination, particularly in the Cu(II) complexes, it is possible to identify the strong -d_0 band between 1295 and 1315cm^{-1} as arising from the planar C-H bend (mode 3). It is also noted that the magnitude of

the shifts on complexation of both the free νN-O and coordinated νN-O is smaller for the labelled complexes, indicating that this vibration is more coupled in the deuterated ligand than it is in ordinary pzO.

In their work on metal(II) complexes with pyrazine *N*-oxide, SPECA and his co-workers concluded that high pzO to metal ratios are attained only in cases involving exclusive O-bonded monodentate pzO, while N-bonded monodendate co-ordination occurs only where the ligand to metal ratio is low [76,77]. As seen below, the present work indicates that the coordination is not as simple to define as this, with bridging of pzO and mixed N- and O-bonded monodendate coordination being observed for the high ligand-metal ratio of 5:1.

Even so, the $Mn(pzO)_6(ClO_4)_2$ hemihydrate and its pz-d_4O analogue are coordinated exclusively through O-bonded monodendate coordination, as indicated by the frequency of the split νN-O (coordinated) (although the deuterated complex does show a band of medium intensity showing no shift to lower frequencies). The complex is therefore likely to have S_6 symmetry as is found for its hexakis (pyridine *N*-oxide) analogue [29]. Two νM-O, four δOMO and two each of δMON, τNO and τMO are expected to be infrared active. From Table 4.16 two νM-O bands are observed for the -d_0 complex, while three are seen in the deuterated complex. The νM-O band at 313cm^{-1}(-d_0) is at the identical frequency to that observed in $[Mn(pyO)_6](ClO_4)_2$ [29]. The presence of the lower band in the deuterated spectrum may indicate a slight distortion from S_6 symmetry, which may also account for the larger splitting of the ligand modes 19b(-d_7), 15(-d_0), 9a(-d_0), 8a(-d_7), 8b(-d_7), 7a and 1, than might be expected from a resolution of localised ligand symmetry employing S_6 symmetry.

With lower ligand to metal ratios than 6 to 1, there exists a possibility of

coordination by solvent molecules or by the counter ion, besides the possibility of bridging by the ligand [75-77].

From the infrared spectra it is clear that the Cu complexes ($-d_0$ and $-d_4$) are the only ones possessing coordinated perchlorate. This is shown by the splitting of the perchlorate bands at *ca.* 1100cm^{-1}, by the strong intensity of the band at 935cm^{-1} and by the appearance of a weak band at 460cm^{-1} (masked in the $-d_4$ spectrum). Furthermore, the absence of a strong band between 1270cm^{-1} and 1247cm^{-1} indicates that the perchlorate is monodendate [67].

The bathochromatic shift of νM-O with a total absence of bands below that of νN-O for the free ligand (1307cm^{-1} for the $-d_0$ isotopomer, 1215cm^{-1} for the $-d_4$ isotopomer) is clear evidence for exclusive terminal N-coordination by Cu(II) perchlorate, as was previously observed by SPECA *et al.* [76]. This being so, the most likely conformation of the complex is that with D_{4h} symmetry. For such symmetry one νM-N and two δMN, and one νM-OClO$_3$ and one δM-OClO$_3$ are expected to be infrared active. From Table 4.16 the bands at 297cm^{-1}($-d_0$) and 288cm^{-1}($-d_4$) are assigned to νM-N on the basis of their relative insensitivity to ligand deuteration, the medium to weak bands at 249cm^{-1}($-d_0$) and 247cm^{-1}($-d_4$), with their lower frequency weaker shoulders, are assigned to νM-OClO$_3$. The low frequency of the metal-perchlorate stretches is indicative of the presence of long Cu-O bonds (suggesting tetragonal distortion) [79,80], while the presence of the lower frequency shoulders possibly shows that two difference M-O bond lengths exist, with a lowering of symmetry. This may also account for the splitting of the ligand modes 19a($-d_4$), 16b($-d_0$), 15($-d_4$), 12($-d_4$), 11($-d_0$), 7a($-d_0$) and 1.

The differentation between lattice and coordinated water from the infrared spectrum is more difficult to establish, than is the identification of co-

ordinated perchlorate. The O-H stretch of water generally gives rise to a very broad continuous absorption between 3650 and 3000cm^{-1} [79], as a result of several maxima. Coordinated water gives rise to a relatively sharp νO-H between 3400 and 3300cm^{-1} [79,81-84]; however, this may be masked by the presence of lattice water.

Coordination of a water molecule gives rise to three new OH_2 fundamental vibrations, the wagging, twisting and rocking modes, as well as giving rise to the M-OH_2 stretch and the M-OH_2 bending modes. Of these, the twisting mode is infrared inactive, while the OH_2 rock gives rise to a weak infrared band between 800 and 600cm^{-1} and the OH_2 wag gives rise to a band of medium to weak intensity between 650 and 400cm^{-1} for M(II) complexes [82-86]. There is, however, a strong likelihood that these vibrations may be masked by other ligand bands, or in the absence of a full infrared assignment, that other ligand modes might be incorrectly assigned to these two OH_2 modes. Furthermore, there is some question as to the expected frequency of the M-OH_2 stretch for M(II) complexes, with deuteration studies supporting both regions of 345 to 280cm^{-1} [31,82] and 440 to 360cm^{-1} [85].

Considering this, the conformation of the rest of the complexes are examined.

For complexes containing a pzO ratio of 5 to 1, several conformations are possible since the complex may be a 5-coordinate monomer, with either a trigonal bipyramidal or a square based pyramidal conformation. Alternatively, it may be monomeric octahedral with a water molecule occupying the sixth coordation site. The ability of the pzO to form bridges gives rise to the possible formation of a dinuclear octahedrally coordinated complex, or to a polymeric chain of octahedrally coordinated metal(II) atoms.

From the infrared spectra it is tentatively suggested that the most likely structure for $Mn(pzO)_5(ClO_4)_2 \cdot 1\frac{1}{2}H_2O$ and its pz-d_4 analogue is the octahedral monomer with exclusive O-monodendate pzO coordination and with the coordination of one molecule of water. The former is supported by the absence of a band above $1307cm^{-1}$(-d_0) which may be attributed to free νN-O. The latter is tentatively indicated by a medium to strong νO-H at $3378cm^{-1}$(-d_4) and by the presence of the $Mn-OH_2$ rock at $769cm^{-1}$(-d_0). Either the weak shoulder at $458cm^{-1}$(-d_0) (its pz-d_4O analogue being masked by mode 15) or the very weak band at $389cm^{-1}$ may be assigned to $\nu M-OH_2$. The latter is more likely in view of its insensitivity to deuteration of pzO; however, its frequency is very similar to that at which the ligand mode 16a is expected to occur (Table 4.16). The similarity of the infrared spectra in the region containing the metal-ligand stretches for the hexakis - and pentakis pyrazine *N*-oxide complexes supports the suggestion that the latter is monomeric octahedral. This complex therefore differs to the previously reported bridged 5-coordinated Mn(II) complexes with pzO [75,76] in which the bridged M-N stretch is observed at *ca.* $240cm^{-1}$.

In this work $Fe(II)(ClO_4)_2$ was found to give rise to two complexes with pzO; the immediate precipitation of the anhydrous red complex of $Fe(pzO)_5(ClO_4)_2$, and the yellow-orange complex of $Fe(pzO)_5(ClO_4)_2 \cdot 2H_2O$ (upon allowing the red complex to stand exposed to the atmosphere). This behaviour is similar to that previously reported by SPECA *et al.* [76] for the red complex $Fe(pzO)_3(ClO_4)_2$ and the orange complex $Fe(pzO)_3(ClO_4)_2 \cdot H_2O$.

The infrared spectra of the red complex indicates the absence of free νN-O, thereby showing either exclusive monodentate O-coordination for a 5-coordinate complex, or a mixture of monodendate O-coordination and bridging by pzO for a 6-coordinate complex.

For penta-coordination two possible coordinations exist, trigonal bipyramidal or square based pyramidal. Considering the $M(ON)_5$ unit, both complexes are expected to give rise to five infrared active M-O stretches (both having C_1 symmetry). Considering the simpler MO_5 unit, two M-O stretches are expected in the infrared band for trigonal bipyramidal symmetry, while three are expected to be Raman active (with the E' vibration being coincidental with its infrared analogue). For square based pyramidal, three M-O stretches are expected in the infrared spectra while four are expected to be Raman active (with two A_1 and an E vibration being coincidental with their infrared analogues).

For the 6-coordinate octahedral dimer having either C_{2h} symmetry (considering the $M_2(ON)_{10}$ unit) or D_{2h} symmetry (considering the ligand as a point mass) six infrared active and six Raman active metal-ligand stretches are expected (with no infrared and Raman coincidences). For the octahedrally coordinated polymeric chain having D_{4d} symmetry (*i.e.* the M_xL_{4x} unit containing a 45° screw axis) four infrared active metal-ligand stretches and eight Raman active metal-ligand stretches (of which four are coincident with the infrared bands) are expected. The polymeric chain having D_{4h} symmetry (*i.e.* the M_xL_{4x} unit having no screw axis) is expected to give rise to two infrared active metal-ligand and to two Raman active metal-ligand bands (with no infrared and Raman coincidence).

Three infrared active metal-ligand stretches are observed, which suggests a square based pyramidal conformation. However, the medium band at 239cm^{-1} ($-d_0$) is typical of a M-N stretch [75-77], which suggests the presence of a bridged molecule of pzO, and so the polymeric structures with D_{4d} and D_{4h} symmetry cannot be excluded purely on the basis of the infrared spectra. (The frequency of the bands at 329cm^{-1} and 269cm^{-1} may also reflect mono co-

ordinated O- and bridged O- stretches). In view of the large difference expected within the Raman spectra for the different structures, future Raman studies of the red Fe(II) complex should clarify the final conformation of this complex.

The yellow complex is clearly monomeric octahedral, with unidendate O-coordinated pzO and with one molecule of coordinated water. This is evident from the absence of free νN-O, and by the loss of the band at 239cm^{-1} (with the lowering of the M-O stretch at 329cm^{-1}) compared with the red complex. (This observation also supports the suggestion that the red Fe(II) complex is bridged polymeric). No analogue to the very weak shoulder at 450cm^{-1} is observed in the yellow complex with pz-d_4O, and the four bands between 400 and 250cm^{-1} show substantial ligand deuteration sensitivity (Table 4.16), so the assignment of νFe-OH$_2$ remains uncertain. SPECA *et al.* [76] assigned Fe-OH$_2$ to the weak band at 390cm^{-1} in the infrared spectrum of [Fe(pzO)$_3$(ClO$_4$)(H$_2$O)](ClO$_4$) However, present labelling studies indicate that bands in this region may well arise from the ligand mode 16a.

The tangerine Co(pzO)$_5$(ClO$_4$)$_2$·1½H$_2$O complex differs from the previously considered pentakis pyrazine *N*-oxide complexes in that monodentate N-coordination is present. This is evident from the presence of a strong broad N-O stretch at 1330cm^{-1}(-d_0). From Tables 4.14 and 4.15, the absence of an OH$_2$ rocking mode and the nature of the broad νO-H bands indicate the absence of coordinated water. Furthermore, the infrared spectra over the metal-ligand stretching region are similar to the red Fe(II) complexes (-d_0 and -d_4), therefore the presence of the strong band at 271cm^{-1}(-d_0) very likely indicates terminal O-coordination (with the higher band reflecting bridged νM-O). However, this may only be clearly established by an ^{18}O labelling study of the pzO.

Therefore, as with the red Fe(II) complex, while the pzO bridged octahedrally coordinated complex is considered the most likely structure, future work, especially investigating the Raman spectra, is required to determine the exact nature of the coordination. The suggestion of the presence of terminal N-coordination, terminal O-coordination and bridged pzO for this Co(II) complex is supported by the literature. $[Co(pzO)_2(NO_2)_2]$ which is octahedral monomeric, shows both terminal O- and terminal N-coordination [74]. The polymeric trigonal bipyramidal $[Co(pzO)_3Cl_4]_x$ (x = 1 or 2) shows both terminal N-coordination and bridging by pzO [75], while $[Co(pzO)_3(H_2O)(ClO_4)](ClO_4)$ (octahedral dimeric) shows terminal O-coordination and bridging by pzO [76].

The last metal complexes which have a ligand to metal ratio of 5 to 1 are those of $Zn(pzO)_5 \cdot H_2O$ and its pz-d_4O analogue. The nature of the νO-H band and the absence of a M-OH_2 rock at *ca.* 760cm^{-1} is indicative of the presence of lattice water. The weak band at 464cm^{-1} (with its medium pz-d_4O analogue at 444cm^{-1}) cannot be considered as νM-OH_2 in view of its large sensitivity to deuteration of pzO. The presence of bands above and below the N-O stretch of the free ligand is indicative of both terminal N-coordination and O-terminal or bridged pzO coordination.

The possible structure of the complex is therefore either trigonal bipyramidal or square based pyramidal monomeric, or octahedrally dimeric or polymeric. The absence of a band at *ca.* 235cm^{-1} (being bridged νM-N) implies that bridging is unlikely, while the high frequency of the band at 264cm ($-d_0$), which is here assigned to νM-N, further supports pentacoordination rather than hexacoordination, being evident of a lower coordination number than the previously considered octahedrally coordinated complexes. Of the two monomeric configurations, the trigonal bipyramidal is favoured by the absence of CFSE, while the presence of terminal N-coordination of pzO, with its ability to

afford π-bonding, favours the square based pyramidal conformation. As two infrared active metal-ligand stretches and three Raman active stretches (with one being *E"* being coincidental in the infrared and Raman spectra) are expected for trigonal bipyramidal, while three infrared active metal-ligand stretches and four Raman active stretches (with two A_1 and one E being coincidental in the infrared and Raman spectra) are expected for square based pyramidal conformation a final conclusion to the structure of the complex must await a Raman investigation.

The final four complexes to consider are the tetrakis pyrazine *N*-oxide complexes of Ni(II) and Co(II), and their pz-d_4O analogues. Apart from the similarity of the infrared spectra for both the N-O stretching and metal-ligand stretching regions for both the Ni(II) and Co(II) complexes, the systematic absence of modes 8a(-d_0) and 18b(-d_4) in these complexes and the presence of these bands in the other complexes suggests that the Ni(II) and the light pink Co(II) complex are isostructural. The light pink $Co(pzO)_4H_2O$ complex differs to that of the tangerine $Co(pzO)_5(ClO_4)_2\cdot 1\frac{1}{2}H_2O$ complex in that there is no terminally coordinated pzO present in the latter, as is evident from the νN-O (Tables 4.14 and 4.15). Furthermore, the nature of the O-H stretch at 3360cm^{-1}(-d_0) and at 3340cm^{-1}(-d_4) for both complexes, as well as the presence of a OH_2 rock at *ca.* 765cm^{-1}(-d_0) and at 760cm^{-1}(-d_4) indicates the presence of coordinated water. However, no clear assignment of the νM-OH_2 can be made since the three bands between 470cm^{-1} and 250cm^{-1} reveals sensitivity to deuteration of pzO in both the Co(II) and Ni(II) complexes. In view of the slight deuteration sensitivity of the OH_2 rock (Tables 4.14 and 4.15), it is possible that there may be strong coupling between νM-OH_2 and νM-O (of pzO). The presence of two metal-ligand stretching bands in the infrared spectra (with a bridged νM-N at 235cm^{-1}) indicates the complexes are octahedrally polymeric with D_{4h} symmetry (*i.e.* without a screw axis). How-

ever, this is subject to confirmation by future Raman investigations.

Finally, the assignments of the vibrations below 200cm^{-1} for the present series of metal(II) complexes with pzO and their fully deuterated analogues (Table 4.16) are tentatively based upon previous infrared studies [4-7,20].

In conclusion, it is necessary to point out the limitations to the isotopic labelling of pzO investigated in this work. While the present deuteration assignment has (*i*) clarified the identification of mode 3($-d_0$), (*ii*) established that mode 14($-d_0$) cannot be confused with the N-O stretching vibration, (*iii*) shown that the weak bands at *ca.* 390cm^{-1} (previously assigned to νM-OH$_2$) are very likely to arise from the ligand mode 16a, and (*iv*) established that the two bands at 249cm^{-1}($-d_0$) and 247cm^{-1}($-d_4$) in the Cu(II) complexes are Cu-OClO$_3$ stretches, it is noted that the nature of the labelling does not enable a distinguishing between the M-N and M-O stretching fundamentals. Since a lower coordination number results in the M-N stretch being raised in frequency to a position similar to the M-O stretch of 6-coordinate complexes (*e.g.* the Cu and Zn complexes), the use of frequency ranges to identify the M-N and M-O stretches must remain very tentative, especially where Raman data is not available. It is possible that future ^{18}O labelling of pzO may establish more exactly not only the assignment of νM-O and νM-N (provided there is no significant coupling between these modes), but may also clarify the assignments of νM-OH$_2$ for the yellow Fe(II) complex, as well as for the tetrakis pyrazine *N*-oxide complexes of Co(II) and Ni(II). The use of a deuteration study of the coordinated water to establish the correct assignment of νM-OH$_2$ is likely to prove impractical in view of the extreme hygroscopicity of these complexes.

1. C.V. BERNEY and J.H. WEBER,
Inorg. Chem., 7 (1968) 283.

2. C.V. BERNEY and J.H. WEBER,
Inorg. Chim. Acta, 5 (1971) 375.

3. S. SUZUKI and W.J. ORVILLE-THOMAS,
J. Mol. Struct., 37 (1977) 321.

4. A.D. VAN INGEN SCHENAU, W.L. GROENEVELD and J. REEDIJK,
Spectrochim. Acta, 30A (1974) 213.

5. A.D. VAN INGEN SCHENAU, C. ROMERS, D. KNETSCH and W.L. GROENEVELD,
Spectrochim. Acta, 33A (1977) 859.

6. A.M. GREENAWAY, C.J. O'CONNOR, E. SINN and J.R. FERRARO,
Spectrochim. Acta, 37A (1981) 575.

7. D.M. ADAMS and W.R. TRUMBLE,
J. Chem. Soc. Dalton, (1975) 30.

8. D.M. ADAMS and W.R. TRUMBLE,
Inorg. Chem., 15 (1976) 1968.

9. C.W. FRANK and L.B. ROGERS,
Inorg. Chem., 5 (1966) 615.

10. J.R. FERRARO, W. WOZNIAK and G. ROCH,
Ric. Sci., 38 (1968) 433.

11. J.R. FERRARO, J. ZIPPER and W. WOZNIAK,
Appl. Spectrosc., 23 (1969) 160.

12. J.R. ALLEN, G.A. BARNS and D.H. BROWN,
J. Inorg. Nucl. Chem., 33 (1971) 3765.

13. I.A. DORRITY and K.G. ORRELL,
J. Inorg. Nucl. Chem., 36 (1974) 230.

14. J.E. RUEDE and D.A. THORNTON,
J. Mol. Struct., 34 (1976) 75.

15. R.J.H. CLARK and C.S. WILLIAMS,
Inorg. Chem., 4 (1965) 350.

16. O. POIZAT and C. SOURISSEAU,
J. Phys. Chem., 88 (1984) 3007.

17. M. GOLDSTEIN, E.F. MOONEY, A. ANDERSON and H.A. GEBBIE,
Spectrochim. Acta, 21 (1965) 105.

18. D.M.L. GOODGAME, M. GOODGAME, P.J. HAYWARD and G.W. RAYNER-CANHAM,
Inorg. Chem., 7 (1968) 2447.

19. M. GOLDSTEIN and W.D. UNSWORTH,
Inorg. Chim. Acta, 4 (1970) 342.

20. M. GOLDSTEIN, F.B. TAYLOR and W.D. UNSWORTH,
J. Chem. Soc. Dalton, (1972) 418.

21. M.D. CHILD and G.C. PERCY,
Spectrosc. Letters, 10 (1977) 71.

22. R.E. MORCOM and C.F. BELL,
J. Inorg. Nucl. Chem., 35 (1973) 1865.

23. B. HUTCHINSON, J. TAKEMOTO and K. NAKAMOTO,
J. Amer. Chem. Soc., 92 (1970) 3335.

24. Y. SAITO, J. TAKEMOTO, B. HUTCHINSON and K. NAKAMOTO,
Inorg. Chem., 11 (1972) 2003.

25. J.H. TAKEMOTO, B. STREUSAND and B. HUTCHINSON,
Spectrochim. Acta, 30A (1974) 827.

26. R.E. WILDE and T.K.K. SRINIVASAN,
J. Inorg. Nucl. Chem., 36 (1974) 323.

27. A.T. KOWAL and J. SKARZEWSKI,
Spectrochim. Acta, 41A (1985) 563.

28. S.A. COTTON and J.F. GIBSON,
J. Chem. Soc. A, (1970) 2105.

29. A.T. HUTTON and D.A. THORNTON,
J. Mol. Struct., 39 (1977) 33.

30. G.A. GRIFFITHS and D.A. THORNTON,
J. Mol. Struct., 52 (1979) 39.

31. T.P.E. AUF DER HEYDE, C.S. GREEN, D.E. NEEDHAM, D.A. THORNTON and G.M. WATKINS,
J. Mol. Struct., 70 (1981) 121.

32. J. PADMOS and A. VAN VEEN,
Spectrochim. Acta, 38A (1982) 97.

33. R.G. INSKEEP,
J. Inorg. Nucl. Chem., 24 (1962) 763.

34. G.C. PERCY abd D.A. THORNTON,
Spectrosc. Letters, 3 (1970) 323.

35. G.C. PERCY and D.A. THORNTON,
J. Mol. Struct., 10 (1971) 39.

36. G.C. PERCY and D.A. THORNTON,
J. Mol. Struct., 14 (1972) 313.

37. O.P. ANDERSON,
J. Chem. Soc. Dalton, (1972) 2597.

38. O.P. ANDERSON,
J. Chem. Soc. Dalton, (1973) 1237.

39. J.S. STRUKL and J.L. WALTER,
Spectrochim. Acta, 27A (1971) 223.

40. S. McCLANAHAN and J. KINCAID,
J. Raman Spectrosc., 15 (1984) 173.

41. H. IRVING and T.J.P. WILLIAMS,
J. Chem. Soc., (1953) 3192.

42. N.N. GREENWOOD and K. WADE,
J. Chem. Soc., (1960) 1130.

43. N.S. GILL, R.H. NUTTAL, D.E. SCAIFE and D.W.A. SHARP,
J. Inorg. Nucl. Chem., 18 (1961) 79.

44. J.R. DURIG, B.R. MITCHELL, D.W. SINK, J.N. WILLIS and A.S. WILSON,
Spectrochim. Acta, 23A (1967) 1121.

45. S. AKYÜZ, A.B. DEMPSTER, R.L. MOREHOUSE and S. SUZUKI,
J. Mol. Struct., 17 (1973) 105.

46. E.D. McKENZIE,
Coord. Chem. Rev., 6 (1971) 187.

47. C. POSTMUS, J.R. FERRARO and W. WOZNIAK,
Inorg. Chem., 6 (1967) 2030.

48. K. KRISHNAN and R.A. PLANE,
Spectrochim. Acta, 25A (1969) 831.

49. N.M. KARAYANNIS, A.N. SPECA, D.E. CHASEN and L.L. PYTLEWSKI,
Coord. Chem. Rev., 20 (1976) 37.

50. P.G. SIMPSON, A. VINCIGUERRA and J.V. QUAGLIANO,
Inorg. Chem., 2 (1963) 282.

51. A. VINCIGUERRA, P.G. SIMPSON, Y. KAKIUTI and J.V. QUAGLIANO,
Inorg. Chem., 2 (1963) 286.

52. S.K. MADAN and W.E. BULL,
J. Inorg. Nucl. Chem., 26 (1964) 2211.

53. I.S. ASHUJA and R. SINGH,
Spectrochim. Acta, 30A (1974) 2055.

54. I.S. ASHUJA, R. SINGH and C.L. YADAVA,
J. Mol. Struct., 74 (1981) 143.

55. I. BERTINI, D. GATTESCHI and L.J. WILSON,
Inorg. Chim. Acta, 4 (1970) 629.

56. A.R. AL-KARAGHOULI, R.O. DAY and J.S. WOOD,
Inorg. Chem., 17 (1978) 3702.

57. S.W. NG, C.L. BARNES, D. VAN DER HELM and J.J. ZUCKERMAN,
Organomet., 2 (1983) 600.

58. M. ORCHIN and P.J. SCHMIDT,
Coord. Chem. Rev., 3 (1968) 345.

59. J.H. NELSON, L.C. NATHAN and R.O. RAGSDALE,
Inorg. Chem., 7 (1968) 1841.

60. J.H. NELSON and R.O. RAGSDALE,
Inorg. Chim. Acta, 2 (1968) 230.

61. J.H. NELSON and R.O. RAGSDALE,
Inorg. Chim. Acta, 3 (1969) 473.

62. V.G.K. DAS, V.C. KEONG, N.G.S. WENG, C. WEI and T.C. MAK,
J. Organomet. Chem., 311 (1986) 289.

63. J.E. HUHEEY,
Inorganic Chemistry : Principles of Structure and Reactivity, (1972)
Harper and Row, New York.

64. N.M. KARAYANNIS, L.L. PYTLEWSKI and M.M. LABES,
Inorg. Chim. Acta, 3 (1969) 415.

65. N.M. KARAYANNIS, C.M. MIKULSKI, M.J. STROCKO, L.L. PYTLEWSKI and M.M. LABES,
J. Inorg. Nucl. Chem., 33 (1971) 3185.

66. J.D. LEE, D.S. BROWN and B.G.A. MELSOM,
Cta. Cryst. B, 25 (1969) 1378.

67. B.J. HATHAWAY and A.E. UNDERHILL,
J. Chem. Soc., (1961) 3091.

68. L.B. ZINNER and G. VICENTINI,
An. Acad. brasil. Ciênc., 47 (1975) 83.

69. C.J. POPP and G.D. GARLOUGH,
J. Inorg. Nucl. Chem., 43 (1981) 501.

70. G. VICENTINI and L.B. ZINNER,
Inorg. Nucl. Chem. Lett., 10 (1974) 629.

71. L.B. ZINNER and G. VICENTINI,
J. Inorg. Nucl. Chem., 37 (1975) 1999.

72. G. VICENTINI, L.B. ZINNER and Y. SHIMIZU,
An. Acad. brasil. Ciênce., 50 (1978) 319.

73. G. VICENTINI and O.J. FENTANES,
An. Acad. brasil. Ciênce., 51 (1979) 451.

74. P.J. HUFFMAN and J.E. HOUSE,
J. Inorg. Nucl. Chem., 36 (1974) 2618.

75. A.N. SPECA, N.M. KARAYANNIS and L.L. PYTLEWSKI,
J. Inorg. Nucl. Chem., 35 (1973) 3113.

76. A.N. SPECA, L.L. PYTLEWSKI and N.M. KARAYANNIS,
J. Inorg. Nucl. Chem., 35 (1973) 4029.

77. A.N. SPECA, N.M. KARAYANNIS, L.L. PYTLEWSKI and C. OWENS,
J. Inorg. Nucl. Chem., 38 (1976) 91.

78. R. WHYMAN and W.E. HATFIELD,
Inorg. Chem., 6 (1967) 1859.

79. D.E. CHASEN, L.L. PYTLEWSKI, C. OWENS and N.M. KARAYANNIS,
J. Inorg. Nucl. Chem., 41 (1979) 13.

80. J.-L. PASCAL, J. POTIER, D.J. JONES, J. ROZIERE and A. MICHALOWICZ,
Inorg. Chem., 23 (1984) 2068.

81. J. FUJITA, K. NAKAMOTO and M. KOBAYASHI,
J. Amer. Chem. Soc., 78 (1956) 3963.

82. D.M. ADAMS and P.J. LOCK,
J. Chem. Soc., A (1971) 2801.

83. D. MICHALSKA-FONG, P.J. McCARTHY and K. NAKAMOTO,
Spectrochim. Acta, 39A (1983) 835.

84. J. DILLEN, A.T.H. LENSTRA, J.G. HAASNOOT and J. REEDIJK,
Polyhedron, 2 (1983) 195.

85. I. NAKAGAWA and T. SHIMANOUCHI,
Spectrochim. Acta, 20 (1964) 429.

86. S. KIDA, J.V. QUAGLIANO, J.A. WALMSLEY and S.Y. TYREE,
Spectrochim. Acta, 19 (1963) 189.

CHAPTER 5

ZEISE'S SALT DERIVATIVES

In this, the final chapter of this work, the full infrared vibrational analyses of a series of mixed ligand complexes, namely Pt(II) organometallic complexes derived from Zeise's salt ($K[Pt(C_2H_4)Cl_3]$) are examined.

These π-acid type complexes have created a great deal of interest in the literature, not only because of the usefulness of the ^{195}Pt satellites ($I=\frac{1}{2}$; 33,6% relative abundance) in nmr studies for determining the thermodynamic data for olefin rotation and ligand exchange [1-6], but also because of the variety of unusual complexes formed with neutral ligands (Figure 5.1).

The *trans*-effect of the π-acid (either C_2H_4 or CO) results in the increased reactivity of normally unreactive ligands with the Pt^{2+} ion. This is illustrated by the immediate reaction of pyridine *N*-oxide with an aqueous solution of $K[Pt(C_2H_4)Cl_3]$ to form *trans*-$[Pt(pyO)(C_2H_4)Cl_2]$, while yielding no reaction with an aqueous K_2PtCl_4 solution [7].

The range of products resulting from the reaction of Zeise's salt with a potentially bidentate ligand reflects the different responses to several competing effects experienced by these complexes.

1 The presence of π-acid species (π-acceptors) stabilises 5-coordination.

2 The *trans*-labilizing effect of η^2-ethene destabilises bidentate chelation.

3 The chelate effects stabilise bidentate chelation and depend upon

   (i) The size of the chelating ring.

   (ii) The gem-dimethyl effect.

   (iii) The strength of the σ donor.

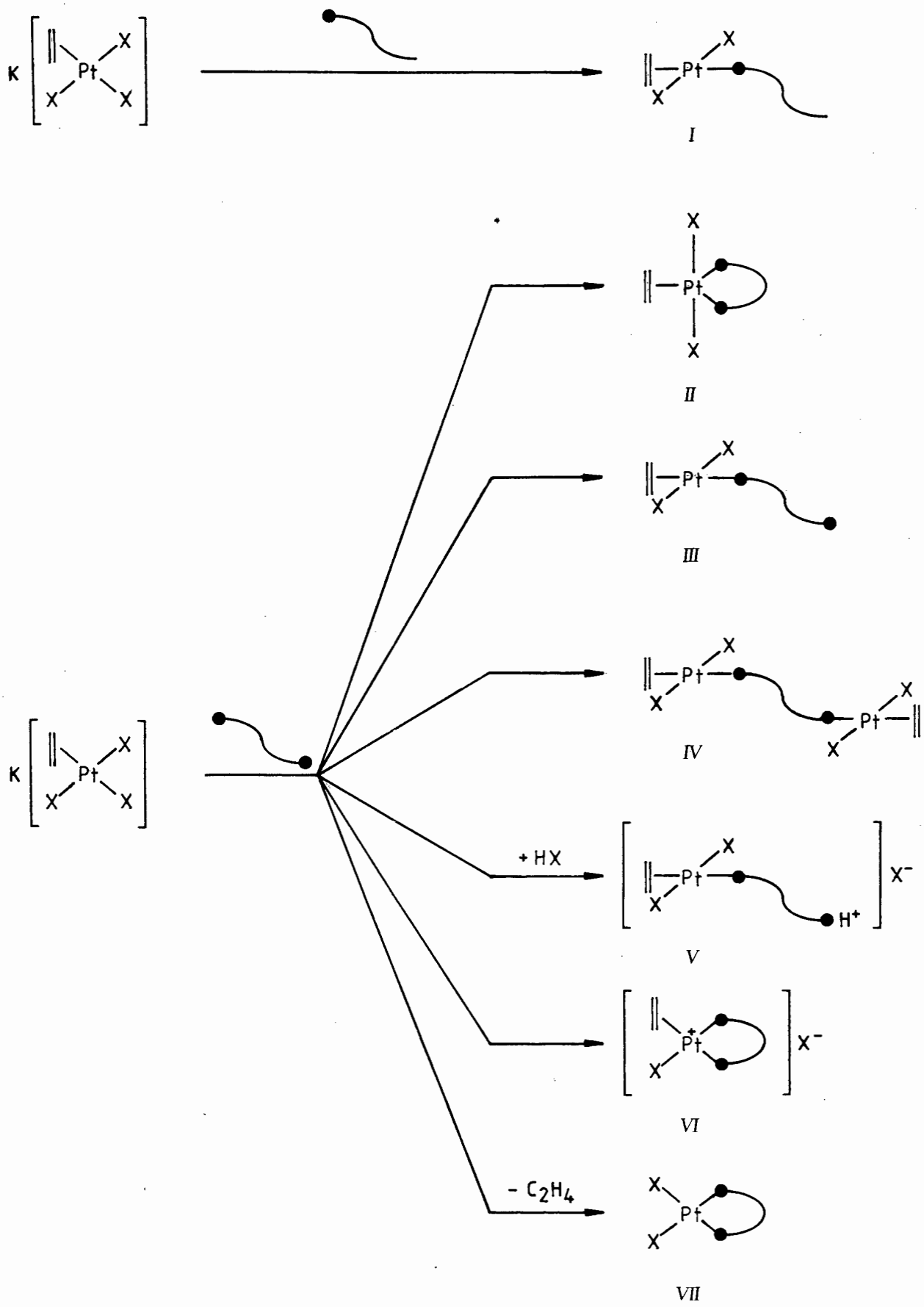

Figure 5.1 Possible products reacting mono- or bidentate ligands with Zeise's salt

The expansion from a coordination number of 4 to 5 is enhanced by an increased π back-donation from the Pt onto both the olefin and the chelating ligand (provided they belong to conjugated moieties), resulting in the Pt atom being more positive in 5- rather than in 4- coordinated complexes with the same ligands [8]. The stabilization of the π-acid species is demonstrated by a number of reported crystal structures of stable 5-coordinated [Pt(N-N)(olefin) Cl_2] complexes [3,9-11].

The *trans*-labelling effect of the olefin is observed in the square planar cationic complex (Type VI), [Pt(tmen)(C_2H_4)Cl]Cl (where tmen = *N*,*N*,*N'*,*N'*-tetramethyl-1,2-diaminoethane), in which the Pt-N *trans* to the ethene is longer by 0,08Å than its *cis* companion [12].

The role which the size of the chelating ring plays in these complexes is seen in that 5-member chelate rings stabilise bidentate chelation more readily than larger rings [12,13]. The 'gem-dimethyl' or 'Thorpe-Ingold effect' - the observation that cyclisation reactions are favoured by the presence of certain substituents on the ring forming atoms - is demonstrated by the importance of substitution on the donor nitrogens of the diamine and diimine complexes of Types II and VI [12,13]. The strength of the σ donation by the nitrogen atoms of the chelating ligands, which increases in the order N(azine) < (hydrazine) < N(imine) < N(amine), dictates whether bidentate or monodentate coordinate occurs [13-15].

Five-coordinate Pt(II) complexes of the Type II involving amine- [3,8,10,13-16], imine- [3,8,11,13-16], hydrazine- [9] and azine- nitrogen donors [8,13-16] have been reported in the literature.

These complexes represent a different class of compound compared with the

four-coordinate Pt(II) complex. HARTLEY [18] has divided metal-olefin complexes into two classes. The square planar Pt(II) complexes are typical of Class S complexes, which contain metal-olefin complexes with a coordination number of 4 or 6 in which the olefin is found perpendicular to the square plane. On the other hand, trigonal bipyramidal Pt(II) complexes are more typical of Class T complexes. This class contains those metal-olefin complexes with a coordination number of 3 or 5, in which the olefin is found to lie in the trigonal plane [18-20].

The criterion for the geometry of the five-coordinate Pt(II) complex is electronic rather than steric, being dependant on the symmetries of the associated orbitals. There is maximum opportunity for π-back donation from the p_x, p_y and $d_{x^2-y^2}$ metal orbitals (which have high electron density resulting from the *trans* equatorial ligands) into the π^* orbital of the ethene [19,20]. Thus the trigonal bipyramidal Pt(II) complexes are more closely allied to the trigonal platinum(0) complex $[Pt(PPh_3)_2(C_2H_4)]$ than to the square planar Pt(II) Zeise's salt derivatives.

The possible alternate four-coordinate configurations that the Pt(II) complexes may adopt with a potentially bidentate ligand are given by Types III to VII (Figure 5.1). Complexes in which the second coordinating site on the ligand remains free (Type III) have been reported for amine- [21], imine- [3,8,15] and azine- nitrogen donors [3,15,22]. These complexes are the result of those ligands in which the chelate ring would be larger than a 5-membered ring [21], or those in which the second coordinating site cannot, for steric reasons, coordinate to the same Pt atom [3,15,22].

The second coordinating site on the ligand may, however, coordinate to a second Pt atom, to yield a binuclear complex of the Type IV. Nitrogen donor

ligands with amine- [23,24], imine- [11,13] and azine- nitrogen [22] have given this type of complex. The ligand requirements to produce these bridged complexes are the same as mentioned for Type III, while the absence of substituents on the donor nitrogens (the 'gem-dimethyl effect') has also been observed to cause bridging [23,24].

The formation of the two cationic complexes (Types V and VI) depends upon the chelation effects. The cationic species in which the ligand is bidentate are those which are stabilised by both a positive gem-dimethyl effect and by having a 5-membered chelate ring [12,25,26]. Where one of these two criteria is absent the open-handed cation species of Type V is produced, in which the second donor is protonated [12]. In the open-handed cationic species, the coordinate site *trans* to the olefin is either taken up by a chloride or another donor atom. In the absence of this, the site is occupied by a solvent molecule which starts off a decomposition process ending in the formation of platinum metal [12]. Cationic species of both types are reported in the literature only for amine- nitrogen donors [12,25,26].

The final configuration which a bidentate ligand may produce with Zeise's salt is chelation with the expulsion of the π-acid; the ethene. This is illustrated by the decomposition of the five-coordinate complex [Pt(bipy)$(C_2H_4)Cl_2$] [27]. In organic solvents like dichloromethane, the decomposition is a single step dissociation process. In an aqueous medium there exist two mechanisms with parallel pathways, the dissociation process above and a two step dissociation (k_1) / association (k_2) process shown below.

$$[Pt(bipy)(C_2H_4)Cl_2] \xrightarrow[\text{fast}]{k_1} [Pt(bipy)(C_2H_4)Cl]^+ + Cl^- \xrightarrow[\text{slow}]{k_2} [Pt(bipy)Cl_2] + C_2H_4$$

The first step, the dissociative formation of the cationic species of Type VI, is rapid. The second step is slow (but is more rapid in the presence of chloride ions) and is thought to proceed via the intermediate 5-coordinate species in which the one chloride is axial while the other is equatorial [27]. This, being less stable than that species with both halides axial, results in the expulsion of the ethene.

In Pt(II) complexes the *trans*-effect of CO is of a similar magnitude to that of ethene, but is slightly weaker [28,29]. This, combined with the facile displacement of ethene from Zeise's salt, would lead to the expectation of carbon monoxide analogues of Zeise's salt derivatives similar to those described in Figure 5.1.

Four-coordinate complexes of the type *trans*-$[PtL(CO)Cl_2]$ with monodentate ligands have been well established [29-36]. Trigonal bipyramidal Pt(II) carbonyl complexes of Type II are, however, not as clearly established. The only five-coordinate Pt(II) carbonyl complex containing a neutral bidentate ligand found in the literature is that of $[Pt(phen)(CO)(SnCl_3)_2]$ [37,38] which was described as 'a very insoluble brown complex, presumably the five-coordinate monomer'. Its bipy analogue could not be isolated in the pure form [39]. Indeed, the only crystal structure of a five-coordinate Pt(II) carbonyl complex found in the literature is that of $[Pt(CH_3)(CO)\{HB(pyz)_3\}]$, which is stabilised by the anionic and geometric characteristics of the hydro tris (1-pyrazolyl)borate ligand [39].

Several attempts to produce the mononuclear complexes of Type III with pyrazine proved unsuccessful, producing either the bridged dinuclear complex or $[Pt(pz)_2Cl_2]$ [36]. Similarly the reaction of bipy with Pt-*carsol* yields the bridged dinuclear complex $[Pt_2(bipy)(CO)_2Cl_4]$ [40]. The presence of HCl in

this reaction yields the salt [Pt(bipy)(CO)Cl] [$Pt(CO)Cl_3$] [40], the cationic complex of Type VI and the only Pt(II) carbonyl cationic species found in the literature.

It is clear that much work, particularly that involving potentially bidentate ligands, still remains to be done in carbonyl analogues of Zeise's salt derivatives. One particular difficulty with these complexes is their sensitivity to water, readily decomposing to platinum metal in its presence [31,36].

It is also to be noted that - apart from the widely investigated *p*-substituted pyridine *N*-oxides [36,41-44] - investigations of *trans*- Zeise's salt derivatives have predominently involved nitrogen donor ligands. This may be understood in terms of the relative extent of the *trans*-effect of C_2H_4 and CO compared with other possible ligand donors.

Two types of ligand have a high *trans*-effect on Pt(II) complexes, those having high *trans*-influence and those with π bonding capacity (and low *trans*-influence) [28]. The *trans*-influence of a given ligand L depends upon

(i) the effect of L on the hybrid orbital used by the metal in its bond to the ligand *trans* to L (ligand A).

(ii) the net charge transfer from ligand to metal (i.e. $\sigma_{covalent} - \pi$).

The tendency of L to deplete metal *s*-character in the *trans* Pt-A bond depends upon the nature of the donor atom, upon the orbital hybridisation of the donor atom and upon the electronegativity of its substituents [28]. This tendency decreases in the order [28,42,44]:

C-donor($sp^3 > sp^2 > sp$)>P-donor >As-donor >S-donor >N-donor >halide >O-donor

Since the relative degree of the *trans*-effect of C_2H_4 and CO is: $CH_3^- \simeq CN^- \simeq C_2H_4 \simeq CO >> PR_3 \simeq AsR_3$ [28], one might expect *trans*-$[PtL(C_2H_4)Cl_2]$ complexes (and their CO analogues) with tertiary phosphines, tertiary arsines and sulphoxides besides those with nitrogen and oxygen donors. However, whether produced by the customary C_2H_4 or CO cleavage of the halide-bridged dimer *trans*-$[Pt_2L_2X_4]$ where L = PR_3 or AsR_3 [45-50], or by halide displacement from Zeise's salt or its CO analogue [51,52], the *cis*-isomer is generally produced. One exception to this is the existence (due to steric considerations) of *trans*-$[Pt\{P(o\text{-tolyl})_3\}(CO)Cl_2]$. The *trans*-isomer for these reactions has been shown to be the initial product [33], but it rapidly undergoes either CO/C_2H_4-catalysed or solvent-assisted *trans*→*cis* isomerisation. Similarly, the three Zeise's salt derivatives with a sulphur donor found in the literature are of the *cis*-isomers [54-56].

Clearly the most suitable donor system (besides that of nitrogen) likely to yield *trans*-Zeise's salt derivatives would be that of oxygen. Apart from the *p*-substituted *N*-oxide derivatives, the only other Pt-O bonded Zeise's salt derivatives in the literature are those with quinoline *N*-oxide; $[Pt(quinO)(C_2H_4)Cl_2]$ [57] and diphenylcyclopropane (dpcp)*; $[Pt(dpcp)(C_2H_4)Cl_2]$ and $[Pt(dpcp)(CO)Cl_2]$ [58]. Both were assumed to be *trans* in the absence of far infrared spectra. The investigation of other *N*-oxide systems is therefore of importance.

---

* dpcp is an unusual ligand in that it acts similarly to pyO [58].

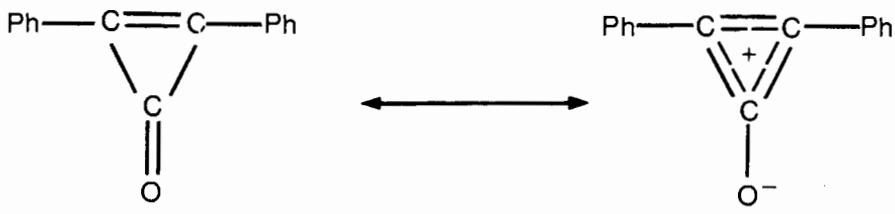

While mixed ligand systems tend to be more complicated (spectroscopically speaking) than single ligand systems, they do offer the potential for a wider variety of labelling studies. In the present study of the series [PtL-$(C_2H_4)X_2$] the use of halogen replacement, of individual deuteration studies of both the ligand and the η^2-ethene, and of CO replacement of the η^2-ethene is employed. Of the forty-one complexes reported in this Chapter, the synthesis of only four has previously been reported in the literature, these being [Pt(quin)$(C_2H_4)Cl_2$] [59], [Pt(quinO)$(C_2H_4)Cl_2$] [57], [Pt(bipy)(C_2H_4) Cl_2] and [Pt(phen)$(C_2H_4)Cl_2$] [16]. The vibrational spectra of these have not been previously reported.

The only other isotopic labelling studies of Zeise's salt derivatives reported in the literature are those for [Pt(en)$(C_2H_4)X_2$] X=Cl or Br, en=ethylenediamine) by KONG and THEOPHANIDES [23] which employ a deuteration study of both the ligand and the ethene, and those by THORNTON and his co-workers [22, 35,36,60] involving deuteration studies of the ethene and of several ligands.

Before the vibrational assignment of these mixed complexes can be made, the vibrational spectra of the coordinated ethene and CO need to be investigated.

The various assignments of Zeise's salt, K[Pt$(C_2H_4)Cl_3$], to be found in the literature are given in Table 5.1. That by POWELL and SHEPPARD [61] is the result of a mid-infrared study. GROGAN and NAKAMOTO [62] reported the infrared spectra and normal coordinate analysis of both the -d_0 and -d_4 analogues of Zeise's salt. PRADILLA-SORANZO and FACKLER [63] presented a far-infrared and normal coordinate analysis of the -d_0 and -d_4 complexes. HIRAISHI [64] extended the work by studying both the infrared and Raman spectra of both isotopomers. The work by ANDREWS [65] represents a refined normal coordinate analysis. Finally, JOBIC [66] completed a new inelastic neutron scattering

		$K[Pt(C_2H_4)Cl_3]$						$K[Pt(C_2D_4)Cl_3]$			
		JOBIC	ANDREWS *et al.*	HITAISHI	PRADILLA-SORZANO & FACKLER	GROGAN & NAKAMOTO	POWELL & SHEPPERD	JOBIC[f]	HITAISHI	PRADILLA-SORZANO & FACKLER	GROGAN & NAKAMOTO
		(1985)	(1975)	(1969)	(1967)	(1966)	(1958)	(1985)	(1969)	(1967)	(1966)
		[66]	[65]	[64]	[63]	[62]	[61]	[66]	[64]	[63]	[62]
ν_1	$\nu C\text{-}H(A_1)$	3005	3013	3013	3013	2920	3020	(2202)	2224	2218	2215
ν_2	$\delta CH_2(A_1)$	1515[c]	1515[c]	1515[c]	1419[c]	1418[c]	1428	(938)	962	1060	978
ν_3	$\nu C\text{-}C(A_1)$	1240[c]	1243[c]	1243[c]	1518[c]	1526[c]	1516	(1382)	1353	(1417)	1428
ν_4	$\tau CH_2(A_2)$	1020	841	-	-	730	975?	(726)	-	-	450
ν_5	$\nu C\text{-}H(A_2)$	3100	3079	3094	-	2975	-	(2326)	2349	-	2219
ν_6	$\rho CH_2(A_2)$	1180	-	841	-	1251	1240	(963)	597	-	1011
ν_7	$\omega CH_2(A_1)$	1010	975	975	1023	1023[c]	1022	(791)	757	820	811
ν_8	$\omega CH_2(B_1)$	975	1010	1010	1012	1023[c]	1010	(808)	812	814	818
ν_9	$\nu C\text{-}H(B_2)$	3080	3094	3079	3079	3098	3085	(2281)	2331	2330	2335
ν_{10}	$\rho CH_2(B_2)$	845[c]	841	720	842	844	810	(612)	525	(582)	536
ν_{11}	$\nu C\text{-}H(B_1)$	3005	2988	2988	2988	3010	-	(2168)	2193	2184	2185
ν_{12}	$\delta CH_2(B_1)$	1425	1426	1426	1426	1428	1402	(1060)	1059	1059	1067
ν_{13}	$\tau CH_2(B_2)$[a]	720[c]	-	1180	720	-	734	(514)	-	532	-
	$\nu_a Pt\text{-}C_2(B_2)$[b]	493	493	493	403	407	-	(426)	451	384	-
	$\nu_s Pt\text{-}C_2(A_1)$	405	405[d]	405	491	-	-	(365)	385	450	387
	$\nu_s PtCl(A_1)$	-	-	338	341	331	-	-	336	339	329
	$\nu_a PtCl(B_2)$	-	-	327	330	339	-	-	326	330	339
	$\nu PtCl_t(A_1)$	-	-	309	305	310	-	-	305	304	305
	$\delta_a C_2PtCl(B_2)$	-	-	219	212	210	-	-	200	198	198
	$\delta ClPtCl(A_1)$	-	-	(152)	181	183	-	-	(151)	181	185
	$\delta_s C_2PtCl(B_2)$	-	-	(46)	161	161	-	-	(46)	161	160
	$\pi_a C_2PtCl(B_1)$	-	-	-	123	121	-	-	-	114	117
	$\pi_s C_2PtCl(B_1)$	-	-	-	-	92	-	-	-	-	92

(a) rotation about z axis

(b) rotation about y axis

(c) highly coupled

(d) coupled inversely (see text)

(e) accidently degenerate

(f) calculated values only

Calculated values in parentheses

Table 5.1 Vibrational assignment of Zeise's salt found in the literature

The literature assignments for $K[Pt(CO)Cl_3]$ and its bromo analogue are given in Table 5.2. That by DENNING and WARE [69] reports the infrared and Raman spectra of $K[Pt(CO)Cl_3]$. Their Raman spectra were later shown to be those of a mixture of $[Pt(CO)Cl_3]^-$ and $[Pt_2(CO)_2X_4]^{2-}$ [49]. The work by CLEARE and GRIFFITH [70] and by BROWNING *et al.* [49] are infrared and Raman studies of both the Cl and Br complexes. GOGGIN and NORTON [71] reported a normal coordinate analysis of the planar fundamentals of the molecule.

	GOGGIN & NORTON (1978) [71]		BROWNING *et al.* (1977) [49]		CLEARE & GRIFFITH (1970) [70]		DENNING & WARE[(a)] (1968) [69]
Assignment	X = Cl	X = Br	X = Cl	X = Br	X = Cl	X = Br	X = Cl
$\nu C \equiv O(A_1)$	2097	2090	2083	2083	2121	2112	2126
$[\nu^{13}C \equiv O(A_1)]$	[2050]	[2043]	[2038]	[2037]	[-]	[-]	[-]
$\delta Pt\text{-}C \equiv O(B_2)$	540	525	543	528	536	524	490
$\pi Pt\text{-}C \equiv O(B_1)$	-	-	508	486	-	-	481
$\nu Pt\text{-}CO(A_1)$	497	496	504	504	495	490	529
$\nu_s Pt\text{-}X(A_1)$	345	227	348	227	346	225	344
$\nu_a Pt\text{-}X(B_2)$	344	246	344	245	339	240	349
$\nu Pt\text{-}X_t(A_1)$	322	204	325	204	317	180	318
$\delta_a CO\text{-}Pt\text{-}X(B_2)$	166	100	164	106	-	-	273
$\delta X\text{-}Pt\text{-}X(A_1)$	152	100	151	112	186	104	175
$\delta_s CO\text{-}Pt\text{-}X(B_2)$	152	100	151	112	-	-	95
$\pi_a CO\text{-}Pt\text{-}X(B_1)$	-	-	129	98	-	-	268
$\pi_s CO\text{-}Pt\text{-}X(B_1)$	-	-	105	-	-	-	109

(a) Assignments uncertain due to mixture of anions $[Pt(CO)Cl_3]^-$ and $[Pt_2(CO)_2Cl_4]^{2-}$

Table 5.2 Vibrational assignment of $K[Pt(CO)X_3]$ (X = Cl, Br) found in the literature

The planar Pt-C ≡ O bend is found at a frequency close to the Pt-CO stretch which makes their assignments difficult [36,49]. For the *trans*-$[Pt(CO)Cl_3]^-$ complexes the planar Pt-C ≡ O bend is found at a higher frequency than its out-of-plane counterpart, πPt-C ≡ O. This is the opposite of the finding for the *cis*-$[Pt(CO)_2X_2]$ complexes [49].

The full infrared assignment of the Zeise's salt derivatives (and their CO analogues) investigated in this work are presented in Tables 5.3 to 5.9. The individual ligand assignments are based upon those made in Chapter 3, with the exception of those made for the complexes pyridazine (pdz) and its -d_4 isotopomer. The latter assignments are based upon the deuteration labelling study of the free ligand made by STIDHAM and TUCCI [72]. The results of the ^{1}H nmr investigation of the η-ethene complexes are given in Table 5.10.

At present, ^{1}H nmr spectroscopy is regarded as the best technique for distinguishing between four- and five-coordination of Pt(II). Four-coordinate Pt(II) complexes yield chemical shifts of 4,40 to 5,00 ppm for the olefin protons, with Pt-H coupling constants of approximately 60 Hz. A substantial upfield shift (> 1 ppm) of the olefin proton resonance, with larger Pt-H coupling constants (> 10 Hz) is generally regarded as evidence of a five-coordinate platinum [3,9,13-17].

While the author agrees with the former criterion, the Pt-H coupling constants of about 70 Hz found for [Pt(quinO)(C_2H_4)X_2] and [Pt(bipyO_2H)X_2]X (which are in agreement with those found for substituted pyO [42,73]) indicate that the Pt-H coupling cannot be used to distinguish between four- and five-coordination. It is also noted here that the chemical shift of the olefin protons provides a suitable means of distinction between nitrogen and oxygen coordination in four-coordinate Pt(II) complexes since the aromatic *N*-oxides yield shifts of ±4,4 ppm while the heterocycles yield shifts of ±4,9 ppm.* Hence, the pzO derivatives show Pt-N rather than Pt-O bonding (Table 5.10).

---

* This does not imply that the most stable complexes are those with highest σvalues for the olefin protons [9,16].

Table 5.3 Infrared assignment (4000-50cm^{-1}) of $[Pt(C_2H_4)(phen)Cl_2]$ and its C_2D_4 and phen-d_8 analogues

[Pt(phen)(C_2H_4)Cl_2]			
phen	C_2D_4	phen-d_8	Assignment
	(4000-2900cm^{-1})		
3084 w	3084 wm	-	23 (νC-H/D)
	2309 wm [a]	-	ν_5 (C_2H_4/D_4)
3066 wsh	3067 wmsh	2284 wm	22 (νC-H/D)
	2309 wm [a]	3064 w	ν_9 (C_2H_4/D_4)
3056 m	3056 m	2274 wm	21 (νC-H/D)
		2264 wm	43 (νC-H/D)
3018 w	2203 w	-	ν_1 (C_2H_4/D_4)
2988 wm	2175 w	2988 wm	ν_{11} (C_2H_4/D_4)
	(1700-50cm^{-1})		
1628 wsh	1635 w	1611 w	comb
1622 ms	1622 s	1600 w	18 (νring)
1604 m	1604 m	1557 s	17 (νring)
		1552 s	
1587 m	1586 m	1585 m	40 (νring)
1579 s	1579 s	1546 ms	39 (νring)
-	1565 w	-	comb
1514 s	1513 vs	1472 vs	16 (νring)
1500 m	1500 m		
1495 s	1494 s	1430 vs	38 (αC-H/D)
-	953 w	1486 w	ν_2 (C_2H_4/D_4)
1460 m	1050 s	1460 m	ν_{12} (C_2H_4/D_4)
1452 m	1452 m	1409 s	15 (αC-H/D)
-	-	1448 vw	comb
-	-	1440 wsh	comb
1429 vs	1429 vs	1343 s [a]	37 (νring)
	1432 mssh	1387 w	14 (νring)
1410 s	1412 ms	1343 s [a]	36 (νring)
1379 vw	1379 vw	-	comb
1357 vw	-	-	comb
1343 ms	1343 ms	1309 mw	13 (νring)
1324 w	1323 w	1245 w	35 (νring)
1318 w	1317 w	1235 w	
1300 w	1306 wm	1154 mw	12 (νring)
1258 wm	1368 vw	1263 mw	ν_3 (C_2H_4/D_4)
	1259 s	1034 w	34 (αC-H/D)

Table 5.3 (continued)

[Pt(phen)(C_2H_4)Cl_2]			
phen	C_2D_4	phen-d_8	Assignment
-	-	1227 mw	comb
1213 w	1213 w	1006 wsh	33 (αC-H/D)
-	-	1208 vw	comb
1206 w	1204 w	894 m	9 (αC-H/D)
1199 vw	1198 wsh	1197 vw	comb
1183 m	930 m	1182 m	ν_6 (C_2H_4/D_4)
-	-	1162 vw	comb
1153 m	1153 ms	849 w	8 (αC-H/D)
-	-	1147 mw	comb
1143 s	1143 s	868 w	31 (αC-H/D)
-	-	1135 w	comb
1129 vw	1125 vw	-	comb
1113 w	1109 w	-	comb
1103 ms	1103 ms	833 m	7 (νring)
1092 w	1092 mw	842 w	30 (νring)
1055 vw	1070 vw	-	comb
1034 w	1033 w	823 vw	6 (νring)
1021 s	770 wmsh	1019 s	ν_4 (C_2H_4/D_4)
1011 mw	814 m	1010 mw	ν_7 (C_2H_4/D_4)
998 m	997 vw	771 vw	46 (γC-H/D)
	760 w	975 wsh	ν_8 (C_2H_4/D_4)
956 ms	956 ms	-	58 (γC-H/D)
-	-	949 vw	comb
925 vw	-	-	comb
-	-	911 w	comb
905 wm	908 w	732 m	28 (νring)
882 vw	882 vw	-	comb
868 ms	867 ms	722 wm	48 (γC-H/D)
852 vs	851 vs	785 m	5 (νring)
841 s	840 s	636 s	49 (γC-H/D)
829 w	828 w	758 w	59 (γC-H/D)
808 w	809 w	667 vw	60 (γC-H/D)
794 w	603 w	795 w	ν_{10} (C_2H_4/D_4)
782 s	782 s	625 s	50 (γring)
770 vw	484 w	-	ν_{13} (C_2H_4/D_4) (?)
745 vw	749 vw	-	61 (γring)

Table 5.3 (continued)

[Pt(phen)(C_2H_4)Cl_2]			
phen	C_2D_4	phen-d_8	Assignment
725 vs	726 vs	694 vs	27 (ν ring)
	721 vs	601 s	51 (γC-H/D)
		590 m	
705 s	705 s	689 ms	4 (ν ring)
-	-	674 vw	comb
656 w	655 w	645 msh	comb
642 s	642 s	542 w	26 (ν ring)
623 vw	-	-	62 (γ ring)
-	-	612 w	comb
558 w	558 w	-	3 (ν ring)
546 w	546 vw	-	63 (γ ring)
510 w	510 w	454 m	52 (γ ring)
503 mw	502 wm	463 wm	25 (ν ring)
486 m	462 wm	489 mw	ν_aPt-C_2
450 wm	449 wm	348 ms	53 (γ ring)
425 ms	425 ms	412 m	24 (ν ring)
-	-	477 vw	comb
352 m	352 m	308 wm	64 (γ ring) (?)
336 s	335 s	335 s	ν_aPt-Cl
322 wm	326 msh	-	ν_aPt-^{37}Cl
294 vw	292 w	279 vw	ν_aM-N
277 vw	275 w	271 w	ν_sM-N
-	-	261 vw	comb
254 vw	254 w	247 vw	65 (γ ring)
235 wsh	235 w	214 w	54 (γ ring)
228 m	215 w	227 w	δPt-C_2
203 w	203 vw	197 w	δ skeletal (?)
190 m	180 m	184 w	δN-Pt-N (?)
174 s	174 m	174 m	δ skeletal
153 ms	152 m	153 mw	δCl-Pt-Cl
137 mw	136 w	131 w	66 (γ ring)
116 m	108 w	106 wm	55 (γ ring)
85 w	72 w	86 wsh	π skeletal
72 m	57 vw	70 w	π skeletal

(a) band assigned twice

s = strong

m = medium

w = weak

v = very

sh = shoulder

br = broad

comb = combination

Table 5.4 Infrared assignment (4000-50cm^{-1}) of $[Pt(C_2H_4)(bipy)Cl_2]$ and its C_2D_4 and bipy-d_8 analogues

[Pt(bipy)(C_2H_4)Cl_2]			
bipy	C_2D_4	bipy-d_8	Assignment
	(4000-2900cm^{-1})		
3102 w	3104 vw	2303 w	2 (νC-H/D)
		2280 w [a]	20b (νC-H/D)
	2340 vw	-	ν_5 (C_2H_4/D_4)
3060 wm	3062 m	2269 w	20a, 7b (νC-H/D)
	2508 wm	3064 w	ν_9 (C_2H_4/D_4)
3030 w	3032 mw	2280 w [a]	20a' (νC-H/D)
3017 w	3017 mw	2280 w [a]	7b' (νC-H/D)
	2201 w	-	ν_1 (C_2H_4/D_4)
2999 wsh	2999 wsh	-	comb
2981 mw	2986 w	-	comb
	2173 wm	2983 wm	ν_{11} (C_2H_4/D_4)
-	2957 vw	-	comb
-	2933 vw	2928 vw	comb
2900 vw	-	2901 vw	comb
	(1700-50cm^{-1})		
-	-	1648 vw	comb
-	-	1636 vw	comb
1612 w	1613 w	-	comb
1601 s	1603 s	1574 ssh	8b' (νring)
1595 s	1596 s	1562 s	8b (νring)
1573 ms	1575 s	1456 vs	8a (νring)
1562 ms	1565 mw	1531 s	8a' (νring)
-	-	1492 vw	comb
1488 s	1488 s	1419 s	19a' (νring)
		1411 s	
1474 s	1471 s	1334 s	19a (νring)
1470 s			
1459 m	1052 ms	1460 wm	ν_{12} (C_2H_4/D_4)
1448 s	1448 vs	1347 w	19b' (νring)
		1343 wm	
-	-	1431 vw	comb
1410 m	1428 m	1328 vs	19b (νring)
	1410 wsh		
1379 w	-	1385 vw	comb
-	-	1370 w	comb

Table 5.4 (continued)

[Pt(bipy)(C_2H_4)Cl_2]			
bipy	C_2D_4	bipy-d_8	Assignment
-	-	1359 w	comb
-	-	1352 w	comb
1313 s	1313 s	955 wsh	3' (αC-H/D)
1289 vw	1282 vw	1258 w	A (νinter-ring)
-	-	1276 w	comb
1274 vw	1274 vw	1204 wm	14' (νring)
-	1264 vw	-	comb
1251 m	1253 ms	978 s	3 (αC-H/D)
1229 m	1228 m	1237 s	14 (νring)
-	-	1214 wm	comb
1212 vw	1211 vw	-	comb
1182 s	922 m	1179 ms	ν_6 (C_2H_4/D_4)
1175 ms	1176 s	848 wm	15' (αC-H/D)
1163 s	1164 s	827 m	15 (αC-H/D)
1141 s	-	1139 s	(?)
1127 w 1118 w	1126 w 1121 w	873 m	9b' (αC-H/D)
1108 wm	1110 m	862 s	9b (αC-H/D)
-	1100 vw	-	comb
-	-	1079 vw	comb
1072 w	1072 wm	788 vw	18b (αC-H/D)
1057 m	1056 wm	774 w	18b' (αC-H/D)
-	-	1043 vw	comb
1042 w	1043 w 1039 m	1029 m 1022 m	12 (νring)
1026	1024 s 1013 m	1013 s 991 s	1 (νring) 12' (νring)
1005 s	811 wm	1008 msh	ν_7 (C_2H_4/D_4)
997 wm	996 vw	808 vw	5 (γC-H/D)
980 w	978 wm	-	5' (γC-H)
965 vw	966 vw	-	ν_8 (C_2H_4) (?)
masked	957 vw	masked	ν_2 (C_2D_4)
-	933 w	-	comb
906 ms	904 ms	659 m	10b (γC-H/D)
891 vw	891 w	-	10b' (γC-H/D)
-	880 w	-	comb

Table 5.4 (continued)

[Pt(bipy)(C_2H_4)Cl_2]			
bipy	C_2D_4	bipy-d_8	Assignment
871 vw	-	-	comb
845 w	843 w	masked	10a' (γC-H/D)
818 wm	605 vw	815 w	ν_{10} (C_2H_4/D_4)
800 w	798 w	617 vw	10a (γC-H/D)
772 vs	773 vs	592 s	1' (νring)
762 s	759 s	732 wm	4 (γring)
748 w	746 w	-	11' (γC-H/D)
735 s	735 s	587 s	11 (γC-H/D)
718 m	716 ms	720 wm	4' (γring)
-	672 w	-	comb
654 s 650 ssh	652 s	627 s	6b (νring)
631 s	630 s	608 m	6a (νring)
-	528 vw	-	comb
495 wm	456 wm	495 wm	ν_aPt-C_2
masked	489 vw	masked	ν_{13} (C_2D_4)
469 wm	468 m	439 wm	E (ring scissors)
457 vw	-	-	comb
447 vw	445 w	410 vw	Γ (ring shear)
421 m	420 ms	376 m	16b (γring)
413 w	415 m	351 wm	16a (γring)
385 vw	385 vw	-	16a' (γring)
350 msh	350 msh	-	comb
336 s	334 s	334 s	ν_aPt-Cl
294 w	294 w	276 w	νPt-N
250 w	259 w	225 m	νPt-N
232 m	234 m	187 wm	16b' (γring)
209 vw	215 wm	-	δ skeletal
199 w	191 w	-	δPt-C_2
171 w	169 wm	167 wm	δ skeletal
157 w	156 m	156 m	δCl-Pt-Cl
-	135 w	132 m	π skeletal
-	111 w	115 w	π skeletal
97 w	91 w	69 w	Z (i. rotation)
74 w	71 w		lattice

(a) band assigned twice

s = strong

m = medium

w = weak

v = very

sh = shoulder

br = broad

comb = combination

Table 5.5 Infrared assignment (4000-50cm^{-1}) of $[Pt(C_2H_4)(pdz)X_2]$ (X = Cl, Br), its C_2D_4, pdz-d_4 analogues and their CO derivatives

$[PtL(C_2H_4)X_2]$				$[PtL(CO)X_2]$			
L = pdz X = Cl	pdz X = Br	pdz C_2D_4	pdz-d_4	pdz X = Cl	pdz X = Br	pdz-d_4	Assignment
			(4000-2900cm^{-1})				
3145 w	3141 w	3144 vw	-	3149 w	3159 w 3143 w	-	comb
3097 m	3091 wm	3097 wm 2323 w	2311 wm 3086 vw	3094 m	3085 m	2305 wm (a)	13 (νC-H/D) ν_5 (C_2H_4/D_4)
3070 wm	3072 w	2310 w 3071 w	3070 w 2300 wsh	- 3079 wm	- 3077 m	- 2305 wm (a)	ν_9 (C_2H_4/D_4) 20b (νC-H/D)
3059 m	3061 wm 3052 wmsh	3059 wm	2278 w	3062 s	3057 w	2277 w	7b (νC-H/D)
-	3010 vw	2219 vw	3009 vw	-	-	-	ν_1 (C_2H_4/D_4)
2997 w	2993 w	2997 w	2287 w	3000 m	2995 w	2290 w	2 (νC-H/D)
2973 w	2975 w	2118 vw 2970 vvw	2975 w	- 2974 vvw	- 2970 vwbr	- -	ν_{11} (C_2H_4/D_4) comb
-	-	-	2928 vvwbr	-	-	2925 vvw	comb
			(2400-2000cm^{-1})				
-	-	-	2345 w	-	-	2348 vw	comb
2320 vw	2320 vvw	-	2335 vvw	2334 vvw	-	-	comb
2260 vw	2260 vw	2252 vw	-	-	-	2266 vw	comb
-	-	-	-	2197 vw	2190 vw	-	comb
-	-	-	-	2115 vs	2127 vs	2120 vs	νC≡O
-	-	-	-	2073 s	2079 s	2075 ms	ν^{13}C≡O
2060 w	-	-	2061 w	-	-	-	comb
2032 w	2034 w	2034 w	2033 w	-	-	-	comb
			(1700-50cm^{-1})				
1579 wm	1574 wm	1579 wm	1544 wm	1579 m	1579 m	1547 wm 1541 wm	8a (νring)
1572 s	1569 s	1572 s	1530 ms	1573 s	1574 s	1533 ms	8b (νring)
-	-	1529 vw	-	-	1523 vw	-	comb
1519 w	1519 w	957 w	1519 w	-	-	-	ν_2 (C_2H_4/D_4)
1472 vw	1472 vw	-	-	1487 vw	1486 vw	1485 vw	comb
1452 s	1445 s	1452 s	1338 ms	1456 s	1453 s	1343 m 1339 m	19a (νring)
1426 vs	1422 vs	1064 s	1425 vs	-	-	-	ν_{12} (C_2H_4/D_4)
1418 s		1418 vs	1285 vs	1416 s	1416 s	1291 s 1288 vs	19b (νring)

Table 5.5 (continued)

[PtL(C_2H_4)X_2]				[PtL(CO)X_2]			
L = pdz X = Cl	pdz X = Br	pdz C_2D_4	pdz-d_4	pdz X = Cl	pdz X = Br	pdz-d_4	Assignment
1401 wm	1401 wm	1404 wm	1172 w	1391 wm	1400 s	1175 w	14 (ν ring)
1365 vw	1360 vw	1366 w	1361 w 1357 w	1362 vw	1363 vw	1366 w 1360 w	comb
1320 vw	1316 vw	1320 vw	-	1318 vw	1324 vw	-	comb
1299 s	1292 s	1299 s	1064 w	1295 s	1294 s	1062 mw	3 (αC-H/D)
-	-	1260 w	-	1260 vw	-	-	comb
1253 w	1254 w	-	1252 wm	-	-	-	ν_3 (C_2H_4/D_4)
-	-	-	-	-	1240 wsh	1240 vw	comb
-	-	-	-	-	1230 vw	1229 w	comb
1214 w	1210 w	1222 vw	1214 w	1215 wm	1217 m	-	comb
1210 vwsh	-	1209 vw	1195 vw	1191 vw	-	-	comb
1172 w	1168 vw	1172 w	-	1168 vw	1164 w	1165 w	9a (αC-H) (?)
1155 w	1154 w	1155 w	1155 vw	1151 vw	1145 m	-	
-	-	1123 vw	-	-	1130 vw	-	18a (C-H) (?)
-	1095 vw	1097 vw	-	1096 vw	1101 w	-	
-	-	-	1073 w	-	1078 vw	1074 vw	comb
-	-	-	861 s	-	-	856 s	9a (αC-D)
-	-	-	848 wm	-	-	850 wsh	18a (αC-D)
1078 s	1075 mw	1079 s	837 s	1076 s	1068 s	835 s	15 (αC-H/D)
1058 ms	1058 ms	1058 ms	1001 mw	1064 ms	1063 m	999 w	12 (ν ring)
1031 s	1018 ms	masked	1030 ms	-	-	-	ν_4 (C_2H_4/D_4)
1018 w	masked	1019 vw	-	1009 vw	1020 vw	-	comb
1009 s	1007 s	814 ms	1009 s	-	-	-	ν_7 (C_2H_4/D_4)
994 w	982 w	763 wm	994 w	-	-	-	ν_8 (C_2H_4/D_4)
972 vs	974 vs	973 vs	957 vs	982 vs	977 vs	961 ms	1 (ν ring)
933 m	932 m	934 m	762 w	935 wm	940 w	760 w	5 (γC-H/D)
-	-	870 vvw	738 wsh	870 vvw	-	742 w	17a (γC-H/D)
855 vvw	-	855 vvw	722 wm	845 vvw	850 vvw	720 w	10a (γC-H/D)
819 wm	813 vw	595 vw	819 w	-	-	-	ν_{10}(C_2H_4/D_4)
-	-	-	800 ms	-	-	801 w	(?)
784 vs	779 vs	783 vs	579 vs	774 vs	779 vs	576 vs	11 (γC-H/D)
732 s	734 s	735 ms	678 wm	737 s	739 m	682 wm	4 (γ ring)
723 w	723 w	723 w	-	721 w	720 w	-	comb
702 w	690 w	513 vw	704 w	-	-	-	ν_{13} (C_2H_4/D_4)
685 wm	684 w	684 w	657 w	689 w	687 wm	655 w	ob (ν ring)

Table 5.5 (continued)

[PtL(C_2H_4)X_2]				[PtL(CO)X_2]			
L = pdz X = Cl	pdz X = Br	pdz C_2D_4	pdz-d_4	pdz X = Cl	pdz X = Br	pdz-d_4	Assignment
668 vw	-	668 vvw	-	-	-	-	comb
-	-	-	630 vw	-	-	629 vw	comb
645 m	644 wm	645 wm	622 wm	645 wm	644 m	621 wm	6a (νring)
623 vw	623 vvw	625 vw	-	-	-	-	comb
-	-	-	609 w	-	-	602 w	comb
-	-	-	-	548 m	542 m	540 wm	δPt-C≡O
-	-	-	-	523 w	528 vwsh	523 m	comb
-	-	-	-	498 ms	500 ms	495 ms	πPt-C≡O
472 w	463 w	430 wm (a)	472 w	-	-	-	ν_aPt-C_2
-	-	-	-	473 wm	483 m	476 m	νPt-CO
432 m	437 w	430 wm (a)	393 wm	424 wm	427 wm	388 wm	16a (γring)
389 s	384 ms	388 m	329 wmsh	386 wm	386 wm	masked	16b (γring)
378 m	376 m	362 mw	379 m	-	-	-	ν_sPt-C_2
348 s	255 m (b)	347 s	347 s	351 s	257 m (b)	350 s	ν_aPt-X
336 msh	-	340 mssh	337 msh	339 msh	-	339 m	ν_aPt-^{37}Cl
235 w	211 m (b)	231 w	227 w	236 vw	205 wm (b)	233 w	νPt-N
224 vwsh	-	223 vwsh	219 vwsh	215 w	195 w	-	δ skeletal
200 vw	193 wm	191 w	198 w	-	-	-	δPt-C_2
-	175 w	-	184 vw	186 w	172 vw	177 w	δ skeletal
165 w	120 w	169 w	165 w	154 w	113 w	155 w	δX-Pt-X
-	152 vw	-	-	-	-	-	
139 w	-	139 w	139 wm	125 wm	97 wm	127 w	πX-Pt-X
105 wm	105 vvw	103 w	-	-	-	113 wm 106 wsh	π skeletal
93 wm	88 wm	89 wm	93 wm	84 w	88 wm	89 w	lattice
-	64 vw	-	68 vw	65 vw	-	63 vw	lattice
59 vw	55 vw	55 vw	-	-	-	56 vw	lattice

(a) band assigned twice

(b) coupled vibration (νPt-N/νPt-Br)

s = strong

m = medium

w = weak

v = very

sh = shoulder

br = broad

comb = combination

Table 5.6 Infrared assignment (4000-50cm^{-1}) of $[Pt(C_2H_4)(quin)X_2]$ (X = Cl, Br), its C_2D_4, quin-d_7 analogues and their CO derivatives

$[PtL(C_2H_4)X_2]$				$[PtL(CO)X_2]$			
L = quin X = Cl	quin X = Br	quin C_2D_4	quin-d_7	quin X = Cl	quin X = Br	quin-d_7	Assignment
			(4000-2900cm^{-1})				
3166 vw	3166 vw	3170 vw	3170 vw	-	-	-	comb
3097 w	3090 w	2333 wm [a]	3095 wm	-	-	-	ν_5 (C_2H_4/D_4)
		3097 w	2280 wm [a]	3087 vw	3080 vwsh	2286 w [a]	41 (νC-H/D)
3074 wsh	3078 wsh	2333 wm [a]	-	-	-	-	ν_9 (C_2H_4/D_4)
		3077 wsh	2280 wm [a]	3067 w	3069 vwbr	2265 wsh	1 (νC-H/D)
3069 wm	3064 wm	3068 wm	2280 wm [a]	3052 vw	3052 w	2286 w [a]	14 (νC-H/D)
3056 wm	3052 w	3054 wm	2258 w [a]	3046 vw	3046 w	2259 w [a]	30 (νC-H/D)
3039 w	3040 wsh	3040 wsh		-	-	-	42 (νC-H/D)
3015 w	3010 w	3014 w	2258 w [a]	3020 vw	3025 vw	2259 w [a]	2 (νC-H/D)
		2226 w	3012 vw	-	-	-	ν_1 (C_2H_4/D_4)
2977 wbr	2973 w	2975 vw	2258 w [a]	3002 vw	-	2259 w [a]	15 (νC-H/D)
		2194 w	2980 vw	-	-	-	ν_{11} (C_2H_4/D_4)
2952 vw	2952 vw	2955 vw	-	2956 vw	2955 vw	-	comb
2920 vw	2924 vvw	2923 vw	-	2923 vvw	2928 vvw	-	comb
			(2400-2000cm^{-1})				
-	-	-	-	2335 vw	-	2300 vw	comb
2266 w	2266 vw	2265 w	-	-	-	-	comb
-	-	-	-	2122 vs	2133 vsbr	2125 vs	ν C≡O
-	-	-	-	2070 m	2070 m	2072 m	ν^{13} C≡O
2040 vw	2039 w	-	2040 vw	-	-	-	comb
2008 vw	2005 w	-	2006 vw	-	-	-	comb
			(1700-50cm^{-1})				
1641 vw	1637 vw	1639 vw	-	-	-	-	comb
1618 s	1616 m	1617 ms	1587 s	1620 m	1621 mw	1592 s	16 (νring)
1608 w	1605 vw	1605 w	1605 w	1602 w	1602 w	1602 vw	comb
1598 mw	1597 mw	-	1592 wmsh	-	-	1598 wmsh	comb
1586 s	1589 ms	1589 ms	1560 s	1588 s	1589 s	1561 s	31 (νring)
	1583 ms	1586 ms					
1565 mw	1565 mw	1565 mw	1543 m	1572 mw	1570 mw	1546 m	4 (νring)
-	-	-	1567 w	-	-	1572 w	comb
1550 w	1550 vw	1551 w	-	1550 vw	1552 w	-	comb
1541 vw	1545 vw	1541 vwsh	-	-	-	-	comb
1508 vs	1507 vs	masked	1515 vw	-	-	-	ν_2 (C_2H_4/D_4)
		1507 vs	1448 vs	1509 vs	1509 vs	1452 vs	44 (νring)

Table 5.6 (continued)

[PtL(C_2H_4)X_2]				[PtL(CO)X_2]			
L = quin X = Cl	quin X = Br	quin C_2D_4	quin-d_7	quin X = Cl	quin X = Br	quin-d_7	Assignment
1462 mssh	1465 wsh 1459 ms	1465 wsh 1461 ms	1289 m	1465 wsh 1462 m	1462 w 1462 wm	1288 ms	8 (νring)
1450 wsh	1446 vw	1450 wsh	-	1450 wsh	1450 wsh	-	comb
1438 ms	1437 ms	1438 ms	1381 s	1438 w	1437 w	1381 s	17 (νring)
1418 vs	1417 vs	1058 vs	1419 vs	-	-	-	ν_{12} (C_2H_4/D_4)
1396 s	1395 s	1397 vs	1246 wm 1241 wm	1393 s	1390 ms	1251 ms 1245 mw	32 (νring)
-	-	-	1397 w	-	-	1399 w	comb
1379 vs	1378 s	1379 vs	1296 s	1378 s	1378 s	1296 vs	3 (νring)
1369 w	1369 wsh	1369 m	1369 w	1369 wsh	1361 w	1365 wm	comb
-	1361 w	-	1363 mw	-	-	-	comb
-	-	-	1347 vvw	-	-	1734 vvw	comb
1330 vw	1328 w	1328 w	-	1332 vvw 1324 vw	1324 vw	-	comb
1312 s	1310 s	1313 s	1227 w	1312 s	1308 s	1228 wbr	43 (νring)
1272 vvw	-	1272 vw	1278 w	1279 w	1272 w	-	comb
1265 w	1265 w	1265 w	1056 w	1266 mw	1263 w	1047 wm	34 (αC-H/D)
1254 m	1252 wm	1369 m	1254 wm	-	-	-	ν_3 (C_2H_4/D_4)
1236 w	1235 w	1236 w	1098 s	1238 w	1239 w	1101 s	46 (αC-H/D)
-	-	-	-	1223 w	1230 w 1230 w	1203 vw	comb
1217 vw	-	1218 vw	1215 vw	-	-	-	comb
1205 m	1205 m	1205 m	-	1208 m	1204 ms	926 vw	18 (αC-H/D)
1186 vvw	1186 vw	1186 vw	-	1185 vw	1185 vw	-	comb and ν_6 (C_2H_4/D_4)
1167 vvw	1166 vw	1168 vw	1169 vw	1168 vvw	-	1172 vwbr	comb
1154 m	1153 wm	1156 wm	1155 vwbr	1159 m	-	1156 vwbr	comb
1139 s	1140 ms	1141 s	833 ms [(a)]	1145 wm	1145 wm	834 ms	5 (αC-H/D)
1133 s	1133 s	1134 s	880 m	1135 ms	1132 s	880 m	33 (αC-H/D)
1087 w	1086 w	1087 w	833 ms [(a)]	1092 w	1090 w	830 wm	19 (αC-H/D)
-	-	-	1090 vwsh	-	-	1089 w	comb
1063 wm	1065 w	1064 wm	-	1065 w	1065 w	-	7 (αC-H/D)
-	1031 vw	1032 vw	-	-	1049 vw	868 vvw	
1020 msh	-	1019 w	840 wsh	1024 wm	1020 wm	843 wm	47 (νring)
1018 s	1019 ms	masked	1021 s	-	-	1014 m	ν_4 (C_2H_4/D_4)
-	1009 sh	1001 vw	989 vw	994 vw	1009 vw	990 vw	comb

Table 5.6 (continued)

[PtL(C_2H_4)X_2]				[PtL(CO)X_2]			
L = quin X = Cl	quin X = Br	quin C_2D_4	quin-d_7	quin X = Cl	quin X = Br	quin-d_7	Assignment
1000 vs	1002 s	812 s	1000 s	-	-	-	ν_7 (C_2H_4/D_4)
982 s	983 mw	984 ms	790 w	982 m	991 m	789 mw	37 (γC-H/D)
masked	masked	752 w	977 vw	-	-	980 vw	ν_8 (C_2H_4/D_4)
964 wm	965 mw	968 w	808 vw	971 mw	968 w	816 vw	10 (γC-H/D)
952 m	953 mw	953 wm	914 m	960 wm	960 w	916 m	21 (νring)
-	-	-	780 m	945 w	-	779 m	26 (γC-H/D)
888 vvw	889 vvw	889 vw	-	889 vvw	-	-	comb
862 w	866 w	864 w	750 w	864 m	865 mw	749 w	39 (γring)
847 vvw	847 vvw	847 vw	678 vw	849 vvw	849 vw	681 vw	11 (γC-H/D)
811 s	812 ms	masked	819 m	-	-	-	ν_{10} (C_2H_4/D_4)
804 s	804 vs	807 vs	639 vs	808 s	810 s	640 vs	38 (γC-H/D)
783 s	784 s	788 m	723 m	789 m	786 m	723 m	36 (νring)
775 s	776 vs	776 vs	617 s 702 (a)	777 s	777 s	619 m 700 vw	23 (γC-H/D) 6 (νring)
-	-	-	760 vw	-	-	760 vw	comb
740 ms	474 mw 742 m	742 ms	580 w	737 ms	738 ms	584 mw	27 (γC-H/D)
720 wm	722 wm	722 wm	-	722 wm	721 wm	-	comb
701 w	701 w	513 ms	702 w (a)	-	-	-	ν_{13} (C_2H_4/D_4)
-	-	-	667 vvw	-	-	667 vvw	comb
-	-	-	649 w	-	-	650 wsh	comb
642 s	642 ms	642 s	544 w	647 m	645 m	masked	12 (γring)
623 mw	631 w 624 w	625 w	594 vw	628 w	624 mw	-	48 (νring)
-	-	-	-	549 s	548 s	552 s	δPt-C O
-	-	-	-	536 ms	536 ms	530 s	πPt-C≡O
531 w	532 w	533 w	515 w	527 mw	527 mw	517 mw	9 (νring)
521 vvw	520 vvw	520 vvw	-	-	-	-	comb
504 s	503 ms	498 ms (a)	505 vw	500 m	500 m	500 vw	20 (νring)
-	-	-	-	486 ms	490 msh	482 ms 473 mw	νPt-CO
486 m	486 mw	498 ms (a)	448 m	478 m	483 ms	443 m	24 (γring)
		447 mw	486 mw	-	-	-	ν_aPt-C_2
465 mw	464 mw	465 mw	410 mw	463 mw	462 mw	408 ms	40 (γring)

Table 5.6 (continued)

[PtL(C_2H_4)X_2]				[PtL(CO)X_2]			
L = quin X = Cl	quin X = Br	quin C_2D_4	quin-d_7	quin X = Cl	quin X = Br	quin-d_7	Assignment
414 mw	413 w	414 mw	374 m	411 mw	412 mw	370 ms	28 (γring)
405 w	404 w	404 mw	368 mw	400 mw	396 m		35 (νring)
388 w	387 w	373 mw	390 ms	-	-	-	ν_sPt-C_2
345 s	259 m (b)	344 s	344 s	352 s	261 m (b)	350 s	ν_aPt-X
340 wsh	-	-	-	355 wsh	-	338 wsh	ν_aPt-^{37}Cl
247 w	232 m (b)	246 wm	230 w	241 vw	241 m (b)	227 w	νPt-N
213 w	202 w	212 wm	207 wm	214 vw	216 vw	209 vw	δ skeletal
-	-	205 wsh	-	-	-	-	comb
-	-	-	197 w	-	-	-	comb
199 wm	189 wm	186 wm	188 wm	192 w	199 vw	176 wm	13 (γring)
-	-	-	-	-	170 vw	-	comb
-	-	-	-	-	154 vw	-	comb
160 w	109 w	159 wm	157 w	149 w	-	147 wm	δX-Pt-X
145 msh	145 w	143 wsh	138 s	140 vw	144 vw	136 w	δ skeletal
135 ms	91 w	135 ms	132 s	123 w	87 wm	123 wm	πX-Pt-X
-	-	114 w	-	-	-	-	
-	-	109 wsh	105 vw	-	-	-	π skeletal
98 vw	85 wsh	-	93 vw	-	-	-	
81 wsh	-	-	-	-	-	-	lattice
74 w	-	-	72 vw	73 w	-	70 w	
70 wsh	-	-	-	68 w	-	-	
56 w	56 w	-	-	62 vwsh	55 w	-	

(a) band assigned twice

(b) coupled vibration (νPt-N/νPt-Br)

s = strong

m = medium

w = weak

v = very

sh = shoulder

br = broad

comb = combination

Table 5.7 Infrared assignment (4000-50cm^{-1}) of [Pt(C_2H_4)(pzO)X_2] (X = Cl, Br), its C_2D_4, pz-d_4O analogues and their CO derivatives

[PtL(C_2H_4)X_2]				[PtL(CO)X_2]			
L = pzO X = Cl	pzO X = Br	pzO C_2D_4	pz-d_4O	pzO X = Cl	pzO X = Br	pz-d_4O	Assignment
			(4000-2900cm^{-1})				
-	-	3120 wm	-	-	-	-	comb
3110 wm	3107 m	3105 m	2330 wm	3116 m	3112 m	2323 s	20b (νC-H/D)
3097 m	3098 msh	2332 w	3098 wm	-	-	-	ν_5 (C_2H_4/D_4)
3079 wsh	3086 m	2298 w	3081 w	3091 m	-	-	ν_9 (C_2H_4/D_4)
		3085 m	2308 wm	3070 mw	3084 wbr	2315 s	20a (νC-H/D)
3053 wm	3049 m	3058 m	2359 w	3048 w	3054 m	2334 wm	2 (νC-H/D)
3042 wm	3039 m	3042 m	2294 m	3039 m		2287 wm	7b (νC-H/D)
masked	masked	2264 w	3013 w	-	-	-	ν_1 (C_2H_4/D_4)
2983 w	2976 vw	2223 vw	2981 w	-	-	-	ν_{11} (C_2H_4/D_4)
2966 vw	-	-	-	-	-	2959 vw	comb
2934 w	-	2936 vw	-	2926 vw	-	2925 vw	comb
			(2400-2000cm^{-1})				
2395 w	2398 w	2408 w	2400 w	2402 w	2410 w	2404 vw	comb
2280 w	2286 vw	2264 w	2274 w	2281 w	2294 w	2298 wsh	comb
2189 vw	2196 vw	2197 vw	2197 vw	-	-	-	comb
-	-	-	-	2123 vs	2136 vs	2151 s 2135 vssh 2121 vs	νC≡O
-	-	-	-	2065 m	2086 m	2067 ms	ν^{13}C≡O
2043 w	2069 vvw	-	2055 vw	-	-	-	comb
			(1700-50cm^{-1})				
1616 s	1611 s	1615 s	1574 vs	1618 s	1623 s	1591 ms 1581 vs 1572 s	8a (νring)
1516 w	1500 w	983 w	1497 w	-	-	-	ν_2 (C_2H_4/D_4)
1489 ms	1478 ms	1486 m	1482 wsh	1487 m 1479 m	1489 m	1480 w 1473 w	8b (νring)
1469 s 1465 s	1463 s	1469 vs	1396 vs	1465 s	1471 vs	1405 vs	19a (νring)
1450 s 1444 vs	1445 vs	1450 s	1368 vs 1362 s	1443 vs	1452 vs	1365 s	19b (νring)
1433 mssh	1427 n	-	1435 vw	-	1431 wm	-	comb
1421 ms	1420 mw	1059 s	1419 ms	-	-	-	ν_{12} (C_2H_4/D_4)
1363 vw	-	-	-	1378 wm	-	-	comb
1337 s	1338 s	1337 vs	1264 m 1254 s	1348 s	1347 vs	1268 s 1255 m	7a (νN-O/νring)

Table 5.7 (continued)

[PtL(C_2H_4)X_2]				[PtL(CO)X_2]			
L = pzO X = Cl	pzO X = Br	pzO C_2D_4	pz-d_4O	pzO X = Cl	pzO X = Br	pz-d_4O	Assignment
1330 vs	1330 s 1321 ms	1329 s	1040 w 1033 wm	1330 ms 1321 s	1329 s	1030 s	3 (αC-H/D)
-	-	-	1290 w	-	-	1291 w	comb
-	-	-	1287 w	-	-	1288 w	comb
1250 ms	1253 w 1250 w	1358 vw	1254 s	-	-	-	ν_3 (C_2H_4/D_4)
1237 w	-	1238 vw	-	-	1240 w	-	comb
1210 vs	1211 s	1210 s	1178 w	1205 s	1201 s	1173 wm	14 (νring)
1204 s	1200 s	1203 s	938 s	1200 m	1185 ms	934 m	9a (αC-H/D)
-	-	-	1200 vw	-	-	1199 vw	comb
-	-	-	1110 vw	-	-	1103 vw	comb
-	-	-	1072 vw	-	-	1072 vw	comb
1089 wm 1083 m	1091 wbr	1091 m	833 wm	1083 s	1084 m	822 ms	18b (αC-H/D)
1076 ms 1071 wm	1072 w	1076 s	864 ms	1073 s	1077 s	859 msh	18a (αC-H/D)
1040 vs	1043 vs	1039 vsbr	1018 s	1049 vs	1052 vs	1021 s	1 (νring)
1028 s	1032 s		804 s	1038 m	1044 ms	800 wm	17a (γC-H/D)
1016 ssh	1025 msh	757 w	1018 s	-	-	-	ν_4 (C_2H_4/D_4)
1004 s	1014 wm	808 m	1002 s	-	-	-	ν_7 (C_2H_4/D_4)
-	-	972 wm	-	-	-	-	ν_6 (C_2D_4)
971 w	-	-	968 w	982 w	975 w	959 w	comb
961 w	959 w	959 w	661 w	961 w	956 w	655 w	10a (γC-H/D) (?)
-	-	-	-	946 wm	943 wm	-	comb
937 vw	938 vw	767 w	masked	-	-	-	ν_8 (C_2H_4)
-	-	-	917 w	-	-	915 vw	comb
-	-	-	883 vw	-	-	886 vw	comb
-	-	-	875 vw	-	-	876 vw	comb
875 s 871 ms	871 m	876 s	855 m	866 m	870 m	852 ms	10b (γC-H/D)
855 s	849 m	858 s 850 wm	790 wm	847 s	848 vs	795 ms 785 w	12 (νring/νN-O)
832 m	840 s	831 ms	740 ms	829 m	832 vs	740 s	11 (γC-H/D)
823 w	826 w	-	-	-	-	-	comb
818 wm	816 w	625 vw	819 w	-	-	-	ν_{10} (C_2H_4/D_4)
-	-	-	-	735 wsh	735 wsh	731 wm	comb
-	-	-	-	722 wm	709 m	-	comb

Table 5.7 (continued)

[PtL(C_2H_4)X_2]				[PtL(CO)X_2]			
L = pzO X = Cl	pzO X = Br	pzO C_2D_4	pz-d_4O	pzO X = Cl	pzO X = Br	pz-d_4O	Assignment
720 sh	728 w	518 vw	721 w	-	-	-	ν_{13} (C_2H_4/D_4)
716 m	716 m	715 m	614 wm	716 m	714 m	614 wm	4 (γring)
683 wv	683 vw	683 w	652 wsh	678 vw	679 wm	655 w	6b (νring)
591 mw	591 w	590 wm	574 w	601 wm	605 m 595 m	582 m	6a (νring)
-	-	-	-	551 wm	523 s	536 ms	δPt-C≡O
535 ms	534 ms	534 m	462 ms	531 s	545 wm	460 s	16b (γring/γN-O)
-	-	-	-	520 w	-	527 w	comb
-	-	-	-	500 m	501 ms (a)	497 wsh	πPt-C≡O
494 s	494 wm	494 ms	472 ms	481 s	481 s	464 s	15 (αN-O)
-	-	-	-	490 wm	501 ms (a)	490 m	νPt-CO
484 m	487 m	446 w	483 w	-	-	-	ν_aPt-C_2
394 m	414 vw	413 vw	395 wsh	410 vw	409 w	387 vw	16a (γring)
401 m	389 m	394 m	401 wm	-	-	-	ν_sPt-C_2
342 s	250 w (a)	342 ms	341 s	359 s	253 mw (b)	358 s	ν_aPt-X
				342 m 335 wm		342 wm 335 wm	ν_aPt-^{37}Cl
283 wm	299 w 289 w	282 w	273 w	282 wm	297 m	274 w	5 (γN-O/γring)
241 ms	215 m (a)	231 ms	238 ms	213 mw	197 m (b)	205 wm	νM-N
231 wsh	-	-	-	236 vw	-	-	comb
198 w	191 w	196 wsh	196 wsh	-	-	-	δPt-C_2
188 wm	152 wm	188 wm	187 wm	168 vwsh	155 m	162 wsh	δ skeletal
152 m	-	159 vwsh 144 w	145 wsh	143 m	-	141 wm	δCl-Pt-Cl
137 w	85 w	135 w	136 w	118 m	88 w	127 ms	πCl-Pt-Cl
115 w	-	122 w	113 w	104 vw	-	103 vw	π skeletal
77 w	75 w	73 vw	84 vw	-	76 vw	71 vw	lattice
66 vw	65 w	58 vw	67 vw	66 vw	63 vw	-	lattice

(a) assigned twice

(b) coupled vibration (νPt-N/νPt-Br)

s = strong

m = medium

w = weak

v = very

sh = shoulder

br = broad

comb = combination

Table 5.8 Infrared assignment (4000-50cm^{-1}) of $[Pt(C_2H_4)(bipyO_2H)X_2]X$ (X = Cl, Br), its C_2D_4, bipy-d_8O_2 analogues and their CO derivatives

$[PtLH(C_2H_4)X_2]X$				$[PtLH(CO)X_2]X$			
L = $bipyO_2$ X = Cl	$bipyO_2$ X = Br	$bipyO_2$ C_2H_4	bipy-d_8O_2	$bipyO_2$ X = Cl	$bipyO_2$ X = Br	bipy-d_8O_2	Assignment
			(400-2900cm^{-1})				
-	3500 vwbr	3500 vwbr	-	3520 vwbr	3536 vwbr	3509 vwbr	comb
3117 mwbr	3110 wsh	3115 mw	2310 m	3109 msh	3118 wm	2312 m	20a (νC-H/D)
3089 mw	3080 mbr	3092 m	2300 ssh	3092 ms	3096 msh	2304 ssh	20b (νC-H/D)
		2324 w [a]	3083 w	-	-	-	ν_5 (C_2H_4/D_4)
		2266 vw		-	-	-	ν_1 (C_2H_4/D_4)
3076 s		3077 ms	2294 s [a]	3077 ms	3081 s	2300 s [a]	20a' and 20b' (νC-H/D)
		2324 w [a]	3064 vw	-	-	-	ν_9 (C_2H_4/D_4)
3064 s	3050 mssh	3054 s	2294 s [a]	3055 s	3062 s	2300 s [a]	2 (νC-H/D)
3037 s	3035 ms	3037 s	2254 wm	3025 wsh	3030 mwsh	2256 wm	2', 7b and 7b' (νC-H/D)
2960 vw	-	2185 vw	2952 vw	-	-	-	ν_{11} (C_2H_4/D_4)
2924 w	2920 w	2925 w	2924 w	2912 w	-	2926 vw	comb
			(2400-2000cm^{-1})				
2264 vw	2262 vw	-	-	2264 vw	2270 vw	-	comb
-	-	-	-	2098 vs	2087 vs	2101 vs	νC≡O
				2090 vs			
-	-	-	-	2047 m	2039 m	2048 s	$\nu^{13}C\equiv O$
2023 w	2000 w	2007 w	-	-	2023 w	2023 wm	comb
			(1700-50cm^{-1})				
1650 wshbr	1650 wbr	1650 wbr	1586 ms	1660 wsh	1650 wbr	1587 ms	8a' (νring)
1615 msh	1615 msh	1610 ms	1529 wm	1617 msh	1616 wm	1528 wm	8a (νring)
1608 m	1607 m	-	1555 vw	1609 ms	1610 m	1554 vw	8b' (νring)
-	-	1568 vw	-	1580 vw	1574 vw	-	comb
1540 w	1543 wm	1541 wm	1514 w	1543 wm	1537 wm	1514 w	8b (νring)
-	-	1503 vw	-	-	1503 vw	-	comb
1478 s	1476 s	1480 ms	1412 wm	1478 s	1477 s	1409 wm	19a' (νring)
			1394 wm			1394 wm	
1463 s	1459 s	1462 s	1362 w	1462	1462 s	1359 w	19a (νring)
1439 w	1441 w	1448 wsh	1374 m	1443 w	-	1373 m	19b' (νring)
1419 vs	1417 s	1052 w	1426 ms	-	-	-	ν_{12} (C_2H_4/D_4)
		1419 vs	1292 ms	1420 vs	1421 vs	1287 ms	19b (νring)
1329 m	1323 m	1329 ms	1323 s	1326 s	1318 ms	1322 vs	$\delta O\text{-}H_{(H_2O)}$
			1275 mbr		1310 s	1287 ms	14' (νring)
-	-	-	1019 m	-	-	1016 m	3' (αC-D)
1294 w	1294 w	1294 w	1033 s	1297 wm	1291 w	1032 s	3 (αC-H/D)
1263 vs	1261 vs	1263 vs	1237 vs	1263 vs	1258 s	1226 vsbr	A (νinter-ring)
1250 s	1250 s	1252 s	1218 s	1250 s	1250 s	1212 s	7a' (νN-O/νring)
1233 w	1231 w	1232 w	-	-	-	-	comb

Table 5.8 (continued)

[PtLH(C_2H_4)X_2]X				[PtLH(CO)X_2]X			
L = bipyO$_2$ X = Cl	bipyO$_2$ X = Br	bipyO$_2$ C_2H_4	bipy-d_2O$_2$	bipyO$_2$ X = Cl	bipyO$_2$ X = Br	bipy-d_2O$_2$	Assignment
1224 s	1223 s	1224 m	1254 s	1224 ms	1221 mssh	1252 ms	14 (ν ring)
1213 s	1209 s	1212 s	1163 ms	1212 s	1208 s	1162 s	7a (νN-O/ν ring)
1159 s	1158 ms	1163 ms	868 ms	1167 wm	1160 m	865 ms	15' (αC-H/D)
			855 s	1160 m		852 s	15 (αC-H/D)
1124 s	1122 ms	1123 ms	909 vs	1124 ms	1126 s	904 vs	9b' (αC-H/D)
-	-	-	1124 vw	-	-	1120 vw	comb
-	-	-	1110 vwsh	-	-	1113 vw	comb
1103 wm	1102 wm	1102 wm	890 s	1103 wm	1104 wm	886 vs	9b (αC-H/D)
-	-	-	1091 vw	-	-	1083 vw	comb
1075 vw	1073 vw	1074 vw	-	1074 w	1069 wm	1074 vw	comb
1064 w	-	1063 w	-	-	-	-	comb
1053 w	1059 vw	1052 wm	826 s	1059 wsh	1054 w	824 s	18b' (αC-H/D)
	1049 w			1050 wm	1046 wm		
1032 m	1031 wm	1030 m	788 s	1023 wm	1030 wm	786 s	18b (αC-H/D)
	1017 w	masked	masked	-	-	-	ν_{14} (C_2H_4/D_4)
1005 m	1004 m	1003 m	1006 ms	1004 wm	1011 wm	1007 ms	1 (ν ring)
	1002 msh		masked	-	-	-	ν_{7} (C_2H_4/D_4)
996 w	988 vw	990 w	-	991 vwsh	996 vw	-	comb
-	-	-	-	-	983 vw	-	comb
975 s	970 m	973 ms	838 vs	970 ms	970 wsh	837 s	5' (γC-H/D)
970 msh	958 w	965 wsh	826 s	966 wsh	959 ms	831 s	5 (γC-H/D)
-	-		949 msh	-	-	940 msh	comb
916 vsbr	912 vsbr	914 vsbr	740 s	916 vsbr	903 vsbr	736 s	10b' (γC-H/D)
894 s	890 ms	893 s	727 ms	893 ms	888 ssh	724 s	10b (γC-H/D)
875 sbr	872 s	876 s	784 s	876 s	877 m	781 s	12 (ν ring/νN-O)
					860 s		
843 s	843 s	843 s	756 vs	843 s	843 s	756 vs	12' (ν ring/νN-O)
792 ssh	790 ssh	790 ssh	549 m	793 ssh		548 m	11' (γC-H/D)
787 vs	784 vs	785 vs		785 vs	781 vs		
773 vs	772 vs	777 vs	600 s	773 vs	774 vs	597 s	11 (γC-H/D)
741 m	740 m	740 m	584 ms	741 m	735 s	682 m	1' (ν ring)
725 ms	725 ms	724 ms	-	725 m	722 s	-	4' (γ ring);
		484 vw	masked	-	-	-	ν_{13} (C_2H_4/D_4)
703 s	701 s	701 s	617 m	703 s	694 s	614 s	4 (γ ring)
656 m	650 m	654 m	652 wm	654 wm	-	648 wm	γO--$H_{(HX)}$
-	-	-	-	-	-	652 w	10a' (γC-D)
640 wm	640 wmsh	639 wmsh	636 wm	640 wsh	639 w	632 wm	10a (γC-H/D)

Table 5.8 (continued)

$[PtLH(C_2H_4)X_2]X$				$[PtLH(CO)X_2]X$			
L = $bipyO_2$ X = Cl	$bipyO_2$ X = Br	$bipyO_2$ C_2H_4	bipy-d_8O_2	$bipyO_2$ X = Cl	$bipyO_2$ X = Br	bipy-d_8O_2	Assignment
577 w	575 w	-	-	575 wsh	577 wm	-	6a (ν ring)
569 s	568 wm	569 s	509 w	569 m	567 wm	497 wsh	6b (ν ring)
550 w	550 w	550 w	-	-	545 w	-	6b' (ν ring)
-	-	-	-	536 ms	529 s	539 ms	δPt-C≡O
502 s	502 s	masked	499 w	-	-	-	ν_aPt-C_2
		502 s	490 w	499 s	499 s	493 m	16b' (γring/γN-O)
			475 w		492 s	474 w	16b (γring/γN-O)
-	-	-	-		484 ssh	493 m	νPt-C≡O
-	-	-	439 vw	-	-	439 vw	comb
-	-	-	454 w	-	-	454 w	18a' (αN-O)
444 s	443 ms	444 ms	406 m [a]	443 ms	440 ms	404 m	18a (αN-O)
407 w	397 mw	392 m	406 m [a]	-	-	-	νPt-C_2
		403 w	389 w	412 vw	406 mw	388 wm	16a and 16a' (γring)
340 ms	242 m	340 ms	341 ms	347 s	244 s	347 s	ν_sPt-X
-	-	-	-	333 msh	-	340 msh	ν_sPt-^{37}Cl
331 s	200 m	331 s	331 s	322 m	205 m	321 m	ν_aPt-X
307 wm	307 wm	307 ms	307 s	308 wm	308 w	301 vw	6a' (ν ring)
			287 wsh			287 w	
-	masked	-	263 vw	-	masked	-	Γ(ring shear)
228 vw	217 m	227 w	213 w	225 w	226 ms	213 w	17a (γN-O/γring)
213 vw		214 w	-	212 vw	-	-	17a' (γN-O/γring)
200 vw	-	200 vw	-	-	-	-	comb
171 w	170 w	170 w	-	172 vw	-	172 vw	
-	-	-	-	158 vw	151 w	156 w	δ skeletal
148 vw	147 vw	148 vw	150 w	145 vw	-	-	
-	130 vw	-	130 vw	-	-	125 wsh	E(ring scissors)
126 wm	-	126 wm	120 vw	122 wm	121 w	118 w	A(ring scissors)
109 vw	110 wbr	109 vw	108 vw	-	107 wm	-	πBr-Pt-Br
89 w	75 w	88 w	87 vw	84 w	81 w	81 w	Z (ring rotation)
65 w	-	65 w	65 w	61 w	-	58 w	lattice

s = strong

m = medium

w = weak

v = very

sh = shoulder

br = broad

comb = combination

Table 5.9 Infrared assignment (4000-50cm^{-1}) of $[Pt(C_2H_4)(quinO)X_2]$ (X = Cl, Br), its C_2D_4, quin-d_7O analogues and their CO derivatives

[PtL(C_2H_4)X_2]				[PtL(CO)X_2]			
L = quinO X = Cl	quinO X = Br	quinO C_2D_4	quin-d_7O	quinO X = Cl	quinO X = Br	quin-d_7O	Assignment
			(4000-2900cm^{-1})				
-	-	3164 vvw	-	3170 vvw	3172 vvw	-	comb
-	3137 vw	3138 vvw	-	3139 vw	-	-	comb
3107 w	3107 w	3108 w	2337 w	3109 wm	3109 w	2335 wm	41 (νC-H/D)
3088 mw	3080 mw	3090 wmsh	2299 w	3091 wm	3090 wm	2316 wmsh	1 (νC-H/D)
3081 m	3076 ms	3085 wm	2294 vwsh	3080 m	3078 m	2309 wm	14 (νC-H/D)
		2320 w (a)	3080 w	-	-	-	ν_5 (C_2H_4/D_4)
3057 wm	3058 wsh	2320 w (a)	3060 w	-	-	-	ν_9 (C_2H_4/D_4)
		3050 wm	2282 w (a)	3056 wm	3057 wm	2296 wm	2 (νC-H/D)
3028 w	3024 w	3030 w	2265 w (a)	3030 wbr	3035 w	2265 w (a)	42 (νC-H/D)
		3018 wsh	2282 w (a)		3025 w	2282 wsh	30 (νC-H/D)
-	3006 w	3008 w	2265 w (a)	3005 vw	-	2265 w (a)	15 (νC-H/D)
		2213 w		-	-	-	ν_1 (C_2H_4/D_4)
2996 w	2998 wbr	2183 w	2290 w	-	-	-	ν_{11} (C_2H_4/D_4)
			(2400-2000cm^{-1})				
-	2326 vw	masked	-	2335 vvw	2335 vvw	-	comb
-	2259 w	2260 vvw	-	2265 vvw	2259 vvw	-	comb
-	-	-	-	2118 vs	2111 vs	2108 vs	νC≡O
					2080 s	2098 vs	
						2071 vs	
-	-	-	-	2060 w	2054 m	2041 m	ν^{13}C≡O
			(1700-50cm^{-1})				
1637 w	1640 vw	1637 w	1620 vw	1640 w	1635 w	1626 vw	16 (νring/νN-O)
1619 m	1621 m	1619 m	1599 m	1621 ms	1621 ms	1600 s	31 (νring)
	1619 m						
1588 s	1586 s	1588 s	1542 ms	1584 s	1586 s	1543 ms	4 (νring)
1584 s		1584 s					
-	1572 w	1572 w	-	-	-	-	comb
-	-	-	1562 vw	-	-	1562 vw	
-	-	-	1526 vw	1548 w	1541 vw	-	
1524 w	-	-	-	-	1526 vw	-	
1514 s	1516 s	1514 vs	1459 s	1515 s	1514 vs	1461 vs	44 (νring)
	1512 mssh	951 w	-	-	-	-	ν_2 (C_2H_4/D_4)

Table 5.9 (continued)

[PtL(C_2H_4)X_2]				[PtL(CO)X_2]			
L = quinO X = Cl	quinO X = Br	quinO C_2D_4	quin-d_7O	quinO X = Cl	quinO X = Br	quin-d_7O	Assignment
1459 m 1450 m 1440 wsh	1458 msh 1449 wm 1440 wm	1457 m 1450 m 1445 msh	1305 ms 1382 vs	1459 mw 1454 mw 1446 mw	1459 mw 1452 w 1447 w	1304 s 1383 vs	8 (ν ring) 17 (ν ring)
1396 vs	1393 s	1397 vs	1363 s	1399 vs	1397 vs	1363 s	3 (ν ring)
1377 s	1378 s	1377 vs	1262 s 1258 msh	1380 vs	1379 vs	1259 s 1255 msh	32 (ν ring)
-	-	-	-	-	1362 w	-	comb
-	1331 w	masked	1329 w	1332 w	1327 w	1329 vw	comb
1324 m	1321 wm	1323 m	1310 ms	1322 m	1319 wm	1311 ms	43 (ν ring/ν N-O)
1308 w	1307 w	1307 w	-	1310 wsh	-	-	comb
1271 s	1269 s	1270 s	1028 ms 810 w	1276 s	1274 ms	1021 ms 816 w	34 (αC-H/D) 18 (αC-H/D)
-	-	-	-	-	1249 vw	1248 wsh	comb
1224 s	1230 wm	1227 m	1132 s	1230 s	1228 s	1137 s	20 (ν N-O/ν ring)
masked	1221 m	1333 m	1224 m	-	-	-	ν_3 (C_2H_4/D_4)
1210 s	1214 s	1211 s	1070 s	1216 vs	1214 s	1072 s	46 (αC-H/D)
-	-	-	1194 w	-	-	1194 w	comb
1187 w	1185 w	masked	1186 w	-	-	-	ν_6 (C_2H_4/D_4)
-	-	-	1172 w	-	-	1176 w	comb
1170 vs	1165 vs	1170 vs	1009 ms	1168 vs	1165 vs	1009 m	19 (αC-H/D)
-	-	-	1153 w	-	-	1154 w	comb
1148 vs	1149 vs 1146 ms	1147 vs	832 m [a]	1158 vs 1144 s	1155 vs 1141 s	833 ms [a]	33 (αC-H/D)
1087 s	1085 s	1088 s	881 w	1085 s	1084 s	879 m	5 (αC-H/D)
-	-	-	1089 w	-	-	1084 w	comb
-	1079 m		-	-	-	-	comb
-	-	-	-	1063 vw	1058 w	-	comb
1046 s	1043 s	1046 s	845 wm	1047 s	1045 s	845 m	7 (αC-H/D)
1028 ms	1020 s	masked	1021 ms	-	-	-	ν_4 (C_2H_4/D_4)
1013 s	1013 s	masked 1015 m	1014 m 832 m [a]	- 1021 m	- 1019 m	- 833 m [a]	ν_7 (C_2H_4/D_4) 10 (γC-H/D)
995 w	999 w	995 w	-	1002 w	999 w	-	comb
989 w 982 w	987 w	965 w masked	875 w 982 vw	988 w	980 w	875 wsh	27 (γC-H/D) ν_8 (C_2H_4/D_4)
-	969 w	-	-	-	-	972 vw	comb

Table 5.9 (continued)

[PtL(C_2H_4)X_2]				[PtL(CO)X_2]			
L = quinO X = Cl	quinO X = Br	quinO C_2D_4	quin-d_7O	quinO X = Cl	quinO X = Br	quin-d_7O	Assignment
964 w	965 wm	965 w	738 wbrsh	968 wm	962 w	730 wbrsh	26 (γC-H/D)
931 w	936 w	938 w	918 vw	952 wm	946 w	915 w	21 (νring/νN-O)
-	-	-	-	935 vw	-	935 vw	comb
876 s	876 s	876 s	790 ms	880 s	878 s	796 ms 789 m	39 (γring)
867 m	867 wm	867 w	770 w	868 w	863 w	772 wsh	47 (νring/νN-O)
805 s	809 vs 800 m	805 vs	682 m 629 s	809 vs 803 s	805 vs 801 s	684 m 629 s	38 (γC-H/D) 23 (γC-H/D)
768 vs	769 vs	768 vs	750 wm	763 vs	768 vs	746 wm	36 (νring)
754 wsh	737 w	735 wsh	722 wm	740 w	735 w	723 m	6 (νring/νN-O)
724 s	722 s	724 s	609 wm	727 s	724 s	609 w	27 (γC-H/D)
-	-	-	-	-	668 vvw	666 w	comb
-	-	-	654 w	660 vw	658 vw	658 w	comb
-	-	-	646 vw	-	-	647 w	comb
641 vw	-	642 vw	640 wsh	-	-	-	comb
626 m	629 m	627 m	571 m	638 m	633 wm	579 m	48 (νring/νN-O)
589 s	591 vs	589 s	529 w	598 s	596 s	521 m	12 (γring)
-	-	-	-	585 wm	582 wm	590 w	δPt-C≡O
575 s	575 s	576 ms	489 w	572 vw	572 vw	487 wm	9 (νring/νN-O)
548 w	548 w	548 w	464 w	542 s	539 s	468 w	20 (νring/νN-O)
-	-	-	541 wm	-	-	541 w	comb
-	-	-	-	522 ms	526 ms	521 ms	πPt-C≡O
517 w	-	-	-	-	-	510 vw	comb
-	-	-	-	506 s	506 s	499 ms	νPt-CO
505 ms	507 ms	504 m	514 m	-	-	-	ν_sPt-C_2
-	-	492 w	-	-	-	-	$\nu_{13}(C_2D_4)$
-	-	-	-	484 vw	484 vw	-	comb
476 w	475 w	475 w	451 w	471 wm	471 wm	447 wm	40 (γring)
462 vw	462 vw	462 vw	408 w	460 w	459 w	408 w	24 (γring)
455 w	453 w	454 w	375 wsh	448 w	447 w	masked	28 (γring)
-	-	-	421 vw	-	-	420 vw	comb
431 ms	418 m	413 m	431 wm	-	-	-	ν_aPt-C_2
-	-	-	-	410 wsh	414 vw	-	comb
390 s	390 s	390 s	359 m	396 s	391 s	359 msh	35 (νring)
346 vs	250 ms	346 vs	346 s	354 vs	255 ms	353 s	ν_aPt-X

Table 5.9 (continued)

[PtL(C_2H_4)X_2]				[PtL(CO)X_2]			
L = quinO X = Cl	quinO X = Br	quinO C_2D_4	quin-d_7O	quinO X = Cl	quinO X = Br	quin-d_7O	Assignment
-	339 vw	-	-	335 w	340 vw	336 wm	νPt-O (?)
321 ms	316 wm	320 ms	306 wm	317 s	315 m	304 ms	45 (αN-O)
-	269 vw	-	-	-	274 vw	-	comb
250 w	masked	249 w	230 w	255 w	masked	238 w	13 (γring)
211 wm	masked	200 wm	209 wm	216 w	211 vw	201 vw	22 (γN-O)
196 wm	198 wm	193 wsh	183 wm	196 wm	193 wm	181 m	25 (γring)
178 vvw	168 vw	170 w	167 vw	173 vvw	165 vw	168 vwsh	δ skeletal (?)
167 vw	160 vw	-		-	-	-	δPt-C_2 (?)
-	-	-	-	162 vvw	154 w	-	δX-Pt-CO (?)
158 vw	129 wm 123 wm	159 vw	151 vw	147 wm	126 wm	146 wm	δX-Pt-X
143 wsh	144 vw	-	-	143 wm	-	139 w	δ skeletal (?)
138 w	111 wm	136 wm	137 w	125 m	100 w	124 w	πX-Pt-X
114 wm	85 wm	108 wm	115 w	-	-	-	π skeletal
-	-	-	-	83 w	83 w	75 w	
80 w	72 wm	80 w	73 vw	-	-	-	Lattice
61 w	60 wsh	60 w	56 vw	64 w	-	61 w	
-	-	-	-	53 w	55 w	50 vw	

s = strong

m = medium

w = weak

v = very

sh = shoulder

br = broad

comb = combination

		X = Cl		X = Br		
	Solvent	Chem. Shift	$J_{(Pt-H)}$	Chem. Shift	$J_{(Pt-H)}$	Conformation
$K[Pt(C_2H_4)X_3]$	$CDCl_3$	4,57 ppm.	37,0 Hz	4,70 ppm.	35,0 Hz	sq. pl.
trans-$[Pt(phen)(C_2H_4)X_2]$	$CDCl_3$	3,76 ppm.	35,0 Hz	-	-	trig. bipy.
trans-$[Pt(bipy)(C_2H_4)X_2]$	$CDCl_3$	3,61 ppm.	34,5 Hz	-	-	trig. bipy.
cis - $[Pt(pdz)(C_2H_4)X_2]$	$CDCl_3$	4,97 ppm.	29,0 Hz	5,10 ppm.	31,5 Hz	sq. pl.
cis - $[Pt(quin)(C_2H_4)X_2]$	$CDCl_3$	5,02 ppm.	33,0 Hz	5,16 ppm.	31,5 Hz	sq. pl.
cis - $[Pt(pzO)(C_2H_4)X_2]$	$CDCl_3$	4,91 ppm.	31,5 Hz	5,06 ppm.	32,0 Hz	sq. pl.
cis - $[Pt(quinO)(C_2H_4)X_2]$	$CDCl_3$	4,39 ppm.	35,0 Hz	4,47 ppm.	38,5 Hz	sq. pl.
cis - $[Pt(bipyO_2H)(C_2H_4)X_2]X$	(a)	-	-	-	-	sq. pl.

(a) complex insoluble in $CDCl_3$, $(CD_3)_2CO$ or D_2O,

sq. pl. = square planar,

trig. bipy. = trigonal bipyramidal.

Table 5.10 ^1H nmr Spectra of various ligand complexes with Zeise's salt

The downfield shift of the olefin protons upon replacement of Cl by Br is a result of a sterically induced polarisation of the C-H bond in ethene by the Br atom [33].

It is clear from Table 5.10 that only the Zeise's salt derivatives with the ligands bipy and phen are five-coordinate. As bipy is a relatively poor π-acceptor compared to aliphatic diimines [74], and as the pyridine nitrogen is a weaker σ-donor, the stabilization of the five-coordinate Pt(II) complexes with bipy and phen must depend predominantly upon that stability inherent in a 5-membered chelate ring. The rapid loss of ethene by these two Zeise's salt derivatives is indicative of the relative instability of these complexes, although the great insolubility of the products undoubtedly helps to drive the reaction to completion.

The inability to produce the pure five-coordinate complexes of bipy and phen from the bromine analogue of Zeise's salt may be understood in terms of the greater *trans*-effect of Br^- to Cl^-. This would increase the relative labilizing of the ethene in the unstable five-coordinate intermediate with its axial/equatorial halogens. The result would then be a rate increase of this, the slow step, of the two step dissociation/association mechanism.

The rapid loss of ethene from the five-coordinate complexes with bipy and phen prevents the preparation of their carbonyl analogues.

That the stabilization of the five-coordinate bipy and phen derivatives is induced by the resultant 5-membered chelate ring is further demonstrated by the four-coordination experienced by the Zeise's salt derivative with pdz. The sterically favoured bidentate coordination by pdz results in the formation of a three-membered chelate ring with the loss, in solution, of ethene,

rather than producing a stable five-coordinate species.

The Zeise's salt derivative (and its CO analogue) with $bipyO_2$ exists as the cationic species of Type V as is evident by the *cis*-coordination (two νPt-Cl are observed in the far infrared spectrum; Table 5.8). Furthermore, the infrared bands of medium to strong intensity at *ca.* 1320cm^{-1} and the strong bands at *ca.* 1700cm^{-1} in these complexes (being δO··H and γO··H respectively [75]) show that the second donor site of the ligand is protonated. This is the first report of such a cationic species for Zeise's salt derivatives with an oxygen donor, and is the only cation of Type V to be reported for platinum-carbonyl complexes.

The inability to form a neutral complex from $bipyO_2$ and Zeise's salt must be attributed to the weaker bonding of oxygen donors to platinum compared with nitrogen donors, and the relative instability of the 7-membered chelate ring which would occur on bidentate coordination. The decomposition of the Zeise's salt derivative to platinum metal in the absence of HCl is typical of the behaviour of the open-handed cationic species in which the coordination site is not taken up by the halogen or by the second donor site [12], and is evidence of the weakness of the oxygen donor.

The Zeise's salt derivative with pzO is clearly coordinated through the nitrogen atom rather than the oxygen. This is evident in the shift of the N-O stretch to higher frequencies on complexation and in the observation of the Pt-N stretch at 241cm^{-1} (Table 5.7), which is typical of that for the pyridine nitrogen [32]. The nitrogen coordination by pzO supports the earlier suggestion that the chemical shift of the olefin protons may be used to determine the site of coordination in molecules with both N-O and aza-nitrogen donors.

The inability to form a bridged dinuclear Pt(II) complex with pzO as well as the absence of reaction of pzO_2 with Zeise's salt to form either the Pt-O bonded mono- or di-nuclear species must be attributed to the weaker oxygen donor capacity of the diazine *N*-oxides compared with that of pyO. This is explained by the greater contribution of the back-donation of the N-O moiety into the ring in diazine *N*-oxides than in pyO [76,77] as is indicated by the higher νN-O frequency of pzO compared to pyO.

Several comments need to be made on the infrared assignments of these Zeise's salt derivatives and their CO analogues. A few assignment difficulties arose.

Firstly, a strong band at 1140cm^{-1} in the spectra of $[Pt(bipy)(C_2H_4)Cl_2]$ (Table 5.4) could not be assigned. Its insensitivity to deuteration of the bipy and its absence from the labelled ethene spectrum would indicate its asassignment to an ethene fundamental. However, there is no suitable fundamental found at this frequency in Zeise's salt-d_0 (Table 5.1).

Secondly, the assignment of the ligand modes 9a and 18a (-d_0 isotopomer) in the series with pdz is uncertain due to the abundance of bands in the frequency range 1100-1200cm^{-1}.

Thirdly, a band of medium to strong intensity at 800cm^{-1} in $[Pt(pdz\text{-}d_4)(C_2H_4)Cl_2]$ with a weak band at 801cm^{-1} in its CO analogue (Table 5.5) can not be assigned employing the vibrational assignment of pdz-d_4 made by STIDHAM and TUCCI [72].

The carbonyl stretch is a vibration sensitive to rotational fine structure in the solid state [23,36]. This accounts for the fine splitting of the carbonyl bands in the spectra of $[Pt(quinO)(CO)Br_2]$, $[Pt(quin\text{-}d_7O)(CO)Cl_2]$,

$[Pt(pz\text{-}d_4O)(CO)Cl_2]$ and $[Pt(bipyO_2H)(CO)Cl_2]Cl$.

A major assignment problem arises in the assignment of the νPt-O for quinO and $bipyO_2$. There is a good deal of uncertainty over the assignment of the Pt-O stretch in pyO (Table 5.11). SHUPACK and ORCHIN originally assigned νPt-O to a very weak shoulder at 325cm^{-1} [43]. MEESTER *et al.* [43] questtioned this assignment since a combination band is observed at this frequency in the free ligand. They preferred to assign νPt-O to a band at 296cm^{-1}. This band might, however, be the γN-O fundamental, mode 17b. AUF DER HEYDE *et al.* [60] did not observe either of these two bands in their labelling studies of $[Pt(pyO)(C_2H_4)X_2]$, but noted two bands reflecting some oxygen sensitivity at 451cm^{-1} and 401cm^{-1} which they tentatively assigned to γPt-O.* The higher frequency band is undoubtedly αN-O, while the latter may be the γring mode 16a (Table 5.11).

The present deuteration labelling studies of the quinO and $bipyO_2$ derivatives of Zeise's salt do not help in locating the Pt-O stretch since in both series a number of internal ligand vibrations are found in the range 410cm^{-1} to 280cm^{-1} (Table 5.11). The presence of the Pt-Cl stretch in this range further complicates the issue.

While an ^{18}O-labelling study of the bromine analogue of one of these Zeise's salt derivatives may in future prove useful in resolving this predicament, a potential difficulty exists in that as a result either of coupling or of the

---

* In following SHINDO's assignment of characteristic N-O frequencies these authors incorrectly assigned γN-O (mode 17b) to the oxygen sensitive band at 511cm^{-1} [60] which is the γring mode 16b with which the former is coupled.

pyO [41,43,60]		quinO (This work)		$bipyO_2 \cdot HX$ (This work)	
Frequency (cm^{-1})	Alternate Assignment	Frequency (cm^{-1})	Alternate Assignment	Frequency (cm^{-1})	Alternate Assignment
451	9b (αN-O)(468)	390 s	35 (νring)(365)	406 vm	νPt-C_2, 16a' or 16a (γring)(402)
401	16b (γring)(401)	339 vw	44 (αN-O)(321)	355 vm	*B* (350) 6a (νring)(320)
325	combination band(325)	321 ms		301 wm	*Γ* (276) 6a (νring)(320)
296	17b (γN-O)(280)				

Free ligand frequencies in parenthesis

B = in-plane shear

Γ = out-of-plane shear

Table 5.11 Alternate assignments to infrared bands assigned to νPt-O

nature of the vibration, all the alternative assignments (except for νPt-C_2 in the bipyO_2 derivative) for the three complexes are potentially ^{18}O-sensitive. Alternatively, an investigation of the far-infrared spectrum of [Pt(dpcp)(C_2H_4)Cl_2] might clarify the assignment of νPt-O.

The assignment of the far-infrared spectra of the complexes under investigation is made difficult by the expected coupling. The nine skeletal vibrations of the square planar Pt(II) complexes were previously described in Figure 1.2 (Chapter 1, page 7). For the trigonal bipyramidal complexes, three additional vibrations are expected, the planar asymmetric Pt-N stretch (B_2) and two bends, one of which has A_2 symmetry and is therefore infrared-forbidden.

From their ligand isotope sensitivity, it is clear that both the Pt-C_2 stretches and the Pt-CO stretch are coupled with the platinum-ligand stretch. They also show slight sensitivity to the halide, but this is not reciprocated by the Pt-Cl stretches. This insensitivity of the νPt-Cl coupling is in accordance with previous observations [43,44].

For the pdz, pzO and quin derivatives of the bromine analogues of Zeise's salt and its CO analogue two bands of similar intensity occur in the νPt-Br region while the νPt-N band appears to be 'absent'. This must be a result of strong coupling between νPt-Br (A_1) (expected frequency *ca.* 245cm^{-1}) and νPt-N (A_1) (expected frequency *ca.* 235cm^{-1}), resulting in one band moving to a higher and one to a lower frequency. Such kinematic coupling would be possible since both vibrations have the same symmetry and similar frequencies, and is further indicated by the mean (for the ethene and CO complexes) of the difference between the two bands ($\Delta\nu$49cm^{-1} for pdz; $\Delta\nu$43cm^{-1} for pzO; $\Delta\nu$24cm^{-1} for quin). As would be expected, this order decreases inversely to

the increase in masses of the ligands((80, 96 and 129 amu, respectively), indicating a reduction in the extent of coupling as the mass of the ligand becomes greater than that of bromide (79,9 amu). The single νPt-Br found in the quinO derivative supports the suggestion of the coupling with the aza-nitrogen. The two νPt-Br found for the bipyO_2 derivative is a result of the *cis*-conformation of this cationic species.

The assignment of the three infrared-active planar skeletal bends (δ skeletal) in the square planar complexes (four for trigonal bipyramidal complexes) and that of the two out-of-plane bends (π skeletal) are very tentative.

The assignments of δX-Pt-X and πX-Pt-X are based upon their greater halogen sensitivity. These assignments agree with other *trans*-Pt(II) chloride complexes in which δCl-Pt-Cl is observed to fall in the range 158 to 168cm^{-1} and πCl-Pt-Cl in the range 125 to 132cm^{-1} [78-80]. There is slight coupling of these modes to the other skeletal bends.

MEESTER *et al.* [32] report a Pt-C_2 deformation at 205cm^{-1} for the Zeise's salt derivatives of substituted pyridines. This ethene vibration is observed at 200cm^{-1} in the pdz and at 198cm^{-1} in the pzO derivatives, and is absent in their CO analogues. It is a coupled vibration showing both ligand-deuteration and halogen sensitivity besides its olefin-deuteration sensitivity. The identification of this band in other derivatives is impossible due to the fact that it is masked by low frequency internal ligand vibrations.

Finally, a comment is needed on the expected band splitting due to natural isotopes. In all the carbonyl complexes a weaker infrared band is observed some 42 to 58cm^{-1} below the very intense carbonyl stretch (Table 5.12). This is assigned to $\nu^{13}C\equiv O$ (^{13}C: 1,11% natural relative abundance). The frequen-

	ligand (L)					
	X^{-}(a)	pdz	quin	pzO	bipyO$_2$HX	quinO
$\nu C \equiv O$	2097	2115	2106	2123	2094(b)	2118
[$\nu^{13}C \equiv O$]]	[2050]	[2073]	[2072]	[2065]	[2047]	[2060]
$\delta Pt\text{-}C \equiv O$	540	548	549	551	536	585
$\pi Pt\text{-}C \equiv O$	508	498	536	500	499	522
$\nu Pt\text{-}CO$	497	473	486	490	499	506
$\nu_a Pt\text{-}Cl$	344	351	351	351(b)	347	354
[$\nu_a Pt\text{-}^{37}Cl$]	[-]	[339]	[335]	[335]	[340]	[-]
$\nu_s Pt\text{-}Cl$	345	-	-	-	322	-
[$\nu_s Pt\text{-}^{37}Cl$]	[-]	[-]	[-]	[-]	[-]	[-]
$\nu_a Pt\text{-}Br$	246	257(c)	259(c)	253(c)	244	255
$\nu_s Pt\text{-}Br$	227	-	-	-	205	-
$\delta Pt\text{-}CO$	166	186?(c)	-	168(c)	158?(c)	173(c)
$\delta Cl\text{-}Pt\text{-}Cl$	152	154	149	143	masked	147
$\pi Cl\text{-}Pt\text{-}Cl$	129	125	123	118	122	125
$\delta Br\text{-}Pt\text{-}Br$	112	113	-	-	masked	126
$\pi Br\text{-}Pt\text{-}Br$	98	97	87	88	masked	100

(a) From GOGGIN and NORTON [71] and BROWNING *et al.* [49]

(b) mean of split band

(c) coupled band

Table 5.12 Characteristic frequencies of ligand complexes $[PtL(CO)X_2]$ (X = Cl, Br)

	Ligand (L)							
	X-	phen	bipy	pdz	quin	pzO	$bipyO_2 \cdot HX$	quinO
ν_1	3013 (2224)	3018 (2203)	3017 (2280)[a]	3010 (2219)	3015 (2226)	3013 (2264)	3089[a] (2266)	3006 (2213)
ν_2	1515 (960)	1486 (951)	m (957)	1519 (957)	1515 (m)	1516 (683)	- (m)	1512 (951)
ν_3	1240 (1380)	1263 (1368)	m (-)	1253 (-)	1254 (1369)	1250 (1358)	m (m)	1221 (1333)
ν_4	1020 (726)	1021 (m)	m (m)	1031 (m)	1019 (m)	1016 (757)	1017 (m)	1028 (m)
ν_5	3100 (2349)	3084 (2309)[a]	3102 (2340)	3097 (2323)	3090 (2333)[a]	3097 (2332)	3089[a] (2324)[a]	3081 (2320)[a]
ν_6	1180 (963?)	1182 (930)	1182 (922)	m (m)	1186?(m)	- (972?)	m (m)	1187 (m)
ν_7	1010 (790)	1010 (814)	1005 (811)	1009 (814)	1000 (812)	1004 (808)	1005 (m)	1014 (m)
ν_8	975 (812)	971 (760)	965?(m)	994 (763)	977 (752)	937 (757)	m (m)	982 (m)
ν_9	3080 (2331)	3066 (2309)[a]	3060 (2308)	3070 (2310)	3071 (2333)[a]	3079 (2298)	3076 (2324)[a]	3057 (2320)[a]
ν_{10}	845 (610)	795 (603)	818 (605)	819 (595)	819 (m)	818 (625)	m (626)	m (m)
ν_{11}	2988 (2184)	2988 (2174)	2981 (2173)	2973 (2188)	2977 (2194)	2983 (2223)	2960 (2185)	2996 (2183)
ν_{12}	1425 (1060)	1460 (1050)	1459 (1052)	1426 (1064)	1418 (1058)	1428 (1059)	1426 (1052)	1416 (1058)
ν_{13}	720 (514)	770?(484)	m (489)	702 (513)	701 (513)	728 (518)	m (484)	m (492)
$\nu_a Pt\text{-}C_2$	493 (430)	486 (462)	495 (456)	472 (430)	486 (447)	484 (446)	499 (m)	507 (505)
$\nu_s Pt\text{-}C_2$	405 (370)	- (-)	- (-)	378 (362)	388 (373)	401 (394)	407 (392)	431 (413)
$\nu_a Pt\text{-}Cl$	338 (336)	336 (335)	336 (334)	348 (347)	345 (344)	342 (342)	340 (341)	346 (346)
$[\nu_a Pt\text{-}^{37}Cl]$	[-] [-]	[322] [m]	[-] [-]	[336] [337]	[340] [-]	[-] [-]	[-] [-]	[-] [-]
$\nu_s Pt\text{-}Cl$	327 (326)	(-) (-)	(-) (-)	(-) (-)	- (-)	- (-)	331 (331)	- (-)
$[\nu_s Pt\text{-}^{37}Cl]$	[-] [-]	[-] [-]	[-] [-]	[-] [-]	[-] [-]	[-] [-]	[-] [-]	[-] [-]
$\nu_a Pt\text{-}Br$	- (-)	- (-)	- (-)	255 (-)[b]	259 (-)[b]	250 (-)[b]	242 (-)	250 (-)
$\nu_s Pt\text{-}Br$	- (-)	- (-)	- (-)	- (-)	- (-)	- (-)	200 (-)	- (-)
$\delta Pt\text{-}C_2$	219 (200)	228 (215)	199 (191)	200 (191)[b]	- (-)	198 (196)[b]	m (-)	m (m)
$\delta Cl\text{-}Pt\text{-}Cl$	152 (151)	153 (152)	157 (156)	165 (169)	160 (159)	152 (151)[c]	m (m)	158 (159)
$\pi Cl\text{-}Pt\text{-}Cl$	123 (114)	m (m)	- (135)	139 (139)	135 (135)	137 (135)	m (m)	138 (136)
$\delta Br\text{-}Pt\text{-}Br$	- (-)	- (-)	- (-)	120 (-)	109 (-)	- (-)	110 (-)	126[c] (-)
$\pi Br\text{-}Pt\text{-}Br$	- (-)	- (-)	- (-)	m (-)	91 (-)	85 (-)	- (-)	111 (-)
% Decrease of $\nu_2+\nu_3$	15,32	-	-	14,00	14,22	14,46	-	17,05

a = band assigned twice

b = coupled vibration

c = mean of split band

m = masked

Table 5.13 Characteristic frequencies of ligand complexes with $K[Pt(C_2H_4)X_3]$ (X = Cl, Br) and their C_2D_4 analogues

cy difference between the two carbonyl stretches is typical of those reported previously [23,32,71]. Similarly, a weak shoulder observed some 12 to 17cm^{-1} below the Pt-Cl stretch in some of the complexes (Tables 5.12 and 5.13) is attributed to νPt-^{37}Cl (^{37}Cl: 24,23% natural relative abundance).

Having completed an in depth assignment of these Zeise's salt derivatives and their CO analogues, the employment of the infrared spectra as a diagnostic tool may be made with more confidence. In Tables 5.12 and 5.13 the five and four coordinate complexes have been arranged in order of increasing νPt-CO, and ν_aPt-C_2 and ν_sPt-C_2. As is expected for mixed ligand systems the assignments of several of the ethene and carbonyl fundamentals are made difficult by masking from the fundamentals associated with the other ligand.

From Table 5.13 it is noted that the absence of the symmetric Pt-C_2 is apparently typical of the five coordinate Pt(II) species, as is the frequency of the Pt-Cl stretch. The latter is found some 6 to 10cm^{-1} lower than that found for the four coordinate Pt(II) complexes as a result of the increased coordination number.

However, a more useful diagnostic tool is the observation that the CH_2 scissor mode ν_{12} (a strong band in the infrared) occurs some 35 to 40cm^{-1} higher in frequency for the five-coordinate species than it does for the four-coordinate species. This can therefore be used to distinguish between the two. Since ν_{12} has been shown to couple with ν_2 and ν_3 in substituted olefins, it is probable that the higher frequency of ν_{12} reflects a difference in coupling within the olefin and that use of this as a diagnostic tool is likely to prove to be limited to complexes with the same olefin.

A final comment is made on the use of the summed percentage decrease of the

$\nu C{=}C/\delta CH_2$ frequencies (ν_2 and ν_3) as a rough estimate of the double bond character of the η-ethene. The summed percentage decrease of ν_2 and ν_3 is a measure of the shift in frequencies of modes ν_2 and ν_3 of the complex with respect to those for the free ethene ($1623cm^{-1}$ and $1343cm^{-1}$ respectively [33]). From Table 5.13 the percentage decrease of 17% for quinO is the largest and is significantly different to those of the nitrogen donors. The decrease for $4CH_3$-pyO [43] (which is calculated to be 16,5%) indicates this to be a typical value for an *N*-oxide donor, while that for substituted pyridines is about 13,5%* [33,43] which is similar for the aza-nitrogen donors observed in this work. The percentage decrease of the $\nu C{=}C/\delta CH_2$ frequencies may therefore be employed to distinguish between nitrogen and oxygen coordination in Pt(II) complexes which contain *N*-oxide and aza-nitrogen donors. However, as is observed for the cationic complex with $bipyO_2$, internal fundamentals may mask either ν_2 or ν_3 to make such a measurement impossible.

In conclusion it is noted that the double bond character of the C-C bond decreases inversely with the increase in the frequency of the two $Pt\text{-}C_2$ stretches. Clearly the weaker the platinum-ligand bond, the stronger the platinum-ethene and the lower the C-C bond order of the ethene.

---

* Incorrectly reported as 12,5% by MEESTER *et al.* [33].

1. J. ASHLEY-SMITH, Z. DOUEK, B.F.G. JOHNSON and J. LEWIS,
J. Chem. Soc. Dalton, (1974) 128.

2. S. MIYA and K. SAITO,
Inorg. Chem., *20* (1981) 287.

3. H. VAN DER POEL, G. VAN KOTEN, M. KOKKES and C.H. STAM,
Inorg. Chem., *20* (1981) 2941.

4. P.D. KAPLAN, P. SCHMIDT and M. ORCHIN,
J. Amer. Chem. Soc., *91* (1969) 85.

5. G.A. FOULDS, G.E. JACKSON and D.A. THORNTON,
J. Mol. Struct., *98* (1983) 323.

6. P.S. HALL,
MSc. Thesis, (1983) University of Cape Town.

7. M. ORCHIN and P.J. SCHMIDT,
Coord. Chem. Rev., *3* (1968) 345.

8. G. MORELLI, G. POLZONETTI and V. SESSA,
Polyhedron, *4* (1985) 1185.

9. L. MARESCA, G. NATILE, M. CALLIGARIS, P. DELISE and L. RANDACCIO,
J. Chem. Soc. Dalton, (1976) 2386.

10. A. DE RENZI, B. DI BLASIO, A. SAPORITO, M. SCALONE and A. VITAGLIANO,
Inorg. Chem., *19* (1980) 960.

11. H. VAN DER POEL, G. VAN KOTEN, K. VRIEZE, M. KOKKES and C.H. STAM,
J. Organometal. Chem., *175* (1979) C21.

12. C. BISI-CASTELLI, L. MARESCA and G. NATILE,
Inorg. Chim. Acta, *89* (1984) 157.

13. V.G. ALBANO, F. DEMARTIN, A. DE RENZI, G. MORELLI and A. SAPORITO,
Inorg. Chem., *24* (1985) 2032.

14. H. VAN DER POEL, G. VAN KOTEN and G.C. VAN STEIN,
J. Chem. Soc. Dalton, (1981) 2164.

15. H. VAN DER POEL and G. VAN KOTEN,
Inorg. Chem., *20* (1981) 2950.

16. L. MARESCA, G. NATILE and L. CATTALINI,
Inorg. Chim. Acta, *14* (1975) 79.

17. A. DE RENZI, A. PANUNZI, A. SAPORITO and G. VITAGLIANO,
Gazz. Chim. Ital., *107* (1977) 549.

18. F.R. HARTLEY,
Platinum Metals Review, *16* (1972) 22.

19. F.R. HARTLEY,
J. Organometal. Chem., *216* (1981) 277.

20. T.A. ALBRIGHT, R. HOFFMAN, J.C. THIBEAULT and D.L. THORN, *J. Amer. Chem. Soc., 101* (1979) 3801.

21. L. MARESCA, G. NATILE and L. CATTALINI, *J. Chem. Soc. Dalton,* (1979) 1140.

22. G.A. FOULDS, D.A. THORNTON and J. YATES, *J. Mol. Struct., 98* (1983) 315.

23. P.C. KONG and T. THEOPHANIDES, *Can. J. Spectrosc., 14* (1969) 105.

24. T. THEOPHANIDES and P.C. KONG, *Can. J. Chem., 48* (1969) 1084.

25. A. TIRIPICCHIO, M. TIRIPICCHIO-CAMELLINI, L. MARESCA, G. NATILE and G. RIZZARDI, *Cryst. Struct. Comm., 8* (1979) 689.

26. L. MARESCA, G. NATILE and G. RIZZARDI, *Inorg. Chim. Acta, 38* (1980) 53.

27. G. NATILE, L. MARESCA, L. CATTALINI, U. BELLUCO, P. UGUAGLIATI and U. CROATTO, *Inorg. Chim. Acta, 20* (1976) 49.

28. T.G. APPLETON, H.C. CLARK and L.E. MANZER, *Coord. Chem. Rev., 10* (1973) 335.

29. A.R. BRAUSE, M. RYCHECK and M. ORCHIN, *J. Amer. Chem. Soc., 89* (1967) 6500.

30. T.A. WEIL, P. SCHMIDT, M. RYCHECK and M. ORCHIN, *Inorg. Chem., 8* (1969) 1002.

31. L. SPAULDING, B.A. REINHARDT and M. ORCHIN, *Inorg. Chem., 11* (1972) 2092.

32. M.A.M. MEESTER, D.J. STUFKENS and K. VRIEZE, *Inorg. Chim. Acta, 14* (1975) 25.

33. M.A.M. MEESTER, D.J. STUFKENS and K. VRIEZE, *Inorg. Chim. Acta, 15* (1975) 137.

34. M.A.M. MEESTER, D.J. STUFKENS and K. VRIEZE, *Proc. 18th. Collog. Spectrosc. Int., 3* (1975) 826.

35. G.A. FOULDS, P.S. HALL and D.A. THORNTON, *J. Mol. Struct., 117* (1984) 95.

36. P.S. HALL, D.A. THORNTON and G.A. FOULDS, *Polyhedron, 6* (1987) in press.

37. J.V. KINGSTON and G.R. SCOLLARY, *J. Chem. Soc. Chem. Commun.,* (1970) 362.

38. J.V. KINGSTON and G.R. SCOLLARY,
J. Chem. Soc. A, (1971) 3765.

39. H.C. CLARK and L.E. MANZER,
Inorg. Chem., 13 (1974) 1996.

40. JU.S. VARSHAVSKY, N.V. KISELEVA, T.G. CHERKASOVA and N.A. BUZINA,
J. Organometal. Chem., 31 (1971) 119.

41. S.I. SHUPACK and M. ORCHIN,
Inorg. Chem., 3 (1964) 374.

42. T. IWAYANAGI and Y. SAITO,
Inorg. Nucl. Chem. Lett., 11 (1975) 459.

43. M.A.M. MEESTER, D.J. STUFKENS and K. VRIEZE,
Inorg. Chim. Acta, 16 (1976) 191.

44. M.A.M. MEESTER, D.J. STUFKENS and K. VRIEZE,
Inorg. Chim. Acta, 21 (1977) 251.

45. K.L. KLASSEN and N.V. DUFFY,
J. Inorg. Nucl. Chem., 35 (1973))2602.

46. L. MANOJLOVIC-MUIR, K.W. MUIR and R. WALKER,
J. Organometal. Chem., 66 (1974) C21.

47. J. CHATT, N.P. JOHNSON and B.L. SHAW,
J. Chem. Soc., (1964) 1662.

48. A.C. SMITHIES, M. RYCHECK and M. ORCHIN,
J. Organometal. Chem., 12 (1968) 199.

49. J. BROWNING, P.L. GOGGIN, R.J. GOODFELLOW, M.G. NORTON,
A.J.M. RATTRAY, B.F. TAYLOR and J. MINK,
J. Chem. Soc. Dalton., (1977) 2061.

50. R.G. GOEL, W.O. OGINI and R.C. SRIVASTAVA,
Inorg. Chem., 20 (1981) 3611.

51. A. DE RENZI, G. PAIARO and A. PANUNZI,
Gazz. Chim. Ital., 102 (1972) 413.

52. M.J. CLEARE and W.P. GRIFFITH,
J. Chem. Soc. A, (1969) 372.

53. G.K. ANDERSON and R.J. CROSS,
J. Chem. Soc. Dalton, (1980) 1988.

54. Y.N. KUKUSHKIN and I.V. PAKOMOVA,
Zh. Neorg. Khim., 15 (1970) 1882.

55. H. BOUCHER and B. BOSNICH,
Inorg. Chem., 16 (1977) 717.

56. H. BOUCHER and B. BOSNICH,
J. Amer. Chem. Soc., 99 (1977) 6253.

57. J.C. DAVIDSON, P.N. PRESTON and M.V. RUSSO,
J. Chem. Soc. Dalton, (1983) 783.

58. W.L. FICHTEMAN, B. SCHMIDT and M. ORCHIN,
J. Organometal. Chem., 12 (1968) 249.

59. D. MANSUY, J.F. BARTOL and J.C. CHOTTARD,
J. Organometal. Chem., 73 (1974) C39.

60. T.P.E. AUF DER HEYDE, G.A. FOULDS, D.A. THORNTON, H.O. DESSEYN and B.J. VAN DER VEKEN,
J. Mol. Struct., 98 (1983) 11.

61. D.B. POWELL and N. SHEPPARD,
Spectrochim. Acta, 13 (1958) 69.

62. M.J. GROGAN and K. NAKAMOTO,
J. Amer. Chem. Soc., 88 (1966) 5454.

63. J. PRADILLA-SORANZO and J.P. FACKLER,
J. Mol. Spectrosc., 22 (1967) 80.

64. J. HIRAISHI,
Spectrochim. Acta, 25A (1969) 749.

65. D.C. ANDREWS, G. DAVIDSON and D.A. DUCE,
J. Organometal. Chem., 101 (1975) 113.

66. H. JOBIC,
J. Mol. Struct., 131 (1985) 167.

67. D.B. POWELL, J.V. SCOTT and N. SHEPPARD,
Spectrochim. Acta, 28A (1972) 327.

68. D.B. POWELL and T.J. LEEDHAM,
Spectrochim. Acta, 28A (1972) 337.

69. R.G. DENNING and M.J. WARE,
Spectrochim. Acta, 24A (1968) 1785.

70. M.J. CLEARE and W.P. GRIFFITH,
J. Chem. Soc. A, (1970) 2788.

71. P.L. GOGGIN and M.G. NORTON,
Inorg. Chim. Acta, 26 (1978) 125.

72. H.D. STIDHAM and J.V. TUCCI,
Spectrochim. Acta, 23A (1967) 2233.

73. G.A. FOULDS,
PhD Thesis, (1982) University of Cape Town.

74. J. REINHOLD, R. BENEDIX, P. BIRNER and H. HENNIG,
Inorg. Chim. Acta, 33 (1979) 209.

75. Z. DEGAN-SZAFRAN,
Rocz. Chem., 44 (1970) 2371.

76. W.W. PAUDLER and M.V. JOVANOVIC,
Heterocycles, 19 (1982) 93.

77. M.V. JOVANOVIC,
Spectrochim. Acta, 41A (1985) 1135.

78. H. POULET, P. DELORME and J.P. MATHIEU,
Spectrochim. Acta, 20 (1964) 1855.

79. J.R. DURIG, B.R. MITCHELL, D.W. SINK, J.N. WILLIS and A.S. WILSON,
Spectrochim. Acta, 23A (1967) 1121.

80. M. PFEFFER, P. BRAUNSTEIN and J. DEHAND,
Spectrochim. Acta, 30A (1974) 341.

APPENDIX 1

Investigations of the mass spectra of aromatic *N*-oxides reveal that they undergo loss of the *N*-oxide through thermal fragmentation and/or electron impact. The mass spectra (pages 378-381) of the pure ligands, pyrazine *N*-oxide (pzO), pyrazine *N,N'*-dioxide (pzO_2), 2,2'bipyridine *N,N'*-dioxide ($bipyO_2$) and quinoline *N*-oxide (quinO) are readily interpreted with the aid of their fully deuterated analogues. The following fragmentation pathways (page 382) are observed. The fragmentation of $bipyO_2$ ($\dot{d}_0$ and $\dot{d}_8$) yielding an (M-17) and (M-18) ion, respectively, is a result of an *ortho* effect similar to that found in alkyl pyridines [3,34], with a molecular rearrangement involving the H/D at the 6 position.

While the presence of an (M-16) ion is possibly ascribed to thermal fragmentation and/or electron impact, it may also result from the presence of starting material. This is illustrated (page 383) by the presence of the double maxima of the m/e 86 mass chromatogram (the trace of a single ion plotted against time) in the product of pzO_2 before recrystallisation (evidence of pzO impurity) *cf.* the single maxima in the sublimed product of pzO_2.

The purity of the ligands was established by doping the product with starting material to establish whether the starting material and product volatalise separately or simultaneously. Where there is sufficient separation between the mass chromatograms of the M and (M-16) ions (*e.g.* with pzO_2 - page 383), the absence of a twin (M-16) maxima of the *undoped* spectrum is evidence of its purity.

PzO_2, pzO and $bipyO_2$ and their fully deuterated analogues show sufficient separation between their M and (M-16) mass chromatograms to allow for purity to be determined. Quinoline *N*-oxide ($\dot{d}_0$ and $\dot{d}_7$) are found to volatalise too closely together to allow the purity to be checked by mass spectroscopy

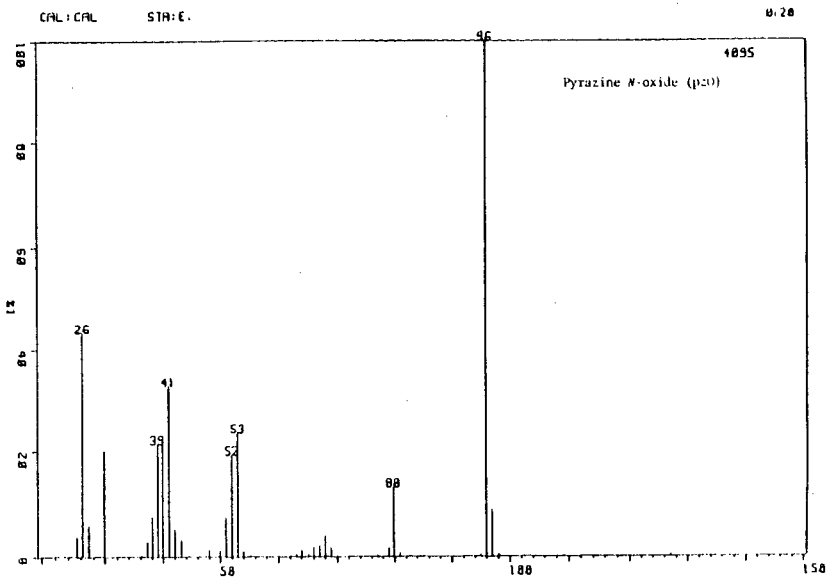
CAL:CAL STA:E. 0:20
4895
Pyrazine N-oxide (pzO)
96
26
41
39
53
52
80
I%
58
100
150

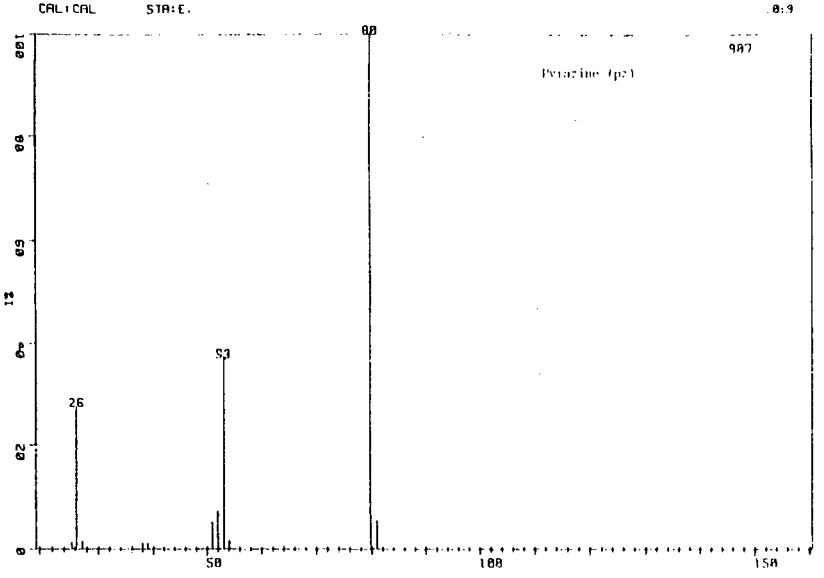
CAL:CAL STA:E. 0:9
9877
Pyrazine (pz)
80
53
26
I%
50
100
150

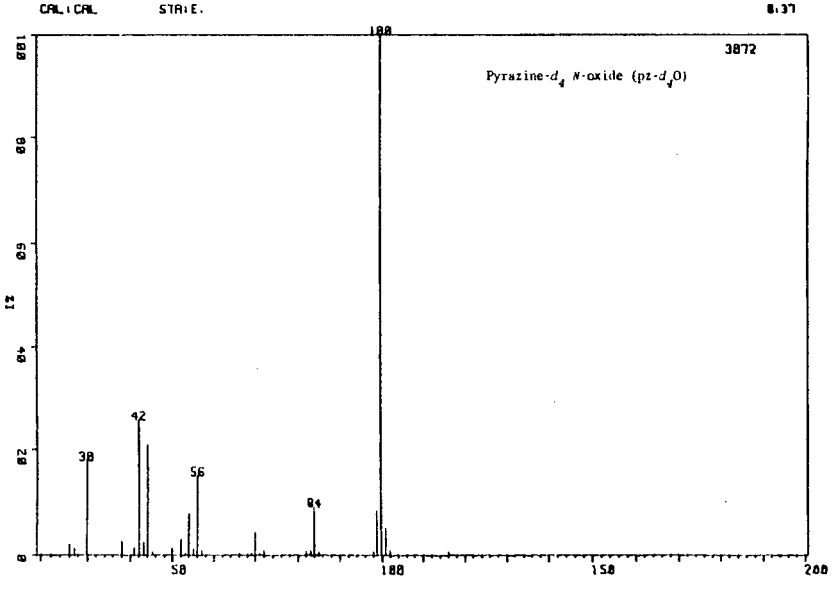
CAL:CAL STA:E. 0:37
3872
Pyrazine-d_4 N-oxide (pz-d_4O)
100
42
38
56
84
I%
50
100
150
200

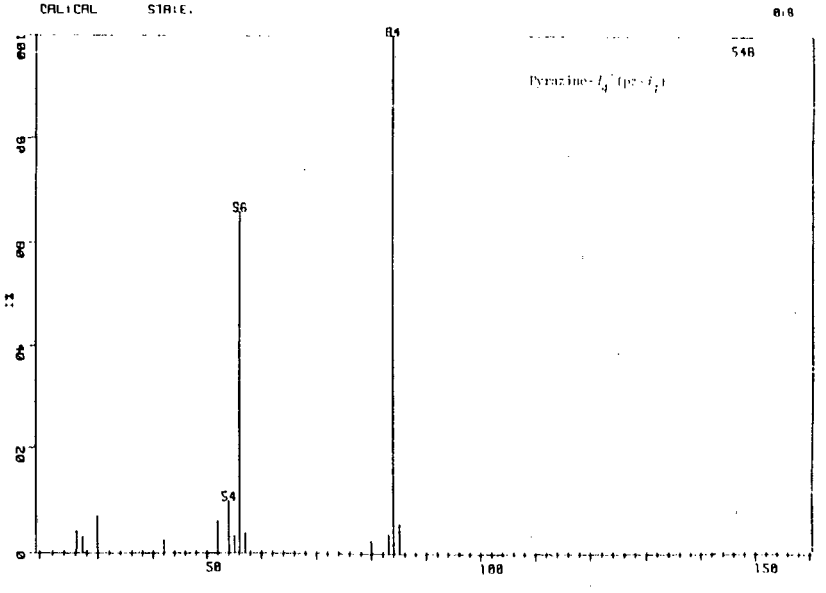
CAL:CAL STA:E. 0:8
548
Pyrazine-d_4 (pz-d_4)
84
56
54
I%
50
100
150

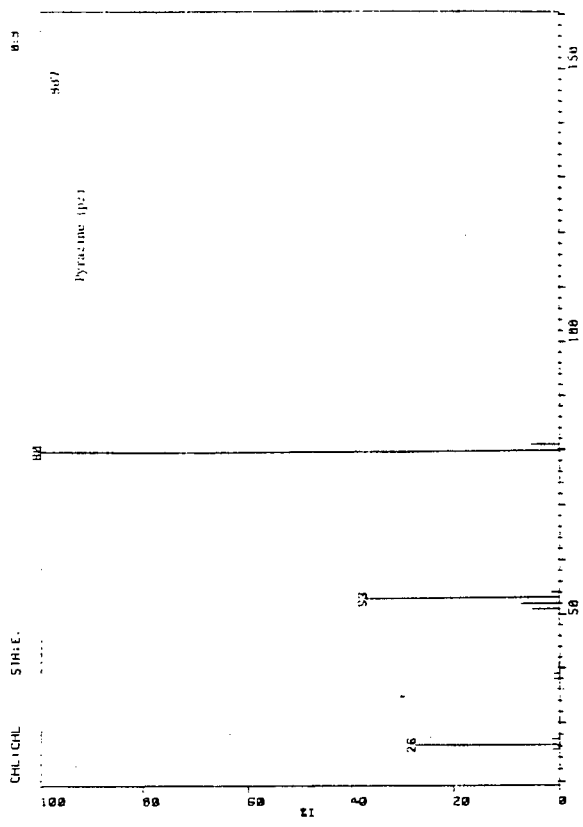

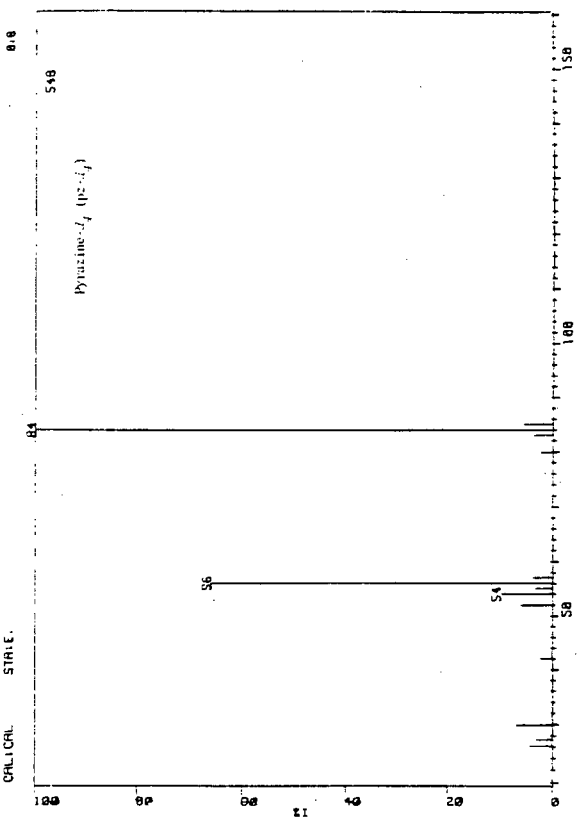

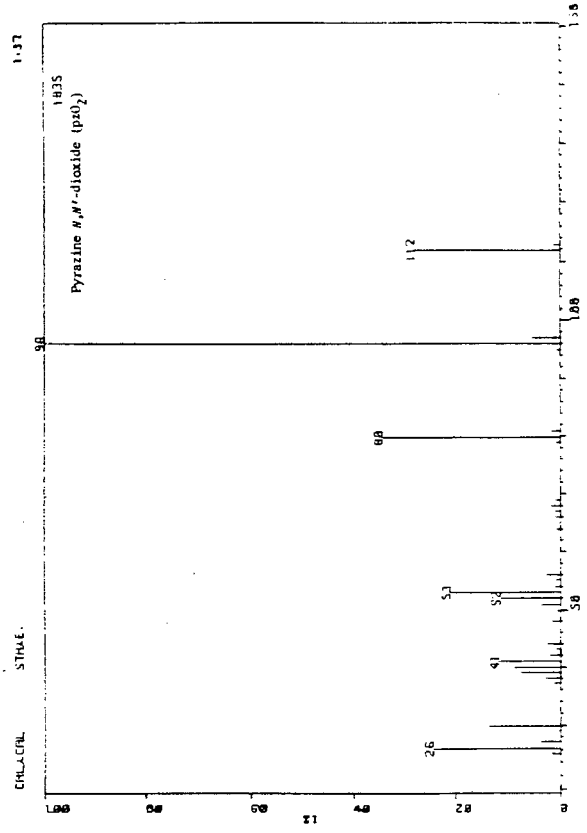
Pyrazine N,N'-dioxide (pzO2)
1435

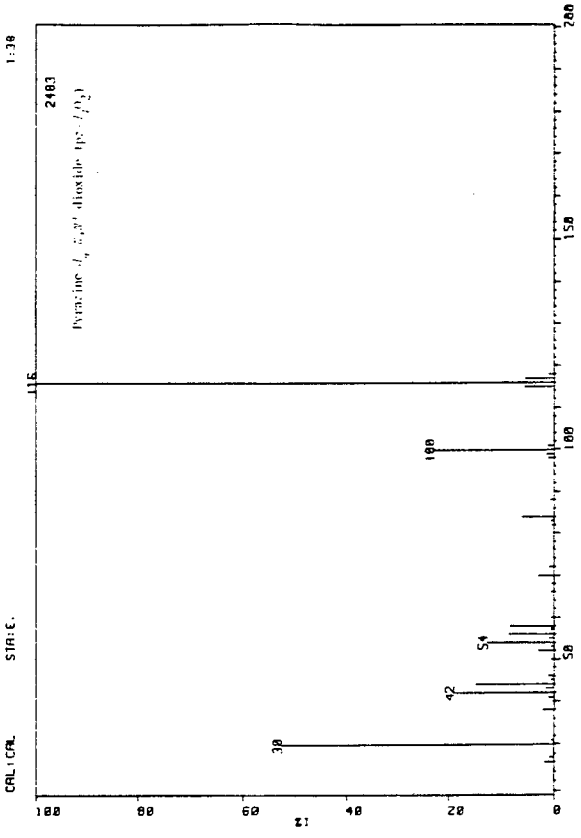
2483

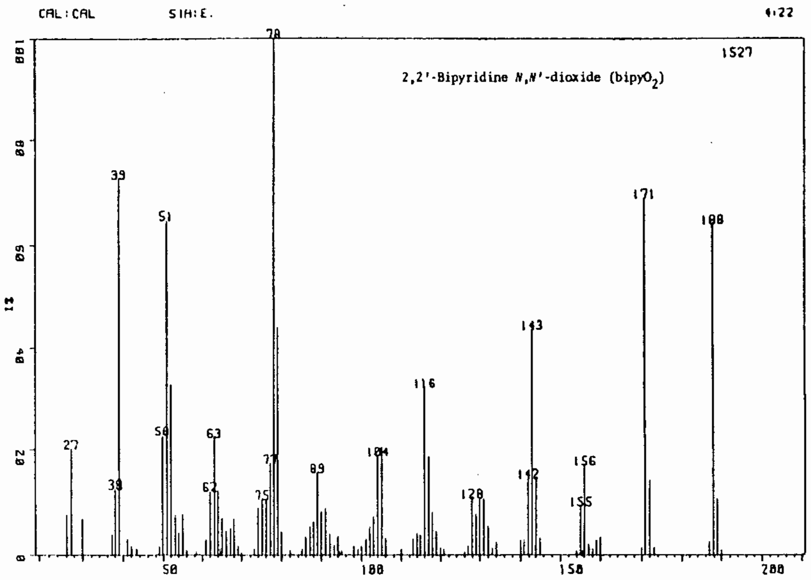
CAL:CAL STA:E.
4:22
1527
2,2'-Bipyridine N,N'-dioxide (bipyO2)
27 38 39 50 51 62 63 75 77 78 89 104 116 128 142 143 155 156 171 188
50 100 150 200

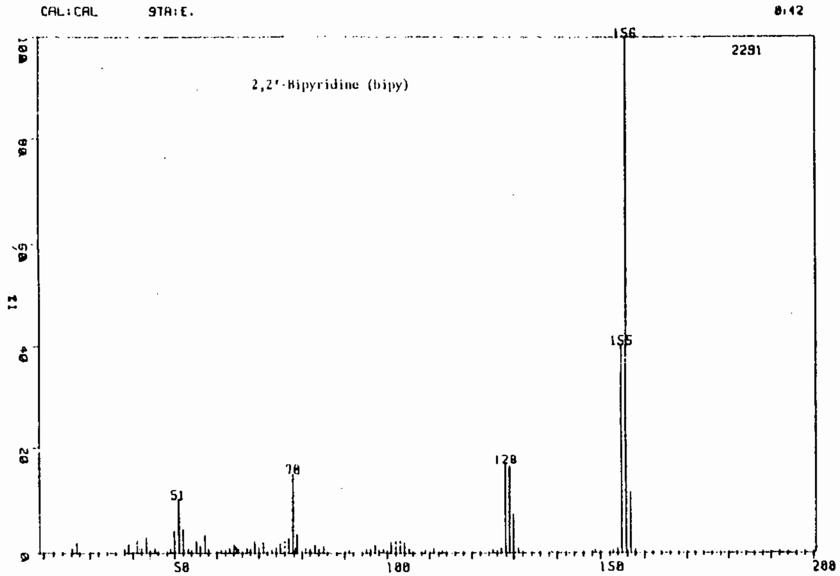
CAL:CAL STA:E.
8:42
2291
2,2'-Bipyridine (bipy)
51 78 128 155 156
50 100 150 200

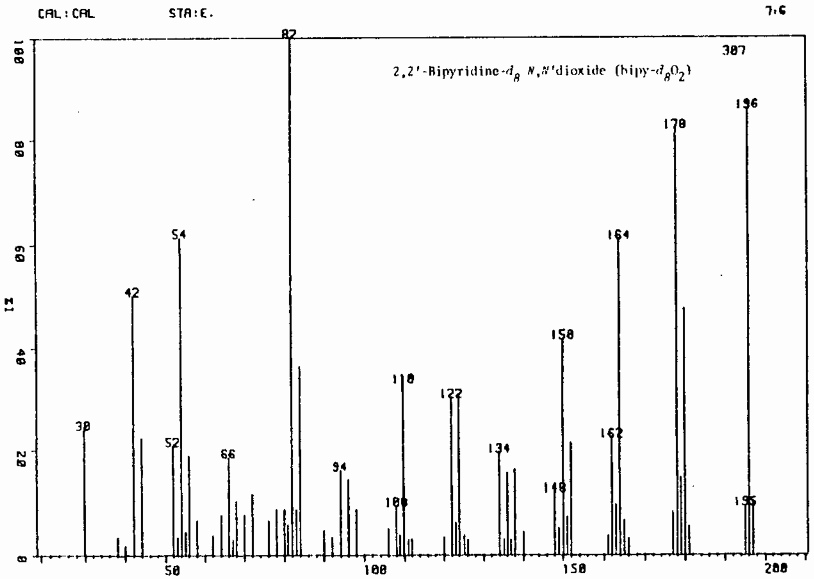
CAL:CAL STA:E.
7:6
387
30 42 52 54 66 82 94 108 110 122 134 148 150 162 164 178 195 196
50 100 150 200

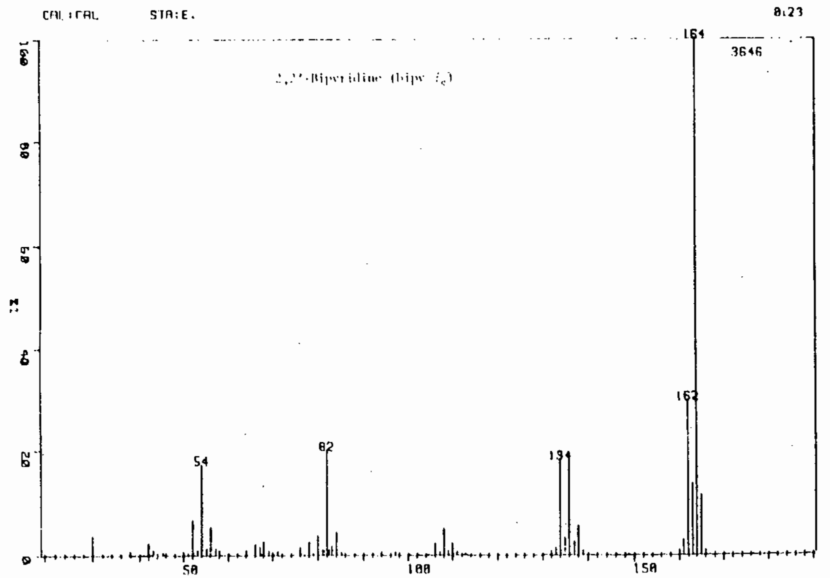
CAL:CAL STA:E.
8:23
3646
54 82 134 162 164
50 100 150

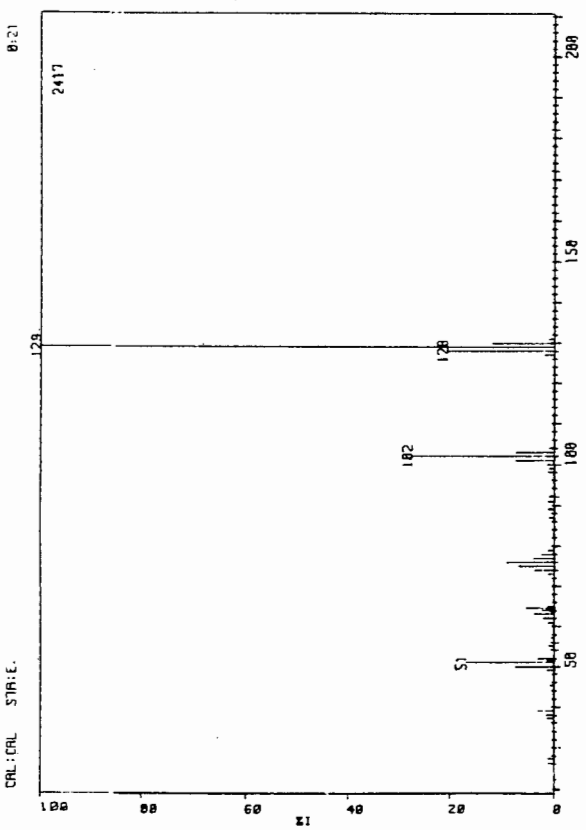
CAL:CAL STA:E.
2417
129
128
182
180
51
50
150
200
100
80
60
40
20
0
%I

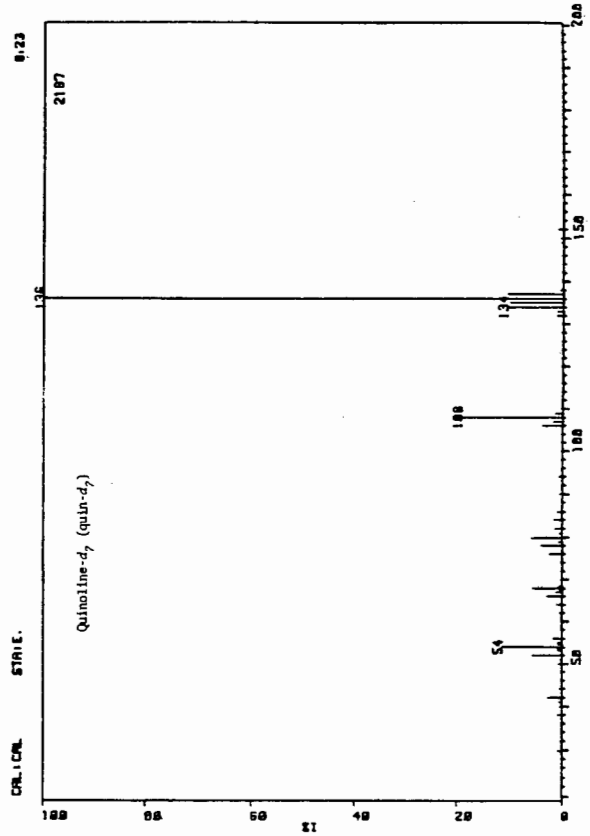
CAL:CAL STA:E.
2197
136
134
108
100
54
50
150
200
100
80
60
40
20
0
%I
Quinoline-d_7 (quin-d_7)

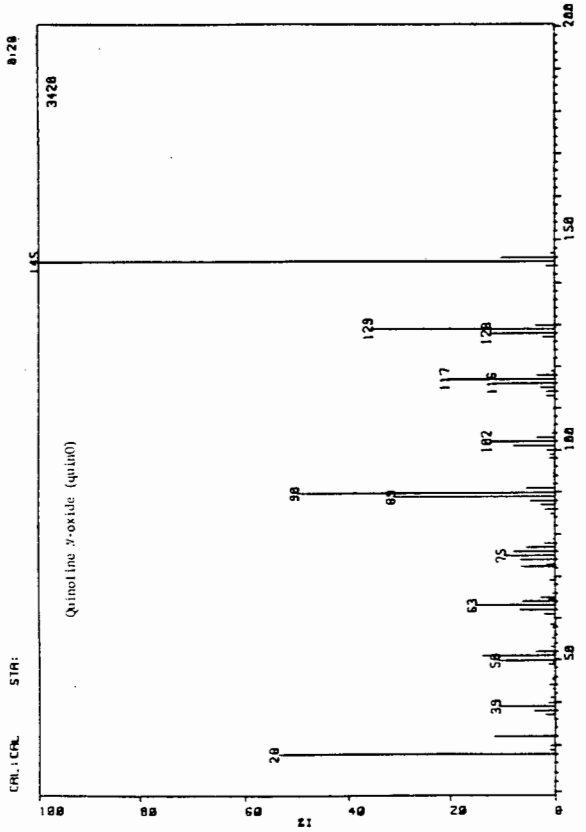
CAL:CAL STA:
3420
145
129
128
117
116
102
100
98
89
75
63
58
50
39
28
150
200
100
80
60
40
20
0
%I
Quinoline 1-oxide (quin0)

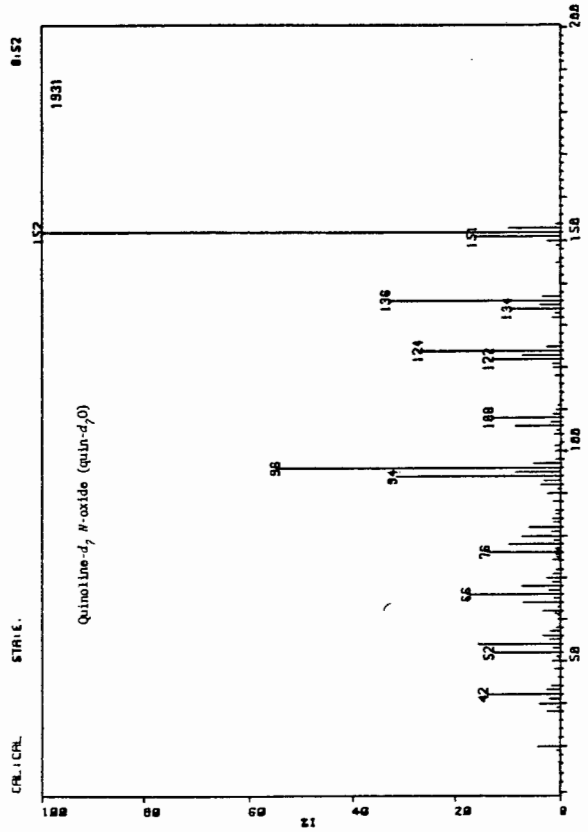
CAL:CAL STA:E.
1931
152
151
136
134
124
122
108
100
98
94
76
66
52
50
42
150
200
100
80
60
40
20
0
%I
Quinoline-d_7 N-oxide (quin-d_7O)

pzO and pz-d_4O

1)

$-d_0$ m/e 96 $\xrightarrow{-[O]}$ m/e 80 $\xrightarrow{-[HCN]}$ m/e 53

$-d_4$ m/e 100 m/e 84 $\xrightarrow{-[DCN]}$ m/e 56

2)

$-d_0$ m/e 96 $\xrightarrow{-[HC_2NO]}$ m/e 41 $\xrightarrow{-[H]}$ m/e 40

$-d_4$ m/e 96 $\xrightarrow{-[DC_2NO]}$ m/e 44 $\xrightarrow{-[D]}$ m/e 42

pzO_2 and pz-d_4O_2

1)

$-d_0$ m/e 112 $\xrightarrow{-[O]}$ m/e 96 $\longrightarrow$ (as above)

$-d_4$ m/e 116 m/e 100

bipyO_2 and bipy-d_8O_2

1)

$-d_0$ m/e 188 $\xrightarrow{-[O]}$ m/e 172 $\xrightarrow{-[O]}$ m/e 156 $\xrightarrow{-[H]}$ m/e 155 $\xrightarrow{-[HCN]}$ m/e 128

$-d_8$ m/e 196 m/e 180 m/e 164 $\xrightarrow{-[D]}$ m/e 162 $\xrightarrow{-[DCN]}$ m/e 134

2)

$-d_0$ m/e 188 $\xrightarrow{-[OH]}$ m/e 171 $\xrightarrow{-[CO]}$ m/e 143 $\xrightarrow{-[HCN]}$ m/e 116

$-d_8$ m/e 196 $\xrightarrow{-[OD]}$ m/e 178 m/e 150 $\xrightarrow{-[DCN]}$ m/e 122

quinO and quin-d_7O

1)

$-d_0$ m/e 145 $\xrightarrow{-[O]}$ m/e 129 $\xrightarrow{-[HCN]}$ m/e 102

$-d_7$ m/e 152 m/e 136 $\xrightarrow{-[DCN]}$ m/e 108

$\xrightarrow{-[C_5H_3N]}$ m/e 51 $\xrightarrow{-[H]}$ m/e 50

$\xrightarrow{-[C_5D_3N]}$ m/e 54 $\xrightarrow{-[D]}$ m/e 52

2)

$-d_0$ m/e 145 $\xrightarrow{-[CO]}$ m/e 117 $\xrightarrow{-[HCN]}$ m/e 90 $\xrightarrow{-[H]}$ m/e 89 $\xrightarrow{-[C_2H_2]}$ m/e 63

$-d_7$ m/e 152 m/e 124 $\xrightarrow{-[DCN]}$ m/e 96 $\xrightarrow{-[D]}$ m/e 94 $\xrightarrow{-[C_2D_2]}$ m/e 66

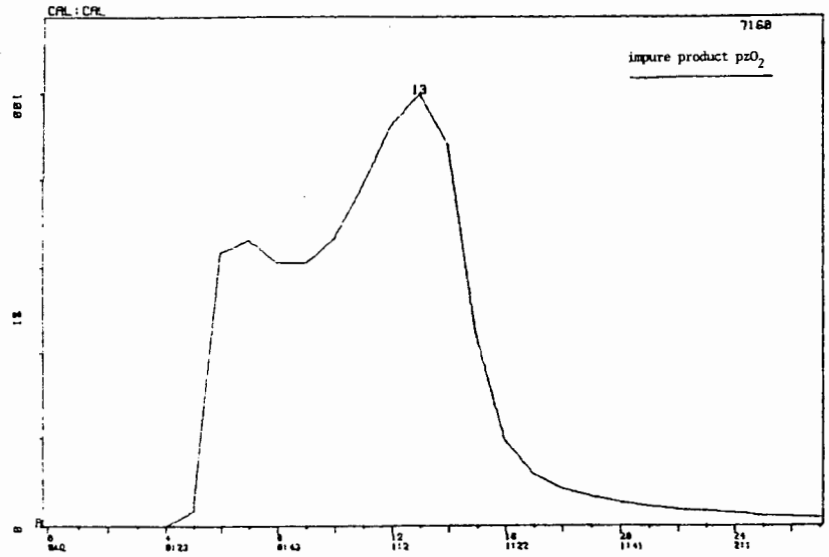
CAL:CAL
7168
impure product pzO_2
13

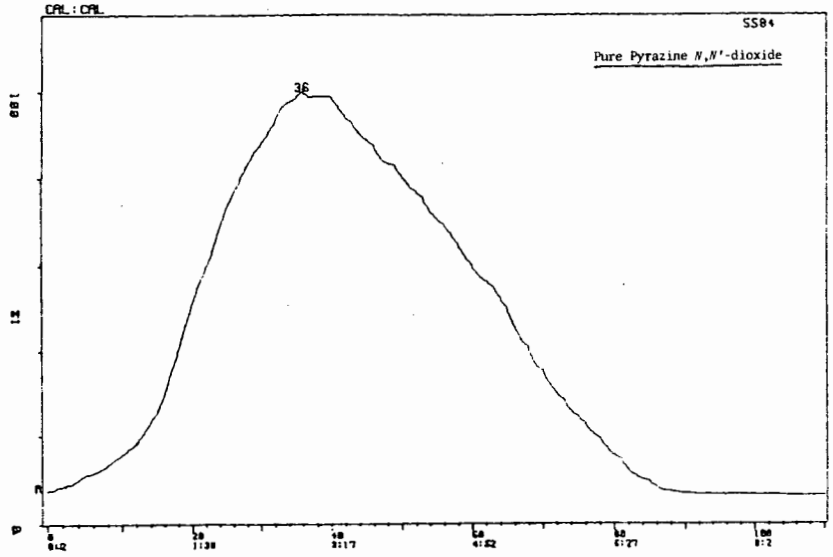
CAL:CAL
5584
Pure Pyrazine N,N'-dioxide
36

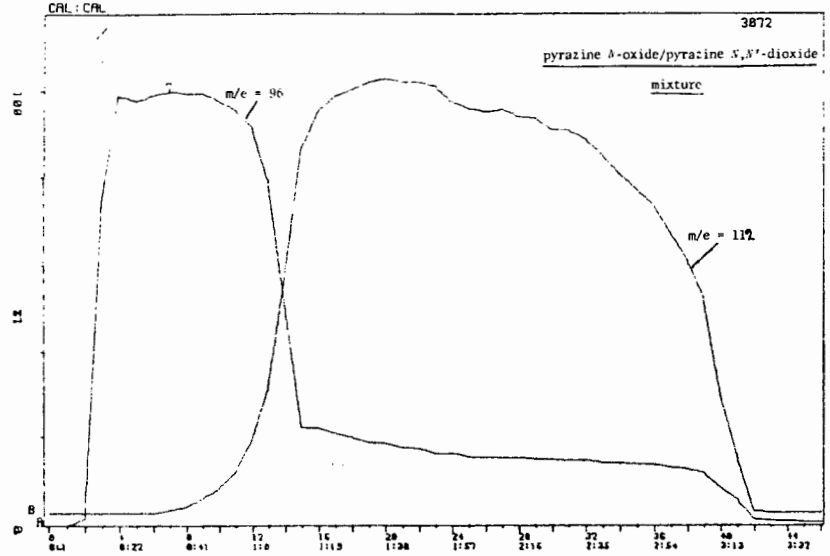
CAL:CAL
3872
pyrazine N-oxide/pyrazine N,N'-dioxide
mixture
m/e = 96
m/e = 112

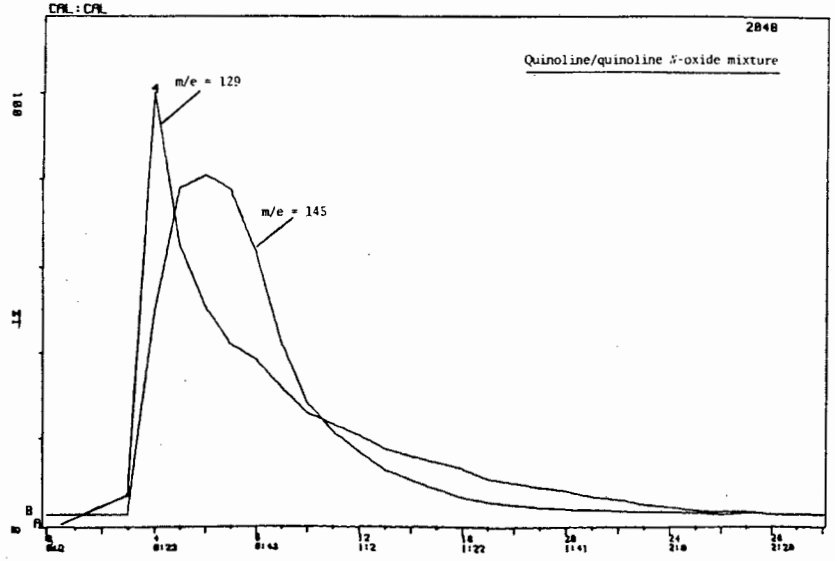
CAL:CAL
2848
Quinoline/quinoline N-oxide mixture
m/e = 129
m/e = 145

(page 383).

[1] A.M. DUFFIELD and O. BUCHARDT, *Acta Chem. Scand.*, *26* (1972) 2423.

[2] O. BUCHARDT, A.M. DUFFIELD and R.H. SHAPIRO, *Tetrahedron*, *24* (1968) 3139.

[3] A. TATEMATSU and H. YOSHIZUMI, *Tetrahedron Letters*, *31* (1967) 2985.

[4] D.A. LIGHTNER, R. NICOLETTI, G.B. QUISTAD and E. IRWIN, *Org. Mass. Spectrom.*, *4* (1970) 571.

APPENDIX 2

1) PYRAZINE *N,N'*-DIOXIDE

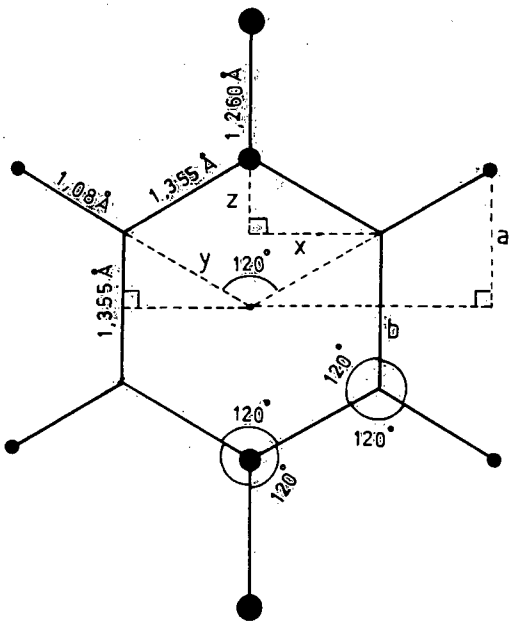

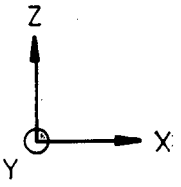

MODEL I

$x = 1{,}355 \sin 60 = 1{,}173$ Å

$y = \dfrac{1{,}355}{2 \cos 60} = 1{,}355$ Å

$z = 1{,}355 \cos 60 = 0{,}6775$ Å

$a = (1{,}355 + 1{,}08) \sin 30 = 1{,}217$ Å

$b = (1{,}355 + 1{,}08) \cos 30 = 2{,}109$ Å

Distance to Axis (Å)

ATOM	X AXIS	Y AXIS	Z AXIS
N	1,355	1,355	0
O	2,615	2,615	0
C	0,677	1,355	1,173
H	1,217	2,435	2,109

MODEL I

B_{1g} species

$$R_{calc} = \left[\left(\frac{116,116}{112,088}\right)^0 \left(\frac{I_x}{I_x'}\right)^0 \left(\frac{I_y}{I_y'}\right)^0 \left(\frac{42,019}{50,977}\right)^1 \left(\frac{1,008}{2,015}\right)^1\right]^{\frac{1}{2}} = 0,793\ (1,261)$$

B_{2g} species

$$R_{calc} = \left[\left(\frac{116,116}{112,088}\right)^0 \left(\frac{I_x}{I_x'}\right)^0 \left(\frac{191,180}{203,122}\right)^1 \left(\frac{I_z}{I_z'}\right)^0 \left(\frac{1,008}{2,015}\right)^1\right]^{\frac{1}{2}} = 0,525\ (1,905)$$

B_{3g} species

$$R_{calc} = \left[\left(\frac{116,116}{112,088}\right)^0 \left(\frac{149,136}{152,122}\right)\left(\frac{I_y}{I_y'}\right)^0 \left(\frac{I_z}{I_z'}\right)^0 \left(\frac{1,008}{2,015}\right)^1\right]^{\frac{1}{2}} = 0,727\ (1,375)$$

B_{1u} species

$$R_{calc} = \left[\left(\frac{116,116}{112,088}\right)^1 \left(\frac{I_x}{I_x'}\right)^0 \left(\frac{I_y}{I_y'}\right)^0 \left(\frac{I_z}{I_z'}\right)^0 \left(\frac{1,008}{2,015}\right)^2\right]^{\frac{1}{2}} = 0,509\ (1,964)$$

B_{2u} species

$$R_{calc} = \left[\left(\frac{116,116}{112,088}\right)^1 \left(\frac{I_x}{I_x'}\right)^0 \left(\frac{I_y}{I_y'}\right)^0 \left(\frac{I_z}{I_z'}\right)^0 \left(\frac{1,008}{2,015}\right)^1\right]^{\frac{1}{2}} = 0,720\ (1,389)$$

B_{3u} species

$$R_{calc} = \left[\left(\frac{116,116}{112,088}\right)^1 \left(\frac{I_x}{I_x'}\right)^0 \left(\frac{I_y}{I_y'}\right)^0 \left(\frac{I_z}{I_z'}\right)^0 \left(\frac{1,008}{2,015}\right)^2\right]^{\frac{1}{2}} = 0,509\ (1,964)$$

A_u species

$$R_{calc} = \left[\left(\frac{116,116}{112,088}\right)^1 \left(\frac{I_x}{I_x'}\right)^0 \left(\frac{I_y}{I_y'}\right)^0 \left(\frac{I_z}{I_z'}\right)^0 \left(\frac{1,008}{2,015}\right)^1\right]^{\frac{1}{2}} = 0,707\ (1,414)$$

A_g species

$$R_{calc} = \left[\left(\frac{116,116}{112,088}\right)^0 \left(\frac{I_x}{I_x'}\right)^0 \left(\frac{I_y}{I_y'}\right)^0 \left(\frac{I_z}{I_z'}\right)^0 \left(\frac{1,008}{2,015}\right)^2\right]^{\frac{1}{2}} = 0,500\ (2,000)$$

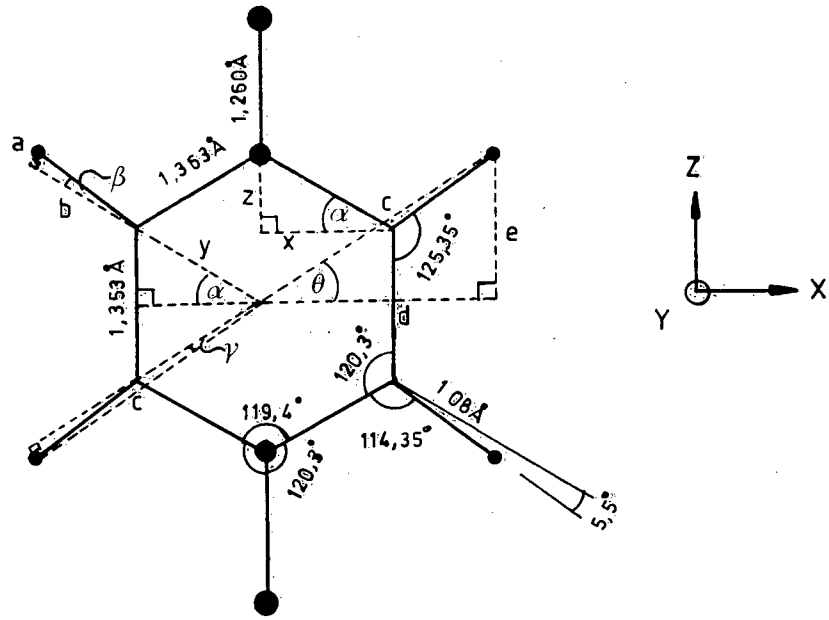

MODEL II

$\alpha = 90 - \left(\frac{120,25}{2}\right) = 29,875°$

$\beta = 5,5°$

$\tan \gamma = \frac{a}{b + h}$; $\gamma = 2,435°$

$\theta = \alpha + \gamma = 32,310°$

$x = 1,363 \sin \left(\frac{119,4}{2}\right) = 1,178$ Å

$y = \frac{1,353}{2} \cos \left(\frac{120,3}{2}\right) = 1,359$ Å

$z = 1,363 \cos \left(\frac{119,4}{2}\right) = 0,688$ Å

$a = 1,08 \sin 5,5 = 0,1035$ Å

$b = 1,08 \cos 5,5 = 1,075$ Å

$c = \frac{a}{\sin \gamma} = (b + y) \cos \gamma = 2,436$ Å

$d = c \cos \theta = 2,059$ Å

$e = c \cos \theta = 1,302$ Å

Distance to Axis (Å)

ATOM	X AXIS	Y AXIS	Z AXIS
N	1,364	1,364	0
O	2,624	2,624	0
C	0,677	1,359	1,178
H	1,302	2,436	2,059

Dimensions adapted from molecular structure of pyO

G.O. SORENSON, Å TANG-PEDERSEN and E.J. PEDERSEN

J. Mol. Struct., 101 (1983) 263.

MODEL II

B_{1g} species

$$R_{calc} = \left[\left(\frac{116,116}{112,088}\right)^0 \left(\frac{I_x}{I_x'}\right)^0 \left(\frac{I_y}{I_y'}\right)^0 \left(\frac{41,882}{50,420}\right)^1 \left(\frac{1,008}{2,015}\right)^1\right]^{\frac{1}{2}} = 0,790\ (1,266)$$

B_{2g} species

$$R_{calc} = \left[\left(\frac{116,116}{112,088}\right)^0 \left(\frac{I_x}{I_x'}\right)^0 \left(\frac{192,548}{204,499}\right)^1 \left(\frac{I_z}{I_z'}\right)^0 \left(\frac{1,008}{2,015}\right)^1\right]^{\frac{1}{2}} = 0,525\ (1,095)$$

B_{3g} species

$$R_{calc} = \left[\left(\frac{116,116}{112,088}\right)^0 \left(\frac{150,646}{154,061}\right)^1 \left(\frac{I_y}{I_y'}\right)^0 \left(\frac{I_z}{I_z'}\right)^0 \left(\frac{1,008}{2,015}\right)^1\right]^{\frac{1}{2}} = 0,728\ (1,374)$$

B_{1u} species

$$R_{calc} = \left[\left(\frac{116,116}{112,088}\right)^1 \left(\frac{I_x}{I_x'}\right)^0 \left(\frac{I_y}{I_y'}\right)^0 \left(\frac{I_z}{I_z'}\right)^0 \left(\frac{1,008}{2,015}\right)^2\right]^{\frac{1}{2}} = 0,509\ (1,964)$$

B_{2u} species

$$R_{calc} = \left[\left(\frac{116,116}{112,088}\right)^1 \left(\frac{I_x}{I_x'}\right)^0 \left(\frac{I_y}{I_y'}\right)^0 \left(\frac{I_z}{I_z'}\right)^0 \left(\frac{1,008}{2,015}\right)^1\right]^{\frac{1}{2}} = 0,720\ (1,389)$$

B_{3u} species

$$R_{calc} = \left[\left(\frac{116,116}{112,088}\right)^1 \left(\frac{I_x}{I_x'}\right)^0 \left(\frac{I_y}{I_y'}\right)^0 \left(\frac{I_z}{I_z'}\right)^0 \left(\frac{1,008}{2,015}\right)^2\right]^{\frac{1}{2}} = 0,509\ (1,964)$$

A_u species

$$R_{calc} = \left[\left(\frac{116,116}{112,088}\right)^0 \left(\frac{I_x}{I_x'}\right)^0 \left(\frac{I_y}{I_y'}\right)^0 \left(\frac{I_z}{I_z'}\right)^0 \left(\frac{1,008}{2,015}\right)^1\right]^{\frac{1}{2}} = 0,707\ (1,414)$$

A_g species

$$R_{calc} = \left[\left(\frac{116,116}{112,088}\right)^0 \left(\frac{I_x}{I_x'}\right)^0 \left(\frac{I_y}{I_y'}\right)^0 \left(\frac{I_z}{I_z'}\right)^0 \left(\frac{1,008}{2,015}\right)^2\right]^{\frac{1}{2}} = 0,500\ (2,000)$$

2) 2,2'BIPYRIDINE *N,N'*-DIOXIDE

syn non-planar model

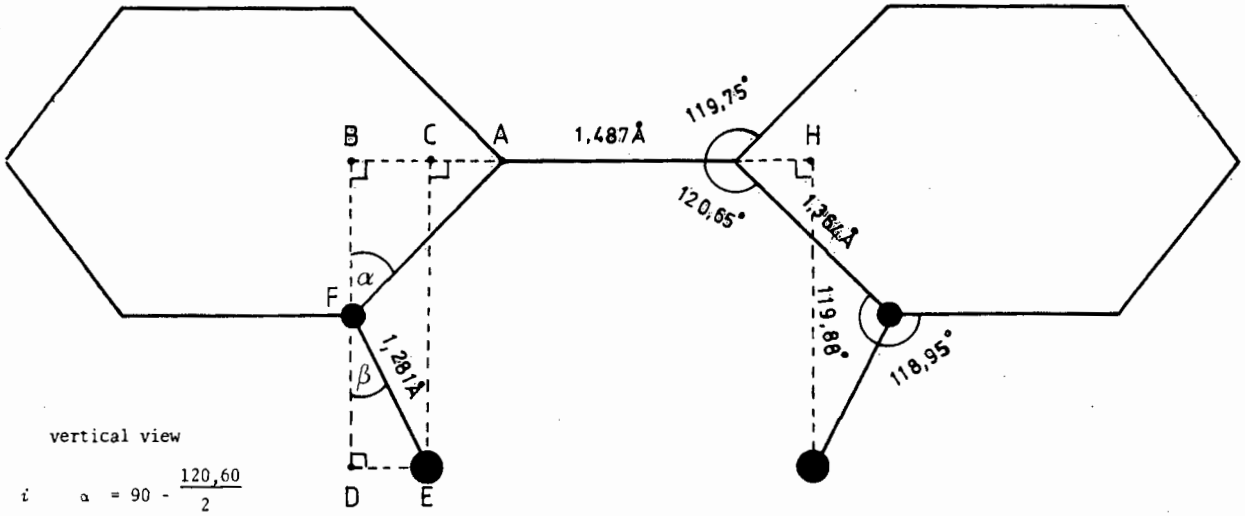

vertical view

i $\alpha = 90 - \frac{120,60}{2}$

$= 29,70°$

$\beta = 180 - (119,88 + \alpha)$

ii $= 30,42°$

iii $AB = 1,364 \cos \frac{120,60}{2}$

$= 0,678$ Å

iv $DE = 1,281 \sin \beta$

$= 0,645$ Å

v $AC = AB - DE$

$= 0,033$ Å

vi $CH = 1,487 + 2\,AC$

$= 1,553$ Å

vii $DF = 1,281 \cos \beta$

$= 1,107$ Å

viii $BF = 1,364 \sin \frac{120,60}{2}$

$= 1,183$ Å

ix $BD = CE_{(horizontal)}$

$= BF + FD$

$= 2,290$ Å

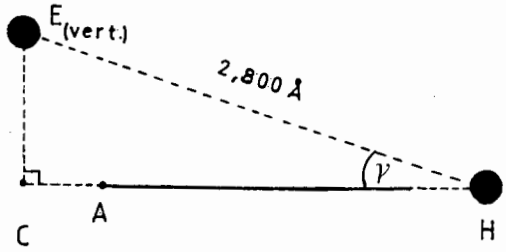

side view *along* inter-ring bond

NB. $CE_{(horizontal)} \neq CE_{(vertical)}$

x $\gamma = \cos^{-1} \frac{CH}{2,80}$

$= 56,54°$

xi $CE_{(vert)} = 2,80 \sin\gamma$

$= 2,330$ Å

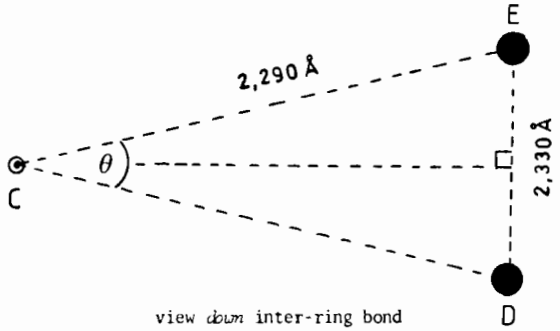

view *down* inter-ring bond

xii $\delta = 2 \sin^{-1} \frac{\frac{CE_{(vert)}}{2}}{BD}$

$= 61,85°$

cis planar model

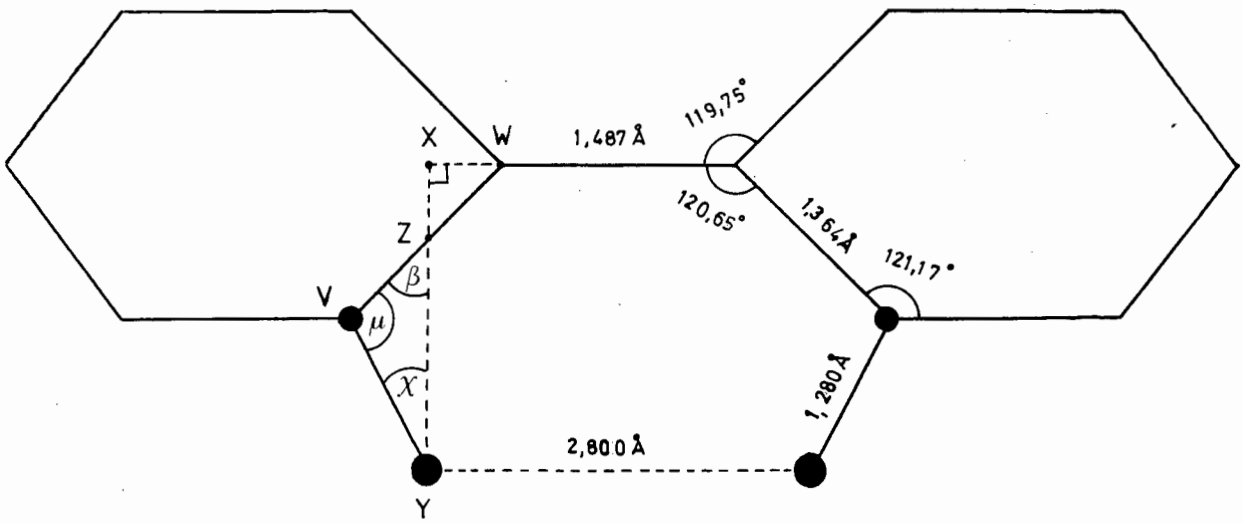

$VY = 1{,}281$ Å

$VW = 1{,}364$ Å

$$XW = \frac{2{,}800 - 1{,}487}{2}$$

$= 0{,}6565$ Å

$$ZW = \frac{XW}{\cos \frac{120{,}60}{2}}$$

$ZW = 1{,}320$ Å

$VZ = VW - ZW$

$= 0{,}044$ Å

$$\beta = 90 - \frac{120{,}60}{2}$$

$= 29{,}70°$

$$\chi = \sin^{-1} \frac{ZV \sin \beta}{YV}$$

$= 0{,}445°$

$\mu_{(distort)} = 180 - (\chi + \beta)$

$= 149{,}87°$

$\mu_{(undist.)} = 119{,}88°$

$\therefore$ distortion $= 29{,}99°$

Dimensions adapted from molecular structures by L.L. MERRITT and E.D. SCHROEDER, *Acta Cryst.*, *9* (1956) 801.

A.R. AL-KARAGHOULI, R.O. DAY and J.S. WOOD, *Inorg. Chem.*, *17* (1978) 3702.